NORMAN S. NISE
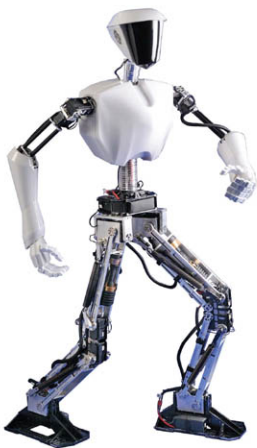
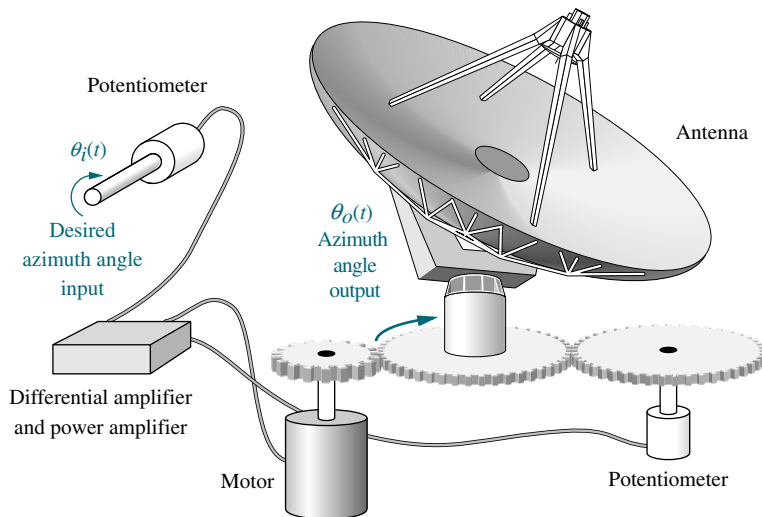# CONTROL SYSTEMS ENGINEERING

SIXTH EDITION
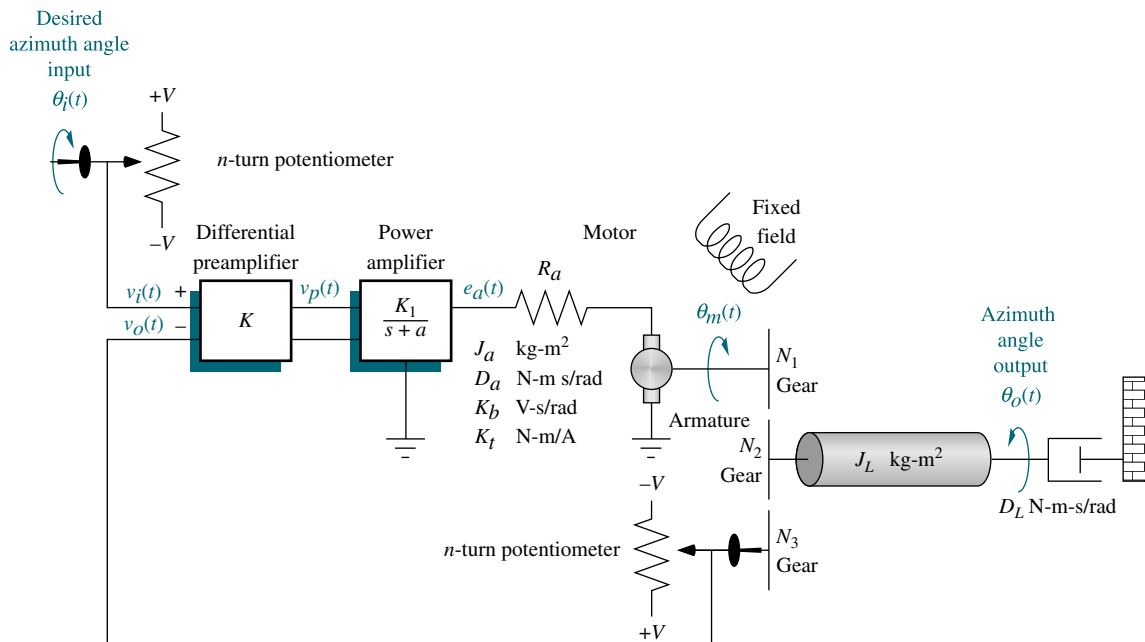
This page intentionally left blank

Antenna Azimuth Position Control System

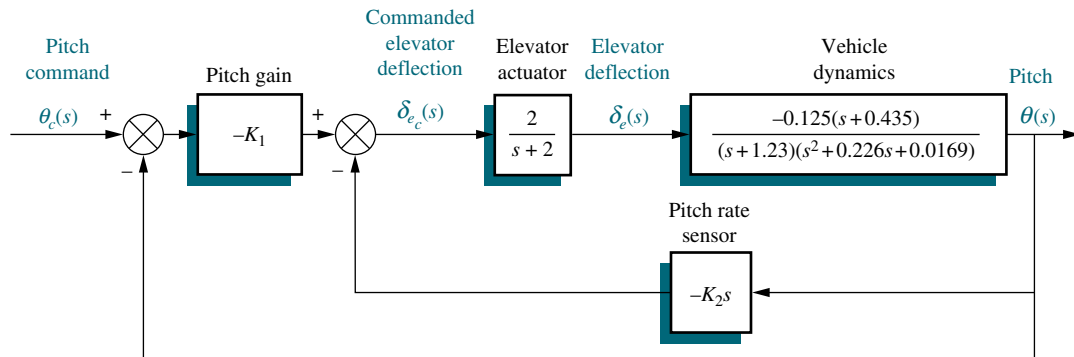## Layout

Potentiometer

$\theta_i(t)$

Desired
azimuth angle
input

Antenna

$\theta_o(t)$
Azimuth
angle
output

Differential amplifier
and power amplifier

Motor

Potentiometer

Schematic

Desired
azimuth angle
input
$\theta_i(t)$ $+V$

n-turn potentiometer

$-V$

Differential
preamplifier

Power
amplifier

Motor

Fixed
field

$v_i(t)$ $+$

$v_o(t)$ $-$

K

$v_p(t)$

$\dfrac{K_1}{s+a}$

$e_a(t)$

R_a

$\theta_m(t)$

J_a kg-m^2
D_a N-m s/rad
K_b V-s/rad
K_t N-m/A

Armature

$-V$

N_1
Gear

N_2
Gear

J_L kg-m^2

Azimuth
angle
output
$\theta_O(t)$

D_L N-m-s/rad

n-turn potentiometer

N_3
Gear

$+V$

Unmanned Free-Swimming Submersible Vehicle

Pitch Control System

Pitch command — $\theta_c(s)$ / Pitch gain $-K_1$ / Commanded elevator deflection $\delta_{e_c}(s)$ / Elevator actuator $\dfrac{2}{s+2}$ / Elevator deflection $\delta_e(s)$ / Vehicle dynamics $\dfrac{-0.125(s+0.435)}{(s+1.23)(s^2+0.226s+0.0169)}$ / Pitch $\theta(s)$ / Pitch rate sensor $-K_2s$

Heading Control System

Heading command — $\psi_c(s)$ / Heading gain $-K_1$ / Commanded rudder deflection $\delta_{r_c}(s)$ / Rudder actuator $\dfrac{2}{s+2}$ / Rudder deflection $\delta_r(s)$ / Vehicle dynamics $\dfrac{-0.125(s+0.437)}{(s+1.29)(s+0.193)}$ / Heading (yaw) rate $\dot{\psi}(s)$ / $\dfrac{1}{s}$ / Heading $\psi(s)$ / Yaw rate sensor $-K_2s$

CONTROL SYSTEMS ENGINEERING
Sixth Edition

Norman S. Nise

California State Polytechnic University, Pomona

WILEY

John Wiley & Sons, Inc.

To my wife, Ellen; sons, Benjamin and Alan; and daughter, Sharon, and their families.

Contents

Online location is www.wiley.com/college/nise

Preface

This book introduces students to the theory and practice of control systems engineering. The text emphasizes the practical application of the subject to the analysis and design of feedback systems.

The study of control systems engineering is essential for students pursuing degrees in electrical, mechanical, aerospace, biomedical, or chemical engineering. Control systems are found in a broad range of applications within these disciplines, from aircraft and spacecraft to robots and process control systems.

Control Systems Engineering is suitable for upper-division college and university engineering students and for those who wish to master the subject matter through self-study. The student using this text should have completed typical lower-division courses in physics and mathematics through differential equations. Other required background material, including Laplace transforms and linear algebra, is incorporated in the text, either within chapter discussions or separately in the appendixes or on the book's Companion Web site. This review material can be omitted without loss of continuity if the student does not require it.

Key Features

The key features of this sixth edition are:

- Standardized chapter organization
- Qualitative and quantitative explanations
- **Examples, Skill-Assessment Exercises,** and **Case Studies** throughout the text
- WileyPLUS content management system for students and professors
- **Cyber Exploration Laboratory and Virtual Experiments**
- Abundant illustrations
- Numerous end-of-chapter problems
- Emphasis on design
- Flexible coverage
- Emphasis on computer-aided analysis and design including MATLAB$^{®}$[1] and LabVIEW$^{®}$[2]

---

[1] MATLAB is a registered trademark of The MathWorks, Inc.

[2] LabVIEW is a registered trademark of National Instruments Corporation.

• Icons identifying major topics

Let us look at each feature in more detail.

◖ Standardized Chapter Organization

Each chapter begins with a list of chapter learning outcomes, followed by a list of case study learning outcomes that relate to specific student performance in solving a practical case study problem, such as an antenna azimuth position control system.

Topics are then divided into clearly numbered and labeled sections containing explanations, examples, and, where appropriate, skill-assessment exercises with answers. These numbered sections are followed by one or more case studies, as will be outlined in a few paragraphs. Each chapter ends with a brief summary, several review questions requiring short answers, a set of homework problems, and experiments.

◖ Qualitative and Quantitative Explanations

Explanations are clear and complete and, where appropriate, include a brief review of required background material. Topics build upon and support one another in a logical fashion. Groundwork for new concepts and terminology is carefully laid to avoid overwhelming the student and to facilitate self-study.

Although quantitative solutions are obviously important, a qualitative or intuitive understanding of problems and methods of solution is vital to producing the insight required to develop sound designs. Therefore, whenever possible, new concepts are discussed from a qualitative perspective before quantitative analysis and design are addressed. For example, in Chapter 8 the student can simply look at the root locus and describe qualitatively the changes in transient response that will occur as a system parameter, such as gain, is varied. This ability is developed with the help of a few simple equations from Chapter 4.

◖ Examples, Skill-Assessment Exercises, and Case Studies

Explanations are clearly illustrated by means of numerous numbered and labeled **Examples** throughout the text. Where appropriate, sections conclude with **Skill-Assessment Exercises**. These are computation drills, most with answers that test comprehension and provide immediate feedback. Complete solutions can be found at www.wiley.com/college/nise.

Broader examples in the form of **Case Studies** can be found after the last numbered section of every chapter, with the exception of Chapter 1. These case studies arc practical application problems that demonstrate the concepts introduced in the chapter. Each case study concludes with a "Challenge" problem that students may work in order to test their understanding of the material.

One of the case studies, an antenna azimuth position control system, is carried throughout the book. The purpose is to illustrate the application of new material in each chapter to the same physical system, thus highlighting the continuity of the design process. Another, more challenging case study, involving

an Unmannered Free-Swimming Submersible Vehicle, is developed over the course of five chapters.

WileyPLUS Content Management System for Students and Professors

WileyPLUS
WPCS
Control Solutions

WileyPLUS is an online suite of resources, including the full text, for students and instructors. For the sixth edition of *Control Systems Engineering*, this suite offers professors who adopt the book with WileyPLUS the ability to create homework assignments based on algorithmic problems or multi-part questions, which guide the student through a problem. Instructors also have the capability to integrate assets, such as the simulations, into their lecture presentations. Students will find a Read, Study, and Practice zone to help them work through problems based on the ones offered in the text.

Control Solutions (prepared by JustAsk) are included in the WileyPLUS platform. The student will find simulations and Control Solutions in the Read, Study, and Practice zone. The Control Solutions are highlighted in the text with a WileyPLUS icon.

A new addition to the WileyPLUS platform for this edition are National Instruments and Quanser Virtual Laboratories. You will find references to them in sidebar entries throughout the textbook.

Visit www.wiley.com or contact your local Wiley representative for information.

Cyber Exploration Laboratory and Virtual Experiments

Computer experiments using MATLAB, Simulink®[3] and the Control System Toolbox are found at the end of the Problems sections under the sub-heading **Cyber Exploration Laboratory**. New to this edition is LabVIEW, which is also used for experiments within the Cyber Exploration Laboratory section of the chapters. The experiments allow the reader to verify the concepts covered in the chapter via simulation. The reader also can change parameters and perform "what if" exploration to gain insight into the effect of parameter and configuration changes. The experiments are written with stated Objectives, Minimum Required Software Packages, as well as Prelab, Lab, and Postlab tasks and questions. Thus, the experiments may be used for a laboratory course that accompanies the class. Cover sheets for these experiments are available at www.wiley.com.college/nise.

In addition, and new to this sixth edition, are **Virtual Experiments**. These experiments are more tightly focused than the **Cyber Exploration Laboratory** experiments and use LabVIEW and Quanser virtual hardware to illustrate immediate discussion and examples. The experiments are referenced in sidebars throughout some chapters.

---

[3] Simulink is a registered trademark of The MathWorks, Inc.

◖ Abundant Illustrations

The ability to visualize concepts and processes is critical to the student's under-standing. For this reason, approximately 800 photos, diagrams, graphs, and tables appear throughout the book to illustrate the topics under discussion.

◖ Numerous End-of-Chapter Problems

Each chapter ends with a variety of homework problems that allow students to test their understanding of the material presented in the chapter. Problems vary in degree of difficulty and complexity, and most chapters include several practical, real-life problems to help maintain students' motivation. Also, the homework problems contain progressive analysis and design problems that use the same practical systems to demonstrate the concepts of each chapter.

◖ Emphasis on Design

Design
D

This textbook places a heavy emphasis on design. Chapters 8, 9, 11, 12 and 13 focus primarily on design. But. even in chapters that emphasize analysis, simple design examples are included wherever possible.

Throughout the book, design examples involving physical systems are identi-fied by the icon shown in the margin. End-of-chapter problems that involve the design of physical systems are included under the separate heading **Design Problems,** and also in chapters covering design, under the heading **Progressive Analysis and Design Problems**. In these examples and problems, a desired response is specified, and the student must evaluate certain system parameters, such as gain, or specify a system configuration along with parameter values. In addition, the text includes numerous design examples and problems (not identified by an icon) that involve purely mathematical systems.

Because visualization is so vital to understanding design, this text carefully relates indirect design specifications to more familiar ones. For example, the less familiar and indirect phase margin is carefully related to the more direct and familiar percent overshoot before being used as a design specification.

For each general type of design problem introduced in the text, a methodology for solving the problem is presented—in many cases in the form of a step-by-step procedure, beginning with a statement of design objectives. Example problems serve to demonstrate the methodology by following the procedure, making simplifying assumptions, and presenting the results of the design in tables or plots that compare the performance of the original system to that of the improved system. This comparison also serves as a check on the simplifying assumptions.

Transient response design topics are covered comprehensively in the text. They include:

- Design via gain adjustment using the root locus
- Design of compensation and controllers via the root locus
- Design via gain adjustment using sinusoidal frequency response methods
- Design of compensation via sinusoidal frequency response methods

- Design of controllers in state space using pole-placement techniques
- Design of observers in state-space using pole-placement techniques
- Design of digital control systems via gain adjustment on the root locus
- Design of digital control system compensation via *s*-plane design and the Tustin transformation

Steady-state error design is covered comprehensively in this textbook and includes:

- Gain adjustment
- Design of compensation via the root locus
- Design of compensation via sinusoidal frequency response methods
- Design of integral control in state space

Finally, the design of gain to yield stability is covered from the following perspectives:

- Routh-Hurwitz criterion
- Root locus
- Nyquist criterion
- Bode plots

Flexible Coverage

The material in this book can be adapted for a one-quarter or a one-semester course. The organization is flexible, allowing the instructor to select the material that best suits the requirements and time constraints of the class.

State Space
SS

Throughout the book, state-space methods are presented along with the classical approach. Chapters and sections (as well as examples, exercises, review questions, and problems) that cover state space are marked by the icon shown in the margin and can be omitted without any loss of continuity. Those wishing to add a basic introduction to state-space modeling can include Chapter 3 in the syllabus.

In a one-semester course, the discussions of slate-space analysis in Chapters 4, 5, 6 and 7, as well as state-space design in Chapter 12, can be covered along with the classical approach. Another option is to teach state space separately by gathering the appropriate chapters and sections marked with the **State Space** icon into a single unit that follows the classical approach. In a one-quarter course, Chapter 13, "Digital Control Systems," could be eliminated.

Emphasis on Computer-Aided Analysis and Design

Control systems problems, particularly analysis and design problems using the root locus, can be tedious, since their solution involves trial and error. To solve these problems, students should be given access to computers or programmable calculators configured with appropriate software. In this sixth edition, MATLAB continues to be integrated into the text as an optional feature. In addition, and new to this

edition, we have included LabVIEW as an option to computer-aided analysis and design.

Many problems in this text can be solved with either a computer or a hand-held programmable calculator. For example, students can use the programmable calculator to (1) determine whether a point on the *s*-plane is also on the root locus, (2) find magnitude and phase frequency response data for Nyquist and Bode diagrams, and (3) convert between the following representations of a second-order system:

- Pole location in polar coordinates
- Pole location in Cartesian coordinates
- Characteristic polynomial
- Natural frequency and damping ratio
- Settling time and percent overshoot
- Peak time and percent overshoot
- Settling time and peak time

Handheld calculators have the advantage of easy accessibility for homework and exams. Please consult Appendix H, located at www.wiley.com/college/nise, for a discussion of computational aids that can be adapted to handheld calculators.

Personal computers are better suited for more computation-intensive applications, such as plotting time responses, root loci, and frequency response curves, as well as finding state-transition matrices. These computers also give the student a real-world environment in which to analyze and design control systems. Those not using MATLAB or LabVIEW can write their own programs or use other programs, such as Program CC. Please consult Appendix H at www.wiley.com/college/nise for a discussion of computational aids that can be adapted for use on computers that do not have MATLAB or LabVIEW installed.

Without access to computers or programmable calculators, students cannot obtain meaningful analysis and design results and the learning experience will be limited.

Icons Identifying Major Topics

WileyPLUS

WPCS

Control Solutions

MATLAB

ML

Simulink

SL

Gui Tool

GUIT

Several icons identify coverage and optional material. The icons are summarized as follows:

Control Solutions for the student are identified with a WileyPLUS icon. These problems, developed by JustAsk, are worked in detail and offer explanations of every facet of the solution.

The MATLAB icon identifies MATLAB discussions, examples, exercises, and problems. MATLAB coverage is provided as an enhancement and is not required to use the text.

The Simulink icon identifies Simulink discussions, examples, exercises, and problems. Simulink coverage is provided as an enhancement and is not required to use the text.

The GUI Tool icon identifies MATLAB GUI Tools discussions, examples, exercises, and problems. The discussion of the tools, which includes the LTI Viewer, the Simulink LTIViewer, and the SISO Design Tool, is provided as an enhancement and is not required to use the text.

The Symbolic Math icon identifies Symbolic Math Toolbox discussions, examples, exercises, and problems. Symbolic Math Toolbox coverage is provided as an enhancement and is not required to use the text.

The LabVIEW icon identifies LabVIEW discussions, examples, exercises, and problems. LabVIEW is provided as an enhancement and is not required to use the text.

The State Space icon highlights state-space discussions, examples, exercises, and problems. State-space material is optional and can be omitted without loss of continuity.

The Design icon clearly identifies design problems involving physical systems.

Symbolic Math
SM

LabVIEW
LV

State Space
SS

Design
D

New to This Edition

The following list describes the key changes in this sixth edition

End-of-chapter problems   More than 20% of the end-of-chapter problems are either new or revised. Also, an additional Progressive Analysis and Design Problem has been added at the end of the chapter problems. The new progressive problem analyzes and designs a hybrid electric vehicle.

MATLAB   The use of MATLAB for computer-aided analysis and design continues to be integrated into discussions and problems as an optional feature in the sixth edition. The MATLAB tutorial has been updated to MATLAB Version 7.9 (R 2009b), the Control System Toolbox Version 8.4, and the Symbolic Math Toolbox Version 5.3

In addition, MATLAB code continues to be incorporated in the chapters in the form of sidebar boxes entitled TryIt.

Virtual Experiments   Virtual experiments, developed by National Instruments and Quanser, are included via sidebar references to experiments on Wiley-PLUS. The experiments are performed with 3-D simulations of Quanser hardware using developed LabVIEW VIs. Virtual Experiments are tightly focused and linked to a discussion or example.

Cyber Exploration Laboratory   Experiments using LabVIEW have been added. Cyber Exploration Laboratory experiments are general in focus and are envisioned to be used in an associated lab class.

MATLAB's Simulink   The use of Simulink to show the effects of nonlinearities upon the time response of open-loop and closed-loop systems appears again in this sixth edition. We also continue to use Simulink to demonstrate how to simulate digital systems. Finally, the Simulink tutorial has been updated to Simulink 7.4

Chapter 11   Lag-lead compensator design using Nichols charts has been added to Section 11.5.

LabVIEW   New to this edition is LabVIEW. A tutorial for this tool is included in Appendix D. LabVIEW is used in Cyber Exploration Laboratory experiments and other problems throughout the textbook.

Book Companion Site (BCS) at www .wiley.com/college/nise

The BCS for the sixth edition includes various student and instructor resources. This free resource can be accessed by going to www.wiley.com/college/nise and clicking on Student Companion Site. Professors also access their password-protected resources on the Instructor Companion Site available through this url. Instructors should contact their Wiley sales representative for access.

For the Student:

- All M-files used in the MATLAB, Simulink, GUI Tools, and Symbolic Math Toolbox tutorials, as well as the TryIt exercises
- Copies of the Cyber Exploration Laboratory experiments for use as experiment cover sheets
- Solutions to the Skill-Assessment Exercises in the text
- LabVIEW Virtual Experiments and LabVIEW VIs used in Appendix D

For the Instructor;

- PowerPoint[®4] files containing the figures from the textbook
- Solutions to end-of-chapter problem sets
- Simulations, developed by JustAsk, for inclusion in lecture presentations

Book Organization by Chapter

Many times it is helpful lo understand an author's reasoning behind the organization of the course material. The following paragraphs hopefully shed light on this topic.

The primary goal of Chapter 1 is to motivate students. In this chapter, students learn about the many applications of control systems in everyday life and about the advantages of study and a career in this field. Control systems engineering design objectives, such as transient response, steady-state error, and stability, are introduced, as is the path to obtaining these objectives. New and unfamiliar terms also are included in the Glossary.

Many students have trouble with an early step in the analysis and design sequence: transforming a physical system into a schematic. This step requires many simplifying assumptions based on experience the typical college student does not yet possess. Identifying some of these assumptions in Chapter 1 helps to fill the experience gap.

Chapters 2, 3, and 5 address the representation of physical systems. Chapters 2 and 3 cover modeling of open-loop systems, using frequency response techniques and state-space techniques, respectively. Chapter 5 discusses the representation and reduction of systems formed of interconnected open-loop subsystems. Only a representative sample of physical systems can be covered in a textbook of this length. Electrical, mechanical (both translational and rotational), and electromechanical systems are used as examples of physical systems that are modeled, analyzed, and designed. Linearization of a nonlinear system—one technique used by the engineer to simplify a system in order to represent it mathematically—is also introduced.

Chapter 4 provides an introduction to system analysis, that is, finding and describing the output response of a system. It may seem more logical to reverse the order of Chapters 4 and 5, to present the material in Chapter 4 along with other chapters covering analysis. However, many years of teaching control systems have taught me that the sooner students see an application of the study of system representation, the higher their motivation levels remain.

Chapters 6, 7, 8, and 9 return to control systems analysis and design with the study of stability (Chapter 6), steady-state errors (Chapter 7), and transient response of higher-order systems using root locus techniques (Chapter 8). Chapter 9 covers design of compensators and controllers using the root locus.

---

[4] PowerPoint is a registered trademark of Microsoft Corporation.

Chapters 10 and 11 focus on sinusoidal frequency analysis and design. Chapter 10, like Chapter 8, covers basic concepts for stability, transient response, and steady-state-error analysis. However, Nyquist and Bode methods are used in place of root locus. Chapter 11, like Chapter 9, covers the design of compensators, but from the point of view of sinusoidal frequency techniques rather than root locus.

An introduction to state-space design and digital control systems analysis and design completes the text in Chapters 12 and 13, respectively. Although these chapters can be used as an introduction for students who will be continuing their study of control systems engineering, they are useful by themselves and as a supplement to the discussion of analysis and design in the previous chapters. The subject matter cannot be given a comprehensive treatment in two chapters, but the emphasis is clearly outlined and logically linked to the rest of the book.

(Acknowledgments

worked behind the scenes, but who should be thanked never the less. Rather than repeating their names and titles here, I refer the reader to the copyright page of this book where they are listed and credited. I am very thankful for their contributions.

Next, I want to acknowledge Integra Software Services, Inc. and its staff for turning the sixth edition manuscript into the finished product you are holding in your hands. Specifically, kudos go out to Heather Johnson, Managing Editor, who, once again, was always there to address my concerns in a timely and professional manner.

My sincere appreciation is extended to Erik Luther of National Instruments Corporation and Paul Gilbert and Michel Levis of Quanser for conceiving, coordinating, and developing the Virtual Experiments that I am sure will enhance your understanding of control systems.

Finally, last but certainly not least, I want to express my appreciation to my wife, Ellen, for her support in ways too numerous to mention during the writing of the past six editions. Specifically though, thanks to her proofing final pages for this sixth edition, you the reader hopefully will find comprehension rather than apprehension in the pages that follow.

<div align="right">Norman S. Nise</div>

Introduction

⟮ Chapter Learning Outcomes ⟯

After completing this chapter, the student will be able to:

- Define a control system and describe some applications (Section 1.1)
- Describe historical developments leading to modern day control theory (Section 1.2)
- Describe the basic features and configurations of control systems (Section 1.3)
- Describe control systems analysis and design objectives (Section 1.4)
- Describe a control system's design process (Sections 1.5–1.6)
- Describe the benefit from studying control systems (Section 1.7)

⟮ Case Study Learning Outcomes ⟯

- You will be introduced to a running case study—an antenna azimuth position control system—that will serve to illustrate the principles in each subsequent chapter. In this chapter, the system is used to demonstrate qualitatively how a control system works as well as to define performance criteria that are the basis for control systems analysis and design.

1.1   Introduction

Control systems are an integral part of modern society. Numerous applications are all around us: The rockets fire, and the space shuttle lifts off to earth orbit; in splashing cooling water, a metallic part is automatically machined; a self-guided vehicle delivering material to workstations in an aerospace assembly plant glides along the floor seeking its destination. These are just a few examples of the automatically controlled systems that we can create.

We are not the only creators of automatically controlled systems; these systems also exist in nature. Within our own bodies are numerous control systems, such as the pancreas, which regulates our blood sugar. In time of "fight or flight," our adrenaline increases along with our heart rate, causing more oxygen to be delivered to our cells. Our eyes follow a moving object to keep it in view; our hands grasp the object and place it precisely at a predetermined location.

Even the nonphysical world appears to be automatically regulated. Models have been suggested showing automatic control of student performance. The input to the model is the student's available study time, and the output is the grade. The model can be used to predict the time required for the grade to rise if a sudden increase in study time is available. Using this model, you can determine whether increased study is worth the effort during the last week of the term.

Control System Definition

A control system consists of *subsystems* and *processes* (or *plants)* assembled for the purpose of obtaining a desired *output* with desired *performance*, given a specified *input*. Figure 1.1 shows a control system in its simplest form, where the input represents a desired output.
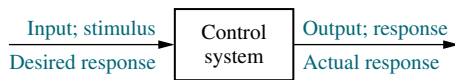
FIGURE 1.1   Simplified description of a control system

For example, consider an elevator. When the fourth-floor button is pressed on the first floor, the elevator rises to the fourth floor with a speed and floor-leveling accuracy designed for passenger comfort. The push of the fourth-floor button is an *input* that represents our desired *output*, shown as a step function in Figure 1.2. The *performance* of the elevator can be seen from the elevator response curve in the figure.

Two major measures of performance are apparent: (1) the transient response and (2) the steady-state error. In our example, passenger comfort and passenger patience are dependent upon the transient response. If this response is too fast, passenger comfort is sacrificed; if too slow, passenger patience is sacrificed. The steady-state error is another important performance specification since passenger safety and convenience would be sacrificed if the elevator did not properly level.
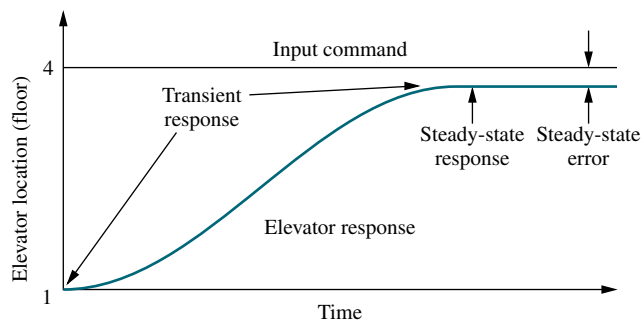
FIGURE 1.2   Elevator response
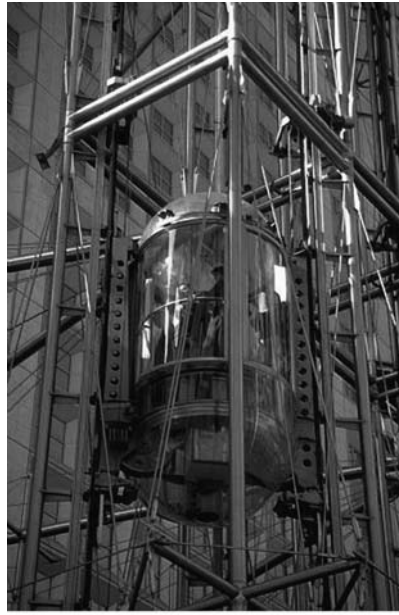
FIGURE 1.3   a. Early elevators were controlled by hand ropes or an elevator operator. Here a rope is cut to demonstrate the safety brake, an innovation in early elevators (© Bettman/ Corbis); **b.** One of two modern Duo-lift elevators makes its way up the Grande Arche in Paris. Two elevators are driven by one motor, with each car acting as a counterbalance to the other. Today, elevators are fully automatic, using control systems to regulate position and velocity.

Advantages of Control Systems

With control systems we can move large equipment with precision that would otherwise be impossible. We can point huge antennas toward the farthest reaches of the universe to pick up faint radio signals; controlling these antennas by hand would be impossible. Because of control systems, elevators carry us quickly to our destination, automatically stopping at the right floor (Figure 1.3). We alone could not provide the power required for the load and the speed; motors provide the power, and control systems regulate the position and speed.

We build control systems for four primary reasons:

1. Power amplification
2. Remote control
3. Convenience of input form
4. Compensation for disturbances

For example, a radar antenna, positioned by the low-power rotation of a knob at the input, requires a large amount of power for its output rotation. A control system can produce the needed power amplification, or power *gain*.

Robots designed by control system principles can compensate for human disabilities. Control systems are also useful in remote or dangerous locations. For example, a remote-controlled robot arm can be used to pick up material in a radioactive environment. Figure 1.4 shows a robot arm designed to work in contaminated environments.

Control systems can also be used to provide convenience by changing the form of the input. For example, in a temperature control system, the input is a *position* on a thermostat. The output is *heat*. Thus, a convenient position input yields a desired thermal output.

Another advantage of a control system is the ability to compensate for disturbances. Typically, we control such variables as temperature in
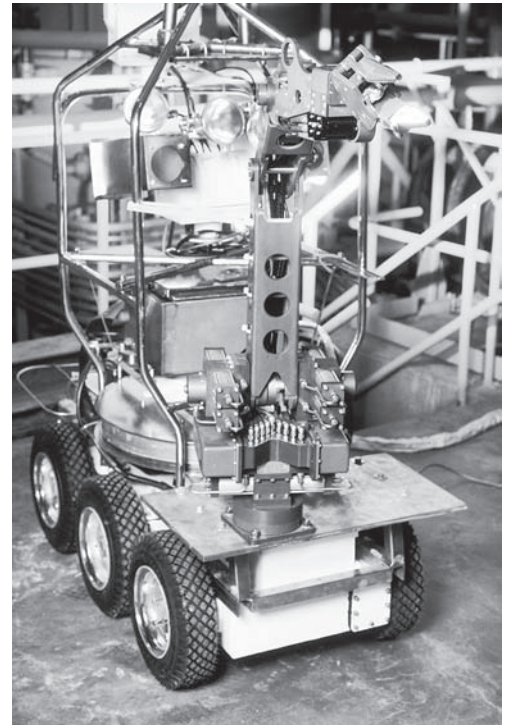
FIGURE 1.4   *Rover* was built to work in contaminated areas at Three Mile Island in Middleton, Pennsylvania, where a nuclear accident occurred in 1979. The remote-controlled robot's long arm can be seen at the front of the vehicle.

thermal systems, position and velocity in mechanical systems, and voltage, current, or frequency in electrical systems. The system must be able to yield the correct output even with a disturbance. For example, consider an antenna system that points in a commanded direction. If wind forces the antenna from its commanded position, or if noise enters internally, the system must be able to detect the disturbance and correct the antenna's position. Obviously, the system's input will not change to make the correction. Consequently, the system itself must measure the amount that the disturbance has repositioned the antenna and then return the antenna to the position commanded by the input.

1.2   A History of Control Systems

Feedback control systems are older than humanity. Numerous biological control systems were built into the earliest inhabitants of our planet. Let us now look at a brief history of human-designed control systems.[1]

Liquid-Level Control

The Greeks began engineering feedback systems around 300 B.C. A water clock invented by Ktesibios operated by having water trickle into a measuring container at a constant rate. The level of water in the measuring container could be used to tell time. For water to trickle at a constant rate, the supply tank had to be kept at a constant level. This was accomplished using a float valve similar to the water-level control in today's flush toilets.

Soon after Ktesibios, the idea of liquid-level control was applied to an oil lamp by Philon of Byzantium. The lamp consisted of two oil containers configured vertically. The lower pan was open at the top and was the fuel supply for the flame. The closed upper bowl was the fuel reservoir for the pan below. The containers were interconnected by two capillary tubes and another tube, called a *vertical riser*, which was inserted into the oil in the lower pan just below the surface. As the oil burned, the base of the vertical riser was exposed to air, which forced oil in the reservoir above to flow through the capillary tubes and into the pan. The transfer of fuel from the upper reservoir to the pan stopped when the previous oil level in the pan was reestablished, thus blocking the air from entering the vertical riser. Hence, the system kept the liquid level in the lower container constant.

Steam Pressure and Temperature Controls

Regulation of steam pressure began around 1681 with Denis Papin's invention of the safety valve. The concept was further elaborated on by weighting the valve top. If the upward pressure from the boiler exceeded the weight, steam was released, and the pressure decreased. If it did not exceed the weight, the valve did not open, and the pressure inside the boiler increased. Thus, the weight on the valve top set the internal pressure of the boiler.

Also in the seventeenth century, Cornelis Drebbel in Holland invented a purely mechanical temperature control system for hatching eggs. The device used a vial of alcohol and mercury with a floater inserted in it. The floater was connected to a damper that controlled a flame. A portion of the vial was inserted into the incubator to sense the heat generated by the fire. As the heat increased, the alcohol and mercury expanded, raising the floater, closing the damper, and reducing the flame. Lower temperature caused the float to descend, opening the damper and increasing the flame.

Speed Control

In 1745, speed control was applied to a windmill by Edmund Lee. Increasing winds pitched the blades farther back, so that less area was available. As the wind

---

[1] See *Bennett* (*1979*) and *Mayr* (*1970*) for definitive works on the history of control systems.

decreased, more blade area was available. William Cubitt improved on the idea in 1809 by dividing the windmill sail into movable louvers.

Also in the eighteenth century, James Watt invented the flyball speed governor to control the speed of steam engines. In this device, two spinning flyballs rise as rotational speed increases. A steam valve connected to the flyball mechanism closes with the ascending flyballs and opens with the descending flyballs, thus regulating the speed.

Stability, Stabilization, and Steering

Control systems theory as we know it today began to crystallize in the latter half of the nineteenth century. In 1868, James Clerk Maxwell published the stability criterion for a third-order system based on the coefficients of the differential equation. In 1874, Edward John Routh, using a suggestion from William Kingdon Clifford that was ignored earlier by Maxwell, was able to extend the stability criterion to fifth-order systems. In 1877, the topic for the Adams Prize was "The Criterion of Dynamical Stability." In response, Routh submitted a paper entitled *A Treatise on the Stability of a Given State of Motion* and won the prize. This paper contains what is now known as the Routh-Hurwitz criterion for stability, which we will study in Chapter 6. Alexandr Michailovich Lyapunov also contributed to the development and formulation of today's theories and practice of control system stability. A student of P. L. Chebyshev at the University of St. Petersburg in Russia, Lyapunov extended the work of Routh to nonlinear systems in his 1892 doctoral thesis, entitled *The General Problem of Stability of Motion*.

During the second half of the 1800s, the development of control systems focused on the steering and stabilizing of ships. In 1874, Henry Bessemer, using a gyro to sense a ship's motion and applying power generated by the ship's hydraulic system, moved the ship's saloon to keep it stable (whether this made a difference to the patrons is doubtful). Other efforts were made to stabilize platforms for guns as well as to stabilize entire ships, using pendulums to sense the motion.

Twentieth-Century Developments

It was not until the early 1900s that automatic steering of ships was achieved. In 1922, the Sperry Gyroscope Company installed an automatic steering system that used the elements of compensation and adaptive control to improve performance. However, much of the general theory used today to improve the performance of automatic control systems is attributed to Nicholas Minorsky, a Russian born in 1885. It was his theoretical development applied to the automatic steering of ships that led to what we call today proportional-plus-integral-plus-derivative (PID), or three-mode, controllers, which we will study in Chapters 9 and 11.

In the late 1920s and early 1930s, H. W. Bode and H. Nyquist at Bell Telephone Laboratories developed the analysis of feedback amplifiers. These contributions evolved into sinusoidal frequency analysis and design techniques currently used for feedback control system, and are presented in Chapters 10 and 11.

In 1948, Walter R. Evans, working in the aircraft industry, developed a graphical technique to plot the roots of a characteristic equation of a feedback system whose parameters changed over a particular range of values. This technique, now known as the root locus, takes its place with the work of Bode and Nyquist in forming the foundation of linear control systems analysis and design theory. We will study root locus in Chapters 8, 9, and 13.

Contemporary Applications

Today, control systems find widespread application in the guidance, navigation, and control of missiles and spacecraft, as well as planes and ships at sea. For example,

modern ships use a combination of electrical, mechanical, and hydraulic components to develop rudder commands in response to desired heading commands. The rudder commands, in turn, result in a rudder angle that steers the ship.

We find control systems throughout the process control industry, regulating liquid levels in tanks, chemical concentrations in vats, as well as the thickness of fabricated material. For example, consider a thickness control system for a steel plate finishing mill. Steel enters the finishing mill and passes through rollers. In the finishing mill, X-rays measure the actual thickness and compare it to the desired thickness. Any difference is adjusted by a screw-down position control that changes the roll gap at the rollers through which the steel passes. This change in roll gap regulates the thickness.

Modern developments have seen widespread use of the digital computer as part of control systems. For example, computers in control systems are for industrial robots, spacecraft, and the process control industry. It is hard to visualize a modern control system that does not use a digital computer.

The space shuttle contains numerous control systems operated by an onboard computer on a time-shared basis. Without control systems, it would be impossible to guide the shuttle to and from earth's orbit or to adjust the orbit itself and support life on board. Navigation functions programmed into the shuttle's computers use data from the shuttle's hardware to estimate vehicle position and velocity. This information is fed to the guidance equations that calculate commands for the shuttle's flight control systems, which steer the spacecraft. In space, the flight control system gimbals (rotates) the orbital maneuvering system (OMS) engines into a position that provides thrust in the commanded direction to steer the spacecraft. Within the earth's atmosphere, the shuttle is steered by commands sent from the flight control system to the aerosurfaces, such as the elevons.

Within this large control system represented by navigation, guidance, and control are numerous subsystems to control the vehicle's functions. For example, the elevons require a control system to ensure that their position is indeed that which was commanded, since disturbances such as wind could rotate the elevons away from the commanded position. Similarly, in space, the gimbaling of the orbital maneuvering engines requires a similar control system to ensure that the rotating engine can accomplish its function with speed and accuracy. Control systems are also used to control and stabilize the vehicle during its descent from orbit. Numerous small jets that compose the reaction control system (RCS) are used initially in the exoatmosphere, where the aerosurfaces are ineffective. Control is passed to the aerosurfaces as the orbiter descends into the atmosphere.

Inside the shuttle, numerous control systems are required for power and life support. For example, the orbiter has three fuel-cell power plants that convert hydrogen and oxygen (reactants) into electricity and water for use by the crew. The fuel cells involve the use of control systems to regulate temperature and pressure. The reactant tanks are kept at constant pressure as the quantity of reactant diminishes. Sensors in the tanks send signals to the control systems to turn heaters on or off to keep the tank pressure constant (*Rockwell International*, *1984*).

Control systems are not limited to science and industry. For example, a home heating system is a simple control system consisting of a thermostat containing a bimetallic material that expands or contracts with changing temperature. This expansion or contraction moves a vial of mercury that acts as a switch, turning the heater on or off. The amount of expansion or contraction required to move the mercury switch is determined by the temperature setting.
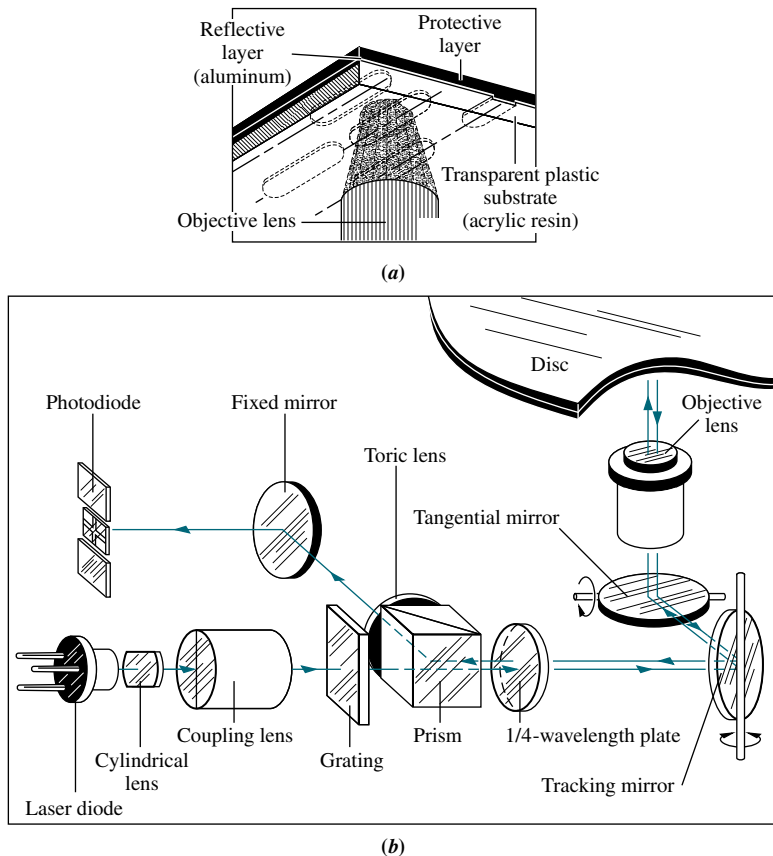
FIGURE 1.5   Optical playback system: **a.** objective lens reading pits on an optical disc; **b.** optical path for playback, showing tracking mirror rotated by a control system to keep the laser beam positioned on the pits (Pioneer Electronics (USA), Inc.)

Home entertainment systems also have built-in control systems. For example, in an optical disk recording system microscopic pits representing the information are burned into the disc by a laser during the recording process. During playback, a reflected laser beam focused on the pits changes intensity (Figure 1.5). The light intensity changes are converted to an electrical signal and processed as sound or picture. A control system keeps the laser beam positioned on the pits, which are cut as concentric circles.

There are countless other examples of control systems, from the everyday to the extraordinary. As you begin your study of control systems engineering, you will become more aware of the wide variety of applications.

1.3   System Configurations

In this section, we discuss two major configurations of control systems: open loop and closed loop. We can consider these configurations to be the internal architecture of the total system shown in Figure 1.1. Finally, we show how a digital computer forms part of a control system's configuration.

Open-Loop Systems

A generic *open-loop system* is shown in Figure 1.6(*a*). It starts with a subsystem called an *input transducer*, which converts the form of the input to that used by the *controller*. The controller drives a *process* or a *plant*. The input is sometimes called the *reference*, while the output can be called the *controlled variable*. Other signals, such as *disturbances*, are shown added to the controller and process outputs via *summing junctions*, which yield the algebraic sum of their input signals using associated signs. For example, the plant can be a furnace or air conditioning system, where the output variable is temperature. The controller in a heating system consists of fuel valves and the electrical system that operates the valves.

The distinguishing characteristic of an open-loop system is that it cannot compensate for any disturbances that add to the controller's driving signal (Disturbance 1 in Figure 1.6(*a*)). For example, if the controller is an electronic amplifier and Disturbance 1 is noise, then any additive amplifier noise at the first summing junction will also drive the process, corrupting the output with the effect of the noise. The output of an open-loop system is corrupted not only by signals that add to the controller's commands but also by disturbances at the output (Disturbance 2 in Figure 1.6(*a*)). The system cannot correct for these disturbances, either.

Open-loop systems, then, do not correct for disturbances and are simply commanded by the input. For example, toasters are open-loop systems, as anyone with burnt toast can attest. The controlled variable (output) of a toaster is the color of the toast. The device is designed with the assumption that the toast will be darker the longer it is subjected to heat. The toaster does not measure the color of the toast; it does not correct for the fact that the toast is rye, white, or sourdough, nor does it correct for the fact that toast comes in different thicknesses.

Other examples of open-loop systems are mechanical systems consisting of a mass, spring, and damper with a constant force positioning the mass. The greater the force, the greater the displacement. Again, the system position will change with a disturbance, such as an additional force, and the system will not detect or correct for the disturbance. Or assume that you calculate the amount of time you need to study

(*a*)

(*b*)
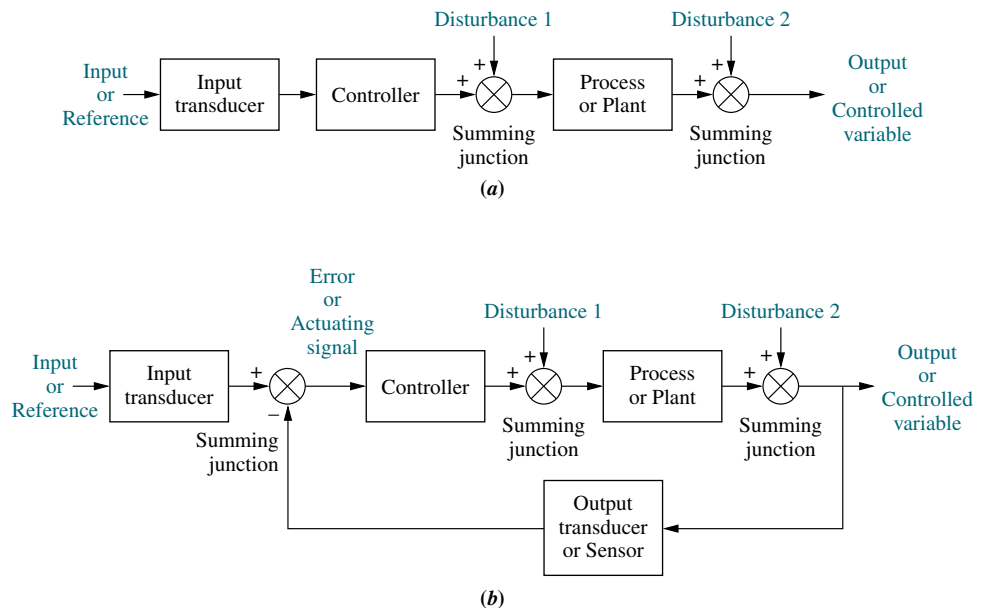
FIGURE 1.6   Block diagrams of control systems: **a.** open-loop system; **b.** closed-loop system

for an examination that covers three chapters in order to get an A. If the professor adds a fourth chapter—a disturbance—you are an open-loop system if you do not detect the disturbance and add study time to that previously calculated. The result of this oversight would be a lower grade than you expected.

Closed-Loop (Feedback Control) Systems

The disadvantages of open-loop systems, namely sensitivity to disturbances and inability to correct for these disturbances, may be overcome in *closed-loop systems*. The generic architecture of a closed-loop system is shown in Figure 1.6(*b*).

The input transducer converts the form of the input to the form used by the controller. An *output transducer*, or *sensor*, measures the output response and converts it into the form used by the controller. For example, if the controller uses electrical signals to operate the valves of a temperature control system, the input position and the output temperature are converted to electrical signals. The input position can be converted to a voltage by a *potentiometer*, a variable resistor, and the output temperature can be converted to a voltage by a *thermistor*, a device whose electrical resistance changes with temperature.

The first summing junction algebraically adds the signal from the input to the signal from the output, which arrives via the *feedback path*, the return path from the output to the summing junction. In Figure 1.6(*b*), the output signal is subtracted from the input signal. The result is generally called the *actuating signal*. However, in systems where both the input and output transducers have *unity gain* (that is, the transducer amplifies its input by 1), the actuating signal's value is equal to the actual difference between the input and the output. Under this condition, the actuating signal is called the *error*.

The closed-loop system compensates for disturbances by measuring the output response, feeding that measurement back through a feedback path, and comparing that response to the input at the summing junction. If there is any difference between the two responses, the system drives the plant, via the actuating signal, to make a correction. If there is no difference, the system does not drive the plant, since the plant's response is already the desired response.

Closed-loop systems, then, have the obvious advantage of greater accuracy than open-loop systems. They are less sensitive to noise, disturbances, and changes in the environment. Transient response and steady-state error can be controlled more conveniently and with greater flexibility in closed-loop systems, often by a simple adjustment of gain (amplification) in the loop and sometimes by redesigning the controller. We refer to the redesign as *compensating* the system and to the resulting hardware as a *compensator*. On the other hand, closed-loop systems are more complex and expensive than open-loop systems. A standard, open-loop toaster serves as an example: It is simple and inexpensive. A closed-loop toaster oven is more complex and more expensive since it has to measure both color (through light reflectivity) and humidity inside the toaster oven. Thus, the control systems engineer must consider the trade-off between the simplicity and low cost of an open-loop system and the accuracy and higher cost of a closed-loop system.

In summary, systems that perform the previously described measurement and correction are called closed-loop, or feedback control, systems. Systems that do not have this property of measurement and correction are called open-loop systems.

Computer-Controlled Systems

In many modern systems, the controller (or compensator) is a digital computer. The advantage of using a computer is that many loops can be controlled or compensated by the same computer through time sharing. Furthermore, any adjustments of the

compensator parameters required to yield a desired response can be made by changes in software rather than hardware. The computer can also perform supervisory functions, such as scheduling many required applications. For example, the space shuttle main engine (SSME) controller, which contains two digital computers, alone controls numerous engine functions. It monitors engine sensors that provide pressures, temperatures, flow rates, turbopump speed, valve positions, and engine servo valve actuator positions. The controller further provides closed-loop control of thrust and propellant mixture ratio, sensor excitation, valve actuators, spark igniters, as well as other functions (*Rockwell International*, *1984*).

1.4   Analysis and Design Objectives

In Section 1.1 we briefly alluded to some control system performance specifications, such as transient response and steady-state error. We now expand upon the topic of performance and place it in perspective as we define our analysis and design objectives.

Analysis is the process by which a system's performance is determined. For example, we evaluate its transient response and steady-state error to determine if they meet the desired specifications. *Design* is the process by which a system's performance is created or changed. For example, if a system's transient response and steady-state error are analyzed and found not to meet the specifications, then we change parameters or add additional components to meet the specifications.

A control system is *dynamic:* It responds to an input by undergoing a transient response before reaching a steady-state response that generally resembles the input. We have already identified these two responses and cited a position control system (an elevator) as an example. In this section, we discuss three major objectives of systems analysis and design: producing the desired transient response, reducing steady-state error, and achieving stability. We also address some other design concerns, such as cost and the sensitivity of system performance to changes in parameters.

Transient Response

Transient response is important. In the case of an elevator, a slow transient response makes passengers impatient, whereas an excessively rapid response makes them uncomfortable. If the elevator oscillates about the arrival floor for more than a second, a disconcerting feeling can result. Transient response is also important for structural reasons: Too fast a transient response could cause permanent physical damage. In a computer, transient response contributes to the time required to read from or write to the computer's disk storage (see Figure 1.7). Since reading and writing cannot take place until the head stops, the speed of the read/write head's movement from one track on the disk to another influences the overall speed of the computer.

In this book, we establish quantitative definitions for transient response. We then analyze the system for its *existing* transient response. Finally, we adjust parameters or design components to yield a *desired* transient response—our first analysis and design objective.

FIGURE 1.7   Computer hard disk drive, showing disks and read/write head

Steady-State Response

Another analysis and design goal focuses on the steady-state response. As we have seen, this response resembles the input and is usually what remains after the transients have decayed to zero. For example, this response may be an elevator stopped near the fourth floor or the head of a disk drive finally stopped at the correct track. We are concerned about the accuracy of the steady-state response. An elevator must be level enough with the floor for the passengers to exit, and a read/write head not positioned over the commanded track results in computer errors. An antenna tracking a satellite must keep the satellite well within its beamwidth in order not to lose track. In this text we define steady-state errors quantitatively, analyze a system's steady-state error, and then design corrective action to reduce the steady-state error—our second analysis and design objective.

Stability

Discussion of transient response and steady-state error is moot if the system does not have *stability*. In order to explain stability, we start from the fact that the total response of a system is the sum of the *natural response* and the *forced response*. When you studied linear differential equations, you probably referred to these responses as the *homogeneous* and the *particular solutions*, respectively. Natural response describes the way the system dissipates or acquires energy. The form or nature of this response is dependent only on the system, not the input. On the other hand, the form or nature of the forced response is dependent on the input. Thus, for a *linear* system, we can write

$$\text{Total response} = \text{Natural response} + \text{Forced response} \qquad (1.1)^{2}$$

For a control system to be useful, the natural response must (1) eventually approach zero, thus leaving only the forced response, or (2) oscillate. In some systems, however, the natural response grows without bound rather than diminish to zero or oscillate. Eventually, the natural response is so much greater than the forced response that the system is no longer controlled. This condition, called *instability*, could lead to self-destruction of the physical device if limit stops are not part of the design. For example, the elevator would crash through the floor or exit through the ceiling; an aircraft would go into an uncontrollable roll; or an antenna commanded to point to a target would rotate, line up with the target, but then begin to oscillate about the target with *growing* oscillations and *increasing* velocity until the motor or amplifiers reached their output limits or until the antenna was damaged structurally. A time plot of an unstable system would show a transient response that grows without bound and without any evidence of a steady-state response.

Control systems must be designed to be stable. That is, their natural response must decay to zero as time approaches infinity, or oscillate. In many systems the transient response you see on a time response plot can be directly related to the natural response. Thus, if the natural response decays to zero as time approaches infinity, the transient response will also die out, leaving only the forced response. If the system is stable, the proper transient response and steady-state error characteristics can be designed. Stability is our third analysis and design objective.

---

[2] You may be confused by the words *transient* vs. *natural*, and *steady-state* vs. *forced*. If you look at Figure 1.2, you can see the transient and steady-state portions of the total response as indicated. The transient response is the sum of the natural and forced responses, while the natural response is large. If we plotted the natural response by itself, we would get a curve that is different from the transient portion of Figure 1.2. The steady-state response of Figure 1.2 is also the sum of the natural and forced responses, but the natural response is small. Thus, the transient and steady-state responses are what you actually see on the plot; the natural and forced responses are the underlying mathematical components of those responses.

Other Considerations

The three main objectives of control system analysis and design have already been enumerated. However, other important considerations must be taken into account. For example, factors affecting hardware selection, such as motor sizing to fulfill power requirements and choice of sensors for accuracy, must be considered early in the design.

Finances are another consideration. Control system designers cannot create designs without considering their economic impact. Such considerations as budget allocations and competitive pricing must guide the engineer. For example, if your product is one of a kind, you may be able to create a design that uses more expensive components without appreciably increasing total cost. However, if your design will be used for many copies, slight increases in cost per copy can translate into many more dollars for your company to propose during contract bidding and to outlay before sales.

Another consideration is *robust* design. System parameters considered constant during the design for transient response, steady-state errors, and stability change over time when the actual system is built. Thus, the performance of the system also changes over time and will not be consistent with your design. Unfortunately, the relationship between parameter changes and their effect on performance is not linear. In some cases, even in the same system, changes in parameter values can lead to small or large changes in performance, depending on the system's nominal operating point and the type of design used. Thus, the engineer wants to create a robust design so that the system will not be sensitive to parameter changes. We discuss the concept of system sensitivity to parameter changes in Chapters 7 and 8. This concept, then, can be used to test a design for robustness.

Case Study

Introduction to a Case Study

Now that our objectives are stated, how do we meet them? In this section we will look at an example of a feedback control system. The system introduced here will be used in subsequent chapters as a running case study to demonstrate the objectives of those chapters. A colored background like this will identify the case study section at the end of each chapter. Section 1.5, which follows this first case study, explores the design process that will help us build our system.

Antenna Azimuth: An Introduction to Position Control Systems

A position control system converts a position input command to a position output response. Position control systems find widespread applications in antennas, robot arms, and computer disk drives. The radio telescope antenna in Figure 1.8 is one example of a system that uses position control systems. In this section, we will look in detail at an antenna azimuth position control system that could be used to position a radio telescope antenna. We will see how the system works and how we can effect changes in its performance. The discussion here will be on a qualitative level, with the objective of getting an intuitive feeling for the systems with which we will be dealing.

An antenna azimuth position control system is shown in Figure 1.9(*a*), with a more detailed layout and schematic in Figures 1.9(*b*) and 1.9(*c*), respectively. Figure 1.9(*d*) shows *a functional block diagram* of the system. The functions are shown above the blocks, and the required hardware is indicated inside the blocks. Parts of Figure 1.9 are repeated on the front endpapers for future reference.

FIGURE 1.8 The search for extraterrestrial life is being carried out with radio antennas like the one pictured here. A radio antenna is an example of a system with position controls.

The purpose of this system is to have the azimuth angle output of the antenna, $\theta_o(t)$, follow the input angle of the potentiometer, $\theta_i(t)$. Let us look at Figure 1.9(*d*) and describe how this system works. The input command is an angular displacement. The potentiometer converts the angular displacement into a voltage.

(*a*)

(*b*)

(*c*)
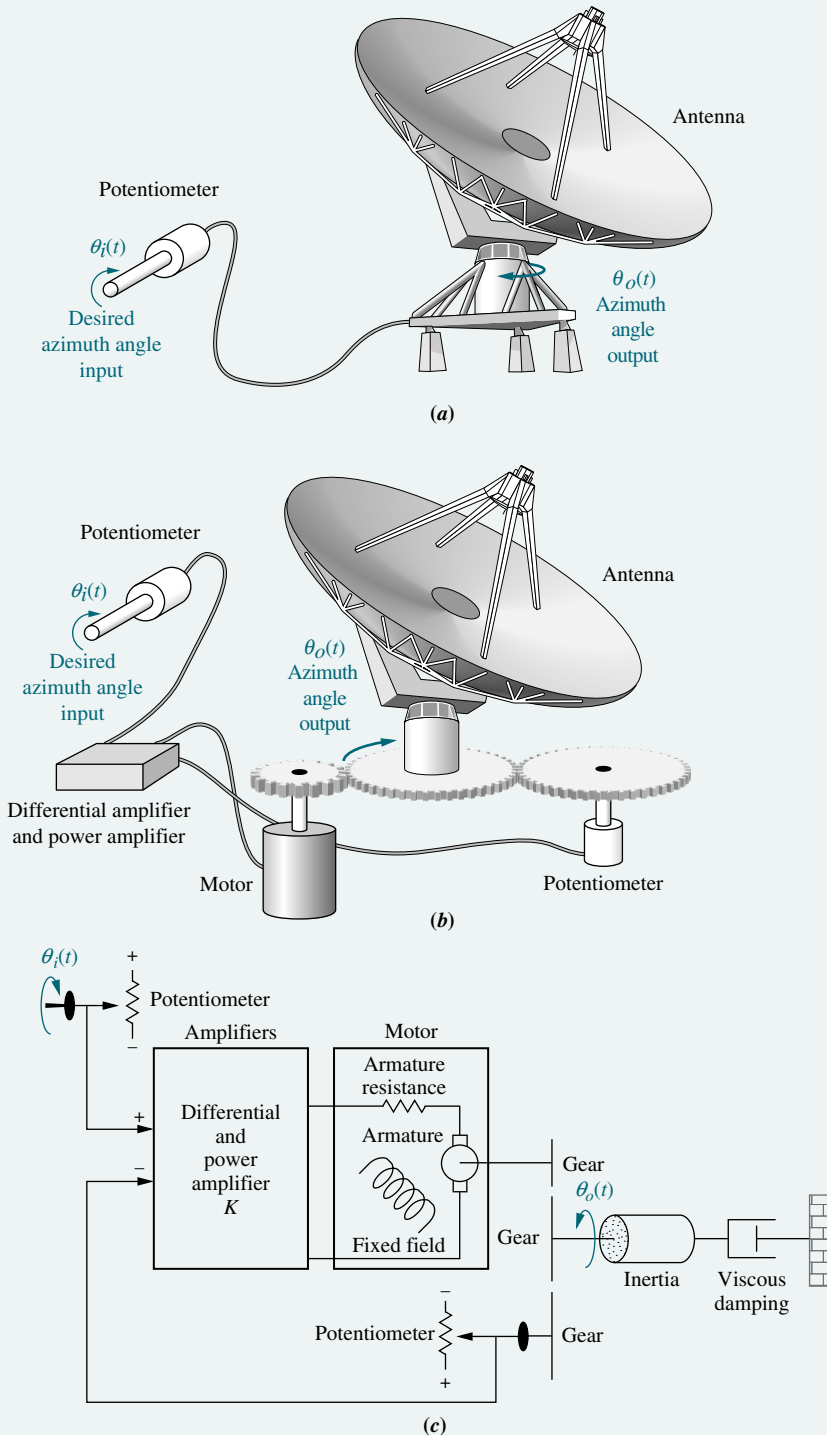
FIGURE 1.9 Antenna azimuth position control system: **a.** system concept; **b.** detailed layout; **c.** schematic; (*figure continues*)
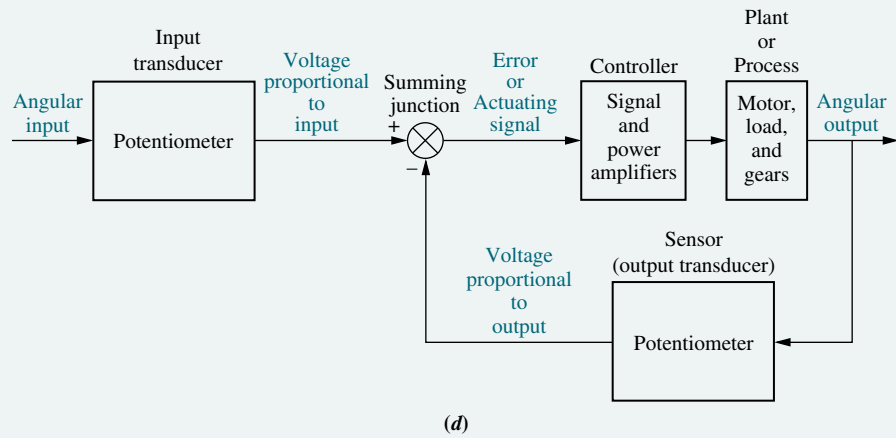
FIGURE 1.9 (*Continued*)
d. functional block diagram

(*d*)

Similarly, the output angular displacement is converted to a voltage by the potentiometer in the feedback path. The signal and power amplifiers boost the difference between the input and output voltages. This amplified actuating signal drives the plant.

The system normally operates to drive the error to zero. When the input and output match, the error will be zero, and the motor will not turn. Thus, the motor is driven only when the output and the input do not match. The greater the difference between the input and the output, the larger the motor input voltage, and the faster the motor will turn.

If we increase the gain of the signal amplifier, will there be an increase in the steady-state value of the output? If the gain is increased, then for a given actuating signal, the motor will be driven harder. However, the motor will still stop when the actuating signal reaches zero, that is, when the output matches the input. The difference in the response, however, will be in the transients. Since the motor is driven harder, it turns faster toward its final position. Also, because of the increased speed, increased momentum could cause the motor to overshoot the final value and be forced by the system to return to the commanded position. Thus, the possibility exists for a transient response that consists of *damped oscillations* (that is, a sinusoidal response whose amplitude diminishes with time) about the steady-state value if the gain is high. The responses for low gain and high gain are shown in Figure 1.10.
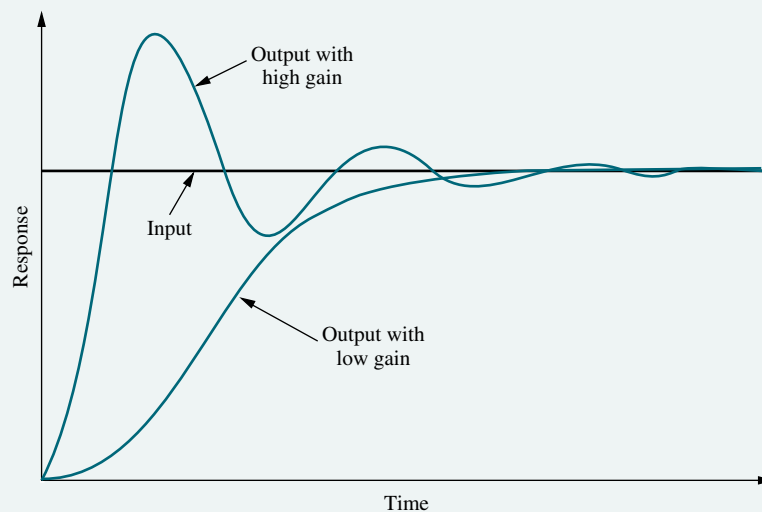
FIGURE 1.10 Response of a position control system, showing effect of high and low controller gain on the output response

We have discussed the transient response of the position control system. Let us now direct our attention to the steady-state position to see how closely the output matches the input after the transients disappear.

We define steady-state error as the difference between the input and the output after the transients have effectively disappeared. The definition holds equally well for step, ramp, and other types of inputs. Typically, the steady-state error decreases with an increase in gain and increases with a decrease in gain. Figure 1.10 shows zero error in the steady-state response; that is, after the transients have disappeared, the output position equals the commanded input position. In some systems, the steady-state error will not be zero; for these systems, a simple gain adjustment to regulate the transient response is either not effective or leads to a trade-off between the desired transient response and the desired steady-state accuracy.

To solve this problem, a controller with a dynamic response, such as an electrical filter, is used along with an amplifier. With this type of controller, it is possible to design both the required transient response and the required steady-state accuracy without the trade-off required by a simple setting of gain. However, the controller is now more complex. The filter in this case is called a compensator. Many systems also use dynamic elements in the feedback path along with the output transducer to improve system performance.

In summary, then, our design objectives and the system's performance revolve around the transient response, the steady-state error, and stability. Gain adjustments can affect performance and sometimes lead to trade-offs between the performance criteria. Compensators can often be designed to achieve performance specifications without the need for trade-offs. Now that we have stated our objectives and some of the methods available to meet those objectives, we describe the orderly progression that leads us to the final system design.

1.5   The Design Process

In this section, we establish an orderly sequence for the design of feedback control systems that will be followed as we progress through the rest of the book. Figure 1.11 shows the described process as well as the chapters in which the steps are discussed.

The antenna azimuth position control system discussed in the last section is representative of control systems that must be analyzed and designed. Inherent in

	Step 1	Step 2	Step 3	Step 4	Step 5	Step 6
	Determine a physical system and specifications from the requirements.	Draw a functional block diagram.	Transform the physical system into a schematic.	Use the schematic to obtain a block diagram, signal-flow diagram, or state-space representation.	If multiple blocks, reduce the block diagram to a single block or closed-loop system.	Analyze, design, and test to see that requirements and specifications are met.

Analog: Chapter 1   Chapters 2, 3   Chapter 5   Chapters 4, 6–12
Digital: Chapter 13   Chapter 13   Chapter 13

FIGURE 1.11   The control system design process

Figure 1.11 is feedback and communication during each phase. For example, if testing (Step 6) shows that requirements have not been met, the system must be redesigned and retested. Sometimes requirements are conflicting and the design cannot be attained. In these cases, the requirements have to be respecified and the design process repeated. Let us now elaborate on each block of Figure 1.11.

Step 1: Transform Requirements Into a Physical System

We begin by transforming the requirements into a physical system. For example, in the antenna azimuth position control system, the requirements would state the desire to position the antenna from a remote location and describe such features as weight and physical dimensions. Using the requirements, design specifications, such as desired transient response and steady-state accuracy, are determined. Perhaps an overall concept, such as Figure 1.9(*a*), would result.

Step 2: Draw a Functional Block Diagram

The designer now translates a qualitative description of the system into a functional block diagram that describes the component parts of the system (that is, function and/or hardware) and shows their interconnection. Figure 1.9(*d*) is an example of a functional block diagram for the antenna azimuth position control system. It indicates functions such as input transducer and controller, as well as possible hardware descriptions such as amplifiers and motors. At this point the designer may produce a detailed layout of the system, such as that shown in Figure 1.9(*b*), from which the next phase of the analysis and design sequence, developing a schematic diagram, can be launched.

Step 3: Create a Schematic

As we have seen, position control systems consist of electrical, mechanical, and electromechanical components. After producing the description of a physical system, the control systems engineer transforms the physical system into a schematic diagram. The control system designer can begin with the physical description, as contained in Figure 1.9(*a*), to derive a schematic. The engineer must make approximations about the system and neglect certain phenomena, or else the schematic will be unwieldy, making it difficult to extract a useful mathematical model during the next phase of the analysis and design sequence. The designer starts with a simple schematic representation and, at subsequent phases of the analysis and design sequence, checks the assumptions made about the physical system through analysis and computer simulation. If the schematic is too simple and does not adequately account for observed behavior, the control systems engineer adds phenomena to the schematic that were previously assumed negligible. A schematic diagram for the antenna azimuth position control system is shown in Figure 1.9(*c*).

When we draw the potentiometers, we make our first simplifying assumption by neglecting their friction or inertia. These mechanical characteristics yield a dynamic, rather than an instantaneous, response in the output voltage. We assume that these mechanical effects are negligible and that the voltage across a potentiometer changes instantaneously as the potentiometer shaft turns.

A differential amplifier and a power amplifier are used as the controller to yield gain and power amplification, respectively, to drive the motor. Again, we assume that the dynamics of the amplifiers are rapid compared to the response time of the motor; thus, we model them as a pure gain, K.

A dc motor and equivalent load produce the output angular displacement. The speed of the motor is proportional to the voltage applied to the motor's *armature circuit*. Both inductance and resistance are part of the armature circuit. In showing

just the armature resistance in Figure 1.9(*c*), we assume the effect of the armature inductance is negligible for a dc motor.

The designer makes further assumptions about the load. The load consists of a rotating mass and bearing friction. Thus, the model consists of *inertia* and *viscous damping* whose resistive torque increases with speed, as in an automobile's shock absorber or a screen door damper.

The decisions made in developing the schematic stem from knowledge of the physical system, the physical laws governing the system's behavior, and *practical experience*. These decisions are not easy; however, as you acquire more design experience, you will gain the insight required for this difficult task.

Step 4: Develop a Mathematical Model (Block Diagram)

Once the schematic is drawn, the designer uses physical laws, such as Kirchhoff's laws for electrical networks and Newton's law for mechanical systems, along with simplifying assumptions, to model the system mathematically. These laws are

Kirchhoff's voltage law   The sum of voltages around a closed path equals zero.

Kirchhoff's current law   The sum of electric currents flowing from a node equals zero.

Newton's laws   The sum of forces on a body equals zero;[3] the sum of moments on a body equals zero.

Kirchhoff's and Newton's laws lead to mathematical models that describe the relationship between the input and output of dynamic systems. One such model is the *linear, time-invariant differential equation*, Eq. (1.2):

$$\frac{d^m c(t)}{dt^n} + d_{n-1}\frac{d^{m-1}c(t)}{dt^{n-1}} + \cdots + d_0 c(t) = b_m \frac{d^m r(t)}{dt^m} + b_{m-1}\frac{d^{m-1}r(t)}{dt^{m-1}} + \cdots + b_0 r(t)$$

$$(1.2)^4$$

Many systems can be approximately described by this equation, which relates the output, $c(t)$, to the input, $r(t)$, by way of the system parameters, a_i and b_j. We assume the reader is familiar with differential equations. Problems and a bibliography are provided at the end of the chapter for you to review this subject.

Simplifying assumptions made in the process of obtaining a mathematical model usually leads to a low-order form of Eq. (1.2). Without the assumptions the system model could be of high order or described with nonlinear, time-varying, or partial differential equations. These equations complicate the design process and reduce the designer's insight. Of course, all assumptions must be checked and all simplifications justified through analysis or testing. If the assumptions for simplification cannot be justified, then the model cannot be simplified. We examine some of these simplifying assumptions in Chapter 2.

In addition to the differential equation, the *transfer function* is another way of mathematically modeling a system. The model is derived from the linear, time-invariant differential equation using what we call the *Laplace transform*. Although the transfer

---

[3] Alternately, $\sum$ forces = Ma. In this text the force, Ma, will be brought to the left-hand side of the equation to yield $\sum$ forces = 0 (D'Alembert's principle). We can then have a consistent analogy between force and voltage, and Kirchhoff's and Newton's laws (that is, $\sum$ forces = 0; $\sum$ voltages = 0).

[4] The right-hand side of Eq. (1.2) indicates differentiation of the input, $r(t)$. In physical systems, differentiation of the input introduces noise. In Chapters 3 and 5 we show implementations and interpretations of Eq. (1.2) that do not require differentiation of the input.

function can be used only for linear systems, it yields more intuitive information than the differential equation. We will be able to change system parameters and rapidly sense the effect of these changes on the system response. The transfer function is also useful in modeling the interconnection of subsystems by forming a block diagram similar to Figure 1.9(*d*) but with a mathematical function inside each block.

Still another model is the *state-space representation*. One advantage of state-space methods is that they can also be used for systems that cannot be described by linear differential equations. Further, state-space methods are used to model systems for simulation on the digital computer. Basically, this representation turns an *n*th-order differential equation into *n* simultaneous first-order differential equations. Let this description suffice for now; we describe this approach in more detail in Chapter 3.

Finally, we should mention that to produce the mathematical model for a system, we require knowledge of the parameter values, such as equivalent resistance, inductance, mass, and damping, which is often not easy to obtain. Analysis, measurements, or specifications from vendors are sources that the control systems engineer may use to obtain the parameters.
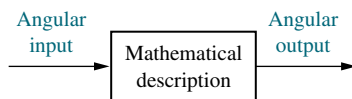
FIGURE 1.12 Equivalent block diagram for the antenna azimuth position control system

Step 5: Reduce the Block Diagram

Subsystem models are interconnected to form block diagrams of larger systems, as in Figure 1.9(*d*), where each block has a mathematical description. Notice that many signals, such as proportional voltages and error, are internal to the system. There are also two signals—angular input and angular output—that are external to the system. In order to evaluate system response in this example, we need to reduce this large system's block diagram to a single block with a mathematical description that represents the system from its input to its output, as shown in Figure 1.12. Once the block diagram is reduced, we are ready to analyze and design the system.

Step 6: Analyze and Design
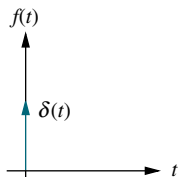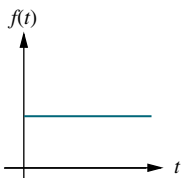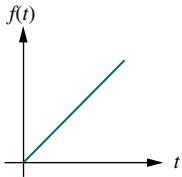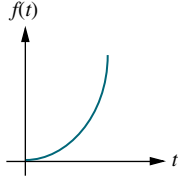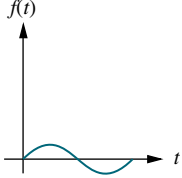
The next phase of the process, following block diagram reduction, is analysis and design. If you are interested only in the performance of an individual subsystem, you can skip the block diagram reduction and move immediately into analysis and design. In this phase, the engineer analyzes the system to see if the response specifications and performance requirements can be met by simple adjustments of system parameters. If specifications cannot be met, the designer then designs additional hardware in order to effect a desired performance.

Test input signals are used, both analytically and during testing, to verify the design. It is neither necessarily practical nor illuminating to choose complicated input signals to analyze a system's performance. Thus, the engineer usually selects standard test inputs. These inputs are impulses, steps, ramps, parabolas, and sinusoids, as shown in Table 1.1.

An *impulse* is infinite at $t = 0$ and zero elsewhere. The area under the unit impulse is 1. An approximation of this type of waveform is used to place initial energy into a system so that the response due to that initial energy is only the transient response of a system. From this response the designer can derive a mathematical model of the system.

A *step* input represents a *constant command*, such as position, velocity, or acceleration. Typically, the step input command is of the same form as the output. For example, if the system's output is position, as it is for the antenna azimuth position control system, the step input represents a desired position, and the output represents the actual position. If the system's output is velocity, as is the spindle speed for a video disc player, the step input represents a constant desired speed, and the output represents the actual speed. The designer uses step inputs because both the transient response and the steady-state response are clearly visible and can be evaluated.

TABLE 1.1   Test waveforms used in control systems

Input	Function	Description	Sketch	Use
Impulse	$\delta(t)$	$\delta(t) = \infty$ for $0- < t < 0+$ $= 0$ elsewhere $\int_{0-}^{0+} \delta(t)dt = 1$		Transient response Modeling
Step	$u(t)$	$u(t) = 1$ for $t > 0$ $= 0$ for $t < 0$		Transient response Steady-state error
Ramp	$tu(t)$	$tu(t) = t$ for $t \geq 0$ $= 0$ elsewhere		Steady-state error
Parabola	$\frac{1}{2}t^2 u(t)$	$\frac{1}{2}t^2 u(t) = \frac{1}{2}t^2$ for $t \geq 0$ $= 0$ elsewhere		Steady-state error
Sinusoid	$\sin \omega t$			Transient response Modeling Steady-state error

The *ramp* input represents a *linearly increasing command*. For example, if the system's output is position, the input ramp represents a linearly increasing position, such as that found when tracking a satellite moving across the sky at constant speed. If the system's output is velocity, the input ramp represents a linearly increasing velocity. The response to an input ramp test signal yields additional information about the steady-state error. The previous discussion can be extended to *parabolic* inputs, which are also used to evaluate a system's steady-state error.

Sinusoidal inputs can also be used to test a physical system to arrive at a mathematical model. We discuss the use of this waveform in detail in Chapters 10 and 11.

We conclude that one of the basic analysis and design requirements is to evaluate the time response of a system for a given input. Throughout the book you will learn numerous methods for accomplishing this goal.

The control systems engineer must take into consideration other characteristics about feedback control systems. For example, control system behavior is altered by fluctuations in component values or system parameters. These variations can be

caused by temperature, pressure, or other environmental changes. Systems must be built so that expected fluctuations do not degrade performance beyond specified bounds. A *sensitivity* analysis can yield the percentage of change in a specification as a function of a change in a system parameter. One of the designer's goals, then, is to build a system with minimum sensitivity over an expected range of environmental changes.

In this section we looked at some control systems analysis and design considerations. We saw that the designer is concerned about transient response, steady-state error, stability, and sensitivity. The text pointed out that although the basis of evaluating system performance is the differential equation, other methods, such as transfer functions and state space, will be used. The advantages of these new techniques over differential equations will become apparent as we discuss them in later chapters.

1.6   Computer-Aided Design

Now that we have discussed the analysis and design sequence, let us discuss the use of the computer as a computational tool in this sequence. The computer plays an important role in the design of modern control systems. In the past, control system design was labor intensive. Many of the tools we use today were implemented through hand calculations or, at best, using plastic graphical aid tools. The process was slow, and the results not always accurate. Large mainframe computers were then used to simulate the designs.

Today we are fortunate to have computers and software that remove the drudgery from the task. At our own desktop computers, we can perform analysis, design, and simulation with one program. With the ability to simulate a design rapidly, we can easily make changes and immediately test a new design. We can play what-if games and try alternate solutions to see if they yield better results, such as reduced sensitivity to parameter changes. We can include nonlinearities and other effects and test our models for accuracy.

MATLAB

The computer is an integral part of modern control system design, and many computational tools are available for your use. In this book we use MATLAB and the MATLAB Control System Toolbox, which expands MATLAB to include control system–specific commands. In addition, presented are several MATLAB enhancements that give added functionality to MATLAB and the Control Systems Toolbox. Included are (1) Simulink, which uses a graphical user interface (GUI); (2) the LTI Viewer, which permits measurements to be made directly from time and frequency response curves; (3) the SISO Design Tool, a convenient and intuitive analysis and design tool; and (4) the Symbolic Math Toolbox, which saves labor when making symbolic calculations required in control system analysis and design. Some of these enhancements may require additional software available from The MathWorks, Inc.

MATLAB is presented as an alternate method of solving control system problems. You are encouraged to solve problems first by hand and then by MATLAB so that insight is not lost through mechanized use of computer programs. To this end, many examples throughout the book are solved by hand, followed by suggested use of MATLAB.

As an enticement to begin using MATLAB, simple program statements that you can try are suggested throughout the chapters at appropriate locations. Throughout the book, various icons appear in the margin to identify MATLAB references that direct you to the proper program in the proper appendix and tell you what you

will learn. Selected end-of-chapter problems and Case Study Challenges to be solved using MATLAB have also been marked with appropriate icons. The following list itemizes the specific components of MATLAB used in this book, the icon used to identify each, and the appendix in which a description can be found:

```
MATLAB/Control System Toolbox tutorials and code are found in
Appendix B and identified in the text with the MATLAB icon shown
in the margin.
```

MATLAB
ML

```
Simulink tutorials and diagrams are found in Appendix C and
identified in the text with the Simulink icon shown in the margin.
```

Simulink
SL

```
MATLAB GUI tools, tutorials, and examples are in Appendix E at
www.wiley.com/college/nise and identified in the text with the GUI
Tool icon shown in the margin. These tools consist of the LTI
Viewer and the SISO Design Tool.
```

Gui Tool
GUIT

```
Symbolic Math Toolbox tutorials and code are found in Appendix F at
www.wiley.com/college/nise and identified in the text with the
Symbolic Math icon shown in the margin.
```

Symbolic Math
SM

MATLAB code itself is not platform specific. The same code runs on PCs and workstations that support MATLAB. Although there are differences in installing and managing MATLAB files, we do not address them in this book. Also, there are many more commands in MATLAB and the MATLAB toolboxes than are covered in the appendixes. Please explore the bibliographies at the end of the applicable appendixes to find out more about MATLAB file management and MATLAB instructions not covered in this textbook.

LabVIEW

LabVIEW is a programming environment presented as an alternative to MATLAB. This graphical alternative produces front panels of virtual instruments on your computer that are pictorial reproductions of hardware instruments, such as wave-form generators or oscilloscopes. Underlying the front panels are block diagrams. The blocks contain underlying code for the controls and indicators on the front panel. Thus, a knowledge of coding is not required. Also, parameters can be easily passed or viewed from the front panel.

```
A LabVIEW tutorial is in Appendix D and all LabVIEW material is
identified with the LabVIEW icon shown in the margin.
```

LabVIEW
LV

You are encouraged to use computational aids throughout this book. Those not using MATLAB or LabVIEW should consult Appendix H at www.wiley.com/college/nise for a discussion of other alternatives. Now that we have introduced control systems to you and established a need for computational aids to perform analysis and design, we will conclude with a discussion of your career as a control systems engineer and look at the opportunities and challenges that await you.

1.7   The Control Systems Engineer

Control systems engineering is an exciting field in which to apply your engineering talents, because it cuts across numerous disciplines and numerous functions within those disciplines. The control engineer can be found at the top level of large projects, engaged at the conceptual phase in determining or implementing

overall system requirements. These requirements include total system performance specifications, subsystem functions, and the interconnection of these functions, including interface requirements, hardware and software design, and test plans and procedures.

Many engineers are engaged in only one area, such as circuit design or software development. However, as a control systems engineer, you may find yourself working in a broad arena and interacting with people from numerous branches of engineering and the sciences. For example, if you are working on a biological system, you will need to interact with colleagues in the biological sciences, mechanical engineering, electrical engineering, and computer engineering, not to mention mathematics and physics. You will be working with these engineers at all levels of project development from concept through design and, finally, testing. At the design level, the control systems engineer can be performing hardware selection, design, and interface, including total subsystem design to meet specified requirements. The control engineer can be working with sensors and motors as well as electronic, pneumatic, and hydraulic circuits.

The space shuttle provides another example of the diversity required of the systems engineer. In the previous section, we showed that the space shuttle's control systems cut across many branches of science: orbital mechanics and propulsion, aerodynamics, electrical engineering, and mechanical engineering. Whether or not you work in the space program, as a control systems engineer you will apply broad-based knowledge to the solution of engineering control problems. You will have the opportunity to expand your engineering horizons beyond your university curriculum.

You are now aware of future opportunities. But for now, what advantages does this course offer to a student of control systems (other than the fact that you need it to graduate)? Engineering curricula tend to emphasize *bottom-up* design. That is, you start from the components, develop circuits, and then assemble a product. In *top-down* design, a high-level picture of the requirements is first formulated; then the functions and hardware required to implement the system are determined. You will be able to take a top-down systems approach as a result of this course.

A major reason for not teaching top-down design throughout the curriculum is the high level of mathematics initially required for the systems approach. For example, control systems theory, which requires differential equations, could not be taught as a lower-division course. However, while progressing through bottom-up design courses, it is difficult to see how such design fits logically into the large picture of the product development cycle.

After completing this control systems course, you will be able to stand back and see how your previous studies fit into the large picture. Your amplifier course or vibrations course will take on new meaning as you begin to see the role design work plays as part of product development. For example, as engineers, we want to describe the physical world mathematically so that we can create systems that will benefit humanity. You will find that you have indeed acquired, through your previous courses, the ability to model physical systems mathematically, although at the time you might not have understood where in the product development cycle the modeling fits. This course will clarify the analysis and design procedures and show you how the knowledge you acquired fits into the total picture of system design.

Understanding control systems enables students from all branches of engineering to speak a common language and develop an appreciation and working knowledge of the other branches. You will find that there really is not much difference among the branches of engineering as far as the goals and applications are concerned. As you study control systems, you will see this commonality.

Summary

Control systems contribute to every aspect of modern society. In our homes we find them in everything from toasters to heating systems to VCRs. Control systems also have widespread applications in science and industry, from steering ships and planes to guiding missiles and the space shuttle. Control systems also exist naturally; our bodies contain numerous control systems. Even economic and psychological system representations have been proposed based on control system theory. Control systems are used where power gain, remote control, or conversion of the form of the input is required.

A control system has an *input*, a *process*, and an *output*. Control systems can be *open loop* or *closed loop*. Open-loop systems do not monitor or correct the output for disturbances; however, they are simpler and less expensive than closed-loop systems. Closed-loop systems monitor the output and compare it to the input. If an error is detected, the system corrects the output and hence corrects the effects of disturbances.

Control systems analysis and design focuses on three primary objectives:

1. Producing the desired transient response
2. Reducing steady-state errors
3. Achieving stability

A system must be stable in order to produce the proper transient and steady-state response. Transient response is important because it affects the speed of the system and influences human patience and comfort, not to mention mechanical stress. Steady-state response determines the accuracy of the control system; it governs how closely the output matches the desired response.

The design of a control system follows these steps:

Step 1   Determine a physical system and specifications from requirements.

Step 2   Draw a functional block diagram.

Step 3   Represent the physical system as a schematic.

Step 4   Use the schematic to obtain a mathematical model, such as a block diagram.

Step 5   Reduce the block diagram.

Step 6   Analyze and design the system to meet specified requirements and specifications that include stability, transient response, and steady-state performance.

In the next chapter we continue through the analysis and design sequence and learn how to use the schematic to obtain a mathematical model.

Review Questions

1. Name three applications for feedback control systems.
2. Name three reasons for using feedback control systems and at least one reason for not using them.
3. Give three examples of open-loop systems.
4. Functionally, how do closed-loop systems differ from open-loop systems?
5. State one condition under which the error signal of a feedback control system would not be the difference between the input and the output.

6. If the error signal is not the difference between input and output, by what general name can we describe the error signal?

7. Name two advantages of having a computer in the loop.

8. Name the three major design criteria for control systems.

9. Name the two parts of a system's response.

10. Physically, what happens to a system that is unstable?

11. Instability is attributable to what part of the total response?

12. Describe a typical control system analysis task.

13. Describe a typical control system design task.

14. Adjustments of the forward path gain can cause changes in the transient response. True or false?

15. Name three approaches to the mathematical modeling of control systems.

16. Briefly describe each of your answers to Question 15.

Problems

1. A variable resistor, called a *potentiometer*, is shown in Figure P1.1. The resistance is varied by moving a wiper arm along a fixed resistance. The resistance from *A* to *C* is fixed, but the resistance from *B* to *C* varies with the position of the wiper arm. If it takes 10 turns to move the wiper arm from *A* to *C*, draw a block diagram of the potentiometer showing the input variable, the output variable, and (inside the block) the gain, which is a constant and is the amount by which the input is multiplied to obtain the output. [Section 1.4: Introduction to a Case Study]

WileyPLUS [5]

WPCS

Control Solutions
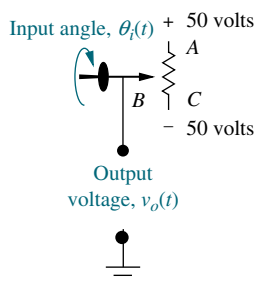
FIGURE P1.1   Potentiometer

2. A temperature control system operates by sensing the difference between the thermostat setting and the actual temperature and then opening a fuel valve an amount proportional to this difference. Draw a functional closed-loop block diagram similar to Figure 1.9(*d*) identifying the input and output transducers, the controller, and the plant. Further, identify the input and output signals of all subsystems previously described. [Section 1.4: Introduction to a Case Study]

3. An aircraft's attitude varies in roll, pitch, and yaw as defined in Figure P1.2. Draw a functional block diagram for a closed-loop system that stabilizes the roll as follows: The system measures the actual roll angle with a gyro and compares the actual roll angle with the desired roll angle. The ailerons respond to the roll-angle error by undergoing an angular deflection. The aircraft responds to this angular deflection, producing a roll angle rate. Identify the input and output transducers, the controller, and the plant. Further, identify the nature of each signal. [Section 1.4: Introduction to a Case Study]
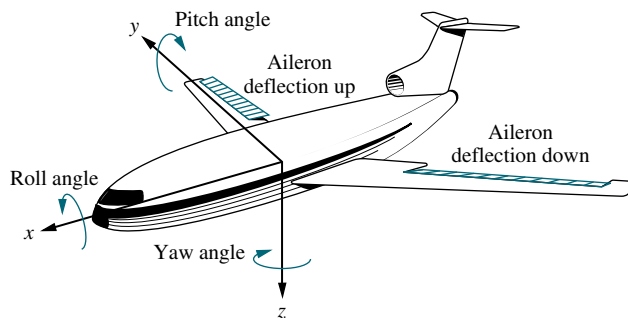
FIGURE P1.2   Aircraft attitude defined

---

4. Many processes operate on rolled material that moves from a supply reel to a take-up reel. Typically, these systems, called *winders*, control the material so that it travels at a constant velocity. Besides velocity, complex winders also control tension, compensate for roll inertia while accelerating or decelerating, and regulate acceleration due to sudden changes. A winder is shown in Figure P1.3. The force transducer measures tension; the winder pulls against the nip rolls, which provide an opposing force; and the bridle provides slip. In order to compensate for changes in speed, the material is looped around a *dancer*. The loop prevents rapid changes from causing excessive slack or damaging the material. If the dancer position is sensed by a potentiometer or other device, speed variations due to buildup on the take-up reel or other causes can be controlled by comparing the potentiometer voltage to the commanded speed. The system then corrects the speed and resets the dancer to the desired position (*Ayers*, 1988). Draw a functional block diagram for the speed control system, showing each component and signal. [Section 1.4: Introduction to a Case Study]
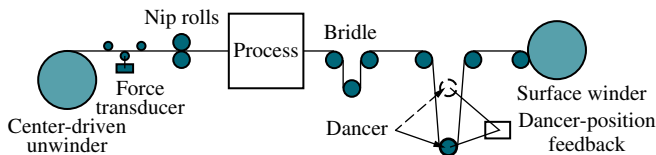
FIGURE P1.3   Winder

5. In a nuclear power generating plant, heat from a reactor is used to generate steam for turbines. The rate of the fission reaction determines the amount of heat generated, and this rate is controlled by rods inserted into the radioactive core. The rods regulate the flow of neutrons. If the rods are lowered into the core, the rate of fission will diminish; if the rods are raised, the fission rate will increase. By automatically
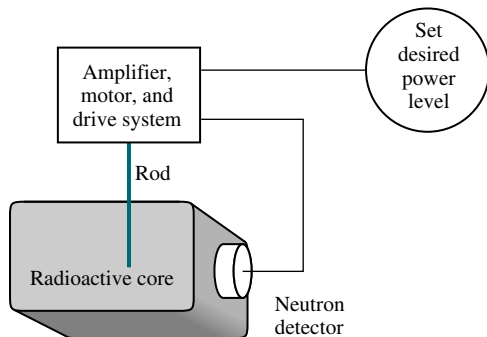
FIGURE P1.4   Control of a nuclear reactor

controlling the position of the rods, the amount of heat generated by the reactor can be regulated. Draw a functional block diagram for the nuclear reactor control system shown in Figure P1.4. Show all blocks and signals. [Section 1.4: Introduction to a Case Study]

6. A university wants to establish a control system model that represents the student population as an output, with the desired student population as an input. The administration determines the rate of admissions by comparing the current and desired student populations. The admissions office then uses this rate to admit students. Draw a functional block diagram showing the administration and the admissions office as blocks of the system. Also show the following signals: the desired student population, the actual student population, the desired student rate as determined by the administration, the actual student rate as generated by the admissions office, the dropout rate, and the net rate of influx. [Section 1.4: Introduction to a Case Study]

7. We can build a control system that will automatically adjust a motorcycle's radio volume as the noise generated by the motorcycle changes. The noise generated by the motorcycle increases with speed. As the noise increases, the system increases the volume of the radio. Assume that the amount of noise can be represented by a voltage generated by the speedometer cable, and the volume of the radio is controlled by a dc voltage (*Hogan*, 1988). If the dc voltage represents the desired volume disturbed by the motorcycle noise, draw the functional block diagram of the automatic volume control system, showing the input transducer, the volume control circuit, and the speed transducer as blocks. Also show the following signals: the desired volume as an input, the actual volume as an output, and voltages representing speed, desired volume, and actual volume. [Section 1.4: Introduction to a Case Study]

WileyPLUS
WPCS
Control Solutions

8. Your bathtub at home is a control system that keeps the water level constant. A constant flow from the tap yields a constant water level, because the flow rate through the drain increases as the water level increases, and decreases as the water level decreases. After equilibrium has been reached, the level can be controlled by controlling the input flow rate. A low input flow rate yields a lower level, while a higher input flow rate yields a higher level. [Section 1.4: Introduction to a Case Study]

a. Sketch a control system that uses this principle to precisely control the fluid level in a tank. Show the intake and drain valves, the tank, any sensors and transducers, and the interconnection of all components.

b. Draw a functional block diagram of the system, identifying the input and output signals of each block.

9. A dynamometer is a device used to measure torque and speed and to vary the load on rotating devices. The dynamometer operates as follows to control the amount of torque: A hydraulic actuator attached to the axle presses a tire against a rotating flywheel. The greater the displacement of the actuator, the more force that is applied to the rotating flywheel. A strain gage load cell senses the force. The displacement of the actuator is controlled by an electrically operated valve whose displacement regulates fluid flowing into the actuator (*D'Souza*, *1988*). Draw a functional block diagram of a closed-loop system that uses the described dynamometer to regulate the force against the tire during testing. Show all signals and systems. Include amplifiers that power the valve, the valve, the actuator and load, and the tire. [Section 1.4: Introduction to a Case Study]

10. During a medical operation an anesthesiologist controls the depth of unconsciousness by controlling the concentration of isoflurane in a vaporized mixture with oxygen and nitrous oxide. The depth of anesthesia is measured by the patient's blood pressure. The anesthesiologist also regulates ventilation, fluid balance, and the administration of other drugs. In order to free the anesthesiologist to devote more time to the latter tasks, and in the interest of the patient's safety, we wish to automate the depth of anesthesia by automating the control of isoflurane concentration. Draw a functional block diagram of the system showing pertinent signals and subsystems (*Meier*, *1992*). [Section 1.4: Introduction to a Case Study]

WileyPLUS
WPCS
Control Solutions

11. The vertical position, $x(t)$, of the grinding wheel shown in Figure P1.5 is controlled by a closed-loop system. The input to the system is the desired depth of grind, and the output is the actual depth of grind. The difference between the desired depth and the actual depth drives the motor, resulting in a force applied to the work. This force results in a feed velocity for the grinding wheel (*Jenkins*, *1997*). Draw a closed-loop functional block diagram for the grinding process, showing the input, output, force, and grinder feed rate. [Section 1.4: Introduction to a Case Study]
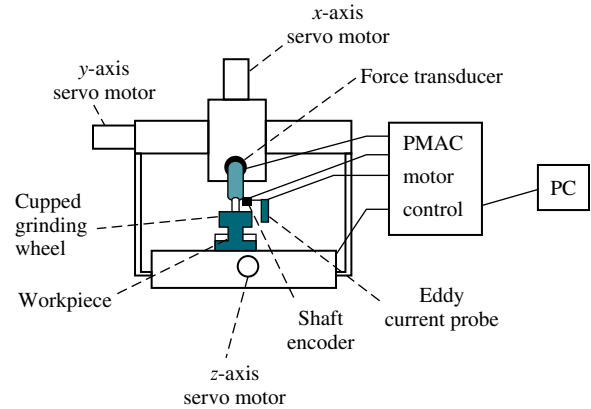
FIGURE P1.5 Grinder system (Reprinted with permission of ASME.)

12. A high-speed proportional solenoid valve is shown in Figure P1.6. A voltage proportional to the desired position of the spool is applied to the coil. The resulting magnetic field produced by the current in the coil causes the armature to move. A push pin connected to the armature moves the spool. A linear voltage differential transformer (LVDT) that outputs a voltage proportional to displacement senses the spool's position. This voltage can be used in a feedback path to implement closed-loop operation (*Vaughan*, *1996*). Draw a functional block diagram of the valve, showing input and output positions, coil voltage, coil current, and spool force. [Section 1.4: Introduction to a Case Study]
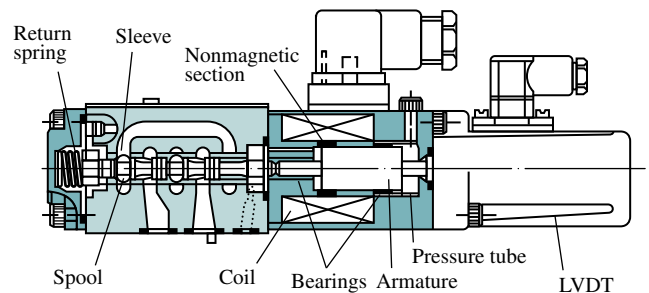
FIGURE P1.6 High-speed proportional solenoid valve (Reprinted with permission of ASME.)

13. The human eye has a biological control system that varies the pupil diameter to maintain constant light

intensity to the retina. As the light intensity increases, the optical nerve sends a signal to the brain, which commands internal eye muscles to decrease the pupil's eye diameter. When the light intensity decreases, the pupil diameter increases.

a. Draw a functional block diagram of the light-pupil system indicating the input, output, and intermediate signals; the sensor; the controller; and the actuator. [Section 1.4: Introduction to a Case Study]

b. Under normal conditions the incident light will be larger than the pupil, as shown in Figure P1.7(*a*). If the incident light is smaller than the diameter of the pupil as shown in Figure P1.7(*b*), the feedback path is broken (*Bechhoefer*, *2005*). Modify your block diagram from Part **a.** to show where the loop is broken. What will happen if the narrow beam of light varies in intensity, say in a sinusoidal fashion?

c. It has been found (*Bechhoefer*, *2005*) that it takes the pupil about 300 milliseconds to react to a change in the incident light. If light shines off center to the retina as shown in Figure P1.7(*c*), describe the response of the pupil with delay present and then without delay present.
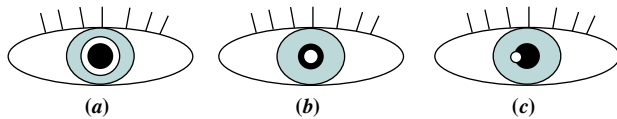
FIGURE P1.7 Pupil is shown black; light beam is shown white. **a.** Light beam diameter is larger than pupil. **b.** Light beam diameter is smaller than pupil. **c.** Narrow light beam is illuminated at pupil's edge.

14. A Segway®[6] Personal Transporter (PT) (Figure P1.8) is a two-wheeled vehicle in which the human operator stands vertically on a platform. As the driver leans left, right, forward, or backward, a set of sensitive gyroscopic sensors sense the desired input. These signals are fed to a computer that amplifies them and commands motors to propel the vehicle in the desired direction. One very important feature of the PT is its safety: The system will maintain its vertical position within a specified angle despite road disturbances, such as uphills and downhills or even if the operator over-leans in any direction. Draw

---

[6] Segway is a registered trademark of Segway, Inc. in the United States and/or other countries.

a functional block diagram of the PT system that keeps the system in a vertical position. Indicate the input and output signals, intermediate signals, and main subsystems. (http://segway.com)

FIGURE P1.8 The Segway Personal Transporter (PT)

15. In humans, hormone levels, alertness, and core body temperature are synchronized through a 24-hour circadian cycle. Daytime alertness is at its best when sleep/wake cycles are in synch with the circadian cycle. Thus alertness can be easily affected with a distributed work schedule, such as the one to which astronauts are subjected. It has been shown that the human circadian cycle can be delayed or advanced through light stimulus. To ensure optimal alertness, a system is designed to track astronauts' circadian cycles and increase the quality of sleep during missions. Core body temperature can be used as an indicator of the circadian cycle. A computer model with optimum circadian body temperature variations can be compared to an astronaut's body temperatures. Whenever a difference is detected, the astronaut is subjected to a light stimulus to advance or delay the astronaut's circadian cycle (*Mott*, *2003*). Draw a functional block diagram of the system. Indicate the input and output signals, intermediate signals, and main subsystems.

WileyPLUS

WPCS

Control Solutions

16. Tactile feedback is an important component in the learning of motor skills such as dancing, sports, and physical rehabilitation. A suit with white dots recognized by a vision system to determine arm joint positions with millimetric precision was developed. This suit is worn by both teacher and

student to provide position information. (*Lieberman, 2007*). If there is a difference between the teacher's positions and that of the student, vibrational feedback is provided to the student through 8 strategically placed vibrotactile actuators in the wrist and arm, which take advantage of a sensory effect known as *cutaneous rabbit* that tricks the subject to feel uniformly spaced stimuli in places where the actuators are not present. These stimuli help the student adjust to correct the motion. In summary, the system consists of an instructor and a student having their movements followed by the vision system. Their movements are fed into a computer that finds the differences between their joint positions and provides proportional vibrational strength feedback to the student. Draw a block diagram describing the system design.

17. Given the electric network shown in Figure P1.9. [Review]

a. Write the differential equation for the network if $v(t) = u(t)$, a unit step.

b. Solve the differential equation for the current, $i(t)$, if there is no initial energy in the network.

c. Make a plot of your solution if $R/L = 1$.
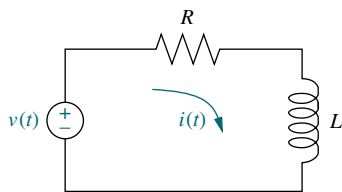
FIGURE P1.9 *RL* network

18. Repeat Problem 17 using the network shown in Figure P1.10. Assume $R = 2\,\Omega$, $L = 1$ H, and $1/LC = 25$. [Review]
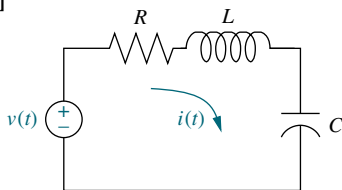
FIGURE P1.10 *RLC* network

19. Solve the following differential equations using classical methods. Assume zero initial conditions. [Review]

a. $\dfrac{dx}{dt} + 7x = 5\cos 2t$

b. $\dfrac{d^2x}{dt^2} + 6\dfrac{dx}{dt} + 8x = 5\sin 3t$

c. $\dfrac{d^2x}{dt^2} + 8\dfrac{dx}{dt} + 25x = 10u(t)$

20. Solve the following differential equations using classical methods and the given initial conditions: [Review]

a. $\dfrac{d^2x}{dt^2} + 2\dfrac{dx}{dt} + 2x = \sin 2t$

$x(0) = 2; \dfrac{dx}{dt}(0) = -3$

b. $\dfrac{d^2x}{dt^2} + 2\dfrac{dx}{dt} + x = 5e^{-2t} + t$

$x(0) = 2; \dfrac{dx}{dt}(0) = 1$

c. $\dfrac{d^2x}{dt^2} + 4x = t^2$

$x(0) = 1; \dfrac{dx}{dt}(0) = 2$

PROGRESSIVE ANALYSIS AND DESIGN PROBLEMS

21. High-speed rail pantograph. Some high-speed rail systems are powered by electricity supplied to a pantograph on the train's roof from a catenary overhead, as shown in Figure P1.11. The force applied by the pantograph to the catenary is regulated to avoid loss of contact due to excessive transient motion. A proposed method to regulate the force uses a closed-loop feedback system, whereby a force, F_{up}, is applied to the bottom of the pantograph, resulting in an output
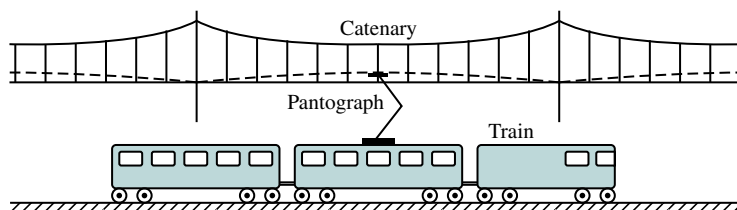
FIGURE P1.11 High-speed rail system showing pantograph and catenary (Reprinted with permission of ASME.)

force applied to the catenary at the top. The contact between the head of the pantograph and the catenary is represented by a spring. The output force is proportional to the displacement of this spring, which is the difference between the catenary and pantograph head vertical positions (*O'Connor*, *1997*). Draw a functional block diagram showing the following signals: the desired output force as the input; the force, F_{up}, applied to the bottom of the pantograph; the difference in displacement between the catenary and pantograph head; and the output contact force. Also, show blocks representing the input transducer, controller, actuator generating F_{up}, pantograph dynamics, spring described above, and output sensor. All forces and displacements are measured from equilibrium.

22. **Contol of HIV/AIDS.** As of 2005, the number of people living worldwide with Human Immunodeficiency Virus/Acquired Immune Deficiency Syndrome (HIV/AIDS) was estimated at 40 million, with 5 million new infections per year and 3 million deaths due to the disease (*UNAIDS*, *2005*). Currently there is no known cure for the disease, and HIV cannot be completely eliminated in an infected individual. Drug combinations can be used to maintain the virus numbers at low levels, which helps prevent AIDS from developing. A common treatment for HIV is the administration of two types of drugs: reverse transcriptase inhibitors (RTIs) and protease inhibitors (PIs). The amount in which each of these drugs is administered is varied according to the amount of HIV viruses in the body (*Craig*, *2004*). Draw a block diagram of a feedback system designed to control the amount of HIV viruses in an infected person. The plant input variables are the amount of RTIs and PIs dispensed. Show blocks representing the controller, the system under control, and the transducers. Label the corresponding variables at the input and output of every block.

23. **Hybrid vehicle.** The use of hybrid cars is becoming increasingly popular. A hybrid electric vehicle (HEV) combines electric machine(s) with an internal combustion engine (ICE), making it possible (along with other fuel consumption–reducing measures, such as stopping the ICE at traffic lights) to use smaller and more efficient gasoline engines. Thus, the efficiency advantages of the electric drivetrain are obtained, while the energy needed to power the electric motor is stored in the onboard fuel tank and not in a large and heavy battery pack.

There are various ways to arrange the flow of power in hybrid car. In a serial HEV (Figure P1.12), the ICE is not connected to the drive shaft. It drives only the generator, which charges the batteries and/or supplies power to the electric motor(s) through an inverter or a converter.
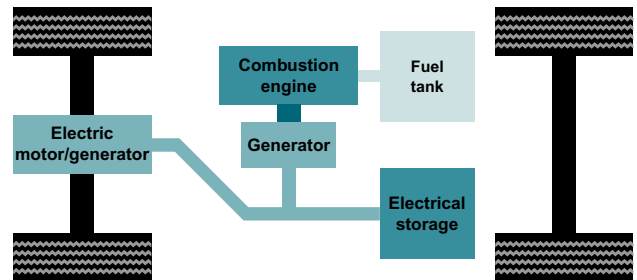
FIGURE P1.12   Serial hybrid-electric vehicle

The HEVs sold today are primarily of the parallel or split-power variety. If the combustion engine can turn the drive wheels as well as the generator, then the vehicle is referred to as a *parallel* hybrid, because both an electric motor and the ICE can drive the vehicle. A parallel hybrid car (Figure P1.13) includes a relatively small battery pack (electrical storage) to put out extra power to the electric motor when fast acceleration is needed. See (*Bosch 5th ed., 2000*), (*Bosch 7th ed., 2007*), (*Edelson, 2008*), (*Anderson, 2009*) for more detailed information about HEV.
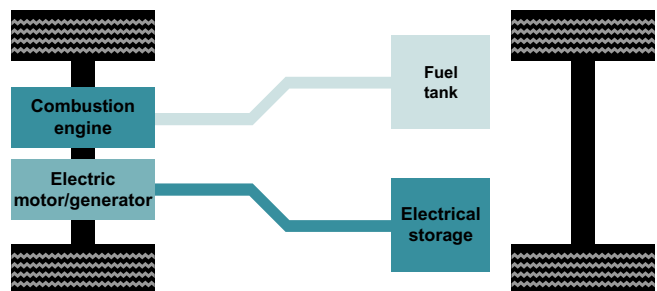
FIGURE P1.13   Parallel hybrid drive

As shown in Figure P1.14, split-power hybrid cars utilize a combination of series and parallel drives (*Bosch, 5th ed., 2007*). These cars use a planetary gear (3) as a split-power transmission to allow some of the ICE power to be applied mechanically to the drive. The other part is converted into electrical energy through the alternator (7) and the inverter (5) to feed the electric motor (downstream of the transmission) and/or to charge the high-voltage

battery (6). Depending upon driving conditions, the ICE, the electric motor, or both propel the vehicle.

1. internal-combustion engine; 2. tank
3. planetary gear; 4. electric motor; 5. inverter;
6. battery; 7. alternator.
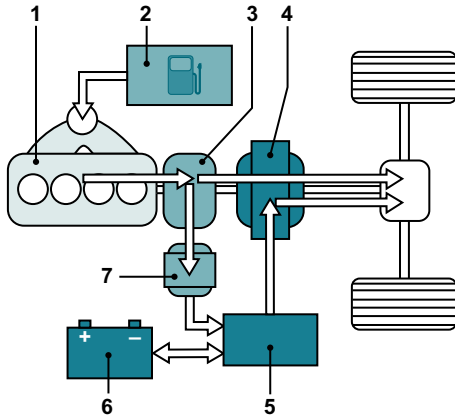
FIGURE P1.14   Split-power hybrid electric vehicle

Draw a functional block diagram for the cruise (speed) control system of:

a. A serial hybrid vehicle, showing its major components, including the speed sensor, electronic control unit (ECU), inverter, electric motor, and vehicle dynamics; as well as all signals, including the desired vehicle speed, actual speed, control command (ECU output), controlled voltage (inverter output), the motive force (provided by the electric motor), and running resistive force[7];

b. A parallel hybrid vehicle, showing its major components, which should include also a block that represents the accelerator, engine, and motor, as well as the signals (including accelerator displacement and combined engine/motor motive force);

c. A split-power HEV, showing its major components and signals, including, in addition to those listed in Parts **a** and **b**, a block representing the planetary gear and its control, which, depending upon driving conditions, would allow the ICE, the electric motor, or both to propel the vehicle, that is, to provide the necessary total motive force.

---

[7] These include the aerodynamic drag, rolling resistance, and climbing resistance. The aerodynamic drag is a function of car speed, whereas the other two are proportional to car weight.

Cyber Exploration Laboratory

Experiment 1.1

Objective   To verify the behavior of closed-loop systems as described in the Chapter 1 Case Study.

Minimum Required Software Packages   LabVIEW and the LabVIEW Control Design and Simulation Module. *Note*: While no knowledge of LabVIEW is required for this experiment, see Appendix D to learn more about LabVIEW, which will be pursued in more detail in later chapters.

Prelab

1. From the discussion in the Case Study, describe the effect of the gain of a closed-loop system upon transient response.
2. From the discussion in the Case Study about steady-state error, sketch a graph of a step input superimposed with a step response output and show the steady-state error. Assume any transient response. Repeat for a ramp input and ramp output response. Describe the effect of gain upon the steady-state error.

Lab

1. Launch LabVIEW and open **Find Examples . . .**

2. In the **NI Example Finder** window, open **CDEx Effect of Controller Type.vi,** found by navigating to it thourgh **Toolkits and Modules/Control and Simulation/ Control Design/Time Analysis/CDEx Effect of Controller Type vi.**

3. On the tool bar click the circulating arrows located next to the solid arrow on the left. The program is now running.

4. Move the slider **Controller Gain** and note the effect of high and low gains.

5. Change the controller by clicking the arrows for **Controller Type** and repeat Step 4.

Postlab

1. Correlate the responses found in the experiment with those described in your Prelab. Explore other examples provided in the LabVIEW example folders.
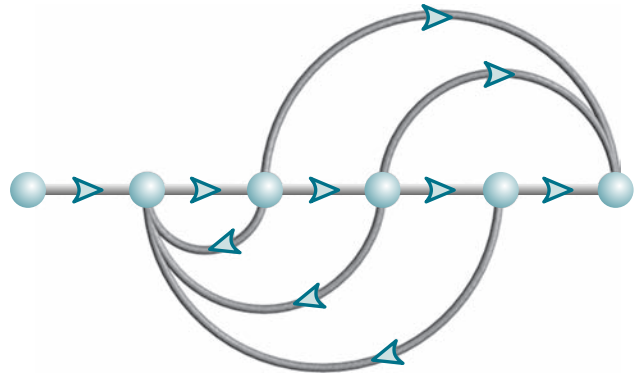
Bibliography

Alternative Drivetrains, July 2005. Available at www.altfuels.org/backgrnd/altdrive.html. Accessed October 13, 2009.

Anderson, S. Field Guide: Hybrid Electric Powertrains, part 4 of 5. *Automotive Design & Production*. Gardner Publication, Inc. Available at http://www.autofieldguide.com/articles/020904.html. Accessed October 13, 2009.

Ayers, J. Taking the Mystery out of Winder Controls. *Power Transmission Design*, April 1988, pp. 27–34.

Bahill, A. T. *Bioengineering: Biomedical, Medical, and Clinical Engineering*. Prentice Hall, Englewood Cliffs, NJ, 1981.

Bechhoefer, J. Feedback for Physicists: A Tutorial Essay on Control. *To Appear in Review of Modern Physics*, July 2005, pp. 42–45. Also available at http://www.sfu.ca/chaos/Publications/papers/RMP_feedback.pdf.

Bennett, S. *A History of Control Engineering, 1800–1930*. Peter Peregrinus, Stevenage, UK, 1979.

Bode, H. W. *Network Analysis and Feedback Amplifier Design*. Van Nostrand, Princeton, NJ, 1945.

Bosch, R. GmbH. *Automotive Electrics and Automotive Electronics*, 5th ed. John Wiley & Sons Ltd., UK, 2007.

Bosch, R. GmbH. *Bosch Automotive Handbook*, 7th ed. John Wiley & Sons Ltd., UK, 2007.

Cannon, R. H., Jr. *Dynamics of Physical Systems*. McGraw-Hill, New York, 1967.

Craig, I. K., Xia, X., and Venter, J. W. Introducing HIV/AIDS Education into the Electrical Engineering Curriculum at the University of Pretoria. *IEEE Transactions on Education*, vol. 47, no. 1, February 2004, pp. 65–73.

D'Azzo, J. J., and Houpis, C. H. *Feedback Control System Analysis and Synthesis*, 2d ed. McGraw-Hill, New York, 1966.

Doebelin, E. O. *Measurement Systems Application and Design*, 4th ed. McGraw-Hill, New York, 1990.

Dorf, R. C. *Modern Control Systems*, 5th ed. Addison-Wesley, Reading, MA, 1989.

D'Souza, A. F. *Design of Control Systems*. Prentice Hall, Upper Saddle River, NJ, 1988.

Edelson, J., et al. Facing the Challenges of the Current Hybrid Electric Drivetrain. *SMMA Technical Conference of the Motor and Motion Association*. Fall 2008. Available at www.ChorusCars.com.

Franklin, G. F., Powell, J. D., and Emami-Naeini, A. *Feedback Control of Dynamic Systems*. Addison-Wesley, Reading, MA, 1986.

Heller, H. C., Crawshaw, L. I., and Hammel, H. T. The Thermostat of Vertebrate Animals. *Scientific American*, August 1978, pp. 102–113.

Hogan, B. J. As Motorcycle's Speed Changes, Circuit Adjusts Radio's Volume. *Design News*, 18, August 1988, pp. 118–119.

Hostetter, G. H., Savant, C. J., Jr., and Stefani, R. T. *Design of Feedback Control Systems*, 2d ed. Saunders College Publishing, New York, 1989.

Jenkins, H. E., Kurfess, T. R., and Ludwick, S. J. Determination of a Dynamic Grinding Model. *Journal of Dynamic Systems, Measurements, and Control*, vol. 119, June 1997, pp. 289–293.

Klapper, J., and Frankle, J. T. *Phase-Locked and Frequency-Feedback Systems*. Academic Press, New York, 1972.

Lieberman, J., and Breazeal, C. Development of a Wearable Vibrotactile Feedback Suit for Accelerated Human Motor Learning. *2007 IEEE Int. Conf. on Robotics and Automation.* Roma, Italy, April 2007.

Martin, R. H., Jr. *Elementary Differential Equations with Boundary Value Problems*. McGraw-Hill, New York, 1984.

Mayr, O. The Origins of Feedback Control. *Scientific American*, October 1970, pp. 110–118.

Mayr, O. *The Origins of Feedback Control*. MIT Press, Cambridge, MA, 1970.

Meier, R., Nieuwland, J., Zbinden, A. M., and Hacisalihzade, S. S. Fuzzy Logic Control of Blood Pressure during Anesthesia. *IEEE Control Systems*, December 1992, pp. 12–17.

Mott, C., et al. *Modifying the Human Circadian Pacemaker Using Model-Based Predictive Control*. Proceedings of the American Control Conference. Denver, CO, June 2003, pp. 453–458.

Novosad, J. P. *Systems, Modeling, and Decision Making*. Kendall/Hunt, Dubuque, IA, 1982.

Nyquist, H. Regeneration Theory. *Bell System Technical Journal*, January 1932.

O'Connor, D. N., Eppinger, S. D., Seering, W. P., and Wormly, D. N. Active Control of a High-Speed Pantograph. *Journal of Dynamic Systems, Measurements, and Control*, vol. 119, March 1997, pp. 1–4.

Ogata, K. *Modern Control Engineering*, 2d ed. Prentice Hall, Upper Saddle River, NJ, 1990.

Rockwell International. *Space Shuttle Transportation System*, 1984 (press information).

Shaw, D. A., and Turnbull, G. A. Modern Thickness Control for a Generation III Hot Strip Mill. *The International Steel Rolling Conference—The Science & Technology of Flat Rolling*, vol. 1. Association Technique de la Siderurgie Francaise, Deauville, France, 1–3, June 1987.

UNAIDS. *AIDS Epidemic Update*. World Health Organization, December 2005. Available at www.unaids.org/Epi2005/doc/EPIupdate2005_pdf_en/epi-update2005_en.pdf. Accessed January 1, 2006.

Vaughan, N. D., and Gamble, J. B. The Modeling and Simulation of a Proportional Solenoid Valve. *Journal of Dynamic Systems, Measurements, and Control*, vol. 118, March 1996, pp. 120–125.

Modeling in the Frequency Domain

2

(Chapter Learning Outcomes)

After completing this chapter, the student will be able to:

- Find the Laplace transform of time functions and the inverse Laplace transform (Sections 2.1–2.2)
- Find the transfer function from a differential equation and solve the differential equation using the transfer function (Section 2.3)
- Find the transfer function for linear, time-invariant electrical networks (Section 2.4)
- Find the transfer function for linear, time-invariant translational mechanical systems (Section 2.5)
- Find the transfer function for linear, time-invariant rotational mechanical systems (Section 2.6)
- Find the transfer functions for gear systems with no loss and for gear systems with loss (Section 2.7)
- Find the transfer function for linear, time-invariant electromechanical systems (Section 2.8)
- Produce analogous electrical and mechanical circuits (Section 2.9)
- Linearize a nonlinear system in order to find the transfer function (Sections 2.10–2.11)

❨ Case Study Learning Outcomes ❩

You will be able to demonstrate your knowledge of the chapter objectives with case studies as follows:

- Given the antenna azimuth position control system shown on the front endpapers, you will be able to find the transfer function of each subsystem.
- Given a model of a human leg or a nonlinear electrical circuit, you will be able to linearize the model and then find the transfer function.

❨ 2.1   Introduction

In Chapter 1, we discussed the analysis and design sequence that included obtaining the system's schematic and demonstrated this step for a position control system. To obtain a schematic, the control systems engineer must often make many simplifying assumptions in order to keep the ensuing model manageable and still approximate physical reality.

The next step is to develop mathematical models from schematics of physical systems. We will discuss two methods: (1) transfer functions in the frequency domain and (2) state equations in the time domain. These topics are covered in this chapter and in Chapter 3, respectively. As we proceed, we will notice that in every case the first step in developing a mathematical model is to apply the fundamental physical laws of science and engineering. For example, when we model electrical networks, Ohm's law and Kirchhoff's laws, which are basic laws of electric networks, will be applied initially. We will sum voltages in a loop or sum currents at a node. When we study mechanical systems, we will use Newton's laws as the fundamental guiding principles. Here we will sum forces or torques. From these equations we will obtain the relationship between the system's output and input.

In Chapter 1 we saw that a differential equation can describe the relationship between the input and output of a system. The form of the differential equation and its coefficients are a formulation or description of the system. Although the differential equation relates the system to its input and output, it is not a satisfying representation from a system perspective. Looking at Eq. (1.2), a general, nth-order, linear, time-invariant differential equation, we see that the system parameters, which are the coefficients, as well as the output, $c(t)$, and the input, $r(t)$, appear throughout the equation.

We would prefer a mathematical representation such as that shown in Figure 2.1(a), where the input, output, and system are distinct and separate parts. Also, we would like to represent conveniently the interconnection of several subsystems. For example, we would like to represent *cascaded* interconnections, as shown

(a)

(b)
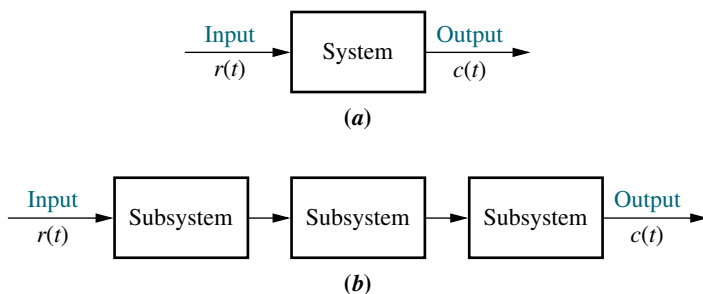
FIGURE 2.1   a. Block diagram representation of a system; **b.** block diagram representation of an interconnection of subsystems

Note: The input, $r(t)$, stands for *reference input*.
The output, $c(t)$, stands for *controlled variable*.

in Figure 2.1(*b*), where a mathematical function, called a transfer function, is inside each block, and block functions can easily be combined to yield Figure 2.1 (*a*) for ease of analysis and design. This convenience cannot be obtained with the differential equation.

◖ **2.2   Laplace Transform Review**

A system represented by a differential equation is difficult to model as a block diagram. Thus, we now lay the groundwork for the Laplace transform, with which we can represent the input, output, and system as separate entities. Further, their interrelationship will be simply algebraic. Let us first define the Laplace transform and then show how it simplifies the representation of physical systems (*Nilsson, 1996*).

The Laplace transform is defined as

$$\mathscr{L}[f(t)] = F(s) = \int_{0-}^{\infty} f(t)e^{-st}\, dt \tag{2.1}$$

where $s = \sigma + j\omega$, a complex variable. Thus, knowing $f(t)$ and that the integral in Eq. (2.1) exists, we can find a function, $F(s)$, that is called the *Laplace transform* of $f(t)$.[1]

The notation for the lower limit means that even if $f(t)$ is discontinuous at $t = 0$, we can start the integration prior to the discontinuity as long as the integral converges. Thus, we can find the Laplace transform of impulse functions. This property has distinct advantages when applying the Laplace transform to the solution of differential equations where the initial conditions are discontinuous at $t = 0$. Using differential equations, we have to solve for the initial conditions after the discontinuity knowing the initial conditions before the discontinuity. Using the Laplace transform we need only know the initial conditions before the discontinuity. See *Kailath (1980)* for a more detailed discussion.

The inverse Laplace transform, which allows us to find $f(t)$ given $F(s)$, is

$$\mathscr{L}^{-1}[F(s)] = \frac{1}{2\pi j} \int_{\sigma - j\infty}^{\sigma + j\infty} F(s)e^{st} ds = f(t)u(t) \tag{2.2}$$

where

$$u(t) = 1 \quad t > 0$$
$$= 0 \quad t < 0$$

is the unit step function. Multiplication of $f(t)$ by $u(t)$ yields a time function that is zero for $t < 0$.

Using Eq. (2.1), it is possible to derive a table relating $f(t)$ to $F(s)$ for specific cases. Table 2.1 shows the results for a representative sample of functions. If we use the tables, we do not have to use Eq. (2.2), which requires complex integration, to find $f(t)$ given $F(s)$.

---

[1] The Laplace transform exists if the integral of Eq. (2.1) converges. The integral will converge if $\int_{0-}^{\infty} |f(t)| e^{-\sigma_1 t}\, dt < \infty$. If $|f(t)| < M e^{\sigma_2 t}, 0 < t < \infty$, the integral will converge if $\infty > \sigma_1 > \sigma_2$. We call σ_2 the *abscissa of convergence*, and it is the smallest value of σ, where $s = \sigma + j\omega$, for which the integral exists.

TABLE 2.1   Laplace transform table

Item no.	$f(t)$	$F(s)$
1.	$\delta(t)$	1
2.	$u(t)$	$\dfrac{1}{s}$
3.	$tu(t)$	$\dfrac{1}{s^2}$
4.	$t^n u(t)$	$\dfrac{n!}{s^{n+1}}$
5.	$e^{-at}u(t)$	$\dfrac{1}{s+a}$
6.	$\sin \omega t u(t)$	$\dfrac{\omega}{s^2 + \omega^2}$
7.	$\cos \omega t u(t)$	$\dfrac{s}{s^2 + \omega^2}$

In the following example we demonstrate the use of Eq. (2.1) to find the Laplace transform of a time function.

Example 2.1

Laplace Transform of a Time Function

PROBLEM: Find the Laplace transform of $f(t) = Ae^{-at}u(t)$.

SOLUTION: Since the time function does not contain an impulse function, we can replace the lower limit of Eq. (2.1) with 0. Hence,

$$F(s) = \int_0^\infty f(t)e^{-st}\, dt = \int_0^\infty Ae^{-at}e^{-st}\, dt = A \int_0^\infty e^{-(s+a)t}\, dt$$

$$= -\frac{A}{s+a} e^{-(s+a)t}\bigg|_{t=0}^\infty = \frac{A}{s+a} \qquad (2.3)$$

In addition to the Laplace transform table, Table 2.1, we can use Laplace transform theorems, listed in Table 2.2, to assist in transforming between $f(t)$ and $F(s)$. In the next example, we demonstrate the use of the Laplace transform theorems shown in Table 2.2 to find $f(t)$ given $F(s)$.

Example 2.2

Inverse Laplace Transform

PROBLEM: Find the inverse Laplace transform of $F_1(s) = 1/(s+3)^2$.

SOLUTION: For this example we make use of the frequency shift theorem, Item 4 of Table 2.2, and the Laplace transform of $f(t) = tu(t)$, Item 3 of Table 2.1. If the inverse transform of $F(s) = 1/s^2$ is $tu(t)$, the inverse transform of $F(s+a) = 1/(s+a)^2$ is $e^{-at}tu(t)$. Hence, $f_1(t) = e^{-3t}tu(t)$.

TABLE 2.2   Laplace transform theorems

Item no.	Theorem	Name
1.	$\mathscr{L}[f(t)] = F(s) \ = \int_{0-}^{\infty} f(t)e^{-st}dt$	Definition
2.	$\mathscr{L}[kf(t)] \qquad = kF(s)$	Linearity theorem
3.	$\mathscr{L}[f_1(t) + f_2(t)] = F_1(s) + F_2(s)$	Linearity theorem
4.	$\mathscr{L}[e^{-at}f(t)] \quad = F(s + a)$	Frequency shift theorem
5.	$\mathscr{L}[f(t - T)] \quad = e^{-sT}F(s)$	Time shift theorem
6.	$\mathscr{L}[f(at)] \qquad = \dfrac{1}{a}F\left(\dfrac{s}{a}\right)$	Scaling theorem
7.	$\mathscr{L}\left[\dfrac{df}{dt}\right] \quad = sF(s) - f(0-)$	Differentiation theorem
8.	$\mathscr{L}\left[\dfrac{d^2f}{dt^2}\right] \quad = s^2F(s) - sf(0-) - f'(0-)$	Differentiation theorem
9.	$\mathscr{L}\left[\dfrac{d^nf}{dt^n}\right] \quad = s^nF(s) - \displaystyle\sum_{k=1}^{n} s^{n-k}f^{k-1}(0-)$	Differentiation theorem
10.	$\mathscr{L}\left[\int_{0-}^{t} f(\tau)d\tau\right] = \dfrac{F(s)}{s}$	Integration theorem
11.	$f(\infty) \qquad = \displaystyle\lim_{s \to 0} sF(s)$	Final value theorem[1]
12.	$f(0+) \qquad = \displaystyle\lim_{s \to \infty} sF(s)$	Initial value theorem[2]

[1]For this theorem to yield correct finite results, all roots of the denominator of $F(s)$ must have negative real parts, and no more than one can be at the origin.

[2]For this theorem to be valid, $f(t)$ must be continuous or have a step discontinuity at $t = 0$ (that is, no impulses or their derivatives at $t = 0$).

Partial-Fraction Expansion

To find the inverse Laplace transform of a complicated function, we can convert the function to a sum of simpler terms for which we know the Laplace transform of each term. The result is called a *partial-fraction expansion*. If $F_1(s) = N(s)/D(s)$, where the order of $N(s)$ is less than the order of $D(s)$, then a partial-fraction expansion can be made. If the order of $N(s)$ is greater than or equal to the order of $D(s)$, then $N(s)$ must be divided by $D(s)$ successively until the result has a remainder whose numerator is of order less than its denominator. For example, if

$$F_1(s) = \frac{s^3 + 2s^2 + 6s + 7}{s^2 + s + 5} \tag{2.4}$$

we must perform the indicated division until we obtain a remainder whose numerator is of order less than its denominator. Hence,

$$F_1(s) = s + 1 + \frac{2}{s^2 + s + 5} \tag{2.5}$$

Taking the inverse Laplace transform, using Item 1 of Table 2.1, along with the differentiation theorem (Item 7) and the linearity theorem (Item 3 of Table 2.2), we obtain

$$f_1(t) = \frac{d\delta(t)}{dt} + \delta(t) + \mathscr{L}^{-1}\left[\frac{2}{s^2 + s + 5}\right] \tag{2.6}$$

Using partial-fraction expansion, we will be able to expand functions like $F(s) = 2/(s^2 + s + 5)$ into a sum of terms and then find the inverse Laplace transform for each term. We will now consider three cases and show for each case how an $F(s)$ can be expanded into partial fractions.

Case 1. Roots of the Denominator of *F(s)* Are Real and Distinct   An example of an $F(s)$ with real and distinct roots in the denominator is

$$F(s) = \frac{2}{(s+1)(s+2)} \tag{2.7}$$

The roots of the denominator are distinct, since each factor is raised only to unity power. We can write the partial-fraction expansion as a sum of terms where each factor of the original denominator forms the denominator of each term, and constants, called *residues*, form the numerators. Hence,

$$F(s) = \frac{2}{(s+1)(s+2)} = \frac{K_1}{(s+1)} + \frac{K_2}{(s+2)} \tag{2.8}$$

To find K_1, we first multiply Eq. (2.8) by $(s+1)$, which isolates K_1. Thus,

$$\frac{2}{(s+2)} = K_1 + \frac{(s+1)K_2}{(s+2)} \tag{2.9}$$

Letting s approach -1 eliminates the last term and yields $K_1 = 2$. Similarly, K_2 can be found by multiplying Eq. (2.8) by $(s+2)$ and then letting s approach -2; hence, $K_2 = -2$.

Each component part of Eq. (2.8) is an $F(s)$ in Table 2.1. Hence, $f(t)$ is the sum of the inverse Laplace transform of each term, or

$$f(t) = (2e^{-t} - 2e^{-2t})u(t) \tag{2.10}$$

In general, then, given an $F(s)$ whose denominator has real and distinct roots, a partial-fraction expansion,

$$F(s) = \frac{N(s)}{D(s)} = \frac{N(s)}{(s+p_1)(s+p_2)\cdots(s+p_m)\cdots(s+p_n)}$$
$$= \frac{K_1}{(s+p_1)} + \frac{K_2}{(s+p_2)} + \cdots + \frac{K_m}{(s+p_m)} + \cdots + \frac{K_n}{(s+p_n)} \tag{2.11}$$

can be made if the order of $N(s)$ is less than the order of $D(s)$. To evaluate each residue, K_i, we multiply Eq. (2.11) by the denominator of the corresponding partial fraction. Thus, if we want to find K_m, we multiply Eq. (2.11) by $(s+p_m)$ and get

$$(s+p_m)F(s) = \frac{(s+p_m)N(s)}{(s+p_1)(s+p_2)\cdots(s+p_m)\cdots(s+p_n)}$$
$$= (s+p_m)\frac{K_1}{(s+p_1)} + (s+p_m)\frac{K_2}{(s+p_2)} + \cdots + K_m + \cdots$$
$$+ (s+p_m)\frac{K_n}{(s+p_n)} \tag{2.12}$$

If we let s approach $-p_m$, all terms on the right-hand side of Eq. (2.12) go to zero except the term K_m, leaving

$$\left. \frac{(s+p_m)N(s)}{(s+p_1)(s+p_2)\cdots(s+p_m)\cdots(s+p_n)} \right|_{s\to -p_m} = K_m \tag{2.13}$$

The following example demonstrates the use of the partial-fraction expansion to solve a differential equation. We will see that the Laplace transform reduces the task of finding the solution to simple algebra.

Example 2.3

Laplace Transform Solution of a Differential Equation

PROBLEM: Given the following differential equation, solve for $y(t)$ if all initial conditions are zero. Use the Laplace transform.

$$\frac{d^2 y}{dt^2} + 12\frac{dy}{dt} + 32y = 32u(t) \tag{2.14}$$

SOLUTION: Substitute the corresponding $F(s)$ for each term in Eq. (2.14), using Item 2 in Table 2.1, Items 7 and 8 in Table 2.2, and the initial conditions of $y(t)$ and $dy(t)/dt$ given by $y(0-) = 0$ and $\dot{y}(0-) = 0$, respectively. Hence, the Laplace transform of Eq. (2.14) is

$$s^2 Y(s) + 12sY(s) + 32Y(s) = \frac{32}{s} \tag{2.15}$$

Solving for the response, $Y(s)$, yields

$$Y(s) = \frac{32}{s(s^2 + 12s + 32)} = \frac{32}{s(s + 4)(s + 8)} \tag{2.16}$$

To solve for $y(t)$, we notice that Eq. (2.16) does not match any of the terms in Table 2.1. Thus, we form the partial-fraction expansion of the right-hand term and match each of the resulting terms with $F(s)$ in Table 2.1. Therefore,

$$Y(s) = \frac{32}{s(s + 4)(s + 8)} = \frac{K_1}{s} + \frac{K_2}{(s + 4)} + \frac{K_3}{(s + 8)} \tag{2.17}$$

where, from Eq. (2.13),

$$K_1 = \frac{32}{(s + 4)(s + 8)}\bigg|_{s \to 0} = 1 \tag{2.18a}$$

$$K_2 = \frac{32}{s(s + 8)}\bigg|_{s \to -4} = -2 \tag{2.18b}$$

$$K_3 = \frac{32}{s(s + 4)}\bigg|_{s \to -8} = 1 \tag{2.18c}$$

Hence,

$$Y(s) = \frac{1}{s} - \frac{2}{(s + 4)} + \frac{1}{(s + 8)} \tag{2.19}$$

Since each of the three component parts of Eq. (2.19) is represented as an $F(s)$ in Table 2.1, $y(t)$ is the sum of the inverse Laplace transforms of each term. Hence,

$$y(t) = (1 - 2e^{-4t} + e^{-8t})u(t) \tag{2.20}$$

Students who are using MATLAB should now run ch2p1 through ch2p8 in Appendix B. This is your first MATLAB exercise. You will learn how to use MATLAB to (1) represent polynomials, (2) find roots of polynomials, (3) multiply polynomials, and (4) find partial-fraction expansions. Finally, Example 2.3 will be solved using MATLAB.

The $u(t)$ in Eq. (2.20) shows that the response is zero until $t = 0$. Unless otherwise specified, all inputs to systems in the text will not start until $t = 0$. Thus, output responses will also be zero until $t = 0$. For convenience, we will leave off the $u(t)$ notation from now on. Accordingly, we write the output response as

$$y(t) = 1 - 2e^{-4t} + e^{-8t} \tag{2.21}$$

TryIt 2.1

Use the following MATLAB and Control System Toolbox statement to form the linear, time-invariant (LTI) transfer function of Eq. (2.22).

`F = zpk([ ], [−1 −2 −2], 2)`

Case 2. Roots of the Denominator of *F(s)* Are Real and Repeated   An example of an $F(s)$ with real and repeated roots in the denominator is

$$F(s) = \frac{2}{(s+1)(s+2)^2} \tag{2.22}$$

The roots of $(s + 2)^2$ in the denominator are repeated, since the factor is raised to an integer power higher than 1. In this case, the denominator root at -2 is a *multiple root* of *multiplicity* 2.

We can write the partial-fraction expansion as a sum of terms, where each factor of the denominator forms the denominator of each term. In addition, each multiple root generates additional terms consisting of denominator factors of reduced multiplicity. For example, if

$$F(s) = \frac{2}{(s+1)(s+2)^2} = \frac{K_1}{(s+1)} + \frac{K_2}{(s+2)^2} + \frac{K_3}{(s+2)} \tag{2.23}$$

then $K_1 = 2$, which can be found as previously described. K_2 can be isolated by multiplying Eq. (2.23) by $(s+2)^2$, yielding

$$\frac{2}{s+1} = (s+2)^2 \frac{K_1}{(s+1)} + K_2 + (s+2)K_3 \tag{2.24}$$

Letting s approach -2, $K_2 = -2$. To find K_3 we see that if we differentiate Eq. (2.24) with respect to s,

$$\frac{-2}{(s+1)^2} = \frac{(s+2)s}{(s+1)^2}K_1 + K_3 \tag{2.25}$$

TryIt 2.2

Use the following MATLAB statements to help you get Eq. (2.26).

`numf = 2;`
`denf = poly([−1 −2 −2]);`
`[k, p, k] = residue...`
` (numf, denf)`

K_3 is isolated and can be found if we let s approach -2. Hence, $K_3 = -2$.

Each component part of Eq. (2.23) is an $F(s)$ in Table 2.1; hence, $f(t)$ is the sum of the inverse Laplace transform of each term, or

$$f(t) = 2e^{-t} - 2te^{-2t} - 2e^{-2t} \tag{2.26}$$

If the denominator root is of higher multiplicity than 2, successive differentiation would isolate each residue in the expansion of the multiple root.

In general, then, given an $F(s)$ whose denominator has real and repeated roots, a partial-fraction expansion,

$$F(s) = \frac{N(s)}{D(s)}$$

$$= \frac{N(s)}{(s + p_1)^r (s + p_2) \cdots (s + p_n)}$$

$$= \frac{K_1}{(s + p_1)^r} + \frac{K_2}{(s + p_1)^{r-1}} + \cdots + \frac{K_r}{(s + p_1)}$$

$$+ \frac{K_{r+1}}{(s + p_2)} + \cdots + \frac{K_n}{(s + p_n)} \tag{2.27}$$

can be made if the order of $N(s)$ is less than the order of $D(s)$ and the repeated roots are of multiplicity r at $-p_1$. To find K_1 through K_r for the roots of multiplicity greater than unity, first multiply Eq. (2.27) by $(s + p_1)^r$ getting $F_1(s)$, which is

$$F_1(s) = (s + p_1)^r F(s)$$

$$= \frac{(s + p_1)^r N(s)}{(s + p_1)^r (s + p_2) \cdots (s + p_n)}$$

$$= K_1 + (s + p_1)K_2 + (s + p_1)^2 K_3 + \cdots + (s + p_1)^{r-1} K_r$$

$$+ \frac{K_{r+1}(s + p_1)^r}{(s + p_2)} + \cdots + \frac{K_n(s + p_1)^r}{(s + p_n)} \tag{2.28}$$

Immediately, we can solve for K_1 if we let s approach $-p_1$. We can solve for K_2 if we differentiate Eq. (2.28) with respect to s and then let s approach $-p_1$. Subsequent differentiation will allow us to find K_3 through K_r. The general expression for K_1 through K_r for the multiple roots is

$$K_i = \frac{1}{(i - 1)!} \frac{d^{i-1} F_1(s)}{ds^{i-1}} \bigg|_{s \to -p_1} \qquad i = 1, 2, \ldots, r; \quad 0! = 1 \tag{2.29}$$

Case 3. Roots of the Denominator of *F(s)* Are Complex or Imaginary   An example of $F(s)$ with complex roots in the denominator is

$$F(s) = \frac{3}{s(s^2 + 2s + 5)} \tag{2.30}$$

This function can be expanded in the following form:

$$\frac{3}{s(s^2 + 2s + 5)} = \frac{K_1}{s} + \frac{K_2 s + K_3}{s^2 + 2s + 5} \tag{2.31}$$

K_1 is found in the usual way to be $\frac{3}{5}$. K_2 and K_3 can be found by first multiplying Eq. (2.31) by the lowest common denominator, $s(s^2 + 2s + 5)$, and clearing the fractions. After simplification with $K_1 = \frac{3}{5}$, we obtain

$$3 = \left(K_2 + \frac{3}{5}\right)s^2 + \left(K_3 + \frac{6}{5}\right)s + 3 \tag{2.32}$$

TryIt 2.3

Use the following MATLAB and Control System Toolbox statement to form the LTI transfer function of Eq. (2.30).

```
F=tf([3],[1 2 5 0])
```

Balancing coefficients, $\left(K_2 + \frac{3}{5}\right) = 0$ and $\left(K_3 + \frac{6}{5}\right) = 0$. Hence $K_2 = -\frac{3}{5}$ and $K_3 = -\frac{6}{5}$. Thus,

$$F(s) = \frac{3}{s(s^2 + 2s + 5)} = \frac{3/5}{s} - \frac{3}{5}\frac{s+2}{s^2 + 2s + 5} \tag{2.33}$$

The last term can be shown to be the sum of the Laplace transforms of an exponentially damped sine and cosine. Using Item 7 in Table 2.1 and Items 2 and 4 in Table 2.2, we get

$$\mathscr{L}[Ae^{-at}\cos \omega t] = \frac{A(s+a)}{(s+a)^2 + \omega^2} \tag{2.34}$$

Similarly,

$$\mathscr{L}[Be^{-at}\sin \omega t] = \frac{B\omega}{(s+a)^2 + \omega^2} \tag{2.35}$$

Adding Eqs. (2.34) and (2.35), we get

$$\mathscr{L}[Ae^{-at}\cos \omega t + Be^{-at}\sin \omega t] = \frac{A(s+a) + B\omega}{(s+a)^2 + \omega^2} \tag{2.36}$$

We now convert the last term of Eq. (2.33) to the form suggested by Eq. (2.36) by completing the squares in the denominator and adjusting terms in the numerator without changing its value. Hence,

$$F(s) = \frac{3/5}{s} - \frac{3}{5}\frac{(s+1) + (1/2)(2)}{(s+1)^2 + 2^2} \tag{2.37}$$

Comparing Eq. (2.37) to Table 2.1 and Eq. (2.36), we find

$$f(t) = \frac{3}{5} - \frac{3}{5}e^{-t}\left(\cos 2t + \frac{1}{2}\sin 2t\right) \tag{2.38}$$

In order to visualize the solution, an alternate form of $f(t)$, obtained by trigonometric identities, is preferable. Using the amplitudes of the cos and sin terms, we factor out $\sqrt{1^2 + (1/2)^2}$ from the term in parentheses and obtain

$$f(t) = \frac{3}{5} - \frac{3}{5}\sqrt{1^2 + (1/2)^2}\,e^{-t}\left(\frac{1}{\sqrt{1^2 + (1/2)^2}}\cos 2t + \frac{1/2}{\sqrt{1^2 + (1/2)^2}}\sin 2t\right) \tag{2.39}$$

Letting $1/\sqrt{1^2 + (1/2)^2} = \cos \phi$ and $(1/2)/\sqrt{1^2 + (1/2)^2} = \sin \phi$,

$$f(t) = \frac{3}{5} - \frac{3}{5}\sqrt{1^2 + (1/2)^2}\,e^{-t}(\cos \phi \cos 2t + \sin \phi \sin 2t) \tag{2.40}$$

or

$$f(t) = 0.6 - 0.671e^{-t}\cos(2t - \phi) \tag{2.41}$$

where $\phi = \arctan 0.5 = 26.57°$. Thus, $f(t)$ is a constant plus an exponentially damped sinusoid.

In general, then, given an $F(s)$ whose denominator has complex or purely imaginary roots, a partial-fraction expansion,

$$F(s) = \frac{N(s)}{D(s)} = \frac{N(s)}{(s+p_1)(s^2+as+b)\cdots}$$
$$= \frac{K_1}{(s+p_1)} + \frac{(K_2 s + K_3)}{(s^2+as+b)} + \cdots \tag{2.42}$$

can be made if the order of $N(s)$ is less than the order of $D(s)$ p_1 is real, and $(s^2 + as + b)$ has complex or purely imaginary roots. The complex or imaginary roots are expanded with $(K_2 s + K_3)$ terms in the numerator rather than just simply K_i, as in the case of real roots. The K_i's in Eq. (2.42) are found through balancing the coefficients of the equation after clearing fractions. After completing the squares on $(s^2 + as + b)$ and adjusting the numerator, $(K_2 s + K_3)/(s^2 + as + b)$ can be put into the form shown on the right-hand side of Eq. (2.36).

Finally, the case of purely imaginary roots arises if $a = 0$ in Eq. (2.42). The calculations are the same.

Another method that follows the technique used for the partial-fraction expansion of $F(s)$ with real roots in the denominator can be used for complex and imaginary roots. However, the residues of the complex and imaginary roots are themselves complex conjugates. Then, after taking the inverse Laplace transform, the resulting terms can be identified as

$$\frac{e^{j\theta} + e^{-j\theta}}{2} = \cos\theta \tag{2.43}$$

and

$$\frac{e^{j\theta} - e^{-j\theta}}{2j} = \sin\theta \tag{2.44}$$

For example, the previous $F(s)$ can also be expanded in partial fractions as

$$F(s) = \frac{3}{s(s^2+2s+5)} = \frac{3}{s(s+1+j2)(s+1-j2)}$$
$$= \frac{K_1}{s} + \frac{K_2}{s+1+j2} + \frac{K_3}{s+1-j2} \tag{2.45}$$

Finding K_2,

$$K_2 = \frac{3}{s(s+1-j2)}\bigg|_{s\to-1-j2} = -\frac{3}{20}(2+j1) \tag{2.46}$$

Similarly, K_3 is found to be the complex conjugate of K_2, and K_1 is found as previously described. Hence,

$$F(s) = \frac{3/5}{s} - \frac{3}{20}\left(\frac{2+j1}{s+1+j2} + \frac{2-j1}{s+1-j2}\right) \tag{2.47}$$

from which

$$f(t) = \frac{3}{5} - \frac{3}{20}\left[(2+j1)e^{-(1+j2)t} + (2-j1)e^{-(1-j2)t}\right]$$
$$= \frac{3}{5} - \frac{3}{20}e^{-t}\left[4\left(\frac{e^{j2t} + e^{-j2t}}{2}\right) + 2\left(\frac{e^{j2t} + e^{-j2t}}{2j}\right)\right] \tag{2.48}$$

TryIt 2.5

Use the following MATLAB statements to help you get Eq. (2.47).

```
numf = 3
denf = [1 2 5 0]
[k,p,k] = residue...
  (numf,denf)
```

Using Eqs. (2.43) and (2.44), we get

$$f(t) = \frac{3}{5} - \frac{3}{5}e^{-t}\left(\cos 2t + \frac{1}{2}\sin 2t\right) = 0.6 - 0.671e^{-t}\cos(2t - \phi) \tag{2.49}$$

where $\phi = \arctan 0.5 = 26.57°$.

Symbolic Math
SM

```
Students who are performing the MATLAB exercises and want to
explore the added capability of MATLAB's Symbolic Math Toolbox
should now run ch2sp1 and ch2sp2 in Appendix F at www.wiley.com/
college/nise. You will learn how to construct symbolic objects and
then find the inverse Laplace and Laplace transforms of frequency
and time functions, respectively. The examples in Case 2 and Case 3
in this section will be solved using the Symbolic Math Toolbox.
```

Skill-Assessment Exercise 2.1

PROBLEM: Find the Laplace transform of $f(t) = te^{-5t}$.

ANSWER: $F(s) = 1/(s + 5)^2$

The complete solution is at www.wiley.com/college/nise.

Skill-Assessment Exercise 2.2

PROBLEM: Find the inverse Laplace transform of $F(s) = 10/[s(s + 2)(s + 3)^2]$.

WileyPLUS
WPCS
Control Solutions

ANSWER: $f(t) = \dfrac{5}{9} - 5e^{-2t} + \dfrac{10}{3}te^{-3t} + \dfrac{40}{9}e^{-3t}$

The complete solution is at www.wiley.com/college/nise.

2.3   The Transfer Function

In the previous section we defined the Laplace transform and its inverse. We presented the idea of the partial-fraction expansion and applied the concepts to the solution of differential equations. We are now ready to formulate the system representation shown in Figure 2.1 by establishing a viable definition for a function that algebraically relates a system's output to its input. This function will allow separation of the input, system, and output into three separate and distinct parts, unlike the differential equation. The function will also allow us to *algebraically* combine mathematical representations of subsystems to yield a total system representation.

Let us begin by writing a general nth-order, linear, time-invariant differential equation,

$$a_n\frac{d^n c(t)}{dt^n} + a_{n-1}\frac{d^{n-1}c(t)}{dt^{n-1}} + \cdots + a_0 c(t) = b_m\frac{d^m r(t)}{dt^m} + b_{m-1}\frac{d^{m-1}r(t)}{dt^{m-1}} + \cdots + b_0 r(t)$$

$$\tag{2.50}$$

where $c(t)$ is the output, $r(t)$ is the input, and the a_i's, b_i's, and the form of the differential equation represent the system. Taking the Laplace transform of both sides,

$$a_n s^n C(s) + a_{n-1} s^{n-1} C(s) + \cdots + a_0 C(s) + \text{initial condition}$$
$$\text{terms involving } c(t)$$
$$= b_m s^m R(s) + b_{m-1} s^{m-1} R(s) + \cdots + b_0 R(s) + \text{initial condition}$$
$$\text{terms involving } r(t) \qquad (2.51)$$

Equation (2.51) is a purely algebraic expression. If we assume that *all initial conditions are zero*, Eq. (2.51) reduces to

$$(a_n s^n + a_{n-1} s^{n-1} + \cdots + a_0) C(s) = (b_m s^m + b_{m-1} s^{m-1} + \cdots + b_0) R(s) \qquad (2.52)$$

Now form the ratio of the output transform, $C(s)$, divided by the input transform, $R(s)$:

$$\frac{C(s)}{R(s)} = G(s) = \frac{(b_m s^m + b_{m-1} s^{m-1} + \cdots + b_0)}{(a_n s^n + a_{n-1} s^{n-1} + \cdots + a_0)} \qquad (2.53)$$

Notice that Eq. (2.53) separates the output, $C(s)$, the input, $R(s)$, and the system, the ratio of polynomials in s on the right. We call this ratio, $G(s)$, the *transfer function* and evaluate it with *zero initial conditions*.

The transfer function can be represented as a block diagram, as shown in Figure 2.2, with the input on the left, the output on the right, and the system transfer function inside the block. Notice that the denominator of the transfer function is identical to the characteristic polynomial of the differential equation. Also, we can find the output, $C(s)$ by using

$$R(s) \longrightarrow \boxed{\dfrac{(b_m s^m + b_{m-1} s^{m-1} + \cdots + b_0)}{(a_n s^n + a_{n-1} s^{n-1} + \cdots + a_0)}} \longrightarrow C(s)$$
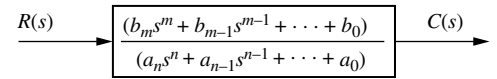
FIGURE 2.2   Block diagram of a transfer function

$$C(s) = R(s) G(s) \qquad (2.54)$$

Let us apply the concept of a transfer function to an example and then use the result to find the response of the system.

Example 2.4

Transfer Function for a Differential Equation

PROBLEM: Find the transfer function represented by

$$\frac{dc(t)}{dt} + 2c(t) = r(t) \qquad (2.55)$$

SOLUTION: Taking the Laplace transform of both sides, assuming zero initial conditions, we have

$$sC(s) + 2C(s) = R(s) \qquad (2.56)$$

The transfer function, $G(s)$, is

$$G(s) = \frac{C(s)}{R(s)} = \frac{1}{s + 2} \qquad (2.57)$$

Students who are using MATLAB should now run ch2p9 through ch2p12 in Appendix B. You will learn how to use MATLAB to create transfer functions with numerators and denominators in polynomial or factored form. You will also learn how to convert between polynomial and factored forms. Finally, you will learn how to use MATLAB to plot time functions.

Students who are performing the MATLAB exercises and want to explore the added capability of MATLAB's Symbolic Math Toolbox should now run ch2sp3 in Appendix F at www.wiley.com/college/nise. You will learn how to use the Symbolic Math Toolbox to simplify the input of complicated transfer functions as well as improve readability. You will learn how to enter a symbolic transfer function and convert it to a linear, time-invariant (LTI) object as presented in Appendix B, ch2p9.

Example 2.5

TryIt 2.6

Use the following MATLAB and Symbolic Math Toolbox statements to help you get Eq. (2.60).

```
syms s
C=1/(s*(s+2))
C=ilaplace(C)
```

TryIt 2.7

Use the following MATLAB statements to plot Eq. (2.60) for t from 0 to 1 s at intervals of 0.01 s.

```
t=0:0.01:1;
plot...
 (t,(1/2-1/2*exp(-2*t)))
```

System Response from the Transfer Function

PROBLEM: Use the result of Example 2.4 to find the response, $c(t)$ to an input, $r(t) = u(t)$, a unit step, assuming zero initial conditions.

SOLUTION: To solve the problem, we use Eq. (2.54), where $G(s) = 1/(s + 2)$ as found in Example 2.4. Since $r(t) = u(t)$, $R(s) = 1/s$, from Table 2.1. Since the initial conditions are zero,

$$C(s) = R(s)G(s) = \frac{1}{s(s+2)} \tag{2.58}$$

Expanding by partial fractions, we get

$$C(s) = \frac{1/2}{s} - \frac{1/2}{s+2} \tag{2.59}$$

Finally, taking the inverse Laplace transform of each term yields

$$c(t) = \frac{1}{2} - \frac{1}{2}e^{-2t} \tag{2.60}$$

Skill-Assessment Exercise 2.3

PROBLEM: Find the transfer function, $G(s) = C(s)/R(s)$, corresponding to the differential equation $\dfrac{d^3c}{dt^3} + 3\dfrac{d^2c}{dt^2} + 7\dfrac{dc}{dt} + 5c = \dfrac{d^2r}{dt^2} + 4\dfrac{dr}{dt} + 3r$.

ANSWER: $G(s) = \dfrac{C(s)}{R(s)} = \dfrac{s^2 + 4s + 3}{s^3 + 3s^2 + 7s + 5}$

The complete solution is at www.wiley.com/college/nise.

Skill-Assessment Exercise 2.4

PROBLEM: Find the differential equation corresponding to the transfer function,

$$G(s) = \frac{2s + 1}{s^2 + 6s + 2}$$

ANSWER: $\dfrac{d^2c}{dt^2} + 6\dfrac{dc}{dt} + 2c = 2\dfrac{dr}{dt} + r$

The complete solution is at www.wiley.com/college/nise.

Skill-Assessment Exercise 2.5

PROBLEM: Find the ramp response for a system whose transfer function is

$$G(s) = \frac{s}{(s + 4)(s + 8)}$$

ANSWER: $c(t) = \dfrac{1}{32} - \dfrac{1}{16}e^{-4t} + \dfrac{1}{32}e^{-8t}$

The complete solution is at www.wiley.com/college/nise.

WileyPLUS

WPCS

Control Solutions

In general, a physical system that can be represented by a linear, time-invariant differential equation can be modeled as a transfer function. The rest of this chapter will be devoted to the task of modeling individual subsystems. We will learn how to represent electrical networks, translational mechanical systems, rotational mechanical systems, and electromechanical systems as transfer functions. As the need arises, the reader can consult the Bibliography at the end of the chapter for discussions of other types of systems, such as pneumatic, hydraulic, and heat-transfer systems (*Cannon, 1967*).

2.4 Electrical Network Transfer Functions
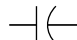
In this section, we formally apply the transfer function to the mathematical modeling of electric circuits including passive networks and operational amplifier circuits. Subsequent sections cover mechanical and electromechanical systems.

Equivalent circuits for the electric networks that we work with first consist of three passive linear components: resistors, capacitors, and inductors.[2] Table 2.3 summarizes the components and the relationships between voltage and current and between voltage and charge under zero initial conditions.

We now combine electrical components into circuits, decide on the input and output, and find the transfer function. Our guiding principles are Kirchhoff's laws. We sum voltages around loops or sum currents at nodes, depending on which technique involves the least effort in algebraic manipulation, and then equate the result to zero. From these relationships we can write the differential equations for the circuit. Then we can take the Laplace transforms of the differential equations and finally solve for the transfer function.

---

[2] *Passive* means that there is no internal source of energy.

TABLE 2.3 Voltage-current, voltage-charge, and impedance relationships for capacitors, resistors, and inductors

Component	Voltage-current	Current-voltage	Voltage-charge	Impedance $Z(s) = V(s)/I(s)$	Admittance $Y(s) = I(s)/V(s)$
⊣⊢ Capacitor	$v(t) = \dfrac{1}{C}\displaystyle\int_0^1 i(\tau)d\tau$	$i(t) = C\dfrac{dv(t)}{dt}$	$v(t) = \dfrac{1}{C}q(t)$	$\dfrac{1}{Cs}$	Cs
⋀⋀⋀ Resistor	$v(t) = Ri(t)$	$i(t) = \dfrac{1}{R}v(t)$	$v(t) = R\dfrac{dq(t)}{dt}$	R	$\dfrac{1}{R} = G$
⌒⌒⌒⌒ Inductor	$v(t) = L\dfrac{di(t)}{dt}$	$i(t) = \dfrac{1}{L}\displaystyle\int_0^1 v(\tau)d\tau$	$v(t) = L\dfrac{d^2q(t)}{dt^2}$	Ls	$\dfrac{1}{Ls}$

Note: The following set of symbols and units is used throughout this book: $v(t)$ – V (volts), $i(t)$ – A (amps), $q(t)$ – Q (coulombs), C – F (farads), R – Ω (ohms), G – Ω (mhos), L – H (henries).

Simple Circuits via Mesh Analysis

Transfer functions can be obtained using Kirchhoff's voltage law and summing voltages around loops or meshes.[3] We call this method *loop* or *mesh analysis* and demonstrate it in the following example.

Example 2.6

Transfer Function—Single Loop via the Differential Equation
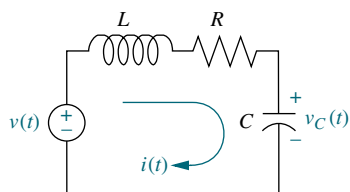
FIGURE 2.3 *RLC* network

PROBLEM: Find the transfer function relating the capacitor voltage, $V_C(s)$, to the input voltage, $V(s)$ in Figure 2.3.

SOLUTION: In any problem, the designer must first decide what the input and output should be. In this network, several variables could have been chosen to be the output—for example, the inductor voltage, the capacitor voltage, the resistor voltage, or the current. The problem statement, however, is clear in this case: We are to treat the capacitor voltage as the output and the applied voltage as the input.

Summing the voltages around the loop, assuming zero initial conditions, yields the integro-differential equation for this network as

$$L\frac{di(t)}{dt} + Ri(t) + \frac{1}{C}\int_0^t i(\tau)d\tau = v(t) \tag{2.61}$$

Changing variables from current to charge using $i(t) = dq(t)/dt$ yields

$$L\frac{d^2q(t)}{dt^2} + R\frac{dq(t)}{dt} + \frac{1}{C}q(t) = v(t) \tag{2.62}$$

From the voltage-charge relationship for a capacitor in Table 2.3,

$$q(t) = Cv_C(t) \tag{2.63}$$

Substituting Eq. (2.63) into Eq. (2.62) yields

$$LC\frac{d^2v_C(t)}{dt^2} + RC\frac{dv_C(t)}{dt} + v_C(t) = v(t) \tag{2.64}$$

---

[3] A particular loop that resembles the spaces in a screen or fence is called a *mesh*.

Taking the Laplace transform assuming zero initial conditions, rearranging terms, and simplifying yields

$$(LCs^2 + RCs + 1)V_C(s) = V(s) \qquad (2.65)$$

Solving for the transfer function, $V_C(s)/V(s)$, we obtain

$$\frac{V_C(s)}{V(s)} = \frac{1/LC}{s^2 + \dfrac{R}{L}s + \dfrac{1}{LC}} \qquad (2.66)$$

as shown in Figure 2.4.
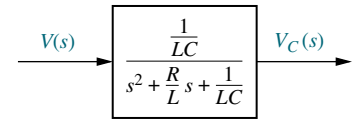
FIGURE 2.4 Block diagram of series RLC electrical network

Let us now develop a technique for simplifying the solution for future problems. First, take the Laplace transform of the equations in the voltage-current column of Table 2.3 assuming zero initial conditions.

For the capacitor,

$$V(s) = \frac{1}{Cs}I(s) \qquad (2.67)$$

For the resistor,

$$V(s) = RI(s) \qquad (2.68)$$

For the inductor,

$$V(s) = LsI(s) \qquad (2.69)$$

Now define the following transfer function:

$$\frac{V(s)}{I(s)} = Z(s) \qquad (2.70)$$

Notice that this function is similar to the definition of resistance, that is, the ratio of voltage to current. But, unlike resistance, this function is applicable to capacitors and inductors and carries information on the dynamic behavior of the component, since it represents an equivalent differential equation. We call this particular transfer function *impedance*. The impedance for each of the electrical elements is shown in Table 2.3.

Let us now demonstrate how the concept of impedance simplifies the solution for the transfer function. The Laplace transform of Eq. (2.61), assuming zero initial conditions, is

$$\left(Ls + R + \frac{1}{Cs}\right)I(s) = V(s) \qquad (2.71)$$

Notice that Eq. (2.71), which is in the form

[Sum of impedances]$I(s)$ = [Sum of applied voltages] (2.72)

suggests the series circuit shown in Figure 2.5. Also notice that the circuit of Figure 2.5 could have been obtained immediately from the circuit of Figure 2.3 simply by replacing each element with its impedance. We call this altered circuit the *transformed circuit*. Finally, notice that the transformed circuit leads immediately to Eq. (2.71) if we add impedances in series as we add resistors in series. Thus, rather than writing the differential equation first and then taking the
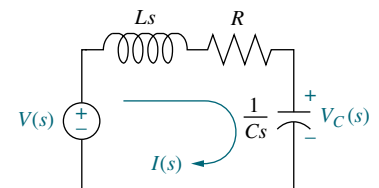
FIGURE 2.5 Laplace-transformed network

Laplace transform, we can draw the transformed circuit and obtain the Laplace transform of the differential equation simply by applying Kirchhoff's voltage law to the transformed circuit. We summarize the steps as follows:

1. Redraw the original network showing all time variables, such as $v(t)$, $i(t)$, and $v_C(t)$, as Laplace transforms $V(s)$, $I(s)$, and $V_C(s)$, respectively.

2. Replace the component values with their impedance values. This replacement is similar to the case of dc circuits, where we represent resistors with their resistance values.

We now redo Example 2.6 using the transform methods just described and bypass the writing of the differential equation.

Example 2.7

Transfer Function—Single Loop via Transform Methods

PROBLEM: Repeat Example 2.6 using mesh analysis and transform methods without writing a differential equation.

SOLUTION: Using Figure 2.5 and writing a mesh equation using the impedances as we would use resistor values in a purely resistive circuit, we obtain

$$\left(Ls + R + \frac{1}{Cs}\right)I(s) = V(s) \tag{2.73}$$

Solving for $I(s)/V(s)$,

$$\frac{I(s)}{V(s)} = \frac{1}{Ls + R + \dfrac{1}{Cs}} \tag{2.74}$$

But the voltage across the capacitor, $V_C(s)$, is the product of the current and the impedance of the capacitor. Thus,

$$V_C(s) = I(s)\frac{1}{Cs} \tag{2.75}$$

Solving Eq. (2.75) for $I(s)$, substituting $I(s)$ into Eq. (2.74), and simplifying yields the same result as Eq. (2.66).

Simple Circuits via Nodal Analysis

Transfer functions also can be obtained using Kirchhoff's current law and summing currents flowing from nodes. We call this method *nodal analysis*. We now demonstrate this principle by redoing Example 2.6 using Kirchhoff's current law and the transform methods just described to bypass writing the differential equation.

Example 2.8

Transfer Function—Single Node via Transform Methods

PROBLEM: Repeat Example 2.6 using nodal analysis and without writing a differential equation.

SOLUTION: The transfer function can be obtained by summing currents flowing out of the node whose voltage is $V_C(s)$ in Figure 2.5. We assume that currents leaving the node are positive and currents entering the node are negative. The currents consist of the current through the capacitor and the current flowing through the series resistor and inductor. From Eq. (2.70), each $I(s) = V(s)/Z(s)$. Hence,

$$\frac{V_C(s)}{I/Cs} + \frac{V_C(s) - V(s)}{R + Ls} = 0 \qquad (2.76)$$

where $V_C(s)/(1/Cs)$ is the current flowing out of the node through the capacitor, and $[V_C(s) - V(s)]/(R + Ls)$ is the current flowing out of the node through the series resistor and inductor. Solving Eq. (2.76) for the transfer function, $V_C(s)/V(s)$, we arrive at the same result as Eq. (2.66).

Simple Circuits via Voltage Division

Example 2.6 can be solved directly by using voltage division on the transformed network. We now demonstrate this technique.

Example 2.9

Transfer Function—Single Loop via Voltage Division

PROBLEM: Repeat Example 2.6 using voltage division and the transformed circuit.

SOLUTION: The voltage across the capacitor is some proportion of the input voltage, namely the impedance of the capacitor divided by the sum of the impedances. Thus,

$$V_C(s) = \frac{1/Cs}{\left(Ls + R + \dfrac{1}{Cs}\right)} V(s) \qquad (2.77)$$

Solving for the transfer function, $V_C(s)/V(s)$, yields the same result as Eq. (2.66).
      Review Examples 2.6 through 2.9. Which method do you think is easiest for this circuit?

The previous example involves a simple, single-loop electrical network. Many electrical networks consist of multiple loops and nodes, and for these circuits we must write and solve simultaneous differential equations in order to find the transfer function, or solve for the output.

Complex Circuits via Mesh Analysis

To solve complex electrical networks—those with multiple loops and nodes—using mesh analysis, we can perform the following steps:

1. Replace passive element values with their impedances.

2. Replace all sources and time variables with their Laplace transform.

3. Assume a transform current and a current direction in each mesh.

4. Write Kirchhoff's voltage law around each mesh.

5. Solve the simultaneous equations for the output.

6. Form the transfer function.

Let us look at an example.

Example 2.10

Transfer Function—Multiple Loops

PROBLEM: Given the network of Figure 2.6(a), find the transfer function, $I_2(s)/V(s)$.

SOLUTION: The first step in the solution is to convert the network into Laplace transforms for impedances and circuit variables, assuming zero initial conditions. The result is shown in Figure 2.6(b). The circuit with which we are dealing requires two simultaneous equations to solve for the transfer function. These equations can be found by summing voltages around each mesh through which the assumed currents, $I_1(s)$ and $I_2(s)$, flow. Around Mesh 1, where $I_1(s)$ flows,

$$R_1 I_1(s) + Ls I_1(s) - Ls I_2(s) = V(s) \tag{2.78}$$

Around Mesh 2, where $I_2(s)$ flows,

$$Ls I_2(s) + R_2 I_2(s) + \frac{1}{Cs} I_2(s) - Ls I_1(s) = 0 \tag{2.79}$$

(*a*)

(*b*)

(*c*)
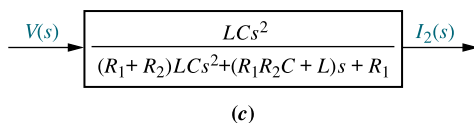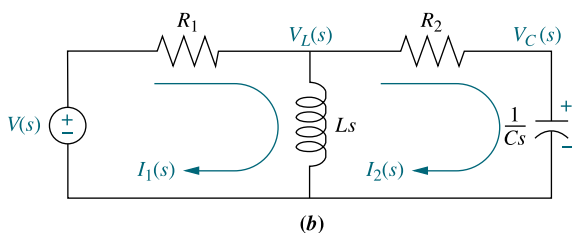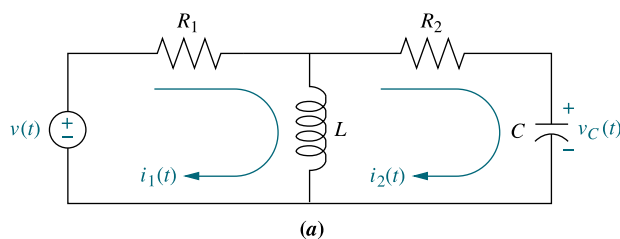
FIGURE 2.6   a. Two-loop electrical network; **b.** transformed two-loop electrical network; **c.** block diagram

Combining terms, Eqs. (2.78) and (2.79) become simultaneous equations in $I_1(s)$ and $I_2(s)$:

$$(R_1 + Ls)I_1(s) \qquad\qquad - LsI_2(s) = V(s) \qquad\qquad (2.80\text{a})$$

$$- LsI_1(s) + \left(Ls + R_2 + \frac{1}{Cs}\right)I_2(s) = 0 \qquad\qquad (2.80\text{b})$$

We can use Cramer's rule (or any other method for solving simultaneous equations) to solve Eq. (2.80) for $I_2(s)$.[4] Hence,

$$I_2(s) = \frac{\begin{vmatrix} (R_1 + Ls) & V(s) \\ -Ls & 0 \end{vmatrix}}{\Delta} = \frac{LsV(s)}{\Delta} \qquad\qquad (2.81)$$

where

$$\Delta = \begin{vmatrix} (R_1 + Ls) & -Ls \\ -Ls & \left(Ls + R_2 + \dfrac{1}{Cs}\right) \end{vmatrix}$$

Forming the transfer function, $G(s)$, yields

$$G(s) = \frac{I_2(s)}{V(s)} = \frac{Ls}{\Delta} = \frac{LCs^2}{(R_1 + R_2)LCs^2 + (R_1R_2C + L)s + R_1} \qquad (2.82)$$

as shown in Figure 2.6(c).

We have succeeded in modeling a physical network as a transfer function: The network of Figure 2.6(a) is now modeled as the transfer function of Figure 2.6(c). Before leaving the example, we notice a pattern first illustrated by Eq. (2.72). The form that Eq. (2.80) take is

$$\begin{bmatrix} \text{Sum of} \\ \text{impedances} \\ \text{around Mesh 1} \end{bmatrix} I_1(s) - \begin{bmatrix} \text{Sum of} \\ \text{impedances} \\ \text{common to the} \\ \text{two meshes} \end{bmatrix} I_2(s) = \begin{bmatrix} \text{Sum of applied} \\ \text{voltages around} \\ \text{Mesh 1} \end{bmatrix} \quad (2.83\text{a})$$

$$- \begin{bmatrix} \text{Sum of} \\ \text{impedances} \\ \text{common to the} \\ \text{two meshes} \end{bmatrix} I_1(s) + \begin{bmatrix} \text{Sum of} \\ \text{impedances} \\ \text{around Mesh 2} \end{bmatrix} I_2(s) = \begin{bmatrix} \text{Sum of applied} \\ \text{voltages around} \\ \text{Mesh 2} \end{bmatrix} \quad (2.83\text{b})$$

Recognizing the form will help us write such equations rapidly; for example, mechanical equations of motion (covered in Sections 2.5 and 2.6) have the same form.

Symbolic Math

SM

```
Students who are performing the MATLAB exercises and want to explore
the added capability of MATLAB's Symbolic Math Toolbox should now
run ch2sp4 in Appendix F at www.wiley.com/college/nise, where
Example 2.10 is solved. You will learn how to use the Symbolic
Math Toolbox to solve simultaneous equations using Cramer's
rule. Specifically, the Symbolic Math Toolbox will be used to solve
for the transfer function in Eq. (2.82) using Eq. (2.80).
```

---

[4] See Appendix G (Section G.4) at www.wiley.com/college/nise for Cramer's rule.

Complex Circuits via Nodal Analysis

Often, the easiest way to find the transfer function is to use nodal analysis rather than mesh analysis. The number of simultaneous differential equations that must be written is equal to the number of nodes whose voltage is unknown. In the previous example we wrote simultaneous mesh equations using Kirchhoff's voltage law. For multiple nodes we use Kirchhoff's current law and sum currents flowing from each node. Again, as a convention, currents flowing from the node are assumed to be positive, and currents flowing into the node are assumed to be negative.

Before progressing to an example, let us first define *admittance*, $Y(s)$, as the reciprocal of impedance, or

$$Y(s) = \frac{1}{Z(s)} = \frac{I(s)}{V(s)} \tag{2.84}$$

When writing nodal equations, it can be more convenient to represent circuit elements by their admittance. Admittances for the basic electrical components are shown in Table 2.3. Let us look at an example.

Example 2.11

Transfer Function—Multiple Nodes

PROBLEM: Find the transfer function, $V_C(s)/V(s)$, for the circuit in Figure 2.6(b). Use nodal analysis.

SOLUTION: For this problem, we sum currents at the nodes rather than sum voltages around the meshes. From Figure 2.6(b) the sum of currents flowing from the nodes marked $V_L(s)$ and $V_C(s)$ are, respectively,

$$\frac{V_L(s) - V(s)}{R_1} + \frac{V_L(s)}{Ls} + \frac{V_L(s) - V_C(s)}{R_2} = 0 \tag{2.85a}$$

$$CsV_C(s) + \frac{V_C(s) - V_L(s)}{R_2} = 0 \tag{2.85b}$$

Rearranging and expressing the resistances as conductances,[5] $G_1 = 1/R_1$ and $G_2 = 1/R_2$, we obtain,

$$\left(G_1 + G_2 + \frac{1}{Ls}\right)V_L(s) \qquad - G_2V_C(s) = V(s)G_1 \tag{2.86a}$$

$$-G_2V_L(s) + (G_2 + Cs)V_C(s) = 0 \tag{2.86b}$$

Solving for the transfer function, $V_C(s)/V(s)$, yields

$$\frac{V_C(s)}{V(s)} = \frac{\dfrac{G_1G_2}{C}s}{(G_1 + G_2)s^2 + \dfrac{G_1G_2L + C}{LC}s + \dfrac{G_2}{LC}} \tag{2.87}$$

as shown in Figure 2.7.

$$V(s) \longrightarrow \boxed{\dfrac{\dfrac{G_1G_2}{C}s}{(G_1+G_2)s^2 + \dfrac{G_1G_2L+C}{LC}s + \dfrac{G_2}{LC}}} \longrightarrow V_C(s)$$
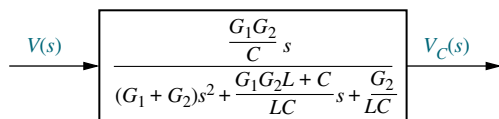
FIGURE 2.7   Block diagram of the network of Figure 2.6

---

[5] In general, admittance is complex. The real part is called conductance and the imaginary part is called susceptance. But when we take the reciprocal of resistance to obtain the admittance, a purely real quantity results. The reciprocal of resistance is called conductance.

Another way to write node equations is to replace voltage sources by current sources. A voltage source presents a constant voltage to any load; conversely, a current source delivers a constant current to any load. Practically, a current source can be constructed from a voltage source by placing a large resistance in series with the voltage source. Thus, variations in the load do not appreciably change the current, because the current is determined approximately by the large series resistor and the voltage source. Theoretically, we rely on *Norton's theorem*, which states that a voltage source, $V(s)$, in series with an impedance, $Z_s(s)$, can be replaced by a current source, $I(s) = V(s)/Z_s(s)$, in parallel with $Z_s(s)$.

In order to handle multiple-node electrical networks, we can perform the following steps:

1. Replace passive element values with their admittances.
2. Replace all sources and time variables with their Laplace transform.
3. Replace transformed voltage sources with transformed current sources.
4. Write Kirchhoff's current law at each node.
5. Solve the simultaneous equations for the output.
6. Form the transfer function.

Let us look at an example.

Example 2.12

Transfer Function—Multiple Nodes with Current Sources

PROBLEM: For the network of Figure 2.6, find the transfer function, $V_C(s)/V(s)$, using nodal analysis and a transformed circuit with current sources.

SOLUTION: Convert all impedances to admittances and all voltage sources in series with an impedance to current sources in parallel with an admittance using Norton's theorem.

Redrawing Figure 2.6(*b*) to reflect the changes, we obtain Figure 2.8, where $G_1 = 1/R_1$, $G_2 = 1/R_2$, and the node voltages—the voltages across the inductor and the capacitor—have been identified as $V_L(s)$ and $V_C(s)$, respectively. Using the general relationship, $I(s) = Y(s)V(s)$, and summing currents at the node $V_L(s)$,

FIGURE 2.8   Transformed network ready for nodal analysis

$$G_1 V_L(s) + \frac{1}{Ls} V_L(s) + G_2[V_L(s) - V_C(s)] = V(s)G_1 \qquad (2.88)$$

Summing the currents at the node $V_C(s)$ yields

$$Cs V_C(s) + G_2[V_C(s) - V_L(s)] = 0 \qquad (2.89)$$

Combining terms, Eqs. (2.88) and (2.89) become simultaneous equations in $V_C(s)$ and $V_L(s)$, which are identical to Eq. (2.86) and lead to the same solution as Eq. (2.87).

An advantage of drawing this circuit lies in the form of Eq. (2.86) and its direct relationship to Figure 2.8, namely

$$\begin{bmatrix} \text{Sum of admittances} \\ \text{connected to Node 1} \end{bmatrix} V_L(s) - \begin{bmatrix} \text{Sum of admittances} \\ \text{common to the two} \\ \text{nodes} \end{bmatrix} V_C(s) = \begin{bmatrix} \text{Sum of applied} \\ \text{currents at Node 1} \end{bmatrix}$$

$$(2.90a)$$

$$- \begin{bmatrix} \text{Sum of admittances} \\ \text{common to the two} \\ \text{nodes} \end{bmatrix} V_L(s) + \begin{bmatrix} \text{Sum of admittances} \\ \text{connected to Node 2} \end{bmatrix} V_C(s) = \begin{bmatrix} \text{Sum of applied} \\ \text{currents at Node 2} \end{bmatrix}$$

$$(2.90b)$$

A Problem-Solving Technique

In all of the previous examples, we have seen a repeating pattern in the equations that we can use to our advantage. If we recognize this pattern, we need not write the equations component by component; we can sum impedances around a mesh in the case of mesh equations or sum admittances at a node in the case of node equations. Let us now look at a three-loop electrical network and write the mesh equations by inspection to demonstrate the process.

Example 2.13

Mesh Equations via Inspection

PROBLEM: Write, but do not solve, the mesh equations for the network shown in Figure 2.9.
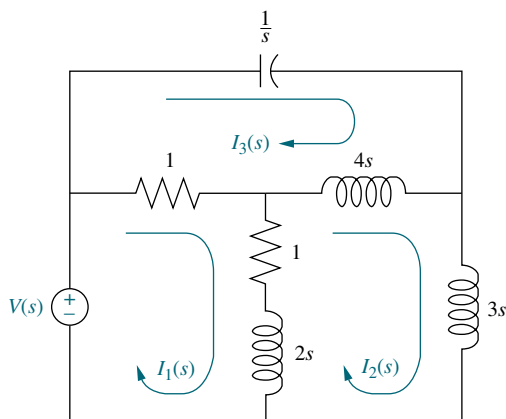
FIGURE 2.9   Three-loop electrical network

SOLUTION: Each of the previous problems has illustrated that the mesh equations and nodal equations have a predictable form. We use that knowledge to solve this three-loop problem. The equation for Mesh 1 will have the following form:

$$\left[\begin{array}{c} \text{Sum of} \\ \text{impedances} \\ \text{around Mesh 1} \end{array}\right] I_1(s) - \left[\begin{array}{c} \text{Sum of} \\ \text{impedances} \\ \text{common to} \\ \text{Mesh 1 and} \\ \text{Mesh 2} \end{array}\right] I_2(s)$$

$$- \left[\begin{array}{c} \text{Sum of} \\ \text{impedances} \\ \text{common to} \\ \text{Mesh 1 and} \\ \text{Mesh 3} \end{array}\right] I_3(s) = \left[\begin{array}{c} \text{Sum of applied} \\ \text{voltages around} \\ \text{Mesh 1} \end{array}\right] \qquad (2.91)$$

Similarly, Meshes 2 and 3, respectively, are

$$- \left[\begin{array}{c} \text{Sum of} \\ \text{impedances} \\ \text{common to} \\ \text{Mesh 1 and} \\ \text{Mesh 2} \end{array}\right] I_1(s) + \left[\begin{array}{c} \text{Sum of} \\ \text{impedances} \\ \text{around Mesh 2} \end{array}\right] I_2(s) - \left[\begin{array}{c} \text{Sum of} \\ \text{impedances} \\ \text{common to} \\ \text{Mesh 2 and} \\ \text{Mesh 3} \end{array}\right] I_3(s) = \left[\begin{array}{c} \text{Sum of appied} \\ \text{voltages around} \\ \text{Mesh 2} \end{array}\right]$$

$$(2.92)$$

and

$$- \left[\begin{array}{c} \text{Sum of} \\ \text{impedances} \\ \text{common to} \\ \text{Mesh 1 and} \\ \text{Mesh 3} \end{array}\right] I_1(s) - \left[\begin{array}{c} \text{Sum of} \\ \text{impedances} \\ \text{common to} \\ \text{Mesh 2 and} \\ \text{Mesh 3} \end{array}\right] I_2(s)$$

$$+ \left[\begin{array}{c} \text{Sum of} \\ \text{impedances} \\ \text{around Mesh 3} \end{array}\right] I_3(s) = \left[\begin{array}{c} \text{Sum of applied} \\ \text{voltages around} \\ \text{Mesh 3} \end{array}\right] \qquad (2.93)$$

Substituting the values from Figure 2.9 into Eqs. (2.91) through (2.93) yields

$$+(2s+2)I_1(s) - (2s+1)I_2(s) \qquad\qquad - I_3(s) = V(s) \qquad (2.94\text{a})$$

$$-(2s+1)I_1(s) + (9s+1)I_2(s) \qquad\qquad - 4sI_3(s) = 0 \qquad (2.94\text{b})$$

$$-I_1(s) \qquad - 4sI_2(s) + \left(4s+1+\tfrac{1}{s}\right)I_3(s) = 0 \qquad (2.94\text{c})$$

which can be solved simultaneously for any desired transfer function, for example, $I_3(s)/V(s)$.

TryIt 2.8

Use the following MATLAB and Symbolic Math Toolbox statements to help you solve for the electrical currents in Eq. (2.94).

```
syms s I1 I2 I3 V
A =[(2*s + 2)  -(2*s + 1)...
   -1
   -(2*s + 1)  (9*s + 1)...
   -4*s
   -1 -4*s...
   (4*s + 1 + 1/s)];
B =[I1;I2;I3];
C =[V;0;0];
B = inv(A)*C;
pretty(B)
```
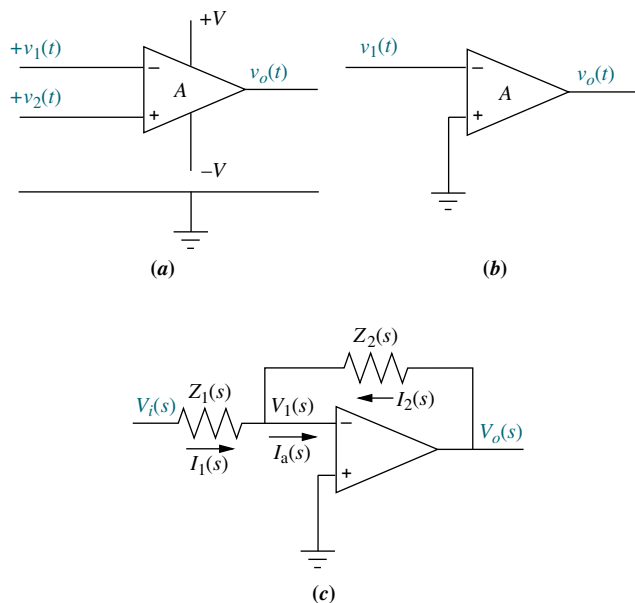
FIGURE 2.10   **a.** Operational amplifier; **b.** schematic for an inverting operational amplifier; **c.** inverting operational amplifier configured for transfer function realization. Typically, the amplifier gain, A, is omitted.

Passive electrical circuits were the topic of discussion up to this point. We now discuss a class of active circuits that can be used to implement transfer functions. These are circuits built around an operational amplifier.

Operational Amplifiers

An *operational amplifier*, pictured in Figure 2.10(a), is an electronic amplifier used as a basic building block to implement transfer functions. It has the following characteristics:

1. Differential input, $V_2(t) - v_1(t)$

2. High input impedance, $Z_i = \infty$ (ideal)

3. Low output impedance, $Z_o = 0$ (ideal)

4. High constant gain amplification, $A = \infty$ (ideal)

The output, $v_o(t)$, is given by

$$v_o(t) = A(v_2(t) - v_1(t)) \tag{2.95}$$

Inverting Operational Amplifier

If $v_2(t)$ is grounded, the amplifier is called an *inverting operational amplifier*, as shown in Figure 2.10(b). For the inverting operational amplifier, we have

$$v_o(t) = -Av_1(t) \tag{2.96}$$

If two impedances are connected to the inverting operational amplifier as shown in Figure 2.10(c), we can derive an interesting result if the amplifier has the characteristics mentioned in the beginning of this subsection. If the input impedance to the amplifier is high, then by Kirchhoff's current law, $I_a(s) = 0$ and $I_1(s) = -I_2(s)$.

Also, since the gain A is large, $v_1(t) \approx 0$. Thus, $I_1(s) = V_i(s)/Z_1(s)$, and $-I_2(s) = -V_o(s)/Z_2(s)$. Equating the two currents, $V_o(s)/Z_2(s) = -V_i(s)/Z_1(s)$, or the transfer function of the inverting operational amplifier configured as shown in Figure 2.10(c) is

$$\boxed{\frac{V_o(s)}{V_i(s)} = -\frac{Z_2(s)}{Z_1(s)}} \qquad (2.97)$$

Example 2.14

Transfer Function—Inverting Operational Amplifier Circuit

PROBLEM: Find the transfer function, $V_o(s)/V_i(s)$, for the circuit given in Figure 2.11.
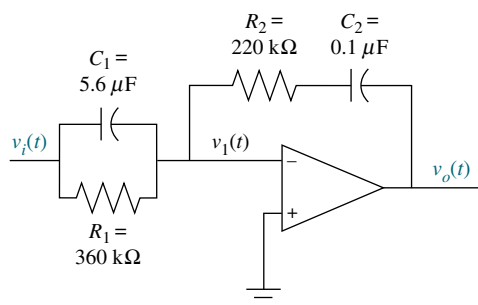
FIGURE 2.11 Inverting operational amplifier circuit for Example 2.14

SOLUTION: The transfer function of the operational amplifier circuit is given by Eq. (2.97). Since the admittances of parallel components add, $Z_1(s)$ is the reciprocal of the sum of the admittances, or

$$Z_1(s) = \frac{1}{C_1 s + \dfrac{1}{R_1}} = \frac{1}{5.6 \times 10^{-6} s + \dfrac{1}{360 \times 10^3}} = \frac{360 \times 10^3}{2.016 s + 1} \qquad (2.98)$$

For $Z_2(s)$ the impedances add, or

$$Z_2(s) = R_2 + \frac{1}{C_2 s} = 220 \times 10^3 + \frac{10^7}{s} \qquad (2.99)$$

Substituting Eqs. (2.98) and (2.99) into Eq. (2.97) and simplifying, we get

$$\frac{V_o(s)}{V_i(s)} = -1.232 \frac{s^2 + 45.95 s + 22.55}{s} \qquad (2.100)$$

The resulting circuit is called a PID controller and can be used to improve the performance of a control system. We explore this possibility further in Chapter 9.

Noninverting Operational Amplifier

Another circuit that can be analyzed for its transfer function is the noninverting operational amplifier circuit shown in Figure 2.12. We now derive the transfer
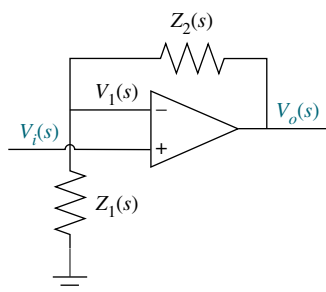
FIGURE 2.12 General noninverting operational amplifier circuit

function. We see that

$$V_o(s) = A(V_i(s) - V_1(s)) \tag{2.101}$$

But, using voltage division,

$$V_1(s) = \frac{Z_1(s)}{Z_1(s) + Z_2(s)} V_o(s) \tag{2.102}$$

Substituting Eq. (2.102) into Eq. (2.101), rearranging, and simplifying, we obtain

$$\frac{V_o(s)}{V_i(s)} = \frac{A}{1 + AZ_1(s)/(Z_1(s) + Z_2(s))} \tag{2.103}$$

For large A, we disregard unity in the denominator and Eq. (2.103) becomes

$$\boxed{\frac{V_o(s)}{V_i(s)} = \frac{Z_1(s) + Z_2(s)}{Z_1(s)}} \tag{2.104}$$

Let us now look at an example.

Example 2.15

Transfer Function—Noninverting Operational Amplifier Circuit
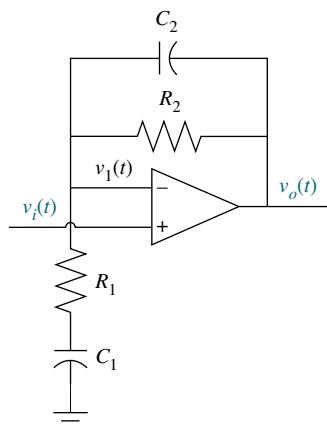
FIGURE 2.13 Noninverting operational amplifier circuit for Example 2.15

PROBLEM: Find the transfer function, $V_o(s)/V_i(s)$, for the circuit given in Figure 2.13.

SOLUTION: We find each of the impedance functions, $Z_1(s)$ and $Z_2(s)$, and then substitute them into Eq. (2.104). Thus,

$$Z_1(s) = R_1 + \frac{1}{C_1 s} \tag{2.105}$$

and

$$Z_2(s) = \frac{R_2(1/C_2 s)}{R_2 + (1/C_2 s)} \tag{2.106}$$

Substituting Eqs. (2.105) and (2.106) into Eq. (2.104) yields

$$\frac{V_o(s)}{V_i(s)} = \frac{C_2 C_1 R_2 R_1 s^2 + (C_2 R_2 + C_1 R_2 + C_1 R_1)s + 1}{C_2 C_1 R_2 R_1 s^2 + (C_2 R_2 + C_1 R_1)s + 1} \tag{2.107}$$

Skill-Assessment Exercise 2.6

PROBLEM: Find the transfer function, $G(s) = V_L(s)/V(s)$, for the circuit given in Figure 2.14. Solve the problem two ways—mesh analysis and nodal analysis. Show that the two methods yield the same result.
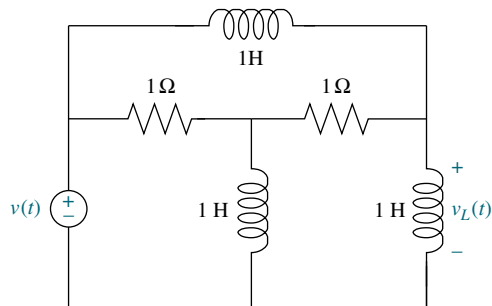
FIGURE 2.14   Electric circuit for Skill-Assessment Exercise 2.6

ANSWER: $V_L(s)/V(s) = (s^2 + 2s + 1)/(s^2 + 5s + 2)$

The complete solution is at www.wiley.com/college/nise.

Skill-Assessment Exercise 2.7

PROBLEM: If $Z_1(s)$ is the impedance of a 10 μF capacitor and $Z_2(s)$ is the impedance of a 100 kΩ resistor, find the transfer function, $G(s) = V_o(s)/V_i(s)$, if these components are used with (a) an inverting operational amplifier and (b) a noninverting amplifier as shown in Figures 2.10(c) and 2.12, respectively.

ANSWER: $G(s) = -s$ for an inverting operational amplifier; $G(s) = s + 1$ for a noninverting operational amplifier.

The complete solution is at www.wiley.com/college/nise.

WileyPLUS

WPCS

Control Solutions
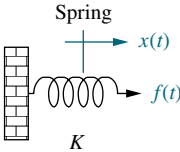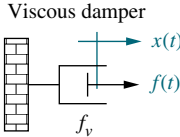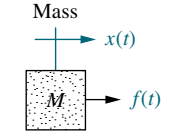
    In this section, we found transfer functions for multiple-loop and multiple-node electrical networks, as well as operational amplifier circuits. We developed mesh and nodal equations, noted their form, and wrote them by inspection. In the next section we begin our work with mechanical systems. We will see that many of the concepts applied to electrical networks can also be applied to mechanical systems via analogies—from basic concepts to writing the describing equations by inspection. This revelation will give you the confidence to move beyond this textbook and study systems not covered here, such as hydraulic or pneumatic systems.

2.5   Translational Mechanical System Transfer Functions

We have shown that electrical networks can be modeled by a transfer function, $G(s)$, that algebraically relates the Laplace transform of the output to the Laplace transform of the input. Now we will do the same for mechanical systems. In this section we concentrate on translational mechanical systems. In the next section we extend the concepts to rotational mechanical systems. Notice that the end product, shown in Figure 2.2, will be mathematically indistinguishable from an electrical network. Hence, an electrical network can be interfaced to a mechanical system by cascading their transfer functions, provided that one system is not loaded by the other.[6]

---

[6] The concept of loading is explained further in Chapter 5.

TABLE 2.4　Force-velocity, force-displacement, and impedance translational relationships for springs, viscous dampers, and mass

Component	Force-velocity	Force-displacement	Impedence $Z_M(s) = F(s)/X(s)$
Spring K	$f(t) = K \int_0^t v(\tau)d\tau$	$f(t) = Kx(t)$	K
Viscous damper f_v	$f(t) = f_v v(t)$	$f(t) = f_v \dfrac{dx(t)}{dt}$	$f_v s$
Mass M	$f(t) = M \dfrac{dv(t)}{dt}$	$f(t) = M \dfrac{d^2 x(t)}{dt^2}$	Ms^2

Note: The following set of symbols and units is used throughout this book: $f(t)$ = N (newtons), $x(t)$ = m (meters), $v(t)$ = m/s (meters/second), K = N/m (newtons/meter), f_v = N-s/m(newton-seconds/meter), M = kg (kilograms = newton-seconds^2/meter).

Mechanical systems parallel electrical networks to such an extent that there are analogies between electrical and mechanical components and variables. Mechanical systems, like electrical networks, have three passive, linear components. Two of them, the spring and the mass, are energy-storage elements; one of them, the viscous damper, dissipates energy. The two energy-storage elements are analogous to the two electrical energy-storage elements, the inductor and capacitor. The energy dissipator is analogous to electrical resistance. Let us take a look at these mechanical elements, which are shown in Table 2.4. In the table, K, f_v, and M are called *spring constant*, *coefficient of viscous friction*, and *mass*, respectively.

We now create analogies between electrical and mechanical systems by comparing Tables 2.3 and 2.4. Comparing the force-velocity column of Table 2.4 to the voltage-current column of Table 2.3, we see that mechanical force is analogous to electrical voltage and mechanical velocity is analogous to electrical current. Comparing the force-displacement column of Table 2.4 with the voltage-charge column of Table 2.3 leads to the analogy between the mechanical displacement and electrical charge. We also see that the spring is analogous to the capacitor, the viscous damper is analogous to the resistor, and the mass is analogous to the inductor. Thus, summing forces written in terms of velocity is analogous to summing voltages written in terms of current, and the resulting mechanical differential equations are analogous to mesh equations. If the forces are written in terms of displacement, the resulting mechanical equations resemble, but are not analogous to, the mesh equations. We, however, will use this model for mechanical systems so that we can write equations directly in terms of displacement.

Another analogy can be drawn by comparing the force-velocity column of Table 2.4 to the current-voltage column of Table 2.3 in reverse order. Here the analogy is between force and current and between velocity and voltage. Also, the

spring is analogous to the inductor, the viscous damper is analogous to the resistor, and the mass is analogous to the capacitor. Thus, summing forces written in terms of velocity is analogous to summing currents written in terms of voltage and the resulting mechanical differential equations are analogous to nodal equations. We will discuss these analogies in more detail in Section 2.9.

We are now ready to find transfer functions for translational mechanical systems. Our first example, shown in Figure 2.15(a), is similar to the simple *RLC* network of Example 2.6 (see Figure 2.3). The mechanical system requires just one differential equation, called the *equation of motion*, to describe it. We will begin by assuming a positive direction of motion, for example, to the right. This assumed positive direction of motion is similar to assuming a current direction in an electrical loop. Using our assumed direction of positive motion, we first draw a free-body diagram, placing on the body all forces that act on the body either in the direction of motion or opposite to it. Next we use Newton's law to form a differential equation of motion by summing the forces and setting the sum equal to zero. Finally, assuming zero initial conditions, we take the Laplace transform of the differential equation, separate the variables, and arrive at the transfer function. An example follows.

Example 2.16

Transfer Function—One Equation of Motion
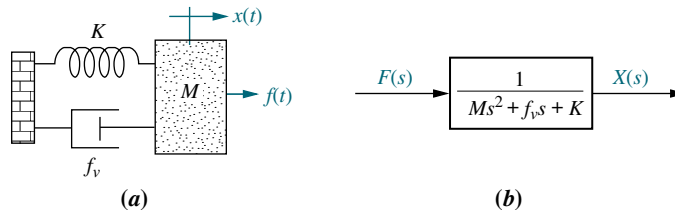
FIGURE 2.15   a. Mass, spring, and damper system; **b.** block diagram

PROBLEM: Find the transfer function, $X(s)/F(s)$, for the system of Figure 2.15(a).

SOLUTION: Begin the solution by drawing the free-body diagram shown in Figure 2.16(a). Place on the mass all forces felt by the mass. We assume the mass is traveling toward the right. Thus, only the applied force points to the right; all other forces impede the motion and act to oppose it. Hence, the spring, viscous damper, and the force due to acceleration point to the left.

We now write the differential equation of motion using Newton's law to sum to zero all of the forces shown on the mass in Figure 2.16(a):

$$M\frac{d^2x(t)}{dt^2} + f_v\frac{dx(t)}{dt} + Kx(t) = f(t) \tag{2.108}$$
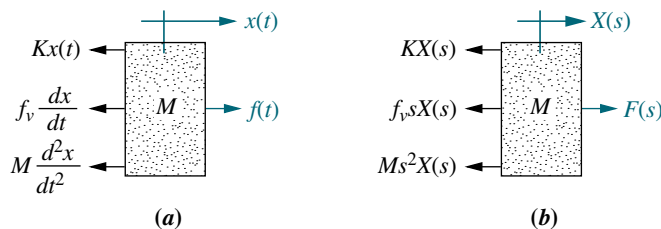
FIGURE 2.16   a. Free-body diagram of mass, spring, and damper system; **b.** transformed free-body diagram

Taking the Laplace transform, assuming zero initial conditions,

$$Ms^2X(s) + f_vsX(s) + KX(s) = F(s) \tag{2.109}$$

or

$$(Ms^2 + f_vs + K)X(s) = F(s) \tag{2.110}$$

Solving for the transfer function yields

$$G(s) = \frac{X(s)}{F(s)} = \frac{1}{Ms^2 + f_vs + K} \tag{2.111}$$

which is represented in Figure 2.15(b).

Now can we parallel our work with electrical networks by circumventing the writing of differential equations and by defining impedances for mechanical components? If so, we can apply to mechanical systems the problem-solving techniques learned in the previous section. Taking the Laplace transform of the force-displacement column in Table 2.4, we obtain for the spring,

$$F(s) = KX(s) \tag{2.112}$$

for the viscous damper,

$$F(s) = f_vsX(s) \tag{2.113}$$

and for the mass,

$$F(s) = Ms^2X(s) \tag{2.114}$$

If we define impedance for mechanical components as

$$Z_M(s) = \frac{F(s)}{X(s)} \tag{2.115}$$

and apply the definition to Eqs. (2.112) through (2.114), we arrive at the impedances of each component as summarized in Table 2.4 (*Raven, 1995*).[7]

Replacing each force in Figure 2.16(a) by its Laplace transform, which is in the format

$$F(s) = Z_M(s)X(s) \tag{2.116}$$

we obtain Figure 2.16(b), from which we could have obtained Eq. (2.109) immediately without writing the differential equation. From now on we use this approach.

---

[7] Notice that the impedance column of Table 2.4 is not a direct analogy to the impedance column of Table 2.3, since the denominator of Eq. (2.115) is displacement. A direct analogy could be derived by defining mechanical impedance in terms of velocity as $F(s)/V(s)$. We chose Eq. (2.115) as a convenient definition for writing the equations of motion in terms of displacement, rather than velocity. The alternative, however, is available.

Finally, notice that Eq. (2.110) is of the form

$$[\text{Sum of impedances}]X(s) = [\text{Sum of applied forces}] \qquad (2.117)$$

which is similar, but not analogous, to a mesh equation (see footnote 7).

Many mechanical systems are similar to multiple-loop and multiple-node electrical networks, where more than one simultaneous differential equation is required to describe the system. In mechanical systems, the number of equations of motion required is equal to the number of *linearly independent* motions. Linear independence implies that a point of motion in a system can still move if all other points of motion are held still. Another name for the number of linearly independent motions is the number of *degrees of freedom.* This discussion is not meant to imply that these motions are not coupled to one another; in general, they are. For example, in a two-loop electrical network, each loop current depends on the other loop current, but if we open-circuit just one of the loops, the other current can still exist if there is a voltage source in that loop. Similarly, in a mechanical system with two degrees of freedom, one point of motion can be held still while the other point of motion moves under the influence of an applied force.

In order to work such a problem, we draw the free-body diagram for each point of motion and then use superposition. For each free-body diagram we begin by holding all other points of motion still and finding the forces acting on the body due only to its own motion. Then we hold the body still and activate the other points of motion one at a time, placing on the original body the forces created by the adjacent motion.

Using Newton's law, we sum the forces on each body and set the sum to zero. The result is a system of simultaneous equations of motion. As Laplace transforms, these equations are then solved for the output variable of interest in terms of the input variable from which the transfer function is evaluated. Example 2.17 demonstrates this problem-solving technique.

Example 2.17

Transfer Function—Two Degrees of Freedom

PROBLEM: Find the transfer function, $X_2(s)/F(s)$, for the system of Figure 2.17(a).

(a)

(b)
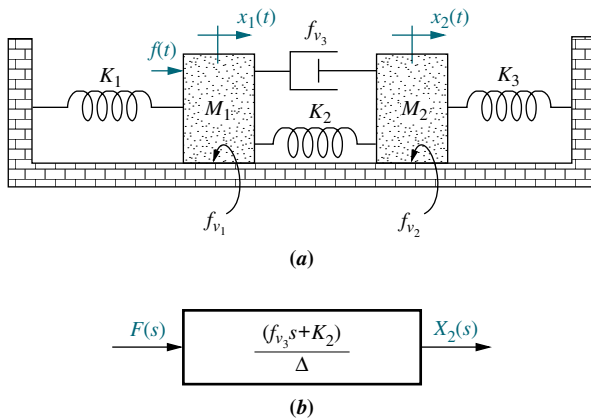
FIGURE 2.17   a. Two-degrees-of-freedom translational mechanical system;[8] **b.** block diagram

Virtual Experiment 2.1 Automobile Suspension

Put theory into practice exploring the dynamics of another two degree of freedom system—an automobile suspension system driving over a bumpy road demonstrated with the Quanser Active Suspension System modeled in LabVIEW.

Virtual experiments are found on WileyPLUS.

---

[8] Friction shown here and throughout the book, unless otherwise indicated, is viscous friction. Thus, f_{v1} and f_{v2} are not Coulomb friction, but arise because of a viscous interface.

SOLUTION: The system has two degrees of freedom, since each mass can be moved in the horizontal direction while the other is held still. Thus, two simultaneous equations of motion will be required to describe the system. The two equations come from free-body diagrams of each mass. Superposition is used to draw the free-body diagrams. For example, the forces on M_1 are due to (1) its own motion and (2) the motion of M_2 transmitted to M_1 through the system. We will consider these two sources separately.

If we hold M_2 still and move M_1 to the right, we see the forces shown in Figure 2.18(a). If we hold M_1 still and move M_2 to the right, we see the forces shown in Figure 2.18(b). The total force on M_1 is the superposition, or sum, of the forces just discussed. This result is shown in Figure 2.18(c). For M_2, we proceed in a similar fashion: First we move M_2 to the right while holding M_1 still; then we move M_1 to the right and hold M_2 still. For each case we evaluate the forces on M_2. The results appear in Figure 2.19.
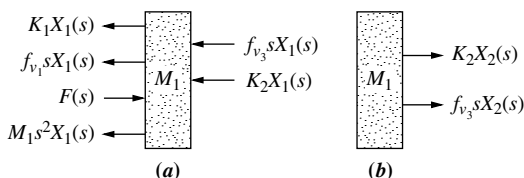
FIGURE 2.18   a. Forces on M_1 due only to motion of M_1; **b.** forces on M_1 due only to motion of M_2; **c.** all forces on M_1
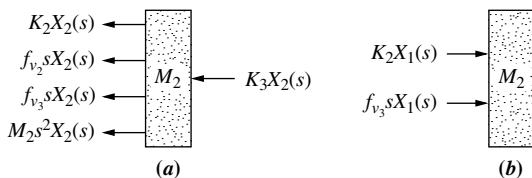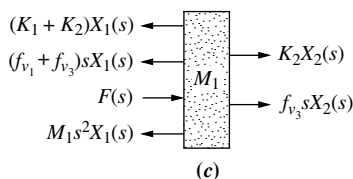
FIGURE 2.19   a. Forces on M_2 due only to motion of M_2; **b.** forces on M_2 due only to motion of M_1; **c.** all forces on M_2
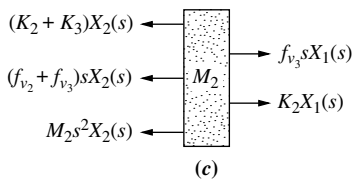
The Laplace transform of the equations of motion can now be written from Figures 2.18(c) and 2.19(c) as

$$\left[M_1 s^2 (f_{v_1} + f_{v_3})s + (K_1 + K_2)\right] X_1(s) - (f_{v_3}s + K_2)X_2(s) = F(s) \qquad (2.118\text{a})$$

$$-(f_{v_3}s + K_2)X_1(s) + \left[M_2 s^2 + (f_{v_2} + f_{v_3})s + (K_2 + K_3)\right] X_2(s) = 0 \qquad (2.118\text{b})$$

From this, the transfer function, $X_2(s)/F(s)$, is

$$\frac{X_2(s)}{F(s)} = G(s) = \frac{(f_{v_3}s + K_2)}{\Delta} \tag{2.119}$$

as shown in Figure 2.17(b) where

$$\Delta = \begin{vmatrix} \left[M_1 s^2 + (f_{v_1} + f_{v_3})s + (K_1 + K_2)\right] & -(f_{v_3}s + K_2) \\ -(f_{v_3}s + K_2) & \left[M_2 s^2 + (f_{v_2} + f_{v_3})s + (K_2 + K_3)\right] \end{vmatrix}$$

Notice again, in Eq. (2.118), that the form of the equations is similar to electrical mesh equations:

$$\begin{bmatrix} \text{Sum of} \\ \text{impedances} \\ \text{connected} \\ \text{to the motion} \\ \text{at } x_1 \end{bmatrix} X_1(s) - \begin{bmatrix} \text{Sum of} \\ \text{impedances} \\ \text{between} \\ x_1 \text{ and } x_2 \end{bmatrix} X_2(s) = \begin{bmatrix} \text{Sum of} \\ \text{applied forces} \\ \text{at } x_1 \end{bmatrix} \tag{2.120a}$$

$$-\begin{bmatrix} \text{Sum of} \\ \text{impedances} \\ \text{between} \\ x_1 \text{ and } x_2 \end{bmatrix} X_1(s) + \begin{bmatrix} \text{Sum of} \\ \text{impedances} \\ \text{connected} \\ \text{to the motion} \\ \text{at } x_2 \end{bmatrix} X_2(s) = \begin{bmatrix} \text{Sum of} \\ \text{applied forces} \\ \text{at } x_2 \end{bmatrix} \tag{2.120b}$$

The pattern shown in Eq. (2.120) should now be familiar to us. Let us use the concept to write the equations of motion of a three-degrees-of-freedom mechanical network by inspection, without drawing the free-body diagram.

Example 2.18

Equations of Motion by Inspection

PROBLEM: Write, but do not solve, the equations of motion for the mechanical network of Figure 2.20.
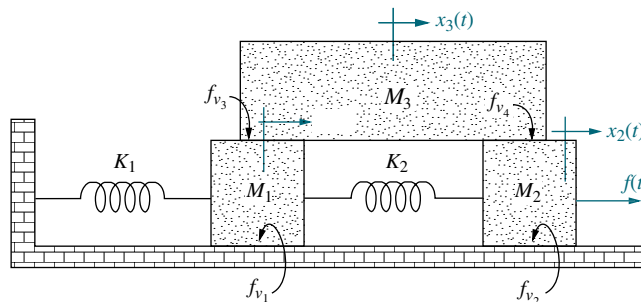
FIGURE 2.20   Three-degrees-of-freedom translational mechanical system

SOLUTION: The system has three degrees of freedom, since each of the three masses can be moved independently while the others are held still. The form of the equations will be similar to electrical mesh equations. For M_1,

$$\begin{bmatrix} \text{Sum of} \\ \text{impedances} \\ \text{connected} \\ \text{to the motion} \\ \text{at } x_1 \end{bmatrix} X_1(s) - \begin{bmatrix} \text{Sum of} \\ \text{impedances} \\ \text{between} \\ x_1 \text{ and } x_2 \end{bmatrix} X_2(s)$$

$$- \begin{bmatrix} \text{Sum of} \\ \text{impedances} \\ \text{between} \\ x_1 \text{ and } x_3 \end{bmatrix} X_3(s) = \begin{bmatrix} \text{Sum of} \\ \text{applied forces} \\ \text{at } x_1 \end{bmatrix} \tag{2.121}$$

Similarly, for M_2 and M_3, respectively,

$$- \begin{bmatrix} \text{Sum of} \\ \text{impedances} \\ \text{between} \\ x_1 \text{ and } x_2 \end{bmatrix} X_1(s) + \begin{bmatrix} \text{Sum of} \\ \text{impedances} \\ \text{connected} \\ \text{to the motion} \\ \text{at } x_2 \end{bmatrix} X_2(s)$$

$$- \begin{bmatrix} \text{Sum of} \\ \text{impedances} \\ \text{between} \\ x_2 \text{ and } x_3 \end{bmatrix} X_3(s) = \begin{bmatrix} \text{Sum of} \\ \text{applied forces} \\ \text{at } x_2 \end{bmatrix} \tag{2.122}$$

$$- \begin{bmatrix} \text{Sum of} \\ \text{impedances} \\ \text{between} \\ x_1 \text{ and } x_3 \end{bmatrix} X_1(s) - \begin{bmatrix} \text{Sum of} \\ \text{impedances} \\ \text{between} \\ x_2 \text{ and } x_3 \end{bmatrix} X_2(s)$$

$$+ \begin{bmatrix} \text{Sum of} \\ \text{impedances} \\ \text{connected} \\ \text{to the motion} \\ \text{at } x_3 \end{bmatrix} X_3(s) = \begin{bmatrix} \text{Sum of} \\ \text{applied forces} \\ \text{at } x_3 \end{bmatrix} \tag{2.123}$$

M_1 has two springs, two viscous dampers, and mass associated with its motion. There is one spring between M_1 and M_2 and one viscous damper between M_1 and M_3. Thus, using Eq. (2.121),

$$[M_1 s^2 + (f_{v_1} + f_{v_3})s + (K_1 + K_2)]X_1(s) - K_2 X_2(s) - f_{v_3} s X_3(s) = 0 \tag{2.124}$$

Similarly, using Eq. (2.122) for M_2,

$$-K_2 X_1(s) + [M_2 s^2 + (f_{v_2} + f_{v_4})s + K_2]X_2(s) - f_{v_4} s X_3(s) = F(s) \tag{2.125}$$

and using Eq. (2.123) for M_3,

$$-f_{v_3}sX_1(s) - f_{v_4}sX_2(s) + \left[M_3s^2 + (f_{v_3} + f_{v_4})s\right]X_3(s) = 0 \qquad (2.126)$$

Equations (2.124) through (2.126) are the equations of motion. We can solve them for any displacement, $X_1(s)$, $X_2(s)$, or $X_3(s)$, or transfer function.

Skill-Assessment Exercise 2.8

PROBLEM: Find the transfer function, $G(s) = X_2(s)/F(s)$, for the translational mechanical system shown in Figure 2.21.
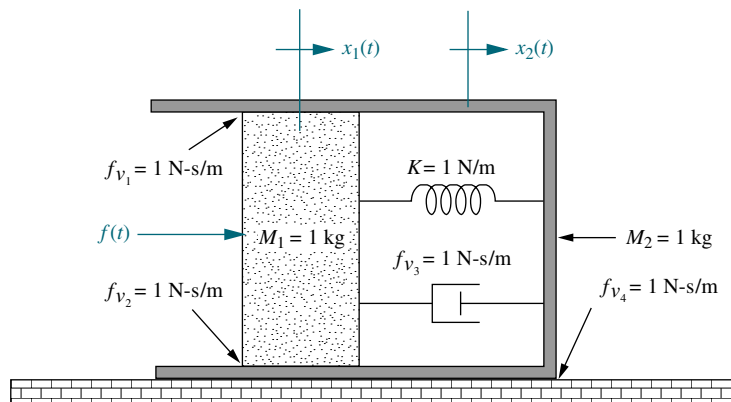
FIGURE 2.21   Translational mechanical system for Skill-Assessment Exercise 2.8

ANSWER: $G(s) = \dfrac{3s + 1}{s(s^3 + 7s^2 + 5s + 1)}$

The complete solution is at www.wiley.com/college/nise.

2.6   Rotational Mechanical System Transfer Functions

Having covered electrical and translational mechanical systems, we now move on to consider rotational mechanical systems. Rotational mechanical systems are handled the same way as translational mechanical systems, except that torque replaces force and angular displacement replaces translational displacement. The mechanical components for rotational systems are the same as those for translational systems, except that the components undergo rotation instead of translation. Table 2.5 shows the components along with the relationships between torque and angular velocity, as well as angular displacement. Notice that the symbols for the

TABLE 2.5 Torque-angular velocity, torque-angular displacement, and impedance rotational relationships for springs, viscous dampers, and inertia

Component	Torque-angular velocity	Torque-angular displacement	Impedence $Z_M(s) = T(s)/\theta(s)$
Spring K	$T(t) = K \int_0^t \omega(\tau)d\tau$	$T(t) = K\theta(t)$	K
Viscous damper D	$T(t) = D\omega(t)$	$T(t) = D\dfrac{d\theta(t)}{dt}$	Ds
Inertia J	$T(t) = J\dfrac{d\omega(t)}{dt}$	$T(t) = J\dfrac{d^2\theta(t)}{dt^2}$	Js^2

Note: The following set of symbols and units is used throughout this book: $T(t)$ – N-m (newton-meters), $\theta(t)$ – rad(radians), $\omega(t)$ – rad/s(radians/second), K – N-m/rad(newton- meters/radian), D – N-m-s/rad (newton- meters-seconds/radian). J – kg-m^2(kilograms-meters^2 – newton-meters-seconds^2/radian).

components look the same as translational symbols, but they are undergoing rotation and not translation.

Also notice that the term associated with the mass is replaced by inertia. The values of K, D, and J are called *spring constant*, *coefficient of viscous friction*, and *moment of inertia*, respectively. The impedances of the mechanical components are also summarized in the last column of Table 2.5. The values can be found by taking the Laplace transform, assuming zero initial conditions, of the torque-angular displacement column of Table 2.5.

The concept of degrees of freedom carries over to rotational systems, except that we test a point of motion by *rotating* it while holding still all other points of motion. The number of points of motion that can be rotated while all others are held still equals the number of equations of motion required to describe the system.

Writing the equations of motion for rotational systems is similar to writing them for translational systems; the only difference is that the free-body diagram consists of torques rather than forces. We obtain these torques using superposition. First, we rotate a body while holding all other points still and place on its free-body diagram all torques due to the body's own motion. Then, holding the body still, we rotate adjacent points of motion one at a time and add the torques due to the adjacent motion to the free-body diagram. The process is repeated for each point of motion. For each free-body diagram, these torques are summed and set equal to zero to form the equations of motion.

Two examples will demonstrate the solution of rotational systems. The first one uses free-body diagrams; the second uses the concept of impedances to write the equations of motion by inspection.

Example 2.19

Transfer Function—Two Equations of Motion

PROBLEM: Find the transfer function, $\theta_2(s)/T(s)$, for the rotational system shown in Figure 2.22(a). The rod is supported by bearings at either end and is undergoing torsion. A torque is applied at the left, and the displacement is measured at the right.

FIGURE 2.22 **a.** Physical system; **b.** schematic; **c.** block diagram

SOLUTION: First, obtain the schematic from the physical system. Even though torsion occurs throughout the rod in Figure 2.22(a),[9] we approximate the system by assuming that the torsion acts like a spring concentrated at one particular point in the rod, with an inertia J_1 to the left and an inertia J_2 to the right.[10] We also assume that the damping inside the flexible shaft is negligible. The schematic is shown in Figure 2.22(b). There are two degrees of freedom, since each inertia can be rotated while the other is held still. Hence, it will take two simultaneous equations to solve the system.

Next, draw a free-body diagram of J_1, using superposition. Figure 2.23(a) shows the torques on J_1 if J_2 is held still and J_1 rotated. Figure 2.23(b) shows the torques on J_1 if J_1 is held still and J_2 rotated. Finally, the sum of Figures 2.23(a) and 2.23(b) is shown in Figure 2.23(c), the final free-body diagram for J_1. The same process is repeated in Figure 2.24 for J_2.

FIGURE 2.23 **a.** Torques on J_1 due only to the motion of J_1; **b.** torques on J_1 due only to the motion of J_2; **c.** final free-body diagram for J_1

---

[9] In this case the parameter is referred to as a *distributed* parameter.

[10] The parameter is now referred to as a *lumped* parameter.

FIGURE 2.24   a. Torques on J_2 due only to the motion of J_2; **b.** torques on J_2 due only to the motion of J_1; **c.** final free-body diagram for J_2
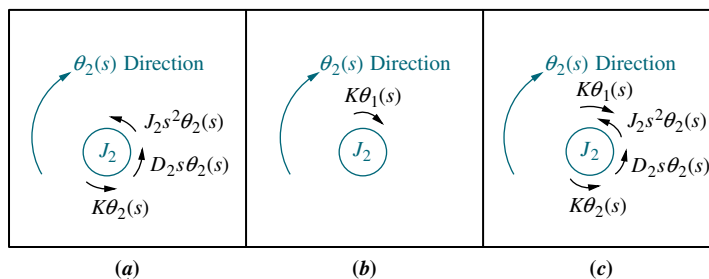
Summing torques respectively from Figures 2.23(c) and 2.24(c) we obtain the equations of motion,

$$(J_1 s^2 + D_1 s + K)\theta_1(s) \qquad\qquad - K\theta_2(s) = T(s) \tag{2.127a}$$

$$-K\theta_1(s) + (J_2 s^2 + D_2 s + K)\theta_2(s) = 0 \tag{2.127b}$$

from which the required transfer function is found to be

$$\frac{\theta_2(s)}{T(s)} = \frac{K}{\Delta} \tag{2.128}$$

as shown in Figure 2.22(c), where

$$\Delta = \begin{vmatrix} (J_1 s^2 + D_1 s + K) & -K \\ -K & (J_2 s^2 + D_2 s + K) \end{vmatrix}$$

Notice that Eq. (2.127) have that now well-known form

$$\begin{bmatrix} \text{Sum of} \\ \text{impedances} \\ \text{connected} \\ \text{to the motion} \\ \text{at } \theta_1 \end{bmatrix}\theta_1(s) - \begin{bmatrix} \text{Sum of} \\ \text{impedances} \\ \text{between} \\ \theta_1 \text{ and } \theta_2 \end{bmatrix}\theta_2(s) = \begin{bmatrix} \text{Sum of} \\ \text{applied torques} \\ \text{at } \theta_1 \end{bmatrix} \tag{2.129a}$$

$$-\begin{bmatrix} \text{Sum of} \\ \text{impedances} \\ \text{between} \\ \theta_1 \text{ and } \theta_2 \end{bmatrix}\theta_1(s) + \begin{bmatrix} \text{Sum of} \\ \text{impedances} \\ \text{connected} \\ \text{to the motion} \\ \text{at } \theta_2 \end{bmatrix}\theta_2(s) = \begin{bmatrix} \text{Sum of} \\ \text{applied torques} \\ \text{at } \theta_2 \end{bmatrix} \tag{2.129b}$$

TryIt 2.9

Use the following MATLAB and Symbolic Math Toolbox statements to help you get Eq. (2.128).

```
syms s J1 D1 K T J2 D2...
  theta1 theta2
A =[(J1*s^2+D1*s+K) −K
    −K (J2*s^2+D2*s+K)];
B =[theta1
    theta2];
C =[T
    0];
B=inv(A)*C;
theta2=B(2);
'theta2'
pretty(theta2)
```

Example 2.20

Equations of Motion By Inspection

PROBLEM: Write, but do not solve, the Laplace transform of the equations of motion for the system shown in Figure 2.25.
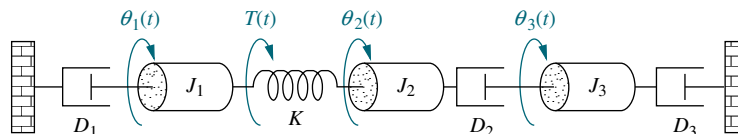
FIGURE 2.25   Three-degrees-of-freedom rotational system

SOLUTION: The equations will take on the following form, similar to electrical mesh equations:

$$
\begin{bmatrix} \text{Sum of} \\ \text{impedances} \\ \text{connected} \\ \text{to the motion} \\ \text{at } \theta_1 \end{bmatrix} \theta_1(s) - \begin{bmatrix} \text{Sum of} \\ \text{impedances} \\ \text{between} \\ \theta_1 \text{ and } \theta_2 \end{bmatrix} \theta_2(s)
$$

(2.130a)

$$
- \begin{bmatrix} \text{Sum of} \\ \text{impedances} \\ \text{between} \\ \theta_1 \text{ and } \theta_3 \end{bmatrix} \theta_3(s) = \begin{bmatrix} \text{Sum of} \\ \text{applied torques} \\ \text{at } \theta_1 \end{bmatrix}
$$

$$
- \begin{bmatrix} \text{Sum of} \\ \text{impedances} \\ \text{between} \\ \theta_1 \text{ and } \theta_2 \end{bmatrix} \theta_1(s) + \begin{bmatrix} \text{Sum of} \\ \text{impedances} \\ \text{connected} \\ \text{to the motion} \\ \text{at } \theta_2 \end{bmatrix} \theta_2(s)
$$

(2.130b)

$$
- \begin{bmatrix} \text{Sum of} \\ \text{impedances} \\ \text{between} \\ \theta_2 \text{ and } \theta_3 \end{bmatrix} \theta_3(s) = \begin{bmatrix} \text{Sum of} \\ \text{applied torques} \\ \text{at } \theta_2 \end{bmatrix}
$$

$$
- \begin{bmatrix} \text{Sum of} \\ \text{impedances} \\ \text{between} \\ \theta_1 \text{ and } \theta_3 \end{bmatrix} \theta_1(s) - \begin{bmatrix} \text{Sum of} \\ \text{impedances} \\ \text{between} \\ \theta_2 \text{ and } \theta_3 \end{bmatrix} \theta_2(s)
$$

(2.130c)

$$
+ \begin{bmatrix} \text{Sum of} \\ \text{impedances} \\ \text{connected} \\ \text{to the motion} \\ \text{at } \theta_3 \end{bmatrix} \theta_3(s) = \begin{bmatrix} \text{Sum of} \\ \text{applied torques} \\ \text{at } \theta_3 \end{bmatrix}
$$

Hence,

$$
\begin{aligned}
(J_1 s^2 + D_1 s + K)\theta_1(s) & & -K\theta_2(s) & & -0\theta_3(s) &= T(s) \\
-K\theta_1(s) & +(J_2 s^2 + D_2 s + K)\theta_2(s) & & -D_2 s\theta_3(s) &= 0 \\
-0\theta_1(s) & & -D_2 s\theta_2(s) & +(J_3 s^2 + D_3 s + D_2 s)\theta_3(s) &= 0
\end{aligned}
$$

(2.131a, b, c)

Skill-Assessment Exercise 2.9

PROBLEM: Find the transfer function, $G(s) = \theta_2(s)/T(s)$, for the rotational mechanical system shown in Figure 2.26.

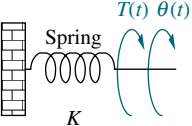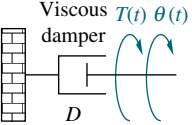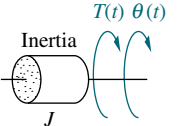**FIGURE 2.26** Rotational mechanical system for Skill-Assessment Exercise 2.9
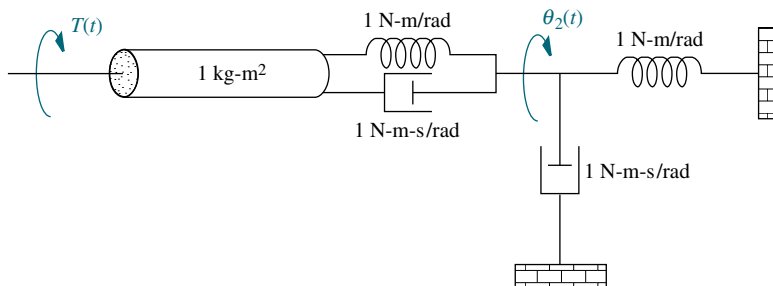
ANSWER: $G(s) = \dfrac{1}{2s^2 + s + 1}$

The complete solution is at www.wiley.com/college/nise.

2.7 Transfer Functions for Systems with Gears

Now that we are able to find the transfer function for rotational systems, we realize that these systems, especially those driven by motors, are rarely seen without associated gear trains driving the load. This section covers this important topic.

Gears provide mechanical advantage to rotational systems. Anyone who has ridden a 10-speed bicycle knows the effect of gearing. Going uphill, you shift to provide more torque and less speed. On the straightaway, you shift to obtain more speed and less torque. Thus, gears allow you to match the drive system and the load—a trade-off between speed and torque.

For many applications, gears exhibit *backlash*, which occurs because of the loose fit between two meshed gears. The drive gear rotates through a small angle before making contact with the meshed gear. The result is that the angular rotation of the output gear does not occur until a small angular rotation of the input gear has occurred. In this section, we idealize the behavior of gears and assume that there is no backlash.
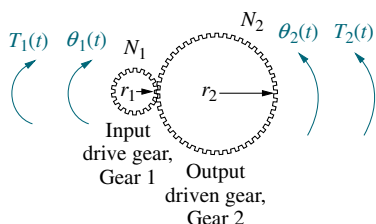
The linearized interaction between two gears is depicted in Figure 2.27. An input gear with radius r_1 and N_1 teeth is rotated through angle $\theta_1(t)$ due to a torque, $T_1(t)$. An output gear with radius r_2 and N_2 teeth responds by rotating through angle $\theta_2(t)$ and delivering a torque, $T_2(t)$. Let us now find the relationship between the rotation of Gear 1, $\theta_1(t)$, and Gear 2, $\theta_2(t)$.

From Figure 2.27, as the gears turn, the distance traveled along each gear's circumference is the same. Thus,

FIGURE 2.27 A gear system

$$r_1\theta_1 = r_2\theta_2 \tag{2.132}$$

or

$$\frac{\theta_2}{\theta_1} = \frac{r_1}{r_2} = \frac{N_1}{N_2} \qquad (2.133)$$

since the ratio of the number of teeth along the circumference is in the same proportion as the ratio of the radii. We conclude that the ratio of the angular displacement of the gears is inversely proportional to the ratio of the number of teeth.

What is the relationship between the input torque, T_1, and the delivered torque, T_2? If we assume the gears are *lossless*, that is they do not absorb or store energy, the energy into Gear 1 equals the energy out of Gear 2.[11] Since the translational energy of force times displacement becomes the rotational energy of torque times angular displacement,

$$T_1\theta_1 = T_2\theta_2 \qquad (2.134)$$

Solving Eq. (2.134) for the ratio of the torques and using Eq. (2.133), we get

$$\frac{T_2}{T_1} = \frac{\theta_1}{\theta_2} = \frac{N_2}{N_1} \qquad (2.135)$$

Thus, the torques are directly proportional to the ratio of the number of teeth. All results are summarized in Figure 2.28.

Let us see what happens to mechanical impedances that are driven by gears. Figure 2.29(*a*) shows gears driving a rotational inertia, spring, and viscous damper. For clarity, the gears are shown by an end-on view. We want to represent Figure 2.29(*a*) as an equivalent system at θ_1 without the gears. In other words, can the mechanical impedances be reflected from the output to the input, thereby eliminating the gears?
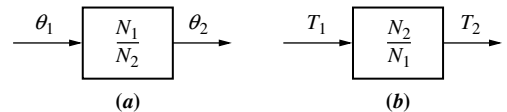
FIGURE 2.28   Transfer functions for **a.** angular displacement in lossless gears and **b.** torque in lossless gears
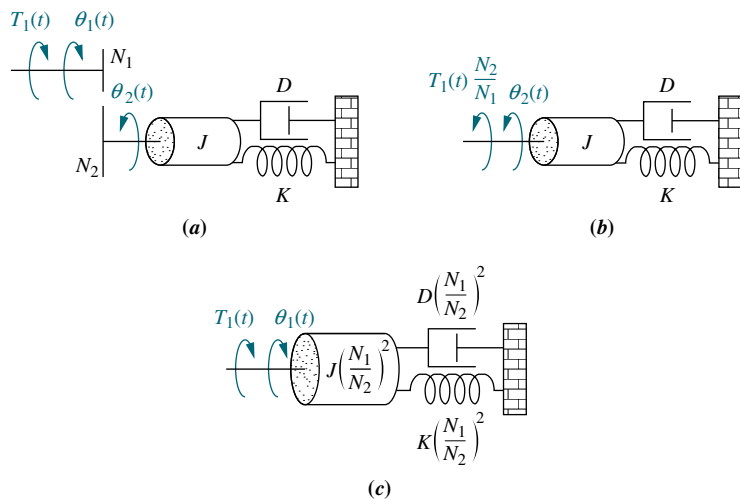
FIGURE 2.29   a. Rotational system driven by gears; **b.** equivalent system at the output after reflection of input torque; **c.** equivalent system at the input after reflection of impedances

---

[11] This is equivalent to saying that the gears have negligible inertia and damping.

From Figure 2.28(b), T_1 can be reflected to the output by multiplying by N_2/N_1. The result is shown in Figure 2.29(b), from which we write the equation of motion as

$$(Js^2 + Ds + K)\theta_2(s) = T_1(s)\frac{N_2}{N_1} \tag{2.136}$$

Now convert $\theta_2(s)$ into an equivalent $\theta_1(s)$, so that Eq. (2.136) will look as if it were written at the input. Using Figure 2.28(a) to obtain $\theta_2(s)$ in terms of $\theta_1(s)$, we get

$$(Js^2 + Ds + K)\frac{N_1}{N_2}\theta_1(s) = T_1(s)\frac{N_2}{N_1} \tag{2.137}$$

After simplification,

$$\left[J\left(\frac{N_1}{N_2}\right)^2 s^2 + D\left(\frac{N_1}{N_2}\right)^2 s + K\left(\frac{N_1}{N_2}\right)^2\right]\theta_1(s) = T_1(s) \tag{2.138}$$

which suggests the equivalent system at the input and without gears shown in Figure 2.29(c). Thus, the load can be thought of as having been reflected from the output to the input.

Generalizing the results, we can make the following statement: *Rotational mechanical impedances can be reflected through gear trains by multiplying the mechanical impedance by the ratio*

$$\left(\frac{\text{Number of teeth of gear on \textit{destination} shaft}}{\text{Number of teeth of gear on \textit{source} shaft}}\right)^2$$

where the impedance to be reflected is attached to the source shaft and is being reflected to the destination shaft. The next example demonstrates the application of the concept of reflected impedances as we find the transfer function of a rotational mechanical system with gears.

Example 2.21

Transfer Function—System with Lossless Gears

PROBLEM: Find the transfer function, $\theta_2(s)/T_1(s)$, for the system of Figure 2.30(a).
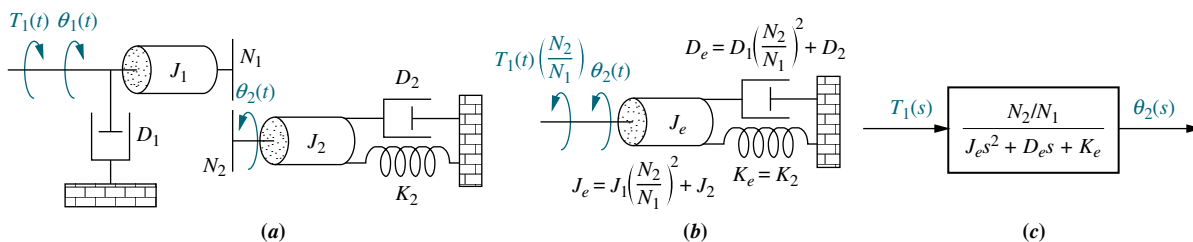
FIGURE 2.30   a. Rotational mechanical system with gears; **b.** system after reflection of torques and impedances to the output shaft; **c.** block diagram

SOLUTION: It may be tempting at this point to search for two simultaneous equations corresponding to each inertia. The inertias, however, do not undergo linearly independent motion, since they are tied together by the gears. Thus, there is only one degree of freedom and hence one equation of motion.

Let us first reflect the impedances (J_1 and D_1) and torque (T_1) on the input shaft to the output as shown in Figure 2.30(b), where the impedances are reflected by $(N_2/N_1)^2$ and the torque is reflected by (N_2/N_1). The equation of motion can now be written as

$$(J_e s^2 + D_e s + K_e)\theta_2(s) = T_1(s)\frac{N_2}{N_1} \tag{2.139}$$

where

$$J_e = J_1\left(\frac{N_2}{N_1}\right)^2 + J_2; \quad D_e = D_1\left(\frac{N_2}{N_1}\right)^2 + D_2; \quad K_e = K_2$$

Solving for $\theta_2(s)/T_1(s)$, the transfer function is found to be

$$G(s) = \frac{\theta_2(s)}{T_1(s)} = \frac{N_2/N_1}{J_e s^2 + D_e s + K_e} \tag{2.140}$$

as shown in Figure 2.30(c).

In order to eliminate gears with large radii, a *gear train* is used to implement large gear ratios by cascading smaller gear ratios. A schematic diagram of a gear train is shown in Figure 2.31. Next to each rotation, the angular displacement relative to θ_1 has been calculated. From Figure 2.31,

$$\theta_4 = \frac{N_1 N_3 N_5}{N_2 N_4 N_6}\theta_1 \tag{2.141}$$

For gear trains, we conclude that the equivalent gear ratio is the product of the individual gear ratios. We now apply this result to solve for the transfer function of a system that does not have lossless gears.
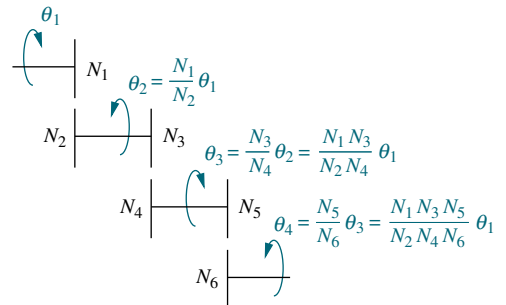
FIGURE 2.31   Gear train

Example 2.22

Transfer Function—Gears with Loss

PROBLEM: Find the transfer function, $\theta_1(s)/T_1(s)$, for the system of Figure 2.32(a).
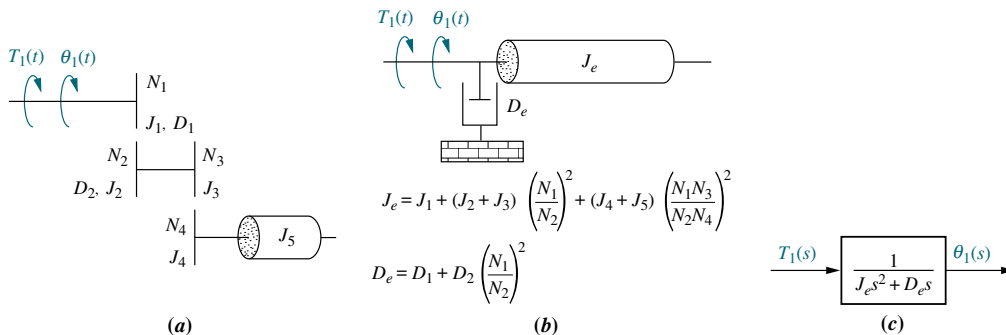
FIGURE 2.32
a. System using a gear train; **b.** equivalent system at the input; **c.** block diagram

SOLUTION: This system, which uses a gear train, does not have lossless gears. All of the gears have inertia, and for some shafts there is viscous friction. To solve the problem, we want to reflect all of the impedances to the input shaft, θ_1. The gear ratio is not the same for all impedances. For example, D_2 is reflected only through one gear ratio as $D_2(N_1/N_2)^2$, whereas J_4 plus J_5 is reflected through two gear ratios as $(J_4 + J_5)[(N_3/N_4)(N_1/N_2)]^2$. The result of reflecting all impedances to θ_1 is shown in Figure 2.32(b), from which the equation of motion is

$$(J_e s^2 + D_e s)\theta_1(s) = T_1(s) \tag{2.142}$$

where

$$J_e = J_1 + (J_2 + J_3)\left(\frac{N_1}{N_2}\right)^2 + (J_4 + J_5)\left(\frac{N_1 N_3}{N_2 N_4}\right)^2$$

and

$$D_e = D_1 + D_2\left(\frac{N_1}{N_2}\right)^2$$

From Eq. (2.142), the transfer function is

$$G(s) = \frac{\theta_1(s)}{T_1(s)} = \frac{1}{J_e s^2 + D_e s} \tag{2.143}$$

as shown in Figure 2.32(c).

Skill-Assessment Exercise 2.10

PROBLEM: Find the transfer function, $G(s) = \theta_2(s)/T(s)$, for the rotational mechanical system with gears shown in Figure 2.33.
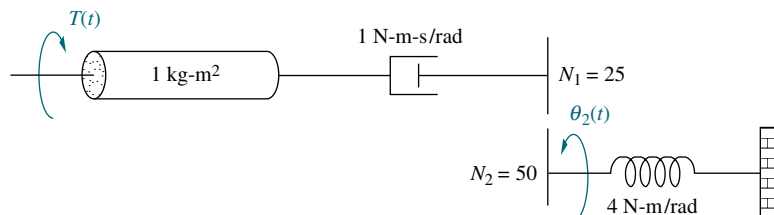
FIGURE 2.33   Rotational mechanical system with gears for Skill-Assessment Exercise 2.10

ANSWER: $G(s) = \dfrac{1/2}{s^2 + s + 1}$

The complete solution is at www.wiley.com/college/nise.

2.8 Electromechanical System Transfer Functions

In the last section we talked about rotational systems with gears, which completed our discussion of purely mechanical systems. Now, we move to systems that are hybrids of electrical and mechanical variables, the *electromechanical systems*. We have seen one application of an electromechanical system in Chapter 1, the antenna azimuth position control system. Other applications for systems with electromechanical components are robot controls, sun and star trackers, and computer tape and disk-drive position controls. An example of a control system that uses electromechanical components is shown in Figure 2.34.

A motor is an electromechanical component that yields a displacement output for a voltage input, that is, a mechanical output generated by an electrical input. We will derive the transfer function for one particular kind of electromechanical system, the armature-controlled dc servomotor (*Mablekos, 1980*). The motor's schematic is shown in Figure 2.35(*a*), and the transfer function we will derive appears in Figure 2.35(*b*).
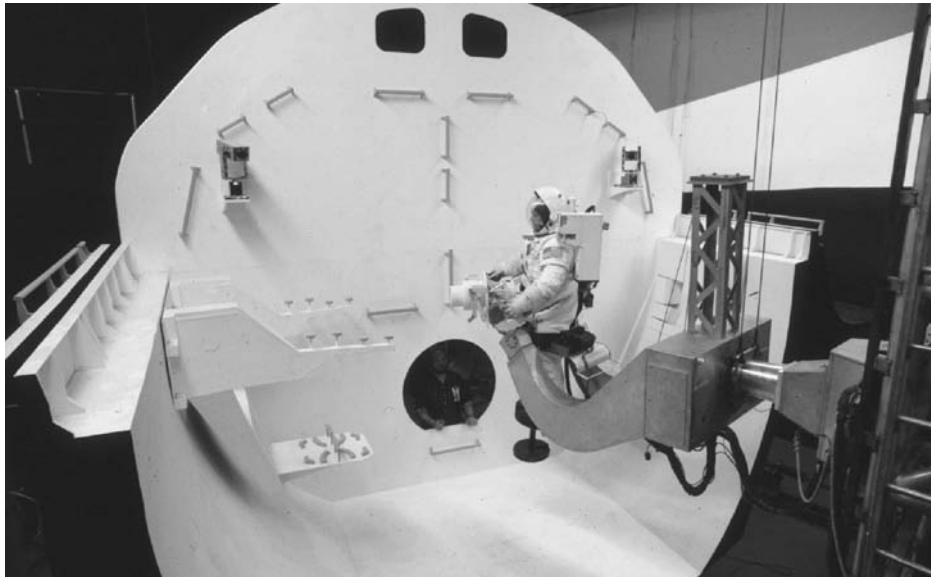
FIGURE 2.34 NASA flight simulator robot arm with electromechanical control system components.
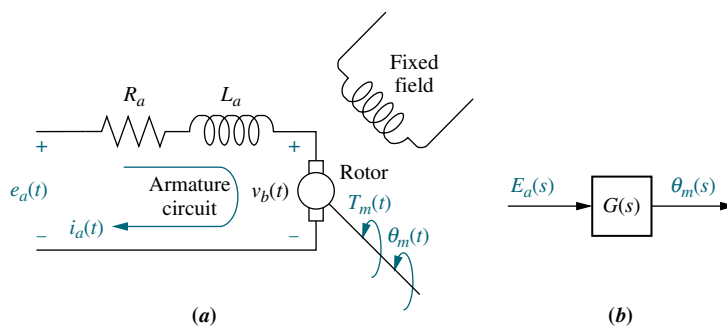
FIGURE 2.35 DC motor: **a.** schematic;[12] **b.** block diagram

---

[12] See Appendix I at www.wiley.com/college/nise for a derivation of this schematic and its parameters.

In Figure 2.35(a) a magnetic field is developed by stationary permanent magnets or a stationary electromagnet called the *fixed field*. A rotating circuit called the *armature*, through which current $i_a(t)$ flows, passes through this magnetic field at right angles and feels a force, $F = Bli_a(t)$, where B is the magnetic field strength and l is the length of the conductor. The resulting torque turns the *rotor*, the rotating member of the motor.

There is another phenomenon that occurs in the motor: A conductor moving at right angles to a magnetic field generates a voltage at the terminals of the conductor equal to $e = Blv$, where e is the voltage and v is the velocity of the conductor normal to the magnetic field. Since the current-carrying armature is rotating in a magnetic field, its voltage is proportional to speed. Thus,

$$v_b(t) = K_b \frac{d\theta_m(t)}{dt} \tag{2.144}$$

We call $v_b(t)$ the *back electromotive force (back emf)*; K_b is a constant of proportionality called the back emf constant; and $d\theta_m(t)/dt = \omega_m(t)$ is the angular velocity of the motor. Taking the Laplace transform, we get

$$V_b(s) = K_b s\theta_m(s) \tag{2.145}$$

The relationship between the armature current, $i_a(t)$, the applied armature voltage, $e_a(t)$, and the back emf, $v_b(t)$, is found by writing a loop equation around the Laplace transformed armature circuit (see Figure 3.5(a)):

$$R_a I_a(s) + L_a s I_a(s) + V_b(s) = E_a(s) \tag{2.146}$$

The torque developed by the motor is proportional to the armature current; thus,

$$T_m(s) = K_t I_a(s) \tag{2.147}$$

where T_m is the torque developed by the motor, and K_t is a constant of proportionality, called the motor torque constant, which depends on the motor and magnetic field characteristics. In a consistent set of units, the value of K_t is equal to the value of K_b. Rearranging Eq. (2.147) yields

$$I_a(s) = \frac{1}{K_t} T_m(s) \tag{2.148}$$

To find the transfer function of the motor, we first substitute Eqs. (2.145) and (2.148) into (2.146), yielding

$$\frac{(R_a + L_a s)T_m(s)}{K_t} + K_b s\theta_m(s) = E_a(s) \tag{2.149}$$

$T_m(t)\ \theta_m(t)$

J_m

D_m
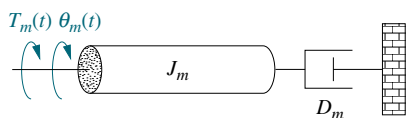
FIGURE 2.36 Typical equivalent mechanical loading on a motor

Now we must find $T_m(s)$ in terms of $\theta_m(s)$ if we are to separate the input and output variables and obtain the transfer function, $\theta_m(s)/E_a(s)$.

Figure 2.36 shows a typical equivalent mechanical loading on a motor. J_m is the equivalent inertia at the armature and includes both the armature inertia and, as we will see later, the load inertia reflected to the armature.

D_m is the equivalent viscous damping at the armature and includes both the armature viscous damping and, as we will see later, the load viscous damping reflected to the armature. From Figure 2.36,

$$T_m(s) = (J_m s^2 + D_m s)\theta_m(s) \tag{2.150}$$

Substituting Eq. (2.150) into Eq. (2.149) yields

$$\frac{(R_a + L_a s)(J_m s^2 + D_m s)\theta_m(s)}{K_t} + K_b s\theta_m(s) = E_a(s) \tag{2.151}$$

If we assume that the armature inductance, L_a, is small compared to the armature resistance, R_a, which is usual for a dc motor, Eq. (2.151) becomes

$$\left[\frac{R_a}{K_t}(J_m s + D_m) + K_b\right]s\theta_m(s) = E_a(s) \tag{2.152}$$

After simplification, the desired transfer function, $\theta_m(s)/E_a(s)$, is found to be

$$\frac{\theta_m(s)}{E_a(s)} = \frac{K_t/(R_a J_m)}{s\left[s + \dfrac{1}{J_m}\left(D_m + \dfrac{K_t K_b}{R_a}\right)\right]} \tag{2.153}^{[13]}$$

Even though the form of Eq. (2.153) is relatively simple, namely

$$\frac{\theta_m(s)}{E_a(s)} = \frac{K}{s(s + \alpha)} \tag{2.154}$$

the reader may be concerned about how to evaluate the constants.

Let us first discuss the mechanical constants, J_m and D_m. Consider Figure 2.37, which shows a motor with inertia J_a and damping D_a at the armature driving a load consisting of inertia J_L and damping D_L. Assuming that all inertia and damping values shown are known, J_L and D_L can be reflected back to the armature as some equivalent inertia and damping to be added to J_a and D_a, respectively. Thus, the equivalent inertia, J_m, and equivalent damping, D_m, at the armature are

FIGURE 2.37 DC motor driving a rotational mechanical load

$$J_m = J_a + J_L\left(\frac{N_1}{N_2}\right)^2; \quad D_m = D_a + D_L\left(\frac{N_1}{N_2}\right)^2 \tag{2.155}^{[14]}$$

Now that we have evaluated the mechanical constants, J_m and D_m, what about the electrical constants in the transfer function of Eq. (2.153)? We will show that these constants can be obtained through a *dynamometer* test of the motor, where a dynamometer measures the torque and speed of a motor under the condition of a

---

[13] The units for the electrical constants are K_t = N-m-A (newton-meters/ampere), and K_b = V-s/rad (volt-seconds/radian).

[14] If the values of the mechanical constants are not known, motor constants can be determined through laboratory testing using transient response or frequency response data. The concept of transient response is covered in Chapter 4; frequency response is covered in Chapter 10.

constant applied voltage. Let us first develop the relationships that dictate the use of a dynamometer.

Substituting Eqs. (2.145) and (2.148) into Eq. (2.146), with $L_a = 0$, yields

$$\frac{R_a}{K_t} T_m(s) + K_b s \theta_m(s) = E_a(s) \tag{2.156}$$

Taking the inverse Laplace transform, we get

$$\frac{R_a}{K_t} T_m(t) + K_b \omega_m(t) = e_a(t) \tag{2.157}$$

where the inverse Laplace transform of $s\theta_m(s)$ is $d\theta_m(t)/dt$ or, alternately, $\omega_m(t)$.

If a dc voltage, e_a, is applied, the motor will turn at a constant angular velocity, ω_m, with a constant torque, T_m. Hence, dropping the functional relationship based on time from Eq. (2.157), the following relationship exists when the motor is operating at steady state with a dc voltage input:

$$\frac{R_a}{K_t} T_m + K_b \omega_m = e_a \tag{2.158}$$

Solving for T_m yields

$$\boxed{T_m = -\frac{K_b K_t}{R_a} \omega_m + \frac{K_t}{R_a} e_a} \tag{2.159}$$
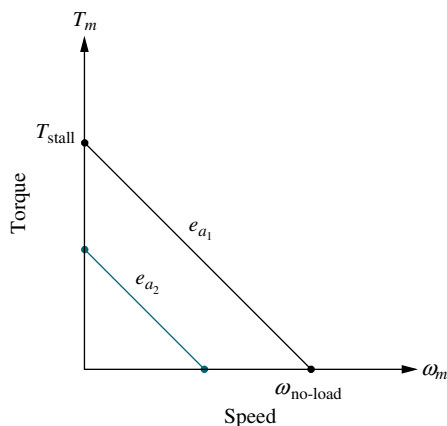
FIGURE 2.38 Torque-speed curves with an armature voltage, e_a, as a parameter

Equation (2.159) is a straight line, T_m vs. ω_m, and is shown in Figure 2.38. This plot is called the *torque-speed curve*. The torque axis intercept occurs when the angular velocity reaches zero. That value of torque is called the *stall torque*, T_{stall}. Thus,

$$T_{stall} = \frac{K_t}{R_a} e_a \tag{2.160}$$

The angular velocity occurring when the torque is zero is called the *no-load speed,* $\omega_{no\text{-}load}$. Thus,

$$\omega_{no\text{-}load} = \frac{e_a}{K_b} \tag{2.161}$$

The electrical constants of the motor's transfer function can now be found from Eqs. (2.160) and (2.161) as

$$\boxed{\frac{K_t}{R_a} = \frac{T_{stall}}{e_a}} \tag{2.162}$$

and

$$\boxed{K_b = \frac{e_a}{\omega_{no\text{-}load}}} \tag{2.163}$$

The electrical constants, K_t/R_a and K_b, can be found from a dynamometer test of the motor, which would yield T_{stall} and $\omega_{no\text{-}load}$ for a given e_a.

Example 2.23

Transfer Function—DC Motor and Load

PROBLEM: Given the system and torque-speed curve of Figure 2.39(a) and (b), find the transfer function, $\theta_L(s)/E_a(s)$.

SOLUTION: Begin by finding the mechanical constants, J_m and D_m, in Eq. (2.153). From Eq. (2.155), the total inertia at the armature of the motor is

$$J_m = J_a + J_L\left(\frac{N_1}{N_2}\right)^2 = 5 + 700\left(\frac{1}{10}\right)^2 = 12 \tag{2.164}$$

and the total damping at the armature of the motor is

$$D_m = D_a + D_L\left(\frac{N_1}{N_2}\right)^2 = 2 + 800\left(\frac{1}{10}\right)^2 = 10 \tag{2.165}$$

Now we will find the electrical constants, K_t/R_a and K_b. From the torque-speed curve of Figure 2.39(b),

$$T_{\text{stall}} = 500 \tag{2.166}$$

$$\omega_{\text{no-load}} = 50 \tag{2.167}$$

$$e_a = 100 \tag{2.168}$$
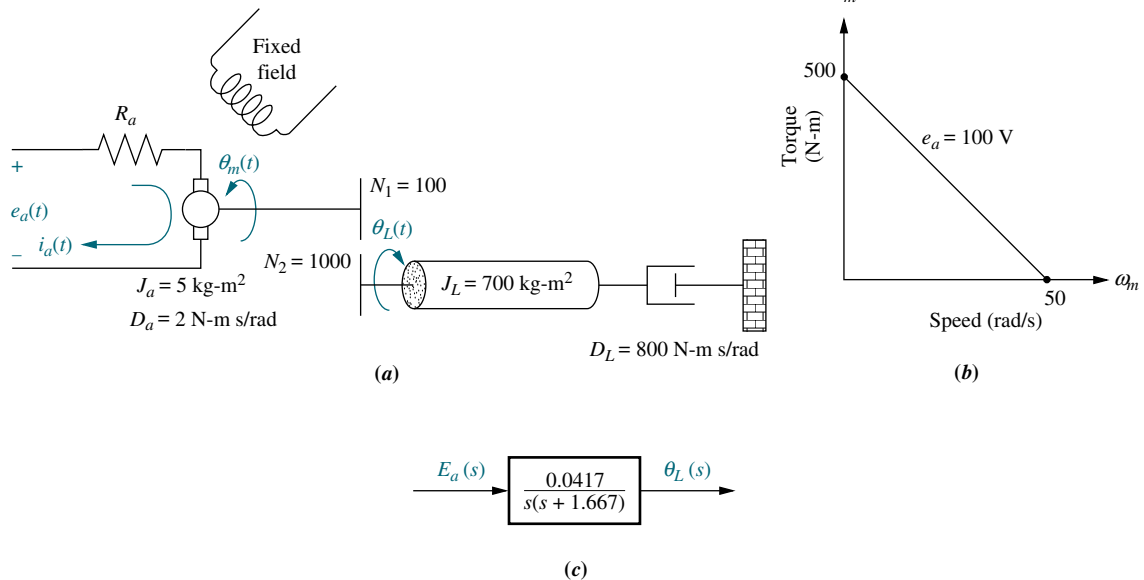
FIGURE 2.39   a. DC motor and load; **b.** torque-speed curve; **c.** block diagram

Hence the electrical constants are

$$\frac{K_t}{R_a} = \frac{T_{\text{stall}}}{e_a} = \frac{500}{100} = 5 \tag{2.169}$$
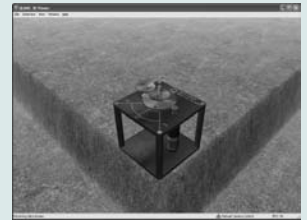
and

$$K_b = \frac{e_a}{\omega_{\text{no-load}}} = \frac{100}{50} = 2 \tag{2.170}$$

Substituting Eqs. (2.164), (2.165), (2.169), and (2.170) into Eq. (2.153) yield

$$\frac{\theta_m(s)}{E_a(s)} = \frac{5/12}{s\left\{s + \dfrac{1}{12}[10 + (5)(2)]\right\}} = \frac{0.417}{s(s + 1.667)} \tag{2.171}$$

In order to find $\theta_L(s)/E_a(s)$, we use the gear ratio, $N_1/N_2 = 1/10$, and find

$$\frac{\theta_L(s)}{E_a(s)} = \frac{0.0417}{s(s + 1.667)} \tag{2.172}$$

as shown in Figure 2.39(c).

Skill-Assessment Exercise 2.11

WileyPLUS

WPCS

Control Solutions

PROBLEM: Find the transfer function, $G(s) = \theta_L(s)/E_a(s)$, for the motor and load shown in Figure 2.40. The torque-speed curve is given by $T_m = -8\omega_m + 200$ when the input voltage is 100 volts.
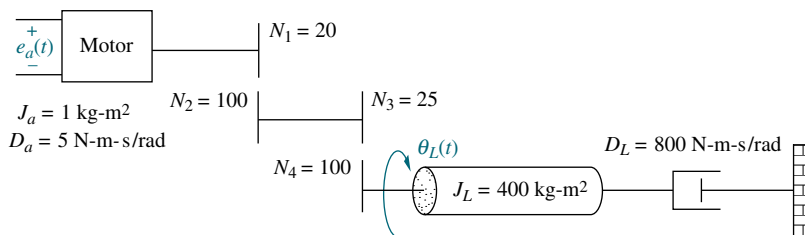
FIGURE 2.40   Electro-mechanical system for Skill-Assessment Exercise 2.11

ANSWER: $G(s) = \dfrac{1/20}{s[s + (15/2)]}$

The complete solution is at www.wiley.com/college/nise.

2.9   Electric Circuit Analogs

In this section, we show the commonality of systems from the various disciplines by demonstrating that the mechanical systems with which we worked can be represented by equivalent electric circuits. We have pointed out the similarity between the equations resulting from Kirchhoff's laws for electrical systems and the equations of motion of mechanical systems. We now show this commonality even more convincingly by producing electric circuit equivalents for mechanical systems. The variables of the electric circuits behave exactly as the analogous

variables of the mechanical systems. In fact, converting mechanical systems to electrical networks before writing the describing equations is a problem-solving approach that you may want to pursue.

An electric circuit that is analogous to a system from another discipline is called an electric circuit *analog*. Analogs can be obtained by comparing the describing equations, such as the equations of motion of a mechanical system, with either electrical mesh or nodal equations. When compared with mesh equations, the resulting electrical circuit is called a *series analog*. When compared with nodal equations, the resulting electrical circuit is called a *parallel analog*.

Series Analog

Consider the translational mechanical system shown in Figure 2.41(*a*), whose equation of motion is

$$(Ms^2 + f_v s + K)X(s) = F(s) \tag{2.173}$$

Kirchhoff's mesh equation for the simple series RLC network shown in Figure 2.41(*b*) is

$$\left(Ls + R + \frac{1}{Cs}\right)I(s) = E(s) \tag{2.174}$$

As we previously pointed out, Eq. (2.173) is not directly analogous to Eq. (2.174) because displacement and current are not analogous. We can create a direct analogy by operating on Eq. (2.173) to convert displacement to velocity by dividing and multiplying the left-hand side by *s*, yielding

$$\frac{Ms^2 + f_v s + K}{s} sX(s) = \left(Ms + f_v + \frac{K}{s}\right)V(s) = F(s) \tag{2.175}$$

Comparing Eqs. 2.174 and 2.175, we recognize the sum of impedances and draw the circuit shown in Figure 2.41(*c*). The conversions are summarized in Figure 2.41(*d*).

When we have more than one degree of freedom, the impedances associated with a motion appear as series electrical elements in a mesh, but

mass = M →	inductor	= M henries
viscous damper = f_v →	resistor	= f_v ohms
spring = K →	capacitor	= $\frac{1}{K}$ farads
applied force = $f(t)$ →	voltage source	= $f(t)$
velocity = $v(t)$ →	mesh current	= $v(t)$

(*d*)
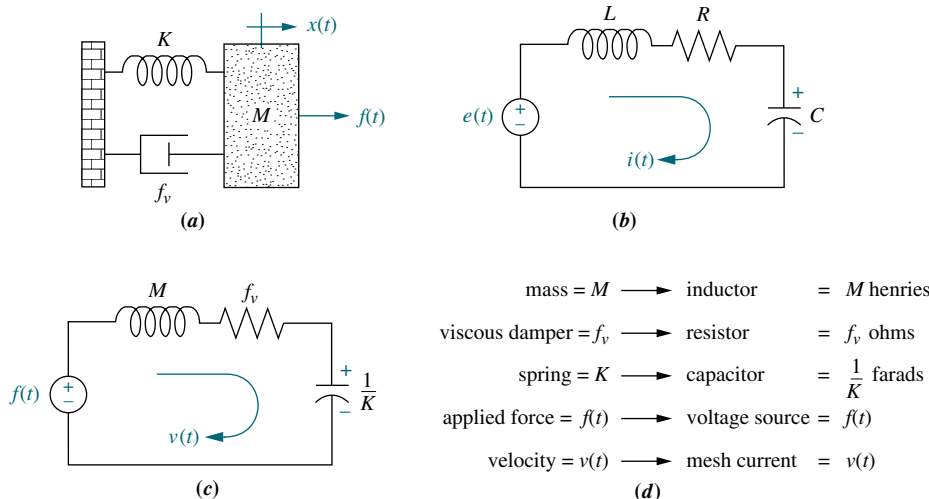
FIGURE 2.41 Development of series analog: **a.** mechanical system; **b.** desired electrical representation; **c.** series analog; **d.** parameters for series analog

the impedances between adjacent motions are drawn as series electrical impedances between the two corresponding meshes. We demonstrate with an example.

Example 2.24

Converting a Mechanical System to a Series Analog

PROBLEM: Draw a series analog for the mechanical system of Figure 2.17(a).

SOLUTION: Equations (2.118) are analogous to electrical mesh equations after conversion to velocity. Thus,

$$\left[M_1 s + (f_{v_1} + f_{v_3}) + \frac{(K_1 + K_2)}{s}\right] V_1(s) - \left(f_{v_3} + \frac{K_2}{s}\right) V_2(s) = F(s) \qquad (2.176a)$$

$$-\left(f_{v_3} + \frac{K_2}{s}\right) V_1(s) + \left[M_2 s + (f_{v_2} + f_{v_3}) + \frac{(K_2 + K_3)}{s}\right] V_2(s) = 0 \qquad (2.176b)$$

Coefficients represent sums of electrical impedance. Mechanical impedances associated with M_1 form the first mesh, where impedances between the two masses are common to the two loops. Impedances associated with M_2 form the second mesh. The result is shown in Figure 2.42, where $v_1(t)$ and $v_2(t)$ are the velocities of M_1 and M_2, respectively.
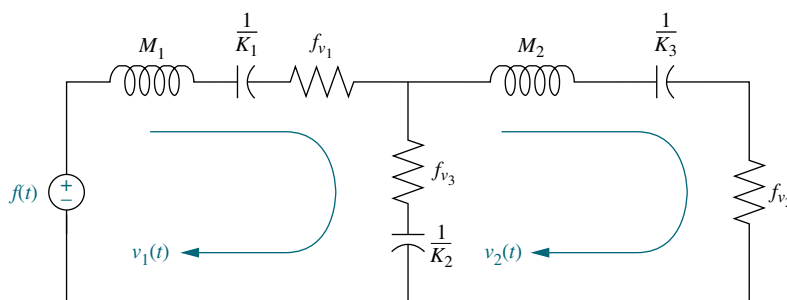
FIGURE 2.42 Series analog of mechanical system of Figure 2.17(a)

Parallel Analog

A system can also be converted to an equivalent parallel analog. Consider the translational mechanical system shown in Figure 2.43(a), whose equation of motion is given by Eq. (2.175). Kirchhoff's nodal equation for the simple parallel *RLC* network shown in Figure 2.43(b) is

$$\left(Cs + \frac{1}{R} + \frac{1}{Ls}\right) E(s) = I(s) \qquad (2.177)$$

Comparing Eqs. (2.175) and (2.177), we identify the sum of admittances and draw the circuit shown in Figure 2.43(c). The conversions are summarized in Figure 2.43(d).

mass = M ⟶ capacitor = M farads

viscous damper = f_v ⟶ resistor = $\frac{1}{f_v}$ ohms

spring = K ⟶ inductor = $\frac{1}{K}$ henries

applied force = $f(t)$ ⟶ current source = $f(t)$

velocity = $v(t)$ ⟶ node voltage = $v(t)$
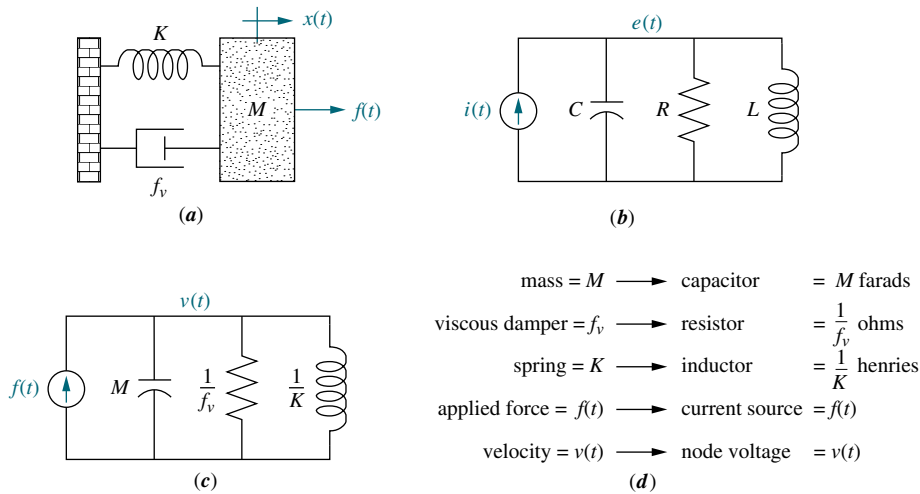
FIGURE 2.43 Development of parallel analog: **a.** mechanical system; **b.** desired electrical representation; **c.** parallel analog; **d.** parameters for parallel analog

When we have more than one degree of freedom, the components associated with a motion appear as parallel electrical elements connected to a node, but the components of adjacent motions are drawn as parallel electrical elements between two corresponding nodes. We demonstrate with an example.

Example 2.25

Converting a Mechanical System to a Parallel Analog

PROBLEM: Draw a parallel analog for the mechanical system of Figure 2.17(*a*).

SOLUTION: Equation (2.176) is also analogous to electrical node equations. Coefficients represent sums of electrical admittances. Admittances associated with M_1 form the elements connected to the first node, where mechanical admittances between the two masses are common to the two nodes. Mechanical admittances associated with M_2 form the elements connected to the second node. The result is shown in Figure 2.44, where $v_1(t)$ and $v_2(t)$ are the velocities of M_1 and M_2, respectively.
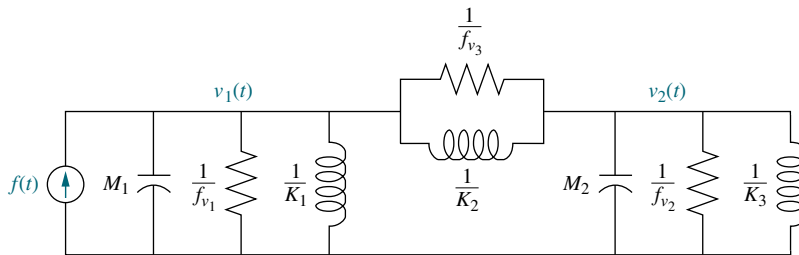
FIGURE 2.44 Parallel analog of mechanical system of Figure 2.17(*a*)

Skill-Assessment Exercise 2.12

PROBLEM: Draw a series and parallel analog for the rotational mechanical system of Figure 2.22.

ANSWER: The complete solution is at www.wiley.com/college/nise.

◖ 2.10 Nonlinearities

The models thus far are developed from systems that can be described approximately by linear, time-invariant differential equations. An assumption of *linearity* was implicit in the development of these models. In this section, we formally define the terms *linear* and *nonlinear* and show how to distinguish between the two. In Section 2.11, we show how to approximate a nonlinear system as a linear system so that we can use the modeling techniques previously covered in this chapter (*Hsu, 1968*).

A linear system possesses two properties: superposition and homogeneity. The property of *superposition* means that the output response of a system to the sum of inputs is the sum of the responses to the individual inputs. Thus, if an input of $r_1(t)$ yields an output of $c_1(t)$ and an input of $r_2(t)$ yields an output of $c_2(t)$, then an input of $r_1(t) + r_2(t)$ yields an output of $c_1(t) + c_2(t)$. The property of *homogeneity* describes the response of the system to a multiplication of the input by a scalar. Specifically, in a linear system, the property of homogeneity is demonstrated if for an input of $r_1(t)$ that yields an output of $c_1(t)$, an input of $Ar_1(t)$ yields an output of $Ac_1(t)$; that is, multiplication of an input by a scalar yields a response that is multiplied by the same scalar.

We can visualize linearity as shown in Figure 2.45. Figure 2.45(*a*) is a linear system where the output is always $\frac{1}{2}$ the input, or $f(x) = 0.5x$, regardless of the value of *x*. Thus each of the two properties of linear systems applies. For example, an input of 1 yields an output of $\frac{1}{2}$ and an input of 2 yields an output of 1. Using superposition, an input that is the sum of the original inputs, or 3, should yield an output that is the sum of the individual outputs, or 1.5. From Figure 2.45(*a*), an input of 3 does indeed yield an output of 1.5.

To test the property of homogeneity, assume an input of 2, which yields an output of 1. Multiplying this input by 2 should yield an output of twice as much, or 2. From Figure 2.45(*a*), an input of 4 does indeed yield an output of 2. The reader can verify that the properties of linearity certainly do not apply to the relationship shown in Figure 2.45(*b*).

FIGURE 2.45 **a.** Linear system; **b.** nonlinear system

Figure 2.46 shows some examples of physical nonlinearities. An electronic amplifier is linear over a specific range but exhibits the nonlinearity called *saturation* at high input voltages. A motor that does not respond at very low input voltages due to frictional forces exhibits a nonlinearity called *dead zone*. Gears that do not fit tightly exhibit a nonlinearity called *backlash:* The input moves over a small range
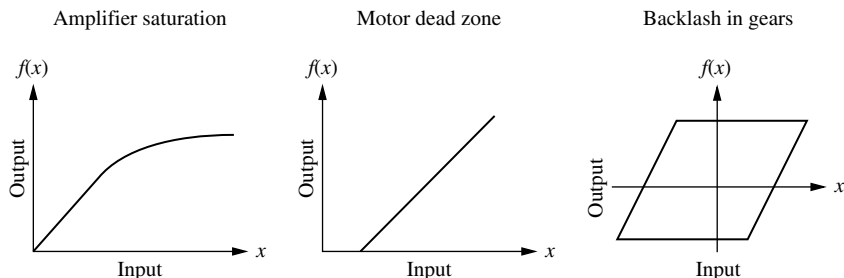
FIGURE 2.46 Some physical nonlinearities

without the output responding. The reader should verify that the curves shown in Figure 2.46 do not fit the definitions of linearity over their entire range. Another example of a nonlinear subsystem is a phase detector, used in a phase-locked loop in an FM radio receiver, whose output response is the sine of the input.

A designer can often make a linear approximation to a nonlinear system. Linear approximations simplify the analysis and design of a system and are used as long as the results yield a good approximation to reality. For example, a linear relationship can be established at a point on the nonlinear curve if the range of input values about that point is small and the origin is translated to that point. Electronic amplifiers are an example of physical devices that perform linear amplification with small excursions about a point.

2.11   Linearization

The electrical and mechanical systems covered thus far were assumed to be linear. However, if any nonlinear components are present, we must linearize the system before we can find the transfer function. In the last section, we defined and discussed nonlinearities; in this section, we show how to obtain linear approximations to nonlinear systems in order to obtain transfer functions.

The first step is to recognize the nonlinear component and write the nonlinear differential equation. When we linearize a nonlinear differential equation, we linearize it for small-signal inputs about the steady-state solution when the small-signal input is equal to zero. This steady-state solution is called *equilibrium* and is selected as the second step in the linearization process. For example, when a pendulum is at rest, it is at equilibrium. The angular displacement is described by a nonlinear differential equation, but it can be expressed with a linear differential equation for small excursions about this equilibrium point.

Next we linearize the nonlinear differential equation, and then we take the Laplace transform of the linearized differential equation, assuming zero initial conditions. Finally, we separate input and output variables and form the transfer function. Let us first see how to linearize a function; later, we will apply the method to the linearization of a differential equation.

If we assume a nonlinear system operating at point A, $[x_0, f(x_0)]$ in Figure 2.47, small changes in the input can be related to changes in the output about the point by way of the slope of the curve at the point A. Thus, if the slope of the curve at point A is m_a, then small excursions of the input about point A, δ_x, yield small changes in the output, $\delta f(x)$, related by the slope at point A. Thus,

$$[f(x) - f(x_0)] \approx m_a(x - x_0) \qquad (2.178)$$

from which

$$\delta f(x) \approx m_a \delta x \qquad (2.179)$$

and

$$f(x) \approx f(x_0) + m_a(x - x_0) \approx f(x_0) + m_a \delta x \qquad (2.180)$$
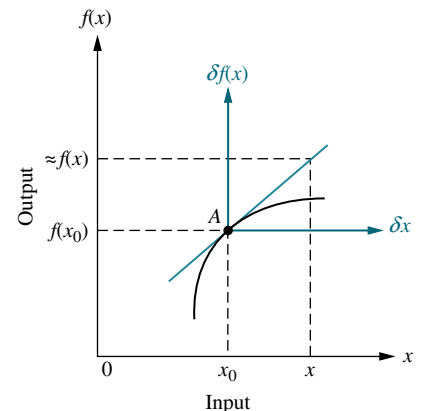
FIGURE 2.47 Linearization about point A

This relationship is shown graphically in Figure 2.47, where a new set of axes, δ_x and $\delta f(x)$, is created at the point A, and $f(x)$ is approximately equal to $f(x_0)$, the ordinate of the new origin, plus small excursions, $m_a \delta x$, away from point A. Let us look at an example.

Example 2.26

Linearizing a Function

PROBLEM: Linearize $f(x) = 5 \cos x$ about $x = \pi/2$.

SOLUTION: We first find that the derivative of $f(x)$ is $df/dx = (-5 \sin x)$. At $x = \pi/2$, the derivative is -5. Also $f(x_0) = f(\pi/2) = 5 \cos(\pi/2) = 0$. Thus, from Eq. (2.180), the system can be represented as $f(x) = -5\,\delta x$ for small excursions of x about $\pi/2$. The process is shown graphically in Figure 2.48, where the cosine curve does indeed look like a straight line of slope -5 near $\pi/2$.
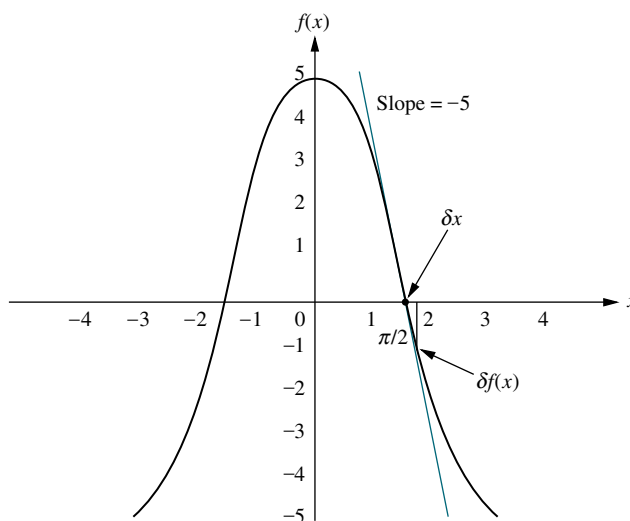
FIGURE 2.48   Linearization of $5 \cos x$ about $x = \pi/2$

The previous discussion can be formalized using the Taylor series expansion, which expresses the value of a function in terms of the value of that function at a particular point, the excursion away from that point, and derivatives evaluated at that point. The Taylor series is shown in Eq. (2.181).

$$f(x) = f(x_0) + \frac{df}{dx}\bigg|_{x=x_0} \frac{(x - x_0)}{1!} + \frac{d^2 f}{dx^2}\bigg|_{x=x_0} \frac{(x - x_0)^2}{2!} + \cdots \tag{2.181}$$

For small excursions of x from x_0, we can neglect higher-order terms. The resulting approximation yields a straight-line relationship between the change in $f(x)$ and the excursions away from x_0. Neglecting the higher-order terms in Eq. (2.181), we get

$$f(x) - f(x_0) \approx \frac{df}{dx}\bigg|_{x=x_0} (x - x_0) \tag{2.182}$$

or

$$\delta f(x) \approx m|_{x=x_0} \delta x \qquad (2.183)$$

which is a linear relationship between $\delta f(x)$ and δx for small excursions away from x_0. It is interesting to note that Eqs. (2.182) and (2.183) are identical to Eqs. (2.178) and (2.179), which we derived intuitively. The following examples illustrate linearization. The first example demonstrates linearization of a differential equation, and the second example applies linearization to finding a transfer function.

Example 2.27

Linearizing a Differential Equation

PROBLEM: Linearize Eq. (2.184) for small excursions about $x = \pi/4$.

$$\frac{d^2x}{dt^2} + 2\frac{dx}{dt} + \cos x = 0 \qquad (2.184)$$

SOLUTION: The presence of the term $\cos x$ makes this equation nonlinear. Since we want to linearize the equation about $x = \pi/4$, we let $x = \delta x + \pi/4$, where δx is the small excursion about $\pi/4$, and substitute x into Eq. (2.184):

$$\frac{d^2\left(\delta x + \dfrac{\pi}{4}\right)}{dt^2} + 2\frac{d\left(\delta x + \dfrac{\pi}{4}\right)}{dt} + \cos\left(\delta x + \frac{\pi}{4}\right) = 0 \qquad (2.185)$$

But

$$\frac{d^2\left(\delta x + \dfrac{\pi}{4}\right)}{dt^2} = \frac{d^2\delta x}{dt^2} \qquad (2.186)$$

and

$$\frac{d\left(\delta x + \dfrac{\pi}{4}\right)}{dt} = \frac{d\delta x}{dt} \qquad (2.187)$$

Finally, the term $\cos\left(\delta x + (\pi/4)\right)$ can be linearized with the truncated Taylor series. Substituting $f(x) = \cos(\delta x + (\pi/4))$, $f(x_0) = f(\pi/4) = \cos(\pi/4)$, and $(x - x_0) = \delta x$ into Eq. (2.182) yields

$$\cos\left(\delta x + \frac{\pi}{4}\right) - \cos\left(\frac{\pi}{4}\right) = \frac{d\cos x}{dx}\bigg|_{x=\frac{\pi}{4}} \delta x = -\sin\left(\frac{\pi}{4}\right)\delta x \qquad (2.188)$$

Solving Eq. (2.188) for $\cos\left(\delta x + (\pi/4)\right)$, we get

$$\cos\left(\delta x + \frac{\pi}{4}\right) = \cos\left(\frac{\pi}{4}\right) - \sin\left(\frac{\pi}{4}\right)\delta x = \frac{\sqrt{2}}{2} - \frac{\sqrt{2}}{2}\delta x \qquad (2.189)$$

Substituting Eqs. (2.186), (2.187), and (2.189) into Eq. (2.185) yields the following linearized differential equation:

$$\frac{d^2\delta x}{dt^2} + 2\frac{d\delta x}{dt} - \frac{\sqrt{2}}{2}\delta x = -\frac{\sqrt{2}}{2} \qquad (2.190)$$

This equation can now be solved for δx, from which we can obtain $x = \delta x + (\pi/4)$.

Even though the nonlinear Eq. (2.184) is homogeneous, the linearized Eq. (2.190) is not homogeneous. Eq. (2.190) has a forcing function on its right-hand side. This additional term can be thought of as an input to a system represented by Eq. (2.184).

Another observation about Eq. (2.190) is the negative sign on the left-hand side. The study of differential equations tells us that since the roots of the characteristic equation are positive, the homogeneous solution grows without bound instead of diminishing to zero. Thus, this system linearized around $x = \pi/4$ is not stable.

Example 2.28

Transfer Function—Nonlinear Electrical Network
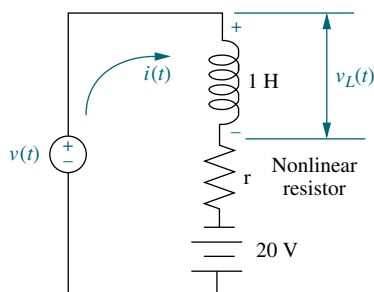
FIGURE 2.49 Nonlinear electrical network

PROBLEM: Find the transfer function, $V_L(s)/V(s)$, for the electrical network shown in Figure 2.49, which contains a nonlinear resistor whose voltage-current relationship is defined by $i_r = 2e^{0.1v_r}$, where i_r and v_r are the resistor current and voltage, respectively. Also, $v(t)$ in Figure 2.49 is a small-signal source.

SOLUTION: We will use Kirchhoff's voltage law to sum the voltages in the loop to obtain the nonlinear differential equation, but first we must solve for the voltage across the nonlinear resistor. Taking the natural log of the resistor's current-voltage relationship, we get $v_r = 10 \ln \frac{1}{2} i_r$. Applying Kirchhoff's voltage law around the loop, where $i_r = i$, yields

$$L\frac{di}{dt} + 10 \ln \frac{1}{2}i - 20 = v(t) \tag{2.191}$$

Next, let us evaluate the equilibrium solution. First, set the small-signal source, $v(t)$, equal to zero. Now evaluate the steady-state current. With $v(t) = 0$, the circuit consists of a 20 V battery in series with the inductor and nonlinear resistor. In the steady state, the voltage across the inductor will be zero, since $v_L(t) = Ldi/dt$ and di/dt is zero in the steady state, given a constant battery source. Hence, the resistor voltage, v_r, is 20 V. Using the characteristics of the resistor, $i_r = 2e^{0.1v_r}$, we find that $i_r = i = 14.78$ amps. This current, i_0, is the equilibrium value of the network current. Hence $i = i_0 + \delta i$. Substituting this current into Eq. (2.191) yields

$$L\frac{d(i_0 + \delta i)}{dt} + 10 \ln \frac{1}{2}(i_0 + \delta i) - 20 = v(t) \tag{2.192}$$

Using Eq. (2.182) to linearize $\ln \frac{1}{2}(i_0 + \delta i)$, we get

$$\ln \frac{1}{2}(i_0 + \delta i) - \ln \frac{1}{2}i_0 = \frac{d\left(\ln \frac{1}{2}i\right)}{di}\bigg|_{i=i_0} \delta i = \frac{1}{i}\bigg|_{i=i_0} \delta i = \frac{1}{i_0}\delta i \tag{2.193}$$

or

$$\ln \frac{1}{2}(i_0 + \delta i) = \ln \frac{i_0}{2} + \frac{1}{i_0}\delta i \tag{2.194}$$

Substituting into Eq. (2.192), the linearized equation becomes

$$L\frac{d\delta i}{dt} + 10 \left(\ln \frac{i_0}{2} + \frac{1}{i_0}\delta i\right) - 20 = v(t) \tag{2.195}$$

Letting $L = 1$ and $i_0 = 14.78$, the final linearized differential equation is

$$\frac{d\delta i}{dt} + 0.677\delta i = v(t) \tag{2.196}$$

Taking the Laplace transform with zero initial conditions and solving for $\delta i(s)$, we get

$$\delta i(s) = \frac{V(s)}{s + 0.677} \tag{2.197}$$

But the voltage across the inductor about the equilibrium point is

$$v_L(t) = L\frac{d}{dt}(i_0 + \delta i) = L\frac{d\delta i}{dt} \tag{2.198}$$

Taking the Laplace transform,

$$V_L(s) = Ls\delta i(s) = s\delta i(s) \tag{2.199}$$

Substituting Eq. (2.197) into Eq. (2.199) yields

$$V_L(s) = s\frac{V(s)}{s + 0.677} \tag{2.200}$$

from which the final transfer function is

$$\frac{V_L(s)}{V(s)} = \frac{s}{s + 0.677} \tag{2.201}$$

for small excursions about $i = 14.78$ or, equivalently, about $v(t) = 0$.

Skill-Assessment Exercise 2.13

PROBLEM: Find the linearized transfer function, $G(s) = V(s)/I(s)$, for the electrical network shown in Figure 2.50. The network contains a nonlinear resistor whose voltage-current relationship is defined by $i_r = e^{v_r}$. The current source, $i(t)$, is a small-signal generator.

WileyPLUS
WPCS
Control Solutions

ANSWER: $G(s) = \dfrac{1}{s + 2}$

The complete solution is at www.wiley.com/college/nise.
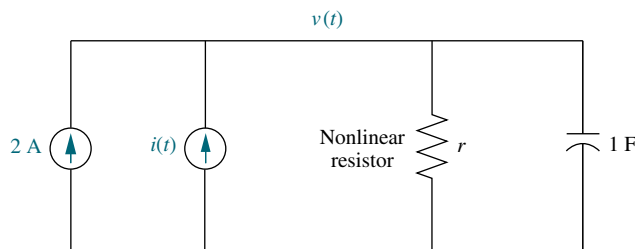
FIGURE 2.50   Nonlinear electric circuit for Skill-Assessment Exercise 2.13

Case Studies

Antenna Control: Transfer Functions

This chapter showed that physical systems can be modeled mathematically with transfer functions. Typically, systems are composed of subsystems of different types, such as electrical, mechanical, and electromechanical.

The first case study uses our ongoing example of the antenna azimuth position control system to show how to represent each subsystem as a transfer function.

PROBLEM: Find the transfer function for each subsystem of the antenna azimuth position control system schematic shown on the front endpapers. Use Configuration 1.

SOLUTION: First, we identify the individual subsystems for which we must find transfer functions; they are summarized in Table 2.6. We proceed to find the transfer function for each subsystem.

TABLE 2.6 Subsystems of the antenna azimuth position control system

Subsystem	Input	Output
Input potentiometer	Angular rotation from user, $\theta_i(t)$	Voltage to preamp, $v_i(t)$
Preamp	Voltage from potentiometers, $v_e(t) = v_i(t) - v_0(t)$	Voltage to power amp, $v_p(t)$
Power amp	Voltage from preamp, $v_p(t)$	Voltage to motor, $e_a(t)$
Motor	Voltage from power amp, $e_a(t)$	Angular rotation to load, $\theta_0(t)$
Output potentiometer	Angular rotation from load, $\theta_0(t)$	Voltage to preamp, $v_0(t)$

Input Potentiometer; Output Potentiometer

Since the input and output potentiometers are configured in the same way, their transfer functions will be the same. We *neglect* the dynamics for the potentiometers and simply find the relationship between the output voltage and the input angular displacement. In the center position the output voltage is zero. Five turns toward either the positive 10 volts or the negative 10 volts yields a voltage change of 10 volts. Thus, the transfer function, $V_i(s)/\theta_i(s)$, for the potentiometers is found by dividing the voltage change by the angular displacement:

$$\frac{V_i(s)}{\theta_i(s)} = \frac{10}{10\pi} = \frac{1}{\pi} \tag{2.202}$$

Preamplifier; Power Amplifier

The transfer functions of the amplifiers are given in the problem statement. Two phenomena are *neglected*. First, we *assume* that saturation is never reached. Second, the dynamics of the preamplifier are *neglected*, since its speed of response is typically much greater than that of the power amplifier. The transfer functions of both amplifiers are given in the problem statement and are the ratio of the Laplace transforms of the output voltage divided by the input voltage. Hence, for the

preamplifier,

$$\frac{V_p(s)}{V_e(s)} = K \qquad (2.203)$$

and for the power amplifier,

$$\frac{E_a(s)}{V_p(s)} = \frac{100}{s + 100} \qquad (2.204)$$

Motor and Load

The motor and its load are next. The transfer function relating the armature displacement to the armature voltage is given in Eq. (2.153). The equivalent inertia, J_m, is

$$J_m = J_a + J_L \left(\frac{25}{250}\right)^2 = 0.02 + 1\frac{1}{100} = 0.03 \qquad (2.205)$$

where $J_L = 1$ is the load inertia at θ_0. The equivalent viscous damping, D_m, at the armature is

$$D_m = D_a + D_L \left(\frac{25}{250}\right)^2 = 0.01 + 1\frac{1}{100} = 0.02 \qquad (2.206)$$

where D_L is the load viscous damping at θ_0. From the problem statement, $K_t = 0.5$ N-m/A, $K_b = 0.5$ V-s/rad, and the armature resistance $R_a = 8$ ohms. These quantities along with J_m and D_m are substituted into Eq. (2.153), yielding the transfer function of the motor from the armature voltage to the armature displacement, or

$$\frac{\theta_m(s)}{E_a(s)} = \frac{K_t/(R_a J_m)}{s\left[s + \frac{1}{J_m}\left(D_m + \frac{K_t K_b}{R_a}\right)\right]} = \frac{2.083}{s(s + 1.71)} \qquad (2.207)$$

To complete the transfer function of the motor, we multiply by the gear ratio to arrive at the transfer function relating load displacement to armature voltage:

$$\frac{\theta_0(s)}{E_a(s)} = 0.1\frac{\theta_m(s)}{E_a(s)} = \frac{0.2083}{s(s + 1.71)} \qquad (2.208)$$

The results are summarized in the block diagram and table of block diagram parameters (Configuration 1) shown on the front endpapers.

CHALLENGE: We now give you a problem to test your knowledge of this chapter's objectives: Referring to the antenna azimuth position control system schematic shown on the front endpapers, evaluate the transfer function of each subsystem. Use Configuration 2. Record your results in the table of block diagram parameters shown on the front endpapers for use in subsequent chapters' case study challenges.

Transfer Function of a Human Leg

In this case study we find the transfer function of a biological system. The system is a human leg, which pivots from the hip joint. In this problem, the component of weight is nonlinear, so the system requires linearization before the evaluation of the transfer function.

Hip joint

T_m

θ

$Mg \sin \theta$

Leg

$L/2$

$L/2$

Mg
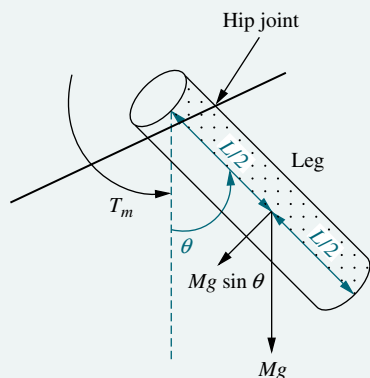
FIGURE 2.51   Cylinder model of a human leg.

PROBLEM: The transfer function of a human leg relates the output angular rotation about the hip joint to the input torque supplied by the leg muscle. A simplified model for the leg is shown in Figure 2.51. The model *assumes* an applied muscular torque, $T_m(t)$, viscous damping, D, at the hip joint, and inertia, J, around the hip joint.[15] Also, a component of the weight of the leg, Mg, where M is the mass of the leg and g is the acceleration due to gravity, creates a nonlinear torque. If we *assume* that the leg is of uniform density, the weight can be applied at $L/2$, where L is the length of the leg (*Milsum, 1966*). Do the following:

a. Evaluate the nonlinear torque.

b. Find the transfer function, $\theta(s)/T_m(s)$, for small angles of rotation, where $\theta(s)$ is the angular rotation of the leg about the hip joint.

SOLUTION: First, calculate the torque due to the weight. The total weight of the leg is Mg acting vertically. The component of the weight in the direction of rotation is $Mg \sin \theta$. This force is applied at a distance $L/2$ from the hip joint. Hence the torque in the direction of rotation, $T_W(t)$, *is* $Mg(L/2) \sin \theta$. Next, draw a free-body diagram of the leg, showing the applied torque, $T_m(t)$, the torque due to the weight, $T_W(t)$, and the opposing torques due to inertia and viscous damping (see Figure 2.52).

θ $J\dfrac{d^2\theta}{dt^2}$ $D\dfrac{d\theta}{dt}$

$T_m(t)$ Leg $T_W(t)$

FIGURE 2.52   Free-body diagram of leg model

Summing torques, we get

$$J\frac{d^2\theta}{dt^2} + D\frac{d\theta}{dt} + Mg\frac{L}{2}\sin\theta = T_m(t) \qquad (2.209)$$

We linearize the system about the equilibrium point, $\theta = 0$, the vertical position of the leg. Using Eq. (2.182), we get

$$\sin\theta - \sin 0 = (\cos 0)\delta\,\theta \qquad (2.210)$$

from which, $\sin\theta = \delta\theta$. Also, $J\,d^2\theta/dt^2 = J\,d^2\delta\theta/dt^2$ and $D\,d\theta/dt = D\,d\delta\theta/dt$. Hence Eq. (2.209) becomes

$$J\frac{d^2\delta\theta}{dt^2} + D\frac{d\delta\theta}{dt} + Mg\frac{L}{2}\delta\theta = T_m(t) \qquad (2.211)$$

Notice that the torque due to the weight approximates a spring torque on the leg. Taking the Laplace transform with zero initial conditions yields

$$\left(Js^2 + Ds + Mg\frac{L}{2}\right)\delta\theta(s) = T_m(s) \qquad (2.212)$$

from which the transfer function is

$$\frac{\delta\theta(s)}{T_m(s)} = \frac{1/J}{s^2 + \frac{D}{J}s + \frac{MgL}{2J}} \qquad (2.213)$$

---

[15] For emphasis, J is not around the center of mass, as we previously assumed for inertia in mechanical rotation.

for small excursions about the equilibrium point, $\theta = 0$.

CHALLENGE: We now introduce a case study challenge to test your knowledge of this chapter's objectives. Although the physical system is different from a human leg, the problem demonstrates the same principles: linearization followed by transfer function evaluation.

Given the nonlinear electrical network shown in Figure 2.53, find the transfer function relating the output nonlinear resistor voltage, $V_r(s)$, to the input source voltage, $V(s)$.
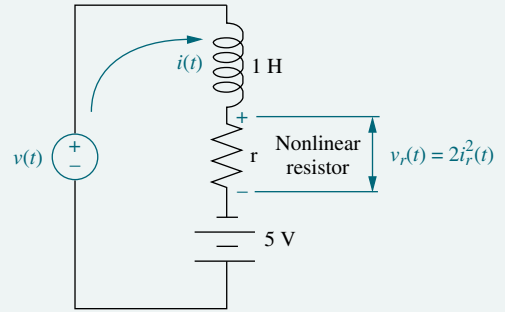
FIGURE 2.53 Nonlinear electric circuit

(Summary)

In this chapter, we discussed how to find a mathematical model, called a *transfer function*, for linear, time-invariant electrical, mechanical, and electromechanical systems. The transfer function is defined as $G(s) = C(s)/R(s)$, or the ratio of the Laplace transform of the output to the Laplace transform of the input. This relationship is algebraic and also adapts itself to modeling interconnected subsystems.

We realize that the physical world consists of more systems than we illustrated in this chapter. For example, we could apply transfer function modeling to hydraulic, pneumatic, heat, and even economic systems. Of course, we must assume these systems to be linear, or make linear approximations, in order to use this modeling technique.

Now that we have our transfer function, we can evaluate its response to a specified input. System response will be covered in Chapter 4. For those pursuing the state-space approach, we continue our discussion of modeling in Chapter 3, where we use the time domain rather than the frequency domain.

(Review Questions)

1. What mathematical model permits easy interconnection of physical systems?
2. To what classification of systems can the transfer function be best applied?
3. What transformation turns the solution of differential equations into algebraic manipulations?
4. Define the transfer function.
5. What assumption is made concerning initial conditions when dealing with transfer functions?
6. What do we call the mechanical equations written in order to evaluate the transfer function?
7. If we understand the form the mechanical equations take, what step do we avoid in evaluating the transfer function?
8. Why do transfer functions for mechanical networks look identical to transfer functions for electrical networks?

9. What function do gears perform?

10. What are the component parts of the mechanical constants of a motor's transfer function?

11. The motor's transfer function relates armature displacement to armature voltage. How can the transfer function that relates load displacement and armature voltage be determined?

12. Summarize the steps taken to linearize a nonlinear system.

Problems

1. Derive the Laplace transform for the following time functions: [Section: 2.2]

  a. $u(t)$

  b. $tu(t)$

  c. $\sin \omega t\, u(t)$

  d. $\cos \omega t\, u(t)$

2. Using the Laplace transform pairs of Table 2.1 and the Laplace transform theorems of Table 2.2, derive the Laplace transforms for the following time functions: [Section: 2.2]

WileyPLUS

WPCS

Control Solutions

  a. $e^{-at}\sin \omega t\, u(t)$

  b. $e^{-at}\cos \omega t\, u(t)$

  c. $t^3 u(t)$

3. Repeat Problem 18 in Chapter 1, using Laplace transforms. Assume that the forcing functions are zero prior to $t = 0-$. [Section: 2.2]

4. Repeat Problem 19 in Chapter 1, using Laplace transforms. Use the following initial conditions for each part as follows: (a) $x(0) = 4$, $x'(0) = -4$; (b) $x(0) = 4$, $x'(0) = 1$; (c) $x(0) = 2$, $x'(0) = 3$, where $x'(0) = \dfrac{dx}{dt}(0)$. Assume that the forcing functions are zero prior to $t = 0-$. [Section: 2.2]

5. Use MATLAB and the Symbolic Math Toolbox to find the Laplace transform of the following time functions: [Section: 2.2]

Symbolic Math

SM

  a. $f(t) = 8t^2\cos(3t + 45°)$

  b. $f(t) = 3te^{-2t}\sin(4t + 60°)$

6. Use MATLAB and the Symbolic Math Toolbox to find the inverse

Symbolic Math

SM

Laplace transform of the following frequency functions: [Section: 2.2]

  a. $G(s) = \dfrac{(s^2 + 3s + 10)(s + 5)}{(s + 3)(s + 4)(s^2 + 2s + 100)}$

  b. $G(s) = \dfrac{s^3 + 4s^2 + 2s + 6}{(s + 8)(s^2 + 8s + 3)(s^2 + 5s + 7)}$

7. A system is described by the following differential equation:

$$\frac{d^3y}{dt^3} + 3\frac{d^2y}{dt^2} + 5\frac{dy}{dt} + y = \frac{d^3x}{dt^3} + 4\frac{d^2x}{dt^2} + 6\frac{dx}{dt} + 8x$$

Find the expression for the transfer function of the system, $Y(s)/X(s)$. [Section: 2.3]

8. For each of the following transfer functions, write the corresponding differential equation. [Section: 2.3]

  a. $\dfrac{X(s)}{F(s)} = \dfrac{7}{s^2 + 5s + 10}$

  b. $\dfrac{X(s)}{F(s)} = \dfrac{15}{(s + 10)(s + 11)}$

  c. $\dfrac{X(s)}{F(s)} = \dfrac{s + 3}{s^3 + 11s^2 + 12s + 18}$

9. Write the differential equation for the system shown in Figure P2.1. [Section: 2.3]

$$R(s) \longrightarrow \boxed{\dfrac{s^5 + 2s^4 + 4s^3 + s^2 + 4}{s^6 + 7s^5 + 3s^4 + 2s^3 + s^2 + 5}} \longrightarrow C(s)$$
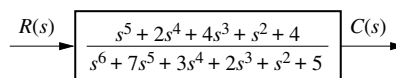
FIGURE P2.1

10. Write the differential equation that is mathematically equivalent to the

WileyPLUS

WPCS

Control Solutions

block diagram shown in Figure P2.2. Assume that $r(t) = 3t^3$. [Section: 2.3]
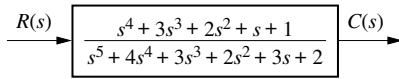
FIGURE P2.2

11. A system is described by the following differential equation: [Section 2.3]

$$\frac{d^2x}{dt^2} + 2\frac{dx}{dt} + 3x = 1$$

with the initial conditions $x(0) = 1$, $\dot{x}(0) = -1$. Show a block diagram of the system, giving its transfer function and all pertinent inputs and outputs. (Hint: the initial conditions will show up as added inputs to an effective system with zero initial conditions.)

12. Use MATLAB to generate the transfer function: [Section: 2.3]   MATLAB **ML**

$$G(s) = \frac{5(s+15)(s+26)(s+72)}{s(s+55)(s^2+5s+30)(s+56)(s^2+27s+52)}$$

in the following ways:

a. the ratio of factors;

b. the ratio of polynomials.

13. Repeat Problem 12 for the following transfer function: [Section: 2.3]   MATLAB **ML**

$$G(s) = \frac{s^4 + 25s^3 + 20s^2 + 15s + 42}{s^5 + 13s^4 + 9s^3 + 37s^2 + 35s + 50}$$

14. Use MATLAB to generate the partial-fraction expansion of the following function: [Section: 2.3]

$$F(s) = \frac{10^4(s+5)(s+70)}{s(s+45)(s+55)(s^2+7s+110)(s^2+6s+95)}$$

15. Use MATLAB and the Symbolic Math Toolbox to input and form LTI objects in polynomial and factored form for the following frequency functions: [Section: 2.3]   Symbolic Math **SM**

a. $G(s) = \frac{45(s^2+37s+74)(s^3+28s^2+32s+16)}{(s+39)(s+47)(s^2+2s+100)(s^3+27s^2+18s+15)}$

b. $G(s) = \frac{56(s+14)(s^3+49s^2+62s+53)}{(s^3+81s^2+76s+65)(s^2+88s+33)(s^2+56s+77)}$

16. Find the transfer function, $G(s) = V_o(s)/V_i(s)$, for each network shown in Figure P2.3. [Section: 2.4]
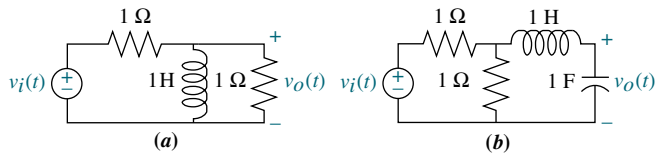
FIGURE P2.3

17. Find the transfer function, $G(s) = V_L(s)/V(s)$, for each network shown in Figure P2.4. [Section: 2.4]
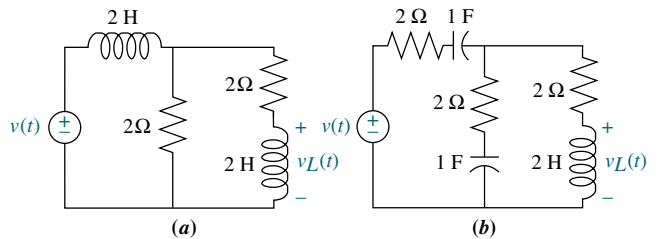
FIGURE P2.4

18. Find the transfer function, $G(s) = V_o(s)/V_i(s)$, for each network shown in Figure P2.5. Solve the problem using mesh analysis. [Section: 2.4]   WileyPLUS **WPCS** Control Solutions
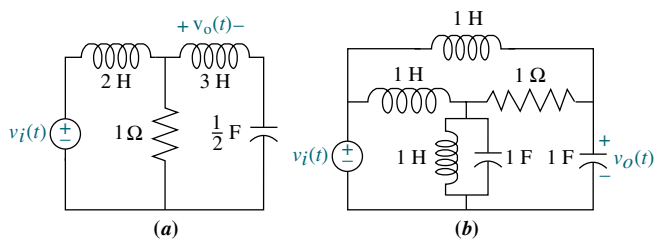
FIGURE P2.5

19. Repeat Problem 18 using nodal equations. [Section: 2.4]

20. a. Write, but do not solve, the mesh and nodal equations for the network of Figure P2.6. [Section: 2.4]

b. Use MATLAB, the Symbolic Math Toolbox, and the equations found in part a to solve for the transfer function, $G(s) = V_o(s)/V(s)$. Use both the   Symbolic Math **SM**

mesh and nodal equations and show
that either set yields the same transfer
function. [Section: 2.4]
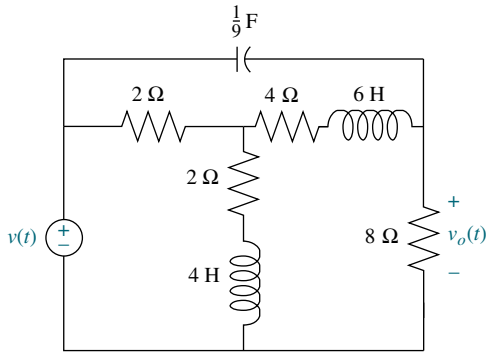
FIGURE P2.6
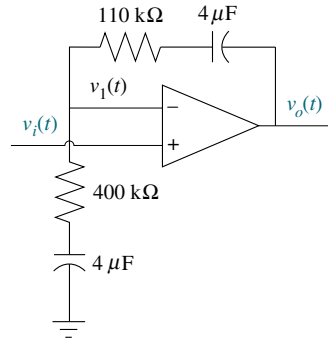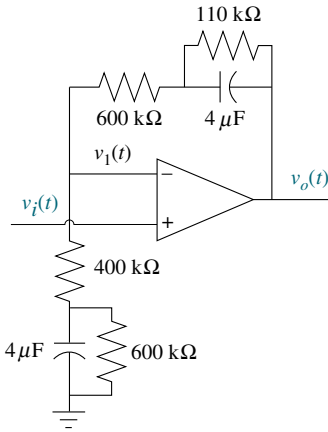
21. Find the transfer function, $G(s) = V_o(s)/V_i(s)$, for
each operational amplifier circuit shown in Figure
P2.7. [Section: 2.4]
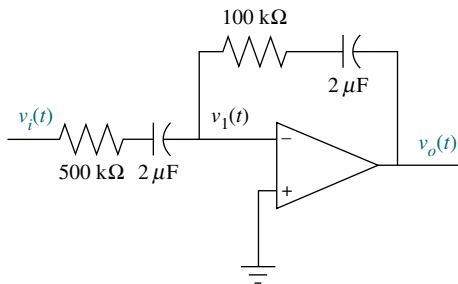
(*a*)
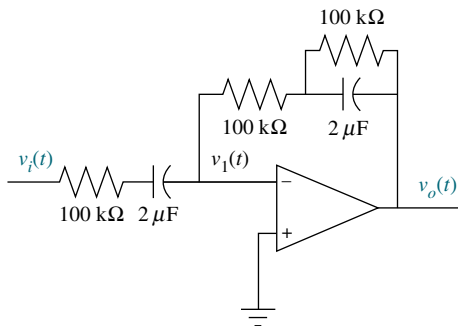
(*b*)

FIGURE P2.7

22. Find the transfer function, $G(s) = V_o(s)/V_i(s)$, for
each operational amplifier circuit shown in Figure
P2.8. [Section: 2.4]

(*a*)

(*b*)

FIGURE P2.8

23. Find the transfer function, $G(s) = X_1(s)/F(s)$, for
the translational mechanical system shown in Figure
P2.9. [Section: 2.5]
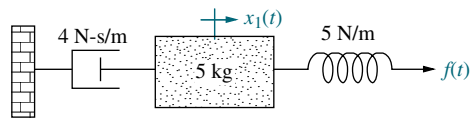
FIGURE P2.9

24. Find the transfer function, $G(s) = X_2(s)/F(s)$, for
the translational mechanical network shown in
Figure P2.10. [Section: 2.5]
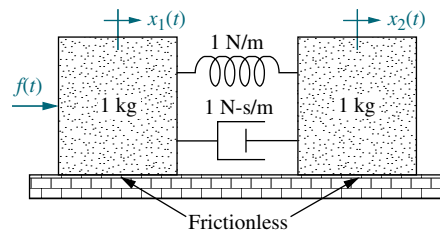
FIGURE P2.10

25. Find the transfer function, $G(s) = X_2(s)/F(s)$, for the translational mechanical system shown in Figure P2.11. (Hint: place a zero mass at $x_2(t)$.) [Section: 2.5]
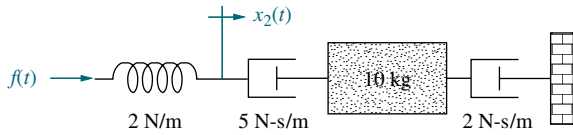
FIGURE P2.11

26. For the system of Figure P2.12 find the transfer function, $G(s) = X_1(s)/F(s)$. [Section: 2.5]
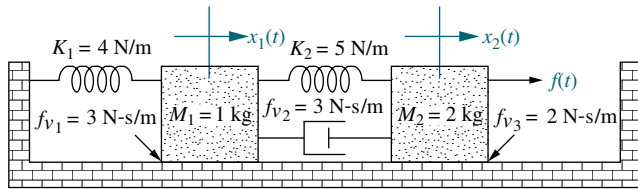
FIGURE P2.12

27. Find the transfer function, $G(s) = X_3(s)/F(s)$, for the translational mechanical system shown in Figure P2.13. [Section: 2.5]
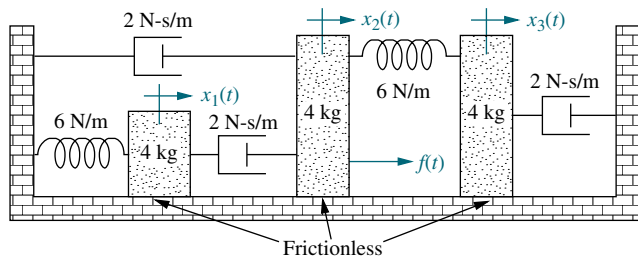
FIGURE P2.13

28. Find the transfer function, $X_3(s)/F(s)$, for each system shown in Figure P2.14. [Section: 2.5]

(*a*)

(*b*)
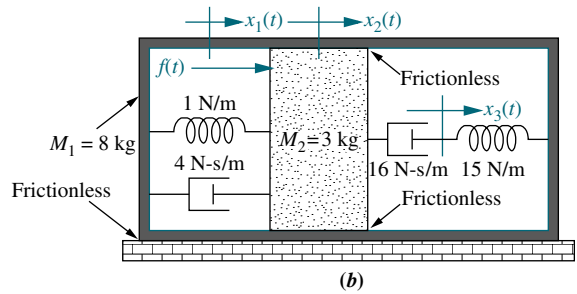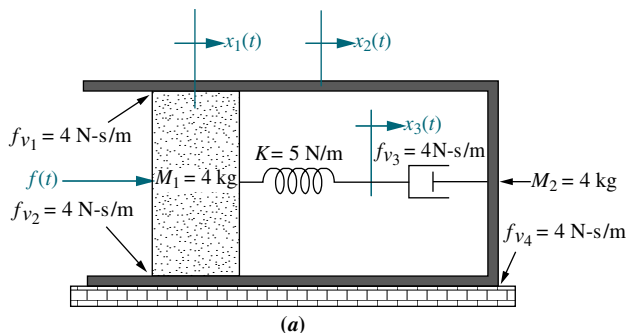
FIGURE P2.14

29. Write, but do not solve, the equations of motion for the translational mechanical system shown in Figure P2.15. [Section: 2.5]
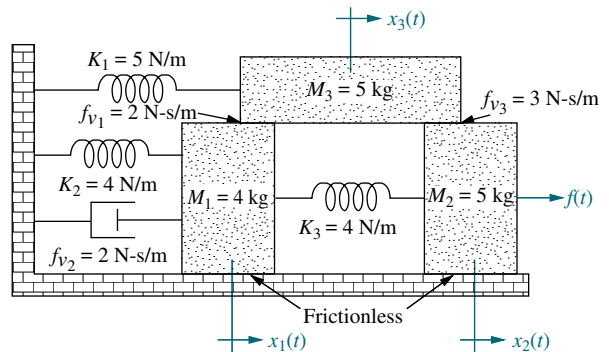
FIGURE P2.15

30. For each of the rotational mechanical systems shown in Figure P2.16, write, but do not solve, the equations of motion. [Section: 2.6]

(*a*)

(*b*)
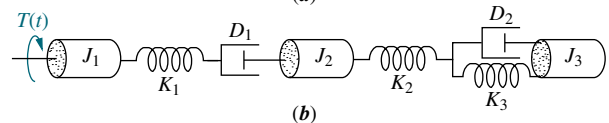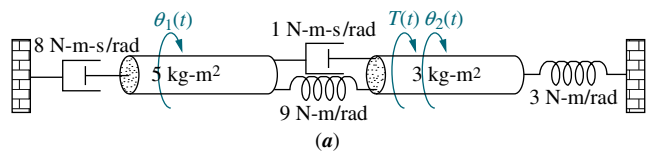
FIGURE P2.16

31. For the rotational mechanical system shown in Figure P2.17, find the transfer function $G(s) = \theta_2(s)/T(s)$ [Section: 2.6]
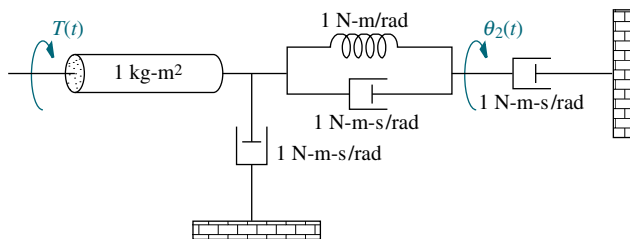
FIGURE P2.17

32. For the rotational mechanical system with gears shown in Figure P2.18, find the transfer function, $G(s) = \theta_3(s)/T(s)$. The gears have inertia and bearing friction as shown. [Section: 2.7]
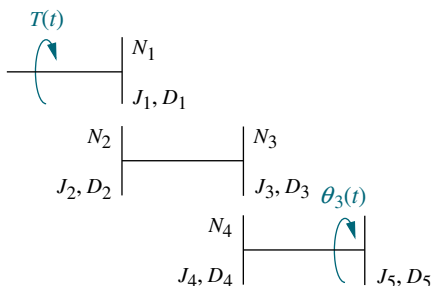
FIGURE P2.18

33. For the rotational system shown in Figure P2.19, find the transfer function, $G(s) = \theta_2(s)/T(s)$. [Section: 2.7]
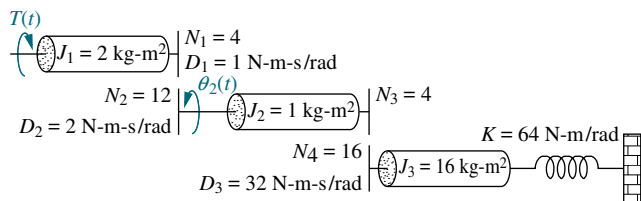
FIGURE P2.19

34. Find the transfer function, $G(s) = \theta_2(s)/T(s)$, for the rotational mechanical system shown in Figure P2.20. [Section: 2.7]
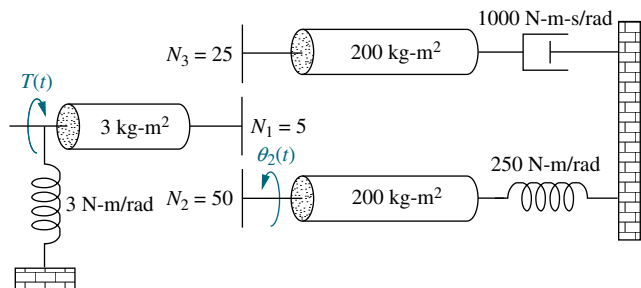
FIGURE P2.20

35. Find the transfer function, $G(s) = \theta_4(s)/T(s)$, for the rotational system shown in Figure P2.21. [Section: 2.7]
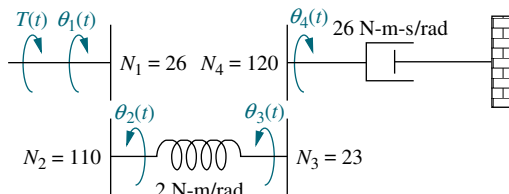
FIGURE P2.21

36. For the rotational system shown in Figure P2.22, find the transfer function, $G(s) = \theta_L(s)/T(s)$. [Section: 2.7]
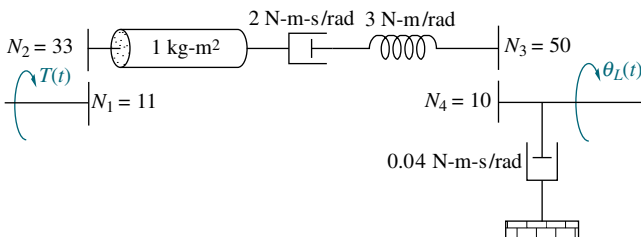
FIGURE P2.22

37. For the rotational system shown in Figure P2.23, write the equations of motion from which the transfer function, $G(s) = \theta_1(s)/T(s)$, can be found. [Section: 2.7]

WileyPLUS
WPCS
Control Solutions
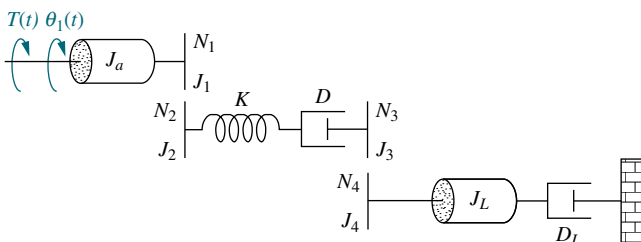
FIGURE P2.23

38. Given the rotational system shown in Figure P2.24, find the transfer function, $G(s) = \theta_6(s)/\theta_1(s)$. [Section: 2.7]
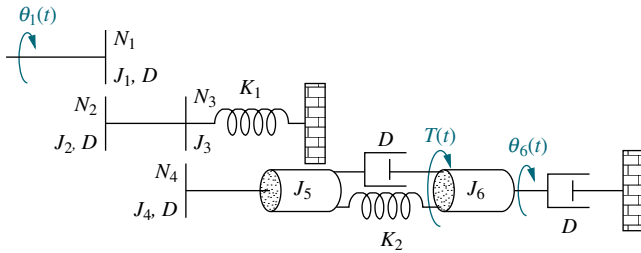
FIGURE P2.24

39. In the system shown in Figure P2.25, the inertia, J, of radius, r, is constrained to move only about the stationary axis A. A viscous damping force of translational value f_v exists between the bodies J and M. If an external force, $f(t)$, is applied to the mass, find the transfer function, $G(s) = \theta(s)/F(s)$. [Sections: 2.5; 2.6]
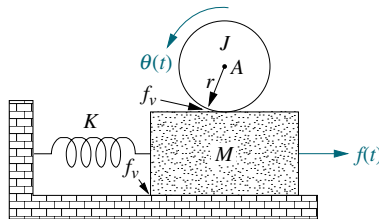
FIGURE P2.25

40. For the combined translational and rotational system shown in Figure P2.26, find the transfer function, $G(s) = X(s)/T(s)$. [Sections: 2.5; 2.6; 2.7]
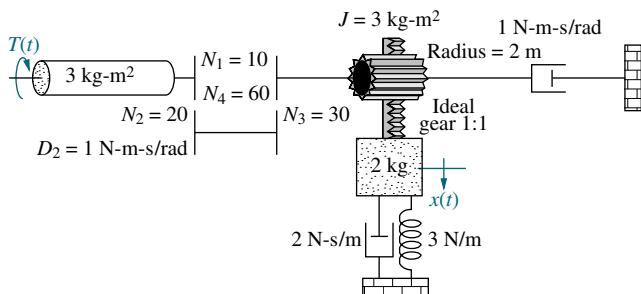
FIGURE P2.26

41. Given the combined translational and rotational system shown in Figure P2.27, find the transfer function, $G(s) = X(s)/T(s)$. [Sections: 2.5; 2.6]

WileyPLUS

WPCS

Control Solutions
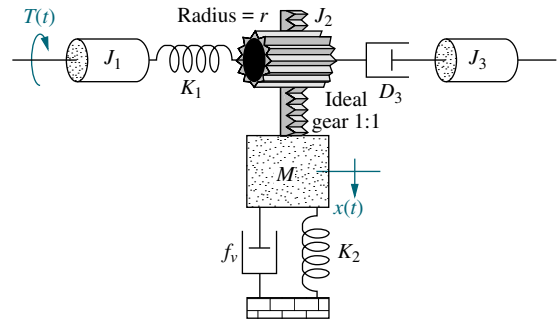
FIGURE P2.27

42. For the motor, load, and torque-speed curve shown in Figure P2.28, find the transfer function, $G(s) = \theta_L(s)/E_a(s)$. [Section: 2.8]
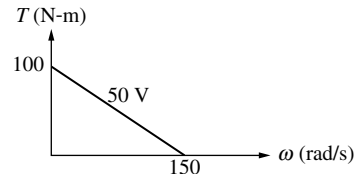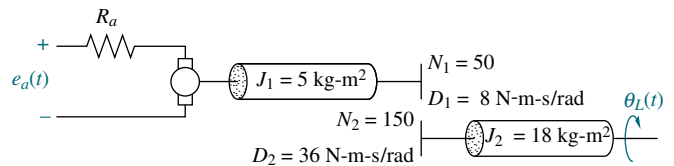
FIGURE P2.28

43. The motor whose torque-speed characteristics are shown in Figure P2.29 drives the load shown in the diagram. Some of the gears have inertia. Find the transfer function, $G(s) = \theta_2(s)/E_a(s)$. [Section: 2.8]
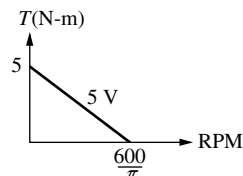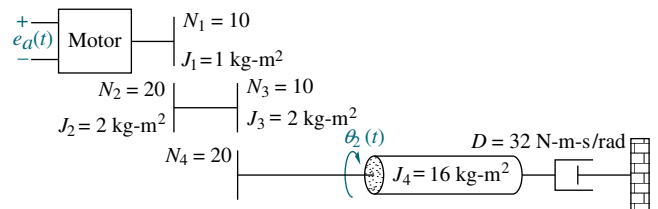
FIGURE P2.29

44. A dc motor develops 55 N-m of torque at a speed of 600 rad/s when 12 volts are applied. It stalls out at this voltage with 100 N-m of torque. If the inertia and damping of the armature are 7 kg-m^2 and 3 N-m-s/rad, respectively, find the transfer function, $G(s) = \theta_L(s)/E_a(s)$, of this motor if it drives an inertia load of 105 kg-m^2 through a gear train, as shown in Figure P2.30. [Section: 2.8]
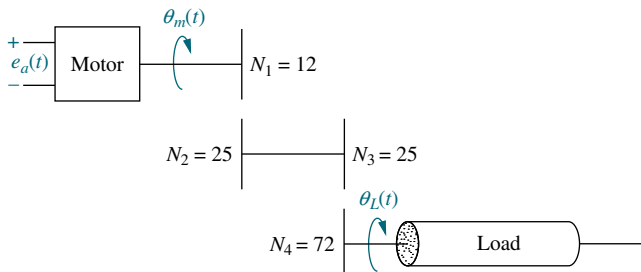
FIGURE P2.30

45. In this chapter, we derived the transfer function of a dc motor relating the angular displacement output to the armature voltage input. Often we want to control the output torque rather than the displacement. Derive the transfer function of the motor that relates output torque to input armature voltage. [Section: 2.8]

WileyPLUS
WPCS
Control Solutions

46. Find the transfer function, $G(s) = X(s)/E_a(s)$, for the system shown in Figure P2.31. [Sections: 2.5–2.8]
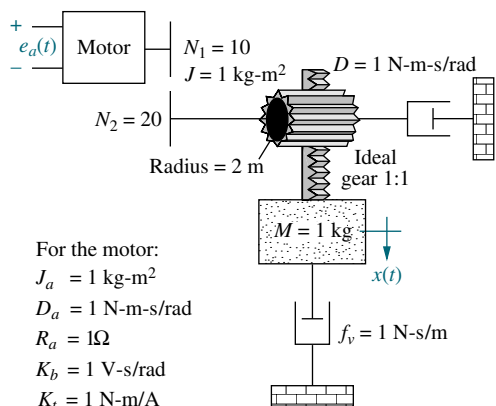
FIGURE P2.31

47. Find the series and parallel analogs for the translational mechanical system shown in Figure 2.20 in the text. [Section: 2.9]

48. Find the series and parallel analogs for the rotational mechanical systems shown in Figure P2.16(*b*) in the problems. [Section: 2.9]

49. A system's output, *c*, is related to the system's input, *r*, by the straight-line relationship, $c = 5r + 7$. Is the system linear? [Section: 2.10]

50. Consider the differential equation

$$\frac{d^2x}{dt^2} + 3\frac{dx}{dt} + 2x = f(x)$$

where $f(x)$ is the input and is a function of the output, *x*. If $f(x) = \sin x$, linearize the differential equation for small excursions. [Section: 2.10]

a. $x = 0$

b. $x = \pi$

51. Consider the differential equation

$$\frac{d^3x}{dt^3} + 10\frac{d^2x}{dt^2} + 31\frac{dx}{dt} + 30x = f(x)$$

where $f(x)$ is the input and is a function of the output, *x*. If $f(x) = e^{-x}$, linearize the differential equation for *x* near 0. [Section: 2.10]

WileyPLUS
WPCS
Control Solutions

52. Many systems are *piecewise* linear. That is, over a *large* range of variable values, the system can be described linearly. A system with amplifier saturation is one such example. Given the differential equation

$$\frac{d^2x}{dt^2} + 17\frac{dx}{dt} + 50x = f(x)$$

assume that $f(x)$ is as shown in Figure P2.32. Write the differential equation for each of the following ranges of *x*: [Section: 2.10]

a. $-\infty < x < -3$

b. $-3 < x < 3$

c. $3 < x < \infty$
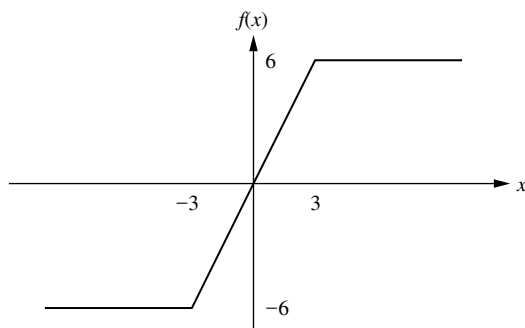
FIGURE P2.32

53. For the translational mechanical system with a nonlinear spring shown in Figure P2.33, find the transfer function, $G(s) = X(s)/F(s)$, for small excursions around $f(t) = 1$. The spring is defined by $x_s(t) = 1 - e^{-f_s(t)}$, where $x_s(t)$ is the spring displacement and $f_s(t)$ is the spring force. [Section: 2.10]

WileyPLUS

WPCS

Control Solutions
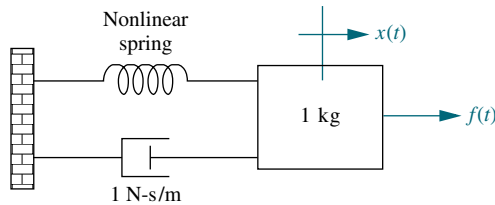
FIGURE P2.33

54. Consider the restaurant plate dispenser shown in Figure P2.34, which consists of a vertical stack of dishes supported by a compressed spring. As each plate is removed, the reduced weight on the dispenser causes the remaining plates to rise. Assume that the mass of the system minus the top plate is M, the viscous friction between the piston and the sides of the cylinder is f_v, the spring constant is K, and the weight of a single plate is W_D. Find the transfer function, $Y(s)/F(s)$, where $F(s)$ is the step reduction in force felt when the top plate is removed, and $Y(s)$ is the vertical displacement of the dispenser in an upward direction.
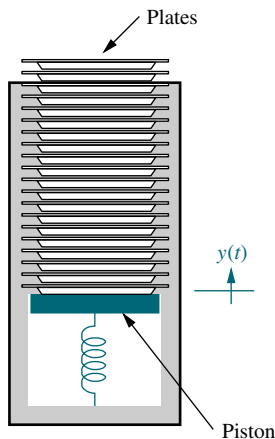
FIGURE P2.34 Plate dispenser

55. Each inner ear in a human has a set of three nearly perpendicular semicircular canals of about 0.28 mm in diameter filled with fluid. Hair-cell transducers that deflect with skull movements and whose main purpose is to work as attitude sensors as well as help us maintain our sense of direction and equilibrium are attached to the canals. As the hair cells move, they deflect a waterproof flap called the *cupula*. It has been shown that the skull and cupula movements are related by the following equation (*Milsum, 1966*):

$$J\ddot{\phi} + b\dot{\phi} + k\phi = (aJ)\ddot{\psi}$$

where

J = moment of inertia of the fluid in the thin tube (constant)

b = torque per unit relative angular velocity (constant)

k = torque per unit relative angular displacement (constant)

a = constant

$\phi(t)$ = angular deflection of the cupula (output)

$\ddot{\psi}(t)$ = skull's angular acceleration (input)

Find the transfer function $\dfrac{\Phi(s)}{\Psi(s)}$.

56. Diabetes is an illness that has risen to epidemic proportions, affecting about 3% of the total world population in 2003. A differential equation model that describes the total population size of diabetics is

$$\frac{dC(t)}{dt} = -(\lambda + \mu + \delta + \gamma + \nu)C(t) + \lambda N(t)$$

$$\frac{dN(t)}{dt} = -(\nu + \delta)C(t) - \mu N(t) + I(t)$$

with the initial conditions $C(0) = C_0$ and $N(0) = N_0$ and

$I(t)$ = the system input: the number of new cases of diabetes

$C(t)$ = number of diabetics with complications

$N(t)$ = the system output: the total number of diabetics with and without complications

μ = natural mortality rate (constant)

λ = probability of developing a complication (constant)

δ = mortality rate due to complications (constant)

ν = rate at which patients with complications become severely disabled (constant)

γ = rate at which complications are cured (constant)

Assume the following values for parameters: $\nu = \delta = 0.05/\text{yr}$, $\mu = 0.02/\text{yr}$, $\gamma = 0.08/\text{yr}$, $\lambda = 0.7$, with initial conditions $C_0 = 47{,}000{,}500$ and $N_0 =, 61{,}100{,}500$. Assume also that diabetic incidence is constant $I(t) = I = 6 \times 10^6$ (*Boutayeb, 2004*).

a. Draw a block diagram of the system showing the output $N(s)$, the input $I(s)$, the transfer function, and the initial conditions.

b. Use any method to find the analytic expression for $N(t)$ for $t \geq 0$.

57. The circuit shown in Figure P2.35(*a*) is excited with the pulse shown in Figure P2.35(*b*).

(a)   **(b)**
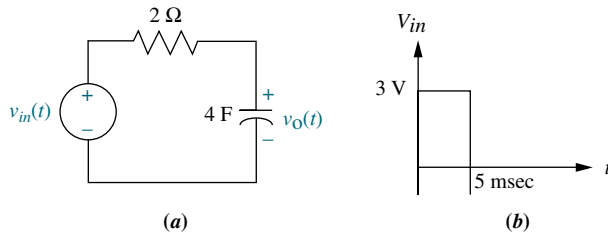
FIGURE P2.35

The Laplace transform can be used to calculate $v_o(t)$ in two different ways: The "exact" method is performed by writing $v_i(t) = 3[u(t) - u(t - 0.005)]$, from which we use the Laplace transform to obtain

$$V_{in}(s) = 3\frac{1 - e^{-0.005s}}{s}$$

(Hint: look at Item 5 in Table 2.2, the time shift theorem.) In the second approach the pulse is approximated by an impulse input having the same area (energy) as the original input. From Figure P2.35(*b*): $v_{in}(t) \approx (3\,\text{V})(5\,\text{msec})\ \delta(t) = 0.015\delta(t)$. In this case, $V_{in}(s) = 0.015$. This approximation can be used as long as the width of the pulse of Figure P2.35(*b*) is much smaller than the circuit's smallest time constant. (Here, $\tau = RC = (2\Omega)(4\,\text{F}) = 8\,\text{sec} \gg 5\,\text{msec}$.)

a. Assuming the capacitor is initially discharged, obtain an analytic expression for $v_o(t)$ using both methods.

b. Plot the results of both methods using any means available to you, and compare both outputs. Discuss the differences.

58. In a magnetic levitation experiment a metallic object is held up in the air suspended under an electromagnet. The vertical displacement of the object can be described by the following nonlinear differential equation (*Galvão, 2003*):

$$m\frac{d^2H}{dt^2} = mg - k\frac{I^2}{H^2}$$

where

$m =$ mass of the metallic object
$g\ =$ gravity acceleration constant
$k\ =$ a positive constant
$H =$ distance between the electromagnet and the metallic object (output signal)
$I\ =$ electromagnet/s current (input signal)

a. Show that a system's equilibrium will be achieved when $H_0 = I_0\sqrt{\frac{k}{mg}}$.

b. Linearize the equation about the equilibrium point found in Part **a** and show that the resulting transfer function obtained from the linearized differential equation can be expressed as

$$\frac{\delta H(s)}{\delta I(s)} = -\frac{a}{s^2 - b^2}$$

with $a > 0$. Hint: to perform the linearization, define $\delta H = H(t) - H_0$ and $\delta I = I(t) - I_0$; substitute into the original equation. This will give

$$m\frac{d^2(H_0 + \delta H)}{dt^2} = mg - k\frac{(I_0 + \delta I)^2}{(H_0 + \delta H)^2} = \gamma$$

Now get a first-order Taylor's series approximation on the right-hand side of the equation. Namely, calculate

$$m\frac{d^2\delta H}{dt^2} = \frac{\partial\gamma}{\partial\delta H}\bigg|_{\delta H=0,\ \delta I=0}\delta H + \frac{\partial\gamma}{\partial\delta I}\bigg|_{\delta H=0,\ \delta I=0}\delta I$$

59. Figure P2.36 shows a quarter-car model commonly used for analyzing suspension systems. The car's tire is considered to act as a spring without damping, as shown. The parameters of the model are (*Lin, 1997*)

$M_b\ =$ car's body mass
$M_{us} =$ wheel's mass
$K_a\ =$ strut's spring constant
$K_t\ =$ tire's spring constant
$f_v\ =$ strut's damping constant
$r\ =$ road disturbance (input)
$x_s\ =$ car's vertical displacement
$x_w =$ wheel's vertical displacement

Obtain the transfer function from the road disturbance to the car's vertical displacement $\frac{X_s(s)}{R(s)}$.
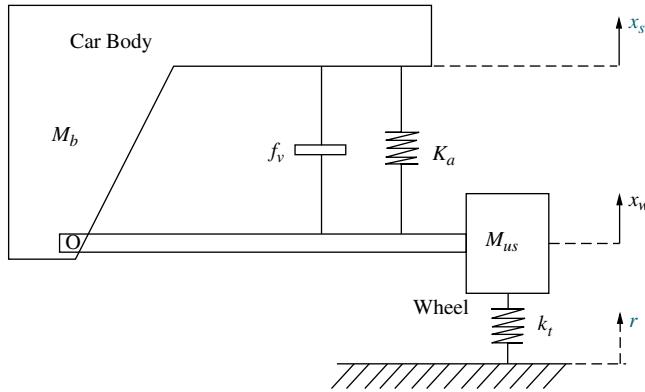
FIGURE P2.36 Quarter-car model used for suspension design. (© 1997 IEEE)

60. Enzymes are large proteins that biological systems use to increase the rate at which reactions occur. For example, food is usually composed of large molecules that are hard to digest; enzymes break down the large molecules into small nutrients as part of the digestive process. One such enzyme is amylase, contained in human saliva. It is commonly known that if you place a piece of uncooked pasta in your mouth its taste will change from paper-like to sweet as amylase breaks down the carbohydrates into sugars. Enzyme breakdown is often expressed by the following relation:

$$S + E \underset{k_1}{\overset{k_s}{\rightleftarrows}} C \overset{k_1}{\to} P$$
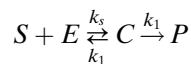
In this expression a substrate (S) interacts with an enzyme (E) to form a combined product (C) at a rate k_1. The intermediate compound is reversible and gets disassociated at a rate k_{-1}. Simultaneously some of the compound is transformed into the final product (P) at a rate k_2. The kinetics describing this reaction are known as the Michaelis-Menten equations and consist of four nonlinear differential equations. However, under some conditions these equations can be simplified. Let E_0 and S_0 be the initial concentrations of enzyme and substrate, respectively. It is generally accepted that under some energetic conditions or when the enzyme concentration is very big ($E_0 \gg S_0$),

the kinetics for this reaction are given by

$$\frac{dS}{dt} = k_\psi(\widetilde{K}_s C - S)$$

$$\frac{dC}{dt} = k_\psi(S - \widetilde{K}_M C)$$

$$\frac{dP}{dt} = k_2 C$$

where the following constant terms are used (*Schnell, 2004*) :

$$k_\psi = k_1 E_0$$

$$\widetilde{K}_s = \frac{k - 1}{k_\psi}$$

and

$$\widetilde{K}_M = \widetilde{K}_s + \frac{k_2}{k_\psi}$$

a. Assuming the initial conditions for the reaction are $S(0) = S_0$, $E(0) = E_0$, $C(0) = P(0) = 0$, find the Laplace transform expressions for S, C, and P: $\mathscr{L}\{S\}$, $\mathscr{L}\{C\}$, and $\mathscr{L}\{P\}$, respectively.

b. Use the final theorem to find $S(\infty)$, $C(\infty)$, and $P(\infty)$.

61. Humans are able to stand on two legs through a complex feedback system that includes several sensory inputs—equilibrium and visual along with muscle actuation. In order to gain a better understanding of the workings of the postural feedback mechanism, an individual is asked to stand on a platform to which sensors are attached at the base. Vibration actuators are attached with straps to the individual's calves. As the vibration actuators are stimulated, the individual sways and movements are recorded. It was hypothesized that the human postural dynamics are analogous to those of a cart with a balancing standing pole attached (inverted pendulum). In that case, the dynamics can be described by the following two equations:

$$J\frac{d^2\theta}{dt^2} = mgl \sin\theta(t) + T_{\text{bal}} + T_d(t)$$

$$T_{\text{bal}}(t) = -mgl \sin\theta(t) + kJ\theta(t) - \eta J\dot{\theta}(t)$$

$$-\rho J \int_0^t \theta(t)dt$$

where m is the individual's mass; l is the height of the individual's center of gravity; g is the gravitational constant; J is the individual's equivalent moment of inertia; η, ρ, and k are constants given by the body's postural control system; $\theta(t)$ is the

individual's angle with respect to a vertical line; $T_{bal}(t)$ is the torque generated by the body muscles to maintain balance; and $T_d(t)$ is the external torque input disturbance. Find the transfer function $\dfrac{\Theta(s)}{T_d(s)}$ (*Johansson, 1988*).

62. Figure P2.37 shows a crane hoisting a load. Although the actual system's model is highly nonlinear, if the rope is considered to be stiff with a fixed length L, the system can be modeled using the following equations:

$$m_L \ddot{x}_{La} = m_L g \phi$$

$$m_T \ddot{x}_T = f_T - m_L g \phi$$

$$x_{La} = x_T - x_L$$

$$x_L = L\phi$$

where m_L is the mass of the load, m_T is the mass of the cart, x_T and x_L are displacements as defined in the figure, ϕ is the rope angle with respect to the vertical, and f_T is the force applied to the cart (*Marttinen, 1990*).

a. Obtain the transfer function from cart velocity to rope angle $\dfrac{\Phi(s)}{V_T(s)}$.

b. Assume that the cart is driven at a constant velocity V_0 and obtain an expression for the resulting $\phi(t)$. Show that under this condition, the load will sway with a frequency $\omega_0 = \sqrt{\dfrac{g}{L}}$.

c. Find the transfer function from the applied force to the cart's position, $\dfrac{X_T(s)}{F_T(s)}$.

d. Show that if a constant force is applied to the cart, its velocity will increase without bound as $t \to \infty$.
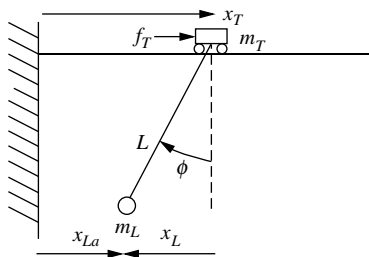
FIGURE P2.37   (© 1990 IEEE)

63. In 1978, Malthus developed a model for human growth population that is also commonly used to model bacterial growth as follows. Let $N(t)$ be the population density observed at time t. Let K be the rate of reproduction per unit time. Neglecting population deaths, the population density at a time $t + \Delta t$ (with small Δt) is given by

$$N(t + \Delta t) \approx N(t) + KN(t)\Delta t$$

which also can be written as

$$\frac{N(t + \Delta t) - N(t)}{\Delta t} = KN(t)$$

Since $N(t)$ can be considered to be a very large number, letting $\Delta t \to 0$ gives the following differential equation (*Edelstein-Keshet, 2005*):

$$\frac{dN(t)}{dt} = KN(t)$$

a. Assuming an initial population $N(0) = N_0$, solve the differential equation by finding $N(t)$.

b. Find the time at which the population is double the initial population.

64. Blood vessel blockages can in some instances be diagnosed through noninvasive techniques such as the use of sensitive microphones to detect flow acoustic anomalies. In order to predict the sound properties of the left coronary artery, a model has been developed that partitions the artery into 14 segments, as shown in Figure P2.38(*a*).

(*a*)

(b)

(c)
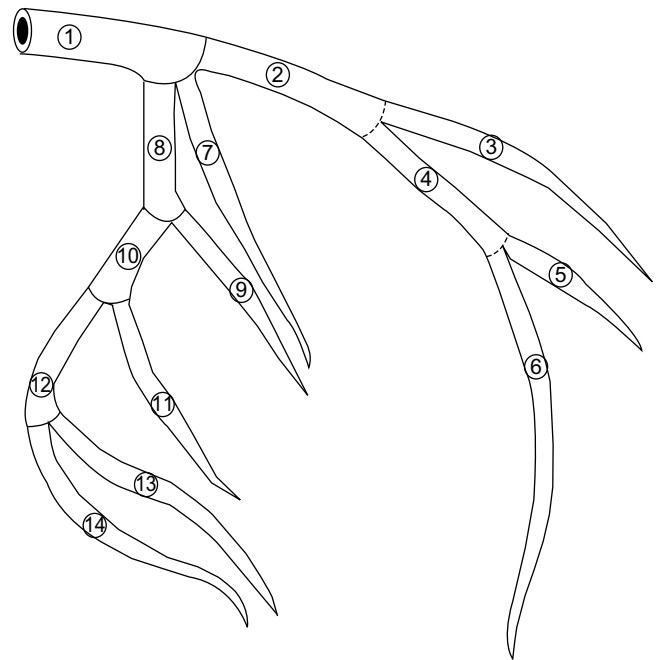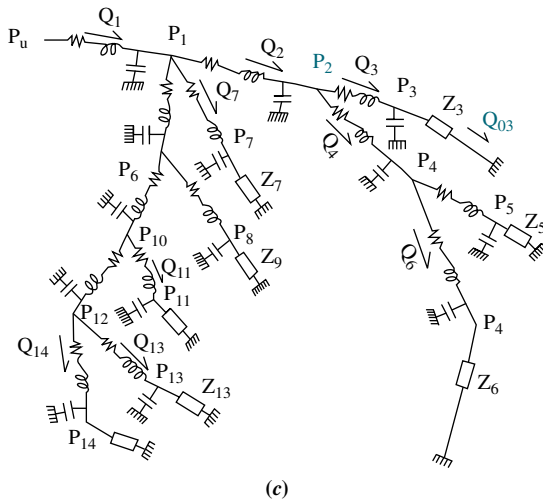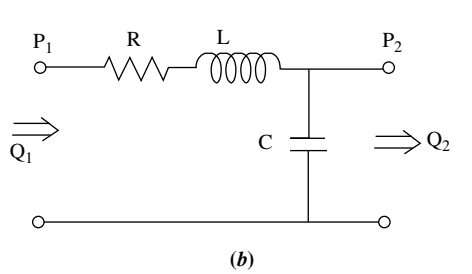
FIGURE P2.38 (© 1990 IEEE)

Each segment is then modeled through the analogous electrical circuit of Figure P2.38(b), resulting in the total model shown in Figure P2.38(c), where eight terminal resistances (Z) have been added. In the electrical model, pressure is analogous to voltage and blood flow is analogous to current. As an example, for Segment 3 it was experimentally verified that $R_3 = 4176\,\Omega$, $C_3 = 0.98\,\mu\text{F}$, $L_3 = 140.6\,\text{H}$, and $Z_3 = 308,163\,\Omega$ (*Wang, 1990*).

a. For Segment 3, find the transfer function from input pressure to blood flow through Z_3, $\dfrac{Q_{03}(s)}{P_2(s)}$.

b. It is well known in circuit analysis that if a constant input is applied to a circuit such as the one of Figure P2.38(b), the capacitor can be substituted by an open circuit and the inductor can be substituted by a short circuit as time approaches infinity. Use this fact to calculate the flow through Z_3 after a constant unit pressure pulse is applied and time approaches infinity.

c. Verify the result obtained in Part **b** using the transfer function obtained in Part **a** and applying the final value theorem.

65. In order to design an underwater vehicle that has the characteristics of both a long-range transit vehicle (torpedo-like) and a highly maneuverable low-speed vehicle (boxlike), researchers have developed a thruster that mimics that of squid jet locomotion (*Krieg, 2008*). It has been demonstrated there that the average normalized thrust due to a command step input, $U(s) = \dfrac{T_{ref}}{s}$, is given by:

$$T(t) = T_{ref}(1 - e^{-\lambda t}) + a\sin(2\pi f t)$$

where T_{ref} is the reference or desired thrust, λ is the system's damping constant, a is the amplitude of the oscillation caused by the pumping action of the actuator, f is the actuator frequency, and $T(t)$ is the average resulting normalized thrust. Find the thruster's transfer function $\dfrac{T(s)}{U(s)}$. Show all steps.

66. The Gompertz growth model is commonly used to model tumor cell growth. Let $v(t)$ be the tumor's volume, then

$$\frac{dv(t)}{dt} = \lambda e^{-\alpha t} v(t)$$

where λ and α are two appropriate constants (*Edelstein-Keshet, 2005*).

a. Verify that the solution to this equation is given by $v(t) = v_0 e^{\lambda/\alpha(1 - e^{-\alpha t})}$, where v_0 is the initial tumor volume.

b. This model takes into account the fact that when nutrients and oxygen are scarce at the tumor's core, its growth is impaired. Find the final predicted tumor volume (let $t \to \infty$).

c. For a specific mouse tumor, it was experimentally found that $\lambda = 2.5$ days, $\alpha = 0.1$ days with $v_0 = 50 \times 10^{-3}\,\text{mm}^3$ (*Chignola, 2005*). Use any method available to make a plot of $v(t)$ vs. t.

d. Check the result obtained in Part **b** with the results from the graph from Part **c**.

PROGRESSIVE ANALYSIS AND DESIGN PROBLEMS

67. **High-speed rail pantograph.** Problem 21 in Chapter 1 discusses active control of a pantograph mechanism for high-speed rail systems. The diagram for the pantograph and catenary coupling is shown in Figure P2.39(a). Assume the simplified model shown in Figure P2.39(b), where the catenary is represented by the spring, K_{ave} (*O'Connor, 1997*).
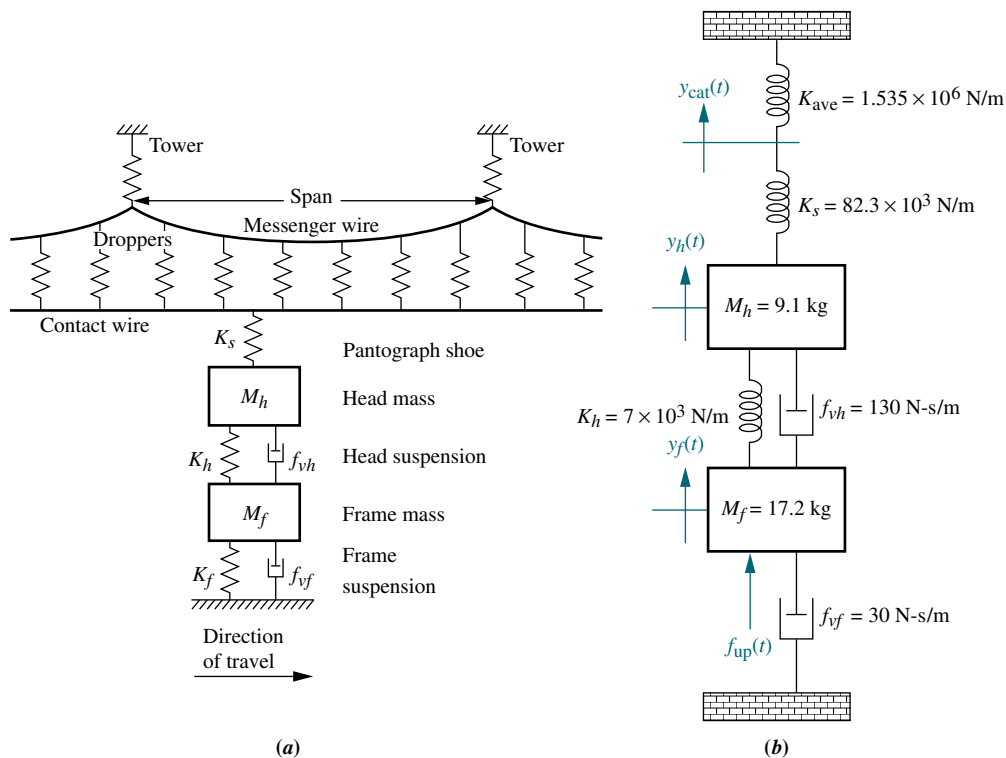
FIGURE P2.39   **a.** Coupling of pantograph and catenary; **b.** simplified representation showing the active-control force (Reprinted with permission of ASME.)

a. Find the transfer function, $G_1(s) = Y_{cat}(s)/F_{up}(s)$, where $y_{cat}(t)$ is the catenary displacement and $f_{up}(t)$ is the upward force applied to the pantograph under active control.

b. Find the transfer function $G_2(s) = Y_h(s)/F_{up}(s)$, where $y_h(t)$ is the pantograph head displacement.

c. Find the transfer function, $G(s) = (Y_h(s) - Y_{cat}(s))/F_{up}(s)$.

68. Control of HIV/AIDS. HIV inflicts its damage by infecting healthy CD4 + T cells (a type of white blood cell) that are necessary to fight infection. As the virus embeds in a T cell and the immune system produces more of these cells to fight the infection, the virus propagates in an opportunistic fashion. As we now develop a simple HIV model, refer to Figure P2.40. Normally T cells are produced at a rate s and die at a rate d. The HIV virus is present in the bloodstream in the infected individual. These viruses in the bloodstream, called *free viruses*, infect healthy T cells at a rate β. Also, the viruses reproduce through the T cell multiplication process or otherwise at a rate k. Free viruses die at a rate c. Infected T cells die at a rate μ.
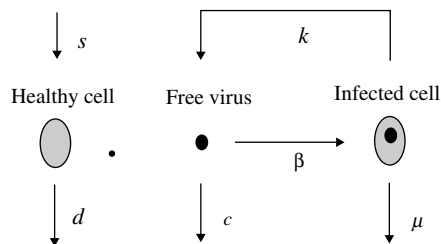
FIGURE P2.40   (© 2004 IEEE)

A simple mathematical model that illustrates these interactions is given by the following equations (*Craig, 2004*):

$$\frac{dT}{dt} = s - dT - \beta Tv$$

$$\frac{dT^*}{dt} = \beta Tv - \mu T^*$$

$$\frac{dv}{dt} = kT^* - cv$$

where

$$T = \text{number of healthy T cells}$$
$$T^* = \text{number of infected T cells}$$
$$v = \text{number of free viruses}$$

a. The system is nonlinear; thus linearization is necessary to find transfer functions as you will do in subsequent chapters. The nonlinear nature of this model can be seen from the above equations. Determine which of these equations are linear, which are nonlinear, and explain why.

b. The system has two equilibrium points. Show that these are given by

$$\left(T_0, \ T_0^*, \ v_0\right) = \left(\frac{s}{d}, \ 0, \ 0\right)$$

and

$$\left(T_0, \ T_0^*, \ v_0\right) = \left(\frac{c\mu}{\beta k}, \ \frac{s}{\mu} - \frac{cd}{\beta k}, \ \frac{sk}{c\mu} - \frac{d}{\beta}\right)$$

69. Hybrid vehicle. Problem 23 in Chapter 1 discusses the cruise control of serial, parallel, and split-power hybrid electric vehicles (HEVs). The functional block diagrams developed for these HEVs indicated that the speed of a vehicle depends upon the balance between the motive forces (developed by the gasoline engine and/or the electric motor) and running resistive forces. The resistive forces include the aerodynamic drag, rolling resistance, and climbing resistance. Figure P2.41 illustrates the running resistances for a car moving uphill (*Bosch, 2007*).
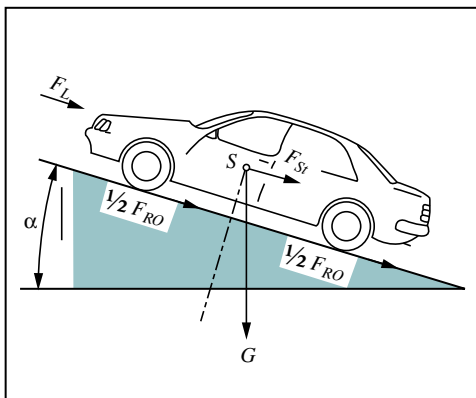
FIGURE P2.41 Running resistances

The total running resistance, F_w, is calculated as $F_w = F_{Ro} + F_L + F_{St}$, where F_{Ro} is the rolling resistance, F_L is the aerodynamic drag, and F_{St} is the climbing resistance. The aerodynamic drag is proportional to the square of the sum of car velocity, v, and the head-wind velocity, v_{hw}, or $v + v_{hw}$. The other two resistances are functions of car weight, G, and the gradient of the road (given by the gradient angle, α), as seen from the following equations:

$$F_{Ro} = fG\cos\alpha = fmg\cos\alpha$$

where

$$f = \text{coefficient of rolling resistance,}$$
$$m = \text{car mass, in kg,}$$
$$g = \text{gravitational acceleration, in m/s}^2.$$
$$F_L = 0.5\rho C_w A(v + v_{hw})^2$$

where

$$\rho = \text{air density, in kg/m}^3,$$
$$C_w = \text{coefficient of aerodynamic drag,}$$
$$A = \text{largest cross-section of the car, in kg/m}^2.$$
$$F_{St} = G\sin\alpha = mg\sin\alpha$$

The motive force, F, available at the drive wheels is:

$$F = \frac{Ti_{tot}}{r}\eta_{tot} = \frac{P\eta_{tot}}{v}$$

where

$$T = \text{motive torque,}$$
$$P = \text{motive power,}$$
$$i_{tot} = \text{total transmission ratio,}$$
$$r = \text{tire radius,}$$
$$\eta_{tot} = \text{total drive-train efficiency.}$$

The surplus force, $F - F_w$, accelerates the vehicle (or retards it when $F_w > F$). Letting $a = \dfrac{F - F_w}{k_m \cdot m}$, where a is the acceleration and k_m is a coefficient that compensates for the apparent increase in vehicle mass due to rotating masses (wheels, flywheel, crankshaft, etc.):

a. Show that car acceleration,[16] a, may be determined from the equation:

$$F = fmg\cos\alpha + mg\sin\alpha + 0.5\rho C_w A(v + v_{hw})^2 + k_m ma$$

---

[16] Other quantities, such as top speed, climbing ability, etc., may also be calculated by manipulation from that equation.

b. Assuming constant acceleration and using the average value for speed, find the average motive force, F_{av} (in N), and power, P_{av} (in kW) the car needs to accelerate from 40 to 60 km/h in 4 seconds on a level road, $(\alpha = 0°)$, under windless conditions, where $v_{hw} = 0$. You are given the following parameters: m = 1590 kg, A = 2 m², $f = 0.011$, $\rho = 1.2$ kg/m³, $C_w = 0.3$, $\eta_{tot} = 0.9$, $k_m = 1.2$. Furthermore, calculate the additional power, P_{add}, the car needs after reaching 60 km/h to maintain its speed while climbing a hill with a gradient $\alpha = 5°$.

c. The equation derived in Part **a** describes the non-linear car motion dynamics where $F(t)$ is the input to the system, and $v(t)$ the resulting output. Given that the aerodynamic drag is proportional to v^2 under

windless conditions, linearize the resulting equation of motion around an average speed, $v_o = 50$ km/h, when the car travels on a level road,[17] where $\alpha = 0°$. (Hint: Expand $v^2 - v_0^2$ in a truncated Taylor series). Write that equation of motion and represent it with a block diagram in which the block G_v represents the vehicle dynamics. The output of that block is the car speed, $v(t)$, and the input is the excess motive force, $F_e(t)$, defined as: $F_e = F - F_{St} - F_{Ro} + F_o$, where F_o the constant component of the linearized aerodynamic drag.

d. Use the equation in Part **c** to find the vehicle transfer function: $G_v(s) = V(s)/F_e(s)$.

---

[17] Note that on a level road the climbing resistance is $F_{St} = 0$, since $\sin \alpha = \sin 0° = 0$.

Cyber Exploration Laboratory

Experiment 2.1

Objectives   To learn to use MATLAB to (1) generate polynomials, (2) manipulate polynomials, (3) generate transfer functions, (4) manipulate transfer functions, and (5) perform partial-fraction expansions.

Minimum Required Software Packages   MATLAB and the Control System Toolbox

Prelab

1. Calculate the following by hand or with a calculator:

   a. The roots of $P_1 = s^6 + 7s^5 + 2s^4 + 9s^3 + 10s^2 + 12s + 15$

   b. The roots of $P_2 = s^6 + 9s^5 + 8s^4 + 9s^3 + 12s^2 + 15s + 20$

   c. $P_3 = P_1 + P_2$; $P_4 = P_1 - P_2$; $P_5 = P_1 P_2$

2. Calculate by hand or with a calculator the polynomial

$$P_6 = (s + 7)(s + 8)(s + 3)(s + 5)(s + 9)(s + 10)$$

3. Calculate by hand or with a calculator the following transfer functions:

   a. $G_1(s) = \dfrac{20(s + 2)(s + 3)(s + 6)(s + 8)}{s(s + 7)(s + 9)(s + 10)(s + 15)}$,

   represented as a numerator polynomial divided by a denominator polynomial.

   b. $G_2(s) = \dfrac{s^4 + 17s^3 + 99s^2 + 223s + 140}{s^5 + 32s^4 + 363s^3 + 2092s^2 + 5052s + 4320}$,

   expressed as factors in the numerator divided by factors in the denominator, similar to the form of $G_1(s)$ in Prelab 3**a.**

   c. $G_3(s) = G_1(s) + G_2(s)$; $G_4(s) = G_1(s) - G_2(s)$; $G_5(s) = G_1(s)G_2(s)$
   expressed as factors divided by factors and expressed as polynomials divided by polynomials.

4. Calculate by hand or with a calculator the partial-fraction expansion of the following transfer functions:

a. $G_6 = \dfrac{5(s+2)}{s(s^2+8s+15)}$

b. $G_7 = \dfrac{5(s+2)}{s(s^2+6s+9)}$

c. $G_8 = \dfrac{5(s+2)}{s(s^2+6s+34)}$

Lab

1. Use MATLAB to find P_3, P_4, and P_5 in Prelab 1.

2. Use only one MATLAB command to find P_6 in Prelab 2.

3. Use only two MATLAB commands to find $G_1(s)$ in Prelab 3**a** represented as a polynomial divided by a polynomial.

4. Use only two MATLAB commands to find $G_2(s)$ expressed as factors in the numerator divided by factors in the denominator.

5. Using various combinations of $G_1(s)$ and $G_2(s)$, find $G_3(s)$, $G_4(s)$, and $G_5(s)$. Various combinations implies mixing and matching $G_1(s)$ and $G_2(s)$ expressed as factors and polynomials. For example, in finding $G_3(s)$, $G_1(s)$ can be expressed in factored form and $G_2(s)$ can be expressed in polynomial form. Another combination is $G_1(s)$ and $G_2(s)$ both expressed as polynomials. Still another combination is $G_1(s)$ and $G_2(s)$ both expressed in factored form.

6. Use MATLAB to evaluate the partial fraction expansions shown in Prelab 4.

Postlab

1. Discuss your findings for Lab 5. What can you conclude?

2. Discuss the use of MATLAB to manipulate transfer functions and polynomials. Discuss any shortcomings in using MATLAB to evaluate partial fraction expansions.

Experiment 2.2

Objectives   To learn to use MATLAB and the Symbolic Math Toolbox to (1) find Laplace transforms for time functions, (2) find time functions from Laplace transforms, (3) create LTI transfer functions from symbolic transfer functions, and (4) perform solutions of symbolic simultaneous equations.

Minimum Required Software Packages   MATLAB, the Symbolic Math Toolbox, and the Control System Toolbox

Prelab

1. Using a hand calculation, find the Laplace transform of:

$f(t) = 0.0075 - 0.00034e^{-2.5t}\cos(22t) + 0.087e^{-2.5t}\sin(22t) - 0.0072e^{-8t}$

2. Using a hand calculation, find the inverse Laplace transform of

$$F(s) = \frac{2(s+3)(s+5)(s+7)}{s(s+8)(s^2+10s+100)}$$

3. Use a hand calculation to solve the circuit for the loop currents shown in Figure P2.42.
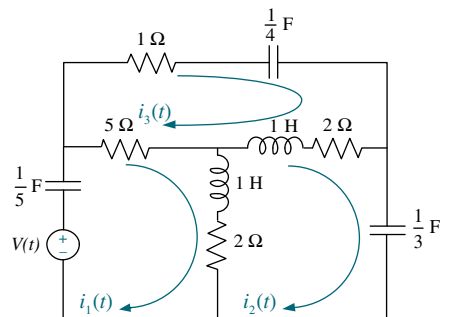
FIGURE P2.42

Lab

1. Use MATLAB and the Symbolic Math Toolbox to
    a. Generate symbolically the time function $f(t)$ shown in Prelab 1.
    b. Generate symbolically $F(s)$ shown in Prelab 2. Obtain your result symbolically in both factored and polynomial forms.
    c. Find the Laplace transform of $f(t)$ shown in Prelab 1.
    d. Find the inverse Laplace transform of $F(s)$ shown in Prelab 2.
    e. Generate an LTI transfer function for your symbolic representation of $F(s)$ in Prelab 2 in both polynomial form and factored form. Start with the $F(s)$ you generated symbolically.
    f. Solve for the loop currents in Prelab 3.

Postlab

1. Discuss the advantages and disadvantages between the Symbolic Math Toolbox and MATLAB alone to convert a transfer function from factored form to polynomial form and vice versa.
2. Discuss the advantages and disadvantages of using the Symbolic Math Toolbox to generate LTI transfer functions.
3. Discuss the advantages of using the Symbolic Math Toolbox to solve simultaneous equations of the type generated by the electrical network in Prelab 3. Is it possible to solve the equations via MATLAB alone? Explain.
4. Discuss any other observations you had using the Symbolic Math Toolbox.

Experiment 2.3

Objective   To learn to use LabVIEW to generate and manipulate polynomials and transfer functions.

Minimum Required Software Packages   LabVIEW and the LabVIEW Control Design and Simulation Module.

Prelab

1. Study Appendix D, Sections D.1 through Section D.4, Example D.1.
2. Perform by hand the calculations stated in Prelab 1 of Experiment 2.1.
3. Find by a hand calculation the polynomial whose roots are: $-7, -8, -3, -5, -9,$ and -10.
4. Perform by hand a partial-fraction expansion of $G(s) = \dfrac{5s + 10}{s^3 + 8s^2 + 15s}$.
5. Find by a hand calculation $G_1(s) + G_2(s)$, $G_1(s) - G_2(s)$, and $G_1(s)G_2(s)$, where $G_1(s) = \dfrac{1}{s^2 + s + 2}$ and $G_2(s) = \dfrac{s + 1}{s^2 + 4s + 3}$.

Lab

1. Open the LabVIEW functions palette and select the **Mathematics/Polynomial** palette.
2. Generate the polynomials enumerated in Prelab 1a and 1b of Experiment 2.1.
3. Generate the polynomial operations stated in Prelab 1c of Experiment 2.1.
4. Generate a polynomial whose roots are those stated in Prelab 3 of this experiment.

5. Generate the partial fraction expansion of the transfer function given in Prelab 4 of this experiment.

6. Using the **Control Design and Simulation/Control Design/Model Construction** palette, construct the two transfer functions enumerated in Prelab 5.

7. Using the **Control Design and Simulation/Control Design/Model Interconnection** palette, display the results of the mathematical operations enumerated in Prelab 5 of this experiment.

Postlab

1. Compare the polynomial operations obtained in Lab 3 to those obtained in Prelab 2.

2. Compare the polynomial displayed in Lab 4 with that calculated in Prelab 3.

3. Compare the partial-fraction expansion obtained in Lab 5 with that calculated in Prelab 4.

4. Compare the results of the mathematical operations found in Lab 7 to those calculated in Prelab 5.

Bibliography

Aggarwal, J. K. *Notes on Nonlinear Systems.* Van Nostrand Reinhold, New York, 1972.

Bosch, R. GmbH, *Bosch Automotive Handbook*, 7th ed. John Wiley & Sons Ltd., UK, 2007.

Boutayeb, A., Twizell, E. H., Achouayb, K., and Chetouani, A. Mathematical Model for the Burden of Diabetes and Its Complications. *BioMedical Engineering OnLine*, 2004, Retrieved from http://www.biomedical-engineering-online.com/content/3/1/20, pp. 1–19.

Cannon, R. H., Jr., *Dynamics of Physical Systems.* McGraw-Hill, New York, 1967.

Carlson, L. E., and Griggs, G. E. *Aluminum Catenary System Quarterly Report.* Technical Report Contract Number DOT-FR-9154, U.S. Department of Transportation, 1980.

Chignola, R., and Foroni, R. I. Estimating the Growth Kinetics of Experimental Tumors from as Few as Two Determinations of Tumor Size: Implications for Clinical Oncology. *IEEE Transactions on Biomedical Engineering*, vol. 52, no. 5, May 2005, pp. 808–815.

Cochin, I. *Analysis and Design of Dynamic Systems.* Harper and Row, New York, 1980.

Cook, P. A. *Nonlinear Dynamical Systems.* Prentice Hall, United Kingdom, 1986.

Craig, I. K., Xia, X., and Venter, J. W. Introducing HIV/AIDS Education into the Electrical Engineering Curriculum at the University of Pretoria. *IEEE Transactions on Education*, vol. 47, no. 1, February 2004, pp. 65–73.

Davis, S. A., and Ledgerwood, B. K. *Electromechanical Components for Servomechanisms.* McGraw-Hill, New York, 1961.

Doebelin, E. O. *Measurement Systems Application and Design.* McGraw-Hill, New York, 1983.

Dorf, R. *Introduction to Electric Circuits*, 2d ed. Wiley, New York, 1993.

D'Souza, A. *Design of Control Systems.* Prentice Hall, Upper Saddle River, NJ, 1988.

Edelstein-Keshet, L. *Mathematical Models in Biology.* Society for Industrial and Applied Mathematics, Philadelphia, PA, 2005.

Elkins, J. A. *A Method for Predicting the Dynamic Response of a Pantograph Running at Constant Speed under a Finite Length of Overhead Equipment.* Technical Report TN DA36, British Railways, 1976.

Franklin, G. F., Powell, J. D., and Emami-Naeini, A. *Feedback Control of Dynamic Systems.* Addison-Wesley, Reading, MA, 1986.

Galvão, R. K. H., Yoneyama, T., and de Araújo, F. M. U. A Simple Technique for Identifying a Linearized Model for a Didactic Magnetic Levitation System. *IEEE Transactions on Education*, vol. 46, no. 1, February 2003, pp. 22–25.

Hsu, J. C., and Meyer, A. U. *Modern Control Principles and Applications*. McGraw-Hill, New York, 1968.

Johansson, R., Magnusson, M., and Åkesson, M. Identification of Human Postural Dynamics. *IEEE Transactions on Biomedical Engineering*, vol. 35, no. 10, October 1988, pp. 858–869.

Kailath, T. *Linear Systems*. Prentice Hall, Upper Saddle River, NJ, 1980.

Kermurjian, A. From the Moon Rover to the Mars Rover. *The Planetary Report*, July/August 1990, pp. 4–11.

Krieg, M., and Mohseni, K. Developing a Transient Model for Squid Inspired Thrusters, and Incorporation into Underwater Robot Control Design. *2008 IEEE/RSJ Int. Conf. on Intelligent Robots and Systems, France*, September 2008.

Kuo, F. F. *Network Analysis and Synthesis*. Wiley, New York, 1966.

Lago, G., and Benningfield, L. M. *Control System Theory*. Ronald Press, New York, 1962.

Lin, J.-S., and Kanellakopoulos, I. Nonlinear Design of Active Suspensions. *IEEE Control Systems Magazine*, vol. 17, issue 3, June 1997, pp. 45–59.

Mablekos, V E. *Electric Machine Theory for Power Engineers*. Harper & Row, Cambridge, MA, 1980.

Marttinen, A., Virkkunen, J., and Salminen, R. T. Control Study with Pilot Crane. *IEEE Transactions on Education*, vol. 33, no. 3, August 1990, pp. 298–305.

Milsum, J. H. *Biological Control Systems Analysis*. McGraw-Hill, New York, 1966.

Minorsky, N. *Theory of Nonlinear Control Systems*. McGraw-Hill, New York, 1969.

Nilsson, J. W., and Riedel, S. A. *Electric Circuits*, 5th ed. Addison-Wesley, Reading, MA, 1996.

O'Connor, D. N., Eppinger, S. D., Seering, W. P., and Wormly, D. N. Active Control of a High-Speed Pantograph. *Journal of Dynamic Systems, Measurements, and Control*, vol. 119, March 1997, pp. l–4.

Ogata, K. *Modern Control Engineering*, 2d ed. Prentice Hall, Upper Saddle River, NJ, 1990.

Raven, F. H. *Automatic Control Engineering*, 5th ed. McGraw-Hill, New York, 1995.

Schnell, S., and Mendoza, C. The Condition for Pseudo-First-Order Kinetics in Enzymatic Reactions Is Independent of the Initial Enzyme Concentration. *Biophysical Chemistry* (107), 2004, pp. 165–174.

Van Valkenburg, M. E. *Network Analysis*. Prentice Hall, Upper Saddle River, NJ, 1974.

Vidyasagar, M. *Nonlinear Systems Analysis*. Prentice Hall, Upper Saddle River, NJ, 1978.

Wang, J. Z., Tie, B., Welkowitz, W., Semmlow, J. L., and Kostis, J. B. Modeling Sound Generation in Stenosed Coronary Arteries. *IEEE Transactions on Biomedical Engineering*, vol. 37, no. 11, November 1990, pp. 1087–1094.

Modeling in the Time Domain
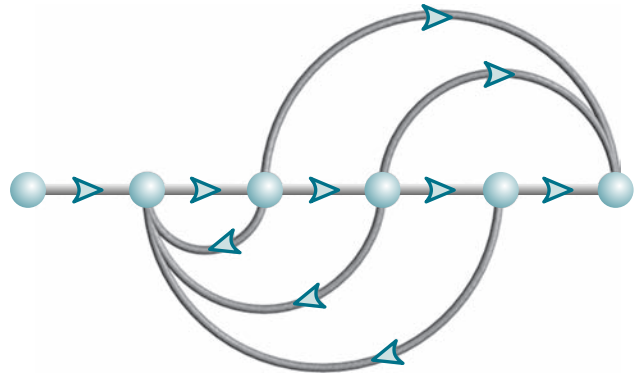
This chapter covers only state-space methods.

State Space
SS

Chapter Learning Outcomes

After completing this chapter, the student will be able to:

- Find a mathematical model, called a *state-space* representation, for a linear, time-invariant system (Sections 3.1–3.3)
- Model electrical and mechanical systems in state space (Section 3.4)
- Convert a transfer function to state space (Section 3.5)
- Convert a state-space representation to a transfer function (Section 3.6)
- Linearize a state-space representation (Section 3.7)

Case Study Learning Outcomes

You will be able to demonstrate your knowledge of the chapter objectives with case studies as follows:

- Given the antenna azimuth position control system shown on the front endpapers, you will be able to find the state-space representation of each subsystem.
- Given a description of the way a pharmaceutical drug flows through a human being, you will be able to find the state-space representation to determine drug concentrations in specified compartmentalized blocks of the process and of the human body. You will also be able to apply the same concepts to an aquifer to find water level.

3.1 Introduction

Two approaches are available for the analysis and design of feedback control systems. The first, which we began to study in Chapter 2, is known as the *classical*, or *frequency-domain*, technique. This approach is based on converting a system's differential equation to a transfer function, thus generating a mathematical model of the system that *algebraically* relates a representation of the output to a representation of the input. Replacing a differential equation with an algebraic equation not only simplifies the representation of individual subsystems but also simplifies modeling interconnected subsystems.

The primary disadvantage of the classical approach is its limited applicability: It can be applied only to linear, time-invariant systems or systems that can be approximated as such.

A major advantage of frequency-domain techniques is that they rapidly provide stability and transient response information. Thus, we can immediately see the effects of varying system parameters until an acceptable design is met.

With the arrival of space exploration, requirements for control systems increased in scope. Modeling systems by using linear, time-invariant differential equations and subsequent transfer functions became inadequate. The *state-space* approach (also referred to as the *modern*, or *time-domain*, approach) is a unified method for modeling, analyzing, and designing a wide range of systems. For example, the state-space approach can be used to represent nonlinear systems that have backlash, saturation, and dead zone. Also, it can handle, conveniently, systems with nonzero initial conditions. Time-varying systems, (for example, missiles with varying fuel levels or lift in an aircraft flying through a wide range of altitudes) can be represented in state space. Many systems do not have just a single input and a single output. Multiple-input, multiple-output systems (such as a vehicle with input direction and input velocity yielding an output direction and an output velocity) can be compactly represented in state space with a model similar in form and complexity to that used for single-input, single-output systems. The time-domain approach can be used to represent systems with a digital computer in the loop or to model systems for digital simulation. With a simulated system, system response can be obtained for changes in system parameters—an important design tool. The state-space approach is also attractive because of the availability of numerous state-space software packages for the personal computer.

The time-domain approach can also be used for the same class of systems modeled by the classical approach. This alternate model gives the control systems designer another perspective from which to create a design. While the state-space approach can be applied to a wide range of systems, it is not as intuitive as the classical approach. The designer has to engage in several calculations before the physical interpretation of the model is apparent, whereas in classical control a few quick calculations or a graphic presentation of data rapidly yields the physical interpretation.

In this book, the coverage of state-space techniques is to be regarded as an introduction to the subject, a springboard to advanced studies, and an alternate approach to frequency-domain techniques. We will limit the state-space approach to linear, time-invariant systems or systems that can be linearized by the methods of Chapter 2. The study of other classes of systems is beyond the scope of this book. Since state-space analysis and design rely on matrices and matrix operations, you may want to review this topic in Appendix G, located at www.wiley.com/college/nise, before continuing.

3.2   Some Observations

We proceed now to establish the state-space approach as an alternate method for representing physical systems. This section sets the stage for the formal definition of the state-space representation by making some observations about systems and their variables. In the discussion that follows, some of the development has been placed in footnotes to avoid clouding the main issues with an excess of equations and to ensure that the concept is clear. Although we use two electrical networks to illustrate the concepts, we could just as easily have used a mechanical or any other physical system.

We now demonstrate that for a system with many variables, such as inductor voltage, resistor voltage, and capacitor charge, we need to use differential equations only to solve for a selected subset of system variables because all other remaining system variables can be evaluated algebraically from the variables in the subset. Our examples take the following approach:

1. We select a particular *subset* of all possible system variables and call the variables in this subset *state variables*.

2. For an *n*th-order system, we write *n simultaneous, first-order differential equations* in terms of the state variables. We call this system of simultaneous differential equations *state equations*.

3. If we know the initial condition of all of the state variables at t_0 as well as the system input for $t \geq t_0$, we can solve the simultaneous differential equations for the state variables for $t \geq t_0$.

4. We *algebraically* combine the state variables with the system's input and find all of the other system variables for $t \geq t_0$. We call this algebraic equation the *output equation*.

5. We consider the state equations and the output equations a viable representation of the system. We call this representation of the system a *state-space representation*.

Let us now follow these steps through an example. Consider the *RL* network shown in Figure 3.1 with an initial current of $i(0)$.

1. We select the current, $i(t)$, for which we will write and solve a differential equation using Laplace transforms.

2. We write the loop equation,

$$L\frac{di}{dt} + Ri = v(t) \tag{3.1}$$

3. Taking the Laplace transform, using Table 2.2, Item 7, and including the initial conditions, yields

$$L[sI(s) - i(0)] + RI(s) = V(s) \tag{3.2}$$

Assuming the input, $v(t)$, to be a unit step, $u(t)$, whose Laplace transform is $V(s) = 1/s$, we solve for $I(s)$ and get

$$I(s) = \frac{1}{R}\left(\frac{1}{s} - \frac{1}{s + \dfrac{R}{L}}\right) + \frac{i(0)}{s + \dfrac{R}{L}} \tag{3.3}$$
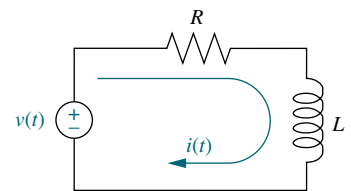
FIGURE 3.1   *RL* network

from which

$$i(t) = \frac{1}{R}\left(1 - e^{-(R/L)t}\right) + i(0)e^{-(R/L)t} \tag{3.4}$$

The function $i(t)$ is a subset of all possible network variables that we are able to find from Eq. (3.4) if we know its initial condition, $i(0)$, and the input, $v(t)$. Thus, $i(t)$ is a state variable, and the differential equation (3.1) is a *state equation*.

4. We can now solve for all of the other network variables *algebraically* in terms of $i(t)$ and the applied voltage, $v(t)$. For example, the voltage across the resistor is

$$v_R(t) = Ri(t) \tag{3.5}$$

The voltage across the inductor is

$$v_L(t) = v(t) - Ri(t) \tag{3.6}^1$$

The derivative of the current is

$$\frac{di}{dt} = \frac{1}{L}[v(t) - Ri(t)] \tag{3.7}^2$$

Thus, knowing the state variable, $i(t)$, and the input, $v(t)$, we can find the value, or *state*, of any network variable at any time, $t \geq t_0$. Hence, the algebraic equations, Eqs. (3.5) through (3.7), are *output equations*.

5. Since the variables of interest are completely described by Eq. (3.1) and Eqs. (3.5) through (3.7), we say that the combined state equation (3.1) and the output equations (3.5 through 3.7) form a viable representation of the network, which we call a *state-space representation*.

Equation (3.1), which describes the dynamics of the network, is not unique. This equation could be written in terms of any other network variable. For example, substituting $i = v_R/R$ into Eq. (3.1) yields

$$\frac{L}{R}\frac{dv_R}{dt} + v_R = v(t) \tag{3.8}$$
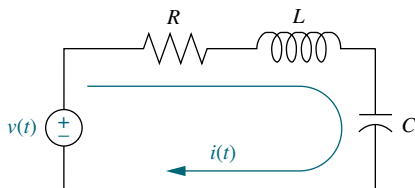
FIGURE 3.2 *RLC* network

which can be solved knowing that the initial condition $v_R(0) = Ri(0)$ and knowing $v(t)$. In this case, the state variable is $v_R(t)$. Similarly, all other network variables can now be written in terms of the state variable, $v_R(t)$, and the input, $v(t)$. Let us now extend our observations to a second-order system, such as that shown in Figure 3.2.

1. Since the network is of second order, two simultaneous, first-order differential equations are needed to solve for two state variables. We select $i(t)$ and $q(t)$, the charge on the capacitor, as the two state variables.

2. Writing the loop equation yields

$$L\frac{di}{dt} + Ri + \frac{1}{C}\int i\,dt = v(t) \tag{3.9}$$

---

[1] Since $v_L(t) = v(t) - v_R(t) = v(t) - Ri(t)$.

[2] Since $\dfrac{di}{dt} = \dfrac{1}{L}v_L(t) = \dfrac{1}{L}[v(t) - Ri(t)]$.

Converting to charge, using $i(t) = dq/dt$, we get

$$L\frac{d^2q}{dt^2} + R\frac{dq}{dt} + \frac{1}{C}q = v(t) \tag{3.10}$$

But an nth-order differential equation can be converted to n simultaneous first-order differential equations, with each equation of the form

$$\frac{dx_i}{dt} = a_{i1}x_1 + a_{i2}x_2 + \cdots + a_{in}x_n + b_i f(t) \tag{3.11}$$

where each x_i is a state variable, and the a_{ij}'s and b_i are constants for linear, time-invariant systems. We say that the right-hand side of Eq. (3.11) is a *linear combination* of the state variables and the input, $f(t)$.

We can convert Eq. (3.10) into two simultaneous, first-order differential equations in terms of $i(t)$ and $q(t)$. The first equation can be $dq/dt = i$. The second equation can be formed by substituting $\int i\, dt = q$ into Eq. (3.9) and solving for di/dt. Summarizing the two resulting equations, we get

$$\frac{dq}{dt} = i \tag{3.12a}$$

$$\frac{di}{dt} = -\frac{1}{LC}q - \frac{R}{L}i + \frac{1}{L}v(t) \tag{3.12b}$$

3. These equations are the state equations and can be solved simultaneously for the state variables, $q(t)$ and $i(t)$, using the Laplace transform and the methods of Chapter 2, if we know the initial conditions for $q(t)$ and $i(t)$ and if we know $v(t)$, the input.

4. From these two state variables, we can solve for all other network variables. For example, the voltage across the inductor can be written in terms of the solved state variables and the input as

$$v_L(t) = -\frac{1}{C}q(t) - Ri(t) + v(t) \tag{3.13}[3]$$

Equation (3.13) is an *output equation*; we say that $v_L(t)$ is a *linear combination* of the state variables, $q(t)$ and $i(t)$, and the input, $v(t)$.

5. The combined state equations (3.12) and the output equation (3.13) form a viable representation of the network, which we call a *state-space representation*.

Another choice of two state variables can be made, for example, $v_R(t)$ and $v_C(t)$, the resistor and capacitor voltage, respectively. The resulting set of simultaneous, first-order differential equations follows:

$$\frac{dv_R}{dt} = -\frac{R}{L}v_R - \frac{R}{L}v_C + \frac{R}{L}v(t) \tag{3.14a}[4]$$

$$\frac{dv_C}{dt} = \frac{1}{RC}v_R \tag{3.14b}$$

---

[3] Since $v_L(t) = L(di/dt) = -(1/C)q - Ri + v(t)$, where di/dt can be found from Eq. (3.9), and $\int i\, dt = q$.
[4] Since $v_R(t) = i(t)R$, and $v_C(t) = (1/C)\int i\, dt$, differentiating $v_R(t)$ yields $dv_R/dt = R(di/dt) = (R/L)v_L = (R/L)[v(t) - v_R - v_C]$, and differentiating $v_C(t)$ yields $dv_C/dt = (1/C)i = (1/RC)v_R$.

Again, these differential equations can be solved for the state variables if we know the initial conditions along with $v(t)$. Further, all other network variables can be found as a linear combination of these state variables.

Is there a restriction on the choice of state variables? Yes! Typically, the minimum number of state variables required to describe a system equals the order of the differential equation. Thus, a second-order system requires a minimum of two state variables to describe it. We can define more state variables than the minimal set; however, within this minimal set the state variables must be linearly independent. For example, if $v_R(t)$ is chosen as a state variable, then $i(t)$ cannot be chosen, because $v_R(t)$ can be written as a linear combination of $i(t)$, namely $v_R(t) = Ri(t)$. Under these circumstances we say that the state variables are *linearly dependent*. State variables must be *linearly independent*; that is, no state variable can be written as a linear combination of the other state variables, or else we would not have enough information to solve for all other system variables, and we could even have trouble writing the simultaneous equations themselves.

The state and output equations can be written in vector-matrix form if the system is linear. Thus, Eq. (3.12), the state equations, can be written as

$$\dot{\mathbf{x}} = \mathbf{A}\mathbf{x} + \mathbf{B}u \tag{3.15}$$

where

$$\dot{\mathbf{x}} = \begin{bmatrix} dq/dt \\ di/dt \end{bmatrix}; \quad \mathbf{A} = \begin{bmatrix} 0 & 1 \\ -1/LC & -R/L \end{bmatrix}$$

$$\mathbf{x} = \begin{bmatrix} q \\ i \end{bmatrix}; \quad \mathbf{B} = \begin{bmatrix} 0 \\ 1/L \end{bmatrix}; \; u = v(t)$$

Equation (3.13), the output equation, can be written as

$$y = \mathbf{C}\mathbf{x} + Du \tag{3.16}$$

where

$$y = v_L(t); \quad \mathbf{C} = [-1/C \quad -R]; \quad \mathbf{x} = \begin{bmatrix} q \\ i \end{bmatrix}; \quad D = 1; \quad u = v(t)$$

We call the combination of Eqs. (3.15) and (3.16) a *state-space representation* of the network of Figure 3.2. A state-space representation, therefore, consists of (1) the simultaneous, first-order differential equations from which the state variables can be solved and (2) the algebraic output equation from which all other system variables can be found. A state-space representation is not unique, since a different choice of state variables leads to a different representation of the same system.

In this section, we used two electrical networks to demonstrate some principles that are the foundation of the state-space representation. The representations developed in this section were for single-input, single-output systems, where y, D, and u in Eqs. (3.15) and (3.16) are scalar quantities. In general, systems have multiple inputs and multiple outputs. For these cases, y and u become vector quantities, and D becomes a matrix. In Section 3.3 we will generalize the representation for multiple-input, multiple-output systems and summarize the concept of the state-space representation.

3.3   The General State-Space Representation

Now that we have represented a physical network in state space and have a good idea of the terminology and the concept, let us summarize and generalize the representation for linear differential equations. First, we formalize some of the definitions that we came across in the last section.

Linear combination. A linear combination of n variables, x_i, for $i = 1$ to n, is given by the following sum, S:

$$S = K_n x_n + K_{n-1} x_{n-1} + \cdots + K_1 x_1 \tag{3.17}$$

where each K_i is a constant.

Linear independence. A set of variables is said to be linearly independent if none of the variables can be written as a linear combination of the others. For example, given x_1, x_2, and x_3, if $x_2 = 5x_1 + 6x_3$, then the variables are not linearly independent, since one of them can be written as a linear combination of the other two. Now, what must be true so that one variable cannot be written as a linear combination of the other variables? Consider the example $K_2 x_2 = K_1 x_1 + K_3 x_3$. If no $x_i = 0$, then any x_i can be written as a linear combination of other variables, unless all $K_i = 0$. Formally, then, variables x_i, for $i = 1$ to n, are said to be linearly independent if their linear combination, S, equals zero *only* if every $K_i = 0$ and no $x_i = 0$ for all $t \geq 0$.

System variable. Any variable that responds to an input or initial conditions in a system.

State variables. The smallest set of linearly independent system variables such that the values of the members of the set at time t_0 along with known forcing functions completely determine the value of all system variables for all $t \geq t_0$.

State vector. A vector whose elements are the state variables.

State space. The n-dimensional space whose axes are the state variables. This is a new term and is illustrated in Figure 3.3, where the state variables are assumed to be a resistor voltage, v_R, and a capacitor voltage, v_C. These variables form the axes of the *state space*. A trajectory can be thought of as being mapped out by the state vector, $\mathbf{x}(t)$, for a range of t. Also shown is the state vector at the particular time $t = 4$.

State equations. A set of n simultaneous, first-order differential equations with n variables, where the n variables to be solved are the state variables.

Output equation. The algebraic equation that expresses the output variables of a system as linear combinations of the state variables and the inputs.

Now that the definitions have been formally stated, we define the state-space representation of a system. A system is represented in state space by the following equations:
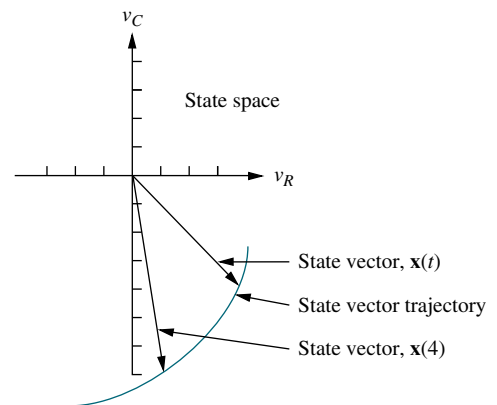
FIGURE 3.3   Graphic representation of state space and a state vector

$$\boxed{\dot{\mathbf{x}} = \mathbf{A}\mathbf{x} + \mathbf{B}\mathbf{u}} \tag{3.18}$$

$$\boxed{\mathbf{y} = \mathbf{C}\mathbf{x} + \mathbf{D}\mathbf{u}} \tag{3.19}$$

for $t \geq t_0$ and initial conditions, $\mathbf{x}(t_0)$, where

$\mathbf{x}$ = state vector
$\dot{\mathbf{x}}$ = derivative of the state vector with respect to time
$\mathbf{y}$ = output vector
$\mathbf{u}$ = input or control vector
$\mathbf{A}$ = system matrix
$\mathbf{B}$ = input matrix
$\mathbf{C}$ = output matrix
$\mathbf{D}$ = feedforward matrix

Equation (3.18) is called the *state equation*, and the vector $\mathbf{x}$, the *state vector*, contains the state variables. Equation (3.18) can be solved for the state variables, which we demonstrate in Chapter 4. Equation (3.19) is called the *output equation*. This equation is used to calculate any other system variables. This representation of a system provides complete knowledge of all variables of the system at any $t \geq t_0$.

As an example, for a linear, time-invariant, second-order system with a single input $v(t)$, the state equations could take on the following form:

$$\frac{dx_1}{dt} = a_{11}x_1 + a_{12}x_2 + b_1 v(t) \tag{3.20a}$$

$$\frac{dx_2}{dt} = a_{21}x_1 + a_{22}x_2 + b_2 v(t) \tag{3.20b}$$

where x_1 and x_2 are the state variables. If there is a single output, the output equation could take on the following form:

$$y = c_1 x_1 + c_2 x_2 + d_1 v(t) \tag{3.21}$$

The choice of state variables for a given system is not unique. The requirement in choosing the state variables is that they be linearly independent and that a minimum number of them be chosen.

3.4   Applying the State-Space Representation

In this section, we apply the state-space formulation to the representation of more complicated physical systems. The first step in representing a system is to select the state vector, which must be chosen according to the following considerations:

1. A minimum number of state variables must be selected as components of the state vector. This minimum number of state variables is sufficient to describe completely the state of the system.

2. The components of the state vector (that is, this minimum number of state variables) must be linearly independent.

Let us review and clarify these statements.

Linearly Independent State Variables

The components of the state vector must be linearly independent. For example, following the definition of linear independence in Section 3.3, if x_1, x_2, and x_3 are chosen as state variables, but $x_3 = 5x_1 + 4x_2$, then x_3 is not linearly independent of x_1

and x_2, since knowledge of the values of x_1 and x_2 will yield the value of x_3. Variables and their successive derivatives are linearly independent. For example, the voltage across an inductor, v_L, is linearly independent of the current through the inductor, i_L, since $v_L = L di_L/dt$. Thus, v_L cannot be evaluated as a linear combination of the current, i_L.

Minimum Number of State Variables

How do we know the minimum number of state variables to select? Typically, the minimum number required equals the order of the differential equation describing the system. For example, if a third-order differential equation describes the system, then three simultaneous, first-order differential equations are required along with three state variables. From the perspective of the transfer function, the order of the differential equation is the order of the denominator of the transfer function after canceling common factors in the numerator and denominator.

In most cases, another way to determine the number of state variables is to count the number of independent energy-storage elements in the system.[5] The number of these energy-storage elements equals the order of the differential equation and the number of state variables. In Figure 3.2 there are two energy-storage elements, the capacitor and the inductor. Hence, two state variables and two state equations are required for the system.

If too few state variables are selected, it may be impossible to write particular output equations, since some system variables cannot be written as a linear combination of the reduced number of state variables. In many cases, it may be impossible even to complete the writing of the state equations, since the derivatives of the state variables cannot be expressed as linear combinations of the reduced number of state variables.

If you select the minimum number of state variables but they are not linearly independent, at best you may not be able to solve for all other system variables. At worst you may not be able to complete the writing of the state equations.

Often the state vector includes more than the minimum number of state variables required. Two possible cases exist. Often state variables are chosen to be physical variables of a system, such as position and velocity in a mechanical system. Cases arise where these variables, although linearly independent, are also *decoupled*. That is, some linearly independent variables are not required in order to solve for any of the other linearly independent variables or any other dependent system variable. Consider the case of a mass and viscous damper whose differential equation is $M\,dv/dt + Dv = f(t)$, where v is the velocity of the mass. Since this is a first-order equation, one state equation is all that is required to define this system in state space with velocity as the state variable. Also, since there is only one energy-storage element, mass, only one state variable is required to represent this system in state space. However, the mass also has an associated position, which is linearly independent of velocity. If we want to include position in the state vector along with velocity, then we add position as a state variable that is linearly independent of the other state variable, velocity. Figure 3.4 illustrates what is happening. The first block is the transfer
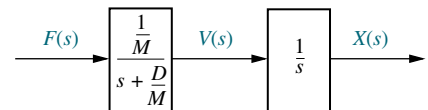
FIGURE 3.4 Block diagram of a mass and damper

---

function equivalent to $M \, dv(t)/dt + Dv(t) = f(t)$. The second block shows that we integrate the output velocity to yield output displacement (see Table 2.2, Item 10). Thus, if we want displacement as an output, the denominator, or characteristic equation, has increased in order to 2, the product of the two transfer functions. Many times, the writing of the state equations is simplified by including additional state variables.

Another case that increases the size of the state vector arises when the added variable is not linearly independent of the other members of the state vector. This usually occurs when a variable is selected as a state variable but its dependence on the other state variables is not immediately apparent. For example, energy-storage elements may be used to select the state variables, and the dependence of the variable associated with one energy-storage element on the variables of other energy-storage elements may not be recognized. Thus, the dimension of the system matrix is increased unnecessarily, and the solution for the state vector, which we cover in Chapter 4, is more difficult. Also, adding dependent state variables affects the designer's ability to use state-space methods for design.[6]

We saw in Section 3.2 that the state-space representation is not unique. The following example demonstrates one technique for selecting state variables and representing a system in state space. Our approach is to write the simple derivative equation for each energy-storage element and solve for each derivative term as a linear combination of any of the system variables and the input that are present in the equation. Next we select each differentiated variable as a state variable. Then we express all other system variables in the equations in terms of the state variables and the input. Finally, we write the output variables as linear combinations of the state variables and the input.

Example 3.1

Representing an Electrical Network

PROBLEM: Given the electrical network of Figure 3.5, find a state-space representation if the output is the current through the resistor.

FIGURE 3.5   Electrical network for representation in state space
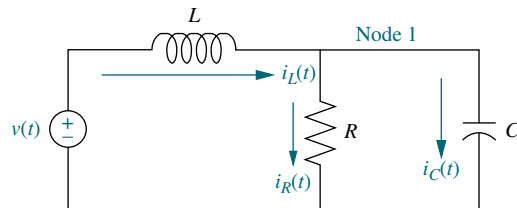
SOLUTION: The following steps will yield a viable representation of the network in state space.

Step 1   Label all of the branch currents in the network. These include i_L, i_R, and i_C, as shown in Figure 3.5.

---

[6] See Chapter 12 for state-space design techniques.

Step 2   Select the state variables by writing the derivative equation for all energy-storage elements, that is, the inductor and the capacitor. Thus,

$$C\frac{dv_C}{dt} = i_C \tag{3.22}$$

$$L\frac{di_L}{dt} = v_L \tag{3.23}$$

From Eqs. (3.22) and (3.23), choose the state variables as the quantities that are differentiated, namely v_C and i_L. Using Eq. (3.20) as a guide, we see that the state-space representation is complete if the right-hand sides of Eqs. (3.22) and (3.23) can be written as linear combinations of the state variables and the input.

Since i_C and v_L are not state variables, our next step is to express i_C and v_L as linear combinations of the state variables, v_C and i_L, and the input, $v(t)$.

Step 3   Apply network theory, such as Kirchhoff's voltage and current laws, to obtain i_C and v_L in terms of the state variables, v_C and i_L. At Node 1,

$$i_C = -i_R + i_L$$
$$= -\frac{1}{R}v_C + i_L \tag{3.24}$$

which yields i_C in terms of the state variables, v_C and i_L.

Around the outer loop,

$$v_L = -v_C + v(t) \tag{3.25}$$

which yields v_L in terms of the state variable, v_C, and the source, $v(t)$.

Step 4   Substitute the results of Eqs. (3.24) and (3.25) into Eqs. (3.22) and (3.23) to obtain the following state equations:

$$C\frac{dv_C}{dt} = -\frac{1}{R}v_C + i_L \tag{3.26a}$$

$$L\frac{di_L}{dt} = \quad -v_C + v(t) \tag{3.26b}$$

or

$$\frac{dv_C}{dt} = -\frac{1}{RC}v_C + \frac{1}{C}i_L \tag{3.27a}$$

$$\frac{di_L}{dt} = \quad -\frac{1}{L}v_C + \frac{1}{L}v(t) \tag{3.27b}$$

Step 5   Find the output equation. Since the output is $i_R(t)$,

$$i_R = \frac{1}{R}v_C \tag{3.28}$$

The final result for the state-space representation is found by representing Eqs. (3.27) and (3.28) in vector-matrix form as follows:

$$\begin{bmatrix} \dot{v}_C \\ \dot{i}_L \end{bmatrix} = \begin{bmatrix} -1/(RC) & 1/C \\ -1/L & 0 \end{bmatrix} \begin{bmatrix} v_C \\ i_L \end{bmatrix} + \begin{bmatrix} 0 \\ 1/L \end{bmatrix} v(t) \tag{3.29a}$$

$$i_R = \begin{bmatrix} 1/R & 0 \end{bmatrix} \begin{bmatrix} v_C \\ i_L \end{bmatrix} \tag{3.29b}$$

where the dot indicates differentiation with respect to time.

In order to clarify the representation of physical systems in state space, we will look at two more examples. The first is an electrical network with a dependent source. Although we will follow the same procedure as in the previous problem, this problem will yield increased complexity in applying network analysis to find the state equations. For the second example, we find the state-space representation of a mechanical system.

Example 3.2

Representing an Electrical Network with a Dependent Source

PROBLEM: Find the state and output equations for the electrical network shown in Figure 3.6 if the output vector is $\mathbf{y} = [\,v_{R_2} \quad i_{R_2}\,]^T$, where T means transpose.[7]
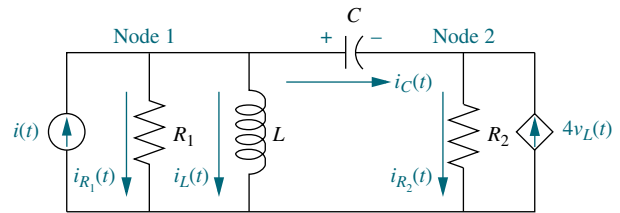
FIGURE 3.6 Electrical network for Example 3.2

SOLUTION: Immediately notice that this network has a voltage-dependent current source.

Step 1 Label all of the branch currents on the network, as shown in Figure 3.6.

Step 2 Select the state variables by listing the voltage-current relationships for all of the energy-storage elements:

$$L\frac{di_L}{dt} = v_L \tag{3.30a}$$

$$C\frac{dv_C}{dt} = i_C \tag{3.30b}$$

From Eqs. (3.30) select the state variables to be the differentiated variables. Thus, the state variables, x_1 and x_2, are

$$x_1 = i_L; \quad x_2 = v_C \tag{3.31}$$

Step 3 Remembering that the form of the state equation is

$$\dot{\mathbf{x}} = \mathbf{Ax} + \mathbf{Bu} \tag{3.32}$$

we see that the remaining task is to transform the right-hand side of Eq. (3.30) into linear combinations of the state variables and input source current. Using Kirchhoff's voltage and current laws, we find v_L and i_C in terms of the state variables and the input current source.

---

[7] See Appendix G for a discussion of the transpose. Appendix G is located at www.wiley.com/college/nise.

Around the mesh containing L and C,

$$v_L = v_C + v_{R_2} = v_C + i_{R_2}R_2 \tag{3.33}$$

But at Node 2, $i_{R_2} = i_C + 4v_L$. Substituting this relationship for i_{R_2} into Eq. (3.33) yields

$$v_L = v_C + (i_C + 4v_L)R_2 \tag{3.34}$$

Solving for v_L, we get

$$v_L = \frac{1}{1 - 4R_2}(v_C + i_C R_2) \tag{3.35}$$

Notice that since v_C is a state variable, we only need to find i_C in terms of the state variables. We will then have obtained v_L in terms of the state variables.

Thus, at Node 1 we can write the sum of the currents as

$$i_C = i(t) - i_{R_1} - i_L$$

$$= i(t) - \frac{v_{R_1}}{R_1} - i_L$$

$$= i(t) - \frac{v_L}{R_1} - i_L \tag{3.36}$$

where $v_{R_1} = v_L$. Equations (3.35) and (3.36) are two equations relating v_L and i_C in terms of the state variables i_L and v_C. Rewriting Eqs. (3.35) and (3.36), we obtain two simultaneous equations yielding v_L and i_C as linear combinations of the state variables i_L and v_C:

$$(1 - 4R_2)v_L - R_2 i_C = v_C \tag{3.37a}$$

$$-\frac{1}{R_1}v_L - i_C = i_L - i(t) \tag{3.37b}$$

Solving Eq. (3.37) simultaneously for v_L and i_C yields

$$v_L = \frac{1}{\Delta}[R_2 i_L - v_C - R_2 i(t)] \tag{3.38}$$

and

$$i_C = \frac{1}{\Delta}\left[(1 - 4R_2)i_L + \frac{1}{R_1}v_C - (1 - 4R_2)i(t)\right] \tag{3.39}$$

where

$$\Delta = -\left[(1 - 4R_2) + \frac{R_2}{R_1}\right] \tag{3.40}$$

Substituting Eqs. (3.38) and (3.39) into (3.30), simplifying, and writing the result in vector-matrix form renders the following state equation:

$$\begin{bmatrix} \dot{i}_L \\ \dot{v}_C \end{bmatrix} = \begin{bmatrix} R_2/(L\Delta) & -1/(L\Delta) \\ (1 - 4R_2)/(C\Delta) & 1/(R_1 C\Delta) \end{bmatrix} \begin{bmatrix} i_L \\ v_C \end{bmatrix}$$

$$+ \begin{bmatrix} -R_2/(L\Delta) \\ -(1 - 4R_2)/(C\Delta) \end{bmatrix} i(t) \tag{3.41}$$

Step 4   Derive the output equation. Since the specified output variables are v_{R_2} and i_{R_2}, we note that around the mesh containing C, L, and R_2,

$$v_{R_2} = -v_C + v_L \tag{3.42a}$$

$$i_{R_2} = i_C + 4v_L \tag{3.42b}$$

Substituting Eqs. (3.38) and (3.39) into Eq. (3.42), v_{R_2} and i_{R_2} are obtained as linear combinations of the state variables, i_L and v_C. In vector-matrix form, the output equation is

$$\begin{bmatrix} v_{R_2} \\ i_{R_2} \end{bmatrix} = \begin{bmatrix} R_2/\Delta & -(1+1/\Delta) \\ 1/\Delta & (1-4R_1)/(\Delta R_1) \end{bmatrix} \begin{bmatrix} i_L \\ v_C \end{bmatrix} + \begin{bmatrix} -R_2/\Delta \\ -1/\Delta \end{bmatrix} i(t) \tag{3.43}$$

In the next example, we find the state-space representation for a mechanical system. It is more convenient when working with mechanical systems to obtain the state equations directly from the equations of motion rather than from the energy-storage elements. For example, consider an energy-storage element such as a spring, where $F = Kx$. This relationship does not contain the derivative of a physical variable as in the case of electrical networks, where $i = C \, dv/dt$ for capacitors, and $v = L \, di/dt$ for inductors. Thus, in mechanical systems we change our selection of state variables to be the position and velocity of each point of linearly independent motion. In the example, we will see that although there are three energy-storage elements, there will be four state variables; an additional linearly independent state variable is included for the convenience of writing the state equations. It is left to the student to show that this system yields a fourth-order transfer function if we relate the displacement of either mass to the applied force, and a third-order transfer function if we relate the velocity of either mass to the applied force.

Example 3.3

Representing a Translational Mechanical System

PROBLEM: Find the state equations for the translational mechanical system shown in Figure 3.7.
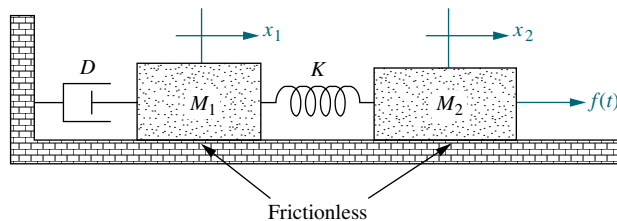
FIGURE 3.7   Translational mechanical system

SOLUTION: First write the differential equations for the network in Figure 3.7, using the methods of Chapter 2 to find the Laplace-transformed equations of motion. Next take the inverse Laplace transform of these equations, assuming zero

initial conditions, and obtain

$$M_1 \frac{d^2 x_1}{dt^2} + D \frac{dx_1}{dt} + K x_1 - K x_2 = 0 \tag{3.44}$$

$$-K x_1 + M_2 \frac{d^2 x_2}{dt^2} + K x_2 = f(t) \tag{3.45}$$

Now let $d^2 x_1 / dt^2 = dv_1 / dt$, and $d^2 x_2 / dt^2 = dv_2 / dt$, and then select x_1, v_1, x_2, and v_2 as state variables. Next form two of the state equations by solving Eq. (3.44) for dv_1 / dt and Eq. (3.45) for dv_2 / dt. Finally, add $dx_1 / dt = v_1$ and $dx_2 / dt = v_2$ to complete the set of state equations. Hence,

$$\frac{dx_1}{dt} = \qquad\qquad + v_1 \tag{3.46a}$$

$$\frac{dv_1}{dt} = -\frac{K}{M_1} x_1 - \frac{D}{M_1} v_1 + \frac{K}{M_1} x_2 \tag{3.46b}$$

$$\frac{dx_2}{dt} = \qquad\qquad\qquad + v_2 \tag{3.46c}$$

$$\frac{dv_2}{dt} = +\frac{K}{M_2} x_1 \qquad\qquad - \frac{K}{M_2} x_2 \qquad + \frac{1}{M_2} f(t) \tag{3.46d}$$

In vector-matrix form,

$$\begin{bmatrix} \dot{x}_1 \\ \dot{v}_1 \\ \dot{x}_2 \\ \dot{v}_2 \end{bmatrix} = \begin{bmatrix} 0 & 1 & 0 & 0 \\ -K/M_1 & -D/M_1 & K/M_1 & 0 \\ 0 & 0 & 0 & 1 \\ K/M_2 & 0 & -K/M_2 & 0 \end{bmatrix} \begin{bmatrix} x_1 \\ v_1 \\ x_2 \\ v_2 \end{bmatrix} + \begin{bmatrix} 0 \\ 0 \\ 0 \\ 1/M_2 \end{bmatrix} f(t) \tag{3.47}$$

where the dot indicates differentiation with respect to time. What is the output equation if the output is $x(t)$?

Skill-Assessment Exercise 3.1

PROBLEM: Find the state-space representation of the electrical network shown in Figure 3.8. The output is $v_o(t)$.
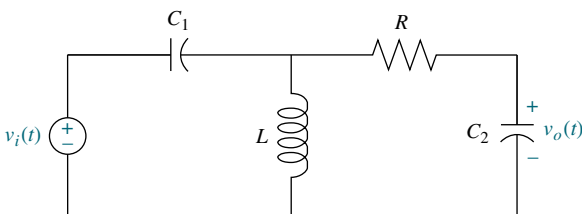
FIGURE 3.8 Electric circuit for Skill-Assessment Exercise 3.1

ANSWER:

$$
\dot{\mathbf{x}} = \begin{bmatrix} 1/C_1 & 1/C_1 & -1/C_1 \\ -1/L & 0 & 0 \\ 1/C_2 & 0 & -1/C_2 \end{bmatrix} \mathbf{x} + \begin{bmatrix} 0 \\ 1 \\ 0 \end{bmatrix} v_i(t)
$$

$$
y = \begin{bmatrix} 0 & 0 & 1 \end{bmatrix} \mathbf{x}
$$

The complete solution is at www.wiley.com/college/nise.

Skill-Assessment Exercise 3.2

PROBLEM: Represent the translational mechanical system shown in Figure 3.9 in state space, where $x_3(t)$ is the output.
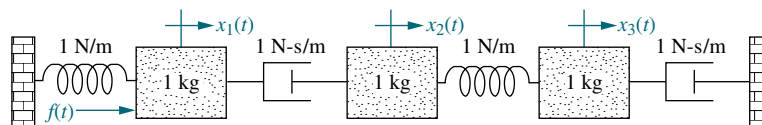
FIGURE 3.9   Translational mechanical system for Skill-Assessment Exercise 3.2

ANSWER:

$$
\dot{\mathbf{z}} = \begin{bmatrix} 0 & 1 & 0 & 0 & 0 & 0 \\ -1 & -1 & 0 & 1 & 0 & 0 \\ 0 & 0 & 0 & 1 & 0 & 0 \\ 0 & 1 & -1 & -1 & 1 & 0 \\ 0 & 0 & 0 & 0 & 0 & 1 \\ 0 & 0 & 1 & 0 & -1 & -1 \end{bmatrix} \mathbf{z} + \begin{bmatrix} 0 \\ 1 \\ 0 \\ 0 \\ 0 \\ 0 \end{bmatrix} f(t)
$$

$$
y = \begin{bmatrix} 0 & 0 & 0 & 0 & 1 & 0 \end{bmatrix} \mathbf{z}
$$

where

$$
\mathbf{z} = \begin{bmatrix} x_1 & \dot{x}_1 & x_2 & \dot{x}_2 & x_3 & \dot{x}_3 \end{bmatrix}^T
$$

The complete solution is at www.wiley.com/college/nise.

3.5   Converting a Transfer Function to State Space

In the last section, we applied the state-space representation to electrical and mechanical systems. We learn how to convert a transfer function representation to a state-space representation in this section. One advantage of the state-space

representation is that it can be used for the simulation of physical systems on the digital computer. Thus, if we want to simulate a system that is represented by a transfer function, we must first convert the transfer function representation to state space.

At first we select a set of state variables, called *phase variables*, where each subsequent state variable is defined to be the derivative of the previous state variable. In Chapter 5 we show how to make other choices for the state variables.

Let us begin by showing how to represent a general, nth-order, linear differential equation with constant coefficients in state space in the phase-variable form. We will then show how to apply this representation to transfer functions.

Consider the differential equation

$$\frac{d^n y}{dt^n} + a_{n-1}\frac{d^{n-1} y}{dt^{n-1}} + \cdots + a_1\frac{dy}{dt} + a_0 y = b_0 u \tag{3.48}$$

A convenient way to choose state variables is to choose the output, $y(t)$, and its $(n-1)$ derivatives as the state variables. This choice is called the *phase-variable choice*. Choosing the state variables, x_i, we get

$$x_1 = y \tag{3.49a}$$

$$x_2 = \frac{dy}{dt} \tag{3.49b}$$

$$x_3 = \frac{d^2 y}{dt^2} \tag{3.49c}$$

$$\vdots \tag{3.49d}$$

$$x_n = \frac{d^{n-1} y}{dt^{n-1}}$$

and differentiating both sides yields

$$\dot{x}_1 = \frac{dy}{dt} \tag{3.50a}$$

$$\dot{x}_2 = \frac{d^2 y}{dt^2} \tag{3.50b}$$

$$\dot{x}_3 = \frac{d^3 y}{dt^3} \tag{3.50c}$$

$$\vdots \tag{3.50d}$$

$$\dot{x}_n = \frac{d^n y}{dt^n}$$

where the dot above the x signifies differentiation with respect to time.

Substituting the definitions of Eq. (3.49) into Eq. (3.50), the state equations are evaluated as

$$\dot{x}_1 = x_2 \tag{3.51a}$$

$$\dot{x}_2 = x_3 \tag{3.51b}$$

$$\vdots \tag{3.51c}$$

$$\dot{x}_{n-1} = x_n$$

$$\dot{x}_n = -a_0 x_1 - a_1 x_2 \cdots - a_{n-1} x_n + b_0 u \tag{3.51d}$$

where Eq. (3.51d) was obtained from Eq. (3.48) by solving for $d^n y/dt^n$ and using Eq. (3.49). In vector-matrix form, Eq. (3.51) become

$$
\begin{bmatrix} \dot{x}_1 \\ \dot{x}_2 \\ \dot{x}_3 \\ \vdots \\ \dot{x}_{n-1} \\ \dot{x}_n \end{bmatrix} = \begin{bmatrix} 0 & 1 & 0 & 0 & 0 & 0 & \cdots & 0 \\ 0 & 0 & 1 & 0 & 0 & 0 & \cdots & 0 \\ 0 & 0 & 0 & 1 & 0 & 0 & \cdots & 0 \\ \vdots & & & & & & & \\ 0 & 0 & 0 & 0 & 0 & 0 & \cdots & 1 \\ -a_0 & -a_1 & -a_2 & -a_3 & -a_4 & -a_5 & \cdots & -a_{n-1} \end{bmatrix} \begin{bmatrix} x_1 \\ x_2 \\ x_3 \\ \vdots \\ x_{n-1} \\ x_n \end{bmatrix} + \begin{bmatrix} 0 \\ 0 \\ 0 \\ \vdots \\ 0 \\ b_0 \end{bmatrix} u
$$

$$(3.52)$$

Equation (3.52) is the phase-variable form of the state equations. This form is easily recognized by the unique pattern of 1's and 0's and the negative of the coefficients of the differential equation written in reverse order in the last row of the system matrix.

Finally, since the solution to the differential equation is $y(t)$, or x_1, the output equation is

$$
y = \begin{bmatrix} 1 & 0 & 0 & \cdots & 0 \end{bmatrix} \begin{bmatrix} x_1 \\ x_2 \\ x_3 \\ \vdots \\ x_{n-1} \\ x_n \end{bmatrix}
$$

$$(3.53)$$

In summary, then, to convert a transfer function into state equations in phase-variable form, we first convert the transfer function to a differential equation by cross-multiplying and taking the inverse Laplace transform, assuming zero initial conditions. Then we represent the differential equation in state space in phase-variable form. An example illustrates the process.

Example 3.4

Converting a Transfer Function with Constant Term in Numerator

PROBLEM: Find the state-space representation in phase-variable form for the transfer function shown in Figure 3.10(*a*).

SOLUTION:

Step 1 Find the associated differential equation. Since

$$\frac{C(s)}{R(s)} = \frac{24}{(s^3 + 9s^2 + 26s + 24)} \tag{3.54}$$

cross-multiplying yields

$$(s^3 + 9s^2 + 26s + 24)C(s) = 24R(s) \tag{3.55}$$

The corresponding differential equation is found by taking the inverse Laplace transform, assuming zero initial conditions:

$$\dddot{c} + 9\ddot{c} + 26\dot{c} + 24c = 24r \tag{3.56}$$

(a)

(b)
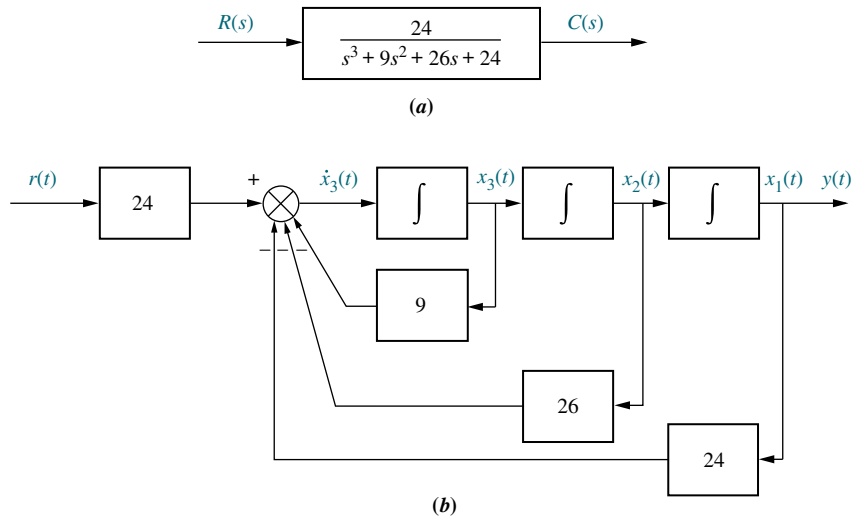
FIGURE 3.10   a. Transfer function; **b.** equivalent block diagram showing phase variables. Note: $y(t) = c(t)$.

Step 2   Select the state variables.
Choosing the state variables as successive derivatives, we get

$$x_1 = c \tag{3.57a}$$

$$x_2 = \dot{c} \tag{3.57b}$$

$$x_3 = \ddot{c} \tag{3.57c}$$

Differentiating both sides and making use of Eq. (3.57) to find $\dot{x}_1$ and $\dot{x}_2$, and Eq. (3.56) to find $\tilde{c} = \dot{x}_3$, we obtain the state equations. Since the output is $c = x_1$, the combined state and output equations are

$$\dot{x}_1 = \qquad\qquad x_2 \tag{3.58a}$$

$$\dot{x}_2 = \qquad\qquad\qquad x_3 \tag{3.58b}$$

$$\dot{x}_3 = -24x_1 - 26x_2 - 9x_3 + 24r \tag{3.58c}$$

$$y = c = x_1 \tag{3.58d}$$

In vector-matrix form,

$$\begin{bmatrix} \dot{x}_1 \\ \dot{x}_2 \\ \dot{x}_3 \end{bmatrix} = \begin{bmatrix} 0 & 1 & 0 \\ 0 & 0 & 1 \\ -24 & -26 & -9 \end{bmatrix} \begin{bmatrix} x_1 \\ x_2 \\ x_3 \end{bmatrix} + \begin{bmatrix} 0 \\ 0 \\ 24 \end{bmatrix} r \tag{3.59a}$$

$$y = \begin{bmatrix} 1 & 0 & 0 \end{bmatrix} \begin{bmatrix} x_1 \\ x_2 \\ x_3 \end{bmatrix} \tag{3.59b}$$

Notice that the third row of the system matrix has the same coefficients as the denominator of the transfer function but negative and in reverse order.

At this point, we can create an equivalent block diagram of the system of Figure 3.10(a) to help visualize the state variables. We draw three integral blocks as shown in Figure 3.10(b) and label each output as one of the state variables, $x_i(t)$, as shown. Since the input to each integrator is $x_i(t)$, use Eqs. (3.58a), (3.58b), and (3.58c) to determine

the combination of input signals to each integrator. Form and label each input. Finally, use Eq. (3.58d) to form and label the output, $y(t) = c(t)$. The final result of Figure 3.10 (b) is a system equivalent to Figure 3.10(a) that explicitly shows the state variables and gives a vivid picture of the state-space representation.

```
Students who are using MATLAB should now run ch3p1 through ch3p4
in Appendix B. You will learn how to represent the system matrix
A, the input matrix B, and the output matrix C using MATLAB. You
will learn how to convert a transfer function to the state-space
representation in phase-variable form. Finally, Example 3.4
will be solved using MATLAB.
```

The transfer function of Example 3.4 has a constant term in the numerator. If a transfer function has a polynomial in s in the numerator that is of order less than the polynomial in the denominator, as shown in Figure 3.11(a), the numerator and denominator can be handled separately. First separate the transfer function into two cascaded transfer functions, as shown in Figure 3.11(b); the first is the denominator, and the second is just the numerator. The first transfer function with just the denominator is converted to the phase-variable representation in state space as demonstrated in the last example. Hence, phase variable x_1 is the output, and the rest of the phase variables are the internal variables of the first block, as shown in Figure 3.11(b). The second transfer function with just the numerator yields

$$Y(s) = C(s) = (b_2 s^2 + b_1 s + b_0)X_1(s) \tag{3.60}$$

where, after taking the inverse Laplace transform with zero initial conditions,

$$y(t) = b_2 \frac{d^2 x_1}{dt^2} + b_1 \frac{dx_1}{dt} + b_0 x_1 \tag{3.61}$$

But the derivative terms are the definitions of the phase variables obtained in the first block. Thus, writing the terms in reverse order to conform to an output equation,

$$y(t) = b_0 x_1 + b_1 x_2 + b_2 x_3 \tag{3.62}$$

Hence, the second block simply forms a specified linear combination of the state variables developed in the first block.

From another perspective, the denominator of the transfer function yields the state equations, while the numerator yields the output equation. The next example demonstrates the process.

(a)
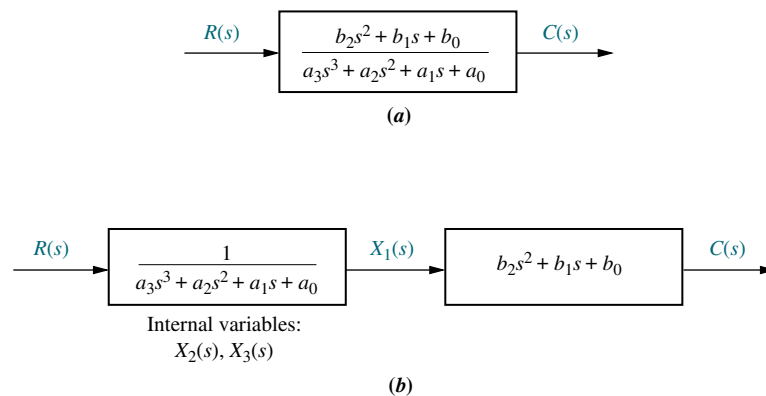
FIGURE 3.11 Decomposing a transfer function

(b)

Example 3.5

Converting a Transfer Function with Polynomial in Numerator

PROBLEM: Find the state-space representation of the transfer function shown in Figure 3.12(*a*).

(*a*)

Internal variables:
$X_2(s)$, $X_3(s)$

(*b*)

(*c*)
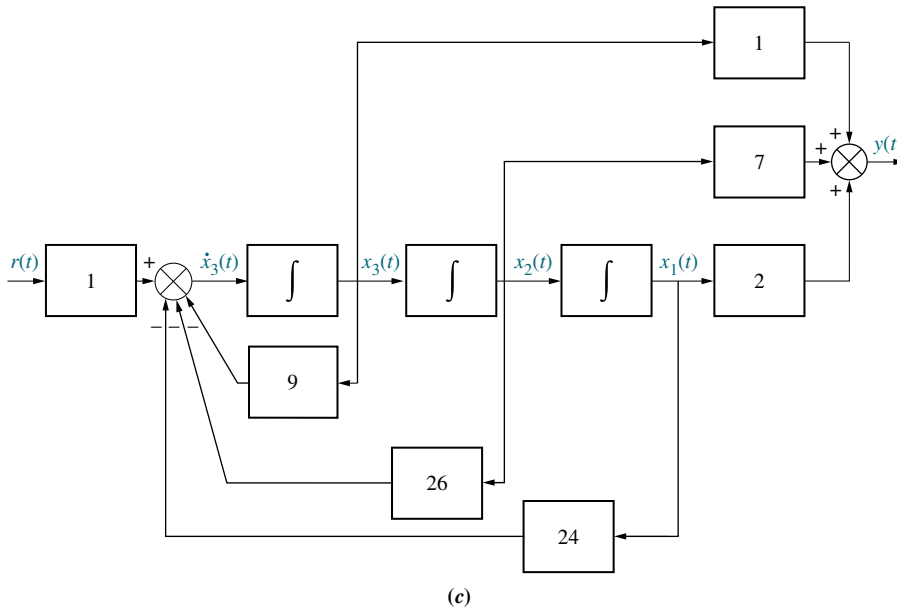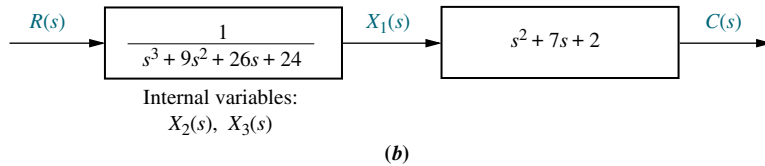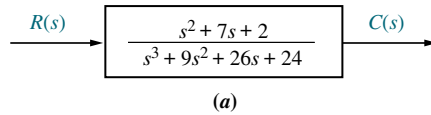
FIGURE 3.12   a. Transfer function; **b.** decomposed transfer function; **c.** equivalent block diagram Note: $y(t) = c(t)$.

SOLUTION: This problem differs from Example 3.4 since the numerator has a polynomial in *s* instead of just a constant term.

Step 1   Separate the system into two cascaded blocks, as shown in Figure 3.12(*b*). The first block contains the denominator and the second block contains the numerator.

Step 2   Find the state equations for the block containing the denominator. We notice that the first block's numerator is 1/24 that of Example 3.4. Thus, the state equations are the same except that this system's input matrix is 1/24 that of Example 3.4. Hence, the state equation is

$$\begin{bmatrix} \dot{x}_1 \\ \dot{x}_2 \\ \dot{x}_3 \end{bmatrix} = \begin{bmatrix} 0 & 1 & 0 \\ 0 & 0 & 1 \\ -24 & -26 & -9 \end{bmatrix} \begin{bmatrix} x_1 \\ x_2 \\ x_3 \end{bmatrix} + \begin{bmatrix} 0 \\ 0 \\ 1 \end{bmatrix} r \qquad (3.63)$$

Step 3   Introduce the effect of the block with the numerator. The second block of Figure 3.12(b), where $b_2 = 1$, $b_1 = 7$, and $b_0 = 2$, states that

$$C(s) = (b_2 s^2 + b_1 s + b_0)X_1(s) = (s^2 + 7s + 2)X_1(s) \qquad (3.64)$$

Taking the inverse Laplace transform with zero initial conditions, we get

$$c = \ddot{x}_1 + 7\dot{x}_1 + 2x_1 \qquad (3.65)$$

But

$$x_1 = x_1$$
$$\dot{x}_1 = x_2$$
$$\ddot{x}_1 = x_3$$

Hence,

$$y = c(t) = b_2 x_3 + b_1 x_2 + b_0 x_1 = x_3 + x_2 + 2x_1 \qquad (3.66)$$

Thus, the last box of Figure 3.11(b) "collects" the states and generates the output equation. From Eq. (3.66),

$$y = \begin{bmatrix} b_0 & b_1 & b_2 \end{bmatrix} \begin{bmatrix} x_1 \\ x_2 \\ x_3 \end{bmatrix} = \begin{bmatrix} 2 & 7 & 1 \end{bmatrix} \begin{bmatrix} x_1 \\ x_2 \\ x_3 \end{bmatrix} \qquad (3.67)$$

Although the second block of Figure 3.12(b) shows differentiation, this block was implemented without differentiation because of the partitioning that was applied to the transfer function. The last block simply collected derivatives that were already formed by the first block.

Once again we can produce an equivalent block diagram that vividly represents our state-space model. The first block of Figure 3.12(b) is the same as Figure 3.10(a) except for the different constant in the numerator. Thus, in Figure 3.12(c) we reproduce Figure 3.10(b) except for the change in the numerator constant, which appears as a change in the input multiplying factor. The second block of Figure 3.12(b) is represented using Eq. (3.66), which forms the output from a linear combination of the state variables, as shown in Figure 3.12(c).

TryIt 3.1

Use the following MATLAB statements to form an LTI state-space representation from the transfer function shown in Figure 3.12(a). The **A** matrix and **B** vector are shown in Eq. (3.63). The **C** vector is shown in Eq. (3.67).

```
num=[1 7 2];
den=[1 9 26 24];
[A,B,C,D]=tf2ss...
 (num,den);
P=[0 0 1;0 1 0;1 0 0];
A=inv(P)*A*P
B=inv(P)*B
C=C*P
```

Skill-Assessment Exercise 3.3

WileyPLUS

WPCS

Control Solutions

PROBLEM: Find the state equations and output equation for the phase-variable representation of the transfer function $G(s) = \dfrac{2s + 1}{s^2 + 7s + 9}$.

ANSWER:

$$\dot{\mathbf{x}} = \begin{bmatrix} 0 & 1 \\ -9 & -7 \end{bmatrix} \mathbf{x} + \begin{bmatrix} 0 \\ 1 \end{bmatrix} r(t)$$
$$y = \begin{bmatrix} 1 & 2 \end{bmatrix} \mathbf{x}$$

The complete solution is at www.wiley.com/college.nise.

3.6   Converting from State Space to a Transfer Function

In Chapters 2 and 3, we have explored two methods of representing systems: the transfer function representation and the state-space representation. In the last section, we united the two representations by converting transfer functions into state-space representations. Now we move in the opposite direction and convert the state-space representation into a transfer function.

Given the state and output equations

$$\dot{\mathbf{x}} = \mathbf{A}\mathbf{x} + \mathbf{B}\mathbf{u} \tag{3.68a}$$

$$\mathbf{y} = \mathbf{C}\mathbf{x} + \mathbf{D}\mathbf{u} \tag{3.68b}$$

take the Laplace transform assuming zero initial conditions:[8]

$$s\mathbf{X}(s) = \mathbf{A}\mathbf{X}(s) + \mathbf{B}\mathbf{U}(s) \tag{3.69a}$$

$$\mathbf{Y}(s) = \mathbf{C}\mathbf{X}(s) + \mathbf{D}\mathbf{U}(s) \tag{3.69b}$$

Solving for $\mathbf{X}(s)$ in Eq. (3.69a),

$$(s\mathbf{I} - \mathbf{A})\mathbf{X}(s) = \mathbf{B}\mathbf{U}(s) \tag{3.70}$$

or

$$\mathbf{X}(s) = (s\mathbf{I} - \mathbf{A})^{-1}\mathbf{B}\mathbf{U}(s) \tag{3.71}$$

where $\mathbf{I}$ is the identity matrix.

Substituting Eq. (3.71) into Eq. (3.69b) yields

$$\mathbf{Y}(s) = \mathbf{C}(s\mathbf{I} - \mathbf{A})^{-1}\mathbf{B}\mathbf{U}(s) + \mathbf{D}\mathbf{U}(s) = [\mathbf{C}(s\mathbf{I} - \mathbf{A})^{-1}\mathbf{B} + \mathbf{D}]\mathbf{U}(s) \tag{3.72}$$

We call the matrix $[\mathbf{C}(s\mathbf{I} - \mathbf{A})^{-1}\mathbf{B} + \mathbf{D}]$ the transfer function matrix, since it relates the output vector, $\mathbf{Y}(s)$, to the input vector, $\mathbf{U}(s)$. However, if $\mathbf{U}(s) = U(s)$ and $\mathbf{Y}(s) = Y(s)$ are scalars, we can find the transfer function,

$$T(s) = \frac{Y(s)}{U(s)} = \mathbf{C}(s\mathbf{I} - \mathbf{A})^{-1}\,\mathbf{B} + \mathbf{D} \tag{3.73}$$

Let us look at an example.

---

[8] The Laplace transform of a vector is found by taking the Laplace transform of each component. Since $\dot{\mathbf{x}}$ consists of the derivatives of the state variables, the Laplace transform of $\dot{\mathbf{x}}$ with zero initial conditions yields each component with the form $sX_i(s)$, where $X_i(s)$ is the Laplace transform of the state variable. Factoring out the complex variable, s, in each component yields the Laplace transform of $\dot{\mathbf{x}}$ as $s\,\mathbf{X}(s)$, where $\mathbf{X}(s)$ is a column vector with components $X_i(s)$.

Example 3.6

State-Space Representation to Transfer Function

PROBLEM: Given the system defined by Eq. (3.74), find the transfer function, $T(s) = Y(s)/U(s)$, where $U(s)$ is the input and $Y(s)$ is the output.

$$\dot{\mathbf{x}} = \begin{bmatrix} 0 & 1 & 0 \\ 0 & 0 & 1 \\ -1 & -2 & -3 \end{bmatrix} \mathbf{x} + \begin{bmatrix} 10 \\ 0 \\ 0 \end{bmatrix} u \tag{3.74a}$$

$$y = \begin{bmatrix} 1 & 0 & 0 \end{bmatrix} \mathbf{x} \tag{3.74b}$$

SOLUTION: The solution revolves around finding the term $(s\mathbf{I} - \mathbf{A})^{-1}$ in Eq. (3.73).[9] All other terms are already defined. Hence, first find $(s\mathbf{I} - \mathbf{A})$:

$$(s\mathbf{I} - \mathbf{A}) = \begin{bmatrix} s & 0 & 0 \\ 0 & s & 0 \\ 0 & 0 & s \end{bmatrix} - \begin{bmatrix} 0 & 1 & 0 \\ 0 & 0 & 1 \\ -1 & -2 & -3 \end{bmatrix} = \begin{bmatrix} s & -1 & 0 \\ 0 & s & -1 \\ 1 & 2 & s+3 \end{bmatrix} \tag{3.75}$$

Now form $(s\mathbf{I} - \mathbf{A})^{-1}$:

$$(s\mathbf{I} - \mathbf{A})^{-1} = \frac{\text{adj}(s\mathbf{I} - \mathbf{A})}{\det(s\mathbf{I} - \mathbf{A})} = \frac{\begin{bmatrix} (s^2 + 3s + 2) & s+3 & 1 \\ -1 & s(s+3) & s \\ -s & -(2s+1) & s^2 \end{bmatrix}}{s^3 + 3s^2 + 2s + 1} \tag{3.76}$$

Substituting $(s\mathbf{I} - \mathbf{A})^{-1}$, $\mathbf{B}$, $\mathbf{C}$, and $\mathbf{D}$ into Eq. (3.73), where

$$\mathbf{B} = \begin{bmatrix} 10 \\ 0 \\ 0 \end{bmatrix}$$

$$\mathbf{C} = \begin{bmatrix} 1 & 0 & 0 \end{bmatrix}$$

$$\mathbf{D} = 0$$

we obtain the final result for the transfer function:

$$T(s) = \frac{10(s^2 + 3s + 2)}{s^3 + 3s^2 + 2s + 1} \tag{3.77}$$

MATLAB

ML

Students who are using MATLAB should now run ch3p5 in Appendix B. You will learn how to convert a state-space representation to a transfer function using MATLAB. You can practice by writing a MATLAB program to solve Example 3.6.

Symbolic Math

SM

Students who are performing the MATLAB exercises and want to explore the added capability of MATLAB's Symbolic Math Toolbox should now run ch3sp1 in Appendix F located at www.wiley.com/college/nise. You will learn how to use the Symbolic Math Toolbox to write matrices and vectors. You will see that the Symbolic Math Toolbox yields an alternative way to use MATLAB to solve Example 3.6.

---

[9] See Appendix G. It is located at www.wiley.com/college/nise and discusses the evaluation of the matrix inverse.

PROBLEM: Convert the state and output equations shown in Eq. (3.78) to a transfer function.

$$\mathbf{x} = \begin{bmatrix} -4 & -1.5 \\ 4 & 0 \end{bmatrix}\mathbf{x} + \begin{bmatrix} 2 \\ 0 \end{bmatrix} u(t) \tag{3.78a}$$

$$y = \begin{bmatrix} 1.5 & 0.625 \end{bmatrix}\mathbf{x} \tag{3.78b}$$

ANSWER:

$$G(s) = \frac{3s + 5}{s^2 + 4s + 6}$$

The complete solution is located at www.wiley.com/college/nise.

TryIt 3.2

Use the following MATLAB and the Control System Toolbox statements to obtain the transfer function shown in Skill-Assessment Exercise 3.4 from the state-space representation of Eq. (3.78).

```
A=[−4 −1.5;4 0];
B=[2 0]';
C=[1.5 0.625];
D=0;
T=ss(A,B,C,D);
T=tf(T)
```

In Example 3.6, the state equations in phase-variable form were converted to transfer functions. In Chapter 5, we will see that other forms besides the phase-variable form can be used to represent a system in state space. The method of finding the transfer function representation for these other forms is the same as that presented in this section.

3.7   Linearization

A prime advantage of the state-space representation over the transfer function representation is the ability to represent systems with nonlinearities, such as the one shown in Figure 3.13. The ability to represent nonlinear systems does not imply the ability to solve their state equations for the state variables and the output. Techniques do exist for the solution of some nonlinear state equations, but this study is beyond the scope of this course. However, in Appendix H, located at www.wiley.com/college/nise,
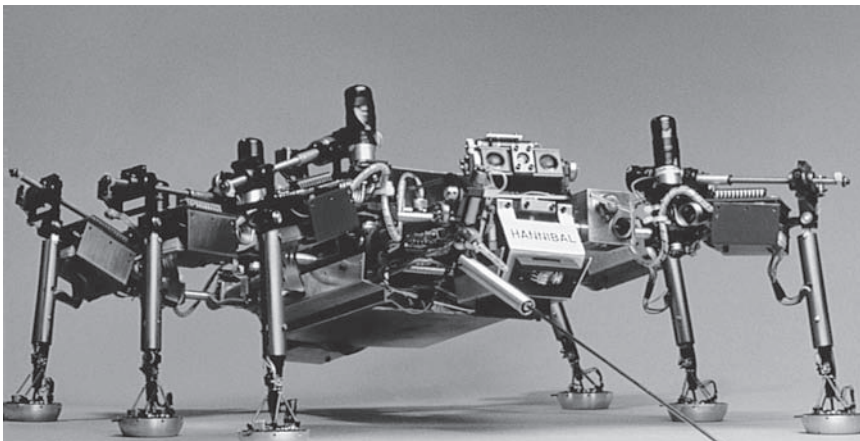
FIGURE 3.13   Walking robots, such as *Hannibal* shown here, can be used to explore hostile environments and rough terrain, such as that found on other planets or inside volcanoes.

you can see how to use the digital computer to solve state equations. This method also can be used for nonlinear state equations.

If we are interested in small perturbations about an equilibrium point, as we were when we studied linearization in Chapter 2, we can also linearize the state equations about the equilibrium point. The key to linearization about an equilibrium point is, once again, the Taylor series. In the following example, we write the state equations for a simple pendulum, showing that we can represent a nonlinear system in state space; then we linearize the pendulum about its equilibrium point, the vertical position with zero velocity.

Example 3.7
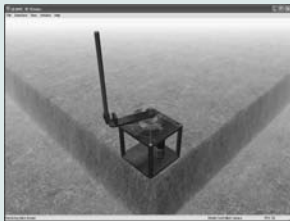
Representing a Nonlinear System

PROBLEM: First represent the simple pendulum shown in Figure 3.14(a) (which could be a simple model for the leg of the robot shown in Figure 3.13) in state space: Mg is the weight, T is an applied torque in the θ direction, and L is the length of the pendulum. Assume the mass is evenly distributed, with the center of mass at $L/2$. Then linearize the state equations about the pendulum's equilibrium point—the vertical position with zero angular velocity.
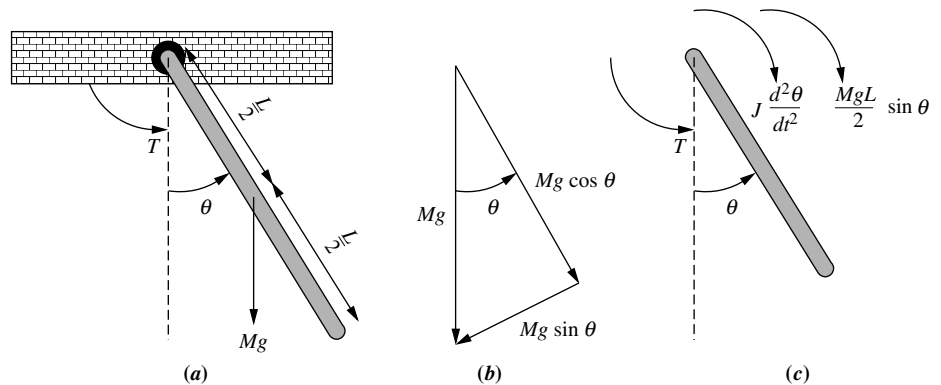
FIGURE 3.14   a. Simple pendulum; **b.** force components of Mg; **c.** free-body diagram

SOLUTION: First draw a free-body diagram as shown in Figure 3.14(c). Summing the torques, we get

$$J\frac{d^2\theta}{dt^2} + \frac{MgL}{2}\sin\theta = T \tag{3.79}$$

where J is the moment of inertia of the pendulum around the point of rotation. Select the state variables x_1 and x_2 as phase variables. Letting $x_1 = \theta$ and $x_2 = d\theta/dt$, we write the state equations as

$$\dot{x}_1 = x_2 \tag{3.80a}$$

$$\dot{x}_2 = -\frac{MgL}{2J}\sin x_1 + \frac{T}{J} \tag{3.80b}$$

where $\dot{x}_2 = d^2\theta/dt^2$ is evaluated from Eq. (3.79).

Thus, we have represented a nonlinear system in state space. It is interesting to note that the nonlinear Eq. (3.80) represent a valid and complete model of the pendulum in state space even under nonzero initial conditions and even if parameters are time varying. However, if we want to apply classical techniques and convert these state equations to a transfer function, we must linearize them.

Let us proceed now to linearize the equation about the equilibrium point, $x_1 = 0$, $x_2 = 0$, that is, $\theta = 0$ and $d\theta/dt = 0$. Let x_1 and x_2 be perturbed about the equilibrium point, or

$$x_1 = 0 + \delta x_1 \tag{3.81a}$$

$$x_2 = 0 + \delta x_2 \tag{3.81b}$$

Using Eq. (2.182), we obtain

$$\sin x_1 - \sin 0 = \left.\frac{d(\sin x_1)}{dx_1}\right|_{x_1=0} \delta x_1 = \delta x_1 \tag{3.82}$$

from which

$$\sin x_1 = \delta x_1 \tag{3.83}$$

Substituting Eqs. (3.81) and (3.83) into Eq. (3.80) yields the following state equations:

$$\dot{\delta x}_1 = \delta x_2 \tag{3.84a}$$

$$\dot{\delta x}_2 = -\frac{MgL}{2J}\delta x_1 + \frac{T}{J} \tag{3.84b}$$

which are linear and a good approximation to Eq. (3.80) for small excursions away from the equilibrium point. What is the output equation?

Skill-Assessment Exercise 3.5

PROBLEM: Represent the translational mechanical system shown in Figure 3.15 in state space about the equilibrium displacement. The spring is nonlinear, where the relationship between the spring force, $f_s(t)$, and the spring displacement, $x_s(t)$, is $f_s(t) = 2x_s^2(t)$. The applied force is $f(t) = 10 + \delta f(t)$, where $\delta f(t)$ is a small force about the 10 N constant value.

Assume the output to be the displacement of the mass, $x(t)$.

ANSWER:

$$\mathbf{x} = \begin{bmatrix} 0 & 1 \\ -4\sqrt{5} & 0 \end{bmatrix}\mathbf{x} + \begin{bmatrix} 0 \\ 1 \end{bmatrix}\delta f(t)$$

$$y = \begin{bmatrix} 1 & 0 \end{bmatrix}\mathbf{x}$$

The complete solution is located at www.wiley.com/college/nise.
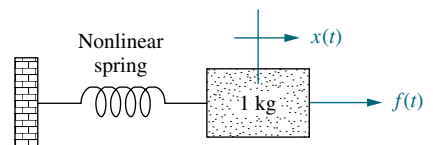
FIGURE 3.15 Nonlinear translational mechanical system for Skill-Assessment Exercise 3.5

Case Studies

Antenna Control: State-Space Representation

We have covered the state-space representation of individual physical subsystems in this chapter. In Chapter 5, we will assemble individual subsystems into feedback control systems and represent the entire feedback system in state space. Chapter 5 also shows how the state-space representation, via signal-flow diagrams, can be used to interconnect these subsystems and permit the state-space representation of the whole closed-loop system. In the following case study, we look at the antenna azimuth position control system and demonstrate the concepts of this chapter by representing each subsystem in state space.

PROBLEM: Find the state-space representation in phase-variable form for each dynamic subsystem in the antenna azimuth position control system shown on the front endpapers, *Configuration 1*. By *dynamic*, we mean that the system does not reach the steady state instantaneously. For example, a system described by a differential equation of first order or higher is a dynamic system. A pure gain, on the other hand, is an example of a nondynamic system, since the steady state is reached instantaneously.

SOLUTION: In the case study problem of Chapter 2, each subsystem of the antenna azimuth position control system was identified. We found that the power amplifier and the motor and load were dynamic systems. The preamplifier and the potentiometers are pure gains and so respond instantaneously. Hence, we will find the state-space representations only of the power amplifier and of the motor and load.

Power amplifier:
The transfer function of the power amplifier is given on the front endpapers as $G(s) = 100/(s + 100)$. We will convert this transfer function to its state-space representation. Letting $v_p(t)$ represent the power amplifier input and $e_a(t)$ represent the power amplifier output,

$$G(s) = \frac{E_a(s)}{V_p(s)} = \frac{100}{(s + 100)} \tag{3.85}$$

Cross-multiplying, $(s + 100)E_a(s) = 100V_p(s)$, from which the differential equation can be written as

$$\frac{de_a}{dt} + 100e_a = 100v_p(t) \tag{3.86}$$

Rearranging Eq. (3.86) leads to the state equation with e_a as the state variable:

$$\frac{de_a}{dt} = -100e_a + 100v_p(t) \tag{3.87}$$

Since the output of the power amplifier is $e_a(t)$, the output equation is

$$y = e_a \tag{3.88}$$

Motor and load:
We now find the state-space representation for the motor and load. We could of course use the motor and load block shown in the block diagram on the front endpapers to obtain the result. However, it is more informative to derive the state-space

representation directly from the physics of the motor without first deriving the transfer function. The elements of the derivation were covered in Section 2.8 but are repeated here for continuity. Starting with Kirchhoff's voltage equation around the armature circuit, we find

$$e_a(t) = i_a(t)R_a + K_b \frac{d\theta_m}{dt} \tag{3.89}$$

where $e_a(t)$ is the armature input voltage, $i_a(t)$ is the armature current, R_a is the armature resistance, K_b is the armature constant, and θ_m is the angular displacement of the armature.

The torque, $T_m(t)$, delivered by the motor is related separately to the armature current and the load seen by the armature. From Section 2.8,

$$T_m(t) = K_t i_a(t) = J_m \frac{d^2\theta_m}{dt^2} + D_m \frac{d\theta_m}{dt} \tag{3.90}$$

where J_m is the equivalent inertia as seen by the armature, and D_m is the equivalent viscous damping as seen by the armature.

Solving Eq. (3.90) for $i_a(t)$ and substituting the result into Eq. (3.89) yields

$$e_a(t) = \left(\frac{R_a J_m}{K_t}\right) \frac{d^2\theta_m}{dt^2} + \left(\frac{D_m R_a}{K_t} + K_b\right) \frac{d\theta_m}{dt} \tag{3.91}$$

Defining the state variables x_1 and x_2 as

$$x_1 = \theta_m \tag{3.92a}$$

$$x_2 = \frac{d\theta_m}{dt} \tag{3.92b}$$

and substituting into Eq. (3.91), we get

$$e_a(t) = \left(\frac{R_a J_m}{K_t}\right) \frac{dx_2}{dt} + \left(\frac{D_m R_a}{K_t} + K_b\right) x_2 \tag{3.93}$$

Solving for dx_2/dt yields

$$\frac{dx_2}{dt} = -\frac{1}{J_m}\left(D_m + \frac{K_t K_b}{R_a}\right)x_2 + \left(\frac{K_t}{R_a J_m}\right)e_a(t) \tag{3.94}$$

Using Eqs. (3.92) and (3.94), the state equations are written as

$$\frac{dx_1}{dt} = x_2 \tag{3.95a}$$

$$\frac{dx_2}{dt} = -\frac{1}{J_m}\left(D_m + \frac{K_t K_b}{R_a}\right)x_2 + \left(\frac{K_t}{R_a J_m}\right)e_a(t) \tag{3.95b}$$

The output, $\theta_o(t)$, is 1/10 the displacement of the armature, which is x_1. Hence, the output equation is

$$y = 0.1x_1 \tag{3.96}$$

In vector-matrix form,

$$\dot{\mathbf{x}} = \begin{bmatrix} 0 & 1 \\ 0 & -\frac{1}{J_m}\left(D_m + \frac{K_t K_b}{R_a}\right) \end{bmatrix}\mathbf{x} + \begin{bmatrix} 0 \\ \frac{K_t}{R_a J_m} \end{bmatrix}e_a(t) \tag{3.97a}$$

$$y = \begin{bmatrix} 0.1 & 0 \end{bmatrix}\mathbf{x} \tag{3.97b}$$

But from the case study problem in Chapter 2, $J_m = 0.03$ and $D_m = 0.02$. Also, $K_t/R_a = 0.0625$ and $K_b = 0.5$. Substituting the values into Eq. (3.97a), we obtain the final state-space representation:

$$\dot{\mathbf{x}} = \begin{bmatrix} 0 & 1 \\ 0 & -1.71 \end{bmatrix} \mathbf{x} + \begin{bmatrix} 0 \\ 2.083 \end{bmatrix} e_a(t) \tag{3.98a}$$

$$y = \begin{bmatrix} 0.1 & 0 \end{bmatrix} \mathbf{x} \tag{3.98b}$$

CHALLENGE: You are now given a problem to test your knowledge of this chapter's objectives. Referring to the antenna azimuth position control system shown on the front endpapers, find the state-space representation of each dynamic subsystem. Use Configuration 2.

Pharmaceutical Drug Absorption

An advantage of state-space representation over the transfer function representation is the ability to focus on component parts of a system and write n simultaneous, first-order differential equations rather than attempt to represent the system as a single, nth-order differential equation, as we have done with the transfer function. Also, multiple-input, multiple-output systems can be conveniently represented in state space. This case study demonstrates both of these concepts.
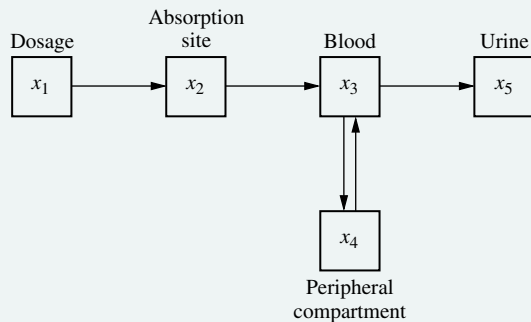
FIGURE 3.16   Pharmaceutical drug-level concentrations in a human

PROBLEM: In the pharmaceutical industry we want to describe the distribution of a drug in the body. A simple model divides the process into compartments: the dosage, the absorption site, the blood, the peripheral compartment, and the urine. The rate of change of the amount of a drug in a compartment is equal to the input flow rate diminished by the output flow rate. Figure 3.16 summarizes the system. Here each x_i is the amount of drug in that particular compartment (*Lordi*, *1972*). Represent the system in state space, where the outputs are the amounts of drug in each compartment.

SOLUTION: The flow rate of the drug into any given compartment is proportional to the concentration of the drug in the previous compartment, and the flow rate out of a given compartment is proportional to the concentration of the drug in its own compartment.

We now write the flow rate for each compartment. The dosage is released to the absorption site at a rate proportional to the dosage concentration, or

$$\frac{dx_1}{dt} = -K_1 x_1 \tag{3.99}$$

The flow into the absorption site is proportional to the concentration of the drug at the dosage site. The flow from the absorption site into the blood is proportional to the concentration of the drug at the absorption site. Hence,

$$\frac{dx_2}{dt} = K_1 x_1 - K_2 x_2 \tag{3.100}$$

Similarly, the net flow rate into the blood and peripheral compartment is

$$\frac{dx_3}{dt} = K_2 x_2 - K_3 x_3 + K_4 x_4 - K_5 x_3 \tag{3.101}$$

$$\frac{dx_4}{dt} = K_5 x_3 - K_4 x_4 \tag{3.102}$$

where $(K_4x_4 - K_5x_3)$ is the net flow rate into the blood from the peripheral compartment. Finally, the amount of the drug in the urine is increased as the blood releases the drug to the urine at a rate proportional to the concentration of the drug in the blood. Thus,

$$\frac{dx_5}{dt} = K_3x_3 \tag{3.103}$$

Equations (3.99) through (3.103) are the state equations. The output equation is a vector that contains each of the amounts, x_i. Thus, in vector-matrix form,

$$\dot{\mathbf{x}} = \begin{bmatrix} -K_1 & 0 & 0 & 0 & 0 \\ K_1 & -K_2 & 0 & 0 & 0 \\ 0 & K_2 & -(K_3 + K_5) & K_4 & 0 \\ 0 & 0 & K_5 & -K_4 & 0 \\ 0 & 0 & K_3 & 0 & 0 \end{bmatrix} \mathbf{x} \tag{3.104a}$$

$$\mathbf{y} = \begin{bmatrix} 1 & 0 & 0 & 0 & 0 \\ 0 & 1 & 0 & 0 & 0 \\ 0 & 0 & 1 & 0 & 0 \\ 0 & 0 & 0 & 1 & 0 \\ 0 & 0 & 0 & 0 & 1 \end{bmatrix} \mathbf{x} \tag{3.104b}$$

You may wonder how there can be a solution to these equations if there is no input. In Chapter 4, when we study how to solve the state equations, we will see that initial conditions will yield solutions without forcing functions. For this problem, an initial condition on the amount of dosage, x_1, will generate drug quantities in all other compartments.

CHALLENGE: We now give you a problem to test your knowledge of this chapter's objectives. The problem concerns the storage of water in aquifers. The principles are similar to those used to model pharmaceutical drug absorption.

Underground water supplies, called aquifers, are used in many areas for agricultural, industrial, and residential purposes. An aquifer system consists of a number of interconnected natural storage tanks. Natural water flows through the sand and sandstone of the aquifer system, changing the water levels in the tanks on its way to the sea. A water conservation policy can be established whereby water is pumped between tanks to prevent its loss to the sea.

A model for the aquifer system is shown in Figure 3.17. In this model, the aquifer is represented by three tanks, with water level h_i called the *head*. Each q_n is the
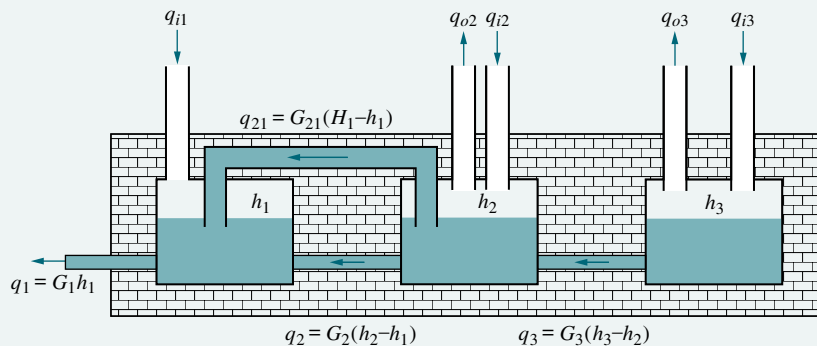
FIGURE 3.17 Aquifer system model

natural water flow to the sea and is proportional to the difference in head between two adjoining tanks, or $q_n = G_n(h_n - h_{n-1})$, where G_n is a constant of proportionality and the units of q_n are m^3/yr.

The engineered flow consists of three components, also measured in m^3/yr: (1) flow from the tanks for irrigation, industry, and homes, q_{on}; (2) replenishing of the tanks from wells, q_{in}; and (3) flow, q_{21}, created by the water conservation policy to prevent loss to the sea. In this model, water for irrigation and industry will be taken only from Tank 2 and Tank 3. Water conservation will take place only between Tank 1 and Tank 2, as follows. Let H_1 be a reference head for Tank 1. If the water level in Tank 1 falls below H_1, water will be pumped from Tank 2 to Tank 1 to replenish the head. If h_1 is higher than H_1, water will be pumped back to Tank 2 to prevent loss to the sea. Calling this *flow for conservation q_{21}*, we can say this flow is proportional to the difference between the head of Tank 1, h_1, and the reference head, H_1, or $q_{21} = G_{21}(H_1 - h_1)$.

The net flow into a tank is proportional to the rate of change of head in each tank. Thus,

$$C_n dh_n/dt = q_{in} - q_{on} + q_{n+1} - q_n + q_{(n+1)n} - q_{n(n-1)}$$

(*Kandel, 1973*).

Represent the aquifer system in state space, where the state variables and the outputs are the heads of each tank.

Summary

This chapter has dealt with the state-space representation of physical systems, which took the form of a state equation,

$$\dot{\mathbf{x}} = \mathbf{A}\mathbf{x} + \mathbf{B}\mathbf{u} \tag{3.105}$$

and an output equation,

$$\mathbf{y} = \mathbf{C}\mathbf{x} + \mathbf{D}\mathbf{u} \tag{3.106}$$

for $t \geq t_0$, and initial conditions $\mathbf{x}(t_0)$. Vector $\mathbf{x}$ is called the *state vector* and contains variables, called *state variables*. The state variables can be combined algebraically with the input to form the output equation, Eq. (3.106), from which any other system variables can be found. State variables, which can represent physical quantities such as current or voltage, are chosen to be linearly independent. The choice of state variables is not unique and affects how the matrices $\mathbf{A, B, C}$, and $\mathbf{D}$ look. We will solve the state and output equations for $\mathbf{x}$ and $\mathbf{y}$ in Chapter 4.

In this chapter, transfer functions were represented in state space. The form selected was the phase-variable form, which consists of state variables that are successive derivatives of each other. In three-dimensional state space, the resulting system matrix, $\mathbf{A}$, for the phase-variable representation is of the form

$$\begin{bmatrix} 0 & 1 & 0 \\ 0 & 0 & 1 \\ -a_0 & -a_1 & -a_2 \end{bmatrix} \tag{3.107}$$

where the a_i's are the coefficients of the characteristic polynomial or denominator of the system transfer function. We also discussed how to convert from a state-space representation to a transfer function.

In conclusion, then, for linear, time-invariant systems, the state-space representation is simply another way of mathematically modeling them. One major advantage of applying the state-space representation to such linear systems is that it allows computer simulation. Programming the system on the digital computer and watching the system's response is an invaluable analysis and design tool. Simulation is covered in Appendix H located at www.wiley.com/college/nise.

Review Questions

1. Give two reasons for modeling systems in state space.
2. State an advantage of the transfer function approach over the state-space approach.
3. Define *state variables*.
4. Define *state*.
5. Define *state vector*.
6. Define *state space*.
7. What is required to represent a system in state space?
8. An eighth-order system would be represented in state space with how many state equations?
9. If the state equations are a system of first-order differential equations whose solution yields the state variables, then the output equation performs what function?
10. What is meant by *linear independence*?
11. What factors influence the choice of state variables in any system?
12. What is a convenient choice of state variables for electrical networks?
13. If an electrical network has three energy-storage elements, is it possible to have a state-space representation with more than three state variables? Explain.
14. What is meant by the phase-variable form of the state-equation?

Problems

1. Represent the electrical network shown in Figure P3.1 in state space, where $v_o(t)$ is the output. [Section: 3.4]
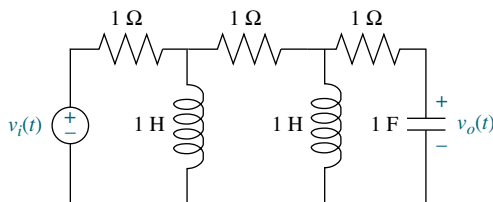
FIGURE P3.1

2. Represent the electrical network shown in Figure P3.2 in state space, where $i_R(t)$ is the output. [Section: 3.4]
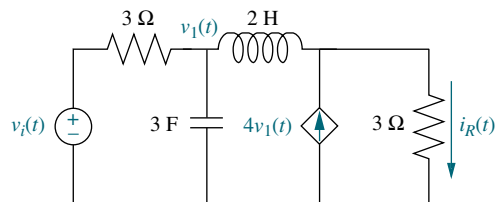
FIGURE P3.2

3. Find the state-space representation of the network shown in Figure P3.3 if the output is $v_o(t)$. [Section: 3.4]
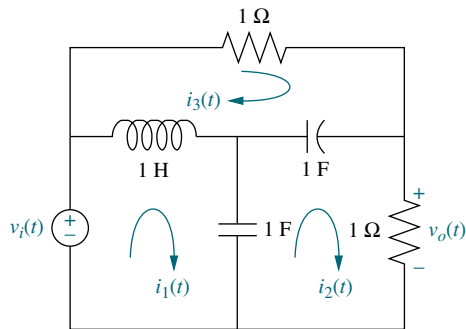
FIGURE P3.3

4. Represent the system shown in Figure P3.4 in state space where the output is $x_3(t)$. [Section: 3.4]
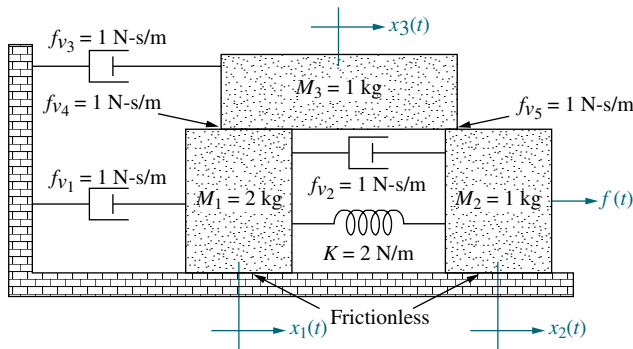
FIGURE P3.4

5. Represent the translational mechanical system shown in Figure P3.5 in state space, where $x_1(t)$ is the output. [Section: 3.4]
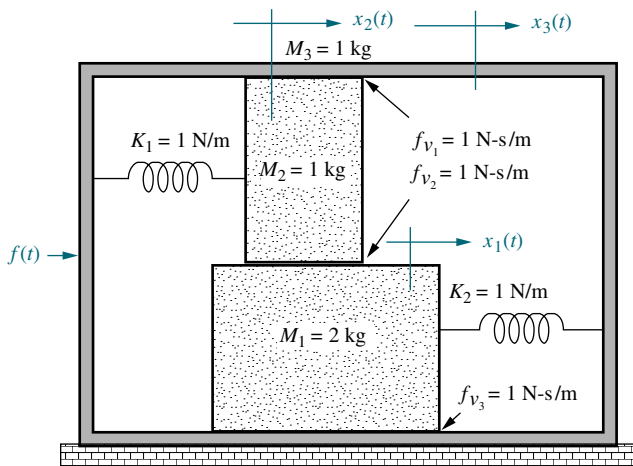
FIGURE P3.5

6. Represent the rotational mechanical system shown in Figure P3.6 in state space, where $\theta_1(t)$ is the output. [Section: 3.4]
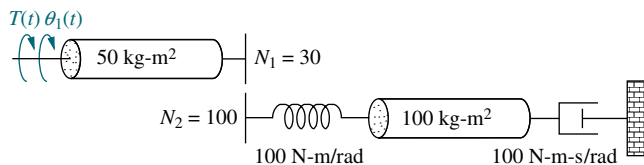
FIGURE P3.6

7. Represent the system shown in Figure P3.7 in state space where the output is $\theta_L(t)$. [Section: 3.4]
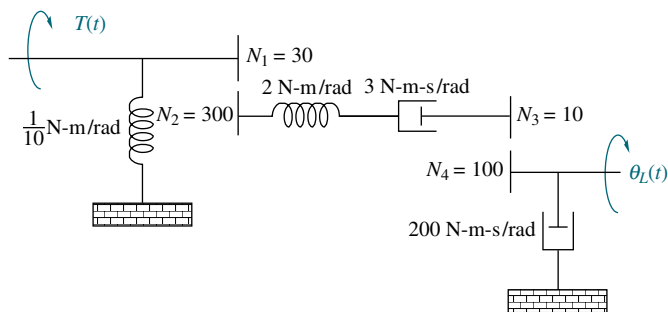
FIGURE P3.7

8. Show that the system of Figure 3.7 in the text yields a fourth-order transfer function if we relate the displacement of either mass to the applied force, and a third-order one if we relate the velocity of either mass to the applied force. [Section: 3.4]

9. Find the state-space representation in phase-variable form for each of the systems shown in Figure P3.8. [Section: 3.5]

(a)

(b)
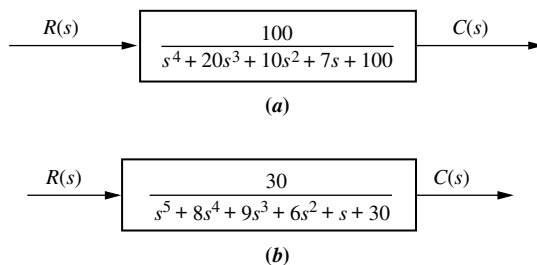
FIGURE P3.8

10. Repeat Problem 9 using MATLAB. [Section: 3.5]

11. For each system shown in Figure P3.9, write the state equations and the output equation for the phase-variable representation. [Section: 3.5]

$R(s)$ → $\dfrac{8s + 10}{s^4 + 5s^3 + s^2 + 5s + 13}$ → $C(s)$

(*a*)

$R(s)$ → $\dfrac{s^4 + 2s3 + 12s^2 + 7s + 6}{s^5 + 9s^4 + 13s^3 + 8s^2}$ → $C(s)$

(*b*)
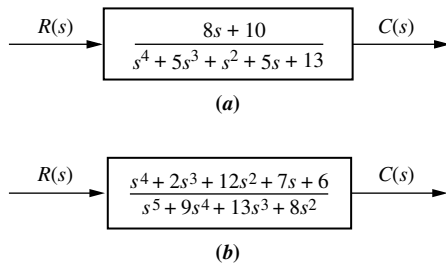
FIGURE P3.9

12. Repeat Problem 11 using MATLAB. [Section: 3.5]

MATLAB
ML

13. Represent the following transfer function in state space. Give your answer in vector-matrix form. [Section: 3.5]

$$T(s) = \frac{(s^2 + 3s + 8)}{(s + 1)(s^2 + 5s + 5)}$$

14. Find the transfer function $G(s) = Y(s)/R(s)$ for each of the following systems represented in state space: [Section: 3.6]

WileyPLUS
WPCS
Control Solutions

a. $\dot{\mathbf{x}} = \begin{bmatrix} 0 & 1 & 0 \\ 0 & 0 & 1 \\ -3 & -2 & -5 \end{bmatrix} \mathbf{x} + \begin{bmatrix} 0 \\ 0 \\ 10 \end{bmatrix} r$

$y = \begin{bmatrix} 1 & 0 & 0 \end{bmatrix} \mathbf{x}$

b. $\dot{\mathbf{x}} = \begin{bmatrix} 2 & -3 & -8 \\ 0 & 5 & 3 \\ -3 & -5 & -4 \end{bmatrix} \mathbf{x} + \begin{bmatrix} 1 \\ 4 \\ 6 \end{bmatrix} r$

$y = \begin{bmatrix} 1 & 3 & 6 \end{bmatrix} \mathbf{x}$

c. $\dot{\mathbf{x}} = \begin{bmatrix} 3 & -5 & 2 \\ 1 & -8 & 7 \\ -3 & -6 & 2 \end{bmatrix} \mathbf{x} + \begin{bmatrix} 5 \\ -3 \\ 2 \end{bmatrix} r$

$y = \begin{bmatrix} 1 & -4 & 3 \end{bmatrix} \mathbf{x}$

15. Use MATLAB to find the transfer function, $G(s) = Y(s)/R(s)$, for each of the following systems represented in state space:[Section: 3.6]

MATLAB
ML

a. $\dot{\mathbf{x}} = \begin{bmatrix} 0 & 1 & 5 & 0 \\ 0 & 0 & 1 & 0 \\ 0 & 0 & 0 & 1 \\ -7 & -9 & -2 & -3 \end{bmatrix} \mathbf{x} + \begin{bmatrix} 0 \\ 5 \\ 8 \\ 2 \end{bmatrix} r$

$y = \begin{bmatrix} 1 & 3 & 6 & 6 \end{bmatrix} \mathbf{x}$

b. $\dot{\mathbf{x}} = \begin{bmatrix} 3 & 1 & 0 & 4 & -2 \\ -3 & 5 & -5 & 2 & -1 \\ 0 & 1 & -1 & 2 & 8 \\ -7 & 6 & -3 & -4 & 0 \\ -6 & 0 & 4 & -3 & 1 \end{bmatrix} \mathbf{x} + \begin{bmatrix} 2 \\ 7 \\ 8 \\ 5 \\ 4 \end{bmatrix} r$

$y = \begin{bmatrix} 1 & -2 & -9 & 7 & 6 \end{bmatrix} \mathbf{x}$

16. Repeat Problem 15 using MATLAB, the Symbolic Math Toolbox, and Eq. (3.73). [Section: 3.6]

Symbolic Math
SM

17. Gyros are used on space vehicles, aircraft, and ships for inertial navigation. The gyro shown in Figure P3.10 is a rate gyro restrained by springs connected between the inner gimbal and the outer gimbal (frame) as shown. A rotational rate about the *z*-axis causes the rotating disk to precess about the *x*-axis. Hence, the input is a rotational rate about the *z*-axis, and the output is an angular displacement about the *x*-axis. Since the outer gimbal is secured to the vehicle, the displacement about the *x*-axis is a measure of the vehicle's angular rate about the *z*-axis. The equation of motion is

WileyPLUS
WPCS
Control Solutions

$$J_x \frac{d^2\theta_x}{dt^2} + D_x \frac{d\theta_x}{dt} + K_x\theta_x = J\omega \frac{d\theta_z}{dt}$$
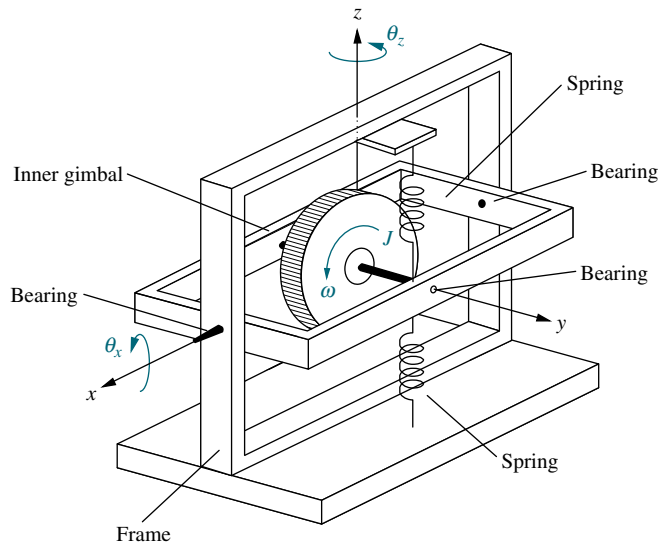
FIGURE P3.10 Gyro system

Represent the gyro in state space. [Section: 3.4]

18. A missile in flight, as shown in Figure P3.11, is subject to several forces: thrust, lift, drag, and gravity. The missile flies at an angle of attack, α, from its longitudinal axis, creating lift. For steering, the body angle from vertical, ϕ, is controlled by rotating the engine at the tail. The transfer function relating the body angle, ϕ, to the angular displacement, δ, of the engine is of the form

$$\frac{\Phi(s)}{\delta(s)} = \frac{K_a s + K_b}{K_3 s^3 + K_2 s^2 + K_1 s + K_0}$$
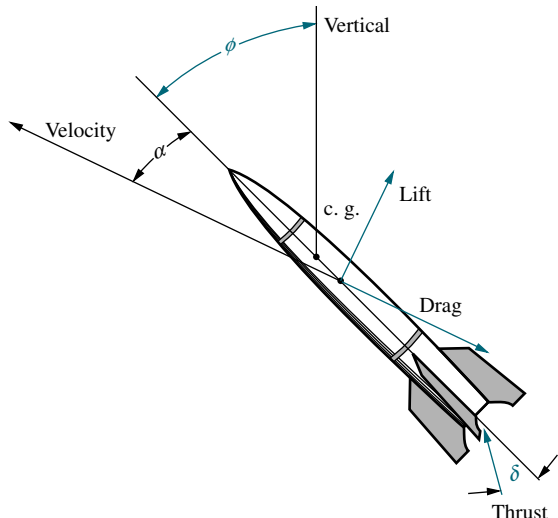
FIGURE P3.11   Missile

Represent the missile steering control in state space. [Section: 3.5]

19. Given the dc servomotor and load shown in Figure P3.12, represent the system in state space, where the state variables are the armature current, i_a, load displacement, θ_L, and load angular velocity, ω_L. Assume that the output is the angular displacement of the armature. Do not neglect armature inductance. [Section: 3.4]
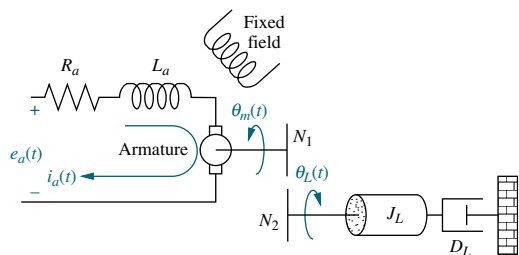
FIGURE P3.12   Motor and load

20. Consider the mechanical system of Figure P3.13. If the spring is nonlinear, and the force, F_s, required to

stretch the spring is $F_s = 2x_1^2$, represent the system in state space linearized about $x_1 = 1$ if the output is x_2. [Section: 3.7]
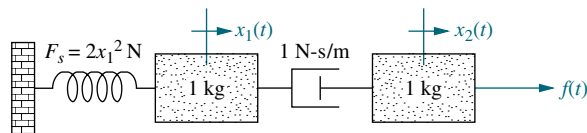
FIGURE P3.13   Nonlinear mechanical system

21. Image-based homing for robots can be implemented by generating heading command inputs to a steering system based on the following guidance algorithm. Suppose the robot shown in Figure P3.14(a) is to go from point R to a target, point T, as shown in Figure P3.14(b). If $\mathbf{R}_x$, $\mathbf{R}_y$, and $\mathbf{R}_z$ are vectors from the robot to each landmark, X, Y, Z, respectively, and $\mathbf{T}_x$, $\mathbf{T}_y$, and $\mathbf{T}_z$ are vectors from the target to each landmark, respectively, then heading commands would drive the robot to minimize $\mathbf{R}_x - \mathbf{T}_x$, $\mathbf{R}_y - \mathbf{T}_y$, and $\mathbf{R}_z - \mathbf{T}_z$ simultaneously, since the differences will be zero when the robot arrives at the target (*Hong, 1992*). If Figure P3.14(c) represents the control system that steers the robot, represent each block—the controller, wheels, and vehicle—in state space. [Section: 3.5]
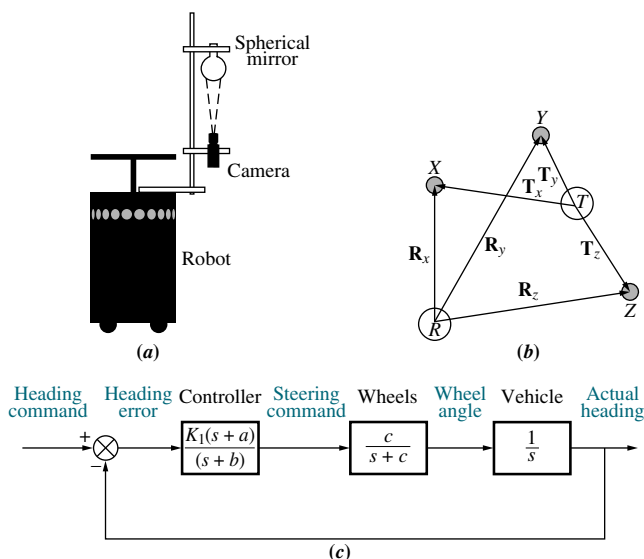
FIGURE P3.14   a. Robot with television imaging system; **b.** vector diagram showing concept behind image-based homing; **c.** heading control system (© 1992 IEEE)

22. Given the F4-E military aircraft shown in Figure P3.15(a), where normal acceleration, a_n, and pitch

rate, q, are controlled by elevator deflection, δ_e, on the horizontal stabilizers and by canard deflection, δ_e. A commanded deflection, δ_{com}, as shown in Figure P3.15(*b*), is used to effect a change in both δ_e and δ_c. The relationships are

$$\frac{\delta_e(s)}{\delta_{com}(s)} = \frac{1/\tau}{s + 1/\tau}$$

$$\frac{\delta_c(s)}{\delta_{com}(s)} = \frac{K_c/\tau}{s + 1/\tau}$$

(a)

(b)
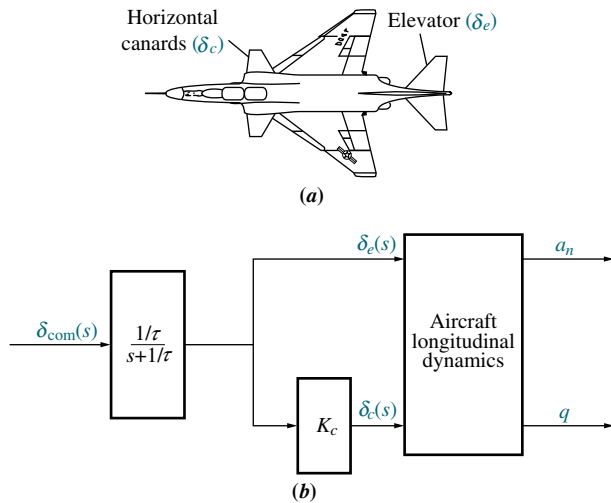
FIGURE P3.15   a. F4-E with canards **b.** open-loop flight control system

These deflections yield, via the aircraft longitudinal dynamics, a_n and q. The state equations describing the effect of δ_{com} on a_n and q is given by (*Cavallo, 1992*)

$$\begin{bmatrix} \dot{a}_n \\ \dot{q} \\ \dot{\delta}_e \end{bmatrix} = \begin{bmatrix} -1.702 & 50.72 & 263.38 \\ 0.22 & -1.418 & -31.99 \\ 0 & 0 & -14 \end{bmatrix} \begin{bmatrix} a_n \\ q \\ \delta_e \end{bmatrix}$$
$$+ \begin{bmatrix} -272.06 \\ 0 \\ 14 \end{bmatrix} \delta_{com}$$

Find the following transfer functions: [Section: 3.5]

$$G_1(s) = \frac{A_n(s)}{\delta_{com}(s)}$$

$$G_2(s) = \frac{Q(s)}{\delta_{com}(s)}$$

23. Modern robotic manipulators that act directly upon their target environments must be controlled so that impact forces as well as steady-state forces do not damage the targets. At the same time, the manipulator must provide sufficient force to perform the task. In order to develop a control system to regulate these forces, the robotic manipulator and target environment must be modeled. Assuming the model shown in Figure P3.16, represent in state space the manipulator and its environment under the following conditions (*Chiu, 1997*). [Section: 3.5]

   a. The manipulator is not in contact with its target environment.

   b. The manipulator is in constant contact with its target environment.
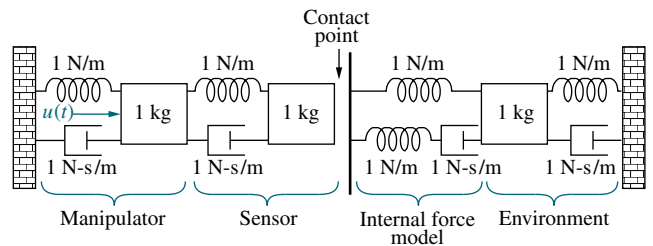
FIGURE P3.16   Robotic manipulator and target environment (© 1997 IEEE)

24. In the past, Type-1 diabetes patients had to inject themselves with insulin three to four times a day. New delayed-action insulin analogues such as insulin Glargine require a single daily dose. A similar procedure to the one described in the Pharmaceutical Drug Absorption case study of this chapter is used to find a model for the concentration-time evolution of plasma for insulin Glargine. For a specific patient, state-space model matrices are given by (*Tarín, 2007*)

$$\mathbf{A} = \begin{bmatrix} -0.435 & 0.209 & 0.02 \\ 0.268 & -0.394 & 0 \\ 0.227 & 0 & -0.02 \end{bmatrix}; \quad \mathbf{B} = \begin{bmatrix} 1 \\ 0 \\ 0 \end{bmatrix};$$

$$\mathbf{C} = [0.0003\ 0\ 0]; \quad \mathbf{D} = 0$$

where the state vector is given by

$$\mathbf{x} = \begin{bmatrix} x_1 \\ x_2 \\ x_3 \end{bmatrix}.$$

The state variables are

x_1 = insulin amount in plasma compartment
x_2 = insulin amount in liver compartment
x_3 = insulin amount in interstitial (in body tissue) compartment

The system's input is u = external insulin flow. The system's output is y = plasma insulin concentration.

a. Find the system's transfer function.

b. `Verify your result using MATLAB.`

MATLAB
ML

25. A linear, time-invariant model of the hypothalamic-pituitary-adrenal axis of the endocrine system with five state variables has been proposed as follows (*Kyrylov, 2005*):

$$\frac{dx_0}{dt} = a_{00}x_0 + a_{02}x_2 + d_0$$

$$\frac{dx_1}{dt} = a_{10}x_0 + a_{11}x_1 + a_{12}x_2$$

$$\frac{dx_2}{dt} = a_{20}x_0 + a_{21}x_1 + a_{22}x_2 + a_{23}x_3 + a_{24}x_4$$

$$\frac{dx_3}{dt} = a_{32}x_2 + a_{33}x_3$$

$$\frac{dx_4}{dt} = a_{42}x_2 + a_{44}x_4$$

where each of the state variables represents circulatory concentrations as follows:

x_0 = corticotropin-releasing hormone
x_1 = corticotropin
x_2 = free cortisol
x_3 = albumin-bound cortisol
x_4 = corticosteroid-binding globulin
d_0 = an external generating factor

Express the system in the form $\dot{\mathbf{x}} = \mathbf{Ax} + \mathbf{Bu}$.

26. In this chapter, we described the state-space representation of single-input, single-output systems. In general, systems can have multiple inputs and multiple outputs. An autopilot is to be designed for a submarine as shown in Figure P3.17 to maintain a constant depth under severe wave disturbances. We will see that this system has two inputs and two outputs and thus the scaler u becomes a vector, $\mathbf{u}$, and the scaler y becomes a vector, $\mathbf{y}$, in the state equations.
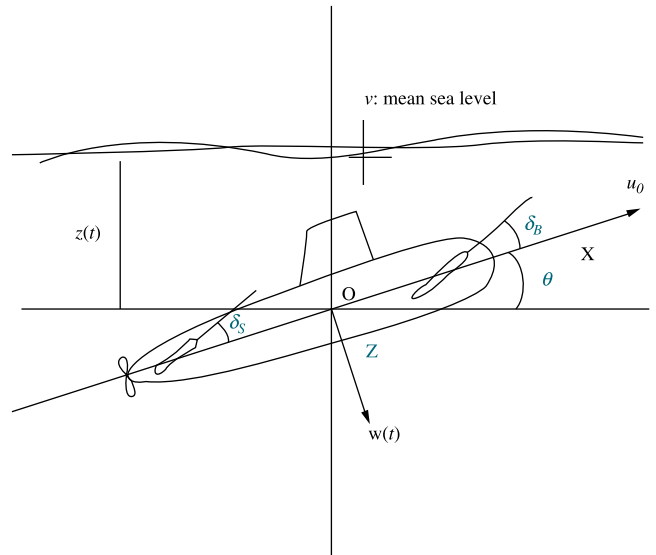
FIGURE P3.17 (© 1995 IEEE)

It has been shown that the system's linearized dynamics under neutral buoyancy and at a given constant speed are given by (*Liceaga-Castro, 2009*):

$$\dot{\mathbf{x}} = \mathbf{Ax} + \mathbf{Bu}$$

$$\mathbf{y} = \mathbf{Cx}$$

where

$$\mathbf{x} = \begin{bmatrix} w \\ q \\ z \\ \theta \end{bmatrix}; \quad \mathbf{y} = \begin{bmatrix} z \\ \theta \end{bmatrix}; \quad \mathbf{u} = \begin{bmatrix} \delta_B \\ \delta_S \end{bmatrix}$$

$$\mathbf{A} = \begin{bmatrix} -0.038 & 0.896 & 0 & 0.0015 \\ 0.0017 & -0.092 & 0 & -0.0056 \\ 1 & 0 & 0 & -3.086 \\ 0 & 1 & 0 & 0 \end{bmatrix};$$

$$\mathbf{B} = \begin{bmatrix} -0.0075 & -0.023 \\ 0.0017 & -0.0022 \\ 0 & 0 \\ 0 & 0 \end{bmatrix}; \quad \mathbf{C} = \begin{bmatrix} 0 & 0 & 1 & 0 \\ 0 & 0 & 0 & 1 \end{bmatrix}$$

and where

w = the heave velocity
q = the pitch rate
z = the submarine depth
θ = the pitch angle
δ_B = the bow hydroplane angle
δ_S = the stern hydroplane angle

Since this system has two inputs and two outputs, four transfer functions are possible.

a. Use MATLAB to calculate the system's matrix transfer function.

b. Using the results from Part **a**, write the transfer function $\dfrac{z(s)}{\delta_B(s)}$, $\dfrac{z(s)}{\delta_S(s)}$, $\dfrac{\theta(s)}{\delta_B(s)}$, and $\dfrac{\theta(s)}{\delta_S(s)}$.

27. Experiments to identify precision grip dynamics between the index finger and thumb have been performed using a ball-drop experiment. A subject holds a device with a small receptacle into which an object is dropped, and the response is measured (*Fagergren*, *2000*). Assuming a step input, it has been found that the response of the motor sub-system together with the sensory system is of the form

$$G(s) = \frac{Y(s)}{R(s)} = \frac{s + c}{(s^2 + as + b)(s + d)}$$

Convert this transfer function to a state-space representation.

28. State-space representations are, in general, not unique. One system can be represented in several possible ways. For example, consider the following systems:

a. $\dot{x} = -5x + 3u$
$y = 7x$

b. $\begin{bmatrix} \dot{x}_1 \\ \dot{x}_2 \end{bmatrix} = \begin{bmatrix} -5 & 0 \\ 0 & -1 \end{bmatrix} \begin{bmatrix} x_1 \\ x_2 \end{bmatrix} + \begin{bmatrix} 3 \\ 1 \end{bmatrix} u$

$y = \begin{bmatrix} 7 & 0 \end{bmatrix} \begin{bmatrix} x_1 \\ x_2 \end{bmatrix}$

c. $\begin{bmatrix} \dot{x}_1 \\ \dot{x}_2 \end{bmatrix} = \begin{bmatrix} -5 & 0 \\ 0 & -1 \end{bmatrix} \begin{bmatrix} x_1 \\ x_2 \end{bmatrix} + \begin{bmatrix} 3 \\ 0 \end{bmatrix} u$

$y = \begin{bmatrix} 7 & 3 \end{bmatrix} \begin{bmatrix} x_1 \\ x_2 \end{bmatrix}$

Show that these systems will result in the same transfer function. We will explore this phenomenon in more detail in Chapter 5.

29. Figure P3.18 shows a schematic description of the global carbon cycle (*Li, 2009*). In the figure, $m_A(t)$ represents the amount of carbon in gigatons (GtC) present in the atmosphere of earth; $m_V(t)$ the amount in vegetation; $m_s(t)$ the amount in soil; $m_{SO}(t)$ the amount in surface ocean; and $m_{IDO}(t)$ the amount in intermediate and deep-ocean reservoirs. Let $u_E(t)$ stand for the human generated CO_2 emissions (GtC/yr). From the figure, the atmospheric mass balance in the atmosphere can be expressed as:

$$\frac{dm_A}{dt}(t) = u_E(t) - (k_{O1} + k_{L1})m_A(t) + k_{L2}m_V(t)$$
$$+ k_{O2}m_{SO}(t) + k_{L4}m_S(t)$$

where the k's are exchange coefficients (yr^{-1}).

a. Write the remaining reservoir mass balances. Namely, write equations for $\dfrac{dm_{SO}(t)}{dt}$, $\dfrac{dm_{IDO}(t)}{dt}$, $\dfrac{dm_V(t)}{dt}$, and $\dfrac{dm_S(t)}{dt}$

b. Express the system in state space form.
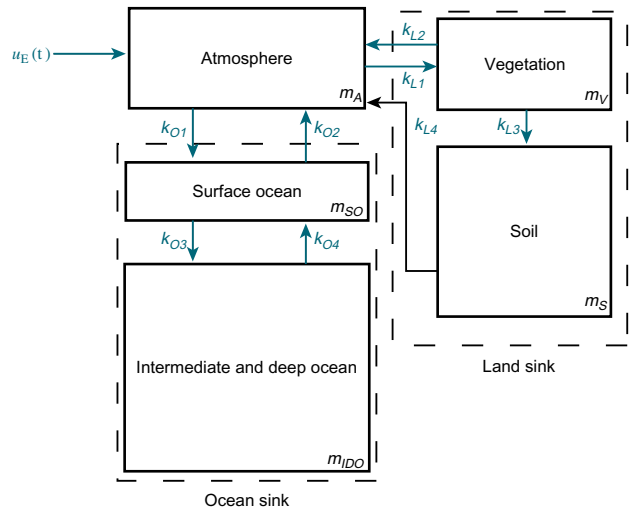
FIGURE P3.18 Global carbon cycle

PROGRESSIVE ANALYSIS AND DESIGN PROBLEMS

30. **High-speed rail pantograph.** A translational mechanical system model for a high-speed rail pantograph, used to supply electricity to a train from an overhead catenary, is shown in Figure P2.39(*b*) (*O'Connor, 1979*). Represent the pantograph in

state space, where the output is the displacement of the top of the pantograph, $y_h(t) - y_{cat}(t)$.

31. Control of HIV/AIDS. Problem 68 in Chapter 2 introduced a model for HIV infection. If retroviral drugs, RTIs and PIs as discussed in Problem 22 in Chapter 1, are used, the model is modified as follows (*Craig, 2004*):

$$\frac{dT}{dt} = s - dT - (1 - u_1)\beta Tv$$

$$\frac{dT^*}{dt} = (1 - u_1)\beta Tv - \mu T^*$$

$$\frac{dv}{dt} = (1 - u_2)kT^* - cv$$

where $0 \leq u_1 \leq 1, 0 \leq u_2 \leq 1$ represent the effectiveness of the RTI and PI medication, respectively.

a. Obtain a state-space representation of the HIV/AIDS model by linearizing the equations about the

$$(T_0, \ T_0^*, \ v_0) = \left(\frac{c\mu}{\beta k}, \frac{s}{\mu} - \frac{cd}{\beta k}, \frac{sk}{c\mu} - \frac{d}{\beta}\right)$$

equilibrium with $u_{10} = u_{20} = 0$. This equilibrium represents the asymptomatic HIV-infected patient. Note that each one of the above equations is of the form $\dot{x}_i = f_i(x_i, u_1, u_2)i = 1, 2, 3$.

b. If Matrices **A** and **B** are given by

$$\mathbf{A} = \begin{bmatrix} \dfrac{\partial f_1}{\partial x_1} & \dfrac{\partial f_1}{\partial x_2} & \dfrac{\partial f_1}{\partial x_3} \\[2mm] \dfrac{\partial f_2}{\partial x_1} & \dfrac{\partial f_2}{\partial x_2} & \dfrac{\partial f_2}{\partial x_3} \\[2mm] \dfrac{\partial f_3}{\partial x_1} & \dfrac{\partial f_3}{\partial x_2} & \dfrac{\partial f_3}{\partial x_3} \end{bmatrix}_{T_0,T_0^*,v_0}; \quad \mathbf{B} = \begin{bmatrix} \dfrac{\partial f_1}{\partial u_1} & \dfrac{\partial f_1}{\partial u_2} \\[2mm] \dfrac{\partial f_2}{\partial u_1} & \dfrac{\partial f_2}{\partial u_2} \\[2mm] \dfrac{\partial f_3}{\partial u_1} & \dfrac{\partial f_3}{\partial u_2} \end{bmatrix}_{T_0,T_0^*,v_0}$$

and we are interested in the number of free HIV viruses as the system's output,

$$\mathbf{C} = \begin{bmatrix} 0 & 0 & 1 \end{bmatrix}$$

show that

$$\mathbf{A} = \begin{bmatrix} -(d + \beta v_0) & 0 & -\beta T_0 \\ \beta v_0 & -\mu & \beta T_0 \\ 0 & k & -c \end{bmatrix}; \quad \mathbf{B} = \begin{bmatrix} \beta T_0 v_0 & 0 \\ -\beta T_0 v_0 & 0 \\ 0 & -kT_0^* \end{bmatrix}$$

c. Typical parameter values and descriptions for the HIV/AIDS model are shown in the following table.

Substitute the values from the table into your model and write as

$$\dot{\mathbf{x}} = \mathbf{Ax} + \mathbf{Bu}$$

$$\mathbf{y} = \mathbf{Cx}$$

t	Time	days
d	Death of uninfected T cells	0.02/day
k	Rate of free viruses produced per infected T cell	100 counts/cell
s	Source term for uninfected T cells	10/mm^3/day
β	Infectivity rate of free virus particles	2.4×10^{-5}/mm^3/day
c	Death rate of viruses	2.4/day
μ	Death rate of infected T cells	0.24/day

(© 2004 IEEE)

32. Hybrid vehicle. For Problem 23 in Chapter 1 we developed the functional block diagrams for the cruise control of serial, parallel, and split-power hybrid electric vehicles (HEV). Those diagrams showed that the engine or electric motor or both may propel the vehicle. When electric motors are the sole providers of the motive force, the forward paths of all HEV topologies are similar. In general, such a forward path can be represented (*Preitl, 2007*) by a block diagram similar to the one of Figure P3.19.

Assume the motor to be an armature-controlled dc motor. In this diagram, K_A is the power amplifier gain; $G_e(s)$ is the transfer function of the motor electric circuit and consists of a series inductor and resistor, L_a and R_a, respectively; K_t is the motor torque constant; J_{tot}, is the sum of the motor inertia, J_m, the inertias of the vehicle, J_{veh}, and the two driven wheels, J_w, both of which are reflected to the motor shaft; k_f is the coefficient of viscous friction; and k_b is the back emf constant.

The input variables are $u_c(t)$, the command voltage from the electronic control unit and $T_c(t)$, the load torque. The output variables in this block diagram are the motor angular speed, $\omega(t)$, and its armature current, $I_a(t)$.

a. Write the basic time-domain equations that characterize the relationships between the state, input, and output variables for the block diagram of Figure P3.19, given that the state variables are the motor armature current, $I_a(t)$, and angular speed, $\omega(t)$.
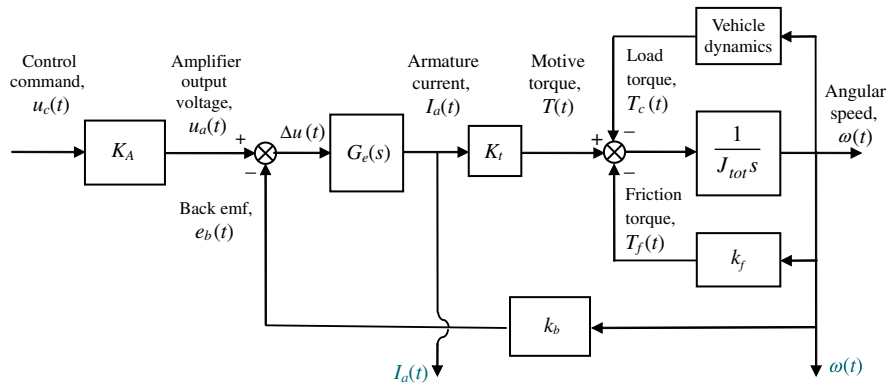
FIGURE P3.19 Block diagram representation of an HEV forward path (© 2007 IEEE)

b. Write the resulting state-space equations and then represent them in matrix form. Regard the load torque $T_c(t)$ as an extra input to the system.

Thus, in your resulting state-space representation, the system will have two inputs and two outputs.

Cyber Exploration Laboratory

Experiment 3.1

Objectives To learn to use MATLAB to (1) generate an LTI state-space representation of a system and (2) convert an LTI state-space representation of a system to an LTI transfer function.

Minimum Required Software Packages MATLAB and the Control System Toolbox

Prelab

1. Derive the state-space representation of the translational mechanical system shown in Skill-Assessment Exercise 3.2 if you have not already done so. Consider the output to be $x_3(t)$.

2. Derive the transfer function, $\frac{X_3(s)}{F(s)}$, from the equations of motion for the translational mechanical system shown in Skill-Assessment Exercise 3.2.

Lab

1. Use MATLAB to generate the LTI state-space representation derived in Prelab 1.

2. Use MATLAB to convert the LTI state-space representation found in Lab 1 to the LTI transfer function found in Prelab 2.

Postlab

1. Compare your transfer functions as found from Prelab 2 and Lab 2.

2. Discuss the use of MATLAB to create LTI state-space representations and the use of MATLAB to convert these representations to transfer functions.

Experiment 3.2

Objectives   To learn to use MATLAB and the Symbolic Math Toolbox to (1) find a symbolic transfer function from the state-space representation and (2) find a state-space representation from the equations of motion.

Minimum Required Software Packages   MATLAB, the Symbolic Math Toolbox, and the Control System Toolbox

Prelab

1. Perform Prelab 1 and Prelab 2 of Experiment 3.1 if you have not already done so.
2. Using the equation $T(s) = \mathbf{C}(s\mathbf{I} - \mathbf{A})^{-1}\mathbf{B}$ to find a transfer function from a state-space representation, write a MATLAB program using the Symbolic Math Toolbox to find the symbolic transfer function from the state-space representation of the translational mechanical system shown in Skill-Assessment Exercise 3.2 and found as a step in Prelab 1.
3. Using the equations of motion of the translational mechanical system shown in Skill-Assessment Exercise 3.2 and found in Prelab 1, write a symbolic MATLAB program to find the transfer function, $\frac{X_3(s)}{F(s)}$, for this system.

Lab

1. Run the programs composed in Prelabs 2 and Prelab 3 and obtain the symbolic transfer functions by the two methods.

Postlab

1. Compare the symbolic transfer function obtained from $T(s) = \mathbf{C}(s\mathbf{I} - \mathbf{A})^{-1}\mathbf{B}$ with the symbolic transfer function obtained from the equations of motion.
2. Discuss the advantages and disadvantages between the two methods.
3. Describe how you would obtain an LTI state-space representation and an LTI transfer function from your symbolic transfer function.

Experiment 3.3

Objectives   To learn to use LabVIEW to (1) generate state-space representations of transfer functions, (2) generate transfer functions from state-space representations, and (3) verify that there are multiple state-space representations for a transfer function.

Minimum Required Software Packages   LabVIEW, the LabVIEW Control Design and Simulation Module, and the MathScript RT Module.

Prelab

1. Study Appendix D, Sections D.1 through Section D.4, Example D.1.
2. Solve Skill-Assessment Exercise 3.3 in Chapter 3.
3. Use your solution to Prelab 2 and convert back to the transfer function.

Lab

1. Use LabVIEW to convert the transfer function, $G(s) = \dfrac{2s + 1}{s^2 + 7s + 9}$, into a state-space representation using both the graphical and MathScript approaches. The front panel will contain controls for the entry of the transfer function and indicators of the transfer function and the two state-space results. Functions for this experiment can be found in the following palettes: (1) **Control Design and Simulation/Control Design/Model Construction,** (2) **Control Design and Simulation/Control Design/Model Conversion,** and (3) **Programming/Structures** Hint: Coefficients are entered in reverse order when using MathScript with MATLAB.

2. Use LabVIEW to convert all state-space representations found in Lab 1 to a transfer function. All state-space conversions should yield the transfer function given in Lab 1. The front panel will contain controls for entering state-space representations and indicators of the transfer function results as well as the state equations used.

Postlab

1. Describe any correlation found between the results of Lab 1 and calculations made in the Prelab.

2. Describe and account for any differences between the results of Lab 1 and calculations made in the Prelab.

3. Explain the results of Lab 2 and draw conclusions from the results.

❨ Bibliography ❩

Carlson, L. E., and Griggs, G. E. *Aluminum Catenary System Quarterly Report.* Technical Report Contract Number DOT-FR-9154, U.S. Department of Transportation, 1980.

Cavallo, A., De Maria, G., and Verde, L. Robust Flight Control Systems: A Parameter Space Design. *Journal of Guidance, Control, and Dynamics*, vol. 15, no. 5, September–October 1992, pp. 1207–1215.

Cereijo, M. R. State Variable Formulations. *Instruments and Control Systems,* December 1969, pp. 87–88.

Chiu, D. K., and Lee, S. Design and Experimentation of a Jump Impact Controller. *IEEE Control Systems*, June 1997, pp. 99–106.

Cochin, I. *Analysis and Design of Dynamic Systems.* Harper & Row, New York, 1980.

Craig, I. K., Xia, X., and Venter, J. W. Introducing HIV/AIDS Education into the Electrical Engineering Curriculum at the University of Pretoria. *IEEE Transactions on Education*, vol. 47, no. 1, February 2004, pp. 65–73.

Elkins, J. A. *A Method for Predicting the Dynamic Response of a Pantograph Running at Constant Speed under a Finite Length of Overhead Equipment*. Technical Report TN DA36, British Railways, 1976.

Fagergren, A., Ekeberg, Ö., and Forssberg, H. Precision Grip Force Dynamics: A System Identification Approach. *IEEE Transactions on Biomedical Engineering*, vol. 47, no. 10, 2000, pp. 1366–1375.

Franklin, G. F., Powell, J. D., and Emami-Naeini, A. *Feedback Control of Dynamic Systems.* Addison-Wesley, Reading, MA, 1986.

Hong, J., Tan, X., Pinette, B., Weiss, R., and Riseman, E. M. Image-Based Homing. *IEEE Control Systems*, February 1992, pp. 38–45.

Inigo, R. M. Observer and Controller Design for D.C. Positional Control Systems Using State Variables. *Transactions, Analog/Hybrid Computer Educational Society*, December 1974, pp. 177–189.

Kailath, T. *Linear Systems*. Prentice Hall, Upper Saddle River, NJ, 1980.

Kandel, A. Analog Simulation of Groundwater Mining in Coastal Aquifers. *Transactions, Analog/Hybrid Computer Educational Society*, November 1973, pp. 175–183.

Kyrylov, V., Severyanova, L. A., and Vieira, A. Modeling Robust Oscillatory Behavior of the Hypothalamic-Pituitary-Adrenal Axis. *IEEE Transactions on Biomedical Engineering*, vol. 52, no. 12, 2005, pp. 1977–1983.

Li, S., Jarvis, A.J., and Leedal, D.T., Are Response Function Representations of the Global Carbon Cycle Ever Interpretable? *Tellus*, vol. 61B, 2009, pp. 361–371.

Liceaga-Castro, E., van der Molen, G. M. Submarine H^∞ Depth Control Under Wave Disturbances. *IEEE Transactions on Control Systems Technology*, vol. 3, no. 3, 1995, pp. 338–346.

Lordi, N. G. Analog Computer Generated Lecture Demonstrations in Pharmacokinetics. *Transactions, Analog/Hybrid Computer Educational Society*, November 1972, pp. 217–222.

O'Connor, D. N., Eppinger, S. D., Seering, W. P., and Wormly, D. N. Active Control of a High-Speed Pantograph. *Journal of Dynamic Systems, Measurements, and Control*, vol. 119, March 1997, pp. 1–4.

Philco Technological Center. *Servomechanism Fundamentals and Experiments*. Prentice Hall, Upper Saddle River, NJ, 1980.

Preitl, Z., Bauer, P., and Bokor, J. A Simple Control Solution for Traction Motor Used in Hybrid Vehicles. *Fourth International Symposium on Applied Computational Intelligence and Informatics. IEEE*. 2007.

Riegelman, S. et al. Shortcomings in Pharmacokinetic Analysis by Conceiving the Body to Exhibit Properties of a Single Compartment. *Journal of Pharmaceutical Sciences*, vol. 57, no. 1, 1968, pp. 117–123.

Tarin, C., Teufel, E., Picó, J., Bondia, J., and Pfleiderer, H. J. Comprehensive Pharmacokinetic Model of Insulin Glargine and Other Insulin Formulations. *IEEE Transactions on Biomedical Engineering*, vol. 52, no. 12, 2005, pp. 1994–2005.

Timothy, L. K., and Bona, B. E. *State Space Analysis: An Introduction*. McGraw-Hill, New York, 1968.
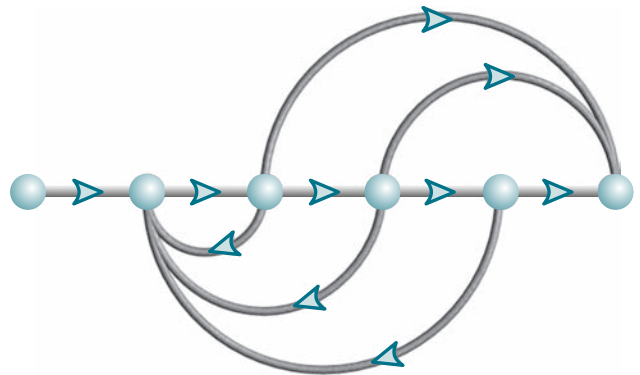
Time Response

Chapter Learning Outcomes

After completing this chapter the student will be able to:

- Use poles and zeros of transfer functions to determine the time response of a control system (Sections 4.1–4.2)
- Describe quantitatively the transient response of first-order systems (Section 4.3)
- Write the general response of second-order systems given the pole location (Section 4.4)
- Find the damping ratio and natural frequency of a second-order system (Section 4.5)
- Find the settling time, peak time, percent overshoot, and rise time for an under-damped second-order system (Section 4.6)
- Approximate higher-order systems and systems with zeros as first- or second-order systems (Sections 4.7–4.8)
- Describe the effects of nonlinearities on the system time response (Section 4.9)
- Find the time response from the state-space representation (Sections 4.10–4.11)

Case Study Learning Outcomes

You will be able to demonstrate your knowledge of the chapter objectives with case studies as follows:

- Given the antenna azimuth position control system shown on the front endpapers, you will be able to (1) predict, by inspection, the form of the open-loop angular velocity response of the load to a step voltage input to the power amplifier;

(2) describe quantitatively the transient response of the open-loop system; (3) derive the expression for the open-loop angular velocity output for a step voltage input; (4) obtain the open-loop state-space representation; (5) plot the open-loop velocity step response using a computer simulation.

● Given the block diagram for the Unmanned Free-Swimming Submersible (UFSS) vehicle's pitch control system shown on the back endpapers, you will be able to predict, find, and plot the response of the vehicle dynamics to a step input command. Further, you will be able to evaluate the effect of system zeros and higher-order poles on the response. You also will be able to evaluate the roll response of a ship at sea.

4.1   Introduction

In Chapter 2, we saw how transfer functions can represent linear, time-invariant systems. In Chapter 3, systems were represented directly in the time domain via the state and output equations. After the engineer obtains a mathematical representation of a subsystem, the subsystem is analyzed for its transient and steady-state responses to see if these characteristics yield the desired behavior. This chapter is devoted to the analysis of system transient response.

It may appear more logical to continue with Chapter 5, which covers the modeling of closed-loop systems, rather than to break the modeling sequence with the analysis presented here in Chapter 4. However, the student should not continue too far into system representation without knowing the application for the effort expended. Thus, this chapter demonstrates applications of the system representation by evaluating the transient response from the system model. Logically, this approach is not far from reality, since the engineer may indeed want to evaluate the response of a subsystem prior to inserting it into the closed-loop system.

After describing a valuable analysis and design tool, poles and zeros, we begin analyzing our models to find the step response of first- and second-order systems. The order refers to the order of the equivalent differential equation representing the system—the order of the denominator of the transfer function after cancellation of common factors in the numerator or the number of simultaneous first-order equations required for the state-space representation.

4.2   Poles, Zeros, and System Response

The output response of a system is the sum of two responses: the *forced response* and the *natural response*.[1] Although many techniques, such as solving a differential equation or taking the inverse Laplace transform, enable us to evaluate this output response, these techniques are laborious and time-consuming. Productivity is aided by analysis and design techniques that yield results in a minimum of time. If the technique is so rapid that we feel we derive the desired result by inspection, we sometimes use the attribute *qualitative* to describe the method. The use of poles and

---

[1] The forced response is also called the *steady-state response* or *particular solution*. The natural response is also called the *homogeneous solution*.

zeros and their relationship to the time response of a system is such a technique. Learning this relationship gives us a qualitative "handle" on problems. The concept of poles and zeros, fundamental to the analysis and design of control systems, simplifies the evaluation of a system's response. The reader is encouraged to master the concepts of poles and zeros and their application to problems throughout this book. Let us begin with two definitions.

Poles of a Transfer Function

The *poles* of a transfer function are (1) the values of the Laplace transform variable, *s,* that cause the transfer function to become infinite or (2) any roots of the denominator of the transfer function that are common to roots of the numerator.

Strictly speaking, the poles of a transfer function satisfy part (1) of the definition. For example, the roots of the characteristic polynomial in the denominator are values of *s* that make the transfer function infinite, so they are thus poles. However, if a factor of the denominator can be canceled by the same factor in the numerator, the root of this factor no longer causes the transfer function to become infinite. In control systems, we often refer to the root of the canceled factor in the denominator as a pole even though the transfer function will not be infinite at this value. Hence, we include part (2) of the definition.

Zeros of a Transfer Function

The *zeros* of a transfer function are (1) the values of the Laplace transform variable, *s*, that cause the transfer function to become zero, or (2) any roots of the numerator of the transfer function that are common to roots of the denominator.

Strictly speaking, the zeros of a transfer function satisfy part (1) of this definition. For example, the roots of the numerator are values of *s* that make the transfer function zero and are thus zeros. However, if a factor of the numerator can be canceled by the same factor in the denominator, the root of this factor no longer causes the transfer function to become zero. In control systems, we often refer to the root of the canceled factor in the numerator as a zero even though the transfer function will not be zero at this value. Hence, we include part (2) of the definition.

Poles and Zeros of a First-Order System: An Example

Given the transfer function $G(s)$ in Figure 4.1(a), a pole exists at $s = -5$, and a zero exists at -2. These values are plotted on the complex *s*-plane in Figure 4.1(b), using an $\times$ for the pole and a $\bigcirc$ for the zero. To show the properties of the poles and zeros, let us find the unit step response of the system. Multiplying the transfer function of Figure 4.1(a) by a step function yields

$$C(s) = \frac{(s+2)}{s(s+5)} = \frac{A}{s} + \frac{B}{s+5} = \frac{2/5}{s} + \frac{3/5}{s+5} \tag{4.1}$$

where

$$A = \frac{(s+2)}{(s+5)}\bigg|_{s\to 0} = \frac{2}{5}$$

$$B = \frac{(s+2)}{s}\bigg|_{s\to -5} = \frac{3}{5}$$

Thus,

$$c(t) = \frac{2}{5} + \frac{3}{5}e^{-5t} \tag{4.2}$$
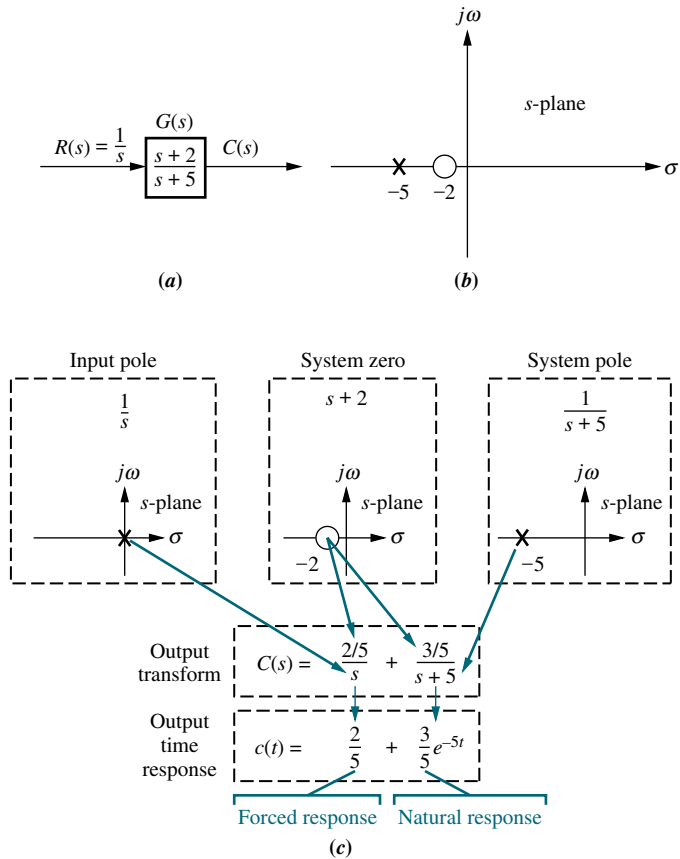
FIGURE 4.1   **a.** System showing input and output; **b.** pole-zero plot of the system; **c.** evolution of a system response. Follow blue arrows to see the evolution of the response component generated by the pole or zero.

From the development summarized in Figure 4.1(c), we draw the following conclusions:

1. A pole of the input function generates the form of the *forced response* (that is, the pole at the origin generated a step function at the output).
2. A pole of the transfer function generates the form of the *natural response* (that is, the pole at -5 generated e^{-5t}).
3. A pole on the real axis generates an *exponential* response of the form $e^{-\alpha t}$, where $-\alpha$ is the pole location on the real axis. Thus, the farther to the left a pole is on the negative real axis, the faster the exponential transient response will decay to zero (again, the pole at -5 generated e^{-5t}; see Figure 4.2 for the general case).
4. The zeros and poles generate the *amplitudes* for both the forced and natural responses (this can be seen from the calculation of A and B in Eq. (4.1)).

Let us now look at an example that demonstrates the technique of using poles to obtain the form of the system response. We will learn to write the form of the response by inspection. Each pole of the system transfer function that is on the real axis generates an exponential response that is a component of the natural response. The input pole generates the forced response.
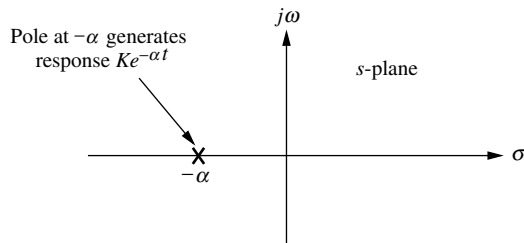
FIGURE 4.2 Effect of a real-axis pole upon transient response.

Example 4.1

Evaluating Response Using Poles

PROBLEM: Given the system of Figure 4.3, write the output, $c(t)$, in general terms. Specify the forced and natural parts of the solution.

SOLUTION: By inspection, each system pole generates an exponential as part of the natural response. The input's pole generates the forced response. Thus,
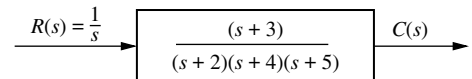
FIGURE 4.3 System for Example 4.1

$$C(s) \equiv \underbrace{\frac{K_1}{s}}_{\substack{\text{Forced} \\ \text{response}}} + \underbrace{\frac{K_2}{s+2} + \frac{K_3}{s+4} + \frac{K_4}{s+5}}_{\substack{\text{Natural} \\ \text{response}}} \qquad (4.3)$$

Taking the inverse Laplace transform, we get

$$c(t) \equiv \underbrace{K_1}_{\substack{\text{Forced} \\ \text{response}}} + \underbrace{K_2 e^{-2t} + K_3 e^{-4t} + K_4 e^{-5t}}_{\substack{\text{Natural} \\ \text{response}}} \qquad (4.4)$$

Skill-Assessment Exercise 4.1

PROBLEM: A system has a transfer function, $G(s) = \dfrac{10(s+4)(s+6)}{(s+1)(s+7)(s+8)(s+10)}$.

Write, by inspection, the output, $c(t)$, in general terms if the input is a unit step.

ANSWER: $c(t) \equiv A + Be^{-t} + Ce^{-7t} + De^{-8t} + Ee^{-10t}$

In this section, we learned that poles determine the nature of the time response: Poles of the input function determine the form of the forced response, and poles of the transfer function determine the form of the natural response. Zeros and poles of the input or transfer function contribute to the amplitudes of the component parts of the total response. Finally, poles on the real axis generate exponential responses.

4.3   First-Order Systems
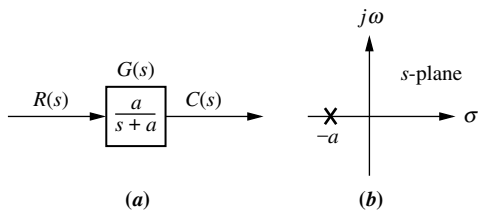
FIGURE 4.4   **a.** First-order system; **b.** pole plot

We now discuss first-order systems without zeros to define a performance specification for such a system. A first-order system without zeros can be described by the transfer function shown in Figure 4.4(a). If the input is a unit step, where $R(s) = 1/s$, the Laplace transform of the step response is $C(s)$, where

$$C(s) = R(s)G(s) = \frac{a}{s(s + a)} \tag{4.5}$$

Taking the inverse transform, the step response is given by

$$c(t) = c_f(t) + c_n(t) = 1 - e^{-at} \tag{4.6}$$

where the input pole at the origin generated the forced response $c_f(t) = 1$, and the system pole at $-a$, as shown in Figure 4.4(b), generated the natural response $c_n(t) = -e^{-at}$. Equation (4.6) is plotted in Figure 4.5.

Let us examine the significance of parameter a, the only parameter needed to describe the transient response. When $t = 1/a$,

$$e^{-at}|_{t=1/a} = e^{-1} = 0.37 \tag{4.7}$$

or

$$c(t)|_{t=1/a} = 1 - e^{-at}|_{t=1/a} = 1 - 0.37 = 0.63 \tag{4.8}$$

We now use Eqs. (4.6), (4.7), and (4.8) to define three transient response performance specifications.

Time Constant

We call $1/a$ the *time constant* of the response. From Eq. (4.7), the time constant can be described as the time for e^{-at} to decay to 37% of its initial value. Alternately, from Eq. (4.8) the time constant is the time it takes for the step response to rise to 63% of its final value (see Figure 4.5).
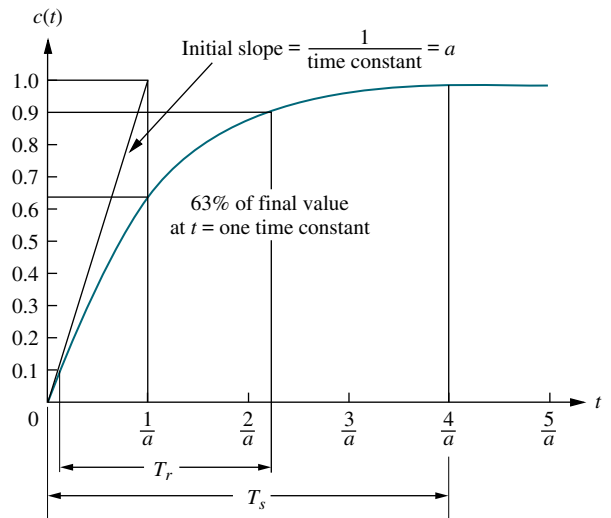
FIGURE 4.5   First-order system response to a unit step
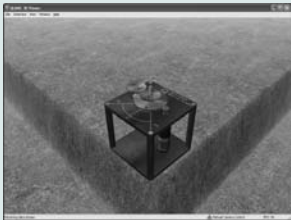
The reciprocal of the time constant has the units (1/seconds), or frequency. Thus, we can call the parameter a the *exponential frequency*. Since the derivative of e^{-at} is $-a$ when $t = 0$, a is the initial rate of change of the exponential at $t = 0$. Thus, the time constant can be considered a transient response specification for a first-order system, since it is related to the speed at which the system responds to a step input.

The time constant can also be evaluated from the pole plot (see Figure 4.4(b)). Since the pole of the transfer function is at $-a$, we can say the pole is located at the *reciprocal* of the time constant, and the farther the pole from the imaginary axis, the faster the transient response.

Let us look at other transient response specifications, such as rise time, T_r, and settling time, T_s, as shown in Figure 4.5.

Rise Time, T_r

Rise time is defined as the time for the waveform to go from 0.1 to 0.9 of its final value. Rise time is found by solving Eq. (4.6) for the difference in time at $c(t) = 0.9$ and $c(t) = 0.1$. Hence,

$$T_r = \frac{2.31}{a} - \frac{0.11}{a} = \frac{2.2}{a} \tag{4.9}$$

Settling Time, T_s

Settling time is defined as the time for the response to reach, and stay within, 2% of its final value.[2] Letting $c(t) = 0.98$ in Eq. (4.6) and solving for time, t, we find the settling time to be

$$T_s = \frac{4}{a} \tag{4.10}$$

First-Order Transfer Functions via Testing

Often it is not possible or practical to obtain a system's transfer function analytically. Perhaps the system is closed, and the component parts are not easily identifiable. Since the transfer function is a representation of the system from input to output, the system's step response can lead to a representation even though the inner construction is not known. With a step input, we can measure the time constant and the steady-state value, from which the transfer function can be calculated.

Consider a simple first-order system, $G(s) = K/(s + a)$, whose step response is

$$C(s) = \frac{K}{s(s + a)} = \frac{K/a}{s} - \frac{K/a}{(s + a)} \tag{4.11}$$

If we can identify K and a from laboratory testing, we can obtain the transfer function of the system.

For example, assume the unit step response given in Figure 4.6. We determine that it has the first-order characteristics we have seen thus far, such as no overshoot and nonzero initial slope. From the response, we measure the time constant, that is, the time for the amplitude to reach 63% of its final value. Since the final value is

---

[2] Strictly speaking, this is the definition of the 2% *setting time*. Other percentages, for example 5%, also can be used. We will use *settling time* throughout the book to mean 2% settling time.
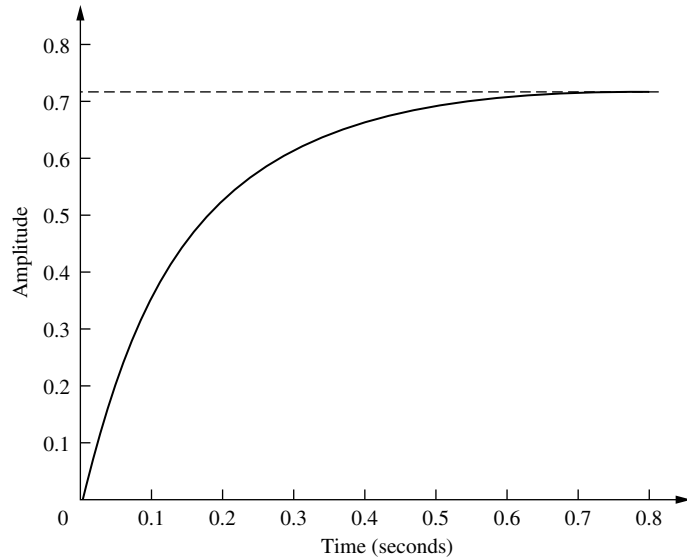
FIGURE 4.6   Laboratory results of a system step response test

about 0.72, the time constant is evaluated where the curve reaches $0.63 \times 0.72 = 0.45$, or about 0.13 second. Hence, $a = 1/0.13 = 7.7$.

To find K, we realize from Eq. (4.11) that the forced response reaches a steady-state value of $K/a = 0.72$. Substituting the value of a, we find $K = 5.54$. Thus, the transfer function for the system is $G(s) = 5.54/(s + 7.7)$. It is interesting to note that the response of Figure 4.6 was generated using the transfer function $G(s) = 5/(s + 7)$.

Skill-Assessment Exercise 4.2

PROBLEM: A system has a transfer function, $G(s) = \dfrac{50}{s + 50}$. Find the time constant, T_c, settling time, T_s, and rise time, T_r.

ANSWER: $T_c = 0.02$ s, $T_s = 0.08$ s, and $T_r = 0.044$ s.

The complete solution is located at www.wiley.com/college/nise.

4.4   Second-Order Systems: Introduction

Let us now extend the concepts of poles and zeros and transient response to second-order systems. Compared to the simplicity of a first-order system, a second-order system exhibits a wide range of responses that must be analyzed and described. Whereas varying a first-order system's parameter simply changes the speed of the response, changes in the parameters of a second-order system can change the *form* of the response. For example, a second-order system can display characteristics much

like a first-order system, or, depending on component values, display damped or pure oscillations for its transient response.

To become familiar with the wide range of responses before formalizing our discussion in the next section, we take a look at numerical examples of the second-order system responses shown in Figure 4.7. All examples are derived from Figure 4.7(*a*), the general case, which has two finite poles and no zeros. The term in the numerator is simply a scale or input multiplying factor that can take on any value without affecting the form of the derived results. By assigning appropriate values to parameters *a* and *b,* we can show all possible second-order transient responses. The unit step response then can be found using $C(s) = R(s)G(s)$, where $R(s) = 1/s$, followed by a partial-fraction expansion and the inverse Laplace transform. Details are left as an end-of-chapter problem, for which you may want to review Section 2.2.
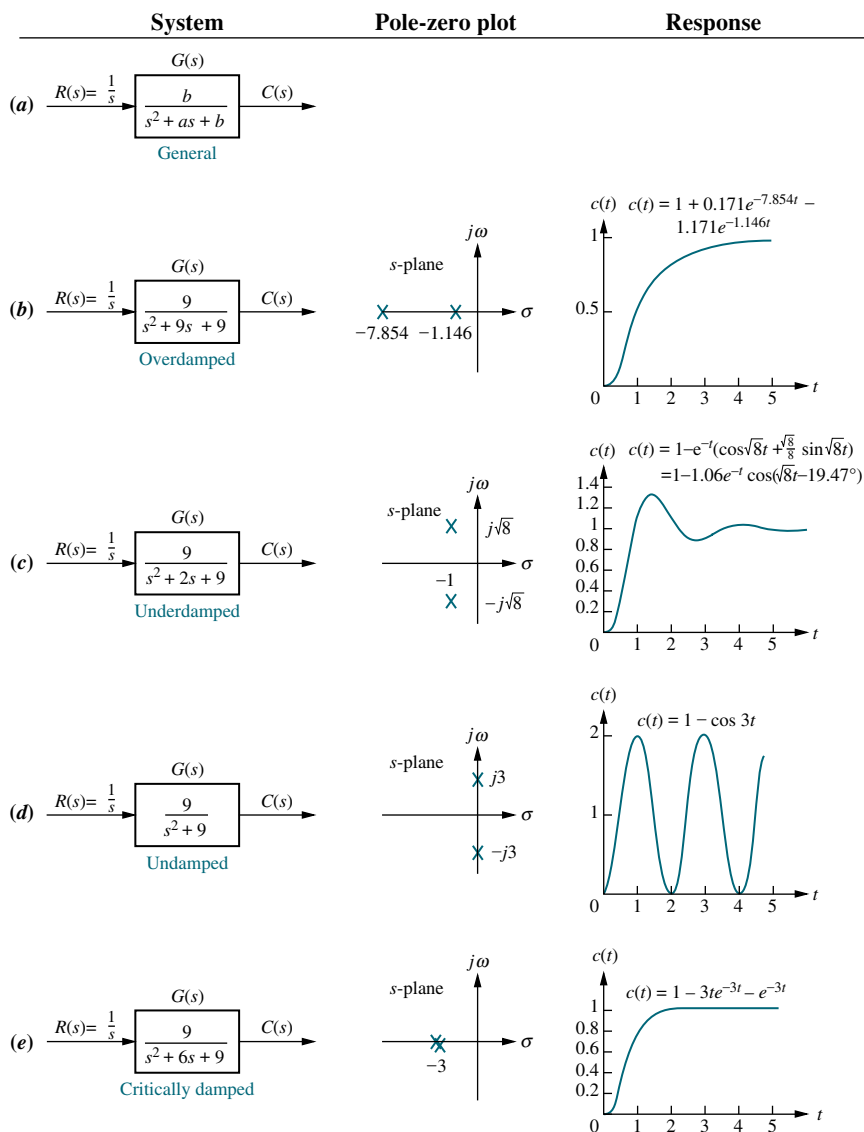
FIGURE 4.7   Second-order systems, pole plots, and step responses

We now explain each response and show how we can use the poles to determine the nature of the response without going through the procedure of a partial-fraction expansion followed by the inverse Laplace transform.

Overdamped Response, Figure 4.7(*b*)

For this response,

$$C(s) = \frac{9}{s(s^2 + 9s + 9)} = \frac{9}{s(s + 7.854)(s + 1.146)} \tag{4.12}$$

This function has a pole at the origin that comes from the unit step input and two real poles that come from the system. The input pole at the origin generates the constant forced response; each of the two system poles on the real axis generates an exponential natural response whose exponential frequency is equal to the pole location. Hence, the output initially could have been written as $c(t) = K_1 + K_2 e^{-7.854t} + K_3 e^{-1.146t}$. This response, shown in Figure 4.7(*b*), is called *overdamped*.[3] We see that the poles tell us the form of the response without the tedious calculation of the inverse Laplace transform.

Underdamped Response, Figure 4.7 (*c*)

For this response,

$$C(s) = \frac{9}{s(s^2 + 2s + 9)} \tag{4.13}$$

This function has a pole at the origin that comes from the unit step input and two complex poles that come from the system. We now compare the response of the second-order system to the poles that generated it. First we will compare the pole location to the time function, and then we will compare the pole location to the plot. From Figure 4.7(*c*), the poles that generate the natural response are at $s = -1 \pm j\sqrt{8}$. Comparing these values to $c(t)$ in the same figure, we see that the real part of the pole matches the exponential decay frequency of the sinusoid's amplitude, while the imaginary part of the pole matches the frequency of the sinusoidal oscillation.

Let us now compare the pole location to the plot. Figure 4.8 shows a general, damped sinusoidal response for a second-order system. The transient response consists of an exponentially decaying amplitude generated by the real part of the system pole times a sinusoidal waveform generated by the imaginary part of the system pole. The time constant of the exponential decay is equal to the reciprocal of the real part of the system pole. The value of the imaginary part is the actual frequency of the sinusoid, as depicted in Figure 4.8. This sinusoidal frequency is given the name *damped frequency of oscillation*, ω_d. Finally, the steady-state response (unit step) was generated by the input pole located at the origin. We call the type of response shown in Figure 4.8 an *underdamped response,* one which approaches a steady-state value via a transient response that is a damped oscillation.

The following example demonstrates how a knowledge of the relationship between the pole location and the transient response can lead rapidly to the response form without calculating the inverse Laplace transform.

FIGURE 4.8   Second-order step response components generated by complex poles

----

[3] So named because *overdamped* refers to a large amount of energy absorption in the system, which inhibits the transient response from overshooting and oscillating about the steady-state value for a step input. As the energy absorption is reduced, an overdamped system will become underdamped and exhibit overshoot.

Example 4.2

Form of Underdamped Response Using Poles

PROBLEM: By inspection, write the form of the step response of the system in Figure 4.9.

SOLUTION: First we determine that the form of the forced response is a step. Next we find the form of the natural response. Factoring the denominator of the transfer function in Figure 4.9, we find the poles to be $s = -5 \pm j13.23$. The real part, -5, is the exponential frequency for the damping. It is also the reciprocal of the time constant of the decay of the oscillations. The imaginary part, 13.23, is the radian frequency for the sinusoidal oscillations. Using our previous discussion and Figure 4.7(*c*) as a guide, we obtain $c(t) = K_1 + e^{-5t}(K_2 \cos 13.23t + K_3 \sin 13.23t) = K_1 + K_4 e^{-5t}(\cos 13.23t - \phi)$, where $\phi = \tan^{-1} K_3 / K_2$, $K_4 = \sqrt{K_2^2 + K_3^2}$, and $c(t)$ is a constant plus an exponentially damped sinusoid.

$R(s) = \dfrac{1}{s}$ → $\boxed{\dfrac{200}{s^2 + 10s + 200}}$ → $C(s)$
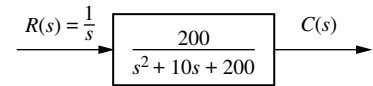
FIGURE 4.9   System for Example 4.2

We will revisit the second-order underdamped response in Sections 4.5 and 4.6, where we generalize the discussion and derive some results that relate the pole position to other parameters of the response.

Undamped Response, Figure 4.7(*d*)

For this response,

$$C(s) = \frac{9}{s(s^2 + 9)} \tag{4.14}$$

This function has a pole at the origin that comes from the unit step input and two imaginary poles that come from the system. The input pole at the origin generates the constant forced response, and the two system poles on the imaginary axis at $\pm j3$ generate a sinusoidal natural response whose frequency is equal to the location of the imaginary poles. Hence, the output can be estimated as $c(t) = K_1 + K_4 \cos(3t - \phi)$. This type of response, shown in Figure 4.7(*d*), is called *undamped*. Note that the absence of a real part in the pole pair corresponds to an exponential that does not decay. Mathematically, the exponential is $e^{-0t} = 1$.

Critically Damped Response, Figure 4.7 (*e*)

For this response,

$$C(s) = \frac{9}{s(s^2 + 6s + 9)} = \frac{9}{s(s + 3)^2} \tag{4.15}$$

This function has a pole at the origin that comes from the unit step input and two multiple real poles that come from the system. The input pole at the origin generates the constant forced response, and the two poles on the real axis at -3 generate a natural response consisting of an exponential and an exponential multiplied by time, where the exponential frequency is equal to the location of the real poles. Hence, the output can be estimated as $c(t) = K_1 + K_2 e^{-3t} + K_3 t e^{-3t}$. This type of response, shown in Figure 4.7(*e*), is called *critically damped*. Critically damped responses are the fastest possible without the overshoot that is characteristic of the underdamped response.

We now summarize our observations. In this section we defined the following natural responses and found their characteristics:

1. *Overdamped responses*

Poles: Two real at $-\sigma_1, \;\; -\sigma_2$

Natural response: Two exponentials with time constants equal to the reciprocal of the pole locations, or
$$c(t) = K_1 e^{-\sigma_1 t} + K_2 e^{-\sigma_2 t}$$

2. *Underdamped responses*

Poles: Two complex at $-\sigma_d \pm j\omega_d$

Natural response: Damped sinusoid with an exponential envelope whose time constant is equal to the reciprocal of the pole's real part. The radian frequency of the sinusoid, the damped frequency of oscillation, is equal to the imaginary part of the poles, or
$$c(t) = A e^{-\sigma_d t} \cos(\omega_d t - \phi)$$

3. *Undamped responses*

Poles: Two imaginary at $\pm j\omega_1$

Natural response: Undamped sinusoid with radian frequency equal to the imaginary part of the poles, or
$$c(t) = A\cos(\omega_1 t - \phi)$$

4. *Critically damped responses*

Poles: Two real at $-\sigma_1$

Natural response: One term is an exponential whose time constant is equal to the reciprocal of the pole location. Another term is the product of time, t, and an exponential with time constant equal to the reciprocal of the pole location, or
$$c(t) = K_1 e^{-\sigma_1 t} + K_2 t e^{-\sigma_1 t}$$

The step responses for the four cases of damping discussed in this section are superimposed in Figure 4.10. Notice that the critically damped case is the division
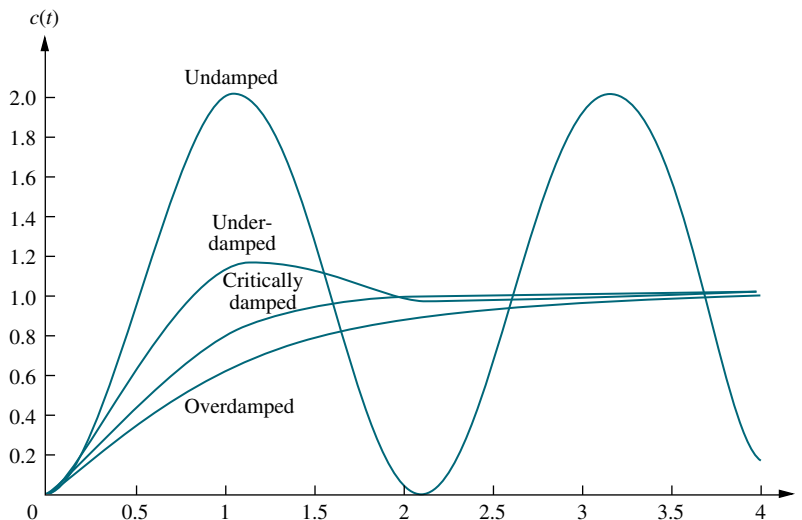
FIGURE 4.10   Step responses for second-order system damping cases

between the overdamped cases and the underdamped cases and is the fastest response without overshoot.

Skill-Assessment Exercise 4.3

PROBLEM: For each of the following transfer functions, write, by inspection, the general form of the step response:

a. $G(s) = \dfrac{400}{s^2 + 12s + 400}$

b. $G(s) = \dfrac{900}{s^2 + 90s + 900}$

c. $G(s) = \dfrac{225}{s^2 + 30s + 225}$

d. $G(s) = \dfrac{625}{s^2 + 625}$

ANSWERS:

a. $c(t) = A + Be^{-6t}\cos(19.08t + \phi)$

b. $c(t) = A + Be^{-78.54t} + Ce^{-11.46t}$

c. $c(t) = A + Be^{-15t} + Cte^{-15t}$

d. $c(t) = A + B\cos(25t + \phi)$

The complete solution is located at www.wiley.com/college/nise.

In the next section, we will formalize and generalize our discussion of second-order responses and define two specifications used for the analysis and design of second-order systems. In Section 4.6, we will focus on the *underdamped* case and derive some specifications unique to this response that we will use later for analysis and design.

4.5   The General Second-Order System

Now that we have become familiar with second-order systems and their responses, we generalize the discussion and establish quantitative specifications defined in such a way that the response of a second-order system can be described to a designer without the need for sketching the response. In this section, we define two physically meaningful specifications for second-order systems. These quantities can be used to describe the characteristics of the second-order transient response just as time constants describe the first-order system response. The two quantities are called natural frequency and damping ratio. Let us formally define them.

Natural Frequency, ω_n

The *natural frequency* of a second-order system is the frequency of oscillation of the system without damping. For example, the frequency of oscillation of a series *RLC* circuit with the resistance shorted would be the natural frequency.

Damping Ratio, ζ

Before we state our next definition, some explanation is in order. We have already seen that a second-order system's underdamped step response is characterized by damped oscillations. Our definition is derived from the need to quantitatively describe this damped oscillation regardless of the time scale. Thus, a system whose transient response goes through three cycles in a millisecond before reaching the steady state would have the same measure as a system that went through three cycles in a millennium before reaching the steady state. For example, the underdamped curve in Figure 4.10 has an associated measure that defines its shape. This measure remains the same even if we change the time base from seconds to microseconds or to millennia.

A viable definition for this quantity is one that compares the exponential decay frequency of the envelope to the natural frequency. This ratio is constant regardless of the time scale of the response. Also, the reciprocal, which is proportional to the ratio of the natural period to the exponential time constant, remains the same regardless of the time base.

We define the *damping ratio*, ζ, to be

$$\zeta = \frac{\text{Exponential decay frequency}}{\text{Natural frequency (rad/second)}} = \frac{1}{2\pi} \frac{\text{Natural period (seconds)}}{\text{Exponential time constant}}$$

Let us now revise our description of the second-order system to reflect the new definitions. The general second-order system shown in Figure 4.7(a) can be transformed to show the quantities ζ and ω_n. Consider the general system

$$G(s) = \frac{b}{s^2 + as + b} \tag{4.16}$$

Without damping, the poles would be on the $j\omega$-axis, and the response would be an undamped sinusoid. For the poles to be purely imaginary, $a = 0$. Hence,

$$G(s) = \frac{b}{s^2 + b} \tag{4.17}$$

By definition, the natural frequency, ω_n, is the frequency of oscillation of this system. Since the poles of this system are on the $j\omega$-axis at $\pm j\sqrt{b}$,

$$\omega_n = \sqrt{b} \tag{4.18}$$

Hence,

$$b = \omega_n^2 \tag{4.19}$$

Now what is the term a in Eq. (4.16)? Assuming an underdamped system, the complex poles have a real part, σ, equal to $-a/2$. The magnitude of this value is then the exponential decay frequency described in Section 4.4. Hence,

$$\zeta = \frac{\text{Exponential decay frequency}}{\text{Natural frequency (rad/second)}} = \frac{|\sigma|}{\omega_n} = \frac{a/2}{\omega_n} \tag{4.20}$$

from which

$$a = 2\zeta\omega_n \tag{4.21}$$

Our general second-order transfer function finally looks like this:

$$G(s) = \frac{\omega_n^2}{s^2 + 2\zeta\omega_n s + \omega_n^2} \tag{4.22}$$

In the following example we find numerical values for ζ and ω_n by matching the transfer function to Eq. (4.22).

Example 4.3

Finding ζ and ω_n For a Second-Order System

PROBLEM: Given the transfer function of Eq. (4.23), find ζ and ω_n.

$$G(s) = \frac{36}{s^2 + 4.2s + 36} \tag{4.23}$$

SOLUTION: Comparing Eq. (4.23) to (4.22), $\omega_n^2 = 36$, from which $\omega_n = 6$. Also, $2\zeta\omega_n = 4.2$. Substituting the value of ω_n, $\zeta = 0.35$.

Now that we have defined ζ and ω_n, let us relate these quantities to the pole location. Solving for the poles of the transfer function in Eq. (4.22) yields

$$s_{1,2} = -\zeta\omega_n \pm \omega_n\sqrt{\zeta^2 - 1} \tag{4.24}$$

From Eq. (4.24) we see that the various cases of second-order response are a function of ζ; they are summarized in Figure 4.11.[4]
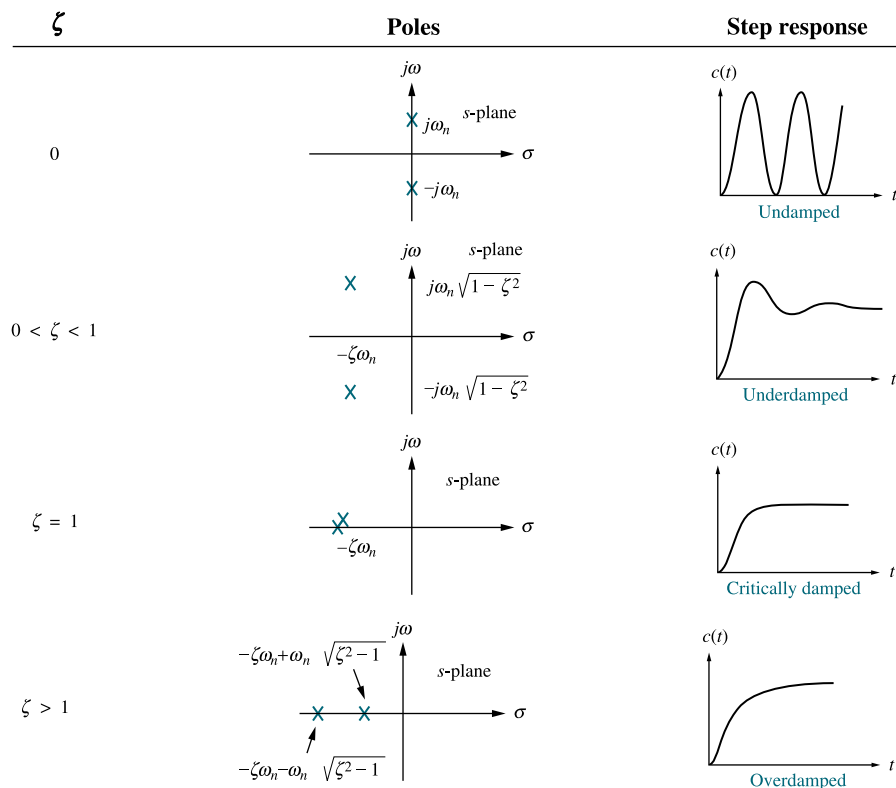
FIGURE 4.11 Second-order response as a function of damping ratio

---

[4] The student should verify Figure 4.11 as an exercise.

In the following example we find the numerical value of ζ and determine the nature of the transient response.

Example 4.4

Characterizing Response from the Value of ζ

PROBLEM: For each of the systems shown in Figure 4.12, find the value of ζ and report the kind of response expected.

$R(s)$ →	$\dfrac{12}{s^2+8s+12}$	→ $C(s)$	$R(s)$ →	$\dfrac{16}{s^2+8s+16}$	→ $C(s)$

(a) (b)

$R(s)$ → $\dfrac{20}{s^2+8s+20}$ → $C(s)$

(c)

FIGURE 4.12   Systems for Example 4.4

SOLUTION: First match the form of these systems to the forms shown in Eqs. (4.16) and (4.22). Since $a = 2\zeta\omega_n$ and $\omega_n = \sqrt{b}$,

$$\zeta = \frac{a}{2\sqrt{b}} \tag{4.25}$$

Using the values of a and b from each of the systems of Figure 4.12, we find $\zeta = 1.155$ for system (a), which is thus overdamped, since $\zeta > 1$; $\zeta = 1$ for system (b), which is thus critically damped; and $\zeta = 0.894$ for system (c), which is thus underdamped, since $\zeta < 1$.

Skill-Assessment Exercise 4.4

PROBLEM: For each of the transfer functions in Skill-Assessment Exercise 4.3, do the following: (1) Find the values of ζ and ω_n; (2) characterize the nature of the response.

ANSWERS:

   a. $\zeta = 0.3$, $\omega_n = 20$; system is underdamped
   b. $\zeta = 1.5$, $\omega_n = 30$; system is overdamped
   c. $\zeta = 1$, $\omega_n = 15$; system is critically damped
   d. $\zeta = 0$, $\omega_n = 25$; system is undamped

The complete solution is located at www.wiley.com/college/nise.

This section defined two specifications, or parameters, of second-order systems: natural frequency, ω_n, and damping ratio, ζ. We saw that the nature of the response obtained was related to the value of ζ. Variations of damping ratio alone yield the complete range of overdamped, critically damped, underdamped, and undamped responses.

◖ 4.6 Underdamped Second-Order Systems

Now that we have generalized the second-order transfer function in terms of ζ and ω_n, let us analyze the step response of an *underdamped* second-order system. Not only will this response be found in terms of ζ and ω_n, but more specifications indigenous to the underdamped case will be defined. The underdamped second-order system, a common model for physical problems, displays unique behavior that must be itemized; a detailed description of the underdamped response is necessary for both analysis and design. Our first objective is to define transient specifications associated with underdamped responses. Next we relate these specifications to the pole location, drawing an association between pole location and the form of the underdamped second-order response. Finally, we tie the pole location to system parameters, thus closing the loop: Desired response generates required system components.

Let us begin by finding the step response for the general second-order system of Eq. (4.22). The transform of the response, $C(s)$, is the transform of the input times the transfer function, or

$$C(s) = \frac{\omega_n^2}{s(s^2 + 2\zeta\omega_n s + \omega_n^2)} = \frac{K_1}{s} + \frac{K_2 s + K_3}{s^2 + 2\zeta\omega_n s + \omega_n^2} \tag{4.26}$$

where it is assumed that $\zeta < 1$ (the underdamped case). Expanding by partial fractions, using the methods described in Section 2.2, Case 3, yields

$$C(s) = \frac{1}{s} - \frac{(s + \zeta\omega_n) + \frac{\zeta}{\sqrt{1-\zeta^2}}\omega_n\sqrt{1-\zeta^2}}{(s + \zeta\omega_n)^2 + \omega_n^2(1-\zeta^2)} \tag{4.27}$$

Taking the inverse Laplace transform, which is left as an exercise for the student, produces

$$c(t) = 1 - e^{-\zeta\omega_n t}\left(\cos\omega_n\sqrt{1-\zeta^2}t + \frac{\zeta}{\sqrt{1-\zeta^2}}\sin\omega_n\sqrt{1-\zeta^2}t\right)$$

$$= 1 - \frac{1}{\sqrt{1-\zeta^2}}e^{-\zeta\omega_n t}\cos(\omega_n\sqrt{1-\zeta^2}t - \phi) \tag{4.28}$$

where $\phi = \tan^{-1}(\zeta/\sqrt{1-\zeta^2})$.

A plot of this response appears in Figure 4.13 for various values of ζ, plotted along a time axis normalized to the natural frequency. We now see the relationship between the value of ζ and the type of response obtained: The lower the value of ζ, the more oscillatory the response. The natural frequency is a time-axis scale factor and does not affect the nature of the response other than to scale it in time.
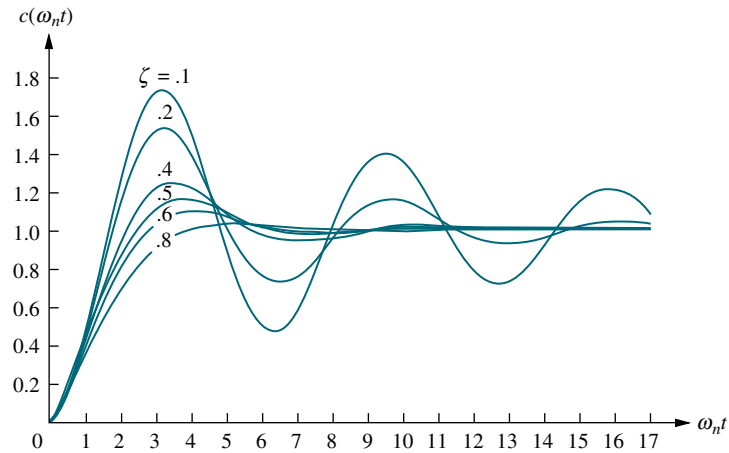
FIGURE 4.13 Second-order underdamped responses for damping ratio values

We have defined two parameters associated with second-order systems, ζ and ω_n. Other parameters associated with the underdamped response are rise time, peak time, percent overshoot, and settling time. These specifications are defined as follows (see also Figure 4.14):

1. *Rise time, T_r.* The time required for the waveform to go from 0.1 of the final value to 0.9 of the final value.

2. *Peak time, T_P.* The time required to reach the first, or maximum, peak.

3. *Percent overshoot, %OS.* The amount that the waveform overshoots the steady-state, or final, value at the peak time, expressed as a percentage of the steady-state value.

4. *Settling time, T_s.* The time required for the transient's damped oscillations to reach and stay within $\pm 2\%$ of the steady-state value.
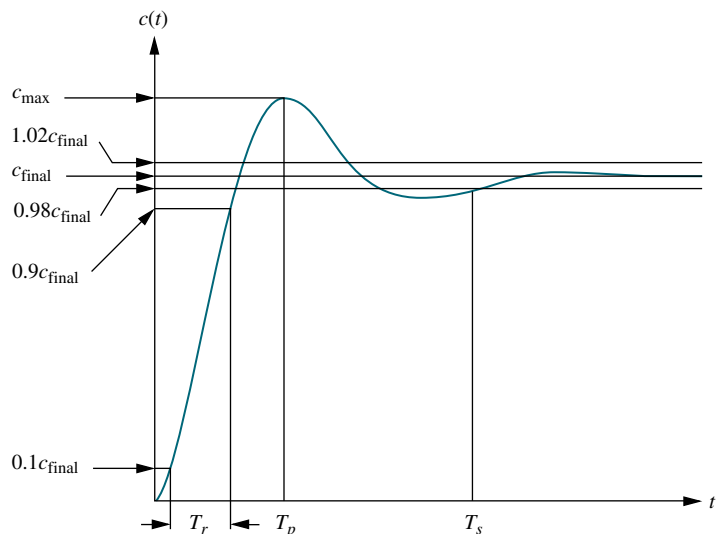
FIGURE 4.14 Second-order underdamped response specifications

Notice that the definitions for settling time and rise time are basically the same as the definitions for the first-order response. All definitions are also valid for systems of order higher than 2, although analytical expressions for these parameters cannot be found unless the response of the higher-order system can be approximated as a second-order system, which we do in Sections 4.7 and 4.8.

Rise time, peak time, and settling time yield information about the speed of the transient response. This information can help a designer determine if the speed and the nature of the response do or do not degrade the performance of the system. For example, the speed of an entire computer system depends on the time it takes for a hard drive head to reach steady state and read data; passenger comfort depends in part on the suspension system of a car and the number of oscillations it goes through after hitting a bump.

We now evaluate T_p, %OS, and T_s as functions of ζ and ω_n. Later in this chapter we relate these specifications to the location of the system poles. A precise analytical expression for rise time cannot be obtained; thus, we present a plot and a table showing the relationship between ζ and rise time.

Evaluation of T_p

T_p is found by differentiating $c(t)$ in Eq. (4.28) and finding the first zero crossing after $t = 0$. This task is simplified by "differentiating" in the frequency domain by using Item 7 of Table 2.2. Assuming zero initial conditions and using Eq. (4.26), we get

$$\mathscr{L}[\dot{c}(t)] = sC(s) = \frac{\omega_n^2}{s^2 + 2\zeta\omega_n s + \omega_n^2} \tag{4.29}$$

Completing squares in the denominator, we have

$$\mathscr{L}[\dot{c}(t)] = \frac{\omega_n^2}{(s + \zeta\omega_n)^2 + \omega_n^2(1 - \zeta^2)} = \frac{\frac{\omega_n}{\sqrt{1-\zeta^2}}\omega_n\sqrt{1 - \zeta^2}}{(s + \zeta\omega_n)^2 + \omega_n^2(1 - \zeta^2)} \tag{4.30}$$

Therefore,

$$\dot{c}(t) = \frac{\omega_n}{\sqrt{1 - \zeta^2}} e^{-\zeta\omega_n t}\sin\omega_n\sqrt{1 - \zeta^2}t \tag{4.31}$$

Setting the derivative equal to zero yields

$$\omega_n\sqrt{1 - \zeta^2}t = n\pi \tag{4.32}$$

or

$$t = \frac{n\pi}{\omega_n\sqrt{1 - \zeta^2}} \tag{4.33}$$

Each value of n yields the time for local maxima or minima. Letting $n = 0$ yields $t = 0$, the first point on the curve in Figure 4.14 that has zero slope. The first peak, which occurs at the peak time, T_p, is found by letting $n = 1$ in Eq. (4.33):

$$T_p = \frac{\pi}{\omega_n\sqrt{1 - \zeta^2}} \tag{4.34}$$

Evaluation of %OS

From Figure 4.14 the percent overshoot, %OS, is given by

$$\%OS = \frac{c_{\max} - c_{\text{final}}}{c_{\text{final}}} \times 100 \tag{4.35}$$

The term $c_{\max}$ is found by evaluating $c(t)$ at the peak time, $c(T_p)$. Using Eq. (4.34) for T_p and substituting into Eq. (4.28) yields

$$c_{\max} = c(T_p) = 1 - e^{-(\zeta\pi/\sqrt{1-\zeta^2})} \left(\cos \pi + \frac{\zeta}{\sqrt{1-\zeta^2}} \sin \pi \right) \tag{4.36}$$

$$= 1 + e^{-(\zeta\pi/\sqrt{1-\zeta^2})}$$

For the unit step used for Eq. (4.28),

$$c_{\text{final}} = 1 \tag{4.37}$$

Substituting Eqs. (4.36) and (4.37) into Eq. (4.35), we finally obtain

$$\boxed{\%OS = e^{-(\zeta\pi/\sqrt{1-\zeta^2})} \times 100} \tag{4.38}$$

Notice that the percent overshoot is a function only of the damping ratio, ζ.

   Whereas Eq. (4.38) allows one to find %OS given ζ, the inverse of the equation allows one to solve for ζ given %OS. The inverse is given by

$$\boxed{\zeta = \frac{-\ln(\%OS/100)}{\sqrt{\pi^2 + \ln^2(\%OS/100)}}} \tag{4.39}$$

The derivation of Eq. (4.39) is left as an exercise for the student. Equation (4.38) (or, equivalently, (4.39)) is plotted in Figure 4.15.
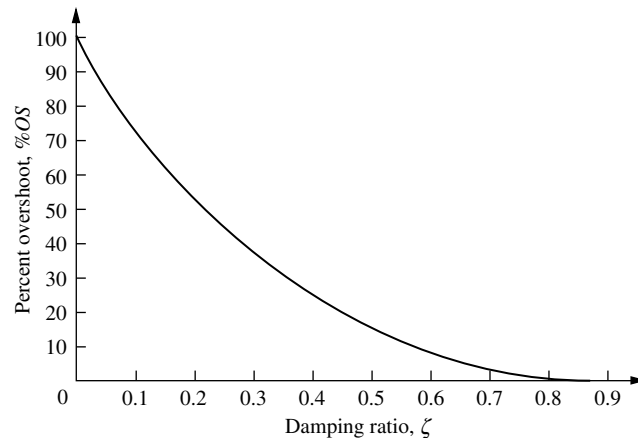
FIGURE 4.15   Percent overshoot versus damping ratio

Evaluation of T_s

In order to find the settling time, we must find the time for which $c(t)$ in Eq. (4.28) reaches and stays within $\pm 2\%$ of the steady-state value, c_{final}. Using our definition, the settling time is the time it takes for the amplitude of the decaying sinusoid in Eq. (4.28) to reach 0.02, or

$$e^{-\zeta\omega_n t} \frac{1}{\sqrt{1-\zeta^2}} = 0.02 \tag{4.40}$$

This equation is a conservative estimate, since we are assuming that $\cos(\omega_n\sqrt{1-\zeta^2}t - \phi) = 1$ at the settling time. Solving Eq. (4.40) for t, the settling time is

$$T_s = \frac{-\ln(0.02\sqrt{1-\zeta^2})}{\zeta\omega_n} \tag{4.41}$$

You can verify that the numerator of Eq. (4.41) varies from 3.91 to 4.74 as ζ varies from 0 to 0.9. Let us agree on an approximation for the settling time that will be used for all values of ζ; let it be

$$\boxed{T_s = \frac{4}{\zeta\omega_n}} \tag{4.42}$$

Evaluation of T_r

A precise analytical relationship between rise time and damping ratio, ζ, cannot be found. However, using a computer and Eq. (4.28), the rise time can be found. We first designate $\omega_n t$ as the normalized time variable and select a value for ζ. Using the computer, we solve for the values of $\omega_n t$ that yield $c(t) = 0.9$ and $c(t) = 0.1$. Subtracting the two values of $\omega_n t$ yields the normalized rise time, $\omega_n T_r$, for that value of ζ. Continuing in like fashion with other values of ζ, we obtain the results plotted in Figure 4.16.[5] Let us look at an example.

Damping ratio	Normalized rise time
0.1	1.104
0.2	1.203
0.3	1.321
0.4	1.463
0.5	1.638
0.6	1.854
0.7	2.126
0.8	2.467
0.9	2.883
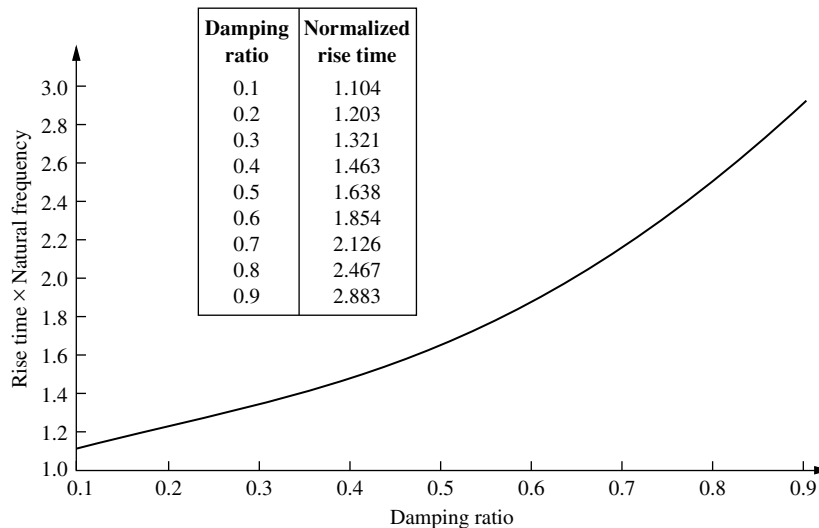
FIGURE 4.16 Normalized rise time versus damping ratio for a second-order underdamped response

---

[5] Figure 4.16 can be approximated by the following polynomials: $\omega_n T_r = 1.76\zeta^3 - 0.417\zeta^2 + 1.039\zeta + 1$ (maximum error less than $\frac{1}{2}\%$ for $0 < \zeta < 0.9$), and $\zeta = 0.115(\omega_n T_r)^3 - 0.883(\omega_n T_r)^2 + 2.504(\omega_n T_r) - 1.738$ (maximum error less than 5% for $0.1 < \zeta < 0.9$). The polynomials were obtained using MATLAB's **polyfit** function.

Example 4.5

Finding T_p, %OS, T_s, and T_r from a Transfer Function
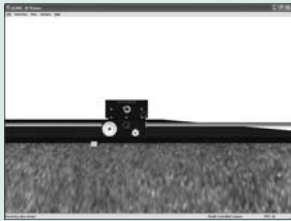
PROBLEM: Given the transfer function

$$G(s) = \frac{100}{s^2 + 15s + 100} \tag{4.43}$$

find T_p, %OS, T_s, and T_r.

SOLUTION: ω_n and ζ are calculated as 10 and 0.75, respectively. Now substitute ζ and ω_n into Eqs. (4.34), (4.38), and (4.42) and find, respectively, that $T_p = 0.475$ second, $\%OS = 2.838$, and $T_s = 0.533$ second. Using the table in Figure 4.16, the normalized rise time is approximately 2.3 seconds. Dividing by ω_n yields $T_r = 0.23$ second. This problem demonstrates that we can find T_p, %OS, T_s, and T_r without the tedious task of taking an inverse Laplace transform, plotting the output response, and taking measurements from the plot.
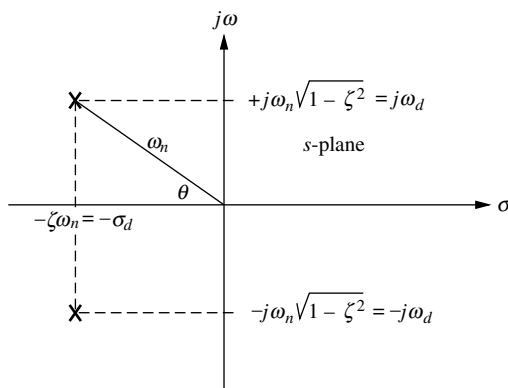
FIGURE 4.17   Pole plot for an underdamped second-order system

We now have expressions that relate peak time, percent overshoot, and settling time to the natural frequency and the damping ratio. Now let us relate these quantities to the location of the poles that generate these characteristics.

The pole plot for a general, underdamped second-order system, previously shown in Figure 4.11, is reproduced and expanded in Figure 4.17 for focus. We see from the Pythagorean theorem that the radial distance from the origin to the pole is the natural frequency, ω_n, and the $\cos \theta = \zeta$.

Now, comparing Eqs. (4.34) and (4.42) with the pole location, we evaluate peak time and settling time in terms of the pole location. Thus,

$$T_p = \frac{\pi}{\omega_n \sqrt{1 - \zeta^2}} = \frac{\pi}{\omega_d} \tag{4.44}$$

$$T_s = \frac{4}{\zeta \omega_n} = \frac{\pi}{\sigma_d} \tag{4.45}$$

where ω_d is the imaginary part of the pole and is called the *damped frequency of oscillation*, and σ_d is the magnitude of the real part of the pole and is the *exponential damping frequency*.
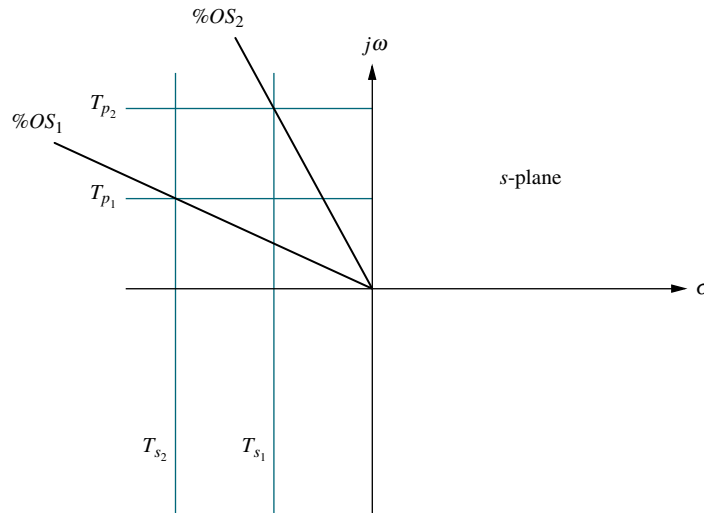
FIGURE 4.18 Lines of constant peak time, T_p, settling time, T_s, and percent overshoot, $\%OS$. Note: $T_{s_2} < T_{s_1}$; $T_{p2} < T_{p1}$; $\%OS_1 < \%OS_2$.

Equation (4.44) shows that T_p is inversely proportional to the imaginary part of the pole. Since horizontal lines on the s-plane are lines of constant imaginary value, they are also lines of constant peak time. Similarly, Eq. (4.45) tells us that settling time is inversely proportional to the real part of the pole. Since vertical lines on the s-plane are lines of constant real value, they are also lines of constant settling time. Finally, since $\zeta = \cos\theta$, radial lines are lines of constant ζ. Since percent overshoot is only a function of ζ, radial lines are thus lines of constant percent overshoot, $\%OS$. These concepts are depicted in Figure 4.18, where lines of constant T_p, T_s, and $\%OS$ are labeled on the s-plane.

At this point, we can understand the significance of Figure 4.18 by examining the actual step response of comparative systems. Depicted in Figure 4.19(a) are the step responses as the poles are moved in a vertical direction, keeping the real part the same. As the poles move in a vertical direction, the frequency increases, but the envelope remains the same since the real part of the pole is not changing. The figure shows a constant exponential envelope, even though the sinusoidal response is changing frequency. Since all curves fit under the same exponential decay curve, the settling time is virtually the same for all waveforms. Note that as overshoot increases, the rise time decreases.

Let us move the poles to the right or left. Since the imaginary part is now constant, movement of the poles yields the responses of Figure 4.19(b). Here the frequency is constant over the range of variation of the real part. As the poles move to the left, the response damps out more rapidly, while the frequency remains the same. Notice that the peak time is the same for all waveforms because the imaginary part remains the same.

Moving the poles along a constant radial line yields the responses shown in Figure 4.19(c). Here the percent overshoot remains the same. Notice also that the responses look exactly alike, except for their speed. The farther the poles are from the origin, the more rapid the response.

We conclude this section with some examples that demonstrate the relationship between the pole location and the specifications of the second-order underdamped response. The first example covers analysis. The second example is a simple design problem consisting of a physical system whose component values we want to design to meet a transient response specification.
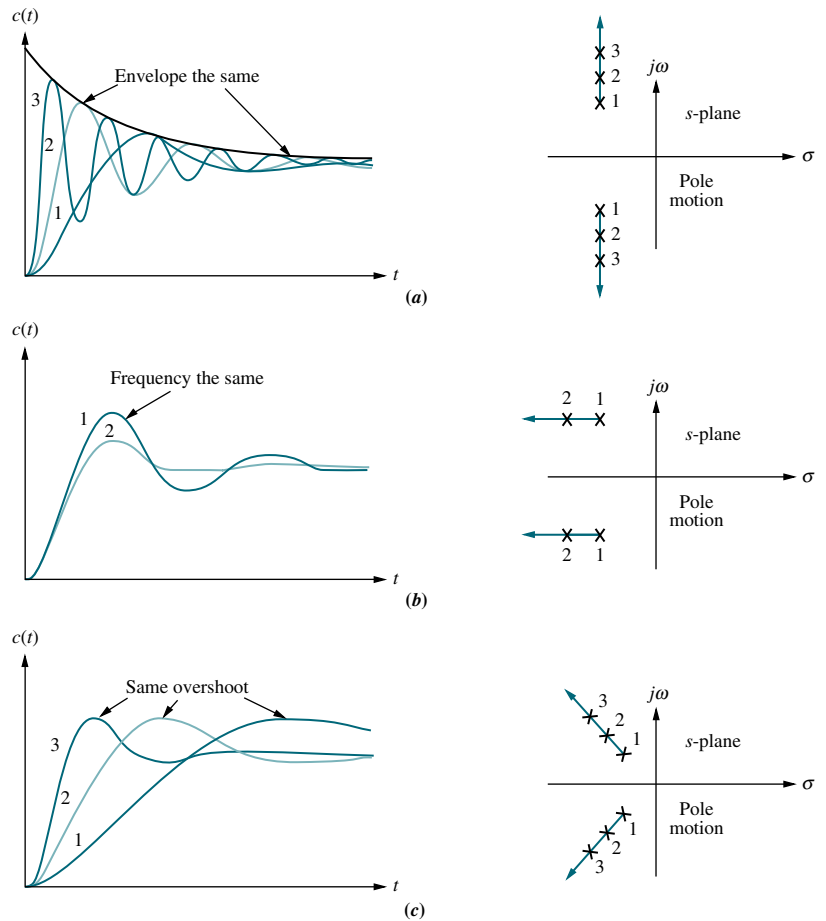
FIGURE 4.19   Step responses of second-order underdamped systems as poles move: **a.** with constant real part; **b.** with constant imaginary part; **c.** with constant damping ratio

Example 4.6

Finding T_p, %OS, and T_s from Pole Location

PROBLEM: Given the pole plot shown in Figure 4.20, find ζ, ω_n, T_p, %OS, and T_s.

SOLUTION: The damping ratio is given by $\zeta = \cos\theta = \cos[\arctan(7/3)] = 0.394$. The natural frequency, ω_n, is the radial distance from the origin to the pole, or $\omega_n = \sqrt{7^2 + 3^2} = 7.616$. The peak time is

$$T_p = \frac{\pi}{\omega_d} = \frac{\pi}{7} = 0.449 \text{ second} \tag{4.46}$$

The percent overshoot is

$$\%OS = e^{-(\zeta\pi/\sqrt{1-\zeta^2})} \times 100 = 26\% \tag{4.47}$$

The approximate settling time is

$$T_s = \frac{4}{\sigma_d} = \frac{4}{3} = 1.333 \text{ seconds} \tag{4.48}$$
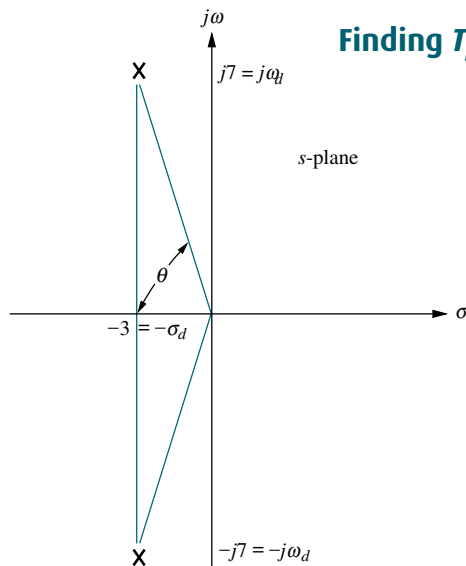
FIGURE 4.20   Pole plot for Example 4.6

Students who are using MATLAB should now run ch4p1 in Appendix B.
You will learn how to generate a second-order polynomial from
two complex poles as well as extract and use the coefficients of
the polynomial to calculate T_p, $\%OS$, and T_s. This exercise uses
MATLAB to solve the problem in Example 4.6.

Example 4.7

Transient Response Through Component Design

Design
D

PROBLEM: Given the system shown in Figure 4.21, find J and D to yield 20%
overshoot and a settling time of 2 seconds for a step input of torque $T(t)$.
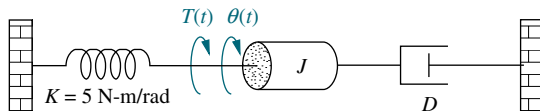
FIGURE 4.21   Rotational mechanical system for Example 4.7

SOLUTION: First, the transfer function for the system is

$$G(s) = \frac{1/J}{s^2 + \dfrac{D}{J}s + \dfrac{K}{J}} \tag{4.49}$$

From the transfer function,

$$\omega_n = \sqrt{\frac{K}{J}} \tag{4.50}$$

and

$$2\zeta\omega_n = \frac{D}{J} \tag{4.51}$$

But, from the problem statement,

$$T_s = 2 = \frac{4}{\zeta\omega_n} \tag{4.52}$$

or $\zeta\omega_n = 2$. Hence,

$$2\zeta\omega_n = 4 = \frac{D}{J} \tag{4.53}$$

Also, from Eqs. (4.50) and (4.52),

$$\zeta = \frac{4}{2\omega_n} = 2\sqrt{\frac{J}{K}} \tag{4.54}$$

From Eq. (4.39), a 20% overshoot implies $\zeta = 0.456$. Therefore, from Eq. (4.54),

$$\zeta = 2\sqrt{\frac{J}{K}} = 0.456 \tag{4.55}$$

Hence,

$$\frac{J}{K} = 0.052 \qquad (4.56)$$

From the problem statement, $K = 5$ N-m/rad. Combining this value with Eqs. (4.53) and (4.56), $D = 1.04$ N-m-s/rad, and $J = 0.26$ kg-m^2.

Second-Order Transfer Functions via Testing

Just as we obtained the transfer function of a first-order system experimentally, we can do the same for a system that exhibits a typical underdamped second-order response. Again, we can measure the laboratory response curve for percent over-shoot and settling time, from which we can find the poles and hence the denominator. The numerator can be found, as in the first-order system, from a knowledge of the measured and expected steady-state values. A problem at the end of the chapter illustrates the estimation of a second-order transfer function from the step response.

Skill-Assessment Exercise 4.5

TryIt 4.1

Use the following MATLAB statements to calculate the answers to Skill-Assessment Exercise 4.5. Ellipses mean code continues on next line.

```
numg=361;
deng=[1 16 361];
omegan=sqrt(deng(3)...
 /deng(1))
zeta=(deng(2)/deng(1))...
 /(2*omegan)
Ts=4/(zeta*omegan)
Tp=pi/(omegan*sqrt...
 (1-zeta^2))
pos=100*exp(-zeta*...
 pi/sqrt(1-zeta^2))
Tr=(1.768*zeta^3 -...
 0.417*zeta^2+1.039*...
 zeta+1)/omegan
```

WileyPLUS
WPCS
Control Solutions

PROBLEM: Find ζ, ω_n, T_s, T_p, T_r, and $\%OS$ for a system whose transfer function is $G(s) = \dfrac{361}{s^2 + 16s + 361}$.

ANSWERS:

$\zeta = 0.421$, $\omega_n = 19$, $T_s = 0.5$ s, $T_p = 0.182$ s, $T_r = 0.079$ s, and $\%OS = 23.3\%$.

The complete solution is located at www.wiley.com/college/nise.

Now that we have analyzed systems with two poles, how does the addition of another pole affect the response? We answer this question in the next section.

4.7 System Response with Additional Poles

In the last section, we analyzed systems with one or two poles. It must be emphasized that the formulas describing percent overshoot, settling time, and peak time were derived only for a system with two complex poles and no zeros. If a system such as that shown in Figure 4.22 has more than two poles or has zeros, we cannot use the formulas to calculate the performance specifications that we derived. However, under certain conditions, a system with more than two poles or with zeros can be

FIGURE 4.22   Robot follows input commands from a human trainer

approximated as a second-order system that has just two complex *dominant poles*. Once we justify this approximation, the formulas for percent overshoot, settling time, and peak time can be applied to these higher-order systems by using the location of the dominant poles. In this section, we investigate the effect of an additional pole on the second-order response. In the next section, we analyze the effect of adding a zero to a two-pole system.

Let us now look at the conditions that would have to exist in order to approximate the behavior of a three-pole system as that of a two-pole system. Consider a three-pole system with complex poles and a third pole on the real axis. Assuming that the complex poles are at $-\zeta\omega_n \pm j\omega_n\sqrt{1 - \zeta^2}$ and the real pole is at $-\alpha_r$, the step response of the system can be determined from a partial-fraction expansion. Thus, the output transform is

$$C(s) = \frac{A}{s} + \frac{B(s + \zeta\omega_n) + C\omega_d}{(s + \zeta\omega_n)^2 + \omega_d^2} + \frac{D}{s + \alpha_r} \tag{4.57}$$

or, in the time domain,

$$c(t) = Au(t) + e^{-\zeta\omega_n t}(B \cos \omega_d t + C \sin \omega_d t) + De^{-\alpha_r t} \tag{4.58}$$

The component parts of $c(t)$ are shown in Figure 4.23 for three cases of α_r. For Case I, $\alpha_r = \alpha_{r_1}$ and is not much larger than $\zeta\omega_n$; for Case II, $\alpha_r = \alpha_{r_2}$ and is much larger than $\zeta\omega_n$; and for Case III, $\alpha_r = \infty$.

Let us direct our attention to Eq. (4.58) and Figure 4.23. If $\alpha_r \gg \zeta\omega_n$ (Case II), the pure exponential will die out much more rapidly than the second-order underdamped step response. If the pure exponential term decays to an insignificant value at the time of the first overshoot, such parameters as percent overshoot, settling time, and peak time will be generated by the second-order underdamped step response component. Thus, the total response will approach that of a pure second-order system (Case III).
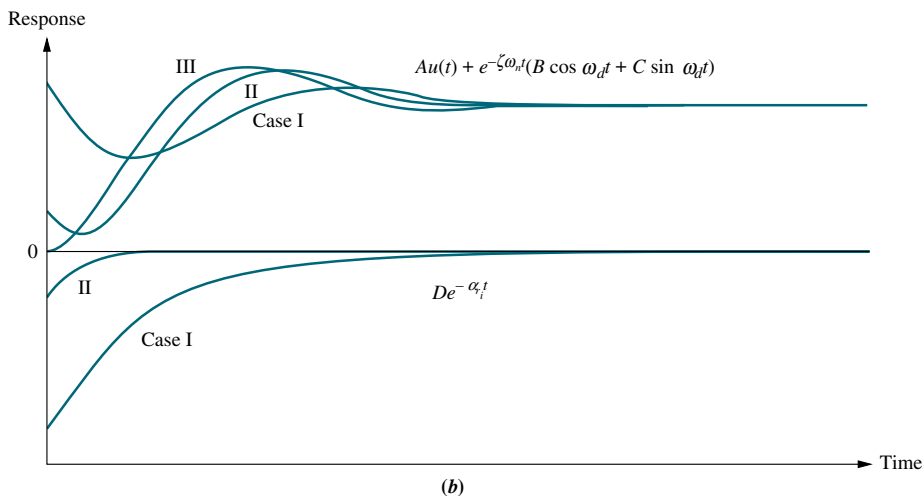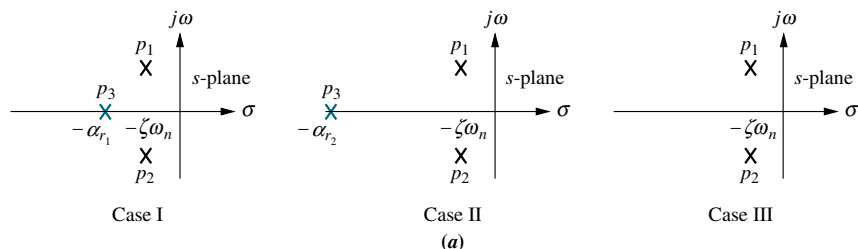
FIGURE 4.23 Component
responses of a three-pole
system: **a.** pole plot;
b. component responses:
Nondominant pole
is near dominant second-order
pair (Case I), far from the pair
(Case II), and at infinity
(Case III)

If α_r is not much greater than $\zeta\omega_n$ (Case I), the real pole's transient response
will not decay to insignificance at the peak time or settling time generated by the
second-order pair. In this case, the exponential decay is significant, and the system
cannot be represented as a second-order system.

The next question is, How much farther from the dominant poles does the third
pole have to be for its effect on the second-order response to be negligible? The
answer of course depends on the accuracy for which you are looking. However, this
book assumes that the exponential decay is negligible after five time constants. Thus,
if the real pole is five times farther to the left than the dominant poles, we assume
that the system is represented by its dominant second-order pair of poles.

What about the magnitude of the exponential decay? Can it be so large that its
contribution at the peak time is not negligible? We can show, through a partial-
fraction expansion, that the residue of the third pole, in a three-pole system with
dominant second-order poles and no zeros, will actually decrease in magnitude as
the third pole is moved farther into the left half-plane. Assume a step response, $C(s)$,
of a three-pole system:

$$C(s) = \frac{bc}{s(s^2 + as + b)(s + c)} = \frac{A}{s} + \frac{Bs + C}{s^2 + as + b} + \frac{D}{s + c} \tag{4.59}$$

where we assume that the nondominant pole is located at $-c$ on the real axis and that
the steady-state response approaches unity. Evaluating the constants in the numer-
ator of each term,

$$A = 1; \qquad B = \frac{ca - c^2}{c^2 + b - ca} \tag{4.60a}$$

$$C = \frac{ca^2 - c^2a - bc}{c^2 + b - ca}; \ \ D = \frac{-b}{c^2 + b - ca} \tag{4.60b}$$

As the nondominant pole approaches ∞, or $c \to \infty$,

$$A = 1; \ B = -1; \ C = -a; \ D = 0 \qquad (4.61)$$

Thus, for this example, D, the residue of the nondominant pole and its response, becomes zero as the nondominant pole approaches infinity.

The designer can also choose to forgo extensive residue analysis, since all system designs should be simulated to determine final acceptance. In this case, the control systems engineer can use the "five times" rule of thumb as a necessary but not sufficient condition to increase the confidence in the second-order approximation during design, but then simulate the completed design.

Let us look at an example that compares the responses of two different three-pole systems with that of a second-order system.

Example 4.8

Comparing Responses of Three-Pole Systems

PROBLEM: Find the step response of each of the transfer functions shown in Eqs. (4.62) through (4.64) and compare them.

$$T_1(s) = \frac{24.542}{s^2 + 4s + 24.542} \qquad (4.62)$$

$$T_2(s) = \frac{245.42}{(s + 10)(s^2 + 4s + 24.542)} \qquad (4.63)$$

$$T_3(s) = \frac{73.626}{(s + 3)(s^2 + 4s + 24.542)} \qquad (4.64)$$

SOLUTION: The step response, $C_i(s)$, for the transfer function, $T_i(s)$, can be found by multiplying the transfer function by $1/s$, a step input, and using partial-fraction expansion followed by the inverse Laplace transform to find the response, $c_i(t)$. With the details left as an exercise for the student, the results are

$$c_1(t) = 1 - 1.09e^{-2t}\cos(4.532t - 23.8°) \qquad (4.65)$$
$$c_2(t) = 1 - 0.29e^{-10t} - 1.189e^{-2t}\cos(4.532t - 53.34°) \qquad (4.66)$$
$$c_3(t) = 1 - 1.14e^{-3t} + 0.707e^{-2t}\cos(4.532t + 78.63°) \qquad (4.67)$$

The three responses are plotted in Figure 4.24. Notice that $c_2(t)$, with its third pole at -10 and farthest from the dominant poles, is the better approximation of $c_1(t)$,
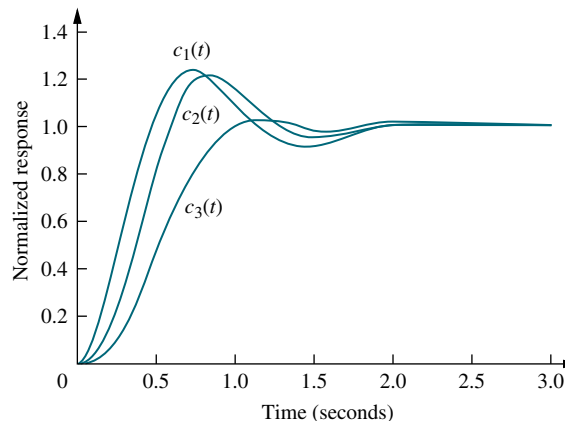
FIGURE 4.24 Step responses of system $T_1(s)$, system $T_2(s)$, and system $T_3(s)$

the pure second-order system response; $c_3(t)$, with a third pole close to the dominant poles, yields the most error.

Students who are using MATLAB should now run ch4p2 in Appendix B. You will learn how to generate a step response for a transfer function and how to plot the response directly or collect the points for future use. The example shows how to collect the points and then use them to create a multiple plot, title the graph, and label the axes and curves to produce the graph in Figure 4.24 to solve Example 4.8.

System responses can alternately be obtained using Simulink. Simulink is a software package that is integrated with MATLAB to provide a graphical user interface (GUI) for defining systems and generating responses. The reader is encouraged to study Appendix C, which contains a tutorial on Simulink as well as some examples. One of the illustrative examples, Example C.1, solves Example 4.8 using Simulink.

Another method to obtain systems responses is through the use of MATLAB's LTI Viewer. An advantage of the LTI Viewer is that it displays the values of settling time, peak time, rise time, maximum response, and the final value on the step response plot. The reader is encouraged to study Appendix E at www.wiley.com/college/nise, which contains a tutorial on the LTI Viewer as well as some examples. Example E.1 solves Example 4.8 using the LTI Viewer.

Skill-Assessment Exercise 4.6

TryIt 4.2

Use the following MATLAB and Control System Toolbox statements to investigate the effect of the additional pole in Skill-Assessment Exercise 4.6(a). Move the higher-order pole originally at −15 to other values by changing "a" in the code.

```
a=15
numga=100*a;
denga=conv([1 a],...
 [1 4 100]);
Ta=tf(numga,denga);
numg=100;
deng=[1 4 100];
T=tf (numg,deng);
step(Ta,'.',T,'-')
```

PROBLEM: Determine the validity of a second-order approximation for each of these two transfer functions:

a. $G(s) = \dfrac{700}{(s + 15)(s^2 + 4s + 100)}$

b. $G(s) = \dfrac{360}{(s + 4)(s^2 + 2s + 90)}$

ANSWERS:

    a. The second-order approximation is valid.

    b. The second-order approximation is not valid.

The complete solution is located at www.wiley.com/college/nise.

4.8   System Response With Zeros

Now that we have seen the effect of an additional pole, let us add a zero to the second-order system. In Section 4.2, we saw that the zeros of a response affect the residue, or amplitude, of a response component but do not affect the nature of the response—exponential, damped sinusoid, and so on. In this section, we add a real-axis zero to a two-pole system. The zero will be added first in the left half-plane and then in the right half-plane and its effects noted and analyzed. We conclude the section by talking about pole-zero cancellation.

Starting with a two-pole system with poles at $(-1 \pm j2.828)$, we consecutively add zeros at -3, -5, and -10. The results, normalized to the steady-state value, are plotted in Figure 4.25. We can see that the closer the zero is to the dominant poles, the greater its effect on the transient response. As the zero moves away from the dominant poles, the response approaches that of the two-pole system. This analysis can be reasoned via the partial-fraction expansion. If we assume a group of poles and a zero far from the poles, the residue of each pole will be affected the same by the zero. Hence, the relative amplitudes remain appreciably the same. For example, assume the partial-fraction expansion shown in Eq. (4.68):

$$
\begin{aligned}
T(s) = \frac{(s+a)}{(s+b)(s+c)} &= \frac{A}{s+b} + \frac{B}{s+c} \\
&= \frac{(-b+a)/(-b+c)}{s+b} + \frac{(-c+a)/(-c+b)}{s+c}
\end{aligned}
\tag{4.68}
$$

If the zero is far from the poles, then a is large compared to b and c, and

$$
T(s) \approx a\left[\frac{1/(-b+c)}{s+b} + \frac{1/(-c+b)}{s+c}\right] = \frac{a}{(s+b)(s+c)}
\tag{4.69}
$$

Hence, the zero looks like a simple gain factor and does not change the relative amplitudes of the components of the response.

Another way to look at the effect of a zero, which is more general, is as follows (*Franklin*, *1991*): Let $C(s)$ be the response of a system, $T(s)$, with unity in the
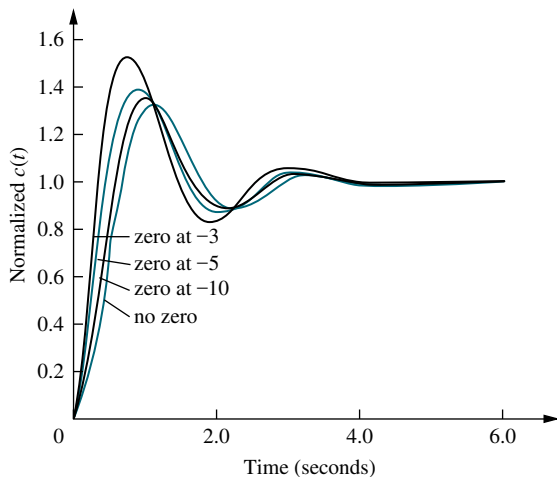
FIGURE 4.25   Effect of adding a zero to a two-pole system
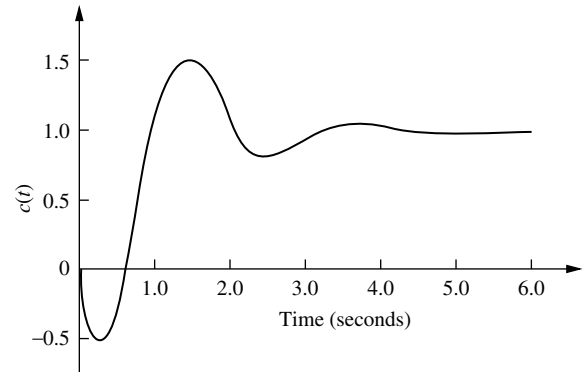
FIGURE 4.26 Step response of a nonminimum-phase system

numerator. If we add a zero to the transfer function, yielding $(s + a)T(s)$, the Laplace transform of the response will be

$$(s + a)C(s) = sC(s) + aC(s) \tag{4.70}$$

Thus, the response of a system with a zero consists of two parts: the derivative of the original response and a scaled version of the original response. If a, the negative of the zero, is very large, the Laplace transform of the response is approximately $aC(s)$, or a scaled version of the original response. If a is not very large, the response has an additional component consisting of the derivative of the original response. As a becomes smaller, the derivative term contributes more to the response and has a greater effect. For step responses, the derivative is typically positive at the start of a step response. Thus, for small values of a, we can expect more overshoot in second-order systems because the derivative term will be additive around the first over-shoot. This reasoning is borne out by Figure 4.25.

An interesting phenomenon occurs if a is negative, placing the zero in the right half-plane. From Eq. (4.70) we see that the derivative term, which is typically positive initially, will be of opposite sign from the scaled response term. Thus, if the derivative term, $sC(s)$, is larger than the scaled response, $aC(s)$, the response will initially follow the derivative in the opposite direction from the scaled response. The result for a second-order system is shown in Figure 4.26, where the sign of the input was reversed to yield a positive steady-state value. Notice that the response begins to turn toward the negative direction even though the final value is positive. A system that exhibits this phenomenon is known as a *nonminimum-phase* system. If a motorcycle or airplane was a nonminimum-phase system, it would initially veer left when commanded to steer right.

Let us now look at an example of an electrical nonminimum-phase network.

Example 4.9

Transfer Function of a Nonminimum-Phase System

PROBLEM:

   a. Find the transfer function, $V_o(s)/V_i(s)$ for the operational amplifier circuit shown in Figure 4.27.

b. If $R_1 = R_2$, this circuit is known as an all-pass filter, since it passes sine waves of a wide range of frequencies without attenuating or amplifying their magnitude (*Dorf, 1993*). We will learn more about frequency response in Chapter 10. For now, let $R_1 = R_2$, $R_3C = 1/10$, and find the step response of the filter. Show that component parts of the response can be identified with those in Eq. (4.70).
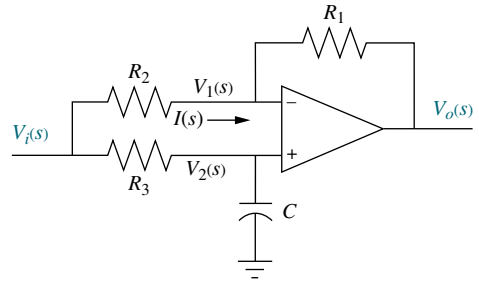
FIGURE 4.27   Nonminimum-phase electric circuit (Reprinted with permission of John Wiley & Sons, Inc.)

SOLUTION:

a. Remembering from Chapter 2 that the operational amplifier has a high input impedance, the current, $I(s)$, through R_1 and R_2, is the same and is equal to

$$I(s) = \frac{V_i(s) - V_o(s)}{R_1 + R_2} \tag{4.71}$$

Also,

$$V_o(s) = A(V_2(s) - V_1(s)) \tag{4.72}$$

But

$$V_1(s) = I(s)R_1 + V_o(s) \tag{4.73}$$

Substituting Eq. (4.71) into (4.73),

$$V_1(s) = \frac{1}{R_1 + R_2}(R_1 V_i(s) + R_2 V_0(s)) \tag{4.74}$$

Using voltage division,

$$V_2(s) = V_i(s)\frac{1/Cs}{R_3 + \dfrac{1}{Cs}} \tag{4.75}$$

Substituting Eqs. (4.74) and (4.75) into Eq. (4.72) and simplifying yields

$$\frac{V_o(s)}{V_i(s)} = \frac{A(R_2 - R_1 R_3 Cs)}{(R_3 Cs + 1)(R_1 + R_2(1 + A))} \tag{4.76}$$

Since the operational amplifier has a large gain, A, let A approach infinity. Thus, after simplification

$$\frac{V_o(s)}{V_i(s)} = \frac{R_2 - R_1 R_3 Cs}{R_2 R_3 Cs + R_2} = -\frac{R_1}{R_2}\frac{\left(s - \dfrac{R_2}{R_1 R_3 C}\right)}{\left(s + \dfrac{1}{R_3 C}\right)} \tag{4.77}$$

b. Letting $R_1 = R_2$ and $R_3C = 1/10$,

$$\frac{V_o(s)}{V_i(s)} = \frac{\left(s - \dfrac{1}{R_3 C}\right)}{\left(s + \dfrac{1}{R_3 C}\right)} = -\frac{(s - 10)}{(s + 10)} \tag{4.78}$$

For a step input, we evaluate the response as suggested by Eq. (4.70):

$$C(s) = -\frac{(s-10)}{s(s+10)} = -\frac{1}{s+10} + 10\frac{1}{s(s+10)} = sC_o(s) - 10C_o(s) \quad (4.79)$$

where

$$C_o(s) = -\frac{1}{s(s+10)} \quad (4.80)$$

is the Laplace transform of the response without a zero. Expanding Eq. (4.79) into partial fractions,

$$C(s) = -\frac{1}{s+10} + 10\frac{1}{s(s+10)} = -\frac{1}{s+10} + \frac{1}{s} - \frac{1}{s+10} = \frac{1}{s} - \frac{2}{s+10} \quad (4.81)$$

or the response with a zero is

$$c(t) = -e^{-10t} + 1 - e^{-10t} = 1 - 2e^{-10t} \quad (4.82)$$

Also, from Eq. (4.80),

$$C_o(s) = -\frac{1/10}{s} + \frac{1/10}{s+10} \quad (4.83)$$

or the response without a zero is

$$c_o(t) = -\frac{1}{10} + \frac{1}{10}e^{-10t} \quad (4.84)$$

The normalized responses are plotted in Figure 4.28. Notice the immediate reversal of the nonminimum-phase response, $c(t)$.
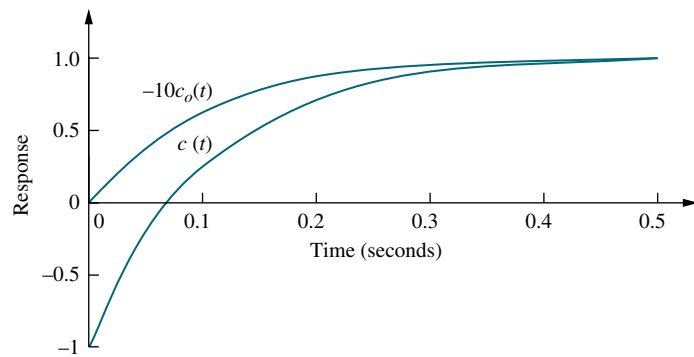
FIGURE 4.28   Step response of the nonminimum-phase network of Figure 4.27 ($c(t)$) and normalized step response of an equivalent network without the zero ($-10c_o(t)$)

We conclude this section by talking about pole-zero cancellation and its effect on our ability to make second-order approximations to a system. Assume a three-pole system with a zero as shown in Eq. (4.85). If the pole term, $(s + p_3)$, and the zero term, $(s + z)$, cancel out, we are left with

$$T(s) = \frac{K(s+z)}{(s+p_3)\,(s^2+as+b)} \quad (4.85)$$

as a second-order transfer function. From another perspective, if the zero at $-z$ is very close to the pole at $-p_3$, then a partial-fraction expansion of Eq. (4.85) will show that the residue of the exponential decay is much smaller than the amplitude of the second-order response. Let us look at an example.

Example 4.10

Evaluating Pole-Zero Cancellation Using Residues

PROBLEM: For each of the response functions in Eqs. (4.86) and (4.87), determine whether there is cancellation between the zero and the pole closest to the zero. For any function for which pole-zero cancellation is valid, find the approximate response.

$$C_1(s) = \frac{26.25(s + 4)}{s(s + 3.5)(s + 5)(s + 6)} \tag{4.86}$$

$$C_2(s) = \frac{26.25(s + 4)}{s(s + 4.01)(s + 5)(s + 6)} \tag{4.87}$$

SOLUTION: The partial-fraction expansion of Eq. (4.86) is

$$C_1(s) = \frac{1}{s} - \frac{3.5}{s + 5} + \frac{3.5}{s + 6} - \frac{1}{s + 3.5} \tag{4.88}$$

The residue of the pole at -3.5, which is closest to the zero at -4, is equal to 1 and is not negligible compared to the other residues. Thus, a second-order step response approximation cannot be made for $C_1(s)$. The partial-fraction expansion for $C_2(s)$ is

$$C_2(s) = \frac{0.87}{s} - \frac{5.3}{s + 5} + \frac{4.4}{s + 6} + \frac{0.033}{s + 4.01} \tag{4.89}$$

The residue of the pole at -4.01, which is closest to the zero at -4, is equal to 0.033, about two orders of magnitude below any of the other residues. Hence, we make a second-order approximation by neglecting the response generated by the pole at -4.01:

$$C_2(s) \approx \frac{0.87}{s} - \frac{5.3}{s + 5} + \frac{4.4}{s + 6} \tag{4.90}$$

and the response $c_2(t)$ is approximately

$$c_2(t) \approx 0.87 - 5.3e^{-5t} + 4.4e^{-6t} \tag{4.91}$$

TryIt 4.4

Use the following MATLAB and Symbolic Math Toolbox statements to evaluate the effect of higher-order poles by finding the component parts of the time response of $c_1(t)$ and $c_2(t)$ in Example 4.10.

```
syms s
C1=26.25*(s+4)/...
   (s*(s + 3.5)*...
   (s+5)*(s+6));
C2=26.25*(s+4)/...
   (s*(s+4.01)*...
   (s+5)*(s + 6));
c1=ilaplace(C1);
c1=vpa(c1,3);
'c1'
pretty (c1)
c2=ilaplace(C2);
c2=vpa(c2,3);
'c2'
pretty(c2);
```

Skill-Assessment Exercise 4.7

PROBLEM: Determine the validity of a second-order step-response approximation for each transfer function shown below.

a. $G(s) = \dfrac{185.71(s + 7)}{(s + 6.5)(s + 10)(s + 20)}$

b. $G(s) = \dfrac{197.14(s + 7)}{(s + 6.9)(s + 10)(s + 20)}$

WileyPLUS

WPCS

Control Solutions

In this section, we have examined the effects of additional transfer function poles and zeros upon the response. In the next section we add nonlinearities of the type discussed in Section 2.10 and see what effects they have on system response.

4.9 Effects of Nonlinearities Upon Time Response

In this section, we qualitatively examine the effects of nonlinearities upon the time response of physical systems. In the following examples, we insert nonlinearities, such as saturation, dead zone, and backlash, as shown in Figure 2.46, into a system to show the effects of these nonlinearities upon the linear responses.

The responses were obtained using Simulink, a simulation software package that is integrated with MATLAB to provide a graphical user interface (GUI). Readers who would like to learn how to use Simulink to generate nonlinear responses should consult the Simulink tutorial in Appendix C. Simulink block diagrams are included with all responses that follow.

Let us assume the motor and load from the Antenna Control Case Study of Chapter 2 and look at the load angular velocity, $\omega_o(s)$, where $\omega_o(s) = 0.1\,s\theta_m(s) = 0.2083\,E_a(s)/(s + 1.71)$ from Eq. (2.208). If we drive the motor with a step input

(*a*)
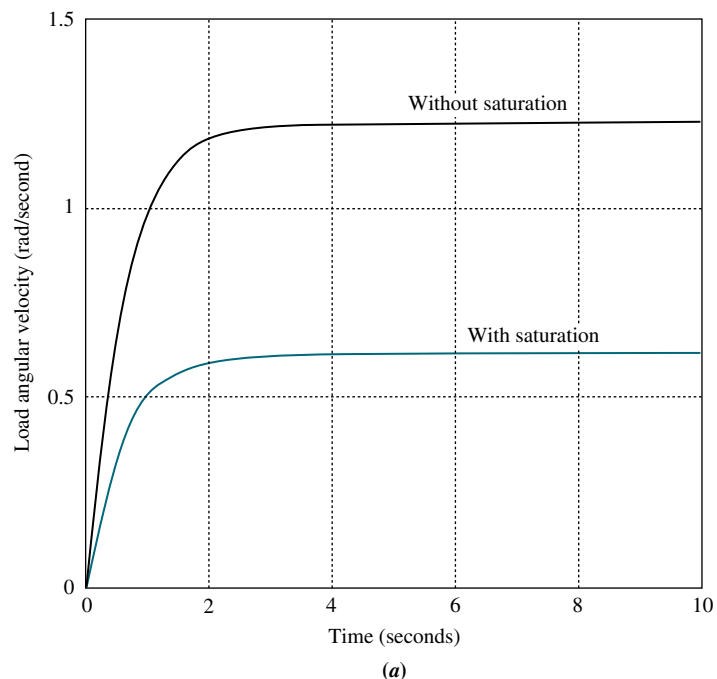
FIGURE 4.29   **a.** Effect of amplifier saturation on load angular velocity response; (*figure continues*)

(*b*)
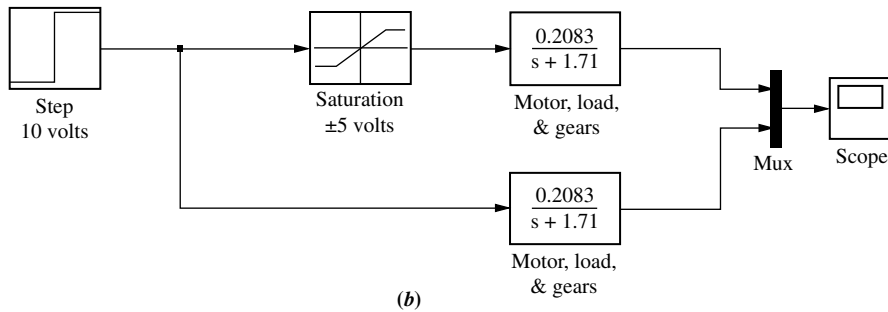
FIGURE 4.29   (*Continued*) **b.** Simulink block diagram

through an amplifier of unity gain that saturates at ±5 volts, Figure 4.29 shows that the effect of amplifier saturation is to limit the obtained velocity.

The effect of dead zone on the output shaft driven by a motor and gears is shown in Figure 4.30. Here we once again assume the motor, load, and gears from Antenna Control Case Study of Chapter 2. Dead zone is present when the motor cannot respond to small voltages. The motor input is a sinusoidal waveform chosen to allow us to see the effects of dead zone vividly. The response begins when the input voltage to the motor exceeds a threshold. We notice a lower amplitude when dead zone is present.

The effect of backlash on the output shaft driven by a motor and gears is shown in Figure 4.31. Again we assume the motor, load, and gears from the Antenna Control Case Study of Chapter 2. The motor input is again a sinusoidal waveform,

(*a*)
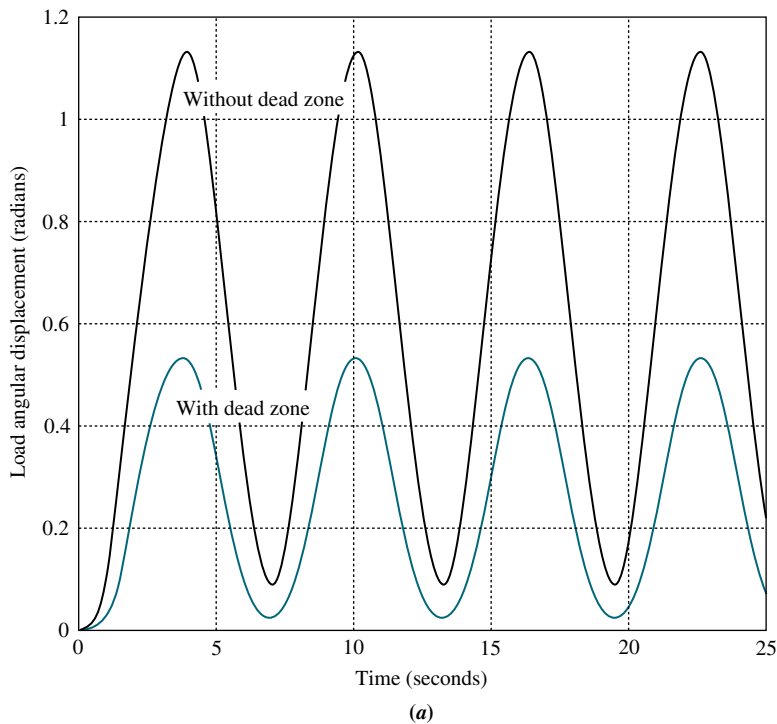
FIGURE 4.30   **a.** Effect of dead zone on load angular displacement response; (*figure continues*)
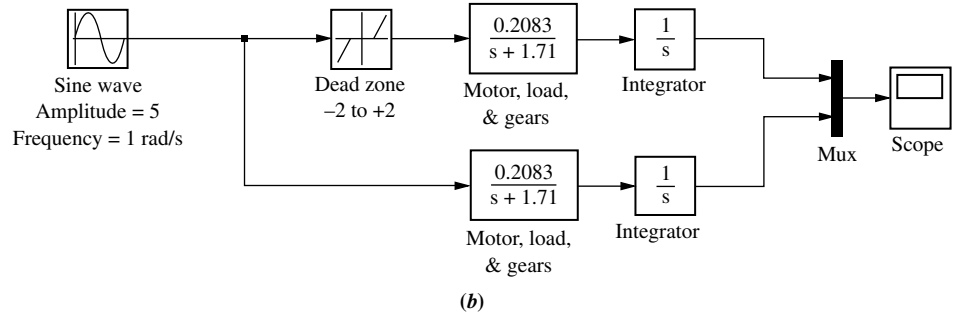
FIGURE 4.30   (*Continued*) **b.** Simulink block diagram
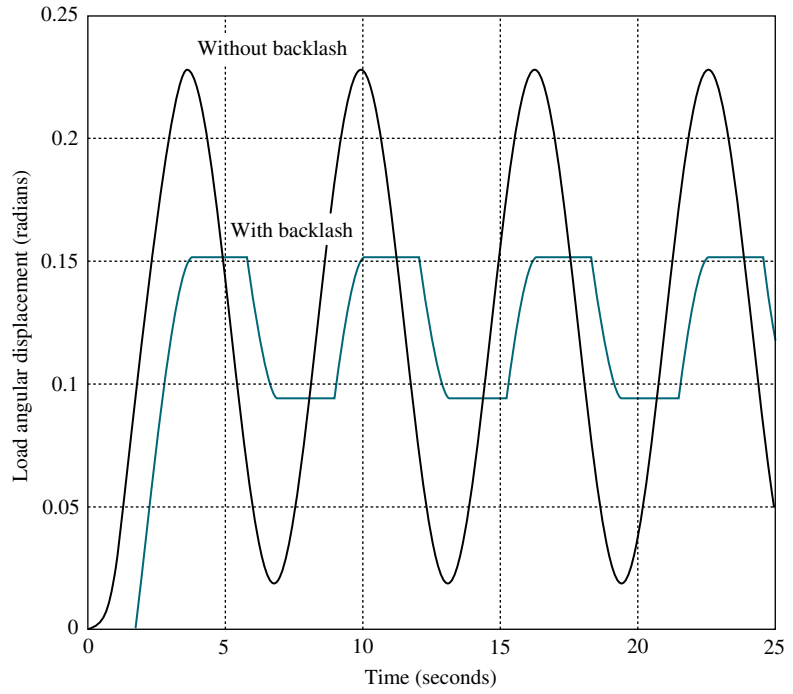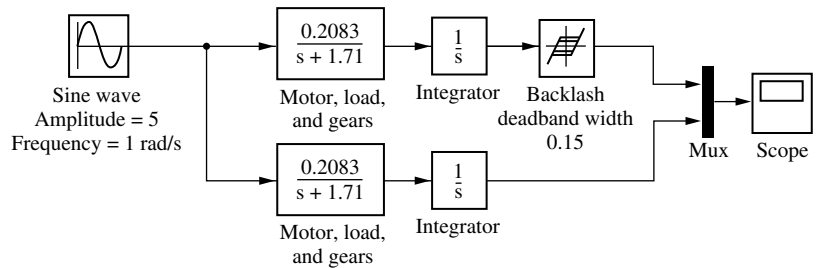
FIGURE 4.31   a. Effect of backlash on load angular displacement response; **b.** Simulink block diagram

which is chosen to allow us to see vividly the effects of backlash in the gears driven by the motor. As the motor reverses direction, the output shaft remains stationary while the motor begins to reverse. When the gears finally connect, the output shaft itself begins to turn in the reverse direction. The resulting response is quite different from the linear response without backlash.

Skill-Assessment Exercise 4.8

Simulink
SL

PROBLEM: Use MATLAB's Simulink to reproduce Figure 4.31.

ANSWER: See Figure 4.31.

Now that we have seen the effects of nonlinearities on the time response, let us return to linear systems. Our coverage so far for linear systems has dealt with finding the time response by using the Laplace transform in the frequency domain. Another way to solve for the response is to use state-space techniques in the time domain. This topic is the subject of the next two sections.

4.10   Laplace Transform Solution of State Equations

In Chapter 3, systems were modeled in state space, where the state-space representation consisted of a state equation and an output equation. In this section, we use the Laplace transform to solve the state equations for the state and output vectors.

State Space
SS

Consider the state equation

$$\dot{\mathbf{x}} = \mathbf{A}\mathbf{x} + \mathbf{B}\mathbf{u} \qquad (4.92)$$

and the output equation

$$\mathbf{y} = \mathbf{C}\mathbf{x} + \mathbf{D}\mathbf{u} \qquad (4.93)$$

Taking the Laplace transform of both sides of the state equation yields

$$s\mathbf{X}(s) - \mathbf{x}(0) = \mathbf{A}\mathbf{X}(s) + \mathbf{B}\mathbf{U}(s) \qquad (4.94)$$

In order to separate $\mathbf{X}(s)$, replace $s\mathbf{X}(s)$ with $s\mathbf{I}\mathbf{X}(s)$, where $\mathbf{I}$ is an $n \times n$ identity matrix, and n is the order of the system. Combining all of the $\mathbf{X}(s)$ terms, we get

$$(s\mathbf{I} - \mathbf{A})\mathbf{X}(s) = \mathbf{x}(0) + \mathbf{B}\mathbf{U}(s) \qquad (4.95)$$

Solving for $\mathbf{X}(s)$ by premultiplying both sides of Eq. (4.95) by $(s\mathbf{I} - \mathbf{A})^{-1}$, the final solution for $\mathbf{X}(s)$ is

$$\mathbf{X}(s) = (s\mathbf{I} - \mathbf{A})^{-1}\mathbf{x}(0) + (s\mathbf{I} - \mathbf{A})^{-1}\mathbf{B}\mathbf{U}(s)$$

$$= \frac{\text{adj}(s\mathbf{I} - \mathbf{A})}{\det(s\mathbf{I} - \mathbf{A})}[\mathbf{x}(0) + \mathbf{B}\mathbf{U}(s)] \qquad (4.96)$$

Taking the Laplace transform of the output equation yields

$$\boxed{\mathbf{Y}(s) = \mathbf{CX}(s) + \mathbf{DU}(s)} \qquad (4.97)$$

Eigenvalues and Transfer Function Poles

We saw that the poles of the transfer function determine the nature of the transient response of the system. Is there an equivalent quantity in the state-space representation that yields the same information? Section 5.8 formally defines the roots of $\det(s\mathbf{I} - \mathbf{A}) = 0$ (see the denominator of Eq. (4.96)) to be *eigenvalues* of the system matrix, $\mathbf{A}$.[6] Let us show that the eigenvalues are equal to the poles of the system's transfer function. Let the output, $\mathbf{Y}(s)$, and the input, $\mathbf{U}(s)$, be scalar quantities $Y(s)$ and $U(s)$, respectively. Further, to conform to the definition of a transfer function, let $\mathbf{x}(0)$, the initial state vector, equal $\mathbf{0}$, the null vector. Substituting Eq. (4.96) into Eq. (4.97) and solving for the transfer function, $Y(s)/U(s)$, yields

$$\frac{Y(s)}{U(s)} = \mathbf{C}\left[\frac{\mathrm{adj}(s\mathbf{I} - \mathbf{A})}{\det(s\mathbf{I} - \mathbf{A})}\right]\mathbf{B} + \mathbf{D}$$

$$= \frac{\mathbf{C}\,\mathrm{adj}(s\mathbf{I} - \mathbf{A})\mathbf{B} + \mathbf{D}\det(s\mathbf{I} - \mathbf{A})}{\det(s\mathbf{I} - \mathbf{A})} \qquad (4.98)$$

The roots of the denominator of Eq. (4.98) are the poles of the system. Since the denominators of Eqs. (4.96) and (4.98) are identical, the system poles equal the eigenvalues. Hence, if a system is represented in state-space, we can find the poles from $\det(s\mathbf{I} - \mathbf{A}) = 0$. We will be more formal about these facts when we discuss stability in Chapter 6.

The following example demonstrates solving the state equations using the Laplace transform as well as finding the eigenvalues and system poles.

Example 4.11

Laplace Transform Solution; Eigenvalues and Poles

PROBLEM: Given the system represented in state space by Eqs. (4.99),

$$\dot{\mathbf{x}} = \begin{bmatrix} 0 & 1 & 0 \\ 0 & 0 & 1 \\ -24 & -26 & -9 \end{bmatrix} \mathbf{x} + \begin{bmatrix} 0 \\ 0 \\ 1 \end{bmatrix} e^{-t} \qquad (4.99a)$$

$$y = \begin{bmatrix} 1 & 1 & 0 \end{bmatrix}\mathbf{x} \qquad (4.99b)$$

$$\mathbf{x}(0) = \begin{bmatrix} 1 \\ 0 \\ 2 \end{bmatrix} \qquad (4.99c)$$

---

[6] Sometimes the symbol λ is used in place of the complex variable s when solving the state equations without using the Laplace transform. Thus, it is common to see the characteristic equation also written as $\det(\lambda\mathbf{I} - \mathbf{A}) = 0$.

do the following:

a. Solve the preceding state equation and obtain the output for the given exponential input.

b. Find the eigenvalues and the system poles.

SOLUTION:

a. We will solve the problem by finding the component parts of Eq. (4.96), followed by substitution into Eq. (4.97). First obtain **A** and **B** by comparing Eq. (4.99a) to Eq. (4.92). Since

$$s\mathbf{I} = \begin{bmatrix} s & 0 & 0 \\ 0 & s & 0 \\ 0 & 0 & s \end{bmatrix} \tag{4.100}$$

then

$$(s\mathbf{I} - \mathbf{A}) = \begin{bmatrix} s & -1 & 0 \\ 0 & s & -1 \\ 24 & 26 & s+9 \end{bmatrix} \tag{4.101}$$

and

$$(s\mathbf{I} - \mathbf{A})^{-1} = \frac{\begin{bmatrix} (s^2 + 9s + 26) & (s+9) & 1 \\ -24 & s^2 + 9s & s \\ -24s & -(26s + 24) & s^2 \end{bmatrix}}{s^3 + 9s^2 + 26s + 24} \tag{4.102}$$

Since $\mathbf{U}(s)$ (the Laplace transform for e^{-t}) is $1/(s+1)$, $\mathbf{X}(s)$ can be calculated. Rewriting Eq. (4.96) as

$$\mathbf{X}(s) = (s\mathbf{I} - \mathbf{A})^{-1}[\mathbf{x}(0) + \mathbf{B}\mathbf{U}(s)] \tag{4.103}$$

and using **B** and $\mathbf{x}(0)$ from Eqs. (4.99a) and (4.99c), respectively, we get

$$X_1(s) = \frac{(s^3 + 10s^2 + 37s + 29)}{(s+1)(s+2)(s+3)(s+4)} \tag{4.104a}$$

$$X_2(s) = \frac{(2s^2 - 21s - 24)}{(s+1)(s+2)(s+3)(s+4)} \tag{4.104b}$$

$$X_3(s) = \frac{s(2s^2 - 21s - 24)}{(s+1)(s+2)(s+3)(s+4)} \tag{4.104c}$$

The output equation is found from Eq. (4.99b). Performing the indicated addition yields

$$Y(s) = \begin{bmatrix} 1 & 1 & 0 \end{bmatrix} \begin{bmatrix} X_1(s) \\ X_2(s) \\ X_3(s) \end{bmatrix} = X_1(s) + X_2(s) \tag{4.105}$$

or

$$Y(s) = \frac{(s^3 + 12s^2 + 16s + 5)}{(s+1)(s+2)(s+3)(s+4)}$$

$$= \frac{-6.5}{s+2} + \frac{19}{s+3} - \frac{11.5}{s+4}$$

(4.106)

where the pole at -1 canceled a zero at -1. Taking the inverse Laplace transform,

$$y(t) = -6.5e^{-2t} + 19e^{-3t} - 11.5e^{-4t}$$

(4.107)

b. The denominator of Eq. (4.102), which is $\det(s\mathbf{I} - \mathbf{A})$, is also the denominator of the system's transfer function. Thus, $\det(s\mathbf{I} - \mathbf{A}) = 0$ furnishes both the poles of the system and the eigenvalues -2, -3, and -4.

Symbolic Math

SM

Students who are performing the MATLAB exercises and want to explore the added capability of MATLAB's Symbolic Math Toolbox should now run ch4sp1 in Appendix F at www.wiley.com/college/ nise. You will learn how to solve state equations for the output response using the Laplace transform. Example 4.11 will be solved using MATLAB and the Symbolic Math Toolbox.

Skill-Assessment Exercise 4.9

WileyPLUS

WPCS

Control Solutions

PROBLEM: Given the system represented in state space by Eqs. (4.108),

$$\dot{\mathbf{x}} = \begin{bmatrix} 0 & 2 \\ -3 & -5 \end{bmatrix} \mathbf{x} + \begin{bmatrix} 0 \\ 1 \end{bmatrix} e^{-t}$$

(4.108a)

$$y = \begin{bmatrix} 1 & 3 \end{bmatrix} \mathbf{x}$$

(4.108b)

TryIt 4.5

Use the following MATLAB and Symbolic Math Toolbox statements to solve Skill-Assessment Exercise 4.9.

```
Syms s
A=[0 2;-3 -5];B=[0;1];
C=[1 3];X0=[2;1];
U=1/(s+1);
I=[1 0;0 1];
X=((s*I-A)^-1)* ...
  (X0+B*U);
Y=C*X;Y=simplify(Y);
y=ilaplace(Y);
pretty(y)
eig(A)
```

$$\mathbf{x}(0) = \begin{bmatrix} 2 \\ 1 \end{bmatrix}$$

(4.108c)

do the following:

a. Solve for $y(t)$ using state-space and Laplace transform techniques.
b. Find the eigenvalues and the system poles.

ANSWERS:

a. $y(t) = -0.5e^{-t} - 12e^{-2t} + 17.5e^{-3t}$
b. -2, -3

The complete solution is located at www.wiley.com/college/nise.

4.11   Time Domain Solution of State Equations

We now look at another technique for solving the state equations. Rather than using the Laplace transform, we solve the equations directly in the time domain using a method closely allied to the classical solution of differential equations. We will find that the final solution consists of two parts that are different from the forced and natural responses.

The solution in the time domain is given directly by

$$
\begin{aligned}
\mathbf{x}(t) &= e^{\mathbf{A}t}\mathbf{x}(0) + \int_0^t e^{\mathbf{A}(t-\tau)}\mathbf{B}\mathbf{u}(\tau)d\tau \\[2mm]
&= \mathbf{\Phi}(t)\mathbf{x}(0) + \int_0^t \mathbf{\Phi}(t-\tau)\mathbf{B}\mathbf{u}(\tau)d\tau
\end{aligned}
\tag{4.109}
$$

where $\mathbf{\Phi}(t) = e^{\mathbf{A}t}$ by definition, and which is called the *state-transition matrix*. Eq. (4.109) is derived in Appendix I located at www.wiley.com/college/nise. Readers who are not familiar with this equation or who may want to refresh their memory should consult Appendix I before proceeding.

Notice that the first term on the right-hand side of the equation is the response due to the initial state vector, $\mathbf{x}(0)$. Notice also that it is the only term dependent on the initial state vector and not the input. We call this part of the response the *zero-input response*, since it is the total response if the input is zero. The second term, called the *convolution integral*, is dependent only on the input, $\mathbf{u}$, and the input matrix, $\mathbf{B}$, not the initial state vector. We call this part of the response the *zero-state response*, since it is the total response if the initial state vector is zero. Thus, there is a partitioning of the response different from the forced/natural response we have seen when solving differential equations. In differential equations, the arbitrary constants of the natural response are evaluated based on the initial conditions and the initial values of the forced response and its derivatives. Thus, the natural response's amplitudes are a function of the initial conditions of the output and the input. In Eq. (4.109), the zero-input response is not dependent on the initial values of the input and its derivatives. It is dependent only on the initial conditions of the state vector. The next example vividly shows the difference in partitioning. Pay close attention to the fact that in the final result the zero-state response contains not only the forced solution but also pieces of what we previously called the natural response. We will see in the solution that the natural response is distributed through the zero-input response and the zero-state response.

Before proceeding with the example, let us examine the form the elements of $\mathbf{\Phi}(t)$ take for linear, time-invariant systems. The first term of Eq. (4.96), the Laplace transform of the response for unforced systems, is the transform of $\Phi(t)\mathbf{x}(0)$, the zero-input response from Eq. (4.109). Thus, for the unforced system

$$
\mathscr{L}[\mathbf{x}(t)] = \mathscr{L}[\mathbf{\Phi}(t)\mathbf{x}(0)] = (s\mathbf{I} - \mathbf{A})^{-1}\mathbf{x}(0)
\tag{4.110}
$$

from which we can see that $(s\mathbf{I} - \mathbf{A})^{-1}$ *is the Laplace transform of the state-transition matrix*, $\mathbf{\Phi}(t)$. We have already seen that the denominator of $(s\mathbf{I} - \mathbf{A})^{-1}$ is a polynomial in s whose roots are the system poles. This polynomial is found from

the equation $\det(s\mathbf{I} - \mathbf{A}) = 0$. Since

$$\mathscr{L}^{-1}[(s\mathbf{I} - \mathbf{A})^{-1}] = \mathscr{L}^{-1}\left[\frac{\text{adj}(s\mathbf{I} - \mathbf{A})}{\det(s\mathbf{I} - \mathbf{A})}\right] = \boldsymbol{\Phi}(t) \qquad (4.111)$$

each term of $\boldsymbol{\Phi}(t)$ would be the sum of exponentials generated by the system's poles.

Let us summarize the concepts with two numerical examples. The first example solves the state equations directly in the time domain. The second example uses the Laplace transform to solve for the state-transition matrix by finding the inverse Laplace transform of $(s\mathbf{I} - \mathbf{A})^{-1}$.

Example 4.12

Time Domain Solution

PROBLEM: For the state equation and initial state vector shown in Eqs. (4.112), where $u(t)$ is a unit step, find the state-transition matrix and then solve for $\mathbf{x}(t)$.

$$\dot{\mathbf{x}}(t) = \begin{bmatrix} 0 & 1 \\ -8 & -6 \end{bmatrix}\mathbf{x}(t) + \begin{bmatrix} 0 \\ 1 \end{bmatrix}u(t) \qquad (4.112\text{a})$$

$$\mathbf{x}(0) = \begin{bmatrix} 1 \\ 0 \end{bmatrix} \qquad (4.112\text{b})$$

SOLUTION: Since the state equation is in the form

$$\dot{\mathbf{x}}(t) = \mathbf{A}\mathbf{x}(t) + \mathbf{B}u(t) \qquad (4.113)$$

find the eigenvalues using $\det(s\mathbf{I} - \mathbf{A}) = 0$. Hence, $s^2 + 6s + 8 = 0$, from which $s_1 = -2$ and $s_2 = -4$. Since each term of the state-transition matrix is the sum of responses generated by the poles (eigenvalues), we assume a state-transition matrix of the form

$$\boldsymbol{\Phi}(t) = \begin{bmatrix} (K_1 e^{-2t} + K_2 e^{-4t}) & (K_3 e^{-2t} + K_4 e^{-4t}) \\ (K_5 e^{-2t} + K_6 e^{-4t}) & (K_7 e^{-2t} + K_8 e^{-4t}) \end{bmatrix} \qquad (4.114)$$

In order to find the values of the constants, we make use of the properties of the state-transition matrix derived in Appendix J located at www.wiley.com/college/nise.

$$\boldsymbol{\Phi}(0) = \mathbf{I} \qquad (4.115)$$

$$K_1 + K_2 = 1 \qquad (4.116\text{a})$$

$$K_3 + K_4 = 0 \qquad (4.116\text{b})$$

$$K_5 + K_6 = 0 \qquad (4.116\text{c})$$

$$K_7 + K_8 = 1 \qquad (4.116\text{d})$$

and since

$$\dot{\mathbf{\Phi}}(0) = \mathbf{A} \tag{4.117}$$

then

$$-2K_1 - 4K_2 = 0 \tag{4.118a}$$

$$-2K_3 - 4K_4 = 1 \tag{4.118b}$$

$$-2K_5 - 4K_6 = -8 \tag{4.118c}$$

$$-2K_7 - 4K_8 = -6 \tag{4.118d}$$

The constants are solved by taking two simultaneous equations four times. For example, Eq. (4.116a) can be solved simultaneously with Eq. (4.118a) to yield the values of K_1 and K_2. Proceeding similarly, all of the constants can be found. Therefore,

$$\mathbf{\Phi}(t) = \begin{bmatrix} (2e^{-2t} - e^{-4t}) & \left(\frac{1}{2}e^{-2t} - \frac{1}{2}e^{-4t}\right) \\ (-4e^{-2t} + 4e^{-4t}) & (-e^{-2t} + 2e^{-4t}) \end{bmatrix} \tag{4.119}$$

Also,

$$\mathbf{\Phi}(t - \tau)\mathbf{B} = \begin{bmatrix} \left(\frac{1}{2}e^{-2(t-\tau)} - \frac{1}{2}e^{-4(t-\tau)}\right) \\ \left(-e^{-2(t-\tau)} + 2e^{-4(t-\tau)}\right) \end{bmatrix} \tag{4.120}$$

Hence, the first term of Eq. (4.109) is

$$\mathbf{\Phi}(t)\mathbf{x}(0) = \begin{bmatrix} (2e^{-2t} - e^{-4t}) \\ (-4e^{-2t} + 4e^{-4t}) \end{bmatrix} \tag{4.121}$$

The last term of Eq. (4.109) is

$$\int_0^t \mathbf{\Phi}(t - \tau)\mathbf{B}u(\tau)d\tau = \begin{bmatrix} \frac{1}{2}e^{-2t}\int_0^t e^{2\tau}d\tau - \frac{1}{2}e^{-4t}\int_0^t e^{4\tau}d\tau \\ \\ -e^{-2t}\int_0^t e^{2\tau}d\tau + 2e^{-4t}\int_0^t e^{4\tau}d\tau \end{bmatrix}$$

$$= \begin{bmatrix} \frac{1}{8} - \frac{1}{4}e^{-2t} + \frac{1}{8}e^{-4t} \\ \\ \frac{1}{2}e^{-2t} - \frac{1}{2}e^{-4t} \end{bmatrix} \tag{4.122}$$

Notice, as promised, that Eq. (4.122), the zero-state response, contains not only the forced response, 1/8, but also terms of the form Ae^{-2t} and Be^{-4t} that are part of

what we previously called the natural response. However, the coefficients, A and B, are not dependent on the initial conditions.

The final result is found by adding Eqs. (4.121) and (4.122). Hence,

$$\mathbf{x}(t) = \mathbf{\Phi}(t)\mathbf{x}(0) + \int_0^t \Phi(t - \tau)\mathbf{B}\mathbf{u}(\tau)d\tau = \begin{bmatrix} \dfrac{1}{8} + \dfrac{7}{4}e^{-2t} - \dfrac{7}{8}e^{-4t} \\[2mm] -\dfrac{7}{2}e^{-2t} + \dfrac{7}{2}e^{-4t} \end{bmatrix} \qquad (4.123)$$

Example 4.13

State-Transition Matrix via Laplace Transform

PROBLEM: Find the state-transition matrix of Example 4.12, using $(s\mathbf{I} - \mathbf{A})^{-1}$.

SOLUTION: We use the fact that $\mathbf{\Phi}(t)$ is the inverse Laplace transform of $(s\mathbf{I} - \mathbf{A})^{-1}$. Thus, first find $(s\mathbf{I} - \mathbf{A})$ as

$$(s\mathbf{I} - \mathbf{A}) = \begin{bmatrix} s & -1 \\ 8 & (s+6) \end{bmatrix} \qquad (4.124)$$

from which

$$(s\mathbf{I} - \mathbf{A})^{-1} = \dfrac{\begin{bmatrix} s+6 & 1 \\ -8 & s \end{bmatrix}}{s^2 + 6s + 8} = \begin{bmatrix} \dfrac{s+6}{s^2+6s+8} & \dfrac{1}{s^2+6s+8} \\[3mm] \dfrac{-8}{s^2+6s+8} & \dfrac{s}{s^2+6s+8} \end{bmatrix} \qquad (4.125)$$

Expanding each term in the matrix on the right by partial fractions yields

$$(s\mathbf{I} - \mathbf{A})^{-1} = \begin{bmatrix} \left(\dfrac{2}{s+2} - \dfrac{1}{s+4}\right) & \left(\dfrac{1/2}{s+2} - \dfrac{1/2}{s+4}\right) \\[3mm] \left(\dfrac{-4}{s+2} + \dfrac{4}{s+4}\right) & \left(\dfrac{-1}{s+2} + \dfrac{2}{s+4}\right) \end{bmatrix} \qquad (4.126)$$

Finally, taking the inverse Laplace transform of each term, we obtain

$$\mathbf{\Phi}(t) = \begin{bmatrix} (2e^{-2t} - e^{-4t}) & \left(\dfrac{1}{2}e^{-2t} - \dfrac{1}{2}e^{-4t}\right) \\[3mm] (-4e^{-2t} + 4e^{-4t}) & (-e^{-2t} + 2e^{-4t}) \end{bmatrix} \qquad (4.127)$$

Symbolic Math
SM

```
Students who are performing the MATLAB exercises and want to
explore the added capability of MATLAB's Symbolic Math Toolbox
should now run ch4sp2 in Appendix F at www.wiley.com/college/
nise. You will learn how to solve state equations for the output
response using the convolution integral. Examples 4.12 and 4.13
will be solved using MATLAB and the Symbolic Math Toolbox.
```

Systems represented in state space can be simulated on the digital computer. Programs such as MATLAB can be used for this purpose. Alternately, the user can write specialized programs, as discussed in Appendix G.1 at www.wiley.com/college/nise.

```
Students who are using MATLAB should now run ch4p3 in Appendix B.
This exercise uses MATLAB to simulate the step response of systems
represented in state space. In addition to generating the step
response, you will learn how to specify the range on the time axis
for the plot.
```

MATLAB
ML

Skill-Assessment Exercise 4.10

PROBLEM: Given the system represented in state space by Eqs. (4.128):

WileyPLUS
WPCS
Control Solutions

$$\dot{\mathbf{x}} = \begin{bmatrix} 0 & 2 \\ -2 & -5 \end{bmatrix} \mathbf{x} + \begin{bmatrix} 0 \\ 1 \end{bmatrix} e^{-2t} \qquad (4.128a)$$

$$y = \begin{bmatrix} 2 & 1 \end{bmatrix} \mathbf{x} \qquad (4.128b)$$

$$\mathbf{x}(0) = \begin{bmatrix} 1 \\ 2 \end{bmatrix} \qquad (4.128c)$$

do the following:

   a. Solve for the state-transition matrix.

   b. Solve for the state vector using the convolution integral.

   c. Find the output, $y(t)$.

ANSWERS:

a. $\Phi(t) = \begin{bmatrix} \left(\dfrac{4}{3}e^{-t} - \dfrac{1}{3}e^{-4t} \right) & \left(\dfrac{2}{3}e^{-t} - \dfrac{2}{3}e^{-4t} \right) \\[2mm] \left(-\dfrac{2}{3}e^{-t} + \dfrac{2}{3}e^{-4t} \right) & \left(-\dfrac{1}{3}e^{-t} + \dfrac{4}{3}e^{-4t} \right) \end{bmatrix}$

b. $\mathbf{x}(t) = \begin{bmatrix} \left(\dfrac{10}{3}e^{-t} - e^{-2t} - \dfrac{4}{3}e^{-4t} \right) \\[2mm] \left(-\dfrac{5}{3}e^{-t} + e^{-2t} + \dfrac{8}{3}e^{-4t} \right) \end{bmatrix}$

c. $y(t) = 5e^{-t} - e^{-2t}$

The complete solution is located at www.wiley.com/college/nise.

Case Studies

Antenna Control: Open-Loop Response

In this chapter, we have made use of the transfer functions derived in Chapter 2 and the state equations derived in Chapter 3 to obtain the output response of an

open-loop system. We also showed the importance of the poles of a system in determining the transient response. The following case study uses these concepts to analyze an open-loop portion of the antenna azimuth position control system. The open-loop function that we will deal with consists of a power amplifier and motor with load.

PROBLEM: For the schematic of the azimuth position control system shown on the front endpapers, Configuration 1, assume an open-loop system (feedback path disconnected).

a. Predict, by inspection, the form of the open-loop angular velocity response of the load to a step-voltage input to the power amplifier.

b. Find the damping ratio and natural frequency of the open-loop system.

c. Derive the complete analytical expression for the open-loop angular velocity response of the load to a step-voltage input to the power amplifier, using transfer functions.

d. Obtain the open-loop state and output equations.

e. Use MATLAB to obtain a plot of the open-loop angular velocity response to a step-voltage input.

State Space

SS

MATLAB

ML

SOLUTION: The transfer functions of the power amplifier, motor, and load as shown on the front endpapers, Configuration 1, were discussed in the Chapter 2 case study. The two subsystems are shown interconnected in Figure 4.32(a). Differentiating the angular position of the motor and load output by multiplying by s, we obtain the output angular velocity, ω_o, as shown in Figure 4.32(a). The equivalent transfer function representing the three blocks in Figure 4.32(a) is the product of the individual transfer functions and is shown in Figure 4.32(b).[7]

a. Using the transfer function shown in Figure 4.32(b), we can predict the nature of the step response. The step response consists of the steady-state response generated by the step input and the transient response, which is the sum of two exponentials generated by each pole of the transfer function. Hence, the form of the response is

$$\omega_o(t) = A + Be^{-100t} + Ce^{-1.71t} \qquad (4.129)$$

b. The damping ratio and natural frequency of the open-loop system can be found by expanding the denominator of the transfer function. Since the open-loop
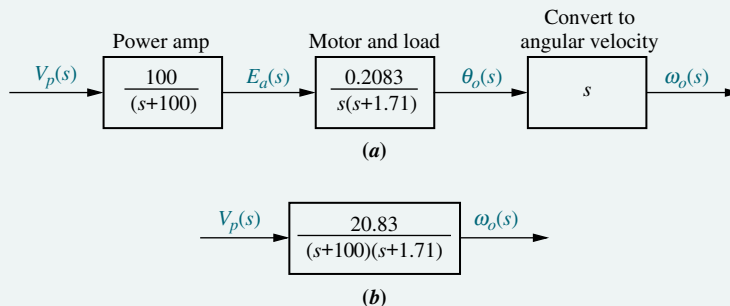
FIGURE 4.32 Antenna azimuth position control system for angular velocity: **a.** forward path; **b.** equivalent forward path

---

[7] This product relationship will be derived in Chapter 5.

transfer function is

$$G(s) = \frac{20.83}{s^2 + 101.71s + 171} \tag{4.130}$$

$\omega_n = \sqrt{171} = 13.08$, and $\zeta = 3.89$ (overdamped).

c. In order to derive the angular velocity response to a step input, we multiply the transfer function of Eq. (4.130) by a step input, $1/s$, and obtain

$$\omega_o(s) = \frac{20.83}{s(s+100)(s+1.71)} \tag{4.131}$$

Expanding into partial fractions, we get

$$\omega_o(s) = \frac{0.122}{s} + \frac{2.12 \times 10^{-3}}{s+100} - \frac{0.124}{s+1.71} \tag{4.132}$$

Transforming to the time domain yields

$$\omega_o(t) = 0.122 + (2.12 \times 10^{-3})e^{-100t} - 0.124e^{-1.71t} \tag{4.133}$$

d. First convert the transfer function into the state-space representation. Using Eq. (4.130), we have

State Space
SS

$$\frac{\omega_o(s)}{V_p(s)} = \frac{20.83}{s^2 + 101.71s + 171} \tag{4.134}$$

Cross-multiplying and taking the inverse Laplace transform with zero initial conditions, we have

$$\ddot{\omega}_o + 101.71\dot{\omega}_o + 171\omega_o = 20.83v_p \tag{4.135}$$

Defining the phase variables as

$$x_1 = \omega_o \tag{4.136a}$$

$$x_2 = \dot{\omega}_o \tag{4.136b}$$

and using Eq. (4.135), the state equations are written as

$$\dot{x}_1 = x_2 \tag{4.137a}$$

$$\dot{x}_2 = -171x_1 - 101.71x_2 + 20.83v_p \tag{4.137b}$$

where $v_p = 1$, a unit step. Since $x_1 = \omega_o$ is the output, the output equation is

$$y = x_1 \tag{4.138}$$

Equations (4.137) and (4.138) can be programmed to obtain the step response using MATLAB or alternative methods described in Appendix H.1 at www.wiley.com/college/nise.

e. `Students who are using MATLAB should now run ch4p4 in Appendix B. This exercise uses MATLAB to plot the step response.`

MATLAB
ML

CHALLENGE: You are now given a problem to test your knowledge of this chapter's objectives. Refer to the antenna azimuth position control system shown on the

front endpapers, Configuration 2. Assume an open-loop system (feedback path disconnected) and do the following:

a. Predict the open-loop angular velocity response of the power amplifier, motor, and load to a step voltage at the input to the power amplifier.

b. Find the damping ratio and natural frequency of the open-loop system.

c. Derive the open-loop angular velocity response of the power amplifier, motor, and load to a step-voltage input using transfer functions.

d. Obtain the open-loop state and output equations.

e. Use MATLAB to obtain a plot of the open-loop angular velocity response to a step-voltage input.

State Space
SS

MATLAB
ML

Unmanned Free-Swimming Submersible Vehicle: Open-Loop Pitch Response

An Unmanned Free-Swimming Submersible (UFSS) vehicle is shown in Figure 4.33. The depth of the vehicle is controlled as follows. During forward motion, an elevator surface on the vehicle is deflected by a selected amount. This deflection causes the vehicle to rotate about the pitch axis. The pitch of the vehicle creates a vertical force that causes the vehicle to submerge or rise. The pitch control system for the vehicle is used here and in subsequent chapters as a case study to demonstrate the covered concepts. The block diagram for the pitch control system is shown in Figure 4.34 and on the back endpapers for future reference (*Johnson*, *1980*). In this case study, we investigate the time response of the vehicle dynamics that relate the pitch angle output to the elevator deflection input.

PROBLEM: The transfer function relating pitch angle, $\theta(s)$, to elevator surface angle, $\delta_e(s)$, for the UFSS vehicle is

$$\frac{\theta(s)}{\delta_e(s)} = \frac{-0.125(s + 0.435)}{(s + 1.23)(s^2 + 0.226s + 0.0169)} \tag{4.139}$$
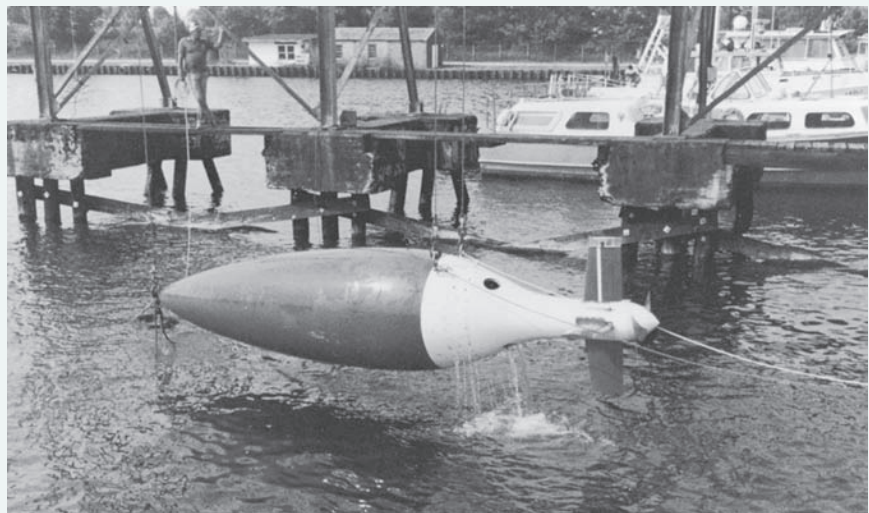
FIGURE 4.33   Unmanned Free-Swimming Submersible (UFSS) vehicle.
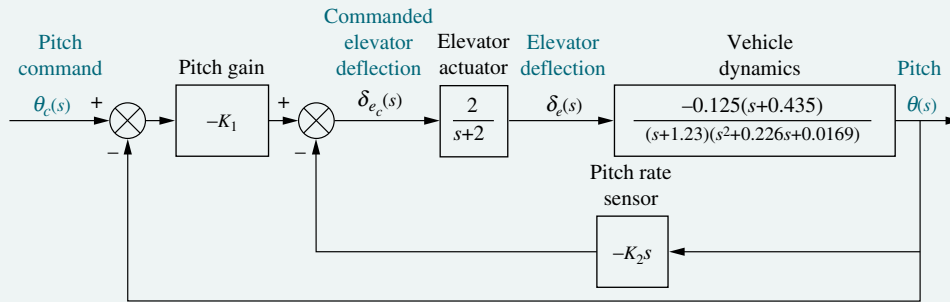
FIGURE 4.34 Pitch control loop for the UFSS vehicle

a. Using only the second-order poles shown in the transfer function, predict percent overshoot, rise time, peak time, and settling time.

b. Using Laplace transforms, find the analytical expression for the response of the pitch angle to a step input in elevator surface deflection.

c. Evaluate the effect of the additional pole and zero on the validity of the second-order approximation.

d. Plot the step response of the vehicle dynamics and verify your conclusions found in (c).

SOLUTION:

a. Using the polynomial $s^2 + 0.226s + 0.0169$, we find that $\omega_n^2 = 0.0169$ and $2\zeta\omega_n = 0.226$. Thus, $\omega_n = 0.13$ rad/s and $\zeta = 0.869$. Hence, $\%OS = e^{-\zeta\pi/\sqrt{1-\zeta^2}} \cdot 100 = 0.399\%$. From Figure 4.16, $\omega_n T_r = 2.75$, or $T_r = 21.2$ s. To find peak time, we use $T_p = \pi/\omega_n\sqrt{1-\zeta^2} = 48.9$ s. Finally, settling time is $T_s = 4/\zeta\omega_n = 35.4$ s.

b. In order to display a positive final value in Part **d**. we find the response of the system to a negative unit step, compensating for the negative sign in the transfer function. Using partial-fraction expansion, the Laplace transform of the response, $\theta(s)$, is

$$\theta(s) = \frac{0.125(s + 0.435)}{s(s + 1.23)(s^2 + 0.226s + 0.0169)}$$

$$= 2.616\frac{1}{s} + 0.0645\frac{1}{s + 1.23}$$

$$- \frac{2.68(s + 0.113) + 3.478\sqrt{0.00413}}{(s + 0.113)^2 + 0.00413} \tag{4.140}$$

Taking the inverse Laplace transform,

$$\theta(t) = 2.616 + 0.0645e^{-1.23t}$$

$$- e^{-0.113t}(2.68 \cos 0.0643t + 3.478 \sin 0.0643t)$$

$$= 2.616 + 0.0645e^{-1.23t} - 4.39e^{-0.113t}\cos(0.0643t + 52.38°) \tag{4.141}$$

c. Looking at the relative amplitudes between the coefficient of the $e^{-1.23t}$ term and the cosine term in Eq. (4.165), we see that there is pole-zero cancellation between the pole at -1.23 and the zero at -0.435. Further, the pole at -1.23 is more than five times farther from the $j\omega$ axis than the second-order dominant
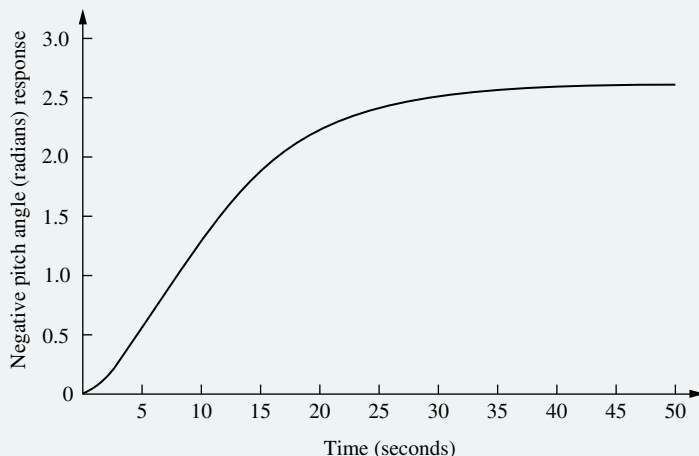
FIGURE 4.35   Negative step response of pitch control for UFSS vehicle

poles at $-0.113 \pm j0.0643$. We conclude that the response will be close to that predicted.

d. Plotting Eq. (4.141) or using a computer simulation, we obtain the step response shown in Figure 4.35. We indeed see a response close to that predicted.

MATLAB
ML

Students who are using MATLAB should now run ch4p5 in Appendix B.
This exercise uses MATLAB to find ζ, ω_n, T_s, T_p, and T_r and plot a step
response. Table lookup is used to find T_r. The exercise applies the
concepts to the problem above.
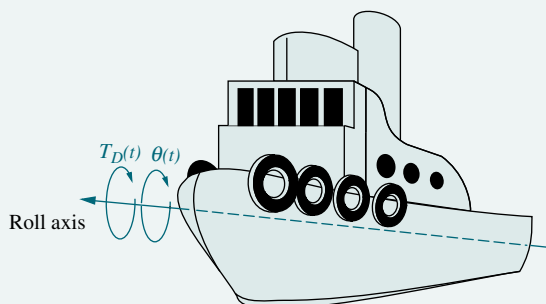
FIGURE 4.36   A ship at sea, showing roll axis

CHALLENGE: You are now given a problem to test your knowledge of this chapter's objectives. This problem uses the same principles that were applied to the Unmanned Free-Swimming Submersible vehicle: Ships at sea undergo motion about their roll axis, as shown in Figure 4.36. Fins called *stabilizers* are used to reduce this rolling motion. The stabilizers can be positioned by a closed-loop roll control system that consists of components, such as fin actuators and sensors, as well as the ship's roll dynamics.

Assume the roll dynamics, which relates the roll-angle output, $\theta(s)$, to a disturbance-torque input, $T_D(s)$, is

$$\frac{\theta(s)}{T_D(s)} = \frac{2.25}{(s^2 + 0.5s + 2.25)} \tag{4.142}$$

Do the following:

a. Find the natural frequency, damping ratio, peak time, settling time, rise time, and percent overshoot.

b. Find the analytical expression for the output response to a unit step input in voltage.

MATLAB
ML

c. Use MATLAB to solve **a** and **b** and to plot the response found in **b**.

Summary

In this chapter, we took the system models developed in Chapters 2 and 3 and found the output response for a given input, usually a step. The step response yields a clear picture of the system's transient response. We performed this analysis for two types of systems, *first order* and *second order*, which are representative of many physical systems. We then formalized our findings and arrived at numerical specifications describing the responses.

For first-order systems having a single pole on the real axis, the specification of transient response that we derived was the *time constant*, which is the reciprocal of the real-axis pole location. This specification gives us an indication of the speed of the transient response. In particular, the time constant is the time for the step response to reach 63% of its final value.

Second-order systems are more complex. Depending on the values of system components, a second-order system can exhibit four kinds of behavior:

1. Overdamped
2. Underdamped
3. Undamped
4. Critically damped

We found that the poles of the input generate the forced response, whereas the system poles generate the transient response. If the system poles are real, the system exhibits *overdamped* behavior. These exponential responses have time constants equal to the reciprocals of the pole locations. Purely imaginary poles yield *undamped* sinusoidal oscillations whose radian frequency is equal to the magnitude of the imaginary pole. Systems with complex poles display *under-damped* responses. The real part of the complex pole dictates the exponential decay envelope, and the imaginary part dictates the sinusoidal radian frequency. The exponential decay envelope has a time constant equal to the reciprocal of the real part of the pole, and the sinusoid has a radian frequency equal to the imaginary part of the pole.

For all second-order cases, we developed specifications called the *damping ratio*, ζ, and *natural frequency*, ω_n. The damping ratio gives us an idea about the nature of the transient response and how much overshoot and oscillation it undergoes, regardless of time scaling. The natural frequency gives an indication of the speed of the response.

We found that the value of ζ determines the form of the second-order natural response:

- If $\zeta = 0$, the response is undamped.
- If $\zeta < 1$, the response is underdamped.
- If $\zeta = 1$, the response is critically damped.
- If $\zeta > 1$, the response is overdamped.

The natural frequency is the frequency of oscillation if all damping is removed. It acts as a scaling factor for the response, as can be seen from Eq. (4.28), in which the independent variable can be considered to be $\omega_n t$.

For the underdamped case we defined several transient response specifications, including these:

- Percent overshoot, $\%OS$
- Peak time, T_p
- Settling time, T_s
- Rise time, T_r

The peak time is inversely proportional to the imaginary part of the complex pole. Thus, horizontal lines on the *s*-plane are lines of constant peak time. Percent overshoot is a function of only the damping ratio. Consequently, radial lines are lines of constant percent overshoot. Finally, settling time is inversely proportional to the real part of the complex pole. Hence, vertical lines on the *s*-plane are lines of constant settling time.

We found that peak time, percent overshoot, and settling time are related to pole location. Thus, we can design transient responses by relating a desired response to a pole location and then relating that pole location to a transfer function and the system's components.

The effects of nonlinearities, such as saturation, dead zone, and backlash were explored using MATLAB's Simulink.

In this chapter, we also evaluated the time response using the state-space approach. The response found in this way was separated into the *zero-input response*, and the *zero-state response*, whereas the frequency response method yielded a total response divided into *natural response* and *forced response* components.

In the next chapter we will use the transient response specifications developed here to analyze and design systems that consist of the interconnection of multiple subsystems. We will see how to reduce these systems to a single transfer function in order to apply the concepts developed in Chapter 4.

Review Questions

1. Name the performance specification for first-order systems.
2. What does the performance specification for a first-order system tell us?
3. In a system with an input and an output, what poles generate the steady-state response?
4. In a system with an input and an output, what poles generate the transient response?
5. The imaginary part of a pole generates what part of a response?
6. The real part of a pole generates what part of a response?
7. What is the difference between the natural frequency and the damped frequency of oscillation?
8. If a pole is moved with a constant imaginary part, what will the responses have in common?
9. If a pole is moved with a constant real part, what will the responses have in common?
10. If a pole is moved along a radial line extending from the origin, what will the responses have in common?

11. List five specifications for a second-order underdamped system.

12. For Question 11 how many specifications completely determine the response?

13. What pole locations characterize (1) the underdamped system, (2) the over-damped system, and (3) the critically damped system?

14. Name two conditions under which the response generated by a pole can be neglected.

15. How can you justify pole-zero cancellation?

16. Does the solution of the state equation yield the output response of the system? Explain.

State Space
SS

17. What is the relationship between $(s\mathbf{I} - \mathbf{A})$, which appeared during the Laplace transformation solution of the state equations, and the state-transition matrix, which appeared during the classical solution of the state equation?

State Space
SS

18. Name a major advantage of using time-domain techniques for the solution of the response.

State Space
SS

19. Name a major advantage of using frequency-domain techniques for the solution of the response.

20. What three pieces of information must be given in order to solve for the output response of a system using state-space techniques?

State Space
SS

21. How can the poles of a system be found from the state equations?

State Space
SS

Problems

1. Derive the output responses for all parts of Figure 4.7. [Section: 4.4]

2. Find the output response, $c(t)$, for each of the systems shown in Figure P4.1. Also find the time constant, rise time, and settling time for each case. [Sections: 4.2, 4.3]

WileyPLUS
WPCS
Control Solutions

$$\frac{5}{s+5}$$

(a)

$$\frac{20}{s+20}$$

(b)
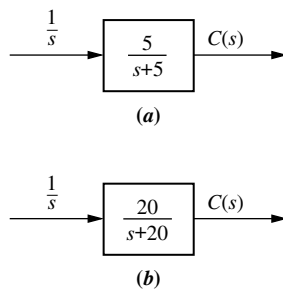
FIGURE P4.1

3. Plot the step responses for Problem 2 using MATLAB.

MATLAB
ML

4. Find the capacitor voltage in the network shown in Figure P4.2 if the switch closes at $t = 0$. Assume zero

initial conditions. Also find the time constant, rise time, and settling time for the capacitor voltage. [Sections: 4.2, 4.3]

1.8 Ω

$t = 0$

5 V

0.79 F
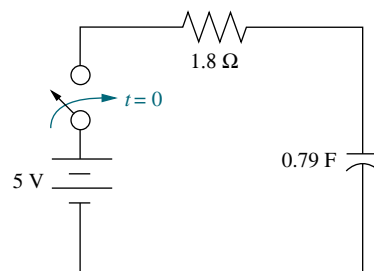
FIGURE P4.2

5. Plot the step response for Problem 4 using MATLAB. From your plots, find the time constant, rise time, and settling time.

MATLAB
ML

6. For the system shown in Figure P4.3, (a) find an equation that relates settling time of the velocity of

the mass to M; (b) find an equation that relates rise time of the velocity of the mass to M. [Sections: 4.2, 4.3]
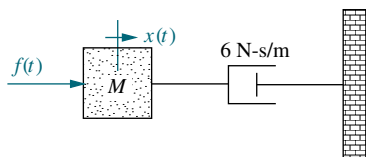
FIGURE P4.3

7. Plot the step response for Problem 6 using MATLAB. From your plots, find the time constant, rise time, and settling time. Use $M = 1$ and $M = 2$. *MATLAB ML*

8. For each of the transfer functions shown below, find the locations of the poles and zeros, plot them on the s-plane, and then write an expression for the general form of the step response without solving for the inverse Laplace transform. State the nature of each response (overdamped, underdamped, and so on). [Sections: 4.3, 4.4]

a. $T(s) = \dfrac{2}{s+2}$

b. $T(s) = \dfrac{5}{(s+3)(s+6)}$

c. $T(s) = \dfrac{10(s+7)}{(s+10)(s+20)}$

d. $T(s) = \dfrac{20}{s^2 + 6s + 144}$

e. $T(s) = \dfrac{s+2}{s^2 + 9}$

f. $T(s) = \dfrac{(s+5)}{(s+10)^2}$

9. Use MATLAB to find the poles of [Section: 4.2]

$$T(s) = \dfrac{s^2 + 2s + 2}{s^4 + 6s^3 + 4s^2 + 7s + 2}$$
MATLAB ML

10. Find the transfer function and poles of the system represented in state space here: [Section: 4.10]

$$\dot{\mathbf{x}} = \begin{bmatrix} 8 & -4 & 1 \\ -3 & 2 & 0 \\ 5 & 7 & -9 \end{bmatrix} \mathbf{x} + \begin{bmatrix} -4 \\ -3 \\ 4 \end{bmatrix} u(t)$$

$$y = \begin{bmatrix} 2 & 8 & -3 \end{bmatrix} \mathbf{x}; \; \mathbf{x}(0) = \begin{bmatrix} 0 \\ 0 \\ 0 \end{bmatrix}$$

11. Repeat Problem 10 using MATLAB. [Section: 4.10]. *MATLAB ML*

WileyPLUS WPCS Control Solutions

12. Write the general form of the capacitor voltage for the electrical network shown in Figure P4.4. [Section: 4.4].
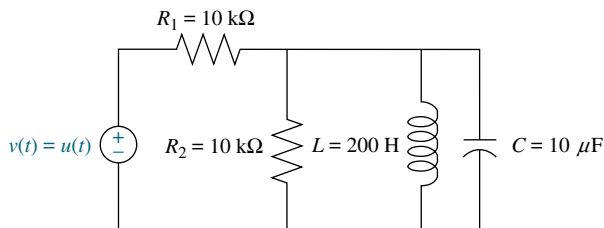
FIGURE P4.4

13. Use MATLAB to plot the capacitor voltage in Problem 12. [Section: 4.4]. *MATLAB ML*

14. Solve for $x(t)$ in the system shown in Figure P4.5 if $f(t)$ is a unit step. [Section: 4.4].
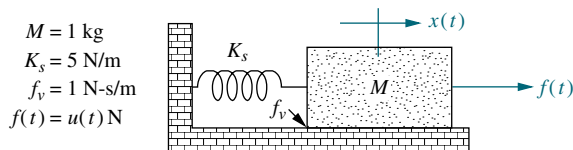
FIGURE P4.5

15. The system shown in Figure P4.6 has a unit step input. Find the output response as a function of time. Assume the system is underdamped. Notice that the result will be Eq. (4.28). [Section: 4.6].
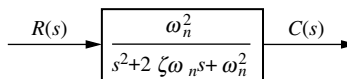
FIGURE P4.6

16. Derive the relationship for damping ratio as a function of percent overshoot, Eq. (4.39). [Section: 4.6].

17. Calculate the exact response of each system of Problem 8 using Laplace transform techniques, and compare the results to those obtained in that problem. [Sections: 4.3, 4.4].

18. Find the damping ratio and natural frequency for each second-order system of Problem 8 and show that the value of the damping ratio conforms to the type of response (underdamped, overdamped, and so on) predicted in that problem. [Section: 4.5].

19. A system has a damping ratio of 0.5, a natural frequency of 100 rad/s, and a dc gain of 1. Find the response of the system to a unit step input. [Section: 4.6].

WileyPLUS WPCS Control Solutions

20. For each of the second-order systems that follow, find ζ, ω_n, T_s, T_p, T_r, and $\%OS$. [Section: 4.6].

   a. $T(s) = \dfrac{16}{s^2 + 3s + 16}$

   b. $T(s) = \dfrac{0.04}{s^2 + 0.02s + 0.04}$

   c. $T(s) = \dfrac{1.05 \times 10^7}{s^2 + 1.6 \times 10^3 s + 1.05 \times 10^7}$

21. Repeat Problem 20 using MATLAB. Have the computer program esti-mate the given specifications and plot the step responses. Estimate the rise time from the plots. [Section: 4.6].

MATLAB
ML

22. Use MATLAB's LTI Viewer and ob-tain settling time, peak time, rise time, and percent overshoot for each of the systems in Problem 20. [Section: 4.6].

Gui Tool
GUIT

23. For each pair of second-order system specifications that follow, find the location of the second-order pair of poles. [Section: 4.6].

   a. $\%OS = 12\%$; $T_s = 0.6$ second

   b. $\%OS = 10\%$; $T_p = 5$ seconds

   c. $T_s = 7$ seconds; $T_p = 3$ seconds

24. Find the transfer function of a second-order system that yields a 12.3% overshoot and a settling time of 1 second. [Section: 4.6]

WileyPLUS
WPCS
Control Solutions

25. For the system shown in Figure P4.7, do the follow-ing: [Section: 4.6]

   a. Find the transfer function $G(s) = X(s)/F(s)$.

   b. Find ζ, ω_n, $\%OS$, T_s, T_p, and T_r.
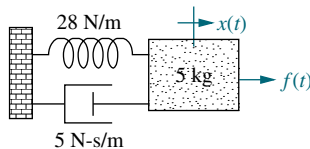
FIGURE P4.7

26. For the system shown in Figure P4.8, a step torque is applied at $\theta_1(t)$. Find

   a. The transfer function, $G(s) = \theta_2(s)/T(s)$.

   b. The percent overshoot, settling time, and peak time for $\theta_2(t)$. [Section: 4.6]
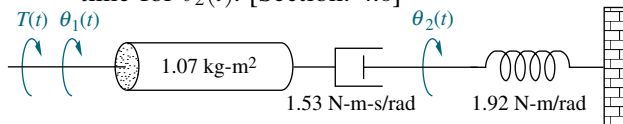
FIGURE P4.8

27. Derive the unit step response for each transfer function in Example 4.8. [Section: 4.7].

28. Find the percent overshoot, settling time, rise time, and peak time for

$$T(s) = \frac{14.145}{(s^2 + 0.842s + 2.829)(s + 5)} \text{ [Section: 4.7]}$$

29. For each of the unit step responses shown in Figure P4.9, find the transfer function of the system. [Sections: 4.3, 4.6].

WileyPLUS
WPCS
Control Solutions
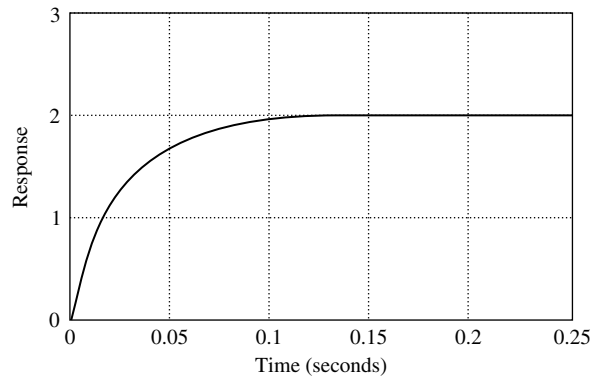
(a)
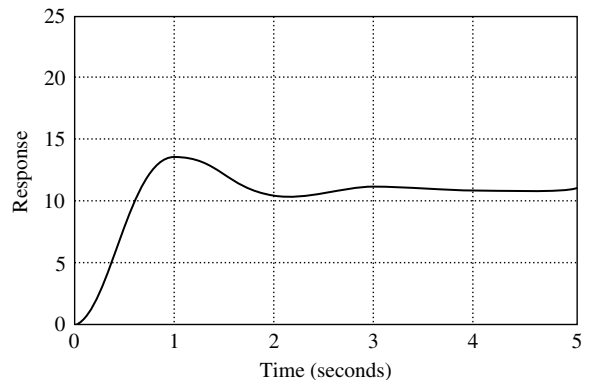
(b)
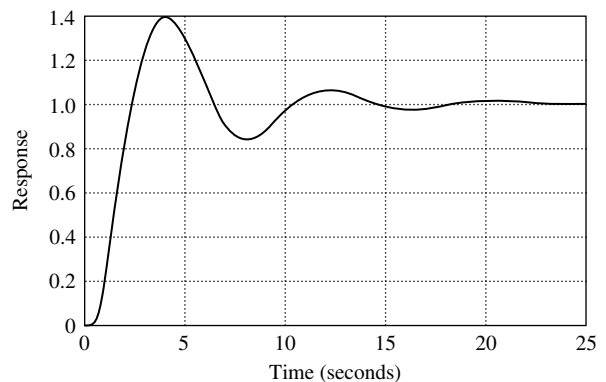
(c)

FIGURE P4.9

30. For the following response functions, determine if pole-zero cancellation can be approximated. If it can, find percent overshoot, settling time, rise time, and peak time. [Section: 4.8].

a. $C(s) = \dfrac{(s+3)}{s(s+2)(s^2+3s+10)}$

b. $C(s) = \dfrac{(s+2.5)}{s(s+2)(s^2+4s+20)}$

c. $C(s) = \dfrac{(s+2.1)}{s(s+2)(s^2+s+5)}$

d. $C(s) = \dfrac{(s+2.01)}{s(s+2)(s^2+5s+20)}$

31. Using MATLAB, plot the time response of Problem 30**a** and from the plot determine percent overshoot, settling time, rise time, and peak time. [Section: 4.8]

$\quad$ MATLAB
$\quad$ **ML**

32. Find peak time, settling time, and percent overshoot for only those responses below that can be approximated as second-order responses. [Section: 4.8].

a. $c(t) = 0.003500 - 0.001524e^{-4t}$
$\qquad -0.001976e^{-3t}\cos(22.16t)$
$\qquad -0.0005427e^{-3t}\sin(22.16t)$

b. $c(t) = 0.05100 - 0.007353e^{-8t}$
$\qquad -0.007647e^{-6t}\cos(8t)$
$\qquad -0.01309e^{-6t}\sin(8t)$

c. $c(t) = 0.009804 - 0.0001857e^{-5.1t}$
$\qquad -0.009990e^{-2t}\cos(9.796t)$
$\qquad -0.001942e^{-2t}\sin(9.796t)$

d. $c(t) = 0.007000 - 0.001667e^{-10t}$
$\qquad -0.008667e^{-2t}\cos(9.951t)$
$\qquad -0.0008040e^{-2t}\sin(9.951t)$

33. For each of the following transfer functions with zeros, find the component parts of the unit step response: (1) the derivative of the response without a zero and (2) the response without a zero, scaled to the negative of the zero value. Also, find and plot the total response. Describe any nonminimum-phase behavior. [Section: 4.8].

a. $G(s) = \dfrac{s+2}{s^2+3s+36}$

b. $G(s) = \dfrac{s-2}{s^2+3s+36}$

34. Use MATLAB's Simulink to obtain the step response of a system,

$\quad$ Simulink
$\quad$ **SL**

$$G(s) = \frac{1}{s^2+3s+10}$$

under the following conditions: [Section: 4.9]

a. The system is linear and driven by an amplifier whose gain is 10.

b. An amplifier whose gain is 10 drives the system. The amplifier saturates at ± 0.25 volts. Describe the effect of the saturation on the system's output.

c. An amplifier whose gain is 10 drives the system. The amplifier saturates at ± 0.25 volts. The system drives a 1:1 gear train that has backlash. The deadband width of the backlash is 0.02 rad. Describe the effect of saturation and backlash on the system's output.

35. A system is represented by the state and output equations that follow. Without solving the state equation, find the poles of the system. [Section: 4.10]

$\quad$ State Space
$\quad$ **SS**

$$\dot{\mathbf{x}} = \begin{bmatrix} -2 & -1 \\ -3 & -5 \end{bmatrix}\mathbf{x} + \begin{bmatrix} 1 \\ 2 \end{bmatrix}u(t)$$

$$y = \begin{bmatrix} 3 & 2 \end{bmatrix}\mathbf{x}$$

36. A system is represented by the state and output equations that follow. Without solving the state equation, find [Section: 4.10]

$\quad$ WileyPLUS
$\quad$ **WPCS**
$\quad$ Control Solutions

$\quad$ State Space
$\quad$ **SS**

a. the characteristic equation;

b. the poles of the system

$$\dot{\mathbf{x}} = \begin{bmatrix} 0 & 2 & 3 \\ 0 & 6 & 5 \\ 1 & 4 & 2 \end{bmatrix}\mathbf{x} + \begin{bmatrix} 0 \\ 1 \\ 1 \end{bmatrix}u(t)$$

$$y = \begin{bmatrix} 1 & 2 & 0 \end{bmatrix}\mathbf{x}$$

37. Given the following state-space representation of a system, find $Y(s)$: [Section: 4.10]

$\quad$ State Space
$\quad$ **SS**

$$\dot{\mathbf{x}} = \begin{bmatrix} 1 & 2 \\ -3 & -1 \end{bmatrix}\mathbf{x} + \begin{bmatrix} 1 \\ 1 \end{bmatrix}\sin 3t$$

$$y = \begin{bmatrix} 1 & 2 \end{bmatrix}\mathbf{x}; \ \mathbf{x}(0) = \begin{bmatrix} 3 \\ 1 \end{bmatrix}$$

38. Given the following system represented in state space, solve for $Y(s)$ using the

$\quad$ State Space
$\quad$ **SS**

Laplace transform method for solution of the state equation: [Section: 4.10]

$$\dot{\mathbf{x}} = \begin{bmatrix} 0 & 1 & 0 \\ -2 & -4 & 1 \\ 0 & 0 & -6 \end{bmatrix} \mathbf{x} + \begin{bmatrix} 0 \\ 0 \\ 1 \end{bmatrix} e^{-t}$$

$$y = \begin{bmatrix} 0 & 0 & 1 \end{bmatrix} \mathbf{x}; \ \mathbf{x}(0) = \begin{bmatrix} 0 \\ 0 \\ 0 \end{bmatrix}$$

39. Solve the following state equation and output equation for $y(t)$, where $u(t)$ is the unit step. Use the Laplace transform method. [Section: 4.10]   State Space **SS**

$$\dot{\mathbf{x}} = \begin{bmatrix} -2 & 0 \\ -1 & -1 \end{bmatrix} \mathbf{x} + \begin{bmatrix} 1 \\ 1 \end{bmatrix} u(t)$$

$$y = \begin{bmatrix} 0 & 1 \end{bmatrix} \mathbf{x}; \ \mathbf{x}(0) = \begin{bmatrix} 3 \\ 0 \end{bmatrix}$$

40. Solve for $y(t)$ for the following system represented in state space, where $u(t)$ is the unit step. Use the Laplace transform approach to solve the state equation. [Section: 4.10]   State Space **SS**

$$\dot{\mathbf{x}} = \begin{bmatrix} -3 & 1 & 0 \\ 0 & -6 & 1 \\ 0 & 0 & -5 \end{bmatrix} \mathbf{x} + \begin{bmatrix} 0 \\ 1 \\ 1 \end{bmatrix} u(t)$$

$$y = \begin{bmatrix} 0 & 1 & 1 \end{bmatrix} \mathbf{x}; \ \mathbf{x}(0) = \begin{bmatrix} 0 \\ 0 \\ 0 \end{bmatrix}$$

41. Use MATLAB to plot the step response of Problem 40. [Section: 4.10]   MATLAB **ML**

42. Repeat Problem 40 using MATLAB's Symbolic Math Toolbox and Eq. (4.96). In addition, run your program with an initial condition,   Symbolic Math **SM**

$$\mathbf{x}(0) = \begin{bmatrix} 1 \\ 1 \\ 0 \end{bmatrix}. \ [\text{Section : } 4.10]$$

43. Using classical (not Laplace) methods only, solve for the state-transition matrix, the state vector, and the output of the   WileyPLUS **WPCS** Control Solutions

system represented here: [Section: 4.11]   State Space **SS**

$$\dot{\mathbf{x}} = \begin{bmatrix} 0 & 1 \\ -1 & -5 \end{bmatrix} \mathbf{x}; \ y = \begin{bmatrix} 1 & 2 \end{bmatrix} \mathbf{x};$$

$$\mathbf{x}(0) = \begin{bmatrix} 1 \\ 0 \end{bmatrix}$$

44. Using classical (not Laplace) methods only, solve for the state-transition matrix, the state vector, and the output of the system represented here, where $u(t)$ is the unit step: [Section: 4.11].   State Space **SS**

$$\dot{\mathbf{x}} = \begin{bmatrix} 0 & 1 \\ -1 & 0 \end{bmatrix} \mathbf{x} + \begin{bmatrix} 0 \\ 1 \end{bmatrix} u(t)$$

$$y = \begin{bmatrix} 3 & 4 \end{bmatrix} \mathbf{x}; \ \mathbf{x}(0) = \begin{bmatrix} 0 \\ 0 \end{bmatrix}$$

45. Solve for $y(t)$ for the following system represented in state space, where $u(t)$ is the unit step. Use the classical approach to solve the state equation. [Section: 4.11]   State Space **SS**

$$\dot{\mathbf{x}} = \begin{bmatrix} -2 & 1 & 0 \\ 0 & 0 & 1 \\ 0 & -6 & -1 \end{bmatrix} \mathbf{x} + \begin{bmatrix} 1 \\ 0 \\ 0 \end{bmatrix} u(t)$$

$$y = \begin{bmatrix} 1 & 0 & 0 \end{bmatrix} \mathbf{x}; \ \mathbf{x}(0) = \begin{bmatrix} 0 \\ 0 \\ 0 \end{bmatrix}$$

46. Repeat Problem 45 using MATLAB's Symbolic Math Toolbox and Eq. (4.109). In addition, run your program with an initial condition,   Symbolic Math **SM**

$$\mathbf{x}(0) = \begin{bmatrix} 1 \\ 1 \\ 0 \end{bmatrix}. \ [\text{Section : } 4.11]$$

47. Using methods described in Appendix H.1 located at www.wiley.com/college/ nise simulate the following system and plot the step response. Verify the expected values of percent overshoot, peak time, and settling time.   State Space **SS**

$$T(s) = \frac{1}{s^2 + 0.8s + 1}$$

48. Using methods described in Appendix H.1 located at www.wiley.com/college/nise, simulate the following system and plot the output, $y(t)$, for a step input:

$$\dot{\mathbf{x}} = \begin{bmatrix} 0 & 1 & 0 \\ -10 & -7 & 1 \\ 0 & 0 & -2 \end{bmatrix} \mathbf{x} + \begin{bmatrix} 0 \\ 0 \\ 1 \end{bmatrix} u(t)$$

$$y(t) = \begin{bmatrix} 1 & 1 & 0 \end{bmatrix} \mathbf{x}; \quad \mathbf{x}(0) = \begin{bmatrix} -1 \\ 0 \\ 0 \end{bmatrix}$$

49. A human responds to a visual cue with a physical response, as shown in Figure P4.10. The transfer function that relates the output physical response, $P(s)$, to the input visual command, $V(s)$, is

$$G(s) = \frac{P(s)}{V(s)} = \frac{(s + 0.5)}{(s + 2)(s + 5)}$$

(*Stefani*, 1973). Do the following:

a. Evaluate the output response for a unit step input using the Laplace transform.

b. Represent the transfer function in state space.

c. Use MATLAB to simulate the system and obtain a plot of the step response.

50. Industrial robots are used for myriad applications. Figure P4.11 shows a robot used to move 55-pound bags of salt pellets; a vacuum head lifts the bags before positioning. The robot can move as many as 12 bags per minute (*Schneider*, 1992). Assume a

FIGURE P4.11   Vacuum robot lifts two bags of salt.

model for the open-loop swivel controller and plant of

$$G_e(s) = \frac{\omega_o(s)}{V_i(s)} = \frac{K}{(s + 10)(s^2 + 4s + 10)}$$

where $\omega_o(s)$ is the Laplace transform of the robot's output swivel velocity and $V_i(s)$ is the voltage applied to the controller.

a. Evaluate percent overshoot, settling time, peak time, and rise time of the response of the open-loop swivel velocity to a step-voltage input. Justify all second-order assumptions.

b. Represent the open-loop system in state space.

Step 1: Light source on   Step 2: Recognize light source   Step 3: Respond to light source
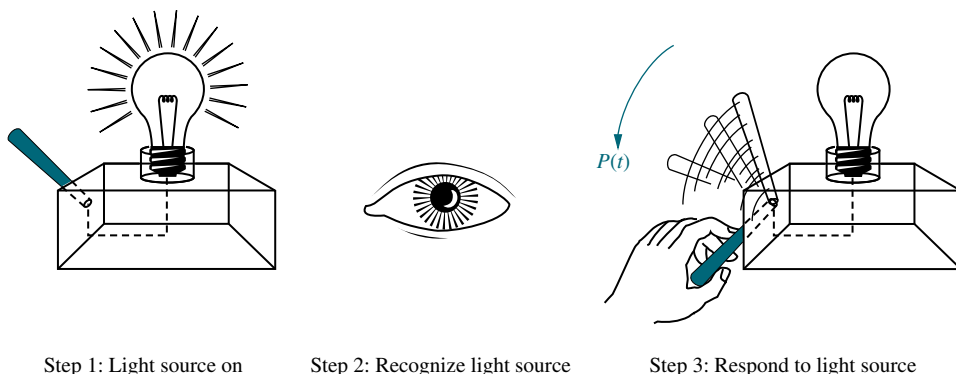
FIGURE P4.10   Steps in determining the transfer function relating output physical response to the input visual command

c. `Use MATLAB or any other com-` `MATLAB` `ML`
`puter program to simulate the`
`system and compare your results to` `a.`

51. Anesthesia induces muscle relaxation (paralysis) and unconsciousness in the patient. Muscle relaxation can be monitored using electromyogram signals from nerves in the hand; unconsciousness can be monitored using the cardiovascular system's mean arterial pressure. The anesthetic drug is a mixture of isoflurane and atracurium. An approximate model relating muscle relaxation to the percent isoflurane in the mixture is

$$\frac{P(s)}{U(s)} = \frac{7.63 \times 10^{-2}}{s^2 + 1.15s + 0.28}$$

where $P(s)$ is muscle relaxation measured as a fraction of total paralysis (normalized to unity) and $U(s)$ is the percent mixture of isoflurane (*Linkens*, *1992*). [Section: 4.6]

a. Find the damping ratio and the natural frequency of the paralysis transient response.

b. Find the maximum possible percent paralysis if a 2% mixture of isoflurane is used.

c. Plot the step response of paralysis if a 1% mixture of isoflurane is used.

d. What percent isoflurane would have to be used for 100% paralysis?

52. To treat acute asthma, the drug theophylline is infused intravenously. The rate of change of the drug concentration in the blood is equal to the difference between the infused concentration and the eliminated concentration. The infused concentration is $i(t)/V_d$, where $i(t)$ is the rate of flow of the drug by weight and V_d is the apparent volume and depends on the patient. The eliminated concentration is given by $k_{10}c(t)$, where $c(t)$ is the current concentration of the drug in the blood and k_{10} is the elimination rate constant. The theophylline concentration in the blood is critical—if it is too low, the drug is ineffective; if too high, the drug is toxic (*Jannett*, *1992*). You will help the doctor with your calculations.

a. Derive an equation relating the desired blood concentration, C_D, to the required infusion rate by weight of the drug, I_R.

b. Derive an equation that will tell how long the drug must be administered to reach the desired

blood concentration. Use both rise time and settling time.

c. Find the infusion rate of theophylline if $V_D = 600$ ml, $k_{10} = 0.07 \, \text{h}^{-1}$, and the required blood level of the drug is 12 mcg/ml ("mcg" means micrograms). See (*Jannett*, *1992*); for a description of parameter values.

d. Find the rise and settling times for the constants in **c**.

53. Upper motor neuron disorder patients can benefit and regain useful function through the use of functional neuroprostheses. The design requires a good understanding of muscle dynamics. In an experiment to determine muscle responses, the identified transfer function was (*Zhou*, *1995*)

$$M(s) = \frac{2.5e^{-0.008s}(1 + 0.172s)(1 + 0.008s)}{(1 + 0.07s)^2(1 + 0.05s)^2}$$

Find the unit step response of this transfer function.

54. When electrodes are attached to the mastoid bones (right behind the ears) and current pulses are applied, a person will sway forward and backward. It has been found that the transfer function from the current to the subject's angle (in degrees) with respect to the vertical is given by (*Nashner*, *1974*)

$$\frac{\theta(s)}{I(s)} = \frac{5.8(0.3s + 1)e^{-0.1s}}{(s + 1)(s^2/1.2^2 + 0.6s/1.2 + 1)}$$

a. Determine whether a dominant pole approximation can be applied to this transfer function.

b. Find the body sway caused by a 250 μA pulse of 150 msec duration.

55. A MOEMS (optical MEMS) is a MEMS (Micro Electromechanical Systems) with an optical fiber channel that takes light generated from a laser diode. It also has a photodetector that measures light intensity variations and outputs voltage variations proportional to small mechanical device deflections. Additionally, a voltage input is capable of deflecting the device. The apparatus can be used as an optical switch or as a variable optical attenuator, and it does not exceed 2000 μm in any dimension. Figure P4.12 shows input-output signal pairs used to identify the parameters of the system. Assume a second-order transfer function and find the system's transfer function (*Borovic*, *2005*).

Open-Loop Responses
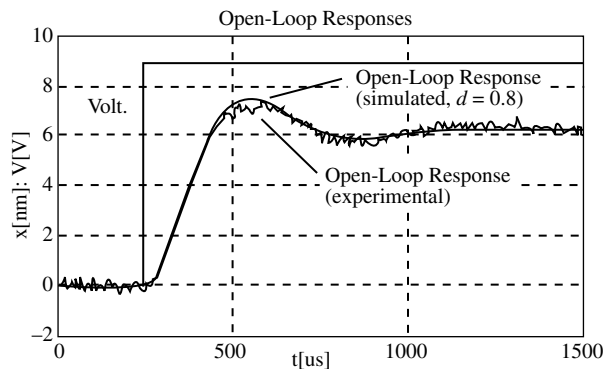
FIGURE P4.12

56. The response of the deflection of a fluid-filled cathe-
ter to changes in pressure can be modeled using a
second-order model. Knowledge of the parameters
of the model is important because in cardiovascular
applications the undamped natural frequency should
be close to five times the heart rate. However, due to
sterility and other considerations, measurement of
the parameters is difficult. A method to obtain trans-
fer functions using measurements of the amplitudes
of two consecutive peaks of the response and their
timing has been developed (*Glantz*, *1979*). Assume
that Figure P4.13 is obtained from catheter measure-
ments. Using the information shown and assuming a
second-order model excited by a unit step input, find
the corresponding transfer function.
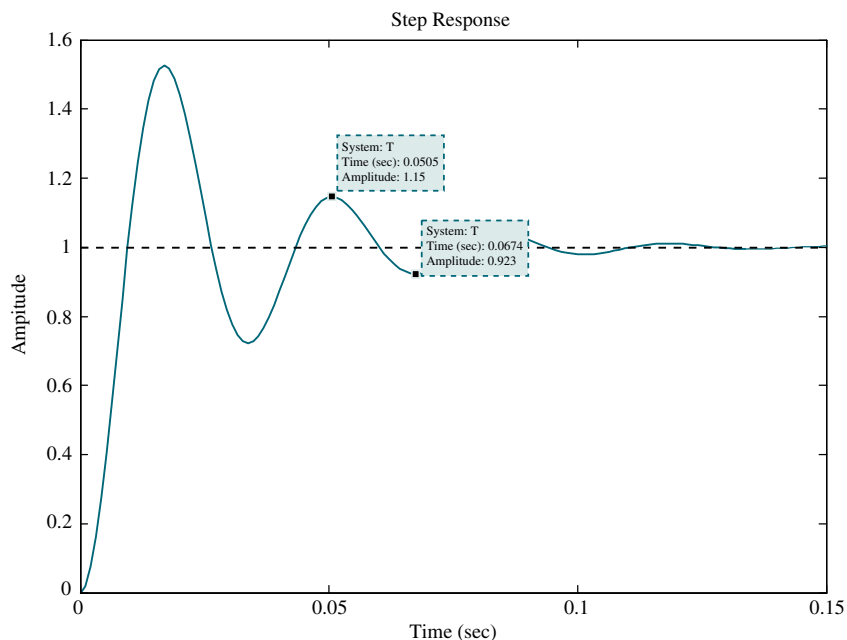
57. Several factors affect the workings of the kidneys.
For example, Figure P4.14 shows how a step change
in arterial flow pressure affects renal blood flow in
rats. In the "hot tail" part of the experiment, pe-
ripheral thermal receptor stimulation is achieved by
inserting the rat's tail in heated water. Variations
between different test subjects are indicated by the
vertical lines. It has been argued that the "control"
and "hot tail" responses are identical except for
their steady-state values (*DiBona*, *2005*).

FIGURE P4.14

Step Response
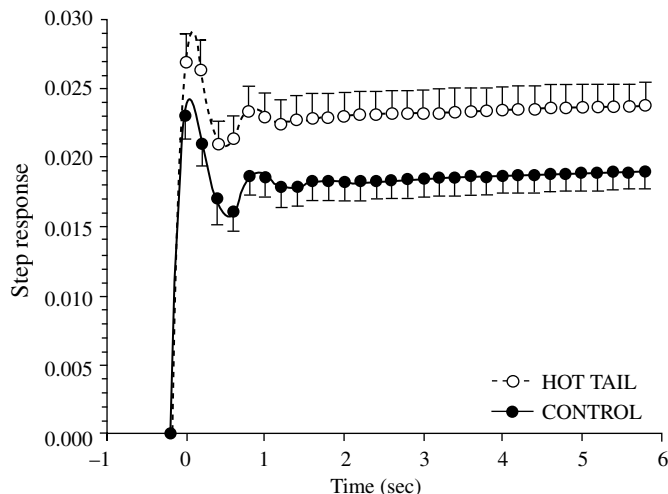
FIGURE P4.13

a. Using Figure P4.14, obtain the normalized ($c_{\text{final}} = 1$) transfer functions for both responses.

b. Use MATLAB to prove or disprove the assertion about the ''control'' and ''hot tail'' responses.

MATLAB
ML

58. The transfer function of a nano-positioning device capable of translating biological samples within a few μm uses a piezoelectric actuator and a linear variable differential transformer (LDVT) as a displacement sensor. The transfer function from input to displacement has been found to be (*Salapaka*, *2002*)

$$G(s) = \frac{9.7 \times 10^4(s^2 - 14400s + 106.6 \times 10^6)}{(s^2 + 3800s + 23.86 \times 10^6)(s^2 + 240s + 2324.8 \times 10^3)}$$

Use a dominant-pole argument to find an equivalent transfer function with the same numerator but only three poles. Use MATLAB to find the actual size and approximate system unit step responses, plotting them on the same graph. Explain the differences between both responses given that both pairs of poles are so far apart.

MATLAB
ML

59. At some point in their lives most people will suffer from at least one onset of low back pain. This disorder can trigger excruciating pain and temporary disability, but its causes are hard to diagnose. It is well known that low back pain alters motor trunk patterns; thus it is of interest to study the causes for these alterations and their extent. Due to the different possible causes of this type of pain, a ''control'' group of people is hard to obtain for laboratory studies. However, pain can be stimulated in healthy people and muscle movement ranges can be compared. Controlled back pain can be induced by injecting saline solution directly into related muscles or ligaments. The transfer function from infusion rate to pain response was obtained experimentally by injecting a 5% saline solution at six different infusion rates over a period of 12 minutes. Subjects verbally rated their pain every 15 seconds on a scale from 0 to 10, with 0 indicating no pain and 10 unbearable pain. Several trials were averaged and the data was fitted to the following transfer function:

$$G(s) = \frac{9.72 \times 10^{-8}(s + 0.0001)}{(s + 0.009)^2(s^2 + 0.018s + 0.0001)}$$

Infusion Pump   Human Response

Constant infusion rate → $M(s)$ → $G(s)$ → Constant back pain
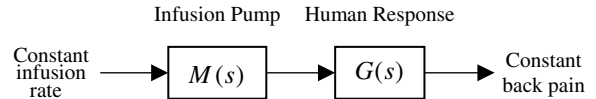
FIGURE P4.15

For experimentation it is desired to build an automatic dispensing system to make the pain level constant as shown in Figure P4.15. It follows that ideally the injection system transfer function has to be

$$M(s) = \frac{1}{G(s)}$$

to obtain an overall transfer function $M(s)G(s) \approx 1$. However, for implementation purposes $M(s)$ must have at least one more pole than zeros (*Zedka*, *1999*). Find a suitable transfer function, $M(s)$ by inverting $G(s)$ and adding poles that are far from the imaginary axis.

**60.** An artificial heart works in closed loop by varying its pumping rate according to changes in signals from the recipient's nervous system. For feedback compensation design it is important to know the heart's open-loop transfer function. To identify this transfer function, an artificial heart is implanted in a calf while the main parts of the original heart are left in place. Then the atrial pumping rate in the original heart is measured while step input changes are effected on the artificial heart. It has been found that, in general, the obtained response closely resembles that of a second-order system. In one such experiment it was found that the step response has a %OS = 30% and a time of first peak $T_p = 127$ sec (*Nakamura*, *2002*). Find the corresponding transfer function.

61. An observed transfer function from voltage potential to force in skeletal muscles is given by (*Ionescu*, *2005*)

$$T(s) = \frac{450}{(s + 5)(s + 20)}$$

a. Obtain the system's impulse response.

b. Integrate the impulse response to find the step response.

c. Verify the result in Part **b** by obtaining the step response using Laplace transform techniques.

62. In typical conventional aircraft, longitudinal flight model linearization results in transfer functions with

two pairs of complex conjugate poles. Consequently, the natural response for these airplanes has two modes in their natural response. The "short period" mode is relatively well-damped and has a high-frequency oscillation. The "plugoid mode" is lightly damped and its oscillation frequency is relatively low. For example, in a specific aircraft the transfer function from wing elevator deflection to nose angle (angle of attack) is (*McRuer, 1973*)

$$\frac{\theta(s)}{\delta_e(s)} =$$

$$-\frac{26.12(s + 0.0098)(s + 1.371)}{(s^2 + 8.99 \times 10^{-3}s + 3.97 \times 10^{-3})(s^2 + 4.21s + 18.23)}$$

a. Find which of the poles correspond to the short period mode and which to the phugoid mode.

b. Peform a "phugoid approximation" (dominant-pole approximation), retaining the two poles and the zero closest to the; ω-axis.

c. Use MATLAB to compare the step responses of the original transfer function and the approximation.

MATLAB
ML

63. A crosslapper is a machine that takes as an input a light fiber fabric and produces a heavier fabric by laying the original fabric in layers rotated by 90 degrees. A feedback system is required in order to maintain consistent product width and thickness by controlling its carriage velocity. The transfer function from servomotor torque, $T_m(s)$, to carriage velocity, $Y(s)$, was developed for such a machine (*Kuo, 2008*). Assume that the transfer function is:

MATLAB
ML

$$G(s) = \frac{Y(s)}{T_m(s)} =$$

$$\frac{33s^4 + 202s^3 + 10061s^2 + 24332s + 170704}{s^7 + 8s^6 + 464s^5 + 2411s^4 + 52899s^3 + 167829s^2 + 913599s + 1076555}$$

a. Use MATLAB to find the partial fraction residues and poles of $G(s)$.

b. Find an approximation to $G(s)$ by neglecting the second-order terms found in **a**.

c. Use MATLAB to plot on one graph the step response of the transfer function

given above and the approximation found in **b**. Explain the differences between the two plots.

64. Although the use of fractional calculus in control systems is not new, in the last decade there is increased interest in its use for several reasons. The most relevant are that fractional calculus differential equations may model certain systems with higher accuracy than integer differential equations, and that fractional calculus compensators might exhibit advantageous properties for control system design. An example of a transfer function obtained through fractional calculus is:

MATLAB
ML

$$G(s) = \frac{1}{s^{2.5} + 4s^{1.7} + 3s^{0.5} + 5}$$

This function can be approximated with an integer rational transfer function (integer powers of s) using Oustaloup's method (*Xue, 2005*). We ask you now to do a little research and consult the aforementioned reference to find and run an M-file that will calculate the integer rational transfer function approximation to $G(s)$ and plot its step response.

65. Mathematical modeling and control of pH processes are quite challenging since the processes are highly nonlinear, due to the logarithmic relationship between the concentration of hydrogen ions [H+] and pH level. The transfer function from input pH to output pH is $G_a(s) = \frac{Y_a(s)}{X_a(s)} = \frac{14.49e^{-4s}}{1478.26s + 1}$. $G_a(s)$ is a model for the anaerobic process in a wastewater treatment system in which methane bacteria need the pH to be maintained in its optimal range from 6.8 to 7.2 (*Jiayu, 2009*). Similarly, (*Elarafi, 2008*) used empirical techniques to model a pH neutralization plant as a second-order system with a pure delay, yielding the following transfer function relating output pH to input pH:

$$G_p(s) = \frac{Y_p(s)}{X_p(s)} = \frac{1.716 \times 10^{-5}e^{-30s}}{s^2 + 6.989 \times 10^{-3}s + 1.185 \times 10^{-6}}$$

a. Find analytical expressions for the unit-step responses $y_a(t)$ and $y_p(t)$ for the two

processes, $G_a(s)$ and $G_p(s)$.
(Hint: Use the time shift theorem in Table 2.2).

b. Use Simulink to plot $y_a(t)$ and $y_p(t)$ on a single graph.

Simulink
SL

66. Using wind tunnel tests, insect flight dynamics can be studied in a very similar fashion to that of man-made aircraft. Linearized longitudinal flight equations for a bumblebee have been found in the unforced case to be

$$
\begin{bmatrix} \dot{u} \\ \dot{w} \\ \dot{q} \\ \dot{\theta} \end{bmatrix} = \begin{bmatrix} -8.792 \times 10^{-3} & 0.56 \times 10^{-3} & -1.0 \times 10^{-3} & -13.79 \times 10^{-3} \\ -0.347 \times 10^{-3} & -11.7 \times 10^{-3} & -0.347 \times 10^{-3} & 0 \\ 0.261 & -20.8 \times 10^{-3} & -96.6 \times 10^{-3} & 0 \\ 0 & 0 & 1 & 0 \end{bmatrix} \begin{bmatrix} u \\ w \\ q \\ \theta \end{bmatrix}
$$

where $u =$ forward velocity; $w =$ vertical velocity, $q =$ angular pitch rate at center of mass, and $\theta =$ pitch angle between the flight direction and the horizontal (*Sun*, 2005).

a. Use MATLAB to obtain the system's eigenvalues.

MATLAB
ML

b. Write the general form of the state-transition matrix. How many constants would have to be found?

67. A dc-dc converter is a device that takes as an input an unregulated dc voltage and provides a regulated dc voltage as its output. The output voltage may be lower (buck converter), higher (boost converter), or the same as the input voltage. Switching dc-dc converters have a semiconductor active switch (BJT or FET) that is closed periodically with a duty cycle d in a pulse width modulated (PWM) manner. For a boost converter, averaging techniques can be used to arrive at the following state equations (*Van Dijk*, 1995):

State Space
SS

$$
L\frac{di_L}{dt} = -(1-d)u_c + E_s
$$

$$
C\frac{du_C}{dt} = (1-d)i_L - \frac{u_C}{R}
$$

where L and C are respectively the values of internal inductance and capacitance; i_L is the current through the internal inductor; R is the resistive load connected to the converter; E_s is the dc input voltage; and the capacitor voltage, u_C, is the converter's output.

a. Write the converter's equations in the form

$$
\dot{x} = \mathbf{Ax} + \mathbf{Bu}
$$
$$
\mathbf{y} = \mathbf{Cx}
$$

assuming d is a constant.

b. Using the $\mathbf{A}$, $\mathbf{B}$, and $\mathbf{C}$ matrices of Part **a**, obtain the converter's transfer function $\dfrac{U_C(s)}{E_s(s)}$.

68. An IPMC (ionic polymer-metal composite) is a Nafion sheet plated with gold on both sides. An IPMC bends when an electric field is applied across its thickness. IPMCs have been used as robotic actuators in several applications and as active catheters in biomedical applications. With the aim of improving actuator settling times, a state-space model has been developed for a 20 mm $\times$ 10 mm $\times$ 0.2 mm polymer sample (*Mallavarapu*, 2001):

State Space
SS

$$
\begin{bmatrix} \dot{x}_1 \\ \dot{x}_2 \end{bmatrix} = \begin{bmatrix} -8.34 & -2.26 \\ 1 & 0 \end{bmatrix} \begin{bmatrix} x_1 \\ x_2 \end{bmatrix} + \begin{bmatrix} 1 \\ 0 \end{bmatrix} u
$$

$$
y = \begin{bmatrix} 12.54 & 2.26 \end{bmatrix} \begin{bmatrix} x_1 \\ x_2 \end{bmatrix}
$$

where u is the applied input voltage and y is the deflection at one of the material's tips when the sample is tested in a cantilever arrangement.

a. Find the state-transition matrix for the system.

b. From Eq. (4.109) in the text, it follows that if a system has zero initial conditions the system output for any input can be directly calculated from the state-space representation and the state-transition matrix using

$$
y(t) = \mathbf{Cx}(t) = \int \mathbf{C}\Phi(t-\tau)\,\mathbf{B}u(\tau)d\tau
$$

Use this equation to find the zero initial condition unit step response of the IPMC material sample.

c. Use MATLAB to verify that your step response calculation in Part **b** is correct.

MATLAB
ML

DESIGN PROBLEMS

69. Find an equation that relates 2% settling time to the value of f_v for the translational mechanical system shown in Figure P4.16. Neglect the mass of all components. [Section: 4.6]

WileyPLUS
WPCS
Control Solutions
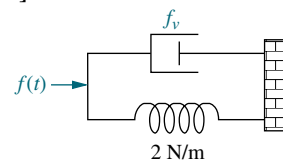
FIGURE P4.16

70. Consider the translational mechanical system shown in Figure P4.17. A 1-pound force, $f(t)$, is applied at $t = 0$. If $f_v = 1$, find K and M such that the response is characterized by a 4-second settling time and a 1-second peak time. Also, what is the resulting percent overshoot? [Section: 4.6]
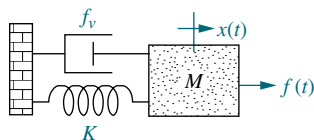
FIGURE P4.17

71. Given the translational mechanical system of Figure P4.17, where $K = 1$ and $f(t)$ is a unit step, find the values of M and f_v to yield a response with 17% overshoot and a settling time of 10 seconds. [Section: 4.6]

72. Find J and K in the rotational system shown in Figure P4.18 to yield a 30% overshoot and a settling time of 3 seconds for a step input in torque. [Section: 4.6]
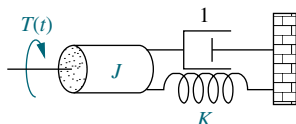
FIGURE P4.18

73. Given the system shown in Figure P4.19, find the damping, D, to yield a 30% overshoot in output angular displacement for a step input in torque. [Section: 4.6]
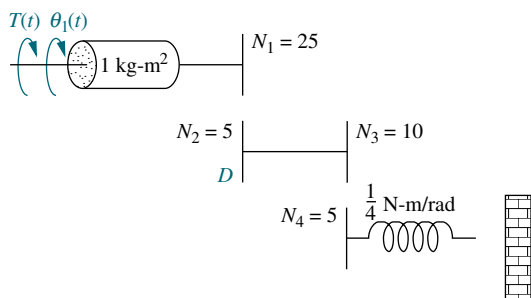
FIGURE P4.19

74. For the system shown in Figure P4.20, find N_1/N_2 so that the settling time for a step torque input is 16 seconds. [Section: 4.6]

WileyPLUS
WPCS
Control Solutions
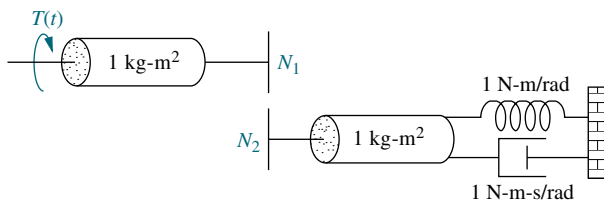
FIGURE P4.20

75. Find M and K, shown in the system of Figure P4.21, to yield $x(t)$ with 10% overshoot and 15 seconds settling time for a step input in motor torque, $T_m(t)$. [Section: 4.6]
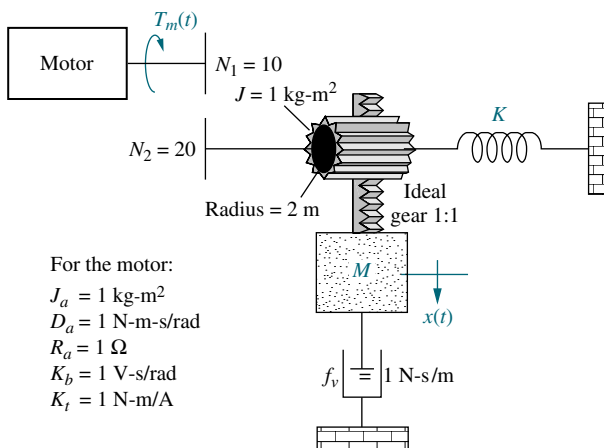
FIGURE P4.21

76. If $v_i(t)$ is a step voltage in the network shown in Figure P4.22, find the value of the resistor such that a 20% overshoot in voltage will be seen across the capacitor if $C = 10^{-6}$ F and $L = 1$ H. [Section: 4.6]
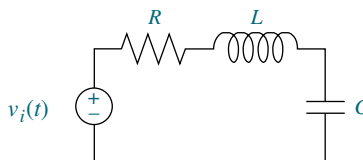
FIGURE P4.22

77. If $v_i(t)$ is a step voltage in the network shown in Figure P4.22, find the values of R and C to yield a 20% overshoot and a 1 ms settling time for $v_c(t)$ if $L = 1$ H. [Section: 4.6]

WileyPLUS
WPCS
Control Solutions

78. Given the circuit of Figure P4.22, where $C = 10\mu$F, find R and L to yield 15% overshoot with a settling time of 7 ms for the capacitor voltage. The input, $v(t)$, is a unit step. [Section: 4.6]

79. For the circuit shown in Figure P4.23, find the values of R_2 and C to yield 8% overshoot with a settling time of 1 ms for the voltage across the capacitor, with $v_i(t)$ as a step input. [Section: 4.6]
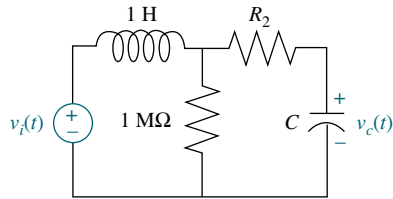
FIGURE P4.23

80. Hydraulic pumps are used as inputs to hydraulic circuits to supply pressure, just as voltage sources supply potential to electric circuits. Applications for hydraulic circuits can be found in the robotics and aircraft industries, where hydraulic actuators are used to move component parts. Figure P4.24 shows the internal parts of the pump. A barrel containing equally spaced pistons rotates about the i-axis. A swashplate, set at an angle, causes the slippers at the ends of the pistons to move the pistons in and out. When the pistons are moving across the intake port, they are extending, and when they are moving across the discharge port, they are retracting and pushing fluid from the port. The large and small actuators at the top and bottom, respectively, control the angle of the swashplate, α. The swashplate angle affects the piston stroke length. Thus, by controlling the swashplate angle, the pump discharge flow rate can be regulated. Assume the state equation for the

State Space **SS**

hydraulic pump is

$$\dot{\mathbf{x}} = \begin{bmatrix} (3.45 - 14000K_c) & -0.255 \times 10^{-9} \\ 0.499 \times 10^{11} & -3.68 \end{bmatrix} \mathbf{x}$$
$$+ \begin{bmatrix} -3.45 + 14000K_c \\ -0.499 \times 10^{11} \end{bmatrix} \alpha_0,$$

where $\mathbf{x} = \begin{bmatrix} \alpha \\ P_d \end{bmatrix}$

and P_d is the pump discharge pressure (*Manring*, *1996*). Find the value of controller flow gain, K_c, so that the damping ratio of the system's poles is 0.9.

PROGRESSIVE ANALYSIS AND DESIGN PROBLEMS

81. High-speed rail pantograph. Problem 67**c** in Chapter 2 asked you to find $G(s) = (Y_h(s) - Y_{cat}(s))/F_{up}(s)$ (*O'Connor*, *1997*).

a. Use the dominant poles from this transfer function and estimate percent overshoot, damping ratio, natural frequency, settling time, peak time, and rise time.

b. Determine if the second-order approximation is valid.

c. Obtain the step response of $G(s)$ and compare the results to Part **a**.

MATLAB **ML**

82. Control of HIV/AIDS. In Chapter 3, Problem 31, we developed a linearized

State Space **SS**
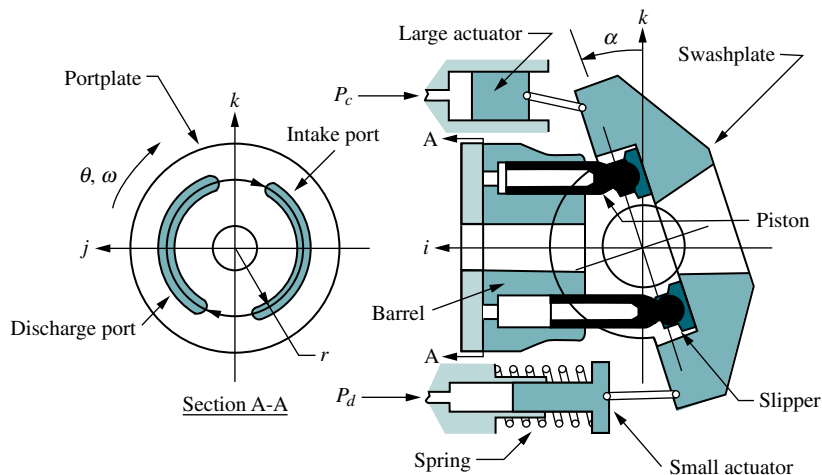
FIGURE P4.24 Pump diagram (Reprinted with permission of ASME.)

state-space model of HIV infection. The model assumed that two different drugs were used to combat the spread of the HIV virus. Since this book focuses on single-input, single-output systems, only one of the two drugs will be considered. We will assume that only RTIs are used as an input. Thus, in the equations of Chapter 3, Problem 31, $u_2 = 0$ (*Craig, 2004*).

a. Show that when using only RTIs in the linearized system of Problem 31 and substituting the typical parameter values given in the table of Problem 31**c**, the resulting state-space representation for the system is given by

$$\begin{bmatrix} \dot{T} \\ \dot{T}^* \\ \dot{v} \end{bmatrix} = \begin{bmatrix} -0.04167 & 0 & -0.0058 \\ 0.0217 & -0.24 & 0.0058 \\ 0 & 100 & -2.4 \end{bmatrix}$$

$$\times \begin{bmatrix} T \\ T^* \\ v \end{bmatrix} + \begin{bmatrix} 5.2 \\ -5.2 \\ 0 \end{bmatrix} u_1$$

$$y = \begin{bmatrix} 0 & 0 & 1 \end{bmatrix} \begin{bmatrix} T \\ T^* \\ v \end{bmatrix}$$

b. Obtain the transfer function from RTI efficiency to virus count; namely find $\dfrac{Y(s)}{U_1(s)}$.

c. Assuming RTIs are 100% effective, what will be the steady-state change of virus count in a given infected patient? Express your answer in virus copies per ml of plasma. Approximately how much time will the medicine take to reach its maximum possible effectiveness?

83. Hybrid vehicle. Assume that the car motive dynamics for a hybrid electric vehicle (HEV) can be described by the transfer function

$$\frac{\Delta V(s)}{\Delta F_e(s)} = \frac{1}{1908s + 10}$$

where AV is the change of velocity in m/sec and ΔF_e is the change in excess motive force in N necessary to propel the vehicle.

a. Find an analytical expression for $\Delta v_{(t)}$ for a step change in excess motive force $\Delta F_e = 2650$ N.

b. Simulate the system using MATLAB. Plot the expression found in Part **a** together with your simulated plot.

MATLAB
ML

Cyber Exploration Laboratory

Experiment 4.1

Objective   To evaluate the effect of pole and zero location upon the time response of first- and second-order systems.

Minimum Required Software Packages   MATLAB, Simulink, and the Control System Toolbox

Prelab

1. Given the transfer function $G(s) = \dfrac{a}{s + a}$, evaluate settling time and rise time for the following values of a: 1, 2, 3, 4. Also, plot the poles.

2. Given the transfer function $G(s) = \dfrac{b}{s^2 + as + b}$:

   a. Evaluate percent overshoot, settling time, peak time, and rise time for the following values: $a = 4$, $b = 25$. Also, plot the poles.

   b. Calculate the values of a and b so that the imaginary part of the poles remains the same but the real part is increased two times over that of Prelab 2**a**, and repeat Prelab 2**a**.

   c. Calculate the values of a and b so that the imaginary part of the poles remains the same but the real part is decreased $\frac{1}{2}$ time over that of Prelab 2**a**, and repeat Prelab 2**a**.

3. a. For the system of Prelab 2**a**, calculate the values of a and b so that the real part of the poles remains the same but the imaginary part is increased two times over that of Prelab 2**a**, and repeat Prelab 2**a**.

   b. For the system of Prelab 2**a**, calculate the values of a and b so that the real part of the poles remains the same but the imaginary part is increased four times over that of Prelab 2**a**, and repeat Prelab 2**a**.

4. a. For the system of Prelab 2**a**, calculate the values of a and b so that the damping ratio remains the same but the natural frequency is increased two times over that of Prelab 2**a**, and repeat Prelab 2**a**.

   b. For the system of Prelab 2**a**, calculate the values of a and b so that the damping ratio remains the same but the natural frequency is increased four times over that of Prelab 2**a**, and repeat Prelab 2**a**.

5. Briefly describe the effects on the time response as the poles are changed in each of Prelab 2, 3, and 4.

Lab

1. Using Simulink, set up the systems of Prelab 1 and plot the step response of each of the four transfer functions on a single graph by using the Simulink LTI Viewer. Also, record the values of settling time and rise time for each step response.

2. Using Simulink, set up the systems of Prelab 2. Using the Simulink LTI Viewer, plot the step response of each of the three transfer functions on a single graph. Also, record the values of percent overshoot, settling time, peak time, and rise time for each step response.

3. Using Simulink, set up the systems of Prelab 2**a** and Prelab 3. Using the Simulink LTI Viewer, plot the step response of each of the three transfer functions on a single graph. Also, record the values of percent overshoot, settling time, peak time, and rise time for each step response.

4. Using Simulink, set up the systems of Prelab 2**a** and Prelab 4. Using the Simulink LTI Viewer, plot the step response of each of the three transfer functions on a single graph. Also, record the values of percent overshoot, settling time, peak time, and rise time for each step response.

Postlab

1. For the first-order systems, make a table of calculated and experimental values of settling time, rise time, and pole location.

2. For the second-order systems of Prelab 2, make a table of calculated and experimental values of percent overshoot, settling time, peak time, rise time, and pole location.

3. For the second-order systems of Prelab 2**a** and Prelab 3, make a table of calculated and experimental values of percent overshoot, settling time, peak time, rise time, and pole location.

4. For the second-order systems of Prelab 2**a** and Prelab 4, make a table of calculated and experimental values of percent overshoot, settling time, peak time, rise time, and pole location.

5. Discuss the effects of pole location upon the time response for both first- and second-order systems. Discuss any discrepancies between your calculated and experimental values.

Experiment 4.2

Objective   To evaluate the effect of additional poles and zeros upon the time response of second-order systems.

Minimum Required Software Packages   MATLAB, Simulink, and the Control System Toolbox

Prelab

1. **a.** Given the transfer function $G(s) = \dfrac{25}{s^2 + 4s + 25}$, evaluate the percent over-shoot, settling time, peak time, and rise time. Also, plot the poles.

   b. Add a pole at -200 to the system of Prelab 1**a**. Estimate whether the transient response in Prelab 1**a** will be appreciably affected.

   c. Repeat Prelab 1**b** with the pole successively placed at $-20, -10$, and -2.

2. A zero is added to the system of Prelab 1**a** at -200 and then moved to $-50, -20, -10, -5$, and -2. List the values of zero location in the order of the greatest to the least effect upon the pure second-order transient response.

3. Given the transfer function $G(s) = \dfrac{(25b/a)(s+a)}{(s+b)(s^2 + 4s + 25)}$, let $a = 3$ and $b = 3.01$, 3.1, 3.3, 3.5, and 4.0. Which values of b will have minimal effect upon the pure second-order transient response?

4. Given the transfer function $G(s) = \dfrac{(2500b/a)(s+a)}{(s+b)(s^2 + 40s + 2500)}$, let $a = 30$ and $b = 30.01$, 30.1, 30.5, 31, 35, and 40. Which values of b will have minimal effect upon the pure second-order transient response?

Lab

1. Using Simulink, add a pole to the second-order system of Prelab 1**a** and plot the step responses of the system when the higher-order pole is nonexistent, at $-200, -20, -10$, and -2. Make your plots on a single graph, using the Simulink LTI Viewer. Normalize all plots to a steady-state value of unity. Record percent overshoot, settling time, peak time, and rise time for each response.

2. Using Simulink, add a zero to the second-order system of Prelab 1**a** and plot the step responses of the system when the zero is nonexistent, at $-200, -50, -20, -10, -5$, and -2. Make your plots on a single graph, using the Simulink LTI Viewer. Normalize all plots to a steady-state value of unity. Record percent overshoot, settling time, peak time, and rise time for each response.

3. Using Simulink and the transfer function of Prelab 3 with $a = 3$, plot the step responses of the system when the value of b is 3, 3.01, 3.1, 3.3, 3.5, and 4.0. Make your plots on a single graph using the Simulink LTI Viewer. Record percent overshoot, settling time, peak time, and rise time for each response.

4. Using Simulink and the transfer function of Prelab 4 with $a = 30$, plot the step responses of the system when the value of b is 30, 30.01, 30.1, 30.5, 31, 35, and 40. Make your plots on a single graph, using the Simulink LTI Viewer. Record percent overshoot, settling time, peak time, and rise time for each response.

Postlab

1. Discuss the effect upon the transient response of the proximity of a higher-order pole to the dominant second-order pole pair.

2. Discuss the effect upon the transient response of the proximity of a zero to the dominant second-order pole pair. Explore the relationship between the length of the vector from the zero to the dominant pole and the zero's effect upon the pure second-order step response.

3. Discuss the effect of pole-zero cancellation upon the transient response of a dominant second-order pole pair. Allude to how close the canceling pole and zero should be and the relationships of (1) the distance between them and (2) the distance between the zero and the dominant second-order poles.

Experiment 4.3

Objective   To use LabVIEW Control Design and Simulation Module for time performance analysis of systems.

Minimum Required Software Packages   LabVIEW with the Control Design and Simulation Module

Prelab   One of the experimental direct drive robotic arms built at the MTT Artificial Intelligence Laboratory and the CMU Robotics Institute can be represented as a feedback control system with a desired angular position input for the robot's joint position and an angular position output representing the actual robot's joint position.

  The forward path consists of three transfer functions in cascade; (1) a compensator, $G_c(s)$, to improve performance; (2) a power amplifier of gain, $K_a = 1$; and (3) the transfer function of the motor and load, $G(s) = 2292/s(s + 75.6)$. Assume a unity-feedback system. Initially the system will be controlled with $G_c(s) = 0.6234$, which is called a proportional controller (*McKerrow, 1991*).

1. Obtain the closed-loop system transfer function and use MATLAB to make a plot of the resulting unit step response.

2. Repeat with $G_c(s) = 3.05 + 0.04s$, which is called a PD controller.

3. Compare both responses and draw conclusions regarding their time domain specifications.

Lab   Create a LabVIEW VI that uses a simulation loop to implement both controllers given in the Prelab. Plot the responses on the same graph for comparison purposes.

Postlab   Compare the responses obtained using your LabVIEW VI with those obtained in the Prelab.

Experiment 4.4

Objective To use the LabVIEW Control Design and Simulation Module to evaluate the effect of pole location upon the time response of second-order systems.

Minimum Required Software Packages LabVIEW with the Control Design and Simulation Module.

Prelab Solve the Cyber Exploration Laboratory Experiment 4.1 Prelab, Part 2.

Lab Build a LabVIEW VI to implement the functions studied in the Prelab of Cyber Exploration Laboratory 4.I, Part 2.

Specifically for Prelab Part **a**, your front panel will have the coefficients of the second-order transfer function as inputs. The front panel will also have the following indicators: (1) the transfer function; (2) the state-space representation; (3) the pole locations; (4) the step response graph; (5) the time response of the two states on the same graph; (6) the time response parametric data including rise time, peak time, settling time, percent overshoot, peak value; and final value.

For Prelab, Part **b**, your front panel will also have the following indicators: (1) the step response graph, and (2) the parametric data listed above for Prelab, Part **a**, but specific to Part **b**.

For Prelab, Part **c**, your front panel will also have the following indicators: (1) the step response graph, and (2) the parametric data listed above for Prelab, Part **a**, but specific to Part **c**.

Run the VI to obtain the data from the indicators.

Postlab Use your results to discuss the effect of pole location upon the step response.

◖ Bibliography ◗
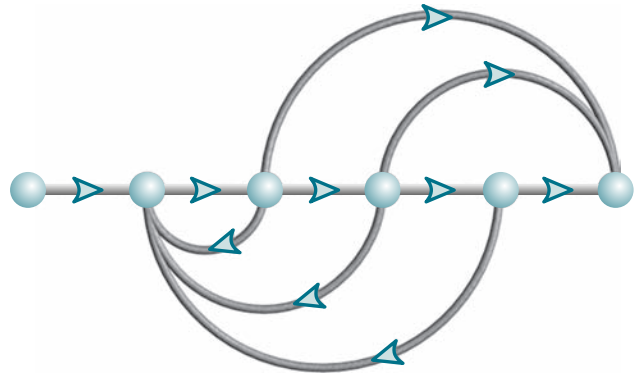
Borovic, B., Liu, A. Q., Popa, D., and Lewis, F. L. Open-Loop versus Closed-Loop Control of MEMS Devices: Choices and Issues. *Journal of Micromechanics, Microengineering*, vol. 15, 2005, pp. 1917–1924.

Craig, I. K., Xia, X., and Venter, J. W.; Introducing HIV/AIDS Education into the Electrical Engineering Curriculum at the University of Pretoria. *IEEE Transactions on Education*, vol. 47, no. 1, February 2004, pp. 65–73.

DiBona, G. F. Physiology in Perspective: The Wisdom of the Body. Neural Control of the Kidney. *American Journal of Physiology–Regulatory, Integrative and Comparative Physiology*, vol. 289, 2005, pp. R633–R641.

Dorf, R. C. *Introduction to Electric Circuits*, 2d ed. Wiley, New York, 1993.

Elarafi, M. G. M. K., and Hisham, S. B. Modeling and Control of pH Neutralization Using Neural Network Predictive Controller. *International Conference on Control, Automation and Systems 2008,* Seoul, Korea. Oct. 14–17, 2008.

Franklin, G. F., Powell, J. D., and Emami-Naeini, A. *Feedback Control of Dynamic Systems*, 2d ed. Addison-Wesley, Reading, MA, 1991.

Glantz, A. S., and Tyberg, V. J. Determination of Frequency Response from Step Response: Application to Fluid-Filled Catheters. *American Journal of Physiology*, vol. 2, 1979, pp. H376–H378.

Good, M. C., Sweet, L. M., and Strobel, K. L. Dynamic Models for Control System Design of Integrated Robot and Drive Systems. *Journal of Dynamic Systems, Measurement, and Control*, March 1985, pp. 53–59.

Ionescu, C., and De Keyser, R. Adaptive Closed-Loop Strategy for Paralyzed Skeletal Muscles. Proceedings of the IASTED International Conference on Biomedical Engineering, 2005.

Jannett, T. C., and Aragula, S. Simulation of Adaptive Control of Theophylline Concentrations. *IEEE Control Systems*, December 1992, pp. 32–37.

Jiayu, K., Mengxiao W., Linan, M., and Zhongjun, X. Cascade Control of pH in an Anaerobic Waste Water Treatment System, *3d International Conference on Bioinformatics and Biomedical Engineering*, 2009.

Johnson, H. et al. *Unmanned Free-Swimming Submersible (UFSS) System Description*. NRL Memorandum Report 4393. Naval Research Laboratory, Washington, D.C. 1980.

Kuo, B. C. *Automatic Control Systems*, 5th ed. Prentice Hall, Upper Saddle River, NJ, 1987.

Kuo, C-F. J., Tsai, C-C., and Tu, H-M. Carriage Speed Control of a Cross-lapper System for Nonwoven Web Quality. *Fibers and Polymers*, vol. 9, no. 4, 2008, pp. 495–502.

Linkens, D. A. Adaptive and Intelligent Control in Anesthesia. *IEEE Control Systems*, December 1992, pp. 6–11.

Mallavarapu, K., Newbury, K., and Leo, D. J. *Feedback Control of the Bending Response of Ionic Polymer-Metal Composite Actuators*. Proceedings of the SPIE, vol. 4329, 2001, pp. 301–310.

Manring, N. D., and Johnson, R. E. Modeling and Designing a Variable-Displacement Open-Loop Pump. *Journal of Dynamic Systems, Measurements, and Control*, vol. 118, June 1996, pp. 267–271.

McKerrow, P. J. *Introduction to Robotics*. Addison-Wesley, Singapore, 1991.

McRuer, D., Ashkenas, I., and Graham, D. *Aircraft Dynamics and Automatic Control*. Princeton University Press, 1973.

Nakamura, M. et al. Transient Response of Remnant Atrial Heart Rate to Step Changes in Total Artificial Heart Output. *Journal of Artificial Organs*, vol. 5, 2002, pp. 6–12.

Nashner, L. M., and Wolfson, P. Influence of Head Position and Proprioceptive Cues on Short Latency Postural Reflexes Evoked by Galvanic Stimulation of the Human Labyrinth. *Brain Research*, vol. 67, 1974, pp. 255–268.

O'Connor, D. N., Eppinger, S. D., Seering, W. P., and Wormly, D. N. Active Control of a High-Speed Pantograph. *Journal of Dynamic Systems, Measurements, and Control*, vol. 119, March 1997, pp. l–4.

Ogata, K. *Modern Control Engineering*, 2d ed. Prentice Hall, Upper Saddle River, NJ, 1990.

Philips, C. L., and Nagle, H. T. *Digital Control Systems Analysis and Design*. Prentice Hall, Upper Saddle River, NJ, 1984.

Salapaka, S., Sebastian, A., Cleveland, J. P., and Salapaka, M. V High Bandwidth Nano-Positioner: A Robust Control Approach. *Review of Scientific Instruments*, vol. 73, No. 9, 2002, pp. 3232–3241.

Sawusch, M. R., and Summers, T. A. *1001 Things to Do with Your Macintosh*. TAB Books, Blue Ridge Summit, PA, 1984.

Schneider, R. T. Pneumatic Robots Continue to Improve. *Hydraulics & Pneumatics*, October 1992, pp. 38–39.

Stefani, R. T. *Modeling Human Response Characteristics*. COED Application Note No. 33. Computers in Education Division of ASEE, 1973.

Sun, M., and Xiong, Y. Dynamic Flight Stability of a Hovering Bumblebee. *Journal of Experimental Biology*, vol. 208, 2005, pp. 447–459.

Timothy, L. K., and Bona, B. E. *State Space Analysis: An Introduction*. McGraw-Hill, New York, 1968.

Van Dijk, E., Spruijt, J. N., O'Sullivan, D. M., and Klaasens, J. B. PWM-Switch Modeling of DC-DC Converters. *IEEE Transactions on Power Electronics*, vol. 10, 1995, pp. 659–665.

Xue, D., and Chen, Y. D. Sub-Optimum H_2 Rational Approximations to Fractional Order Linear Systems. *Proceedings of IDET/CIE 2005*. ASME 2005 International Design Engineering Technical Conferences & Computers and Information in Engineering Conference, Long Beach. CA, 2005. pp. 1–10.

Zedka, M., Prochazka, A., Knight, B., Gillard, D., and Gauthier, M. Voluntary and Reflex Control of Human Back Muscles During Induced Pain. *Journal of Physiology*, vol. 520, 1999, pp. 591–604.

Zhou, B. H., Baratta, R. V., Solomonow, M., and D'Ambrosia, R. D. The Dynamic Response of the Cat Ankle Joint During Load-Moving Contractions. *IEEE Transactions on Biomedical Engineering*, vol. 42, no. 4, 1995, pp. 386–393.

Reduction of Multiple Subsystems

5

Chapter Learning Outcomes

After completing this chapter the student will be able to:

- Reduce a block diagram of multiple subsystems to a single block representing the transfer function from input to output (Sections 5.1–5.2)
- Analyze and design transient response for a system consisting of multiple subsystems (Section 5.3)
- Convert block diagrams to signal-flow diagrams (Section 5.4)
- Find the transfer function of multiple subsystems using Mason's rule (Section 5.5)
- Represent state equations as signal-flow graphs (Section 5.6)
- Represent multiple subsystems in state space in cascade, parallel, controller canonical, and observer canonical forms (Section 5.7)
- Perform transformations between similar systems using transformation matrices; and diagonalize a system matrix (Section 5.8)

State Space
SS

State Space
SS

State Space
SS

Case Study Learning Outcomes

You will be able to demonstrate your knowledge of the chapter objectives with case studies as follows:

- Given the antenna azimuth position control system shown on the front endpapers, you will be able to (a) find the closed-loop transfer function that represents the system from input to output; (b) find a state-space representation for the closed-loop system; (c) predict, for a simplified system model, the percent overshoot,

235

settling time, and peak time of the closed-loop system for a step input; (d) calculate the step response for the closed-loop system; and (e) for the simplified model, design the system gain to meet a transient response requirement.

- Given the block diagrams for the Unmanned Free-Swimming Submersible (UFSS) vehicle's pitch and heading control systems on the back endpapers, you will be able to represent each control system in state space.

State Space
SS

5.1 Introduction

We have been working with individual subsystems represented by a block with its input and output. More complicated systems, however, are represented by the interconnection of many subsystems. Since the response of a single transfer function can be calculated, we want to represent multiple subsystems as a single transfer function. We can then apply the analytical techniques of the previous chapters and obtain transient response information about the entire system.

In this chapter, multiple subsystems are represented in two ways: as block diagrams and as signal-flow graphs. Although neither representation is limited to a particular analysis and design technique, block diagrams are usually used for frequency-domain analysis and design, and signal-flow graphs for state-space analysis.

Signal-flow graphs represent transfer functions as lines, and signals as small-circular nodes. Summing is implicit. To show why it is convenient to use signal-flow graphs for state-space analysis and design, consider Figure 3.10. A graphical representation of a system's transfer function is as simple as Figure 3.10(*a*). However, a graphical representation of a system in state space requires representation of each state variable, as in Figure 3.10(*b*). In that example, a single-block transfer function requires seven blocks and a summing junction to show the state variables explicitly. Thus, signal-flow graphs have advantages over block diagrams, such as Figure 3.10(*b*): They can be drawn more quickly, they are more compact, and they emphasize the state variables.

We will develop techniques to reduce each representation to a single transfer function. Block diagram algebra will be used to reduce block diagrams and Mason's rule to reduce signal-flow graphs. Again, it must be emphasized that these methods are typically used as described. As we shall see, however, either method can be used for frequency-domain or state-space analysis and design.

5.2 Block Diagrams

As you already know, a subsystem is represented as a block with an input, an output, and a transfer function. Many systems are composed of multiple subsystems, as in Figure 5.1. When multiple subsystems are interconnected, a few more schematic elements must be added to the block diagram. These new elements are *summing junctions* and *pickoff points*. All component parts of a block diagram for a linear, time-invariant system are shown in Figure 5.2. The characteristic of the summing junction shown in Figure 5.2(*c*) is that the output signal, $C(s)$, is the algebraic sum of the input signals, $R_1(s)$, $R_2(s)$, and $R_3(s)$. The figure shows three inputs, but any
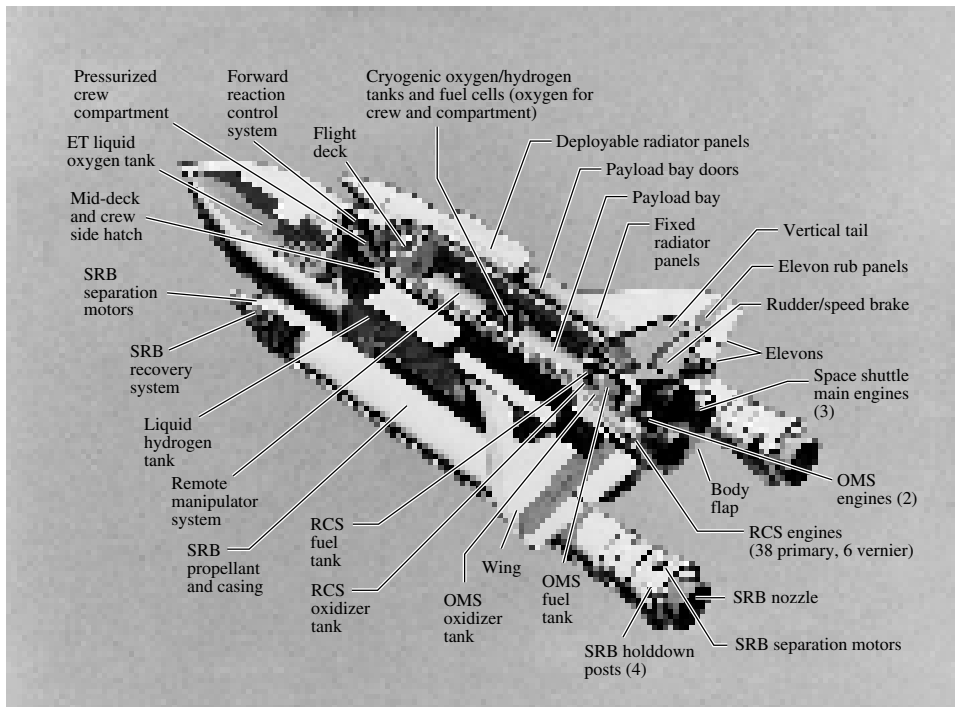
FIGURE 5.1 The space shuttle consists of multiple subsystems. Can you identify those that are control systems or parts of control systems?
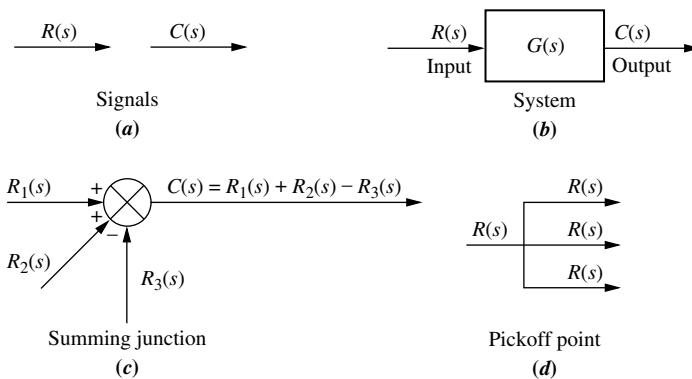
FIGURE 5.2 Components of a block diagram for a linear, time-invariant system

number can be present. A pickoff point, as shown in Figure 5.2(*d*), distributes the input signal, $R(s)$, undiminished, to several output points.

We will now examine some common topologies for interconnecting subsystems and derive the single transfer function representation for each of them. These common topologies will form the basis for reducing more complicated systems to a single block.

Cascade Form

Figure 5.3(*a*) shows an example of cascaded subsystems. Intermediate signal values are shown at the output of each subsystem. Each signal is derived from the product of the input times the transfer function. The equivalent transfer function, $G_e(s)$, shown in Figure 5.3(*b*), is the output Laplace transform divided by the input Laplace
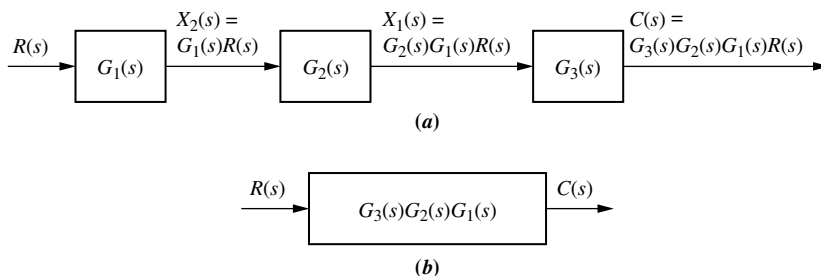
FIGURE 5.3 **a.** Cascaded subsystems; **b.** equivalent transfer function

transform from Figure 5.3(*a*), or

$$G_e(s) = G_3(s)G_2(s)G_1(s) \tag{5.1}$$

which is the product of the subsystems' transfer functions.

Equation (5.1) was derived under the assumption that interconnected subsystems do not load adjacent subsystems. That is, a subsystem's output remains the same whether or not the subsequent subsystem is connected. If there is a change in the output, the subsequent subsystem loads the previous subsystem, and the equivalent transfer function is not the product of the individual transfer functions. The network of Figure 5.4(*a*) demonstrates this concept. Its transfer function is

$$G_1(s) = \frac{V_1(s)}{V_i(s)} = \frac{\dfrac{1}{R_1 C_1}}{s + \dfrac{1}{R_1 C_1}} \tag{5.2}$$

Similarly, the network of Figure 5.4(*b*) has the following transfer function:

$$G_2(s) = \frac{V_2(s)}{V_1(s)} = \frac{\dfrac{1}{R_2 C_2}}{s + \dfrac{1}{R_2 C_2}} \tag{5.3}$$
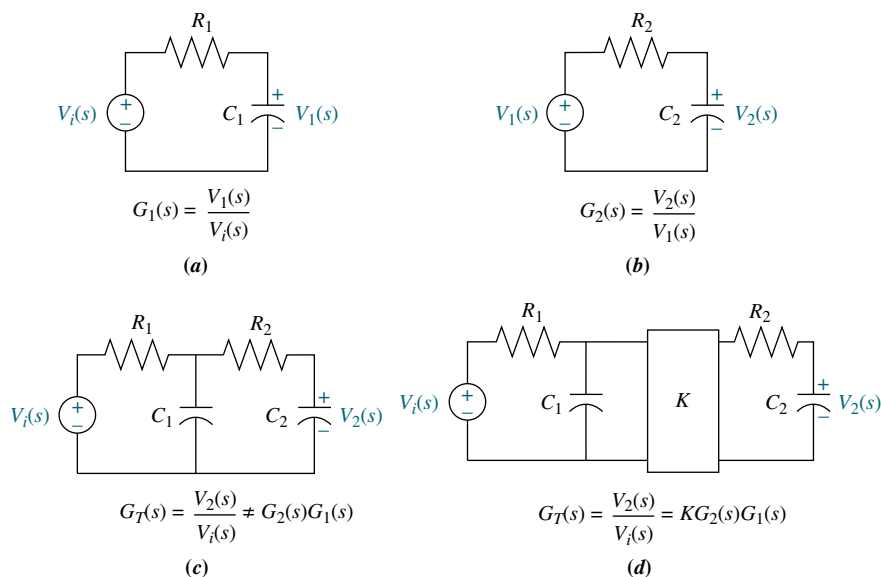
FIGURE 5.4 Loading in cascaded systems

If the networks are placed in cascade, as in Figure 5.4(*c*), you can verify that the transfer function found using loop or node equations is

$$G(s) = \frac{V_2(s)}{V_i(s)} = \frac{\dfrac{1}{R_1 C_1 R_2 C_2}}{s^2 + \left(\dfrac{1}{R_1 C_1} + \dfrac{1}{R_2 C_2} + \dfrac{1}{R_2 C_1}\right)s + \dfrac{1}{R_1 C_1 R_2 C_2}} \tag{5.4}$$

But, using Eq. (5.1),

$$G(s) = G_2(s)G_1(s) = \frac{\dfrac{1}{R_1 C_1 R_2 C_2}}{s^2 + \left(\dfrac{1}{R_1 C_1} + \dfrac{1}{R_2 C_2}\right)s + \dfrac{1}{R_1 C_1 R_2 C_2}} \tag{5.5}$$

Equations (5.4) and (5.5) are not the same: Eq. (5.4) has one more term for the coefficient of *s* in the denominator and is correct.

One way to prevent loading is to use an amplifier between the two networks, as shown in Figure 5.4(*d*). The amplifier has a high-impedance input, so that it does not load the previous network. At the same time it has a low-impedance output, so that it looks like a pure voltage source to the subsequent network. With the amplifier included, the equivalent transfer function is the product of the transfer functions and the gain, *K*, of the amplifier.

Parallel Form

Figure 5.5 shows an example of parallel subsystems. Again, by writing the output of each subsystem, we can find the equivalent transfer function. Parallel subsystems have a common input and an output formed by the algebraic sum of the outputs from all of the subsystems. The equivalent transfer function, $G_e(s)$, is the output transform divided by the input transform from Figure 5.5(*a*), or

$$G_e(s) = \pm G_1(s) \pm G_2(s) \pm G_3(s) \tag{5.6}$$

which is the algebraic sum of the subsystems' transfer functions; it appears in Figure 5.5(*b*).

(*a*)

(*b*)
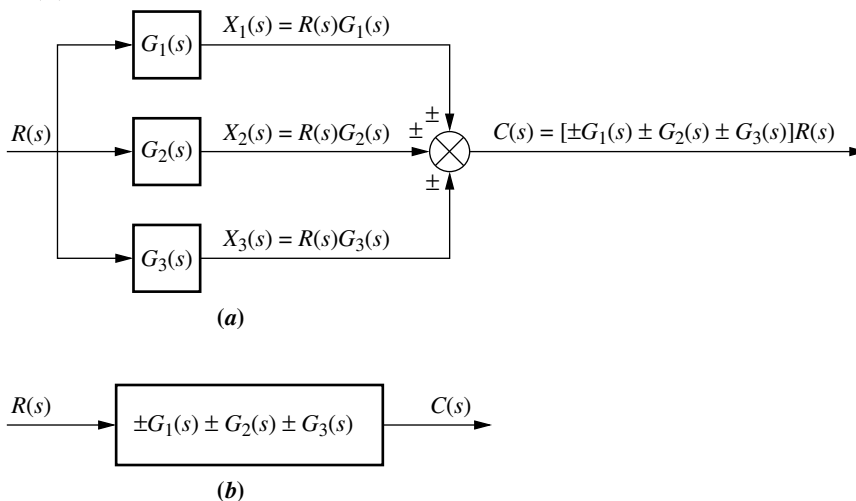
FIGURE 5.5 **a.** Parallel subsystems; **b.** equivalent transfer function

Feedback Form

The third topology is the feedback form, which will be seen repeatedly in subsequent chapters. The feedback system forms the basis for our study of control systems engineering. In Chapter 1, we defined open-loop and closed-loop systems and pointed out the advantage of closed-loop, or feedback control, systems over open-loop systems. As we move ahead, we will focus on the analysis and design of feedback systems.

Let us derive the transfer function that represents the system from its input to its output. The typical feedback system, described in detail in Chapter 1, is shown in Figure 5.6(a); a simplified model is shown in Figure 5.6(b).[1] Directing our attention to the simplified model,

$$E(s) = R(s) \mp C(s)H(s) \tag{5.7}$$

But since $C(s) = E(s)G(s)$,

$$E(s) = \frac{C(s)}{G(s)} \tag{5.8}$$

(a)

(b)

$$\begin{array}{c} R(s) \\ \text{Input} \end{array} \rightarrow \boxed{\dfrac{G(s)}{1 \pm G(s)H(s)}} \rightarrow \begin{array}{c} C(s) \\ \text{Output} \end{array}$$
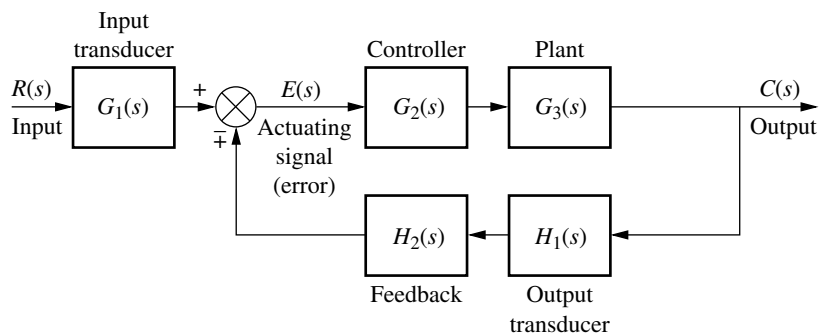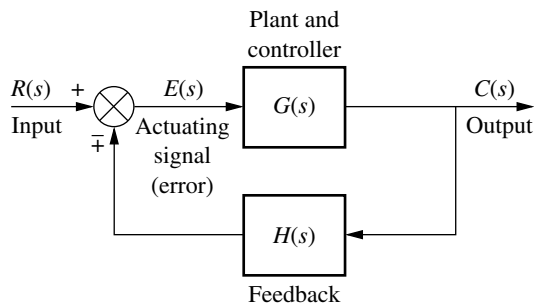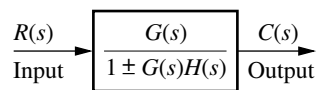
(c)

FIGURE 5.6 **a.** Feedback control system; **b.** simplified model; **c.** equivalent transfer function

---

[1] The system is said to have *negative feedback* if the sign at the summing junction is negative and *positive feedback* if the sign is positive.

Substituting Eq. (5.8) into Eq. (5.7) and solving for the transfer function, $C(s)/R(s) = G_e(s)$, we obtain the equivalent, or *closed-loop*, transfer function shown in Figure 5.6(*c*),

$$G_e(s) = \frac{G(s)}{1 \pm G(s)H(s)} \tag{5.9}$$

The product, $G(s)H(s)$, in Eq. (5.9) is called the *open-loop transfer function*, or *loop gain*.

So far, we have explored three different configurations for multiple subsystems. For each, we found the equivalent transfer function. Since these three forms are combined into complex arrangements in physical systems, recognizing these topologies is a prerequisite to obtaining the equivalent transfer function of a complex system. In this section, we will reduce complex systems composed of multiple subsystems to single transfer functions.

Moving Blocks to Create Familiar Forms

Before we begin to reduce block diagrams, it must be explained that the familiar forms (cascade, parallel, and feedback) are not always apparent in a block diagram. For example, in the feedback form, if there is a pickoff point after the summing junction, you cannot use the feedback formula to reduce the feedback system to a single block. That signal disappears, and there is no place to reestablish the pickoff point.

This subsection will discuss basic block moves that can be made to order to establish familiar forms when they almost exist. In particular, it will explain how to move blocks left and right past summing junctions and pickoff points.

Figure 5.7 shows equivalent block diagrams formed when transfer functions are moved left or right past a summing junction, and Figure 5.8 shows equivalent block diagrams formed when transfer functions are moved left or right past a pickoff point. In the diagrams the symbol $\equiv$ means "equivalent to." These equivalences,
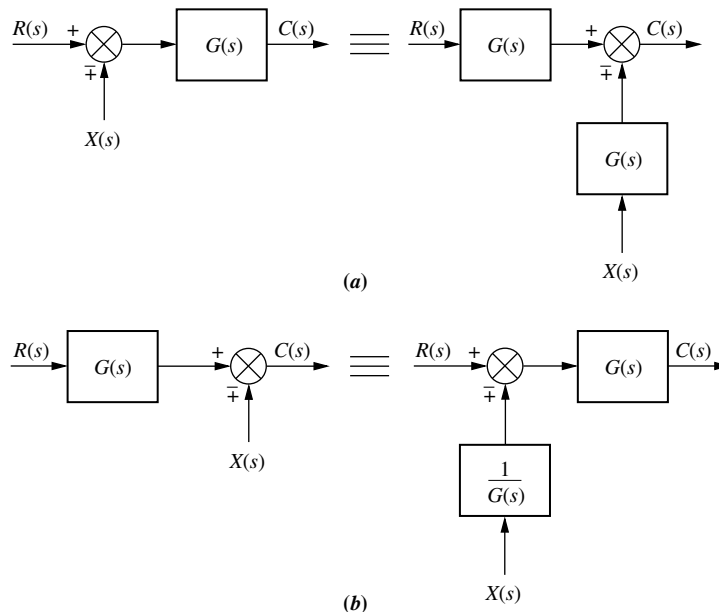
FIGURE 5.7   Block diagram algebra for summing junctions—equivalent forms for moving a block **a.** to the left past a summing junction; **b.** to the right past a summing junction
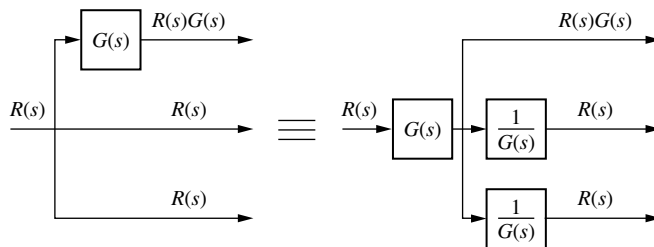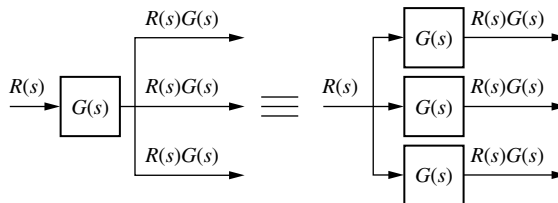
FIGURE 5.8 Block diagram algebra for pickoff points— equivalent forms for moving a block **a.** to the left past a pickoff point; **b.** to the right past a pickoff point

along with the forms studied earlier in this section, can be used to reduce a block diagram to a single transfer function. In each case of Figures 5.7 and 5.8, the equivalence can be verified by tracing the signals at the input through to the output and recognizing that the output signals are identical. For example, in Figure 5.7(a), signals $R(s)$ and $X(s)$ are multiplied by $G(s)$ before reaching the output. Hence, both block diagrams are equivalent, with $C(s) = R(s)G(s) \mp X(s)G(s)$. In Figure 5.7($b$), $R(s)$ is multiplied by $G(s)$ before reaching the output, but $X(s)$ is not. Hence, both block diagrams in Figure 5.7(b) are equivalent, with $C(s) = R(s)G(s) \mp X(s)$. For pickoff points, similar reasoning yields similar results for the block diagrams of Figure 5.8(a) and (b).

Let us now put the whole story together with examples of block diagram reduction.

Example 5.1

Block Diagram Reduction via Familiar Forms

PROBLEM: Reduce the block diagram shown in Figure 5.9 to a single transfer function.
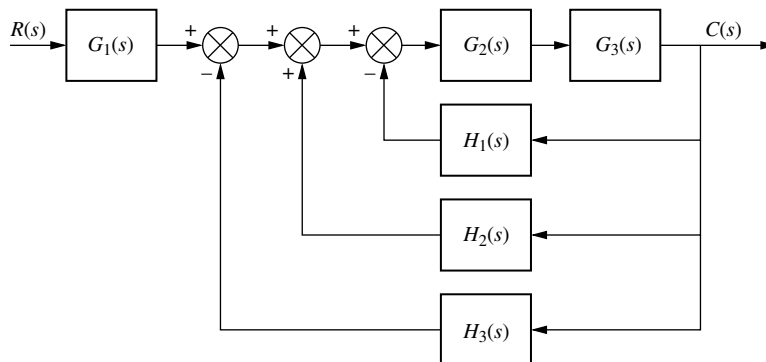
FIGURE 5.9 Block diagram for Example 5.1

SOLUTION: We solve the problem by following the steps in Figure 5.10. First, the three summing junctions can be collapsed into a single summing junction, as shown in Figure 5.10(a).

Second, recognize that the three feedback functions, $H_1(s)$, $H_2(s)$, and $H_3(s)$, are connected in parallel. They are fed from a common signal source, and their outputs are summed. The equivalent function is $H_1(s) - H_2(s) + H_3(s)$. Also recognize that $G_2(s)$ and $G_3(s)$ are connected in cascade. Thus, the equivalent transfer function is the product, $G_3(s)G_2(s)$. The results of these steps are shown in Figure 5.10(b).

Finally, the feedback system is reduced and multiplied by $G_1(s)$ to yield the equivalent transfer function shown in Figure 5.10(c).
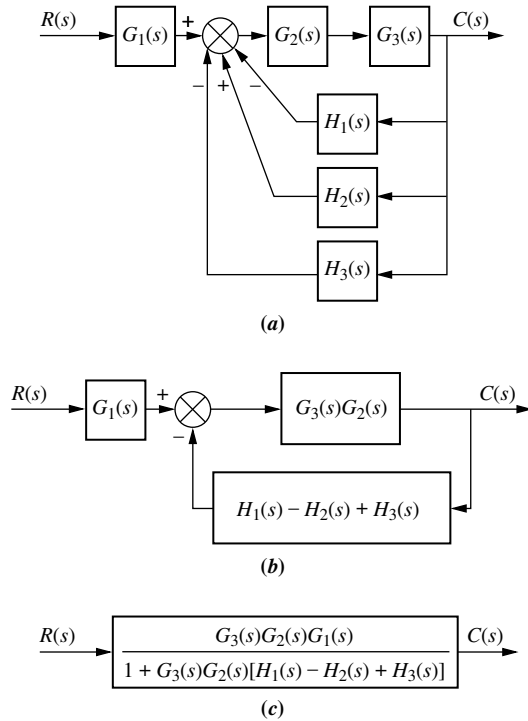
FIGURE 5.10 Steps in solving Example 5.1: **a.** Collapse summing junctions; **b.** form equivalent cascaded system in the forward path and equivalent parallel system in the feedback path; **c.** form equivalent feedback system and multiply by cascaded $G_1(s)$

Example 5.2

Block Diagram Reduction by Moving Blocks

PROBLEM: Reduce the system shown in Figure 5.11 to a single transfer function.
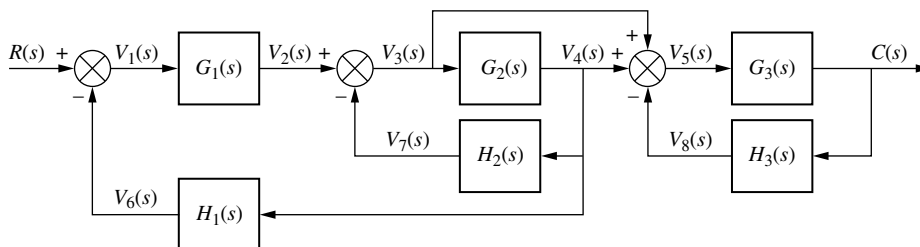
FIGURE 5.11 Block diagram for Example 5.2

SOLUTION: In this example we make use of the equivalent forms shown in Figures 5.7 and 5.8. First, move $G_2(s)$ to the left past the pickoff point to create parallel subsystems, and reduce the feedback system consisting of $G_3(s)$ and $H_3(s)$. This result is shown in Figure 5.12(a).

Second, reduce the parallel pair consisting of $1/G_2(s)$ and unity, and push $G_1(s)$ to the right past the summing junction, creating parallel subsystems in the feedback. These results are shown in Figure 5.12(b).

(a)

(b)

(c)

(d)

(e)
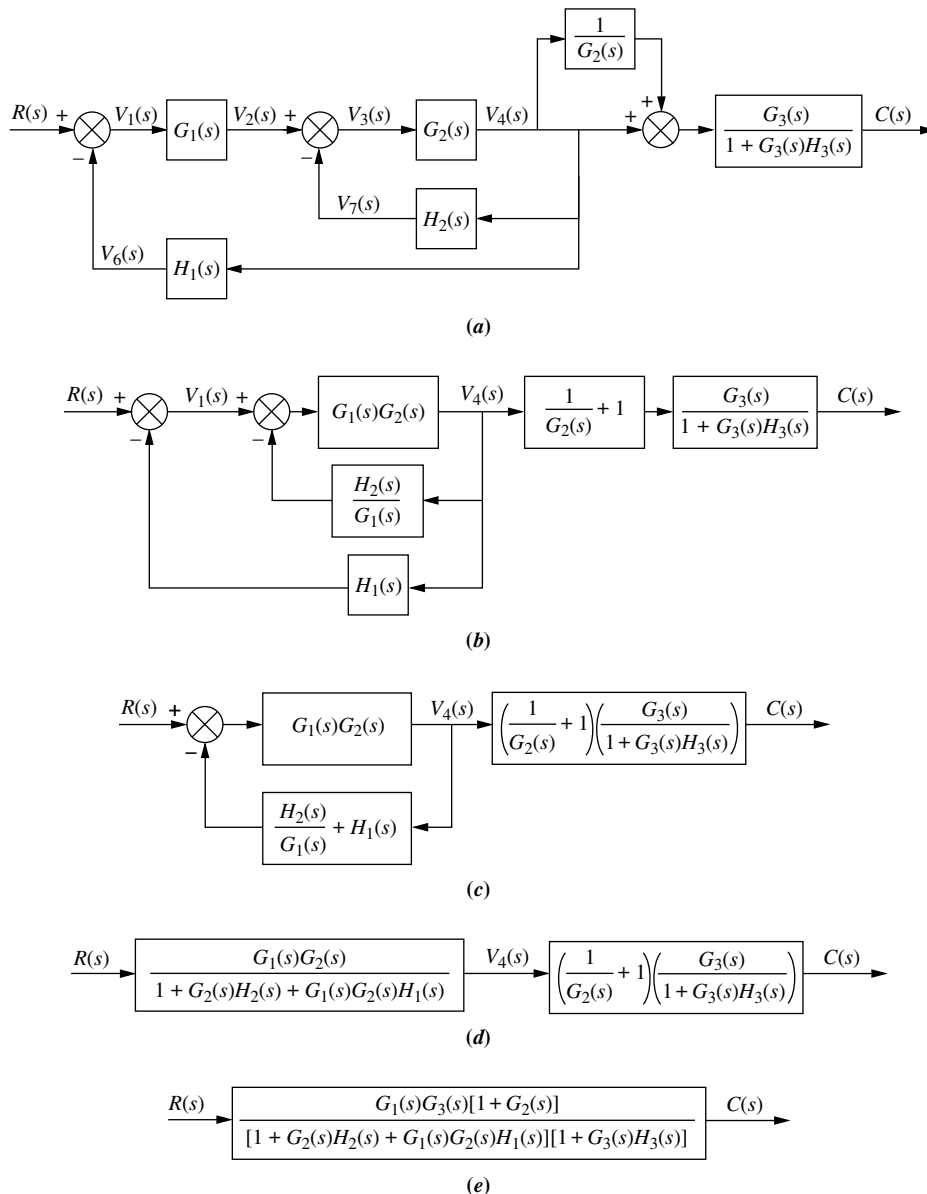
FIGURE 5.12 Steps in the block diagram reduction for Example 5.2

Third, collapse the summing junctions, add the two feedback elements together, and combine the last two cascaded blocks. Figure 5.12(*c*) shows these results.

Fourth, use the feedback formula to obtain Figure 5.12(*d*).

Finally, multiply the two cascaded blocks and obtain the final result, shown in Figure 5.12(*e*).

Skill-Assessment Exercise 5.1

PROBLEM: Find the equivalent transfer function, $T(s) = C(s)/R(s)$, for the system shown in Figure 5.13.
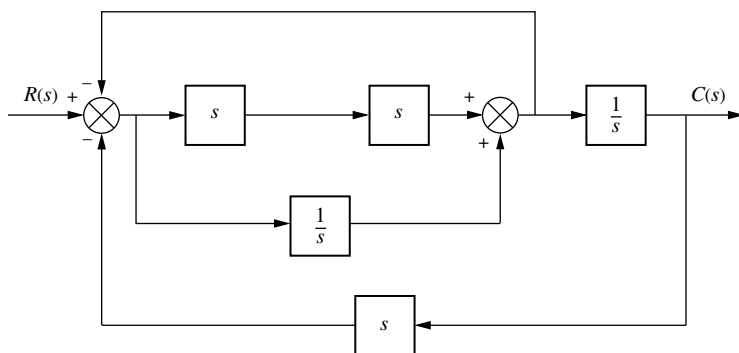
FIGURE 5.13   Block diagram for Skill-Assessment Exercise 5.1

ANSWER:

$$T(s) = \frac{s^3 + 1}{2s^4 + s^2 + 2s}$$

The complete solution is at www.wiley.com/college/nise.

TryIt 5.1

Use the following MATLAB and Control System Toolbox statements to find the closed-loop transfer function of the system in Example 5.2 if all $G_i(s) = 1/(s+1)$ and all $H_i(s) = 1/s$.

```
G1=tf(1,[1 1]);
G2=G1;G3=G1;
H1=tf(1,[1 0]);
H2=H1;H3=H1;
System=append...
 (G1,G2,G3,H1,H2,H3);
input=1;output=3;
Q=[1  -4   0   0   0
   2   1  -5   0   0
   3   2   1  -5  -6
   4   2   0   0   0
   5   2   0   0   0
   6   3   0   0   0];
T=connect(System,...
 Q,input,output);
T=tf(T);T=minreal(T)
```

In this section, we examined the equivalence of several block diagram configurations containing signals, systems, summing junctions, and pickoff points. These configurations were the cascade, parallel, and feedback forms. During block diagram reduction, we attempt to produce these easily recognized forms and then reduce the block diagram to a single transfer function. In the next section, we will examine some applications of block diagram reduction.

5.3   Analysis and Design of Feedback Systems

An immediate application of the principles of Section 5.2 is the analysis and design of feedback systems that reduce to second-order systems. Percent overshoot, settling time, peak time, and rise time can then be found from the equivalent transfer function.
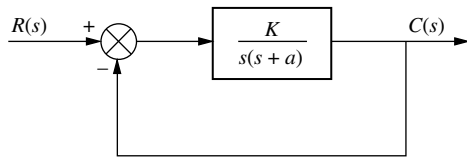
FIGURE 5.14 Second-order feedback control system

Consider the system shown in Figure 5.14, which can model a control system such as the antenna azimuth position control system. For example, the transfer function, $K/s(s + a)$, can model the amplifiers, motor, load, and gears. From Eq. (5.9), the closed-loop transfer function, $T(s)$, for this system is

$$T(s) = \frac{K}{s^2 + as + K} \tag{5.10}$$

where K models the amplifier gain, that is, the ratio of the output voltage to the input voltage. As K varies, the poles move through the three ranges of operation of a second-order system: overdamped, critically damped, and underdamped. For example, for K between 0 and $a^2/4$, the poles of the system are real and are located at

$$s_{1,2} = -\frac{a}{2} \pm \frac{\sqrt{a^2 - 4K}}{2} \tag{5.11}$$

As K increases, the poles move along the real axis, and the system remains overdamped until $K = a^2/4$. At that gain, or amplification, both poles are real and equal, and the system is critically damped.

For gains above $a^2/4$, the system is underdamped, with complex poles located at

$$s_{1,2} = -\frac{a}{2} \pm j\frac{\sqrt{4K - a^2}}{2} \tag{5.12}$$

Now as K increases, the real part remains constant and the imaginary part increases. Thus, the peak time decreases and the percent overshoot increases, while the settling time remains constant.

Let us look at two examples that apply the concepts to feedback control systems. In the first example, we determine a system's transient response. In the second example, we design the gain to meet a transient response requirement.

Example 5.3

Finding Transient Response
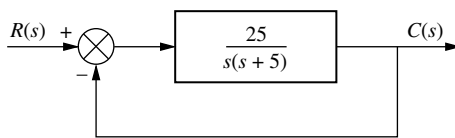
FIGURE 5.15 Feedback system for Example 5.3

PROBLEM: For the system shown in Figure 5.15, find the peak time, percent overshoot, and settling time.

SOLUTION: The closed-loop transfer function found from Eq. (5.9) is

$$T(s) = \frac{25}{s^2 + 5s + 25} \tag{5.13}$$

From Eq. (4.18),

$$\omega_n = \sqrt{25} = 5 \tag{5.14}$$

From Eq. (4.21),

$$2\zeta\omega_n = 5 \tag{5.15}$$

Substituting Eq. (5.14) into (5.15) and solving for ζ yields

$$\zeta = 0.5 \tag{5.16}$$

Using the values for ζ and ω_n along with Eqs (4.34), (4.38), and (4.42), we find respectively,

$$T_p = \frac{\pi}{\omega_n \sqrt{1 - \zeta^2}} = 0.726 \text{ second} \tag{5.17}$$

$$\%OS = e^{-\zeta\pi/\sqrt{1-\zeta^2}} \times 100 = 16.303 \tag{5.18}$$

$$T_s = \frac{4}{\zeta\omega_n} = 1.6 \text{ seconds} \tag{5.19}$$

```
Students who are using MATLAB should now run ch5p2 in Appendix B. You
will learn how to perform block diagram reduction followed by an
evaluation of the closed-loop system's transient response by find-
ing, Tₚ,%OS, and Tₛ. Finally, you will learn how to use MATLAB to
generate a closed-loop step response. This exercise uses MATLAB to
do Example 5.3.
```

```
MATLAB's Simulink provides an alternative method of simulating
feedback systems to obtain the time response. Students who are
performing the MATLAB exercises and want to explore the added
capability of MATLAB's Simulink should now consult Appendix C.
Example C.3 includes a discussion about, and an example of, the use
of Simulink to simulate feedback systems with nonlinearities.
```

Example 5.4

Gain Design for Transient Response

PROBLEM: Design the value of gain. K, for the feedback control system of Figure 5.16 so that the system will respond with a 10% overshoot.
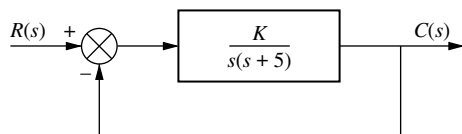
FIGURE 5.16   Feedback system for Example 5.4

SOLUTION: The closed-loop transfer function of the system is

$$T(s) = \frac{K}{s^2 + 5s + K} \tag{5.20}$$

From Eq. (5.20),

$$2\zeta\omega_n = 5 \tag{5.21}$$

and

$$\omega_n = \sqrt{K} \tag{5.22}$$

Thus,

$$\zeta = \frac{5}{2\sqrt{K}} \tag{5.23}$$

Since percent overshoot is a function only of ζ, Eq. (5.23) shows that the percent overshoot is a function of K.

Virtual Experiment 5.1 Position Control Gain Design

Put theory into practice designing the position control gain for the Quanser Linear Servo and simulating its closed-loop response in LabVIEW. This concept is used, for instance, to control a rover exploring the terrain of a planet.
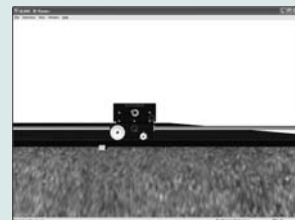
Virtual experiment are found on WileyPLUS.

A 10% overshoot implies that $\zeta = 0.591$. Substituting this value for the damping ratio into Eq. (5.23) and solving for K yields

$$K = 17.9 \qquad (5.24)$$

Although we are able to design for percent overshoot in this problem, we could not have selected settling time as a design criterion because, regardless of the value of K, the real parts, -2.5, of the poles of Eq. (5.20) remain the same.

Skill-Assessment Exercise 5.2

PROBLEM: For a unity feedback control system with a forward-path transfer function $G(s) = \dfrac{16}{s(s + a)}$, design the value of a to yield a closed-loop step response that has 5% overshoot.

ANSWER:

$$a = 5.52$$

The complete solution is at www.wiley.com/college/nise.

TryIt 5.2

Use the following MATLAB and Control System Toolbox statements to find ζ, ω_n, %OS, T_s, T_p, and T_r for the closed-loop unity feedback system described in Skill-Assessment Exercise 5.2. Start with $a = 2$ and try some other values. A step response for the closed-loop system will also be produced.

```
a=2;
numg=16;
deng=poly([0 -a]);
G=tf(numg,deng);
T=feedback(G,1);
```

```
[numt,dent]=...
  tfdata(T,'v');
wn=sqrt(dent)3))
z=dent(2)/(2*wn)
Ts=4/(z*wn)
Tp=pi/(wn*...
  sqrt(1-z^2))
pos=exp(-z*pi...
  /sqrt(1-z^2))*100
Tr=(1.76*z^3 - ...
  0.417*z^2 + 1.039*...
  z + 1)/wn
step(T)
```

5.4 Signal-Flow Graphs

Signal-flow graphs are an alternative to block diagrams. Unlike block diagrams, which consist of blocks, signals, summing junctions, and pickoff points, a signal-flow graph consists only of *branches*, which represent systems, and *nodes*, which represent signals. These elements are shown in Figure 5.17(*a*) and (*b*), respectively. A system is represented by a line with an arrow showing the direction of signal flow through the

FIGURE 5.17 Signal-flow graph components: **a.** system; **b.** signal; **c.** interconnection of systems and signals
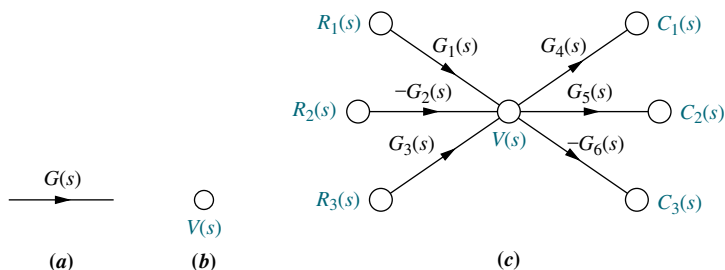
system. Adjacent to the line we write the transfer function. A signal is a node with the signal's name written adjacent to the node.

Figure 5.17(c) shows the interconnection of the systems and the signals. Each signal is the sum of signals flowing into it. For example, the signal $V(s) = R_1(s)G_1(s) - R_2(s)G_2(s) + R_3(s)G_3(s)$. The signal $C_2(s) = V(s)G_5(s) = R_1(s)G_1(s)G_5(s) - R_2(s)G_2(s)G_5(s) + R_3(s)G_3(s)G_5(s)$. The signal $C_3(s) = -V(s)G_6(s) = -R_1(s)G_1(s)G_6(s) + R_2(s)G_2(s)G_6(s) - R_3(s)G_3(s)G_6(s)$. Notice that in summing negative signals we associate the negative sign with the system and not with a summing junction, as in the case of block diagrams.

To show the parallel between block diagrams and signal-flow graphs, we will take some of the block diagram forms from Section 5.2 and convert them to signal-flow graphs in Example 5.5. In each case, we will first convert the signals to nodes and then interconnect the nodes with system branches. In Example 5.6, we will convert an intricate block diagram to a signal-flow graph.

Example 5.5

Converting Common Block Diagrams to Signal-Flow Graphs

PROBLEM: Convert the cascaded, parallel, and feedback forms of the block diagrams shown in Figures 5.3(a), 5.5(a), and 5.6(b), respectively, into signal-flow graphs.

SOLUTION: In each case, we start by drawing the signal nodes for that system. Next we interconnect the signal nodes with system branches. The signal nodes for the cascaded, parallel, and feedback forms are shown in Figure 5.18(a), (c), and (e), respectively. The interconnection of the nodes with branches that represent the subsystems is shown in Figure 5.18(b), (d), and (f) for the cascaded, parallel, and feedback forms, respectively.
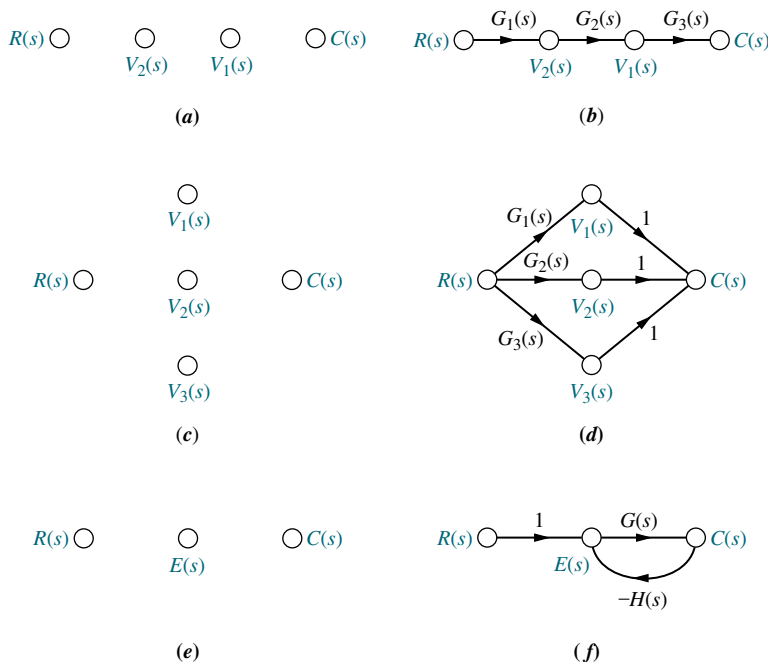
FIGURE 5.18   Building signal-flow graphs: **a.** cascaded system nodes (from Figure 5.3(a)); **b.** cascaded system signal-flow graph; **c.** parallel system nodes (from Figure 5.5(a)); **d.** parallel system signal-flow graph; **e.** feedback system nodes (from Figure 5.6(b)); **f.** feedback system signal-flow graph

Example 5.6

Converting a Block Diagram to a Signal-Flow Graph

PROBLEM: Convert the block diagram of Figure 5.11 to a signal-flow graph.

SOLUTION: Begin by drawing the signal nodes, as shown in Figure 5.19(a). Next, interconnect the nodes, showing the direction of signal flow and identifying each transfer function. The result is shown in Figure 5.19(b). Notice that the negative signs at the summing junctions of the block diagram are represented by the negative transfer functions of the signal-flow graph. Finally, if desired, simplify the signal-flow graph to the one shown in Figure 5.19(c) by eliminating signals that have a single flow in and a single flow out, such as $V_2(s)$, $V_6(s)$, $V_7(s)$, and $V_8(s)$.
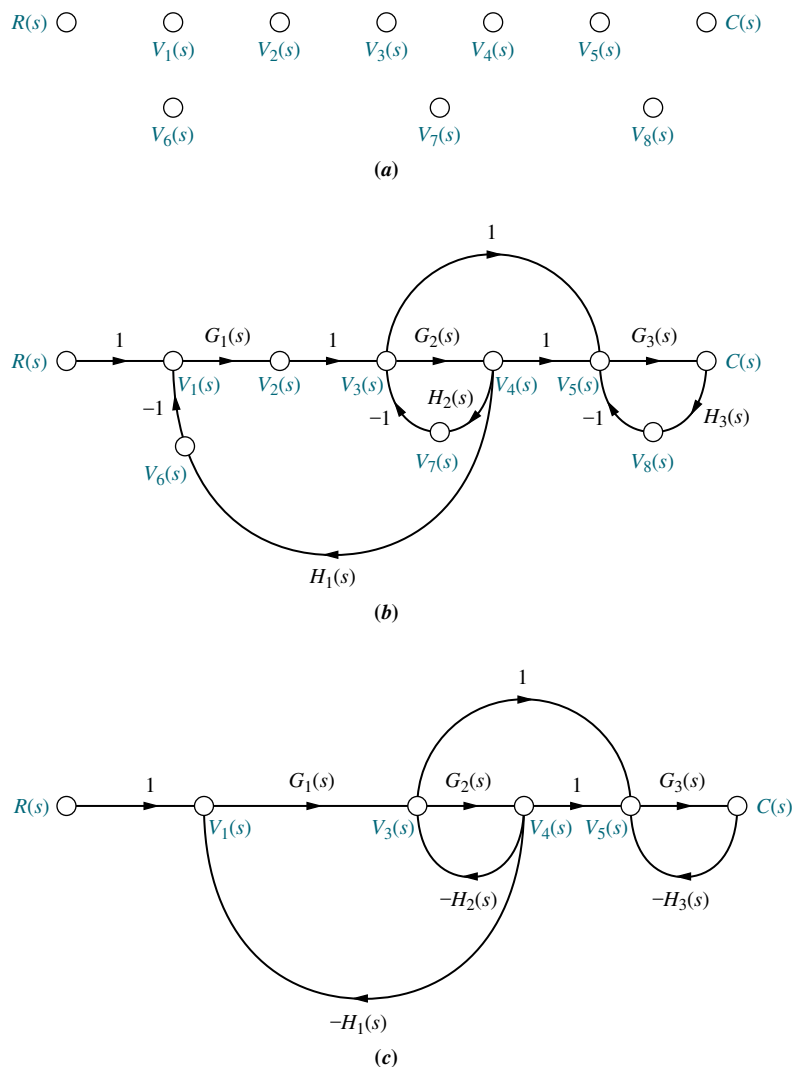
FIGURE 5.19   Signal-flow graph development: **a.** signal nodes; **b.** signal-flow graph; **c.** simplified signal-flow graph

---

Skill-Assessment Exercise 5.3

PROBLEM: Convert the block diagram of Figure 5.13 to a signal-flow graph.

ANSWER: The complete solution is at www.wiley.com/college/nise.

◖ 5.5   Mason's Rule

Earlier in this chapter, we discussed how to reduce block diagrams to single transfer functions. Now we are ready to discuss a technique for reducing signal-flow graphs to single transfer functions that relate the output of a system to its input.

The block diagram reduction technique we studied in Section 5.2 requires successive application of fundamental relationships in order to arrive at the system transfer function. On the other hand, Mason's rule for reducing a signal-flow graph to a single transfer function requires the application of one formula. The formula was derived by S. J. Mason when he related the signal-flow graph to the simultaneous equations that can be written from the graph (*Mason*, *1953*).

In general, it can be complicated to implement the formula without making mistakes. Specifically, the existence of what we will later call nontouching loops increases the complexity of the formula. However, many systems do not have non-touching loops. For these systems, you may find Mason's rule easier to use than block diagram reduction.

Mason's formula has several components that must be evaluated. First, we must be sure that the definitions of the components are well understood. Then we must exert care in evaluating the components. To that end, we discuss some basic definitions applicable to signal-flow graphs; then we state Mason's rule and do an example.

Definitions

Loop gain. The product of branch gains found by traversing a path that starts at a node and ends at the same node, following the direction of the signal flow, without passing through any other node more than once. For examples of loop gains, see Figure 5.20. There are four loop gains:

1. $G_2(s)H_1(s)$ (5.25a)

2. $G_4(s)H_2(s)$ (5.25b)

3. $G_4(s)G_5(s)H_3(s)$ (5.25c)

4. $G_4(s)G_6(s)H_3(s)$ (5.25d)
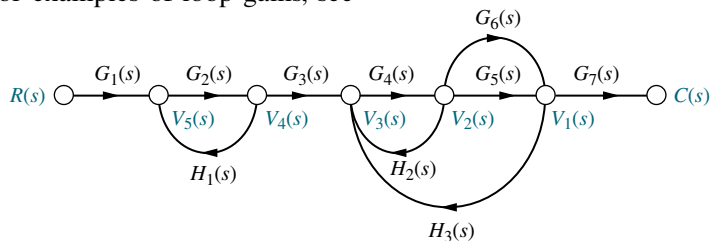
FIGURE 5.20   Signal-flow graph for demonstrating Mason's rule

Forward-path gain. The product of gains found by traversing a path from the input node to the output node of the signal-flow graph in the direction of signal flow. Examples of forward-path gains are also shown in Figure 5.20. There are two forward-path gains:

1. $G_1(s)G_2(s)G_3(s)G_4(s)G_5(s)G_7(s)$ (5.26a)

2. $G_1(s)G_2(s)G_3(s)G_4(s)G_6(s)G_7(s)$ (5.26b)

Nontouching loops. Loops that do not have any nodes in common. In Figure 5.20, loop $G_2(s)H_1(s)$ does not touch loops $G_4(s)H_2(s)$, $G_4(s)G_5(s)H_3(s)$, and $G_4(s)G_6(s)H_3(s)$.

Nontouching-loop gain. The product of loop gains from nontouching loops taken two, three, four, or more at a time. In Figure 5.20 the product of loop gain $G_2(s)H_1(s)$ and loop gain $G_4(s)H_2(s)$ is a nontouching-loop gain taken two at a time. In summary, all three of the nontouching-loop gains taken two at a time are

1. $[G_2(s)H_1(s)][G_4(s)H_2(s)]$ $\qquad\qquad\qquad\qquad\qquad\qquad\qquad\qquad$ (5.27a)

2. $[G_2(s)H_1(s)][G_4(s)G_5(s)H_3(s)]$ $\qquad\qquad\qquad\qquad\qquad\qquad\quad$ (5.27b)

3. $[G_2(s)H_1(s)][G_4(s)G_6(s)H_3(s)]$ $\qquad\qquad\qquad\qquad\qquad\qquad\quad$ (5.27c)

The product of loop gains $[G_4(s)G_5(s)H_3(s)][G_4(s)G_6(s)H_3(s)]$ is not a nontouching-loop gain since these two loops have nodes in common. In our example there are no nontouching-loop gains taken three at a time since three nontouching loops do not exist in the example.

We are now ready to state Mason's rule.

Mason's Rule

The transfer function, $C(s)/R(s)$, of a system represented by a signal-flow graph is

$$G(s) = \frac{C(s)}{R(s)} = \frac{\sum_k T_k \Delta_k}{\Delta}$$ (5.28)

where

k = number of forward paths
T_k = the kth forward-path gain
Δ = $1 - \Sigma$ loop gains $+ \Sigma$ nontouching-loop gains taken two at a time $- \Sigma$ nontouching-loop gains taken three at a time $+ \Sigma$ nontouching-loop gains taken four at a time $- \ldots$
Δ_k = $\Delta - \Sigma$ loop gain terms in Δ that touch the kth forward path. In other words, Δ_k is formed by eliminating from Δ those loop gains that touch the kth forward path.

Notice the alternating signs for the components of Δ. The following example will help clarify Mason's rule.

Example 5.7

Transfer Function via Mason's Rule

PROBLEM: Find the transfer function, $C(s)/R(s)$, for the signal-flow graph in Figure 5.21.
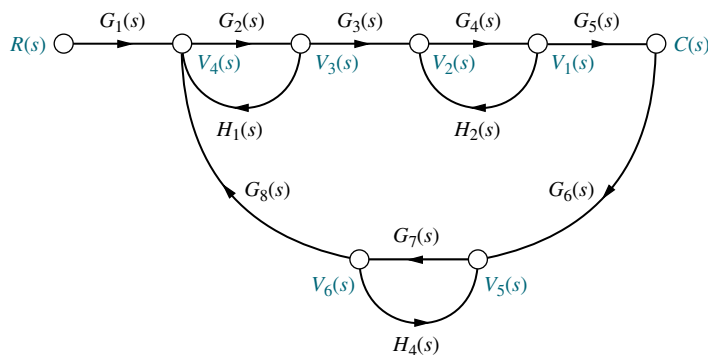
FIGURE 5.21 Signal-flow graph for Example 5.7

SOLUTION: First, identify the *forward-path gains*. In this example there is only one:

$$G_1(s)G_2(s)G_3(s)G_4(s)G_5(s) \tag{5.29}$$

Second, identify the *loop gains*. There are four, as follows:

1. $G_2(s)H_1(s)$ (5.30a)

2. $G_4(s)H_2(s)$ (5.30b)

3. $G_7(s)H_4(s)$ (5.30c)

4. $G_2(s)G_3(s)G_4(s)G_5(s)G_6(s)G_7(s)G_8(s)$ (5.30d)

Third, identify the *nontouching loops taken two at a time*. From Eqs. (5.30) and Figure 5.21, we can see that loop 1 does not touch loop 2, loop 1 does not touch loop 3, and loop 2 does not touch loop 3. Notice that loops 1, 2, and 3 all touch loop 4. Thus, the combinations of nontouching loops taken two at a time are as follows:

$$\text{Loop 1 and loop 2}: \ G_2(s)H_1(s)G_4(s)H_2(s) \tag{5.31a}$$

$$\text{Loop 1 and loop 3}: \ G_2(s)H_1(s)G_7(s)H_4(s) \tag{5.31b}$$

$$\text{Loop 2 and loop 3}: \ G_4(s)H_2(s)G_7(s)H_4(s) \tag{5.31c}$$

Finally, the *nontouching loops taken three at a time* are as follows:

$$\text{Loops 1, 2, and 3}: \ G_2(s)H_1(s)G_4(s)H_2(s)G_7(s)H_4(s) \tag{5.32}$$

Now, from Eq. (5.28) and its definitions, we form Δ and Δ_k. Hence,

$$\begin{aligned}
\Delta = 1 &-[G_2(s)H_1(s) + G_4(s)H_2(s) + G_7(s)H_4(s) \\
&\qquad\qquad + G_2(s)G_3(s)G_4(s)G_5(s)G_6(s)G_7(s)G_8(s)] \\
&+[G_2(s)H_1(s)G_4(s)H_2(s) + G_2(s)H_1(s)G_7(s)H_4(s) \\
&\qquad\qquad + G_4(s)H_2(s)G_7(s)H_4(s)] \\
&-[G_2(s)H_1(s)G_4(s)H_2(s)G_7(s)H_4(s)]
\end{aligned} \tag{5.33}$$

We form Δ_k by eliminating from Δ the loop gains that touch the kth forward path:

$$\Delta_1 = 1 - G_7(s)H_4(s) \tag{5.34}$$

Expressions (5.29), (5.33), and (5.34) are now substituted into Eq. (5.28), yielding the transfer function:

$$G(s) = \frac{T_1\Delta_1}{\Delta} = \frac{[G_1(s)G_2(s)G_3(s)G_4(s)G_5(s)][1 - G_7(s)H_4(s)]}{\Delta} \tag{5.35}$$

Since there is only one forward path, $G(s)$ consists of only one term, rather than a sum of terms, each coming from a forward path.

Skill-Assessment Exercise 5.4

PROBLEM: Use Mason's rule to find the transfer function of the signal-flow diagram shown in Figure 5.19(*c*). Notice that this is the same system used in Example 5.2 to find the transfer function via block diagram reduction.

ANSWER:

$$T(s) = \frac{G_1(s)G_3(s)[1 + G_2(s)]}{[1 + G_2(s)H_2(s) + G_1(s)G_2(s)H_1(s)][1 + G_3(s)H_3(s)]}$$

The complete solution is at www.wiley.com/college/nise.

5.6 Signal-Flow Graphs of State Equations

State Space

SS

In this section, we draw signal-flow graphs from state equations. At first this process will help us visualize state variables. Later we will draw signal-flow graphs and then write alternate representations of a system in state space.

Consider the following state and output equations:

$$\dot{x}_1 = 2x_1 - 5x_2 + 3x_3 + 2r \tag{5.36a}$$

$$\dot{x}_2 = -6x_1 - 2x_2 + 2x_3 + 5r \tag{5.36b}$$

$$\dot{x}_3 = x_1 - 3x_2 - 4x_3 + 7r \tag{5.36c}$$

$$y = -4x_1 + 6x_2 + 9x_3 \tag{5.36d}$$

First, identify three nodes to be the three state variables, x_1, x_2, and x_3; also identify three nodes, placed to the left of each respective state variable, to be the derivatives of the state variables, as in Figure 5.22(*a*). Also identify a node as the input, *r*, and another node as the output, *y*.

Next interconnect the state variables and their derivatives with the defining integration, $1/s$, as shown in Figure 5.22(*b*). Then using Eqs. (5.36), feed to each node the indicated signals. For example, from Eq. (5.36*a*), $\dot{x}_1$ receives $2x_1 - 5x_2 + 3x_3 + 2r$, as shown in Figure 5.22(*c*). Similarly, $\dot{x}_2$ receives $-6x_1 - 2x_2 + 2x_3 + 5r$, as shown in Figure 5.22(*d*), and $\dot{x}_3$ receives $x_1 - 3x_2 - 4x_3 + 7r$, as shown in Figure 5.22(*e*). Finally, using Eq. (5.36*d*), the output, *y*, receives $-4x_1 + 6x_2 + 9x_3$, as shown in Figure 5.19(*f*), the final phase-variable representation, where the state variables are the outputs of the integrators.
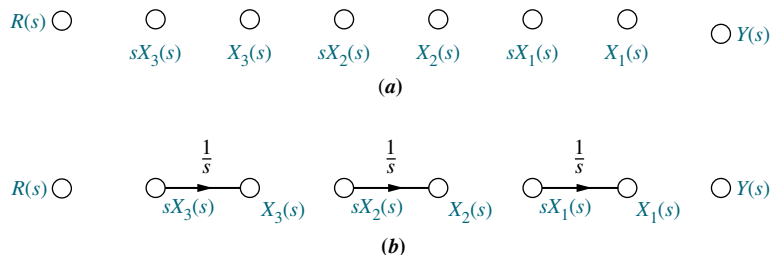
FIGURE 5.22   Stages of development of a signal-flow graph for the system of Eqs. (5.36):
a. Place nodes; **b.** interconnect state variables and derivatives; (*figure continues*)
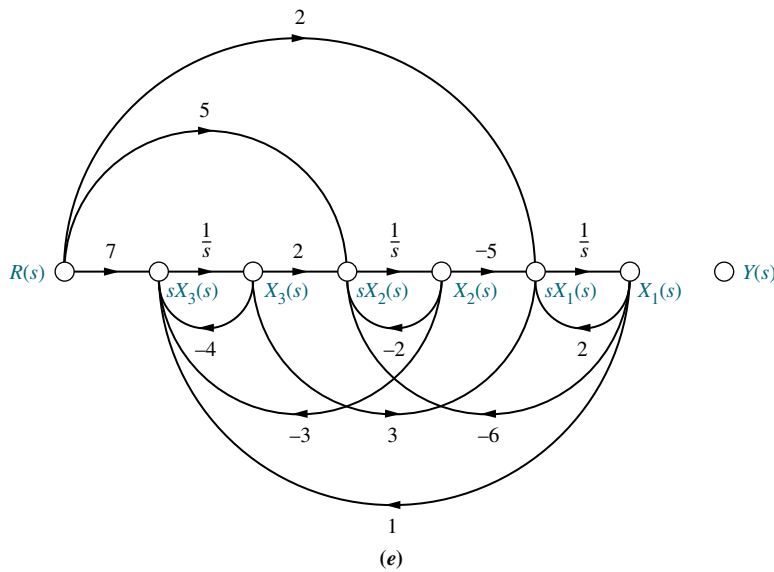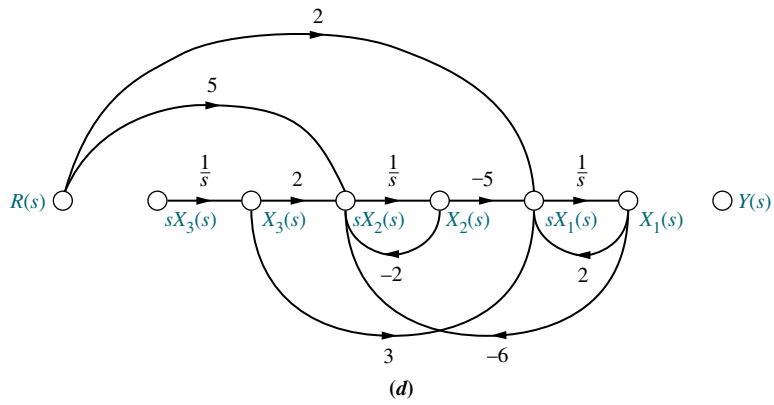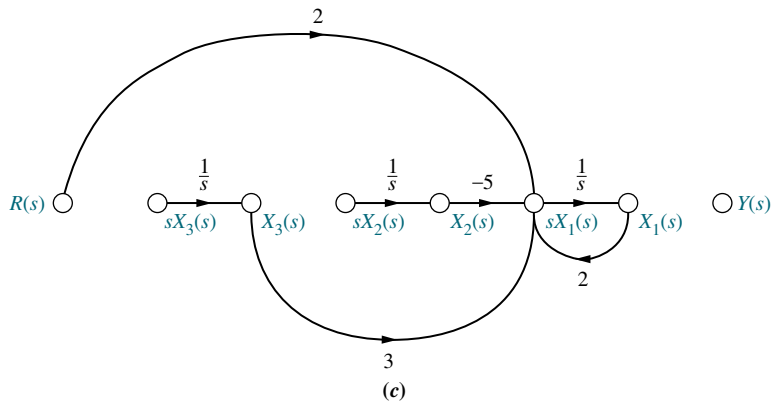
FIGURE 5.22 (*Continued*) **c.** form dx_1/dt; **d.** form dx_2/dt; **e.** form dx_3/dt; (*figure continues*)
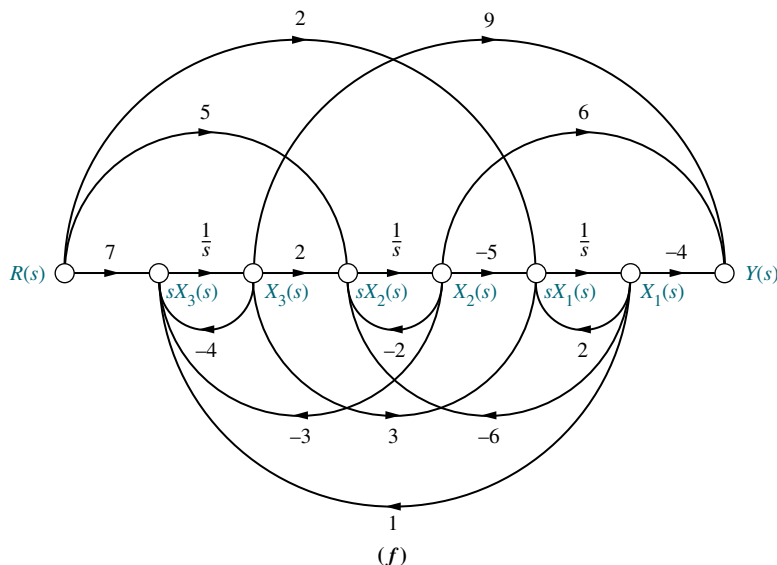
FIGURE 5.22   (*Continued*) **f.** form output (*figure end*)

Skill-Assessment Exercise 5.5

PROBLEM: Draw a signal-flow graph for the following state and output equations:

$$\dot{\mathbf{x}} = \begin{bmatrix} -2 & 1 & 0 \\ 0 & -3 & 1 \\ -3 & -4 & -5 \end{bmatrix} \mathbf{x} + \begin{bmatrix} 0 \\ 0 \\ 1 \end{bmatrix} r$$

$$y = \begin{bmatrix} 0 & 1 & 0 \end{bmatrix} \mathbf{x}$$

ANSWER: The complete solution is at www.wiley.com/college/nise.

In the next section, the signal-flow model will help us visualize the process of determining alternative representations in state space of the same system. We will see that even though a system can be the same with respect to its input and output terminals, the state-space representations can be many and varied.

5.7   Alternative Representations in State Space

State Space
SS

In Chapter 3, systems were represented in state space in phase-variable form. However, system modeling in state space can take on many representations other than the phase-variable form. Although each of these models yields the same output for a given input, an engineer may prefer a particular one for several reasons. For example, one set of state variables, with its unique representation, can model actual physical variables of a system, such as amplifier and filter outputs.

Another motive for choosing a particular set of state variables and state-space model is ease of solution. As we will see, a particular choice of state variables can decouple the system of simultaneous differential equations. Here each equation is written in terms of only one state variable, and the solution is effected by solving n first-order differential equations individually.

Ease of modeling is another reason for a particular choice of state variables. Certain choices may facilitate converting the subsystem to the state-variable representation by using recognizable features of the model. The engineer learns quickly how to write the state and output equations and draw the signal-flow graph, both by inspection. These converted subsystems generate the definition of the state variables.

We will now look at a few representative forms and show how to generate the state-space representation for each.

Cascade Form

We have seen that systems can be represented in state space with the state variables chosen to be the phase variables, that is, variables that are successive derivatives of each other. This is by no means the only choice. Returning to the system of Figure 3.10(a), the transfer function can be represented alternately as

$$\frac{C(s)}{R(s)} = \frac{24}{(s+2)(s+3)(s+4)} \tag{5.37}$$

Figure 5.23 shows a block diagram representation of this system formed by cascading each term of Eq. (5.37). The output of each first-order system block has been labeled as a state variable. These state variables are not the phase variables.
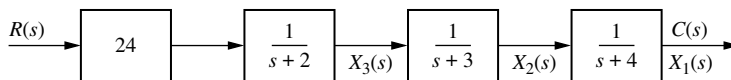
FIGURE 5.23   Representation of Figure 3.10 system as cascaded first-order systems

We now show how the signal-flow graph can be used to obtain a state-space representation of this system. In order to write the state equations with our new set of state variables, it is helpful to draw a signal-flow graph first, using Figure 5.23 as a guide. The signal flow for each first-order system of Figure 5.23 can be found by transforming each block into an equivalent differential equation. Each first-order block is of the form

$$\frac{C_i(s)}{R_i(s)} = \frac{1}{(s+a_i)} \tag{5.38}$$

Cross-multiplying, we get

$$(s+a_i)C_i(s) = R_i(s) \tag{5.39}$$

After taking the inverse Laplace transform, we have

$$\frac{dc_i(t)}{dt} + a_i c_i(t) = r_i(t) \tag{5.40}$$

Solving for $dc_i(t)/dt$ yields

$$\frac{dc_i(t)}{dt} = -a_i c_i(t) + r_i(t) \tag{5.41}$$
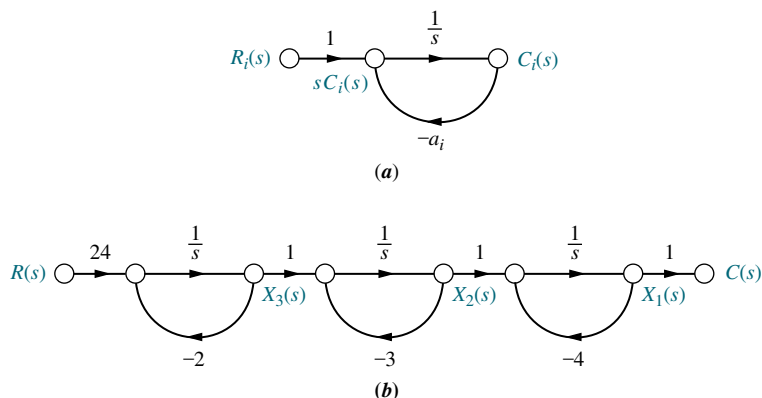
FIGURE 5.24 **a.** First-order subsystem; **b.** Signal-flow graph for Figure 5.23 system

Figure 5.24(*a*) shows the implementation of Eq. (5.41) as a signal-flow graph. Here again, a node was assumed for $c_i(t)$ at the output of an integrator, and its derivative was formed at the input.

Cascading the transfer functions shown in Figure 5.24(*a*), we arrive at the system representation shown in Figure 5.24(*b*).[2] Now write the state equations for the new representation of the system. Remember that the derivative of a state variable will be at the input to each integrator:

$$\dot{x}_1 = -4x_1 + x_2 \tag{5.42a}$$

$$\dot{x}_2 = \qquad -3x_2 + x_3 \tag{5.42b}$$

$$\dot{x}_3 = \qquad\qquad -2x_3 + 24r \tag{5.42c}$$

The output equation is written by inspection from Figure 5.24(*b*):

$$y = c(t) = x_1 \tag{5.43}$$

The state-space representation is completed by rewriting Eqs. (5.42) and (5.43) in vector-matrix form:

$$\dot{\mathbf{x}} = \begin{bmatrix} -4 & 1 & 0 \\ 0 & -3 & 1 \\ 0 & 0 & -2 \end{bmatrix} \mathbf{x} + \begin{bmatrix} 0 \\ 0 \\ 24 \end{bmatrix} r \tag{5.44a}$$

$$y = \begin{bmatrix} 1 & 0 & 0 \end{bmatrix} \mathbf{x} \tag{5.44b}$$

Comparing Eqs. (5.44) with Figure 5.24(*b*), you can form a vivid picture of the meaning of some of the components of the state equation. For the following discussion, please refer back to the general form of the state and output equations, Eqs. (3.18) and (3.19).

For example, the **B** matrix is the input matrix since it contains the terms that couple the input, $r(t)$, to the system. In particular, the constant 24 appears in both the signal-flow graph at the input, as shown in Figure 5.24(*b*), and the input matrix in Eqs. (5.44). The **C** matrix is the output matrix since it contains the constant that couples the state variable, x_1, to the output, $c(t)$. Finally, the **A** matrix is the system

---

[2] Note that node $X_3(s)$ and the following node cannot be merged, or else the input to the first integrator would be changed by the feedback from $X_2(s)$, and the signal $X_3(s)$ would be lost. A similar argument can be made for $X_2(s)$ and the following node.

matrix since it contains the terms relative to the internal system itself. In the form of Eqs. (5.44), the system matrix actually contains the system poles along the diagonal.

Compare Eqs. (5.44) to the phase-variable representation in Eqs. (3.59). In that representation, the coefficients of the system's characteristic polynomial appeared along the last row, whereas in our current representation, the roots of the characteristic equation, the system poles, appear along the diagonal.

Parallel Form

Another form that can be used to represent a system is the parallel form. This form leads to an **A** matrix that is purely diagonal, provided that no system pole is a repeated root of the characteristic equation.

Whereas the previous form was arrived at by cascading the individual first-order subsystems, the parallel form is derived from a partial-fraction expansion of the system transfer function. Performing a partial-fraction expansion on our example system, we get

$$\frac{C(s)}{R(s)} = \frac{24}{(s+2)(s+3)(s+4)} = \frac{12}{(s+2)} - \frac{24}{(s+3)} + \frac{12}{(s+4)} \tag{5.45}$$

Equation (5.45) represents the sum of the individual first-order subsystems. To arrive at a signal-flow graph, first solve for $C(s)$,

$$C(s) = R(s)\frac{12}{(s+2)} - R(s)\frac{24}{(s+3)} + R(s)\frac{12}{(s+4)} \tag{5.46}$$

and recognize that $C(s)$ is the sum of three terms. Each term is a first-order subsystem with $R(s)$ as the input. Formulating this idea as a signal-flow graph renders the representation shown in Figure 5.25.

Once again, we use the signal-flow graph as an aid to obtaining the state equations. By inspection the state variables are the outputs of each integrator, where the derivatives of the state variables exist at the integrator inputs. We write the state equations by summing the signals at the integrator inputs:

$$\dot{x}_1 = -2x_1 \qquad\qquad\qquad + 12r \tag{5.47a}$$

$$\dot{x}_2 = \qquad -3x_2 \qquad - 24r \tag{5.47b}$$

$$\dot{x}_3 = \qquad\qquad -4x_3 + 12r \tag{5.47c}$$

FIGURE 5.25   Signal-flow representation of Eq. (5.45)

The output equation is found by summing the signals that give $c(t)$:

$$y = c(t) = x_1 + x_2 + x_3 \tag{5.48}$$

In vector-matrix form, Eqs. (5.47) and (5.48) become

$$\dot{\mathbf{x}} = \begin{bmatrix} -2 & 0 & 0 \\ 0 & -3 & 0 \\ 0 & 0 & -4 \end{bmatrix} \mathbf{x} + \begin{bmatrix} 12 \\ -24 \\ 12 \end{bmatrix} r \tag{5.49}$$

and

$$y = \begin{bmatrix} 1 & 1 & 1 \end{bmatrix} \mathbf{x} \tag{5.50}$$

Thus, our third representation of the system of Figure 3.10(a) yields a diagonal system matrix. What is the advantage of this representation? Each equation is a

first-order differential equation in only one variable. Thus, we would solve these equations independently. The equations are said to be *decoupled*.

Students who are using MATLAB should now run ch5p3 in Appendix B. You will learn how to use MATLAB to convert a transfer function to state space in a specified form. The exercise solves the previous example by representing the transfer function in Eq. (5.45) by the state-space representation in parallel form of Eq. (5.49).

If the denominator of the transfer function has repeated real roots, the parallel form can still be derived from a partial-fraction expansion. However, the system matrix will not be diagonal. For example, assume the system

$$\frac{C(s)}{R(s)} = \frac{(s+3)}{(s+1)^2(s+2)} \tag{5.51}$$

which can be expanded as partial fractions:

$$\frac{C(s)}{R(s)} = \frac{2}{(s+1)^2} - \frac{1}{(s+1)} + \frac{1}{(s+2)} \tag{5.52}$$

Proceeding as before, the signal-flow graph for Eq. (5.52) is shown in Figure 5.26. The term $-1/(s+1)$ was formed by creating the signal flow from $X_2(s)$ to $C(s)$. Now the state and output equations can be written by inspection from Figure 5.26 as follows:

$$\dot{x}_1 = -x_1 \quad + x_2 \tag{5.53a}$$

$$\dot{x}_2 = \quad - x_2 \quad + 2r \tag{5.53b}$$

$$\dot{x}_3 = \quad - 2x_3 + r \tag{5.53c}$$

$$y = c(t) = \quad x_1 \quad -\frac{1}{2}x_2 \quad + x_3 \tag{5.53d}$$

or, in vector-matrix form,

$$\dot{\mathbf{x}} = \begin{bmatrix} -1 & 1 & 0 \\ 0 & -1 & 0 \\ 0 & 0 & -2 \end{bmatrix} \mathbf{x} + \begin{bmatrix} 0 \\ 2 \\ 1 \end{bmatrix} r \tag{5.54a}$$

$$y = \begin{bmatrix} 1 & -\frac{1}{2} & 1 \end{bmatrix} \mathbf{x} \tag{5.54b}$$

FIGURE 5.26 Signal-flow representation of Eq. (5.52)

This system matrix, although not diagonal, has the system poles along the diagonal. Notice the 1 off the diagonal for the case of the repeated root. The form of the system matrix is known as the *Jordan canonical form*.

Controller Canonical Form

Another representation that uses phase variables is called the *controller canonical form*, so named for its use in the design of controllers, which is covered in Chapter 12. This form is obtained from the phase-variable form simply by ordering the phase variables in the reverse order. For example, consider the transfer function

$$G(s) = \frac{C(s)}{R(s)} = \frac{s^2 + 7s + 2}{s^3 + 9s^2 + 26s + 24} \tag{5.55}$$

The phase-variable form was derived in Example 3.5 as

$$
\begin{bmatrix} \dot{x}_1 \\ \dot{x}_2 \\ \dot{x}_3 \end{bmatrix} = \begin{bmatrix} 0 & 1 & 0 \\ 0 & 0 & 1 \\ -24 & -26 & -9 \end{bmatrix} \begin{bmatrix} x_1 \\ x_2 \\ x_3 \end{bmatrix} + \begin{bmatrix} 0 \\ 0 \\ 1 \end{bmatrix} r \tag{5.56a}
$$

$$
y = \begin{bmatrix} 2 & 7 & 1 \end{bmatrix} \begin{bmatrix} x_1 \\ x_2 \\ x_3 \end{bmatrix} \tag{5.56b}
$$

where $y = c(t)$. Renumbering the phase variables in reverse order yields

$$
\begin{bmatrix} \dot{x}_3 \\ \dot{x}_2 \\ \dot{x}_1 \end{bmatrix} = \begin{bmatrix} 0 & 1 & 0 \\ 0 & 0 & 1 \\ -24 & -26 & -9 \end{bmatrix} \begin{bmatrix} x_3 \\ x_2 \\ x_1 \end{bmatrix} + \begin{bmatrix} 0 \\ 0 \\ 1 \end{bmatrix} r \tag{5.57a}
$$

$$
y = \begin{bmatrix} 2 & 7 & 1 \end{bmatrix} \begin{bmatrix} x_3 \\ x_2 \\ x_1 \end{bmatrix} \tag{5.57b}
$$

Finally, rearranging Eqs. (5.57) in ascending numerical order yields the controller canonical form[3] as

$$
\begin{bmatrix} \dot{x}_1 \\ \dot{x}_2 \\ \dot{x}_3 \end{bmatrix} = \begin{bmatrix} -9 & -26 & -24 \\ 1 & 0 & 0 \\ 0 & 1 & 0 \end{bmatrix} \begin{bmatrix} x_1 \\ x_2 \\ x_3 \end{bmatrix} + \begin{bmatrix} 1 \\ 0 \\ 0 \end{bmatrix} r \tag{5.58a}
$$

$$
y = \begin{bmatrix} 1 & 7 & 2 \end{bmatrix} \begin{bmatrix} x_1 \\ x_2 \\ x_3 \end{bmatrix} \tag{5.58b}
$$

Figure 5.27 shows the steps we have taken on a signal-flow graph. Notice that the controller canonical form is obtained simply by renumbering the phase variables in the opposite order. Equations (5.56) can be obtained from Figure 5.27(*a*), and Eqs. (5.58) from Figure 5.27(*b*).

Notice that the phase-variable form and the controller canonical form contain the coefficients of the characteristic polynomial in the bottom row and in the top row,
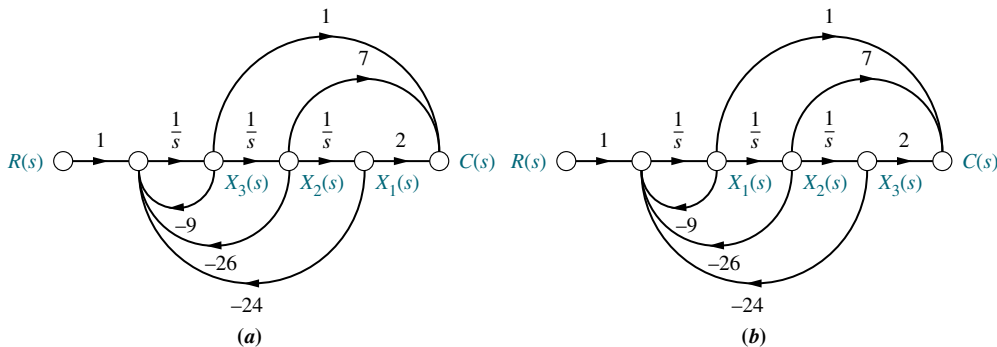
FIGURE 5.27   Signal-flow graphs for obtaining forms for $G(s) = C(s)/R(s) = (s^2 + 7s + 2)/(s^3 + 9s^2 + 26s + 24)$: **a.** phase-variable form; **b.** controller canonical form

---

[3] Students who are using MATLAB to convert from transfer functions to state space using the command **tf2ss** will notice that MATLAB reports the results in controller canonical form.

respectively. System matrices that contain the coefficients of the characteristic polynomial are called *companion matrices* to the characteristic polynomial. The phase-variable and controller canonical forms result in a lower and an upper companion system matrix, respectively. Companion matrices can also have the coefficients of the characteristic polynomial in the left or right column. In the next subsection, we discuss one of these representations.

Observer Canonical Form

The *observer canonical form*, so named for its use in the design of observers (covered in Chapter 12), is a representation that yields a left companion system matrix. As an example, the system modeled by Eq. (5.55) will be represented in this form. Begin by dividing all terms in the numerator and denominator by the highest power of s, s^3, and obtain

$$\frac{C(s)}{R(s)} = \frac{\dfrac{1}{s} + \dfrac{7}{s^2} + \dfrac{2}{s^3}}{1 + \dfrac{9}{s} + \dfrac{26}{s^2} + \dfrac{24}{s^3}} \tag{5.59}$$

Cross-multiplying yields

$$\left[\frac{1}{s} + \frac{7}{s^2} + \frac{2}{s^3}\right] R(s) = \left[1 + \frac{9}{s} + \frac{26}{s^2} + \frac{24}{s^3}\right] C(s) \tag{5.60}$$

Combining terms of like powers of integration gives

$$C(s) = \frac{1}{s}[R(s) - 9C(s)] + \frac{1}{s^2}[7R(s) - 26C(s)] + \frac{1}{s^3}[2R(s) - 24C(s)] \tag{5.61}$$

or

$$C(s) = \frac{1}{s}\left[[R(s) - 9C(s)] + \frac{1}{s}\left([7R(s) - 26C(s)] + \frac{1}{s}[2R(s) - 24C(s)]\right)\right] \tag{5.62}$$

Equation (5.61) or (5.62) can be used to draw the signal-flow graph. Start with three integrations, as shown in Figure 5.28(*a*).

Using Eq. (5.61), the first term tells us that output $C(s)$ is formed, in part, by integrating $[R(s) - 9C(s)]$. We thus form $[R(s) - 9C(s)]$ at the input to the integrator closest to the output, $C(s)$, as shown in Figure 5.28(*b*). The second term tells us that the
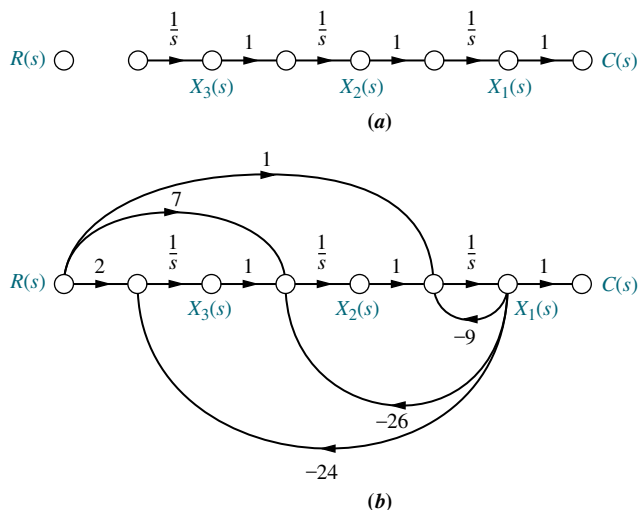
FIGURE 5.28 Signal-flow graph for observer canonical form variables: **a.** planning; **b.** implementation

term $[7R(s) - 26C(s)]$ must be integrated twice. Now form $[7R(s) - 26C(s)]$ at the input to the second integrator. Finally, the last term of Eq. (5.61) says $[2R(s) - 24C(s)]$ must be integrated three times. Form $[2R(s) - 24C(s)]$ at the input to the first integrator.

Identifying the state variables as the outputs of the integrators, we write the following state equations:

$$\dot{x}_1 = -9x_1 + x_2 \qquad\qquad + r \qquad\qquad (5.63a)$$

$$\dot{x}_2 = -26x_1 \qquad\quad + x_3 + 7r \qquad\qquad (5.63b)$$

$$\dot{x}_3 = -24x_1 \qquad\qquad\quad + 2r \qquad\qquad (5.63c)$$

The output equation from Figure 5.28(b) is

$$y = c(t) = x_1 \qquad\qquad (5.64)$$

In vector-matrix form, Eqs. (5.63) and (5.64) become

$$\dot{\mathbf{x}} = \begin{bmatrix} -9 & 1 & 0 \\ -26 & 0 & 1 \\ -24 & 0 & 0 \end{bmatrix} \mathbf{x} + \begin{bmatrix} 1 \\ 7 \\ 2 \end{bmatrix} r \qquad\qquad (5.65a)$$

$$y = \begin{bmatrix} 1 & 0 & 0 \end{bmatrix} \mathbf{x} \qquad\qquad (5.65b)$$

Notice that the form of Eqs. (5.65) is similar to the phase-variable form, except that the coefficients of the denominator of the transfer function are in the first column, and the coefficients of the numerator form the input matrix, **B**. Also notice that the observer canonical form has an **A** matrix that is the transpose of the controller canonical form, a **B** vector that is the transpose of the controller canonical form's **C** vector, and a **C** vector that is the transpose of the controller canonical form's **B** vector. We therefore say that these two forms are *duals*. Thus, if a system is described by **A, B,** and **C**, its dual is described by $\mathbf{A_D} = \mathbf{A}^T$, $\mathbf{B_D} = \mathbf{C}^T$, $\mathbf{C_D} = \mathbf{B}^T$. You can verify the significance of duality by comparing the signal-flow graphs of a system and its dual, Figures 5.27(b) and 5.28(b), respectively. The signal-flow graph of the dual can be obtained from that of the original by reversing all arrows, changing state variables to their derivatives and vice versa, and interchanging $C(s)$ and $R(s)$, thus reversing the roles of the input and the output.

We conclude this section with an example that demonstrates the application of the previously discussed forms to a feedback control system.

Example 5.8

State-Space Representation of Feedback Systems

PROBLEM: Represent the feedback control system shown in Figure 5.29 in state space. Model the forward transfer function in cascade form.

FIGURE 5.29 Feedback control system for Example 5.8

SOLUTION: First we model the forward transfer function in cascade form. The gain of 100, the pole at -2, and the pole at -3 are shown cascaded in Figure 5.30(a). The zero at -5 was obtained using the method for implementing zeros for a system represented in phase-variable form, as discussed in Section 3.5.

Next add the feedback and input paths, as shown in Figure 5.30(b). Now, by inspection, write the state equations:

$$\dot{x}_1 = -3x_1 + x_2 \qquad\qquad (5.66a)$$

$$\dot{x}_2 = \qquad\quad -2x_2 + 100(r - c) \qquad\qquad (5.66b)$$

FIGURE 5.30 Creating a signal-flow graph for the Figure 5.29 system: **a.** forward transfer function; **b.** complete system

But, from Figure 5.30(b),

$$c = 5x_1 + (x_2 - 3x_1) = 2x_1 + x_2 \tag{5.67}$$

Substituting Eq. (5.67) into (5.66b), we find the state equations for the system:

$$\dot{x}_1 = \quad -3x_1 \quad + x_2 \tag{5.68a}$$

$$\dot{x}_2 = -200x_1 - 102x_2 + 100r \tag{5.68b}$$

The output equation is the same as Eq. (5.67), or

$$y = c(t) = 2x_1 + x_2 \tag{5.69}$$

In vector-matrix form

$$\dot{\mathbf{x}} = \begin{bmatrix} -3 & 1 \\ -200 & -102 \end{bmatrix} \mathbf{x} + \begin{bmatrix} 0 \\ 100 \end{bmatrix} r \tag{5.70a}$$

$$y = [\,2 \quad 1\,]\mathbf{x} \tag{5.70b}$$

Skill-Assessment Exercise 5.6

PROBLEM: Represent the feedback control system shown in Figure 5.29 in state space. Model the forward transfer function in controller canonical form.

ANSWER:

$$\dot{\mathbf{x}} = \begin{bmatrix} -105 & -506 \\ 1 & 0 \end{bmatrix} \mathbf{x} + \begin{bmatrix} 1 \\ 0 \end{bmatrix} r$$

$$y = [\,100 \quad 500\,]\mathbf{x}$$

The complete solution is at www.wiley.com/college/nise.

In this section, we used transfer functions and signal-flow graphs to represent systems in parallel, cascade, controller canonical, and observer canonical forms, in addition to the phase-variable form. Using the transfer function $C(s)/R(s) = (s+3)/[(s+4)(s+6)]$ as an example, Figure 5.31 compares the aforementioned forms. Notice the duality of the controller and observer canonical forms, as demonstrated by their respective signal-flow graphs and state equations. In the next section, we will explore the possibility of transforming between representations without using transfer functions and signal-flow graphs.

Form	Transfer function	Signal-flow diagram	State equations
Phase variable	$\dfrac{1}{(s^2 + 10s + 24)} * (s+3)$		$\dot{\mathbf{x}} = \begin{bmatrix} 0 & 1 \\ -24 & -10 \end{bmatrix}\mathbf{x} + \begin{bmatrix} 0 \\ 1 \end{bmatrix}r$ $y = [3\ 1]\,\mathbf{x}$
Parallel	$\dfrac{-1/2}{(s+4)} + \dfrac{3/2}{s+6}$		$\dot{\mathbf{x}} = \begin{bmatrix} -4 & 0 \\ 0 & -6 \end{bmatrix}\mathbf{x} + \begin{bmatrix} -\frac{1}{2} \\ \frac{3}{2} \end{bmatrix}r$ $y = [1\ 1]\,\mathbf{x}$
Cascade	$\dfrac{1}{(s+4)} * \dfrac{(s+3)}{(s+6)}$		$\dot{\mathbf{x}} = \begin{bmatrix} -6 & 1 \\ 0 & -4 \end{bmatrix}\mathbf{x} + \begin{bmatrix} 0 \\ 1 \end{bmatrix}r$ $y = [-3\ 1]\,\mathbf{x}$
Controller canonical	$\dfrac{1}{(s^2 + 10s + 24)} * (s+3)$		$\dot{\mathbf{x}} = \begin{bmatrix} -10 & -24 \\ 1 & 0 \end{bmatrix}\mathbf{x} + \begin{bmatrix} 1 \\ 0 \end{bmatrix}r$ $y = [1\ 3]\,\mathbf{x}$
Observer canonical	$\dfrac{\dfrac{1}{s} + \dfrac{3}{s^2}}{1 + \dfrac{10}{s} + \dfrac{24}{s^2}}$		$\dot{\mathbf{x}} = \begin{bmatrix} -10 & 1 \\ -24 & 0 \end{bmatrix}\mathbf{x} + \begin{bmatrix} 1 \\ 3 \end{bmatrix}r$ $y = [1\ 0]\,\mathbf{x}$

FIGURE 5.31   State-space forms for $C(s)/R(s) = (s+3)/[(s+4)(s+6)]$. Note: $y = c(t)$

5.8   Similarity Transformations

In Section 5.7, we saw that systems can be represented with different state variables even though the transfer function relating the output to the input remains the same. The various forms of the state equations were found by manipulating the transfer function, drawing a signal-flow graph, and then writing the state equations from the signal-flow graph. These systems are called *similar systems*. Although their state-space representations are different, similar systems have the same transfer function and hence the same poles and eigenvalues.

We can make transformations between similar systems from one set of state equations to another without using the transfer function and signal-flow graphs. The results are presented in this section along with examples. Students who have not broached this subject in the past or who wish to refresh their memories are encouraged to study Appendix L at www.wiley.com/college/nise for the derivation. The result of the derivation states: A system represented in state space as

$$\mathbf{x} = \mathbf{Ax} + \mathbf{Bu} \tag{5.71a}$$

$$\mathbf{y} = \mathbf{Cx} + \mathbf{Du} \tag{5.71b}$$

can be transformed to a similar system,

$$\mathbf{z} = \mathbf{P}^{-1}\mathbf{APz} + \mathbf{P}^{-1}\mathbf{Bu} \tag{5.72a}$$

$$\mathbf{y} = \mathbf{CPz} + \mathbf{Du} \tag{5.72b}$$

where, for 2-space,

$$\mathbf{P} = [\mathbf{U}_{z_1}\,\mathbf{U}_{z_2}] = \begin{bmatrix} p_{11} & p_{12} \\ p_{21} & p_{22} \end{bmatrix} \tag{5.72c}$$

$$\mathbf{x} = \begin{bmatrix} p_{11} & p_{12} \\ p_{21} & p_{22} \end{bmatrix} \begin{bmatrix} z_1 \\ z_2 \end{bmatrix} = \mathbf{Pz} \tag{5.72d}$$

and

$$\mathbf{z} = \mathbf{P}^{-1}\mathbf{x} \tag{5.72e}$$

Thus, **P** is a transformation matrix whose columns are the coordinates of the basis vectors of the $z_1 z_2$ space expressed as linear combinations of the $x_1 x_2$ space. Let us look at an example.

Example 5.9

Similarity Transformations on State Equations

PROBLEM: Given the system represented in state space by Eqs. (5.73),

$$\dot{\mathbf{x}} = \begin{bmatrix} 0 & 1 & 0 \\ 0 & 0 & 1 \\ -2 & -5 & -7 \end{bmatrix} \mathbf{x} + \begin{bmatrix} 0 \\ 0 \\ 1 \end{bmatrix} u \tag{5.73a}$$

$$y = \begin{bmatrix} 1 & 0 & 0 \end{bmatrix} \mathbf{x} \tag{5.73b}$$

transform the system to a new set of state variables, $\mathbf{z}$, where the new state variables are related to the original state variables, $\mathbf{x}$, as follows:

$$z_1 = 2x_1 \tag{5.74a}$$

$$z_2 = 3x_1 + 2x_2 \tag{5.74b}$$

$$z_3 = x_1 + 4x_2 + 5x_3 \tag{5.74c}$$

SOLUTION: Expressing Eqs. (5.74) in vector-matrix form,

$$\mathbf{z} = \begin{bmatrix} 2 & 0 & 0 \\ 3 & 2 & 0 \\ 1 & 4 & 5 \end{bmatrix} \mathbf{x} = \mathbf{P}^{-1}\mathbf{x} \tag{5.75}$$

Using Eqs. (5.72) as a guide,

$$\mathbf{P}^{-1}\mathbf{AP} = \begin{bmatrix} 2 & 0 & 0 \\ 3 & 2 & 0 \\ 1 & 4 & 5 \end{bmatrix} \begin{bmatrix} 0 & 1 & 0 \\ 0 & 0 & 1 \\ -2 & -5 & -7 \end{bmatrix} \begin{bmatrix} 0.5 & 0 & 0 \\ -0.75 & 0.5 & 0 \\ 0.5 & -0.4 & 0.2 \end{bmatrix}$$
$$= \begin{bmatrix} -1.5 & 1 & 0 \\ -1.25 & 0.7 & 0.4 \\ -2.5 & 0.4 & -6.2 \end{bmatrix} \tag{5.76}$$

$$\mathbf{P}^{-1}\mathbf{B} = \begin{bmatrix} 2 & 0 & 0 \\ 3 & 2 & 0 \\ 1 & 4 & 5 \end{bmatrix} \begin{bmatrix} 0 \\ 0 \\ 1 \end{bmatrix} = \begin{bmatrix} 0 \\ 0 \\ 5 \end{bmatrix} \tag{5.77}$$

$$\mathbf{CP} = \begin{bmatrix} 1 & 0 & 0 \end{bmatrix} \begin{bmatrix} 0.5 & 0 & 0 \\ -0.75 & 0.5 & 0 \\ 0.5 & -0.4 & 0.2 \end{bmatrix} = \begin{bmatrix} 0.5 & 0 & 0 \end{bmatrix} \tag{5.78}$$

Therefore, the transformed system is

$$\dot{\mathbf{z}} = \begin{bmatrix} -1.5 & 1 & 0 \\ -1.25 & 0.7 & 0.4 \\ -2.55 & 0.4 & -6.2 \end{bmatrix} \mathbf{z} + \begin{bmatrix} 0 \\ 0 \\ 5 \end{bmatrix} u \tag{5.79a}$$

$$y = \begin{bmatrix} 0.5 & 0 & 0 \end{bmatrix} \mathbf{z} \tag{5.79b}$$

MATLAB
ML

```
Students who are using MATLAB should now run ch5p4 in Appendix B.
You will learn how to perform similarity transformations. This
exercise uses MATLAB to do Example 5.9.
```

Thus far we have talked about transforming systems between basis vectors in a different state space. One major advantage of finding these similar systems is apparent in the transformation to a system that has a diagonal matrix.

Diagonalizing a System Matrix

In Section 5.7, we saw that the parallel form of a signal-flow graph can yield a diagonal system matrix. A diagonal system matrix has the advantage that each state equation is a function of only one state variable. Hence, each differential equation can be solved independently of the other equations. We say that the equations are *decoupled*.

Rather than using partial fraction expansion and signal-flow graphs, we can decouple a system using matrix transformations. If we find the correct matrix, **P**, the transformed system matrix, $\mathbf{P}^{-1}\mathbf{AP}$, will be a diagonal matrix. Thus, we are looking for a transformation to another state space that yields a diagonal matrix in that space. This new state space also has basis vectors that lie along its state variables. We give a special name to any vectors that are collinear with the basis vectors of the new system that yields a diagonal system matrix: they are called *eigenvectors*. Thus, the coordinates of the eigenvectors form the columns of the transformation matrix, **P**, as we demonstrate in Eq. L.7 in Appendix L at www.wiley.com/college/nise.

First, let us formally define eigenvectors from another perspective and then show that they have the property just described. Then we will define eigenvalues. Finally, we will show how to diagonalize a matrix.

Definitions

Eigenvector. The eigenvectors of the matrix **A** are all vectors, $\mathbf{x_i} \neq \mathbf{0}$, which under the transformation **A** become multiples of themselves; that is,

$$\mathbf{Ax_i} = \lambda_i \mathbf{x_i} \tag{5.80}$$

where λ_i's are constants.

Figure 5.32 shows this definition of eigenvectors. If **Ax** is not collinear with **x** after the transformation, as in Figure 5.32(*a*), **x** is not an eigenvector. If **Ax** is collinear with **x** after the transformation, as in Figure 5.32(*b*), **x** is an eigenvector.

Eigenvalue. The eigenvalues of the matrix **A** are the values of λ_i that satisfy Eq. (5.80) for $\mathbf{x_i} \neq \mathbf{0}$.

To find the eigenvectors, we rearrange Eq. (5.80). Eigenvectors, $\mathbf{x_i}$, satisfy

$$\mathbf{0} = (\lambda_i \mathbf{I} - \mathbf{A})\mathbf{x_i} \tag{5.81}$$
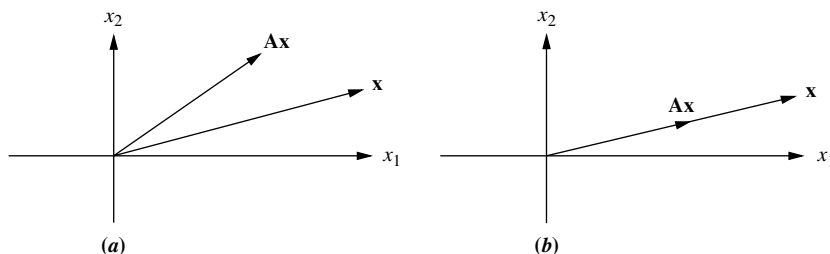
FIGURE 5.32   To be an eigenvector, the transformation **Ax** must be collinear with **x**; thus, in (*a*), **x** is not an eigenvector; in (*b*), it is

Solving for $\mathbf{x_i}$ by premultiplying both sides by $(\lambda_i\mathbf{I} - \mathbf{A})^{-1}$ yields

$$\mathbf{x_i} = (\lambda_i\mathbf{I} - \mathbf{A})^{-1}\mathbf{0} = \frac{\text{adj}(\lambda_i\mathbf{I} - \mathbf{A})}{\det(\lambda_i\mathbf{I} - \mathbf{A})}\mathbf{0} \qquad (5.82)$$

Since $\mathbf{x_i} \neq \mathbf{0}$, a nonzero solution exists if

$$\boxed{\det(\lambda_i\mathbf{I} - \mathbf{A}) = \mathbf{0}} \qquad (5.83)$$

from which λ_i, the eigenvalues, can be found.

We are now ready to show how to find the eigenvectors, $\mathbf{x_i}$. First we find the eigenvalues, λ_i, using $\det(\lambda_i\mathbf{I} - \mathbf{A}) = \mathbf{0}$, and then we use Eq. (5.80) to find the eigenvectors.

Example 5.10

Finding Eigenvectors

PROBLEM: Find the eigenvectors of the matrix

$$\mathbf{A} = \begin{bmatrix} -3 & 1 \\ 1 & -3 \end{bmatrix} \qquad (5.84)$$

SOLUTION: The eigenvectors, $\mathbf{x_i}$, satisfy Eq. (5.81). First, use $\det(\lambda_i\mathbf{I} - \mathbf{A}) = 0$ to find the eigenvalues, λ_i, for Eq. (5.81):

$$\begin{aligned} \det(\lambda\mathbf{I} - \mathbf{A}) &= \left| \begin{bmatrix} \lambda & 0 \\ 0 & \lambda \end{bmatrix} - \begin{bmatrix} -3 & 1 \\ 1 & -3 \end{bmatrix} \right| \\ &= \begin{vmatrix} \lambda + 3 & -1 \\ -1 & \lambda + 3 \end{vmatrix} \\ &= \lambda^2 + 6\lambda + 8 \end{aligned} \qquad (5.85)$$

from which the eigenvalues are $\lambda = -2$, and -4.

Using Eq. (5.80) successively with each eigenvalue, we have

$$\mathbf{Ax_i} = \lambda\mathbf{x_i}$$

$$\begin{bmatrix} -3 & 1 \\ 1 & -3 \end{bmatrix}\begin{bmatrix} x_1 \\ x_2 \end{bmatrix} = -2\begin{bmatrix} x_1 \\ x_2 \end{bmatrix} \qquad (5.86)$$

or

$$-3x_1 + x_2 = -2x_1 \qquad (5.87a)$$
$$x_1 - 3x_2 = -2x_2 \qquad (5.87b)$$

from which $x_1 = x_2$. Thus,

$$\mathbf{x} = \begin{bmatrix} c \\ c \end{bmatrix} \qquad (5.88)$$

Using the other eigenvalue, -4, we have

$$\mathbf{x} = \begin{bmatrix} c \\ -c \end{bmatrix} \qquad (5.89)$$

Using Eqs. (5.88) and (5.89), one choice of eigenvectors is

$$\mathbf{x_1} = \begin{bmatrix} 1 \\ 1 \end{bmatrix} \quad \text{and} \quad \mathbf{x_2} = \begin{bmatrix} 1 \\ -1 \end{bmatrix} \qquad (5.90)$$

We now show that if the eigenvectors of the matrix **A** are chosen as the basis vectors of a transformation, **P**, the resulting system matrix will be diagonal. Let the transformation matrix **P** consist of the eigenvectors of **A, x$_i$**.

$$\mathbf{P} = [\mathbf{x_1}, \mathbf{x_2}, \mathbf{x_3}, \ldots, \mathbf{x_n}] \tag{5.91}$$

Since **x$_i$** are eigenvectors, $\mathbf{Ax_i} = \lambda_i \mathbf{x_i}$, which can be written equivalently as a set of equations expressed by

$$\mathbf{AP} = \mathbf{PD} \tag{5.92}$$

where **D** is a diagonal matrix consisting of λ_i's, the eigenvalues, along the diagonal, and **P** is as defined in Eq. (5.91). Solving Eq. (5.92) for **D** by premultiplying by $\mathbf{P}^{-1}$, we get

$$\mathbf{D} = \mathbf{P}^{-1}\mathbf{AP} \tag{5.93}$$

which is the system matrix of Eq. (5.72).

In summary, under the transformation **P**, consisting of the eigenvectors of the system matrix, the transformed system is diagonal, with the eigenvalues of the system along the diagonal. The transformed system is identical to that obtained using partial-fraction expansion of the transfer function with distinct real roots.

In Example 5.10, we found eigenvectors of a second-order system. Let us continue with this problem and diagonalize the system matrix.

Example 5.11

Diagonalizing a System in State Space

PROBLEM: Given the system of Eqs. (5.94), find the diagonal system that is similar.

$$\dot{\mathbf{x}} = \begin{bmatrix} -3 & 1 \\ 1 & -3 \end{bmatrix}\mathbf{x} + \begin{bmatrix} 1 \\ 2 \end{bmatrix}u \tag{5.94a}$$

$$y = [\,2 \quad 3\,]\mathbf{x} \tag{5.94b}$$

SOLUTION: First find the eigenvalues and the eigenvectors. This step was performed in Example 5.10. Next form the transformation matrix **P**, whose columns consist of the eigenvectors.

$$\mathbf{P} = \begin{bmatrix} 1 & 1 \\ 1 & -1 \end{bmatrix} \tag{5.95}$$

Finally, form the similar system's system matrix, input matrix, and output matrix, respectively.

$$\mathbf{P}^{-1}\mathbf{AP} = \begin{bmatrix} 1/2 & 1/2 \\ 1/2 & -1/2 \end{bmatrix}\begin{bmatrix} -3 & 1 \\ 1 & -3 \end{bmatrix}\begin{bmatrix} 1 & 1 \\ 1 & -1 \end{bmatrix} = \begin{bmatrix} -2 & 0 \\ 0 & -4 \end{bmatrix} \tag{5.96a}$$

$$\mathbf{P}^{-1}\mathbf{B} = \begin{bmatrix} 1/2 & 1/2 \\ 1/2 & -1/2 \end{bmatrix}\begin{bmatrix} 1 \\ 2 \end{bmatrix} = \begin{bmatrix} 3/2 \\ -1/2 \end{bmatrix} \tag{5.96b}$$

$$\mathbf{CP} = [\,2 \quad 3\,]\begin{bmatrix} 1 & 1 \\ 1 & -1 \end{bmatrix} = [\,5 \quad -1\,] \tag{5.96c}$$

Substituting Eqs. (5.96) into Eqs. (5.72), we get

$$\dot{\mathbf{z}} = \begin{bmatrix} -2 & 0 \\ 0 & -4 \end{bmatrix} \mathbf{z} + \begin{bmatrix} 3/2 \\ -1/2 \end{bmatrix} u \qquad (5.97\text{a})$$

$$y = \begin{bmatrix} 5 & -1 \end{bmatrix} \mathbf{z} \qquad (5.97\text{b})$$

Notice that the system matrix is diagonal, with the eigenvalues along the diagonal.

Students who are using MATLAB should now run ch5p5 in Appendix B. This problem, which uses MATLAB to diagonalize a system, is similar (but not identical) to Example 5.11.

MATLAB
ML

Skill-Assessment Exercise 5.7

PROBLEM: For the system represented in state space as follows:

$$\dot{\mathbf{x}} = \begin{bmatrix} 1 & 3 \\ -4 & -6 \end{bmatrix} \mathbf{x} + \begin{bmatrix} 1 \\ 3 \end{bmatrix} u$$
$$y = \begin{bmatrix} 1 & 4 \end{bmatrix} \mathbf{x}$$

convert the system to one where the new state vector, **z**, is

$$\mathbf{z} = \begin{bmatrix} 3 & -2 \\ 1 & -4 \end{bmatrix} \mathbf{x}$$

WileyPLUS
WPCS
Control Solutions

ANSWER:

$$\dot{\mathbf{z}} = \begin{bmatrix} 6.5 & -8.5 \\ 9.5 & -11.5 \end{bmatrix} \mathbf{z} + \begin{bmatrix} -3 \\ -11 \end{bmatrix} u$$
$$y = \begin{bmatrix} 0.8 & -1.4 \end{bmatrix} \mathbf{z}$$

The complete solution is at www.wiley.com/college/nise.

Skill-Assessment Exercise 5.8

PROBLEM: For the original system of Skill-Assessment Exercise 5.7, find the diagonal system that is similar.

ANSWER:

$$\dot{\mathbf{z}} = \begin{bmatrix} -2 & 0 \\ 0 & -3 \end{bmatrix} \mathbf{z} + \begin{bmatrix} 18.39 \\ 20 \end{bmatrix} u$$
$$y = \begin{bmatrix} -2.121 & 2.6 \end{bmatrix} \mathbf{z}$$

The complete solution is at www.wiley.com/college/nise.

TryIt 5.5

Use the following MATLAB and Control System Toolbox statements to do Skill-Assessment Exercise 5.8.

```
A=[1 3;-4 -6];
B=[1;3];
C=[1 4];
D=0;S=ss(A,B,C,D);
Sd=canon(S,'modal')
```
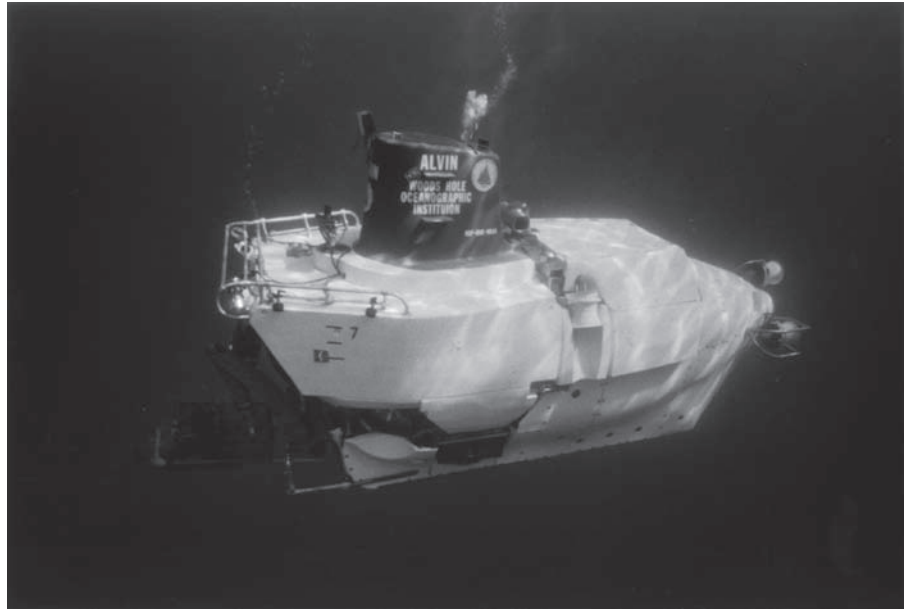
FIGURE 5.33   *Alvin*, a manned submersible, explored the wreckage of the *Titanic* with a tethered robot, *Jason Junior*.

In this section, we learned how to move between different state-space representations of the same system via matrix transformations rather than transfer function manipulation and signal-flow graphs. These different representations are called *similar*. The characteristics of similar systems are that the transfer functions relating the output to the input are the same, as are the eigenvalues and poles. A particularly useful transformation was converting a system with distinct, real eigenvalues to a diagonal system matrix.

We now summarize the concepts of block diagram and signal-flow representations of systems, first through case study problems and then in a written summary. Our case studies include the antenna azimuth position control system and the Unmanned Free-Swimming Submersible vehicle (UFSS). Block diagram reduction is important for the analysis and design of these systems as well as the control systems on board *Alvin* (Figure 5.33), used to explore the wreckage of the *Titanic* 13,000 feet under the Atlantic in July 1986 (*Ballard*, *1987*).

Case Studies

Antenna Control: Designing a Closed-Loop Response

Design
D

This chapter has shown that physical subsystems can be modeled mathematically with transfer functions and then interconnected to form a feedback system. The interconnected mathematical models can be reduced to a single transfer function representing the system from input to output. This transfer function, the closed-loop transfer function, is then used to determine the system response.

The following case study shows how to reduce the subsystems of the antenna azimuth position control system to a single, closed-loop transfer function in order to analyze and design the transient response characteristics.

PROBLEM: Given the antenna azimuth position control system shown on the front endpapers, Configuration 1, do the following:

a. Find the closed-loop transfer function using block diagram reduction.

b. Represent each subsystem with a signal-flow graph and find the state-space representation of the closed-loop system from the signal-flow graph.

c. Use the signal-flow graph found in **b** along with Mason's rule to find the closed-loop transfer function.

d. Replace the power amplifier with a transfer function of unity and evaluate the closed-loop peak time, percent overshoot, and settling time for $K = 1000$.

e. For the system of **d**, derive the expression for the closed-loop step response of the system.

f. For the simplified model of **d**, find the value of K that yields a 10% overshoot.

SOLUTION: Each subsystem's transfer function was evaluated in the case study in Chapter 2. We first assemble them into the closed-loop, feedback control system block diagram shown in Figure 5.34(*a*).

a. The steps taken to reduce the block diagram to a single, closed-loop transfer function relating the output angular displacement to the input angular displacement are shown in Figure 5.34(*a–d*). In Figure 5.34(*b*), the input potentiometer was pushed to the right past the summing junction, creating a unity feedback

(*a*)

(*b*)

(*c*)

(*d*)
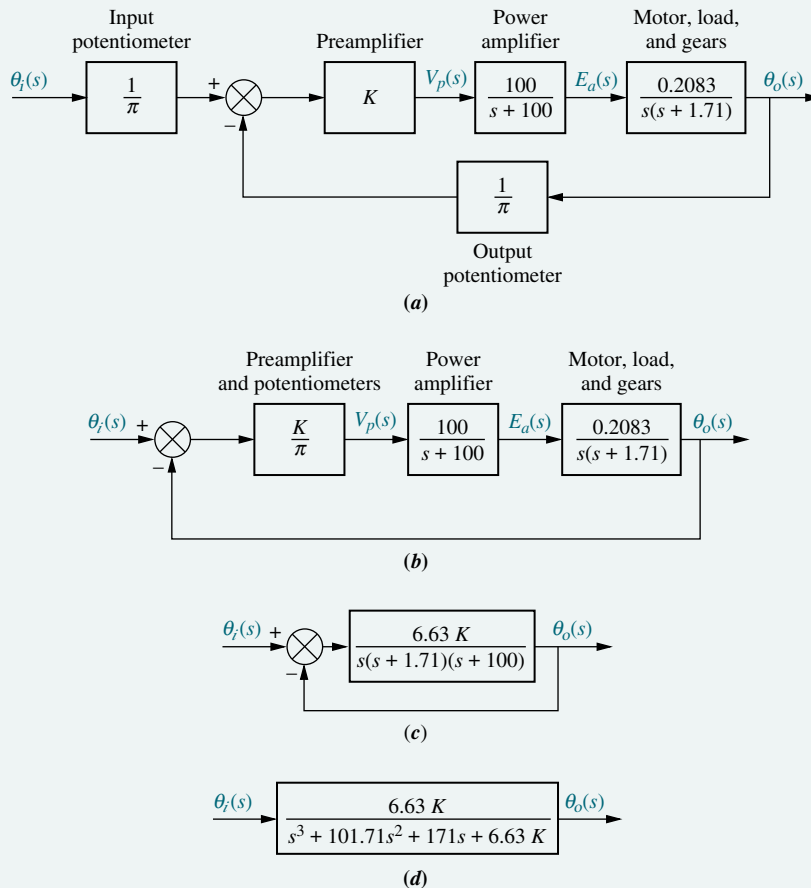
FIGURE 5.34 Block diagram reduction for the antenna azimuth position control system: **a.** original; **b.** pushing input potentiometer to the right past the summing junction; **c.** showing equivalent forward transfer function; **d.** final closed-loop transfer function
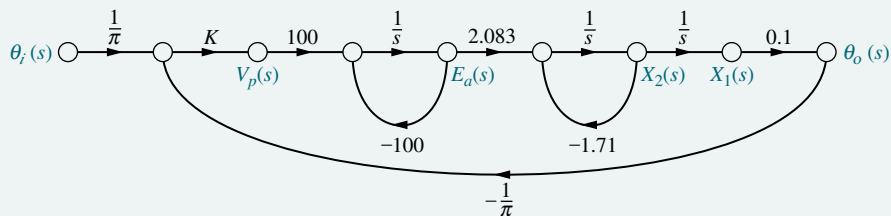
FIGURE 5.35   Signal-flow graph for the antenna azimuth position control system

system. In Figure 5.34(c), all the blocks of the forward transfer function are multiplied together, forming the equivalent forward transfer function. Finally, the feedback formula is applied, yielding the closed-loop transfer function in Figure 5.34(d).

b. In order to obtain the signal-flow graph of each subsystem, we use the state equations derived in the case study of Chapter 3. The signal-flow graph for the power amplifier is drawn from the state equations of Eqs. (3.87) and (3.88), and the signal-flow graph of the motor and load is drawn from the state equation of Eq. (3.98). Other subsystems are pure gains. The signal-flow graph for Figure 5.34(a) is shown in Figure 5.35 and consists of the interconnected subsystems.

The state equations are written from Figure 5.35. First define the state variables as the outputs of the integrators. Hence, the state vector is

$$\mathbf{x} = \begin{bmatrix} x_1 \\ x_2 \\ e_a \end{bmatrix} \tag{5.98}$$

Using Figure 5.35, we write the state equations by inspection:

$$\dot{x}_1 = \qquad\qquad +x_2 \tag{5.99a}$$

$$\dot{x}_2 = \qquad -1.71x_2 + 2.083e_a \tag{5.99b}$$

$$\dot{e}_a = -3.18Kx_1 \qquad - 100e_a + 31.8K\theta_i \tag{5.99c}$$

along with the output equation,

$$y = \theta_o = 0.1x_1 \tag{5.100}$$

where $1/\pi = 0.318$.

In vector-matrix form,

$$\dot{\mathbf{x}} = \begin{bmatrix} 0 & 1 & 0 \\ 0 & -1.71 & 2.083 \\ -3.18K & 0 & -100 \end{bmatrix} \mathbf{x} + \begin{bmatrix} 0 \\ 0 \\ 31.8K \end{bmatrix} \theta_i \tag{5.101a}$$

$$y = \begin{bmatrix} 0.1 & 0 & 0 \end{bmatrix} \mathbf{x} \tag{5.101b}$$

c. We now apply Mason's rule to Figure 5.35 to derive the closed-loop transfer function of the antenna azimuth position control system. First find the forward-path gains. From Figure 5.35 there is only one forward-path gain:

$$T_1 = \left(\frac{1}{\pi}\right)(K)(100)\left(\frac{1}{s}\right)(2.083)\left(\frac{1}{s}\right)\left(\frac{1}{s}\right)(0.1) = \frac{6.63K}{s^3} \tag{5.102}$$

Next identify the closed-loop gains. There are three: the power amplifier loop, $G_{L1}(s)$, with e_a at the output; the motor loop, $G_{L2}(s)$, with x_2 at the output; and the entire system loop, $G_{L3}(s)$, with θ_0 at the output.

$$G_{L1}(s) = \frac{-100}{s} \tag{5.103a}$$

$$G_{L2}(s) = \frac{-1.71}{s} \tag{5.103b}$$

$$G_{L3}(s) = (K)(100)\left(\frac{1}{s}\right)(2.083)\left(\frac{1}{s}\right)\left(\frac{1}{s}\right)(0.1)\left(\frac{-1}{\pi}\right) = \frac{-6.63K}{s^3} \tag{5.103c}$$

Only $G_{L1}(s)$ and $G_{L2}(s)$ are nontouching loops. Thus, the nontouching-loop gain is

$$G_{L1}(s)G_{L2}(s) = \frac{171}{s^2} \tag{5.104}$$

Forming Δ and Δ_k in Eq. (5.28), we have

$$\begin{aligned}\Delta &= 1 - [G_{L1}(s) + G_{L2}(s) + G_{L3}(s)] + [G_{L1}(s)G_{L2}(s)] \\ &= 1 + \frac{100}{s} + \frac{1.71}{s} + \frac{6.63K}{s^3} + \frac{171}{s^2}\end{aligned} \tag{5.105}$$

and

$$\Delta_1 = 1 \tag{5.106}$$

Substituting Eqs. (5.102), (5.105), and (5.106) into Eq. (5.28), we obtain the closed-loop transfer function as

$$T(s) = \frac{C(s)}{R(s)} = \frac{T_1\Delta_1}{\Delta} = \frac{6.63K}{s^3 + 101.71s^2 + 171s + 6.63K} \tag{5.107}$$

d. Replacing the power amplifier with unity gain and letting the preamplifier gain, K, in Figure 5.34(b) equal 1,000 yield a forward transfer function, $G(s)$, of

$$G(s) = \frac{66.3}{s(s + 1.71)} \tag{5.108}$$

Using the feedback formula to evaluate the closed-loop transfer function, we obtain

$$T(s) = \frac{66.3}{s^2 + 1.71s + 66.3} \tag{5.109}$$

From the denominator, $\omega_n = 8.14$, $\zeta = 0.105$. Using Eqs. (4.34), (4.38), and (4.42), the peak time $= 0.388$ second, the percent overshoot $= 71.77\%$, and the settling time $= 4.68$ seconds.

e. The Laplace transform of the step response is found by first multiplying‘ Eq. (5.109) by $1/s$, a unit-step input, and expanding into partial fractions:

$$\begin{aligned}C(s) &= \frac{66.3}{s(s^2 + 1.71s + 66.3)} = \frac{1}{s} - \frac{s + 1.71}{s^2 + 1.71s + 66.3} \\ &= \frac{1}{s} - \frac{(s + 0.855) + 0.106(8.097)}{(s + 0.855)^2 + (8.097)^2}\end{aligned} \tag{5.110}$$

Taking the inverse Laplace transform, we find

$$c(t) = 1 - e^{-0.855r}(\cos 8.097t + 0.106 \sin 8.097t) \tag{5.111}$$

f. For the simplified model we have

$$G(s) = \frac{0.0663K}{s(s + 1.71)} \tag{5.112}$$

from which the closed-loop transfer function is calculated to be

$$T(s) = \frac{0.0663K}{s^2 + 1.71s + 0.0663K} \tag{5.113}$$

From Eq. (4.39) a 10% overshoot yields $\zeta = 0.591$. Using the denominator of Eq. (5.113), $\omega_n = \sqrt{0.0663K}$ and $2\zeta\omega_n = 1.71$. Thus,

$$\zeta = \frac{1.71}{2\sqrt{0.0663K}} = 0.591 \tag{5.114}$$

from which $K = 31.6$.

CHALLENGE: You are now given a problem to test your knowledge of this chapter's objectives: Referring to the antenna azimuth position control system shown on the front endpapers, Configuration 2, do the following:

a. Find the closed-loop transfer function using block diagram reduction.

b. Represent each subsystem with a signal-flow graph and find the state-space representation of the closed-loop system from the signal-flow graph.

c. Use the signal-flow graph found in (b) along with Mason's rule to find the closed-loop transfer function.

d. Replace the power amplifier with a transfer function of unity and evaluate the closed-loop percent overshoot, settling time, and peak time for $K = 5$.

e. For the system used for (d), derive the expression for the closed-loop step response.

f. For the simplified model in (d), find the value of preamplifier gain, K, to yield 15% overshoot.

UFSS Vehicle: Pitch-Angle Control Representation

We return to the Unmanned Free-Swimming Submersible (UFSS) vehicle introduced in the case studies in Chapter 4 (*Johnson*, *1980*). We will represent in state space the pitch-angle control system that is used for depth control.

PROBLEM: Consider the block diagram of the pitch control loop of the UFSS vehicle shown on the back endpapers. The pitch angle, θ, is controlled by a commanded pitch angle, θ_e, which along with pitch-angle and pitch-rate feedback determines the elevator deflection, δ_e, which acts through the vehicle dynamics to determine the pitch angle. Let $K_1 = K_2 = 1$ and do the following:

a. Draw the signal-flow graph for each subsystem, making sure that pitch angle, pitch rate, and elevator deflection are represented as state variables. Then interconnect the subsystems.

b. Use the signal-flow graph obtained in **a** to represent the pitch control loop in state space.
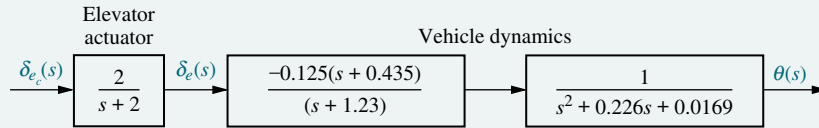
FIGURE 5.36   Block diagram of the UFSS vehicle's elevator and vehicle dynamics, from which a signal-flow graph can be drawn

SOLUTION:

a. The vehicle dynamics are split into two transfer functions, from which the signal-flow graph is drawn. Figure 5.36 shows the division along with the elevator actuator. Each block is drawn in phase-variable form to meet the requirement that particular system variables be state variables. This result is shown in Figure 5.37(*a*). The feedback paths are then added to complete the signal-flow graph, which is shown in Figure 5.37(*b*).

b. By inspection, the derivatives of state variables x_1 through x_4 are written as

$$\dot{x}_1 = x_2 \tag{5.115a}$$

$$\dot{x}_2 = -0.0169x_1 - 0.226x_2 + 0.435x_3 - 1.23x_3 - 0.125x_4 \tag{5.115b}$$

$$\dot{x}_3 = -1.23x_3 - 0.125x_4 \tag{5.115c}$$

$$\dot{x}_4 = 2x_1 + 2x_2 - 2x_4 - 2\theta c \tag{5.115d}$$

Finally, the output $y = x_1$.
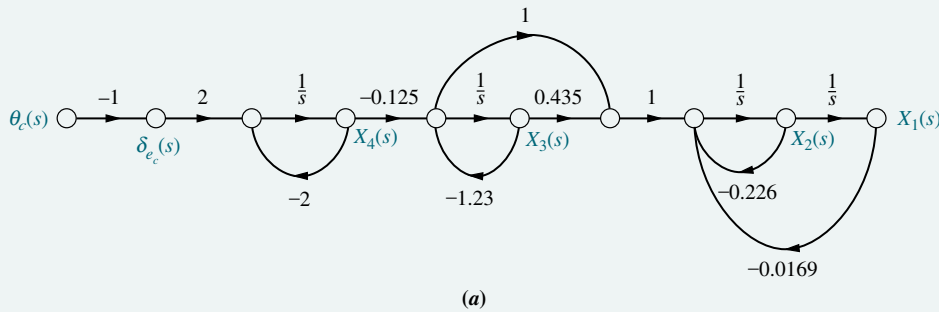
(*a*)
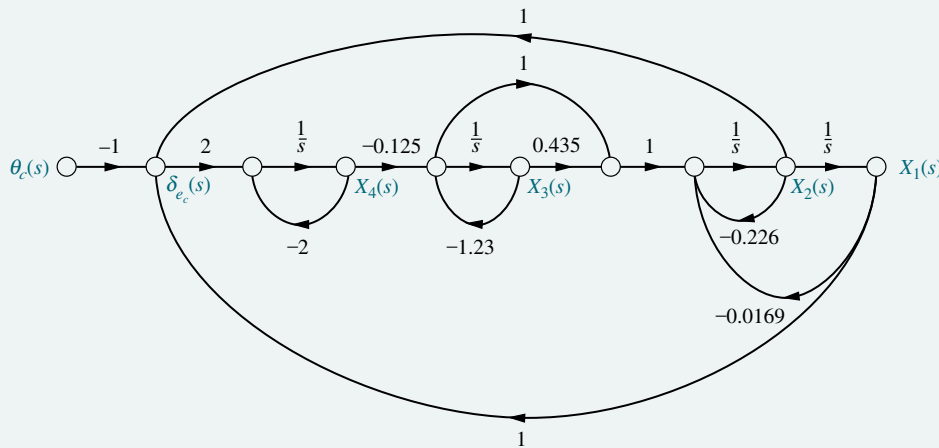
(*b*)

FIGURE 5.37   Signal-flow graph representation of the UFSS vehicle's pitch control system: **a.** without position and rate feedback; **b.** with position and rate feedback. (Note: Explicitly required variables are $x_1 = \theta, x_2 = d\theta/dt$, and $x_4 = \delta_e$.)
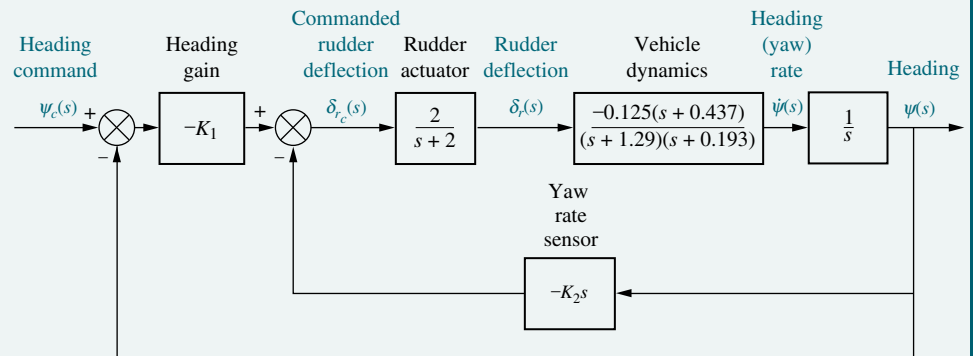
FIGURE 5.38   Block diagram of the heading control system for the UFSS vehicle

In vector-matrix form the state and output equations are

$$\dot{\mathbf{x}} = \begin{bmatrix} 0 & 1 & 0 & 0 \\ -0.0169 & -0.226 & -0.795 & -0.125 \\ 0 & 0 & -1.23 & -0.125 \\ 2 & 2 & 0 & -2 \end{bmatrix} \mathbf{x} + \begin{bmatrix} 0 \\ 0 \\ 0 \\ -2 \end{bmatrix} \theta_c \tag{5.116a}$$

$$y = \begin{bmatrix} 1 & 0 & 0 & 0 \end{bmatrix} \mathbf{x} \tag{5.116b}$$

CHALLENGE: We now give you a problem to test your knowledge of this chapter's objectives. The UFSS vehicle steers via the heading control system shown in Figure 5.38 and repeated on the back endpapers. A heading command is the input. The input and feedback from the submersible's heading and yaw rate are used to generate a rudder command that steers the submersible (*Johnson, 1980*). Let $K_1 = K_2 = 1$ and do the following:

a. Draw the signal-flow graph for each subsystem, making sure that heading angle, yaw rate, and rudder deflection are represented as state variables. Then interconnect the subsystems.

b. Use the signal-flow graph obtained in **a** to represent the heading control loop in state space.

MATLAB
ML

c. Use MATLAB to represent the closed-loop UFSS heading control system in state space in controller canonical form.

(**Summary**)

One objective of this chapter has been for you to learn how to represent multiple subsystems via block diagrams or signal-flow graphs. Another objective has been to be able to reduce either the block diagram representation or the signal-flow graph representation to a single transfer function.

    We saw that the block diagram of a linear, time-invariant system consisted of four elements: *signals*, *systems*, *summing junctions*, and *pickoff points*. These

elements were assembled into three basic forms: *cascade*, *parallel*, and *feedback*. Some basic operations were then derived: moving systems across summing junctions and across pickoff points.

Once we recognized the basic forms and operations, we could reduce a complicated block diagram to a single transfer function relating input to output. Then we applied the methods of Chapter 4 for analyzing and designing a second-order system for transient behavior. We saw that adjusting the gain of a feedback control system gave us partial control of the transient response.

The signal-flow representation of linear, time-invariant systems consists of two elements: nodes, which represent signals, and lines with arrows, which represent subsystems. Summing junctions and pickoff points are implicit in signal-flow graphs. These graphs are helpful in visualizing the meaning of the state variables. Also, they can be drawn first as an aid to obtaining the state equations for a system.

Mason's rule was used to derive the system's transfer function from the signal-flow graph. This formula replaced block diagram reduction techniques. Mason's rule seems complicated, but its use is simplified if there are no nontouching loops. In many of these cases, the transfer function can be written by inspection, with less labor than in the block diagram reduction technique.

Finally, we saw that systems in state space can be represented using different sets of variables. In the last three chapters, we have covered *phase-variable*, *cascade*, *parallel*, *controller canonical*, and *observer canonical* forms. A particular representation may be chosen because one set of state variables has a different physical meaning than another set, or because of the ease with which particular state equations can be solved.

In the next chapter, we discuss system stability. Without stability we cannot begin to design a system for the desired transient response. We will find out how to tell whether a system is stable and what effect parameter values have on a system's stability.

❨ Review Questions ❩

1. Name the four components of a block diagram for a linear, time-invariant system.
2. Name three basic forms for interconnecting subsystems.
3. For each of the forms in Question 2, state (respectively) how the equivalent transfer function is found.
4. Besides knowing the basic forms as discussed in Questions 2 and 3, what other equivalents must you know in order to perform block diagram reduction?
5. For a simple, second-order feedback control system of the type shown in Figure 5.14, describe the effect that variations of forward-path gain, K, have on the transient response.
6. For a simple, second-order feedback control system of the type shown in Figure 5.14, describe the changes in damping ratio as the gain, K, is increased over the underdamped region.
7. Name the two components of a signal-flow graph.
8. How are summing junctions shown on a signal-flow graph?
9. If a forward path touched all closed loops, what would be the value of Δ_k?
10. Name five representations of systems in state space.

State Space

SS

11. Which two forms of the state-space representation are found using the same method?

12. Which form of the state-space representation leads to a diagonal matrix?

13. When the system matrix is diagonal, what quantities lie along the diagonal?

14. What terms lie along the diagonal for a system represented in Jordan canonical form?

15. What is the advantage of having a system represented in a form that has a diagonal system matrix?

16. Give two reasons for wanting to represent a system by alternative forms.

17. For what kind of system would you use the observer canonical form?

18. Describe state-vector transformations from the perspective of different bases.

19. What is the definition of an eigenvector?

20. Based upon your definition of an eigenvector, what is an eigenvalue?

21. What is the significance of using eigenvectors as basis vectors for a system transformation?

Problems

1. Reduce the block diagram shown in Figure P5.1 to a single transfer function, $T(s) = C(s)/R(s)$ Use the following methods:

   a. Block diagram reduction [Section: 5.2]

   b. MATLAB
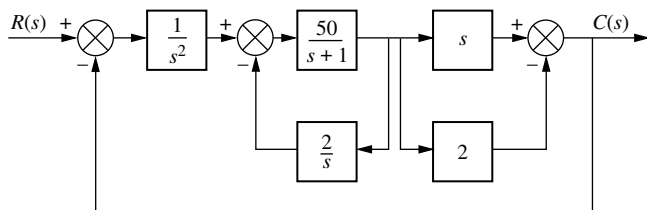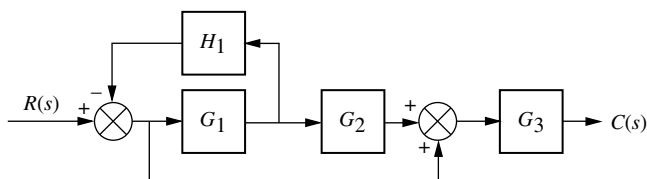
2. Find the closed-loop transfer function, $T(s) = C(s)/R(s)$ for the system shown in Figure P5.2, using block diagram reduction. [Section: 5.2]

FIGURE P5.2

3. Find the equivalent transfer function, $T(s) = C(s)/R(s)$, for the system shown in Figure P5.3. [Section: 5.2]

FIGURE P5.1

FIGURE P5.3

FIGURE P5.5

4. Reduce the system shown in Figure P5.4 to a single transfer function, $T(s) = C(s)/R(s)$. [Section: 5.2]

6. Reduce the block diagram shown in Figure P5.6 to a single block, $T(s) = C(s)/R(s)$. [Section: 5.2]

FIGURE P5.4

FIGURE P5.6

7. Find the unity feedback system that is equivalent to the system shown in Figure P5.7. [Section: 5.2].
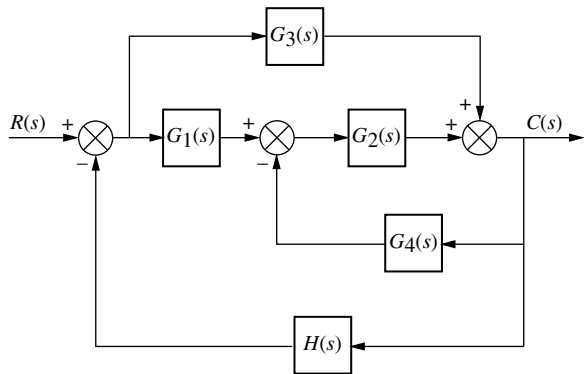
5. Find the transfer function, $T(s) = C(s)/R(s)$, for the system shown in Figure P5.5. Use the following methods:

   a. Block diagram reduction [Section: 5.2]

   b. MATLAB. Use the following   MATLAB
      transfer functions: **ML**
      $G_1(s) = 1/(s+7)$, $G_2(s) = 1/(s^2 + 2s + 3)$,
      $G_3(s) = 1/(s+4)$, $G_4(s) = 1/s$,
      $G_5(s) = 5/(s+7)$, $G_6(s) = 1/(s^2 + 5s + 10)$,
      $G_7(s) = 3/(s+2)$, $G_8(s) = 1/(s+6)$.
      Hint: Use the **append** and **connect**
      commands in MATLAB's Control System
      Toolbox.
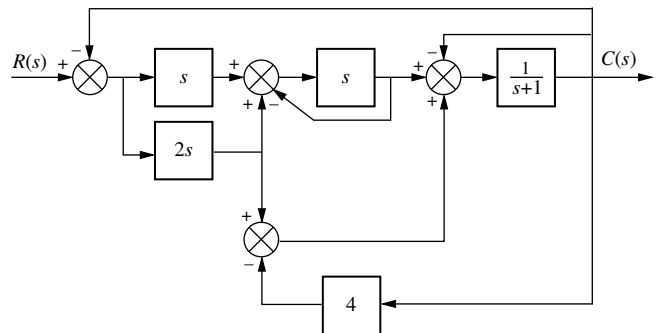
FIGURE P5.7

8. Given the block diagram of a system shown in Figure P5.8, find the transfer function $G(s) = \theta_{22}(s)/\theta_{11}(s)$. [Section: 5.2]
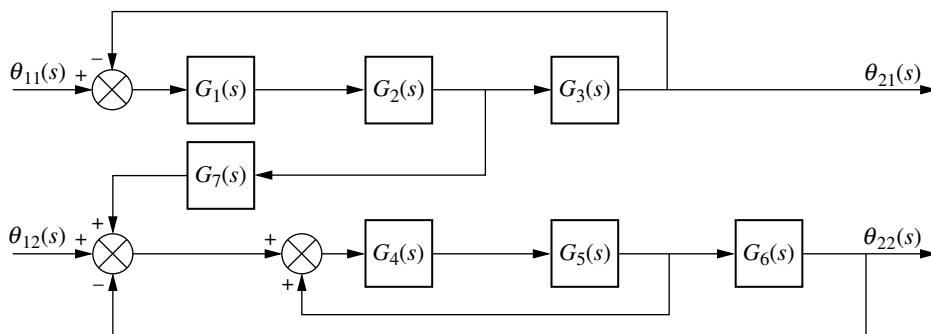
FIGURE P5.8

9. Reduce the block diagram shown in Figure P5.9 to a single transfer function, $T(s) = C(s)/R(s)$. [Section: 5.2]
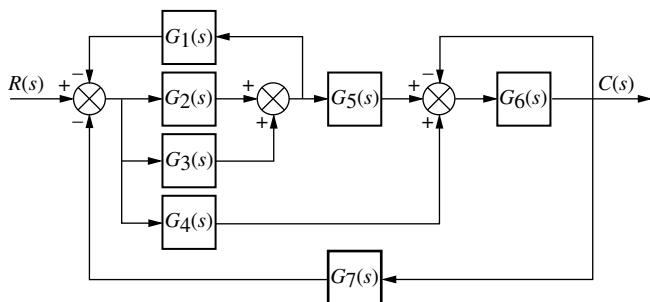
FIGURE P5.9

10. Reduce the block diagram shown in Figure P5.10 to a single block representing the transfer function, $T(s) = C(s)/R(s)$. [Section: 5.2]

WileyPLUS

WPCS

Control Solutions
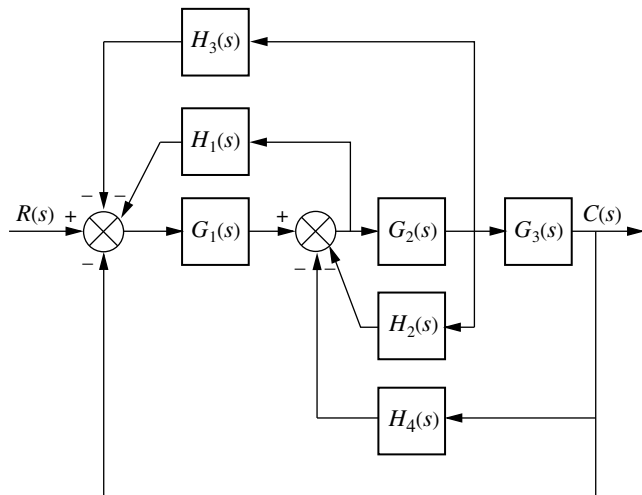
FIGURE P5.10

11. For the system shown in Figure P5.11, find the percent overshoot, settling time, and peak time for a step input if the system's response is underdamped. (Is it? Why?) [Section: 5.3]
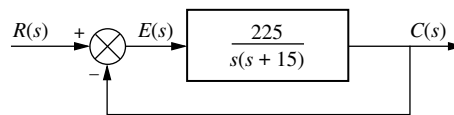
FIGURE P5.11

12. For the system shown in Figure P5.12, find the output, $c(t)$, if the input, $r(t)$, is a unit step. [Section: 5.3]
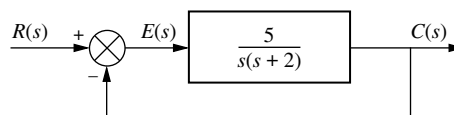
FIGURE P5.12

13. For the system shown in Figure P5.13, find the poles of the closed-loop transfer function, $T(s) = C(s)/R(s)$. [Section: 5.3]
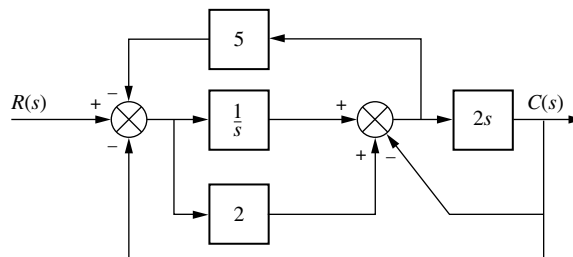
FIGURE P5.13

14. For the system of Figure P5.14, find the value of K that yields 10% overshoot for a step input. [Section: 5.3]
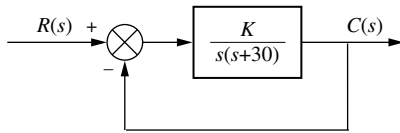
FIGURE P5.14

15. For the system shown in Figure P5.15, find K and α to yield a settling time of 0.15 second and a 30% overshoot. [Section: 5.3]
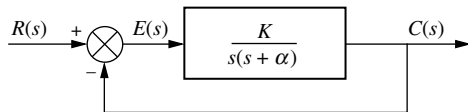
FIGURE P5.15

16. For the system of Figure P5.16, find the values of K_1 and K_2 to yield a peak time of 1.5 second and a settling time of 3.2 seconds for the closed-loop system's step response. [Section: 5.3]
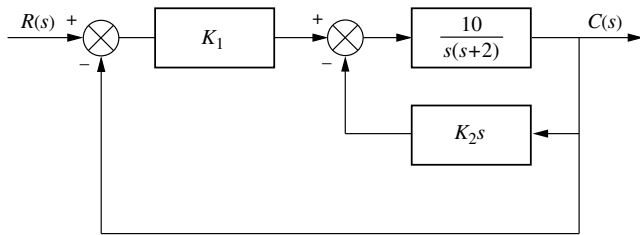
FIGURE P5.16

17. Find the following for the system shown in Figure P5.17: [Section: 5.3]

WileyPLUS
WPCS
Control Solutions

a. The equivalent single block that represents the transfer function, $T(s) = C(s)/R(s)$.

b. The damping ratio, natural frequency, percent overshoot, settling time, peak time, rise time, and damped frequency of oscillation.
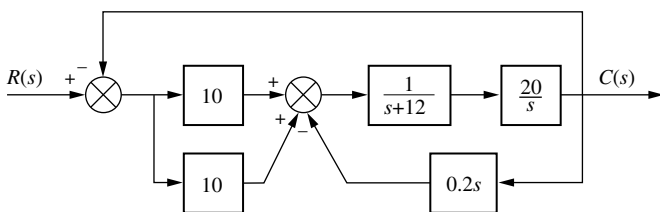
FIGURE P5.17

18. For the system shown in Figure P5.18, find ζ, ω_n, percent overshoot, peak time, rise time, and settling time. [Section: 5.3]
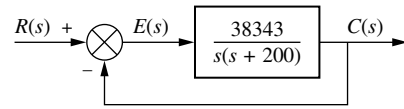
FIGURE P5.18

19. A motor and generator are set up to drive a load as shown in Figure P5.19. If the generator output voltage is $e_g(t) = K_f i_f(t)$, where $i_f(t)$ is the generator's field current, find the transfer function $G(s) = \theta_o(s)/E_i(s)$. For the generator, $K_f = 2\,\Omega$. For the motor, $K_t = 1$ N-m/A, and $K_b = 1$ V-s/rad.
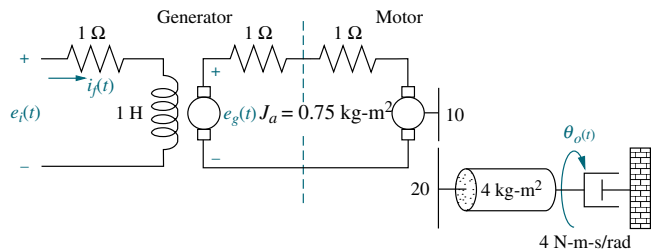
FIGURE P5.19

20. Find $G(s) = E_0(s)/T(s)$ for the system shown in Figure P5.20.

WileyPLUS
WPCS
Control Solutions
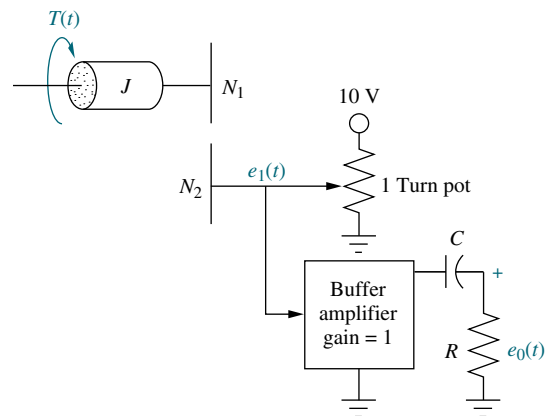
FIGURE P5.20

21. Find the transfer function $G(s) = E_o(s)/T(s)$ for the system shown in Figure P5.21.
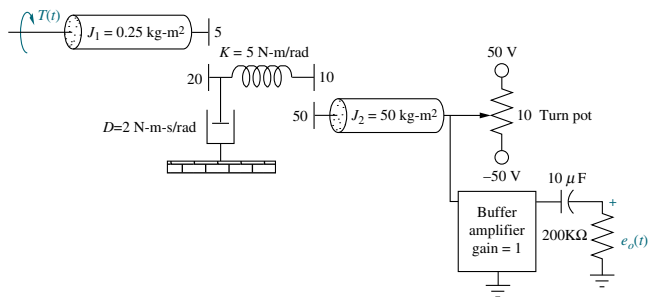
22. Label signals and draw a signal-flow graph for each of the block diagrams shown in the following problems: [Section: 5.4]

   a. Problem 1

   b. Problem 3

   c. Problem 5

23. Draw a signal-flow graph for each of the following state equations: [Section: 5.6]   State Space   SS

   a. $\dot{\mathbf{x}} = \begin{bmatrix} 0 & 1 & 0 \\ 0 & 0 & 1 \\ -2 & -4 & -6 \end{bmatrix} \mathbf{x} + \begin{bmatrix} 0 \\ 0 \\ 1 \end{bmatrix} r$

   $y = \begin{bmatrix} 1 & 1 & 0 \end{bmatrix} \mathbf{x}$

   b. $\dot{\mathbf{x}} = \begin{bmatrix} 0 & 1 & 0 \\ 0 & -3 & 1 \\ -3 & -4 & -5 \end{bmatrix} \mathbf{x} + \begin{bmatrix} 0 \\ 1 \\ 1 \end{bmatrix} r$

   $y = \begin{bmatrix} 1 & 2 & 0 \end{bmatrix} \mathbf{x}$

   c. $\dot{\mathbf{x}} = \begin{bmatrix} 7 & 1 & 0 \\ -3 & 2 & -1 \\ -1 & 0 & 2 \end{bmatrix} \mathbf{x} + \begin{bmatrix} 1 \\ 2 \\ 1 \end{bmatrix} r$

   $y = \begin{bmatrix} 1 & 3 & 2 \end{bmatrix} \mathbf{x}$

24. Given the system below, draw a signal-flow graph and represent the system in state space in the following forms: [Section: 5.7]   State Space   SS   WileyPLUS   WPCS   Control Solutions

   a. Phase-variable form

   b. Cascade form

   $$G(s) = \frac{10}{(s+7)(s+8)(s+9)}$$

25. Repeat Problem 24 for   State Space   SS

   $$G(s) = \frac{20}{s(s-2)(s+5)(s+8)}$$

   [Section: 5.7]

26. Using Mason's rule, find the transfer function, $T(s) = C(s)/R(s)$, for the system represented in Figure P5.22. [Section: 5.5]
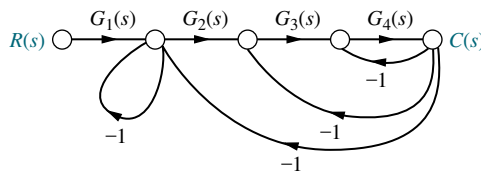
27. Using Mason's rule, find the transfer function, $T(s) = C(s)/R(s)$, for the system represented by Figure P5.23. [Section: 5.5]
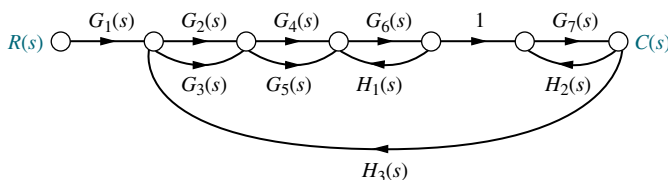
28. Use Mason's rule to find the transfer function of Figure 5.13 in the text. [Section: 5.5]

29. Use block diagram reduction to find the transfer function of Figure 5.21 in the text, and compare your answer with that obtained by Mason's rule. [Section: 5.5]

30. Represent the following systems in state space in Jordan canonical form. Draw the signal-flow graphs. [Section: 5.7]   State Space   SS

   a. $G(s) = \dfrac{(s+1)(s+2)}{(s+3)^2(s+4)}$

   b. $G(s) = \dfrac{(s+2)}{(s+5)^2(s+7)^2}$

   c. $G(s) = \dfrac{(s+3)}{(s+2)^2(s+4)(s+5)}$

31. Represent the systems below in state space in phase-variable form. Draw the signal-flow graphs. [Section: 5.7]   State Space   SS   WileyPLUS   WPCS   Control Solutions

   a. $G(s) = \dfrac{s+3}{s^2 + 2s + 7}$

b. $G(s) = \dfrac{s^2 + 2s + 6}{s^3 + 5s^2 + 2s + 1}$

c. $G(s) = \dfrac{s^3 + 2s^2 + 7s + 1}{s^4 + 3s^3 + 5s^2 + 6s + 4}$

32. Repeat Problem 31 and represent each system in controller canonical and observer canonical forms. [Section: 5.7]

State Space
SS

33. Represent the feedback control systems shown in Figure P5.24 in state space. When possible, represent the open-loop transfer functions separately in cascade and complete the feedback loop with the signal path from output to input. Draw your signal-flow graph to be in one-to-one correspondence to the block diagrams (as close as possible). [Section: 5.7]

State Space
SS

(a)

(b)

(c)

(d)
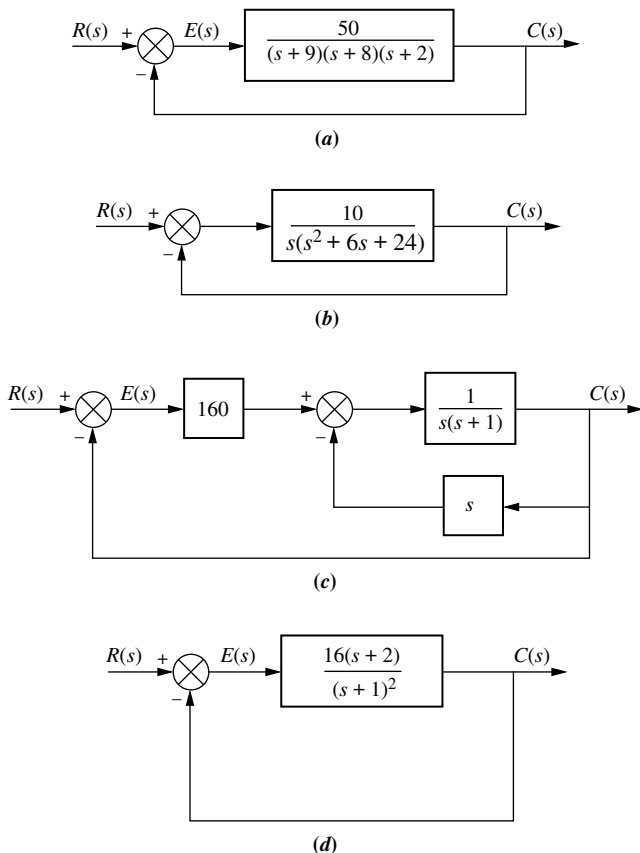
FIGURE P5.24

34. You are given the system shown in Figure P5.25. [Section: 5.7]

State Space
SS

a. Represent the system in state space in phase-variable form.

b. Represent the system in state space in any other form besides phase-variable.
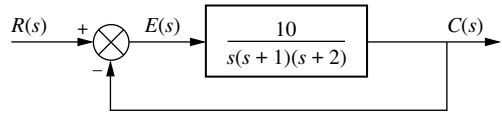
FIGURE P5.25

35. Repeat Problem 34 for the system shown in Figure P5.26. [Section: 5.7]
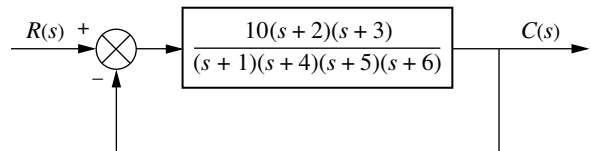
FIGURE P5.26

36. Use MATLAB to solve Problem 35.

MATLAB
ML

37. Represent the system shown in Figure P5.27 in state space where $x_1(t)$, $x_3(t)$, and $x_4(t)$, as shown, are among the state variables, $c(t)$ is the output, and $x_2(t)$ is internal to $X_1(s)/X_3(s)$. [Section: 5.7]

State Space
SS
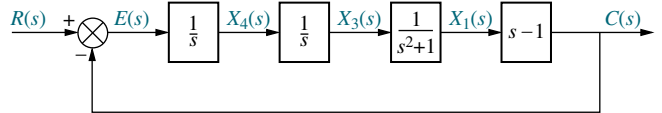
FIGURE P5.27

38. Consider the rotational mechanical system shown in Figure P5.28.

State Space
SS

a. Represent the system as a signal-flow graph.

b. Represent the system in state space if the output is $\theta_2(t)$.
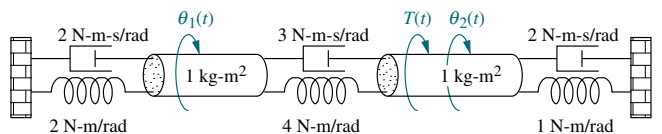
FIGURE P5.28

39. Given a unity feedback system with the forward-path transfer function

MATLAB
ML

State Space
SS

$$G(s) = \frac{7}{s(s+9)(s+12)}$$

use MATLAB to represent the closed loop
system in state space in

a. phase-variable form;

b. parallel form.

40. Consider the cascaded subsystems shown
in Figure P5.29. If $G_1(s)$ is represented in
state space as

State Space

SS

WileyPLUS

WPCS

Control Solutions

$$\dot{\mathbf{x}}_1 = \mathbf{A}_1\mathbf{x}_1 + \mathbf{B}_1 r$$
$$y_1 = \mathbf{C}_1\mathbf{x}_1$$

and $G_2(s)$ is represented in state space as

$$\dot{\mathbf{x}}_2 = \mathbf{A}_2\mathbf{x}_2 + \mathbf{B}_2 y_1$$
$$y_2 = \mathbf{C}_2\mathbf{x}_2$$

show that the entire system can be represented in state
space as

$$
\begin{bmatrix} \dot{\mathbf{x}}_1 \\ \cdots \\ \dot{\mathbf{x}}_2 \end{bmatrix} =
\begin{bmatrix} \mathbf{A}_1 & \vdots & \mathbf{0} \\ \cdots & \cdots & \cdots \\ \mathbf{B}_2\mathbf{C}_1 & \vdots & \mathbf{A}_2 \end{bmatrix}
\begin{bmatrix} \mathbf{x}_1 \\ \cdots \\ \mathbf{x}_2 \end{bmatrix} +
\begin{bmatrix} \mathbf{B}_1 \\ \cdots \\ \mathbf{0} \end{bmatrix} r
$$

$$
y_2 = \begin{bmatrix} \mathbf{0} & \vdots & \mathbf{C}_2 \end{bmatrix}
\begin{bmatrix} \mathbf{x}_1 \\ \cdots \\ \mathbf{x}_2 \end{bmatrix}
$$
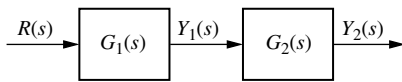
FIGURE P5.29

41. Consider the parallel subsystems shown in
Figure P5.30. If $G_1(s)$ is represented in state
space as

State Space

SS

$$\dot{\mathbf{x}}_1 = \mathbf{A}_1\mathbf{x}_1 + \mathbf{B}_1 r$$
$$y_1 = \mathbf{C}_1\mathbf{x}_1$$

and $G_2(s)$ is represented in state space as

$$\dot{\mathbf{x}}_2 = \mathbf{A}_2\mathbf{x}_2 + \mathbf{B}_2 r$$
$$y_2 = \mathbf{C}_2\mathbf{x}_2$$

show that the entire system can be represented in state
space as

$$
\begin{bmatrix} \dot{\mathbf{x}}_1 \\ \cdots \\ \dot{\mathbf{x}}_2 \end{bmatrix} =
\begin{bmatrix} \mathbf{A}_1 & \vdots & \mathbf{0} \\ \cdots & \cdots & \cdots \\ \mathbf{0} & \vdots & \mathbf{A}_2 \end{bmatrix}
\begin{bmatrix} \mathbf{x}_1 \\ \cdots \\ \mathbf{x}_2 \end{bmatrix} +
\begin{bmatrix} \mathbf{B}_1 \\ \cdots \\ \mathbf{B}_2 \end{bmatrix} r
$$

$$
y = \begin{bmatrix} \mathbf{C}_1 & \vdots & \mathbf{C}_2 \end{bmatrix}
\begin{bmatrix} \mathbf{x}_1 \\ \cdots \\ \mathbf{x}_2 \end{bmatrix}
$$
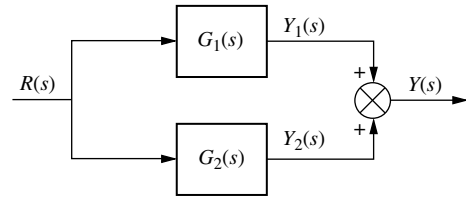
FIGURE P5.30

42. Consider the subsystems shown in Figure
P5.31 and connected to form a feedback
system. If $G(s)$ is represented in state space as

State Space

SS

$$\dot{\mathbf{x}}_1 = \mathbf{A}_1\mathbf{x}_1 + \mathbf{B}_1 e$$
$$y = \mathbf{C}_1\mathbf{x}_1$$

and $H_2(s)$ is represented in state space as

$$\dot{\mathbf{x}}_2 = \mathbf{A}_2\mathbf{x}_2 + \mathbf{B}_2 y$$
$$\rho = \mathbf{C}_2\mathbf{x}_2$$

show that the closed-loop system can be represented
in state space as

$$
\begin{bmatrix} \dot{\mathbf{x}}_1 \\ \cdots \\ \dot{\mathbf{x}}_2 \end{bmatrix} =
\begin{bmatrix} \mathbf{A}_1 & \vdots & -\mathbf{B}_1\mathbf{C}_2 \\ \cdots & \cdots & \cdots \\ \mathbf{B}_2\mathbf{C}_1 & \vdots & \mathbf{A}_2 \end{bmatrix}
\begin{bmatrix} \mathbf{x}_1 \\ \cdots \\ \mathbf{x}_2 \end{bmatrix} +
\begin{bmatrix} \mathbf{B}_1 \\ \cdots \\ \mathbf{0} \end{bmatrix} r
$$

$$
y = \begin{bmatrix} \mathbf{C}_1 & \vdots & \mathbf{0} \end{bmatrix}
\begin{bmatrix} \mathbf{x}_1 \\ \cdots \\ \mathbf{x}_2 \end{bmatrix}
$$
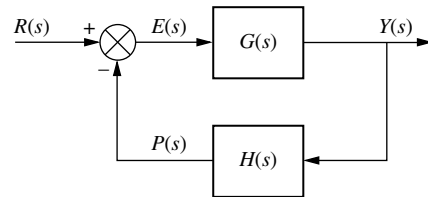
FIGURE P5.31

43. Given the system represented in state
space as follows: [Section: 5.8]

State Space

SS

$$
\dot{\mathbf{x}} = \begin{bmatrix} -1 & -7 & 6 \\ -8 & 4 & 8 \\ 4 & 7 & -8 \end{bmatrix} \mathbf{x} +
\begin{bmatrix} -5 \\ -7 \\ 5 \end{bmatrix} r
$$

$$
y = \begin{bmatrix} -9 & -9 & -8 \end{bmatrix} \mathbf{x}
$$

convert the system to one where the new state
vector, $\mathbf{z}$, is

$$
\mathbf{z} = \begin{bmatrix} -4 & 9 & -3 \\ 0 & -4 & 7 \\ -1 & -4 & -9 \end{bmatrix} \mathbf{x}
$$

44. Repeat Problem 43 for the following system: [Section: 5.8]

State Space
SS

$$\dot{\mathbf{x}} = \begin{bmatrix} -5 & 1 & 1 \\ 9 & -9 & -9 \\ -9 & -1 & 8 \end{bmatrix} \mathbf{x} + \begin{bmatrix} 9 \\ -4 \\ 0 \end{bmatrix} r$$

$$y = \begin{bmatrix} -2 & -4 & 1 \end{bmatrix} \mathbf{x}$$

and the following state-vector transformation:

$$\mathbf{z} = \begin{bmatrix} 5 & -4 & 9 \\ 6 & -7 & 6 \\ 6 & -5 & -3 \end{bmatrix} \mathbf{x}$$

45. Diagonalize the following system: [Section: 5.8]

State Space
SS

WileyPLUS
WPCS
Control Solutions

$$\dot{\mathbf{x}} = \begin{bmatrix} -5 & -5 & 4 \\ 2 & 0 & -2 \\ 0 & -2 & -1 \end{bmatrix} \mathbf{x} + \begin{bmatrix} -1 \\ 2 \\ -2 \end{bmatrix} r$$

$$y = \begin{bmatrix} -1 & 1 & 2 \end{bmatrix} \mathbf{x}$$

46. Repeat Problem 45 for the following system: [Section: 5.8]

State Space
SS

$$\dot{\mathbf{x}} = \begin{bmatrix} -10 & -3 & 7 \\ 18.25 & 6.25 & -11.75 \\ -7.25 & -2.25 & 5.75 \end{bmatrix} \mathbf{x} + \begin{bmatrix} 1 \\ 3 \\ 2 \end{bmatrix} r$$

$$y = \begin{bmatrix} 1 & -2 & 4 \end{bmatrix} \mathbf{x}$$

47. Diagonalize the system in Problem 46 using MATLAB.

MATLAB
ML

48. During ascent the space shuttle is steered by commands generated by the computer's guidance calculations. These commands are in the form of vehicle attitude, attitude rates, and attitude accelerations obtained through measurements made by the vehicle's inertial measuring unit, rate gyro assembly, and accelerometer assembly, respectively. The ascent digital autopilot uses the errors between the actual and commanded attitude, rates, and accelerations to gimbal the space shuttle main engines (called thrust vectoring) and the solid rocket boosters to effect the desired vehicle attitude. The space shuttle's attitude control system employs the same method in the pitch, roll, and yaw control systems. A simplified model of the pitch control system is shown in Figure P5.32.[4]

a. Find the closed-loop transfer function relating actual pitch to commanded pitch. Assume all other inputs are zero.

b. Find the closed-loop transfer function relating actual pitch rate to commanded pitch rate. Assume all other inputs are zero.

c. Find the closed-loop transfer function relating actual pitch acceleration to commanded pitch acceleration. Assume all other inputs are zero.
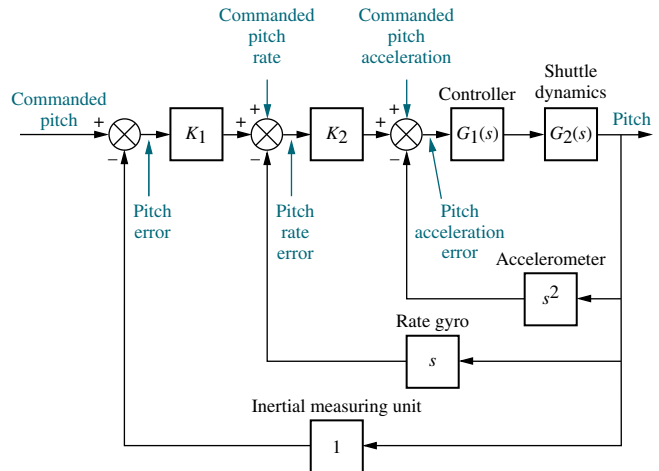
FIGURE P5.32 Space shuttle pitch control system (simplified)

49. An AM radio modulator generates the product of a carrier waveform and a message waveform, as shown in Figure P5.33 (*Kurland, 1971*). Represent the system in state space if the carrier is a sinusoid of frequency $\omega = a$, and the message is a sinusoid of frequency $\omega = b$. Note that this system is nonlinear because of the multiplier.

State Space
SS
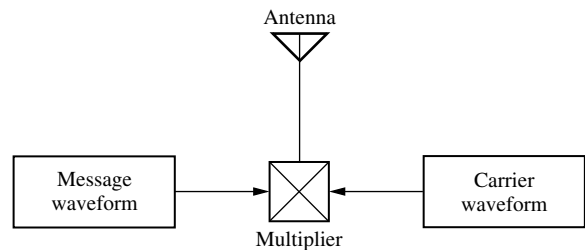
FIGURE P5.33 AM modulator

50. A model for human eye movement consists of the closed-loop system shown in Figure P5.34, where an

[4] Source of background information for this problem: Rockwell International.
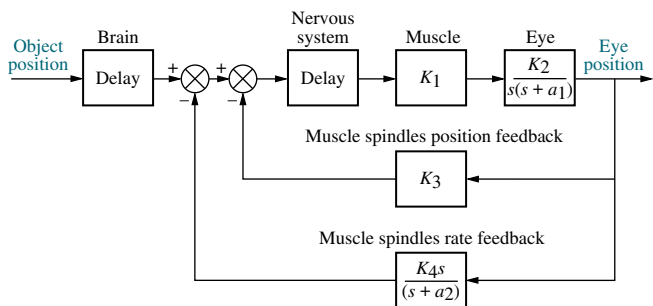
FIGURE P5.34 Feedback control system representing human eye movement

object's position is the input and the eye position is the output. The brain sends signals to the muscles that move the eye. These signals consist of the difference between the object's position and the position and rate information from the eye sent by the muscle spindles. The eye motion is modeled as an inertia and viscous damping and assumes no elasticity (spring) (*Milhorn*, *1966*). Assuming that the delays in the brain and nervous system are negligible, find the closed-loop transfer function for the eye position control.

51. A HelpMate transport robot, shown in Figure P5.35(*a*), is used to deliver goods in a hospital setting. The robot can deliver food, drugs, laboratory materials, and patients' records (*Evans*, *1992*). Given the simplified block diagram of the robot's bearing angle control system, as shown in Figure P5.35(*b*), do the following:

WileyPLUS

WPCS

Control Solutions

(*a*)

(*b*)
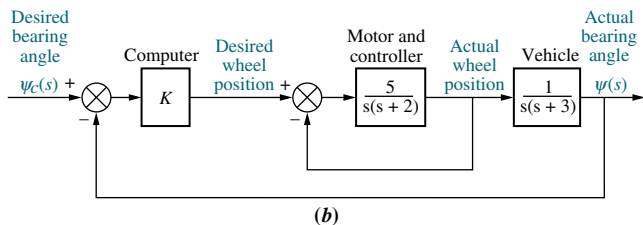
FIGURE P5.35 **a**. HelpMate robot used for in-hospital deliveries; **b**. simplified block diagram for bearing angle control

a. Find the closed-loop transfer function.

b. Represent the system in state space, where the input is the desired bearing angle, the output is the actual bearing angle, and the actual wheel position and actual bearing angle are among the state variables.

State Space

SS

c. Simulate the closed-loop system using MATLAB. Obtain the unit step response for different values of *K* that yield responses from overdamped to underdamped to unstable.

MATLAB

ML

52. Automatically controlled load testers can be used to test product reliability under real-life conditions. The tester consists of a load frame and specimen as shown in Figure P5.36(*a*). The desired load is
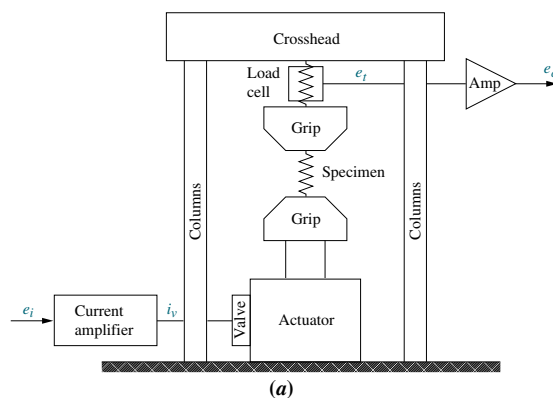
(*a*)
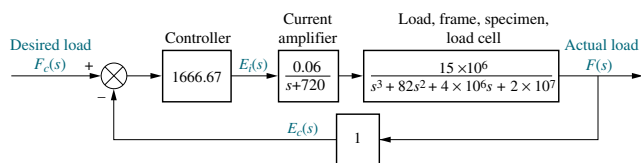
(*b*)

FIGURE P5.36 **a**. Load tester, (© 1992 IEEE) **b.** approximate block diagram

input via a voltage, $e_i(t)$, to a current amplifier. The output load is measured via a voltage, $e_i(t)$, from a load cell measuring the load on the specimen. Figure P5.36(*b*) shows an approximate model of a load testing system without compensation (*Bailey*, 1992).

a. Model the system in state space.

State Space
SS

b. Simulate the step response using MATLAB. Is the response predominantly first or second order? Describe the characteristics of the response that need correction.

MATLAB
ML

53. Consider the F4-E aircraft of Problem 22, Chapter 3. If the open-loop transfer function relating normal acceleration, $A_n(s)$, to the input deflection command, $\delta_c(s)$, is approximated as

State Space
SS

$$\frac{A_n(s)}{\delta_c(s)} = \frac{-272(s^2 + 1.9s + 84)}{(s + 14)(s - 1.8)(s + 4.9)}$$

(*Cavallo*, 1992), find the state-space representation in

a. Phase-variable form
b. Controller canonical form
c. Observer canonical form
d. Cascade form
e. Parallel form

54. Find the closed-loop transfer function of the Unmanned Free-Swimming Submersible vehicle's pitch control system shown on the back endpapers (*Johnson*, 1980).

55. Repeat Problem 54 using MATLAB.

MATLAB
ML

56. Use Simulink to plot the effects of nonlinearities upon the closed-loop step response of the antenna azimuth position control system shown on the front endpapers, Configuration 1. In particular, consider individually each of the following nonlinearities: saturation (±5 volts), backlash (dead-band width 0.15), deadzone (−2 to +2), as well as the linear response. Assume the preamplifier gain is 100 and the step input is 2 radians.

Simulink
SL

57. Problem 12 in Chapter 1 describes a high-speed proportional solenoid valve. A subsystem of the valve is the solenoid coil shown in Figure P5.37. Current through the coil, L, generates a magnetic field that produces a force to operate the valve. Figure P5.37can be represented as a block diagram (*Vaughan*, 1996)
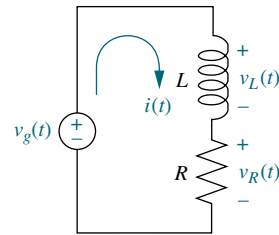
FIGURE P5.37 Solenoid coil circuit

a. Derive a block diagram of a feedback system that represents the coil circuit, where the applied voltage, $v_g(t)$, is the input, the coil voltage, $v_L(t)$, is the error voltage, and the current, $i(t)$, is the output.

b. For the block diagram found in Part **a**, find the Laplace transform of the output current, $I(s)$.

c. Solve the circuit of Figure P5.37 for $I(s)$, and compare to your result in Part **b**.

58. Ktesibios' water clock (see Section 1.2) is probably the first man-made system in which feedback was used in a deliberate manner. Its operations are shown in Figure P5.38(*a*). The clock indicates time progressively on scale D as water falls from orifice A toward vessel B. Clock accuracy depends mainly on water height h_f in the water reservoir G, which must be maintained at a constant level h_r by means of the conical float F that moves up or down to control the water inflow. Figure P5.38(*b*) shows a block diagram describing the system (*Lepschy*, 1992).

Let $q_i(t)$ and $q_o(t)$ represent the input and output water flow, respectively, and h_m the height of water in vessel B. Use Mason's rule to find the following transfer functions, assuming α and β are constants:

a. $\dfrac{H_m(s)}{H_r(s)}$

b. $\dfrac{H_f(s)}{H_r(s)}$

c. $\dfrac{Q_i(s)}{H_r(s)}$

d. $\dfrac{Q_o(s)}{H_r(s)}$

e. Using the above transfer functions, show that if $h_r(t) = $ constant, then $q_o(t) = $ constant and $h_m(t)$ increases at a constant speed.

(a)

(b)
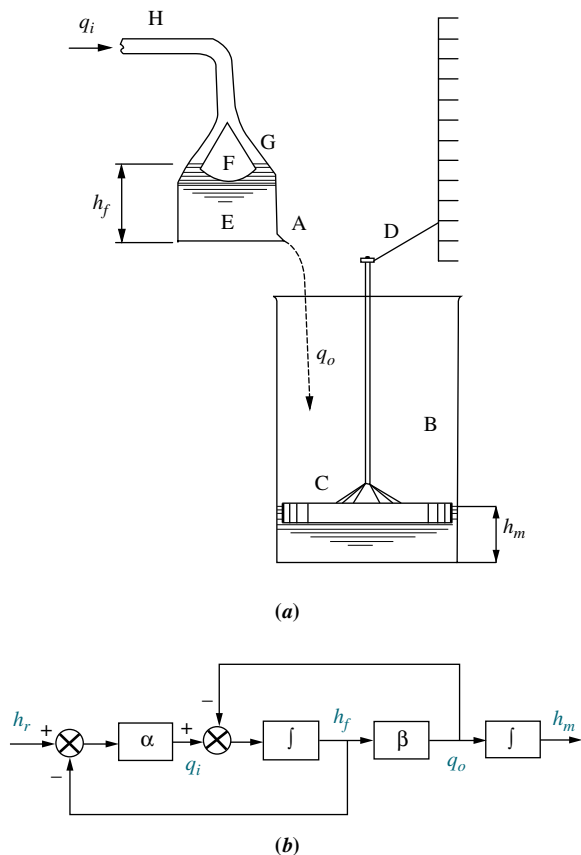
FIGURE P5.38   **a.** Ktesibios' water clock; **b.** water clock block diagram (© 1992 IEEE)

59. Some robotic applications can benefit from actuators in which load position as well as exerted force are controlled. Figure P5.39 shows the block diagram of such an actuator, where u_1 and u_2 are voltage inputs to two coils, each of which controls a pneumatic piston, and y represents the load displacement.

The system's output is u, the differential pressure acting on the load. The system also has a disturbance input f_{ext}, which represents external forces that are not system generated, but are acting on the load. A is a constant (*Ben-Dov, 1995*). Use any method to obtain:

a. An expression for the system's output in terms of the inputs u_1 and u_2 (Assume $f_{\text{ext}} = 0$.)

b. An expression for the effect of f_{ext} on the output u (Assume u_1 and $u_2 = 0$.)

c. What condition on the inputs u_1 and u_2 will result in $u = 0$?
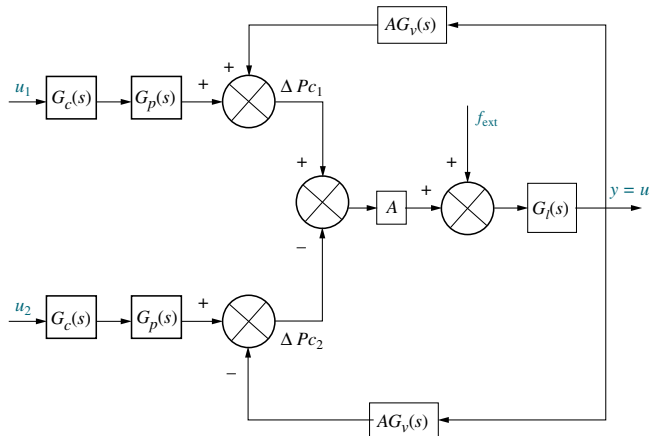
FIGURE P5.39   Actuator block diagram (© 1995 IEEE)

60. Figure P5.40 shows a noninverting operational amplifier.

(a)   **(b)**
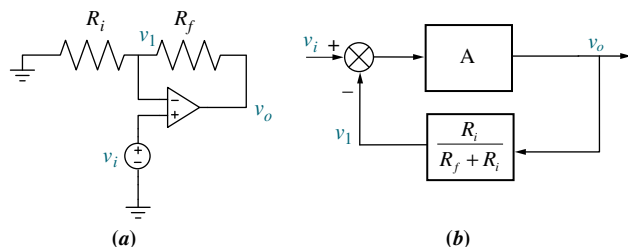
FIGURE P5.40   **a.** Noninverting amplifier; **b.** block diagram

Assuming the operational amplifier is ideal,

a. Verify that the system can be described by the following two equations:

$$v_o = A(v_i - v_o)$$

$$v_1 = \frac{R_i}{R_i + R_f} v_o$$

b. Check that these equations can be described by the block diagram of Figure P5.40(*b*)

c. Use Mason's rule to obtain the closed-loop system transfer function $\dfrac{V_o(s)}{V_i(s)}$

d. Show that when $A \to \infty$, $\dfrac{V_o(s)}{V_i(s)} = 1 + \dfrac{R_f}{R_i}$

61. Figure P5.41 shows the diagram of an inverting operational amplifier.
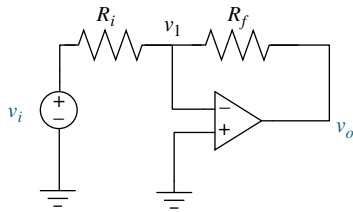
FIGURE P5.41 Inverting operational amplifier

a. Assuming an ideal operational amplifier, use a similar procedure to the one outlined in Problem 60 to find the system equations.

b. Draw a corresponding block diagram and obtain the transfer function $\dfrac{V_o(s)}{V_i(s)}$.

c. Show that when $A \to \infty$, $\dfrac{V_o(s)}{V_i(s)} = -\dfrac{R_f}{R_i}$.

62. Figure P5.42(a) shows an n-channel enhancement-mode MOSFET source follower circuit. Figure P5.42(b) shows its small-signal equivalent (where $R_i = R_1 \| R_2$) (*Neamen, 2001*).

a. Verify that the equations governing this circuit are

$$\frac{v_{in}}{v_i} = \frac{R_i}{R_i + R_s}; \quad v_{gs} = v_{in} - v_o; \quad v_o = g_m(R_s \| r_o)v_{gs}$$

b. Draw a block diagram showing the relations between the equations.

c. Use the block diagram in Part **b** to find $\dfrac{V_o(s)}{V_i(s)}$.
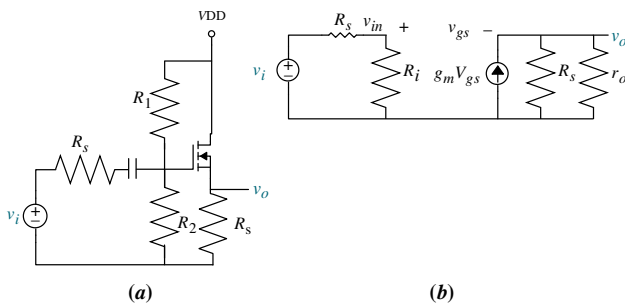
FIGURE P5.42 **a.** An n-channel enhancement-mode MOSFET source follower circuit; **b.** small-signal equivalent

63. A car active suspension system adds an active hydraulic actuator in parallel with the passive damper and spring to create a dynamic impedance that responds to road variations. The block diagram of Figure P5.43 depicts such an actuator with closed-loop control.
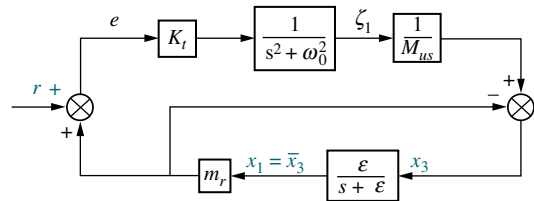
FIGURE P5.43 (© 1997 IEEE)

In the figure, K_t is the spring constant of the tire, M_{US} is the wheel mass, r is the road disturbance, x_1 is the vertical car displacement, x_3 is the wheel vertical displacement, $\omega_0^2 = \frac{K_t}{M_{US}}$ is the natural frequency of the unsprung system and ε is a filtering parameter to be judiciously chosen (*Lin, 1997*). Find the two transfer functions of interest:

a. $\dfrac{X_3(s)}{R(s)}$

b. $\dfrac{X_1(s)}{R(s)}$

64. The basic unit of skeletal and cardiac muscle cells is a *sarcomere*, which is what gives such cells a striated (parallel line) appearance. For example, one bicep cell has about 10^5 sarcomeres. In turn, sarcomeres are composed of protein complexes. Feedback mechanisms play an important role in sarcomeres and thus muscle contraction. Namely, Fenn's law says that the energy liberated during muscle contraction depends on the initial conditions and the load encountered. The following linearized model describing sarcomere contraction has been developed for cardiac muscle:

$$\begin{bmatrix} \dot{A} \\ \dot{T} \\ \dot{U} \\ \dot{SL} \end{bmatrix} = \begin{bmatrix} -100.2 & -20.7 & -30.7 & 200.3 \\ 40 & -20.22 & 49.95 & 526.1 \\ 0 & 10.22 & -59.95 & -526.1 \\ 0 & 0 & 0 & 0 \end{bmatrix} \begin{bmatrix} A \\ T \\ U \\ SL \end{bmatrix} + \begin{bmatrix} 208 \\ -208 \\ -108.8 \\ -1 \end{bmatrix} u(t)$$

$$y = \begin{bmatrix} 0 & 1570 & 1570 & 59400 \end{bmatrix} \begin{bmatrix} A \\ T \\ U \\ SL \end{bmatrix} - 6240u(t)$$

where

$A =$ density of regulatory units with bound calcium and adjacent weak cross bridges (μM)

$T =$ density of regulatory units with bound calcium and adjacent strong cross bridges (M)

$U =$ density of regulatory units without bound calcium and adjacent strong cross bridges (M)

$SL =$ sarcomere length (m)

The system's input is $u(t) =$ the shortening muscle velocity in meters/second and the output is $y_{(t)} =$ muscle force output in Newtons (*Yaniv*, *2006*).

Do the following:

a. Use MATLAB to obtain the transfer function $\dfrac{Y(s)}{U(s)}$.

`MATLAB`
`ML`

b. Use MATLAB to obtain a partial-fraction expansion for $\dfrac{Y(s)}{U(s)}$.

`MATLAB`
`ML`

c. Draw a signal-flow diagram of the system in parallel form.

`State Space`
`SS`

d. Use the diagram of Part **c** to express the system in state-variable form with decoupled equations.

`State Space`
`SS`

65. An electric ventricular assist device (EVAD) has been designed to help patients with diminished but still functional heart pumping action to work in parallel with the natural heart. The device consists of a brushless dc electric motor that actuates on a pusher plate. The plate movements help the ejection of blood in systole and sac filling in diastole. System dynamics during systolic mode have been found to be:

$$\begin{bmatrix} \dot{x} \\ \dot{v} \\ \dot{P}_{ao} \end{bmatrix} = \begin{bmatrix} 0 & 1 & 0 \\ 0 & -68.3 & -7.2 \\ 0 & 3.2 & -0.7 \end{bmatrix} \begin{bmatrix} x \\ v \\ P_{ao} \end{bmatrix} + \begin{bmatrix} 0 \\ 425.4 \\ 0 \end{bmatrix} e_m$$

The state variables in this model are x, the pusher plate position, v, the pusher plate velocity, and P_{ao}, the aortic blood pressure. The input to the system is e_m, the motor voltage (*Tasch*, *1990*).

a. Use MATLAB to find a similarity transformation to diagonalize the system.

`MATLAB`
`ML`

b. Use MATLAB and the obtained similarity transformation of Part a to obtain a diagonalized expression for the system.

`MATLAB`
`ML`

66. In an experiment to measure and identify postural arm reflexes, subjects hold with their hands a linear hydraulic manipulator. A load cell is attached to the actuator handle to measure resulting forces. At the application of a force, subjects try to maintain a fixed posture. Figure P5.44 shows a block diagram for the combined arm-environment system.
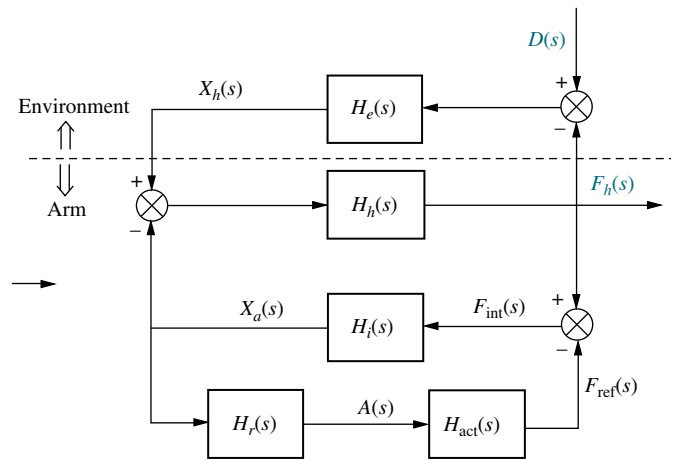
FIGURE P5.44

In the diagram, $H_r(s)$ represents the reflexive length and velocity feedback dynamics; $H_{act}(s)$ the activation dynamics, $H_i(s)$ the intrinsic act dynamics; $H_h(s)$ the hand dynamics; $H_e(s)$ the environmental dynamics; $X_a(s)$ the position of the arm; $X_h(s)$ the measured position of the hand; $F_h(s)$ the measured interaction force applied by the hand; $F_{int}(s)$ the intrinsic force; $F_{ref}(s)$ the reflexive force; $A(s)$ the reflexive activation; and $D(s)$ the external force perturbation (*de Vlugt*, *2002*).

a. Obtain a signal-flow diagram from the block diagram.

b. Find $\dfrac{F_h(s)}{D(s)}$.

67. Use LabVIEW's Control Design and Simulation Module to obtain the controller and the observer canonical forms for:

`State Space`
`SS`

`LabVIEW`
`LV`

$$G(s) = \frac{s^2 + 7s + 2}{s^3 + 9s^2 + 26s + 24}$$

68. A virtual reality simulator with haptic (sense of touch) feedback was developed to simulate the control of a submarine driven through a joystick input. Operator haptic feedback is provided through joystick position constraints and simulator movement (*Karkoub*, *2010*). Figure P5.45 shows the block diagram of the haptic feedback system in which the input u_h is the force exerted by the muscle of the human arm; and the outputs are y_s, the position of the simulator, and y_j, the position of the joystick.
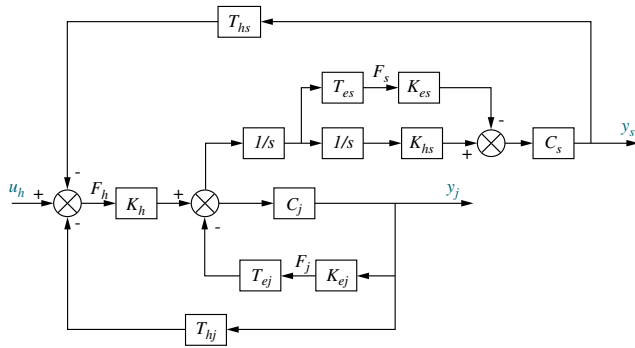
FIGURE P5.45 Copyright © 2010 Cambridge University Press. Reprinted with permission.

a. Find the transfer function $\dfrac{Y_s(s)}{U_h(s)}$.

b. Find the transfer function $\dfrac{Y_j(s)}{U_h(s)}$.

69. Some medical procedures require the insertion of a needle under a patient's skin using CT scan monitoring guidance for precision. CT scans emit radiation, posing some cumulative risks for medical personnel. To avoid this problem, a remote control robot has been developed (*Piccin, 2009*). The robot controls the needle in position and angle in the constraint space of a CT scan machine and also provides the physician with force feedback commensurate with the insertion opposition encountered by the type of tissue in which the needle is inserted. The robot has other features that give the operator the
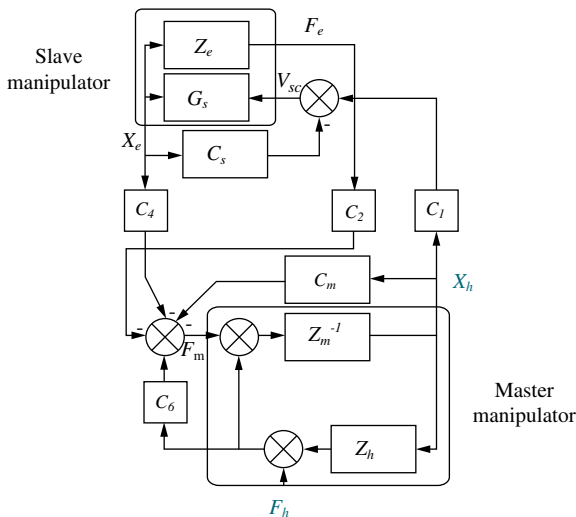
similar sensations and maneuverability as if the needle was inserted directly. Figure P5.46 shows the block diagram of the force insertion mechanism, where F_h is the input force and X_h is the output displacement. Summing junction inputs are positive unless indicated with a negative sign. By way of explanation, $Z =$ impedance; $G =$ transfer function; $C_i =$ communication channel transfer functions; $F =$ force; $X =$ position. Subscripts h and m refer to the master manipulator. Subscripts s and e refer to the slave manipulator.

a. Assuming $Z_h = 0$, $C_1 = C_s$, $C_2 = 1 + C_6$ and $C_4 = -C_m$ use Mason's Rule to show that the transfer function from the operators force input F_h to needle displacement X_h is given by

$$Y(s) = \frac{X_h(s)}{F_h(s)} = \frac{Z_m^{-1}C_2(1 + G_sC_s)}{1 + G_sC_s + Z_m^{-1}(c_m + C_2Z_eG_sC_s)}$$

b. Now with $Z_h \neq 0$ show that $\dfrac{X_h(s)}{F_h(s)} = \dfrac{Y(s)}{1 + Y(s)Z_h}$

70. A hybrid solar cell and diesel power distribution system has been proposed and tested (*Lee, 2007*). The system has been shown to have a very good uninterruptible power supply as well as line voltage regulation capabilities. Figure P5.47 shows a signal-flow diagram of the system. The output, V_{Load}, is the voltage across the load. The two inputs are I_{Cf}, the reference current, and I_{Dist}, the disturbance representing current changes in the supply.

a. Refer to Figure P5.47 and find the transfer function $\dfrac{V_{Load}(s)}{I_{Cf}(s)}$.

b. Find the transfer function $\dfrac{V_{Load}(s)}{I_{Dist}(s)}$.

71. Continuous casting in steel production is essentially a solidification process by which molten steel is
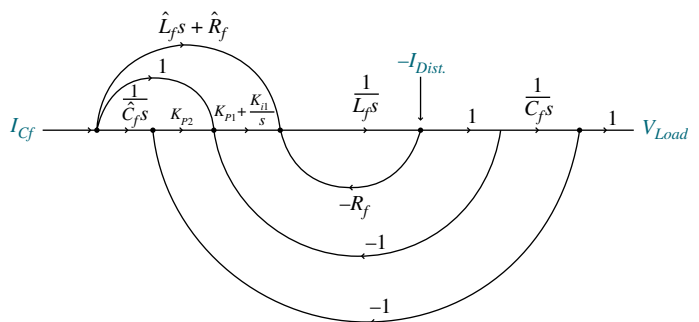
FIGURE P5.46

FIGURE P5.47

solidified into a steel slab after passing through a mold, as shown in Figure P5.48(a). Final product dimensions depend mainly on the casting speed V_p (in m/min), and on the stopper position X (in %) that controls the flow of molten material into the mold (*Kong, 1993*). A simplified model of a casting system is shown in Figure P5.48(b) (*Kong, 1993*) and (*Graebe, 1995*). In the model, H_m = mold level (in mm); H_t = assumed constant height of molten steel in the tundish; D_z = mold thickness = depth of nozzle immerged into molten steel; and W_t = weight of molten steel in the tundish.

For a specific setting let $A_m = 0.5$ and

$$G_x(s) = \frac{0.63}{s + 0.926}$$

Also assume that the valve positioning loop may be modeled by the following second-order transfer function:

$$G_V(s) = \frac{X(s)}{Y_C(s)} = \frac{100}{s^2 + 10s + 100}$$

and the controller is modeled by the following transfer function:

$$G_C(s) = \frac{1.6(s^2 + 1.25s + 0.25)}{s}$$

(*a*)

(*b*)
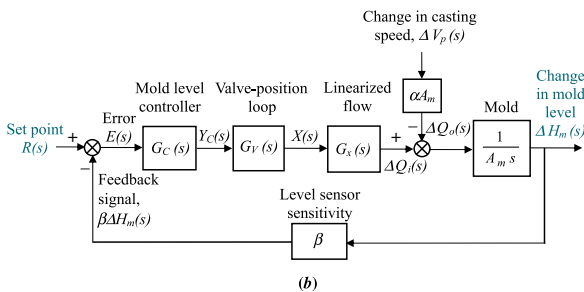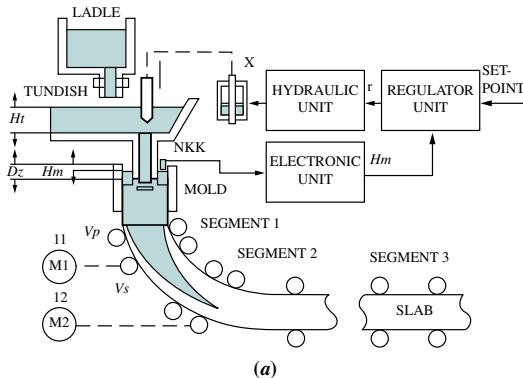
FIGURE P5.48   Steel mold process: **a.** process (© 1993 IEEE); **b.** block diagram

The sensitivity of the mold level sensor is $\beta = 0.5$ and the initial values of the system variables at $t = 0^-$ are: $R(0^-) = 0; Y_C(0^-) = X(0^-) = 41.2; \Delta H_m(0^-) = 0;$ $H_m(0^-) = -75; \Delta V_p(0^-) = 0;$ and $V_p(0^-) = 0$. Do the following:

a. Assuming $v_p(t)$ is constant $\left[\Delta v_p = 0\right]$, find the closed-loop transfer function $T(s) = \Delta H_m(s)/R(s)$.

b. For $r(t) = 5\,u(t), v_p(t) = 0.97\,u(t),$ and $H_m(0^-) = -75\,\text{mm}$, use Simulink to simulate the system. Record the time and mold level (in array format) by connecting them to **Workspace** sinks, each of which should carry the respective variable name. After the simulation ends, utilize MATLAB plot commands to obtain and edit the graph of $h_m(t)$ from $t = 0$ to 80 seconds.

72. A simplified second-order transfer function model for bicycle dynamics is given by

$$\frac{\varphi(s)}{\delta(s)} = \frac{aV}{bh}\frac{\left(s + \dfrac{V}{a}\right)}{\left(s^2 - \dfrac{g}{h}\right)}$$

The input is $\delta(s)$, the steering angle, and the output is $\varphi(s)$, the tilt angle (between the floor and the bicycle longitudinal plane). In the model parameter a is the horizontal distance from the center of the back wheel to the bicycle center of mass; b is the horizontal distance between the centers of both wheels; h is the vertical distance from the center of mass to the floor; V is the rear wheel velocity (assumed constant); and g is the gravity constant. It is also assumed that the rider remains at a fixed position with respect to the bicycle so that the steer axis is vertical and that all angle deviations are small (*Åstrom, 2005*).

a. Obtain a state-space representation for the bicycle model in phase-variable form.

b. Find system eigenvalues and eigenvectors.

c. Find an appropriate similarity transformation matrix to diagonalize the system and obtain the state-space system's diagonal representation.

73. It is shown in Figure 5.6(c) that when negative feedback is used, the overall transfer function for the system of Figure 5.6(b) is

$$\frac{C(s)}{R(s)} = \frac{G(s)}{1 + G(s)H(s)}$$

Develop the block diagram of an alternative feedback system that will result in the same closed-loop transfer function, $C(s)/R(s)$, with $G(s)$ unchanged and unmoved. In addition, your new block diagram must have unity gain in the feedback path. You can add input transducers and/or controllers in the main forward path as required.

DESIGN PROBLEMS

74. The motor and load shown in Figure P5.49(a) are used as part of the unity feedback system shown in Figure P5.49(b). Find the value of the coefficient of viscous damping, D_L, that must be used in order to yield a closed-loop transient response having a 20% overshoot.

(a)

(b)
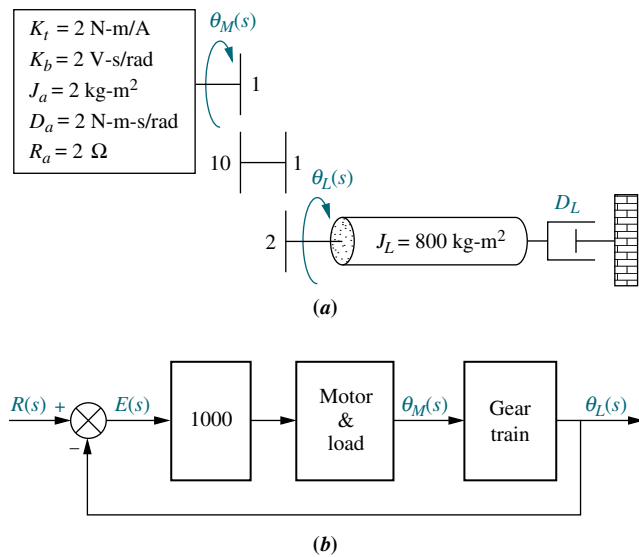
FIGURE P5.49 Position control: **a.** motor and load; **b.** block diagram

75. Assume that the motor whose transfer function is shown in Figure P5.50(a) is used as the forward path of a closed-loop, unity feedback system.

  a. Calculate the percent overshoot and settling time that could be expected.

  b. You want to improve the response found in Part **a**. Since the motor and the motor constants cannot be changed, an amplifier and a tachometer (voltage generator) are inserted into the loop, as shown in Figure P5.50. Find the values of K_1 and K_2 to yield a 16% overshoot and a settling time of 0.2 second.

(a)

(b)
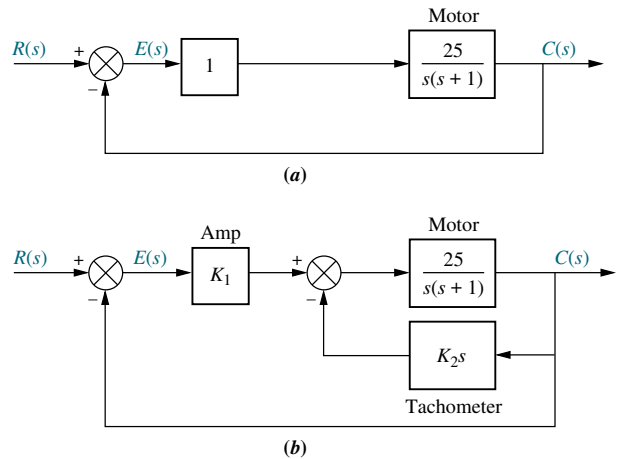
FIGURE P5.50 **a.** Position control; **b.** position control with tachometer

76. The system shown in Figure P5.51 will have its transient response altered by adding a tachometer. Design K and K_2 in the system to yield a damping ratio of 0.69. The natural frequency of the system before the addition of the tachometer is 10 rad/s.
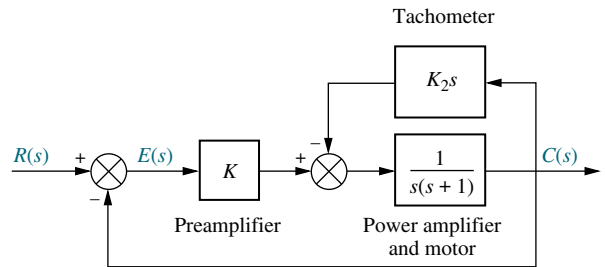
FIGURE P5.51 Position control

77. The mechanical system shown in Figure P5.52(a) is used as part of the unity feedback system shown in Figure P5.52(b). Find the values of M and D to yield 20% overshoot and 2 seconds settling time.

WileyPLUS
WPCS
Control Solutions

(a)
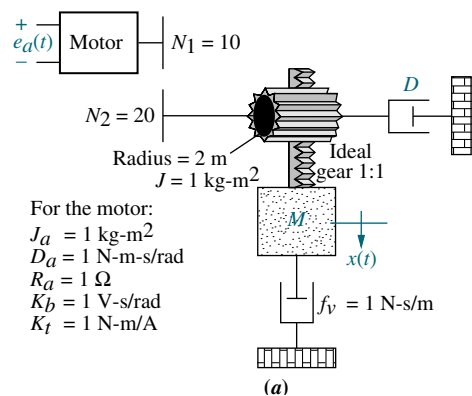
FIGURE P5.52 **a.** Motor and load; (*figure continues*)

(b)
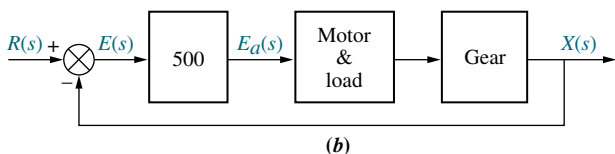
FIGURE P5.52 (*Continued*) **b.** motor and load in feedback system

78. Assume ideal operational amplifiers in the circuit of Figure P5.53.

   a. Show that the leftmost operational amplifier works as a subtracting amplifier. Namely, $v_1 = v_o - v_{in}$.

   b. Draw a block diagram of the system, with the subtracting amplifier represented with a summing junction, and the circuit of the rightmost operational amplifier with a transfer function in the forward path. Keep R as a variable.

   c. Obtain the system's closed-loop transfer function.

   d. For a unit step input, obtain the value of R that will result in a settling time $T_s = 1$ msec.

   e. Using the value of R calculated in Part **d**, make a sketch of the resulting unit step response.
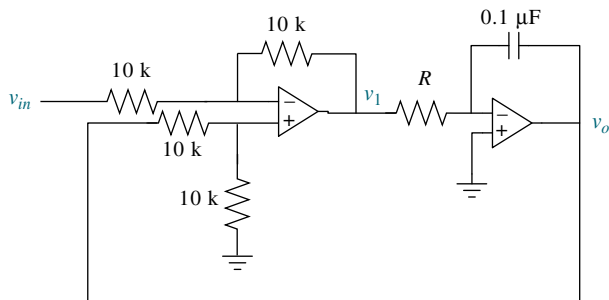
FIGURE P5.53

PROGRESSIVE ANALYSIS AND DESIGN PROBLEMS

79. High-speed rail pantograph. Problem 21 in Chapter 1 discusses the active control of a pantograph mechanism for high-speed rail systems. In this problem you found a functional block diagram relating the output force (*actual*) to the input force (*desired* output). In Problem 67, Chapter 2, you found the transfer function for the pantograph dynamics, that is, the transfer function relating the displacement of the spring that models the head to the applied force, or $G(s) = (Y_h(s) - Y_{cat}(s))/F_{up}(s)$ (*O'Connor, 1997*). We now create a pantograph active-control loop by adding the following components and following your functional block diagram found in Problem 21, Chapter 1: input transducer $(G_i(s) = 1/100)$, controller $(G_c(s) = K)$, actuator

$(G_a(s) = 1/1000)$, pantograph spring $(K_s = 82.3 \times 10^3 \text{N/m})$, and sensor $(H_o(s) = 1/100)$.

   a. Using the functional block diagram from your solution of Problem 21 in Chapter 1, and the pantograph dynamics, $G(s)$, found in Problem 67, Chapter 2, assemble a block diagram of the active pantograph control system.

   b. Find the closed-loop transfer function for the block diagram found in Part **a** if $K = 1000$.

   c. Represent the pantograph dynamics in phase-variable form and find a state-space representation for the closed-loop system if $K = 1000$). State Space **SS**

80. Control of HIV/AIDS. Given the HIV system of Problem 82 in Chapter 4 and repeated here for convenience (*Craig, 2004*): State Space **SS**

$$\begin{bmatrix} \dot{T} \\ \dot{T}^* \\ \dot{v} \end{bmatrix} = \begin{bmatrix} -0.04167 & 0 & -0.0058 \\ 0.0217 & -0.24 & 0.0058 \\ 0 & 100 & -2.4 \end{bmatrix} \begin{bmatrix} T \\ T^* \\ v \end{bmatrix}$$
$$+ \begin{bmatrix} 5.2 \\ -5.2 \\ 0 \end{bmatrix} u_1$$

$$y = \begin{bmatrix} 0 & 0 & 1 \end{bmatrix} \begin{bmatrix} T \\ T^* \\ v \end{bmatrix}$$

Express the system in the following forms:

   a. Phase-variable form

   b. Controller canonical form

   c. Observer canonical form

Finally,

   d. Use MATLAB to obtain the system's diagonalized representation. MATLAB **ML**

81. Hybrid vehicle. Figure P5.54 shows the block diagram of a possible cascade control scheme for an HEV driven by a dc motor (*Preitl, 2007*).
   Let the speed controller $G_{SC}(s) = 100 + \frac{40}{s}$, the torque controller and power amp $K_A G_{TC}(s) = 10 + \frac{6}{s}$, the current sensor sensitivity $K_{CS} = 0.5$, the speed sensor sensitivity $K_{SS} = 0.0433$. Also following the development in previous chapters $\frac{1}{R_a} = 1; \eta_{tot} K_t = 1.8; k_b = 2; D = k_f = 0.1; \frac{1}{J_{tot}} = \frac{1}{7.226}; \frac{r}{i_{tot}} = 0.0615;$ and $\rho C_w A v_0 \frac{r}{i_{tot}} = 0.6154$.

   a. Substitute these values in the block diagram, and find the transfer function, $T(s) = V(s)/R_v(s)$, using block-diagram reduction rules. [Hint: Start
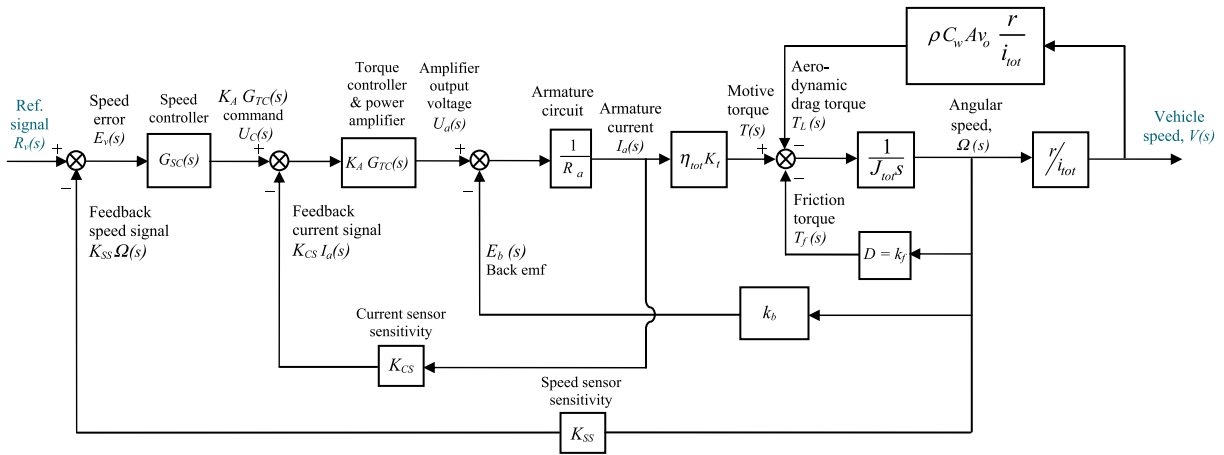
by moving the last $\frac{r}{i_{tot}}$ block to the right past the pickoff point.]

b. Develop a Simulink model for the original system in Figure P5.54. Set the reference signal input, $r_v(t) = 4\,u(t)$, as a step input with a zero initial value, a step time = 0 seconds, and a final value of 4 volts. Use X-Y graphs to display (over the period from 0 to 8 seconds) the response of the

Simulink
SL
MATLAB
ML

following variables to the step input: (1) change in car speed (m/s), (2) car acceleration (m/s^2), and (3) motor armature current (A).

To record the time and the above three variables (in array format), connect them to four **Workspace** sinks, each of which carry the respective variable name. After the simulation ends, utilize MATLAB plot commands to obtain and edit the three graphs of interest.

Cyber Exploration Laboratory

Experiment 5.1

Objectives   To verify the equivalency of the basic forms, including cascade, parallel, and feedback forms. To verify the equivalency of the basic moves, including moving blocks past summing junctions, and moving blocks past pickoff points.

Minimum Required Software Packages   MATLAB, Simulink, and the Control System Toolbox

Prelab

1. Find the equivalent transfer function of three cascaded blocks, $G_1(s) = \dfrac{1}{s+1}$. $G_2(s) = \dfrac{1}{s+4}$, and $G_3(s) = \dfrac{s+3}{s+5}$.

2. Find the equivalent transfer function of three parallel blocks, $G_1(s) = \dfrac{1}{s+4}$. $G_2(s) = \dfrac{1}{s+4}$, and $G_3(s) = \dfrac{s+3}{s+5}$.

3. Find the equivalent transfer function of the negative feedback system of Figure P5.55 if $G(s) = \dfrac{s+1}{s(s+2)}$, and $H(s) = \dfrac{s+3}{s+4}$.
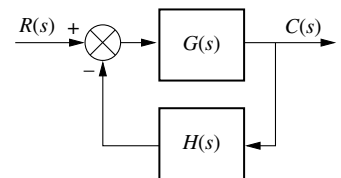
FIGURE P5.55

4. For the system of Prelab 3, push $H(s)$ to the left past the summing junction and draw the equivalent system.

5. For the system of Prelab 3, push $H(s)$ to the right past the pickoff point and draw the equivalent system.

Lab

1. Using Simulink, set up the cascade system of Prelab 1 and the equivalent single block. Make separate plots of the step response of the cascaded system and its equivalent single block. Record the values of settling time and rise time for each step response.

2. Using Simulink, set up the parallel system of Prelab 2 and the equivalent single block. Make separate plots of the step response of the parallel system and its equivalent single block. Record the values of settling time and rise time for each step response.

3. Using Simulink, set up the negative feedback system of Prelab 3 and the equivalent single block. Make separate plots of the step response of the negative feedback system and its equivalent single block. Record the values of settling time and rise time for each step response.

4. Using Simulink, set up the negative feedback systems of Prelabs 3, 4, and 5. Make separate plots of the step response of each of the systems. Record the values of settling time and rise time for each step response.

Postlab

1. Using your lab data, verify the equivalent transfer function of blocks in cascade.

2. Using your lab data, verify the equivalent transfer function of blocks in parallel.

3. Using your lab data, verify the equivalent transfer function of negative feedback systems.

4. Using your lab data, verify the moving of blocks past summing junctions and pickoff points.

5. Discuss your results. Were the equivalencies verified?

Experiment 5.2

Objective   To use the various functions within LabVIEW's Control Design and Simulation Module to implement block diagram reduction.

Minimum Required Software Package   LabVIEW with the Control Design Simulation Module

Prelab   Given the block diagram from Example 5.2, replace $G_1, G_2, G_3, H_1, H_2, H_3$ with the following transfer functions and obtain an equivalent transfer function.

$$G_1 = \frac{1}{s+10}; G_2 = \frac{1}{s+1}; G_3 = \frac{s+1}{s^2+4s+4}; H_1 = \frac{s+1}{s+2}; H_2 = 2; H_3 = 1$$

Lab Use LabVIEW to implement the block diagram from Example 5.2 using the transfer functions given in the Prelab.

Postlab   Verify your calculations from the Prelab with that of the equivalent transfer function obtained with LabVIEW.

Experiment 5.3

Objective   To use the various functions within LabVIEW's Control Design and Simulation Module and the Mathematics/Polynomial palette to implement Mason's rule for block diagram reduction.

Minimum Required Software Package   LabVIEW with Control Design and Simulation Module, Math Script RT Module, and the Mathematics/Polynomial palette.

Prelab   Given the block diagram created in the Prelab of Cyber Exploration Laboratory 5.2, use Mason's rule to obtain an equivalent transfer function.

Lab   Use LabVIEW's Control Design and Simulation Module as well as the Mathematics/Polynomial functions to implement block diagram reduction using Mason's rule.

Postlab   Verify your calculations from the Prelab with that of the equivalent transfer function obtained with LabVIEW.

Bibliography

Åstrom, K., Klein, R. E., and Lennartsson, A. Bicycle Dynamics and Control. *IEEE Control Systems*, August 2005, pp. 26–47.

Bailey, F. N., Cockburn, J. C., and Dee, A. Robust Control for High-Performance Materials Testing. *IEEE Control Systems*, April 1992, pp. 63–70.

Ballard, R. D. *The Discovery of the Titanic*, Warner Books, New York, 1987.

Ben-Dov, D., and Salcudean, S. E. A Force-Controlled Pneumatic Actuator. *IEEE Transactions on Robotics and Automation*, vol. 11, 1995, pp. 906–911.

Cavallo, A., De Maria, G., and Verde, L. Robust Flight Control Systems: A Parameter Space Design. *Journal of Guidance, Control, and Dynamics*, vol. 15, no. 5, September-October 1992, pp. 1207–1215.

Craig, I. K., Xia, X., and Venter, J. W., Introducing HIV/AIDS Education into the Electrical Engineering Curriculum at the University of Pretoria, *IEEE Transactions on Education*, vol. 47, no. 1, February 2004, pp. 65–73.

de Vlugt, E., Schouten, A. C., and van derHelm, F.C.T. Adaptation of Reflexive Feedback during Arm Posture to Different Environments. *Biological Cybernetics*, vol. 87, 2002, pp. 10–26.

Evans, J., Krishnamurthy, B., Barrows, B., Skewis, T., and Lumelsky, V. Handling Real-World Motion Planning: A Hospital Transport Robot. *IEEE Control Systems*, February 1992, pp. 15–20.

Graebe, S. F., Goodwin, G. C., and Elsley, G., Control Design and Implementation in Continuous Steel Casting. *IEEE Control Systems*, August 1995, pp. 64–71.

Hostetter, G. H., Savant, C. J., Jr. and Stefani, R. T. *Design of Feedback Control Systems*. 2d ed. Saunders College Publishing, New York, 1989.

Johnson, H. et al. *Unmanned Free-Swimming Submersible (UFSS) System Description*. NRL Memorandum Report 4393. Naval Research Laboratory, Washington, DC, 1980.

Karkoub, M., Her, M.-G., and Chen, J. M. Design and Control of a Haptic Interactive Motion Simulator for Virtual Entertainment Systems, *Robonica*, vol. 28, 2010, pp. 47–56.

Kong, F., and de Keyser, R. Identification and Control of the Mould Level in a Continuous Casting Machine. *Second IEEE Conference on Control Application*, Vancouver, B.C., 1993. pp. 53–58.

Kurland, M., and Papson, T. P. Analog Computer Simulation of Linear Modulation Systems. *Transactions of the Analog/Hybrid Computer Educational Society*, January 1971, pp. 9–18.

Lee, S.-R., Ko, S.-H., Dehbonei, H., Jeon, C.-H., and Kwon, O.-S., Operational Characteristics of PV/Diesel Hybrid Distributed Generation System Using Dual Voltage Source Inverter for Weak Grid, *ISIS 2007 Proceedings,* Eighth Symposium on Advanced Intelligent Systems. 2007.

Lepschy, A. M., Mian, G. A., and Viaro, U. Feedback Control in Ancient Water and Mechanical Clocks. *IEEE Transactions on Education*, vol. 35, 1992, pp. 3–10.

Lin, J.-S., and Kanellakopoulos, I., Nonlinear Design of Active Suspensions. *IEEE Control Systems*, vol. 17, issue 3, June 1997, pp. 45–59.

Mason, S. J. Feedback Theory—Some Properties of Signal-Flow Graphs. *Proc. IRE*, September 1953, pp. 1144–1156.

Milhorn, H. T., Jr. *The Application of Control Theory to Physiological Systems*. W. B. Saunders, Philadelphia, 1966.

Neamen, D. A. *Electronic Circuit Analysis and Design*. McGraw-Hill, 2d ed., 2001, p. 334.

O'Connor, D. N., Eppinger, S. D., Seering, W. P., and Wormly, D. N. Active Control of a High-Speed Pantograph. *Journal of Dynamic Systems, Measurements, and Control*, vol. 119, March 1997, pp. 1–4.

Piccin, O., Barbé L., Bayle B., and de Mathelin, M. A Force Feedback Teleoperated Needle Insertion Device for Percutaneous Procedures. *Int. J. of Robotics Research*, vol. 28, 2009, p. 1154.

Preitl, Z., Bauer, P., and Bokor, J. A Simple Control Solution for Traction Motor Used in Hybrid Vehicles. *Fourth International Symposium on Applied Computational Intelligence and Informatics*. IEEE, 2007.

Tasch, U., Koontz, J. W., Ignatoski, M. A., and Geselowitz, D. B. An Adaptive Aortic Pressure Observer for the Penn State Electric Ventricular Assist Device. *IEEE Transactions on Biomedical Engineering*, vol. 37, 1990, pp. 374–383.

Timothy, L. K., and Bona, B. E. *State Space Analysis: An Introduction*. McGraw-Hill, New York, 1968.

Vaughan, N. D., and Gamble, J. B. The Modeling and Simulation of a Proportional Solenoid Valve. *Journal of Dynamic Systems, Measurements, and Control*, vol. 118, March 1996, pp. 120–125.

Yaniv, Y., Sivan, R., and Landesberg, A. Stability, Controllability and Observability of the "Four State" Model for the Sarcomeric Control of Contraction. *Annals of Biomedical Engineering*, vol. 34, 2006, pp. 778–789.

Stability

6
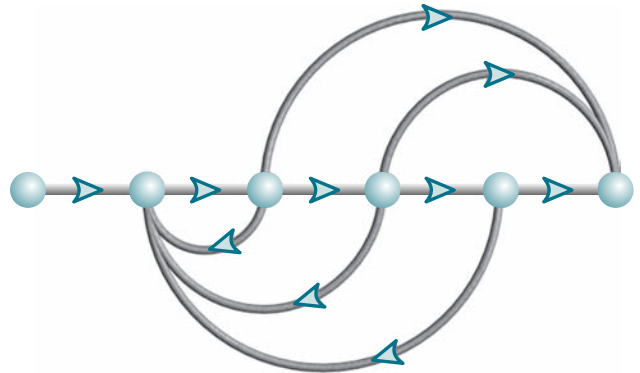
(**Chapter Learning Outcomes**)

After completing this chapter the student will be able to:

- Make and interpret a basic Routh table to determine the stability of a system (Sections 6.1–6.2)
- Make and interpret a Routh table where either the first element of a row is zero or an entire row is zero (Sections 6.3–6.4)
- Use a Routh table to determine the stability of a system represented in state space (Section 6.5)

State Space
SS

(**Case Study Learning Outcomes**)

You will be able to demonstrate your knowledge of the chapter objectives with case studies as follows:

- Given the antenna azimuth position control system shown on the front endpapers, you will be able to find the range of preamplifier gain to keep the system stable.
- Given the block diagrams for the UFSS vehicle's pitch and heading control systems on the back endpapers, you will be able to determine the range of gain for stability of the pitch or heading control system.

6.1 Introduction

In Chapter 1, we saw that three requirements enter into the design of a control system: transient response, stability, and steady-state errors. Thus far we have covered transient response, which we will revisit in Chapter 8. We are now ready to discuss the next requirement, stability.

Stability is the most important system specification. If a system is unstable, transient response and steady-state errors are moot points. An unstable system cannot be designed for a specific transient response or steady-state error requirement. What, then, is stability? There are many definitions for stability, depending upon the kind of system or the point of view. In this section, we limit ourselves to linear, time-invariant systems.

In Section 1.5, we discussed that we can control the output of a system if the steady-state response consists of only the forced response. But the total response of a system is the sum of the forced and natural responses, or

$$c(t) = c_{\text{forced}}(t) + c_{\text{natural}}(t) \tag{6.1}$$

Using these concepts, we present the following definitions of stability, instability, and marginal stability:

A linear, time-invariant system is *stable* if the natural response approaches zero as time approaches infinity.

A linear, time-invariant system is *unstable* if the natural response grows without bound as time approaches infinity.

A linear, time-invariant system is *marginally stable* if the natural response neither decays nor grows but remains constant or oscillates as time approaches infinity.

Thus, the definition of stability implies that only the forced response remains as the natural response approaches zero.

These definitions rely on a description of the natural response. When one is looking at the total response, it may be difficult to separate the natural response from the forced response. However, we realize that if the input is bounded and the total response is not approaching infinity as time approaches infinity, then the natural response is obviously not approaching infinity. If the input is unbounded, we see an unbounded total response, and we cannot arrive at any conclusion about the stability of the system; we cannot tell whether the total response is unbounded because the forced response is unbounded or because the natural response is unbounded. Thus, our alternate definition of *stability*, one that regards the total response and implies the first definition based upon the natural response, is this:

A system is stable if *every* bounded input yields a bounded output.

We call this statement the bounded-input, bounded-output (BIBO) definition of stability.

Let us now produce an alternate definition for instability based on the total response rather than the natural response. We realize that if the input is bounded but the total response is unbounded, the system is unstable, since we can conclude that the natural response approaches infinity as time approaches infinity. If the input is unbounded, we will see an unbounded total response, and we cannot draw any conclusion about the stability of the system; we cannot tell whether the total response is unbounded because the forced response is unbounded or because the

natural response is unbounded. Thus, our alternate definition of *instability*, one that regards the total response, is this:

A system is unstable if *any* bounded input yields an unbounded output.

These definitions help clarify our previous definition of *marginal stability*, which really means that the system is stable for some bounded inputs and unstable for others. For example, we will show that if the natural response is undamped, a bounded sinusoidal input of the same frequency yields a natural response of growing oscillations. Hence, the system appears stable for all bounded inputs except this one sinusoid. Thus, marginally stable systems by the natural response definitions are included as unstable systems under the BIBO definitions.

Let us summarize our definitions of stability for linear, time-invariant systems. Using the natural response:

1. A system is stable if the natural response approaches zero as time approaches infinity.
2. A system is unstable if the natural response approaches infinity as time approaches infinity.
3. A system is marginally stable if the natural response neither decays nor grows but remains constant or oscillates.

Using the total response (BIBO):

1. A system is stable if *every* bounded input yields a bounded output.
2. A system is unstable if *any* bounded input yields an unbounded output.

Physically, an unstable system whose natural response grows without bound can cause damage to the system, to adjacent property, or to human life. Many times systems are designed with limited stops to prevent total runaway. From the perspective of the time response plot of a physical system, instability is displayed by transients that grow without bound and, consequently, a total response that does not approach a steady-state value or other forced response.[1]

How do we determine if a system is stable? Let us focus on the natural response definitions of stability. Recall from our study of system poles that poles in the left half-plane (lhp) yield either pure exponential decay or damped sinusoidal natural responses. These natural responses decay to zero as time approaches infinity. Thus, if the closed-loop system poles are in the left half of the plane and hence have a negative real part, the system is stable. That is, *stable systems have closed-loop transfer functions with poles only in the left half-plane.*

Poles in the right half-plane (rhp) yield either pure exponentially increasing or exponentially increasing sinusoidal natural responses. These natural responses approach infinity as time approaches infinity. Thus, if the closed-loop system poles are in the right half of the *s*-plane and hence have a positive real part, the system is unstable. Also, poles of multiplicity greater than 1 on the imaginary axis lead to the sum of responses of the form $At^n \cos(\omega t + \phi)$, where $n = 1, 2, \ldots$, which also approaches infinity as time approaches infinity. Thus, *unstable systems have closed-loop transfer functions with at least one pole in the right half-plane and/or poles of multiplicity greater than 1 on the imaginary axis.*

---

[1] Care must be taken here to distinguish between natural responses growing without bound and a forced response, such as a ramp or exponential increase, that also grows without bound. A system whose forced response approaches infinity is stable as long as the natural response approaches zero.

Finally, a system that has imaginary axis poles of multiplicity 1 yields pure sinusoidal oscillations as a natural response. These responses neither increase nor decrease in amplitude. Thus, *marginally stable systems have closed-loop transfer functions with only imaginary axis poles of multiplicity 1 and poles in the left half-plane.*

As an example, the unit step response of the stable system of Figure 6.1(*a*) is compared to that of the unstable system of Figure 6.1(*b*). The responses, also shown in Figure 6.1, show that while the oscillations for the stable system diminish, those for the unstable system increase without bound. Also notice that the stable system's response in this case approaches a steady-state value of unity.

It is not always a simple matter to determine if a feedback control system is stable. Unfortunately, a typical problem that arises is shown in Figure 6.2. Although we know the poles of the forward transfer function in Figure 6.2(*a*), we do not know the location of the poles of the equivalent closed-loop system of Figure 6.2(*b*) without factoring or otherwise solving for the roots.

However, under certain conditions, we can draw some conclusions about the stability of the system. First, if the closed-loop transfer function has only
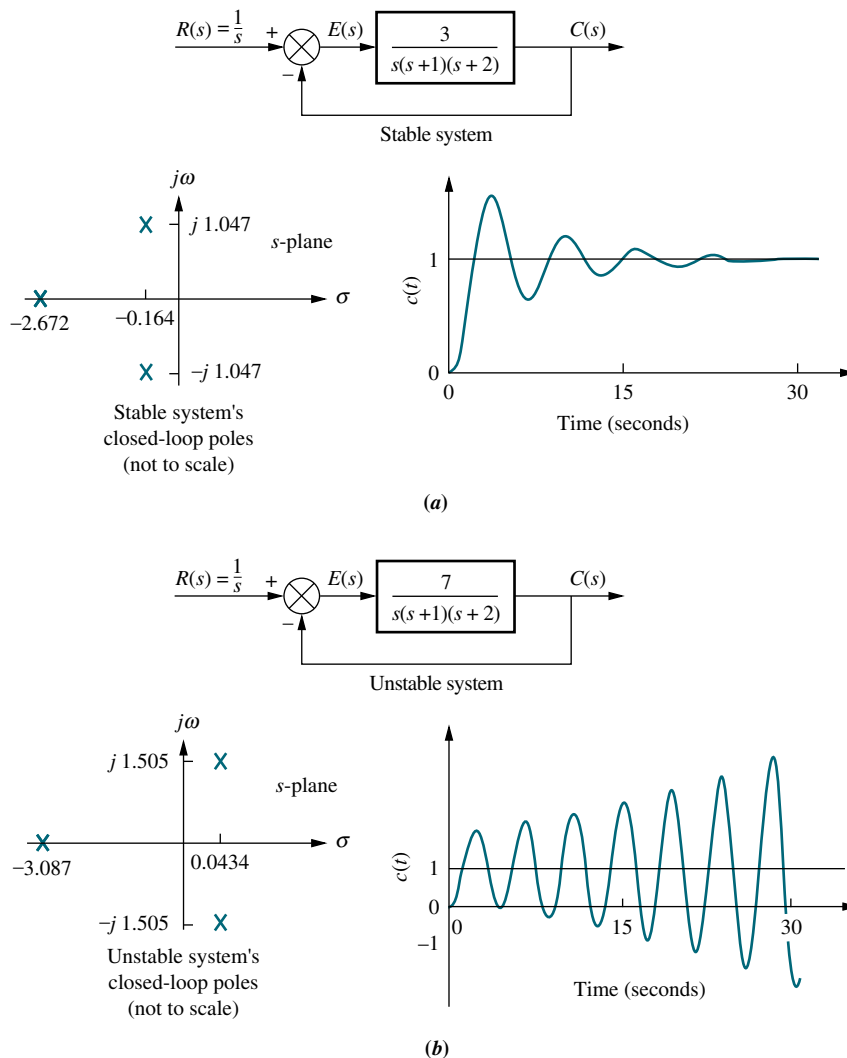
FIGURE 6.1 Closed-loop poles and response:
a. stable system;
b. unstable system
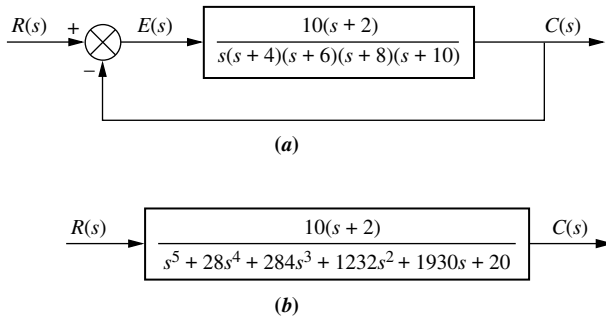
FIGURE 6.2 Common cause of problems in finding closed-loop poles: **a.** original system; **b.** equivalent system

left–half-plane poles, then the factors of the denominator of the closed-loop system transfer function consist of products of terms such as $(s + a_i)$, where a_i is real and positive, or complex with a positive real part. The product of such terms is a polynomial with all positive coefficients.[2] No term of the polynomial can be missing, since that would imply cancellation between positive and negative coefficients or imaginary axis roots in the factors, which is not the case. Thus, a sufficient condition for a system to be unstable is that all signs of the coefficients of the denominator of the closed-loop transfer function are not the same. If powers of s are missing, the system is either unstable or, at best, marginally stable. Unfortunately, if all coefficients of the denominator are positive and not missing, we do not have definitive information about the system's pole locations.

If the method described in the previous paragraph is not sufficient, then a computer can be used to determine the stability by calculating the root locations of the denominator of the closed-loop transfer function. Today some hand-held calculators can evaluate the roots of a polynomial. There is, however, another method to test for stability without having to solve for the roots of the denominator. We discuss this method in the next section.

6.2   Routh-Hurwitz Criterion

In this section, we learn a method that yields stability information without the need to solve for the closed-loop system poles. Using this method, we can tell how many closed-loop system poles are in the left half-plane, in the right half-plane, and on the $j\omega$-axis. (Notice that we say *how many*, not *where*.) We can find the number of poles in each section of the s-plane, but we cannot find their coordinates. The method is called the *Routh-Hurwitz criterion* for stability (*Routh*, *1905*).

The method requires two steps: (1) Generate a data table called a *Routh table* and (2) interpret the Routh table to tell how many closed-loop system poles are in the left half-plane, the right half-plane, and on the $j\omega$-axis. You might wonder why we study the Routh-Hurwitz criterion when modern calculators and computers can tell us the exact location of system poles. The power of the method lies in design rather than analysis. For example, if you have an unknown parameter in the denominator of a transfer function, it is difficult to determine via a calculator the range of this parameter to yield stability. You would probably rely on trial and error to answer the

---

[2] The coefficients can also be made all negative by multiplying the polynomial by -1. This operation does not change the root location.

stability question. We shall see later that the Routh-Hurwitz criterion can yield a closed-form expression for the range of the unknown parameter.

In this section, we make and interpret a basic Routh table. In the next section, we consider two special cases that can arise when generating this data table.

Generating a Basic Routh Table
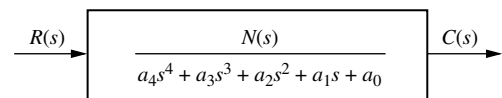
FIGURE 6.3 Equivalent closed-loop transfer function

Look at the equivalent closed-loop transfer function shown in Figure 6.3. Since we are interested in the system poles, we focus our attention on the denominator. We first create the Routh table shown in Table 6.1. Begin by labeling the rows with powers of s from the highest power of the denominator of the closed-loop transfer function to s^0. Next start with the coefficient of the highest power of s in the denominator and list, horizontally in the first row, every other coefficient. In the second row, list horizontally, starting with the next highest power of s, every coefficient that was skipped in the first row.

The remaining entries are filled in as follows. Each entry is a negative determinant of entries in the previous two rows divided by the entry in the first column directly above the calculated row. The left-hand column of the determinant is always the first column of the previous two rows, and the right-hand column is the elements of the column above and to the right. The table is complete when all of the rows are completed down to s^0. Table 6.2 is the completed Routh table. Let us look at an example.

TABLE 6.1   Initial layout for Routh table

s^4	a_4	a_2	a_0
s^3	a_3	a_1	0
s^2			
s^1			
s^0			

TABLE 6.2   Completed Routh table

s^4	a_4	a_2	a_0
s^3	a_3	a_1	0
s^2	$\dfrac{-\begin{vmatrix} a_4 & a_2 \\ a_3 & a_1 \end{vmatrix}}{a_3} = b_1$	$\dfrac{-\begin{vmatrix} a_4 & a_0 \\ a_3 & 0 \end{vmatrix}}{a_3} = b_2$	$\dfrac{-\begin{vmatrix} a_4 & 0 \\ a_3 & 0 \end{vmatrix}}{a_3} = 0$
s^1	$\dfrac{-\begin{vmatrix} a_3 & a_1 \\ b_1 & b_2 \end{vmatrix}}{b_1} = c_1$	$\dfrac{-\begin{vmatrix} a_3 & 0 \\ b_1 & 0 \end{vmatrix}}{b_1} = 0$	$\dfrac{-\begin{vmatrix} a_3 & 0 \\ b_1 & 0 \end{vmatrix}}{b_1} = 0$
s^0	$\dfrac{-\begin{vmatrix} b_1 & b_2 \\ c_1 & 0 \end{vmatrix}}{c_1} = d_1$	$\dfrac{-\begin{vmatrix} b_1 & 0 \\ c_1 & 0 \end{vmatrix}}{c_1} = 0$	$\dfrac{-\begin{vmatrix} b_1 & 0 \\ c_1 & 0 \end{vmatrix}}{c_1} = 0$

Example 6.1

Creating a Routh Table

PROBLEM: Make the Routh table for the system shown in Figure 6.4(a).

SOLUTION: The first step is to find the equivalent closed-loop system because we want to test the denominator of this function, not the given forward transfer
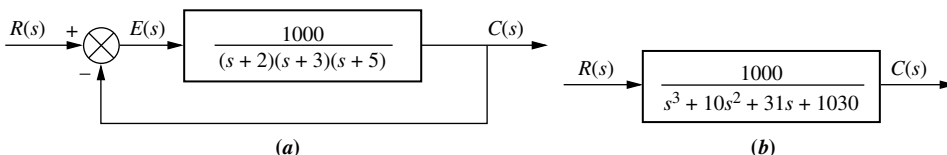
FIGURE 6.4   a. Feedback system for Example 6.1; **b.** equivalent closed-loop system

TABLE 6.3   Completed Routh table for Example 6.1

s^3	1	31	0
s^2	~~10~~ 1	~~1030~~ 103	0
s^1	$\dfrac{-\begin{vmatrix} 1 & 31 \\ 1 & 103 \end{vmatrix}}{1} = -72$	$\dfrac{-\begin{vmatrix} 1 & 0 \\ 0 & 0 \end{vmatrix}}{1} = 0$	$\dfrac{-\begin{vmatrix} 1 & 0 \\ 1 & 0 \end{vmatrix}}{1} = 0$
s^0	$\dfrac{-\begin{vmatrix} 1 & 103 \\ -72 & 0 \end{vmatrix}}{-72} = 103$	$\dfrac{-\begin{vmatrix} 1 & 0 \\ -72 & 0 \end{vmatrix}}{-72} = 0$	$\dfrac{-\begin{vmatrix} 1 & 0 \\ -72 & 0 \end{vmatrix}}{-72} = 0$

function, for pole location. Using the feedback formula, we obtain the equivalent system of Figure 6.4(b). The Routh-Hurwitz criterion will be applied to this denominator. First label the rows with powers of s from s^3 down to s^0 in a vertical column, as shown in Table 6.3. Next form the first row of the table, using the coefficients of the denominator of the closed-loop transfer function. Start with the coefficient of the highest power and skip every other power of s. Now form the second row with the coefficients of the denominator skipped in the previous step. Subsequent rows are formed with determinants, as shown in Table 6.2.

For convenience, any row of the Routh table can be multiplied by a positive constant without changing the values of the rows below. This can be proved by examining the expressions for the entries and verifying that any multiplicative constant from a previous row cancels out. In the second row of Table 6.3, for example, the row was multiplied by 1/10. We see later that care must be taken not to multiply the row by a negative constant.

Interpreting the Basic Routh Table

Now that we know how to generate the Routh table, let us see how to interpret it. The basic Routh table applies to systems with poles in the left and right half-planes. Systems with imaginary poles and the kind of Routh table that results will be discussed in the next section. Simply stated, the Routh-Hurwitz criterion declares that *the number of roots of the polynomial that are in the right half-plane is equal to the number of sign changes in the first column.*

If the closed-loop transfer function has all poles in the left half of the s-plane, the system is stable. Thus, a system is stable if there are no sign changes in the first column of the Routh table. For example, Table 6.3 has two sign changes in the first column. The first sign change occurs from 1 in the s^2 row to -72 in the s^1 row. The second occurs from -72 in the s^1 row to 103 in the s^0 row. Thus, the system of Figure 6.4 is unstable since two poles exist in the right half-plane.

Skill-Assessment Exercise 6.1

PROBLEM: Make a Routh table and tell how many roots of the following polynomial are in the right half-plane and in the left half-plane.

$$P(s) = 3s^7 + 9s^6 + 6s^5 + 4s^4 + 7s^3 + 8s^2 + 2s + 6$$

ANSWER: Four in the right half-plane (rhp), three in the left half-plane (lhp).

The complete solution is at www.wiley.com/college/nise.

Now that we have described how to generate and interpret a basic Routh table, let us look at two special cases that can arise.

6.3   Routh-Hurwitz Criterion: Special Cases

Two special cases can occur: (1) The Routh table sometimes will have a zero *only in the first column* of a row, or (2) the Routh table sometimes will have an *entire row* that consists of zeros. Let us examine the first case.

Zero Only in the First Column

If the first element of a row is zero, division by zero would be required to form the next row. To avoid this phenomenon, an epsilon, ϵ, is assigned to replace the zero in the first column. The value ϵ is then allowed to approach zero from either the positive or the negative side, after which the signs of the entries in the first column can be determined. Let us look at an example.

Example 6.2

Stability via Epsilon Method

TryIt 6.1

Use the following MATLAB statement to find the poles of the closed-loop transfer function in Eq. (6.2).

```
roots([1 2 3 6 5 3])
```

PROBLEM: Determine the stability of the closed-loop transfer function

$$T(s) = \frac{10}{s^5 + 2s^4 + 3s^3 + 6s^2 + 5s + 3} \tag{6.2}$$

SOLUTION: The solution is shown in Table 6.4. We form the Routh table by using the denominator of Eq. (6.2). Begin by assembling the Routh table down to the row where a zero appears *only* in the first column (the s^3 row). Next replace the zero by a small number, ϵ, and complete the table. To begin the interpretation, we must first assume a sign, positive or negative, for the quantity ϵ. Table 6.5 shows the first column of Table 6.4 along with the resulting signs for choices of ϵ positive and ϵ negative.

TABLE 6.4   Completed Routh table for Example 6.2

s^5	1	3	5
s^4	2	6	3
s^3	~~0~~ ϵ	$\dfrac{7}{2}$	0
s^2	$\dfrac{6\epsilon - 7}{\epsilon}$	3	0
s^1	$\dfrac{42\epsilon - 49 - 6\epsilon^2}{12\epsilon - 14}$	0	0
s^0	3	0	0

TABLE 6.5   Determining signs in first column of a Routh table with zero as first element in a row

Label	First column	$\epsilon = +$	$\epsilon = -$
s^5	1	+	+
s^4	2	+	+
s^3	~~0~~ ϵ	+	−
s^2	$\dfrac{6\epsilon - 7}{\epsilon}$	−	+
s^1	$\dfrac{42\epsilon - 49 - 6\epsilon^2}{12\epsilon - 14}$	+	+
s^0	3	+	+

If ϵ is chosen positive, Table 6.5 will show a sign change from the s^3 row to the s^2 row, and there will be another sign change from the s^2 row to the s^1 row. Hence, the system is unstable and has two poles in the right half-plane.

Alternatively, we could choose ϵ negative. Table 6.5 would then show a sign change from the s^4 row to the s^3 row. Another sign change would occur from the s^3 row to the s^2 row. Our result would be exactly the same as that for a positive choice for ϵ. Thus, the system is unstable, with two poles in the right half-plane.

```
Students who are performing the MATLAB exercises and want to
explore the added capability of MATLAB's Symbolic Math Toolbox
should now run ch6sp1 in Appendix F at www.wiley.com/college/
nise. You will learn how to use the Symbolic Math Toolbox to
calculate the values of cells in a Routh table even if the table
contains symbolic objects, such as ε. You will see that the
Symbolic Math Toolbox and MATLAB yield an alternate way to gen-
erate the Routh table for Example 6.2.
```

Symbolic Math

SM

Another method that can be used when a zero appears only in the first column of a row is derived from the fact that a polynomial that has the reciprocal roots of the original polynomial has its roots distributed the same—right half-plane, left half-plane, or imaginary axis—because taking the reciprocal of the root value does not move it to another region. Thus, if we can find the polynomial that has the reciprocal roots of the original, it is possible that the Routh table for the new polynomial will not have a zero in the first column. This method is usually computationally easier than the epsilon method just described.

We now show that the polynomial we are looking for, the one with the reciprocal roots, is simply the original polynomial with its coefficients written in reverse order (*Phillips, 1991*). Assume the equation

$$s^n + a_{n-1}s^{n-1} + \cdots + a_1 s + a_0 = 0 \tag{6.3}$$

If s is replaced by $1/d$, then d will have roots which are the reciprocal of s. Making this substitution in Eq. (6.3),

$$\left(\frac{1}{d}\right)^n + a_{n-1}\left(\frac{1}{d}\right)^{n-1} + \cdots + a_1\left(\frac{1}{d}\right) + a_0 = 0 \tag{6.4}$$

Factoring out $(1/d)^n$,

$$\left(\frac{1}{d}\right)^n \left[1 + a_{n-1}\left(\frac{1}{d}\right)^{-1} + \cdots + a_1\left(\frac{1}{d}\right)^{(1-n)} + a_0\left(\frac{1}{d}\right)^{-n}\right]$$

$$= \left(\frac{1}{d}\right)^n [1 + a_{n-1}d + \cdots + a_1 d^{(n-1)} + a_0 d^n] = 0 \tag{6.5}$$

Thus, the polynomial with reciprocal roots is a polynomial with the coefficients written in reverse order. Let us redo the previous example to show the computational advantage of this method.

Example 6.3

Stability via Reverse Coefficients

PROBLEM: Determine the stability of the closed-loop transfer function

$$T(s) = \frac{10}{s^5 + 2s^4 + 3s^3 + 6s^2 + 5s + 3} \qquad (6.6)$$

SOLUTION: First write a polynomial that has the reciprocal roots of the denominator of Eq. (6.6). From our discussion, this polynomial is formed by writing the denominator of Eq. (6.6) in reverse order. Hence,

$$D(s) = 3s^5 + 5s^4 + 6s^3 + 3s^2 + 2s + 1 \qquad (6.7)$$

We form the Routh table as shown in Table 6.6 using Eq. (6.7). Since there are two sign changes, the system is unstable and has two right-half-plane poles. This is the same as the result obtained in Example 6.2. Notice that Table 6.6 does not have a zero in the first column.

TABLE 6.6   Routh table for Example 6.3

s^5	3	6	2
s^4	5	3	1
s^3	4.2	1.4	
s^2	1.33	1	
s^1	−1.75		
s^0	1		

Entire Row is Zero

We now look at the second special case. Sometimes while making a Routh table, we find that an entire row consists of zeros because there is an even polynomial that is a factor of the original polynomial. This case must be handled differently from the case of a zero in only the first column of a row. Let us look at an example that demonstrates how to construct and interpret the Routh table when an entire row of zeros is present.

Example 6.4

Stability via Routh Table with Row of Zeros

PROBLEM: Determine the number of right-half-plane poles in the closed-loop transfer function

$$T(s) = \frac{10}{s^5 + 7s^4 + 6s^3 + 42s^2 + 8s + 56} \qquad (6.8)$$

SOLUTION: Start by forming the Routh table for the denominator of Eq. (6.8) (see Table 6.7). At the second row we multiply through by 1/7 for convenience. We stop at the third row, since the entire row consists of zeros, and use the following

TABLE 6.7   Routh table for Example 6.4

s^5		1			6			8
s^4	~~7~~	1		~~42~~	6		~~56~~	8
s^3	~~0~~ ~~4~~	1	~~0~~	~~12~~	3	~~0~~	~~0~~	0
s^2		3			8			0
s^1		$\dfrac{1}{3}$			0			0
s^0		8			0			0

procedure. First we return to the row immediately above the row of zeros and form an auxiliary polynomial, using the entries in that row as coefficients. The polynomial will start with the power of s in the label column and continue by skipping every other power of s. Thus, the polynomial formed for this example is

$$P(s) = s^4 + 6s^2 + 8 \tag{6.9}$$

Next we differentiate the polynomial with respect to s and obtain

$$\frac{dP(s)}{ds} = 4s^3 + 12s + 0 \tag{6.10}$$

Finally, we use the coefficients of Eq. (6.10) to replace the row of zeros. Again, for convenience, the third row is multiplied by 1/4 after replacing the zeros.

The remainder of the table is formed in a straightforward manner by following the standard form shown in Table 6.2. Table 6.7 shows that all entries in the first column are positive. Hence, there are no right–half-plane poles.

Let us look further into the case that yields an entire row of zeros. An entire row of zeros will appear in the Routh table when a purely even or purely odd polynomial is a factor of the original polynomial. For example, $s^4 + 5s^2 + 7$ is an even polynomial; it has only even powers of s. Even polynomials only have roots that are symmetrical about the origin.[3] This symmetry can occur under three conditions of root position: (1) The roots are symmetrical and real, (2) the roots are symmetrical and imaginary, or (3) the roots are quadrantal. Figure 6.5 shows examples of these cases. Each case or combination of these cases will generate an even polynomial.

It is this even polynomial that causes the row of zeros to appear. Thus, the row of zeros tells us of the existence of an even polynomial whose roots are symmetric about the origin. Some of these roots could be on the $j\omega$-axis. On the other hand, since $j\omega$ roots are symmetric about the origin, if we do not have a row of zeros, we cannot possibly have $j\omega$ roots.

Another characteristic of the Routh table for the case in question is that the row previous to the row of zeros contains the even polynomial that is a factor of the original polynomial. Finally, everything from the row containing the even polynomial down to the end of the Routh table is a test of only the even polynomial. Let us put these facts together in an example.
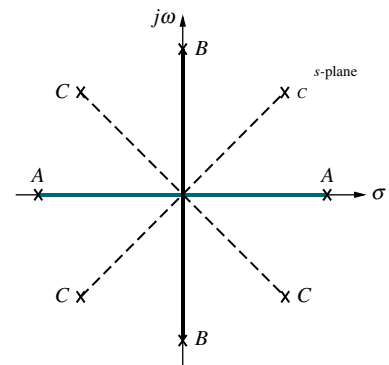
A: Real and symmetrical about the origin
B: Imaginary and symmetrical about the origin
C: Quadrantal and symmetrical about the origin

FIGURE 6.5   Root positions to generate even polynomials: A, B, C, or any combination

---

[3] The polynomial $s^5 + 5s^3 + 7s$ is an example of an odd polynomial; it has only odd powers of s. Odd polynomials are the product of an even polynomial and an odd power of s. Thus, the constant term of an odd polynomial is always missing.

Example 6.5

Pole Distribution via Routh Table with Row of Zeros

PROBLEM:　For the transfer function

$$T(s) = \frac{20}{s^8 + s^7 + 12s^6 + 22s^5 + 39s^4 + 59s^3 + 48s^2 + 38s + 20} \tag{6.11}$$

tell how many poles are in the right half-plane, in the left half-plane, and on the $j\omega$-axis.

SOLUTION:　Use the denominator of Eq. (6.11) and form the Routh table in Table 6.8. For convenience the s^6 row is multiplied by 1/10, and the s^5 row is multiplied by 1/20. At the s^3 row we obtain a row of zeros. Moving back one row to s^4, we extract the even polynomial, $P(s)$, as

$$P(s) = s^4 + 3s^2 + 2 \tag{6.12}$$

TABLE 6.8　Routh table for Example 6.5

s^8		1		12		39	48	20
s^7		1		22		59	38	0
s^6		~~−10~~ −1		~~−20~~ −2	~~10~~	1	~~20~~ 2	0
s^5		~~20~~ 1		~~60~~ 3	~~40~~	2	0	0
s^4		1		3		2	0	0
s^3	~~0~~ ~~4~~	2	~~0~~ ~~6~~	3	~~0~~ ~~0~~	0	0	0
s^2		$\dfrac{3}{2}$ 3		~~2~~ 4		0	0	0
s^1		$\dfrac{1}{3}$		0		0	0	0
s^0		4		0		0	0	0

This polynomial will divide evenly into the denominator of Eq. (6.11) and thus is a factor. Taking the derivative with respect to s to obtain the coefficients that replace the row of zeros in the s^3 row, we find

$$\frac{dP(s)}{ds} = 4s^3 + 6s + 0 \tag{6.13}$$

Replace the row of zeros with 4, 6, and 0 and multiply the row by 1/2 for convenience. Finally, continue the table to the s^0 row, using the standard procedure.

　　How do we now interpret this Routh table? Since all entries from the even polynomial at the s^4 row down to the s^0 row are a test of the even polynomial, we begin to draw some conclusions about the roots of the even polynomial. No sign changes exist from the s^4 row down to the s^0 row. Thus, the even polynomial does not have right–half-plane poles. Since there are no right–half-plane poles, no left–half-plane poles are present because of the requirement for symmetry. Hence, the even polynomial, Eq. (6.12), must have all four of its poles on the $j\omega$-axis.[4] These results are summarized in the first column of Table 6.9.

---

[4] A necessary condition for stability is that the $j\omega$ roots have unit multiplicity. The even polynomial must be checked for multiple $j\omega$ roots. For this case, the existence of multiple $j\omega$ roots would lead to a perfect, fourth-order square polynomial. Since Eq. (6.12) is not a perfect square, the four $j\omega$ roots are distinct.

TABLE 6.9   Summary of pole locations for Example 6.5

| | Polynomial | | |
	Even (fourth-order)	Other (fourth-order)	Total (eighth-order)
Location			
Right half-plane	0	2	2
Left half-plane	0	2	2
$j\omega$	4	0	4

The remaining roots of the total polynomial are evaluated from the s^8 row down to the s^4 row. We notice two sign changes: one from the s^7 row to the s^6 row and the other from the s^6 row to the s^5 row. Thus, the other polynomial must have two roots in the right half-plane. These results are included in Table 6.9 under "Other". The final tally is the sum of roots from each component, the even polynomial and the other polynomial, as shown under "Total" in Table 6.9. Thus, the system has two poles in the right half-plane, two poles in the left half-plane, and four poles on the $j\omega$-axis; it is unstable because of the right–half-plane poles.

We now summarize what we have learned about polynomials that generate entire rows of zeros in the Routh table. These polynomials have a purely even factor with roots that are symmetrical about the origin. The even polynomial appears in the Routh table in the row directly above the row of zeros. Every entry in the table from the even polynomial's row to the end of the chart applies only to the even polynomial. Therefore, the number of sign changes from the even polynomial to the end of the table equals the number of right-half-plane roots of the even polynomial. Because of the symmetry of roots about the origin, the even polynomial must have the same number of left–half-plane roots as it does right–half-plane roots. Having accounted for the roots in the right and left half-planes, we know the remaining roots must be on the $j\omega$-axis.

Every row in the Routh table from the beginning of the chart to the row containing the even polynomial applies only to the other factor of the original polynomial. For this factor, the number of sign changes, from the beginning of the table down to the even polynomial, equals the number of right–half-plane roots. The remaining roots are left–half-plane roots. There can be no $j\omega$ roots contained in the other polynomial.
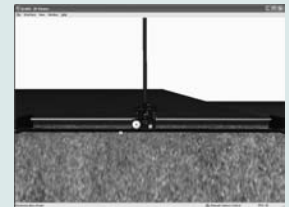
Skill-Assessment Exercise 6.2

PROBLEM: Use the Routh-Hurwitz criterion to find how many poles of the following closed-loop system, $T(s)$, are in the rhp, in the lhp, and on the $j\omega$-axis:

$$T(s) = \frac{s^3 + 7s^2 - 21s + 10}{s^6 + s^5 - 6s^4 + 0s^3 - s^2 - s + 6}$$

ANSWER: Two rhp, two lhp, and two $j\omega$

The complete solution is at www.wiley.com/college/nise.

Let us demonstrate the usefulness of the Routh-Hurwitz criterion with a few additional examples.

6.4   Routh-Hurwitz Criterion: Additional Examples

The previous two sections have introduced the Routh-Hurwitz criterion. Now we need to demonstrate the method's application to a number of analysis and design problems.

Example 6.6

Standard Routh-Hurwitz

PROBLEM: Find the number of poles in the left half-plane, the right half-plane, and on the $j\omega$-axis for the system of Figure 6.6.

FIGURE 6.6   Feedback control system for Example 6.6
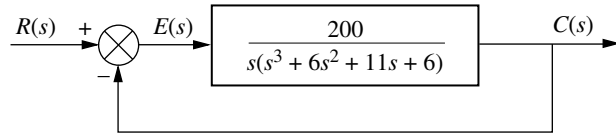
SOLUTION: First, find the closed-loop transfer function as

$$T(s) = \frac{200}{s^4 + 6s^3 + 11s^2 + 6s + 200} \tag{6.14}$$

The Routh table for the denominator of Eq. (6.14) is shown as Table 6.10. For clarity, we leave most zero cells blank. At the s^1 row there is a negative coefficient; thus, there are two sign changes. The system is unstable, since it has two right–half-plane poles and two left–half-plane poles. The system cannot have $j\omega$ poles since a row of zeros did not appear in the Routh table.

TABLE 6.10   Routh table for Example 6.6

s^4	1	11	200
s^3	~~6~~ 1	~~6~~ 1	
s^2	~~10~~ 1	~~200~~ 20	
s^1	−19		
s^0	20		

The next example demonstrates the occurrence of a zero in only the first column of a row.

Example 6.7

Routh-Hurwitz with Zero in First Column

PROBLEM: Find the number of poles in the left half-plane, the right half-plane, and on the $j\omega$-axis for the system of Figure 6.7.

FIGURE 6.7   Feedback control system for Example 6.7
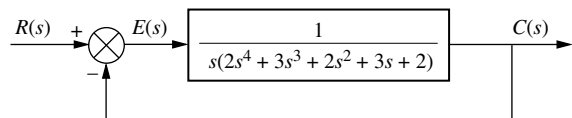
SOLUTION: The closed-loop transfer function is

$$T(s) = \frac{1}{2s^5 + 3s^4 + 2s^3 + 3s^2 + 2s + 1} \tag{6.15}$$

Form the Routh table shown as Table 6.11, using the denominator of Eq. (6.15). A zero appears in the first column of the s^3 row. Since the entire row is not zero, simply replace the zero with a small quantity, ϵ, and continue the table. Permitting ϵ to be a small, positive quantity, we find that the first term of the s^2 row is negative. Thus, there are two sign changes, and the system is unstable, with two poles in the right half-plane. The remaining poles are in the left half-plane.

TABLE 6.11   Routh table for Example 6.7

s^5	2	2	2
s^4	3	3	1
s^3	$\cancel{0}$ ϵ	$\dfrac{4}{3}$	
s^2	$\dfrac{3\epsilon - 4}{\epsilon}$	1	
s^1	$\dfrac{12\epsilon - 16 - 3\epsilon^2}{9\epsilon - 12}$		
s^0	1		

We also can use the alternative approach, where we produce a polynomial whose roots are the reciprocal of the original. Using the denominator of Eq. (6.15), we form a polynomial by writing the coefficients in reverse order,

$$s^5 + 2s^4 + 3s^3 + 2s^2 + 3s + 2 \tag{6.16}$$

The Routh table for this polynomial is shown as Table 6.12. Unfortunately, in this case we also produce a zero only in the first column at the s^2 row. However, the table is easier to work with than Table 6.11. Table 6.12 yields the same results as Table 6.11: three poles in the left half-plane and two poles in the right half-plane. The system is unstable.

TABLE 6.12   Alternative Routh table for Example 6.7

s^5	1	3	3
s^4	2	2	2
s^3	2	2	
s^2	$\cancel{0}$ ϵ	2	
s^1	$\dfrac{2\epsilon - 4}{\epsilon}$		
s^0	2		

```
Students who are using MATLAB should now run ch6p1 in Appendix B.
You will learn how to perform block diagram reduction to find T(s),
followed by an evaluation of the closed-loop system's poles to
determine stability. This exercise uses MATLAB to do Example 6.7.
```

MATLAB
ML

In the next example, we see an entire row of zeros appear along with the possibility of imaginary roots.

Example 6.8

Routh-Hurwitz with Row of Zeros

PROBLEM: Find the number of poles in the left half-plane, the right half-plane, and on the $j\omega$-axis for the system of Figure 6.8. Draw conclusions about the stability of the closed-loop system.

FIGURE 6.8
Feedback control system for Example 6.8
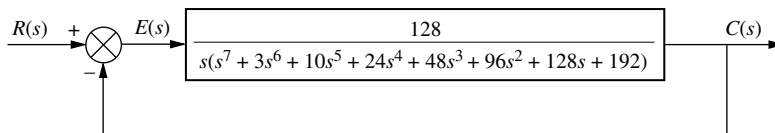
$R(s)$ $+$ $\bigotimes$ $-$ $E(s)$ $\dfrac{128}{s(s^7 + 3s^6 + 10s^5 + 24s^4 + 48s^3 + 96s^2 + 128s + 192)}$ $C(s)$

SOLUTION: The closed-loop transfer function for the system of Figure 6.8 is

$$T(s) = \frac{128}{s^8 + 3s^7 + 10s^6 + 24s^5 + 48s^4 + 96s^3 + 128s^2 + 192s + 128} \tag{6.17}$$

Using the denominator, form the Routh table shown as Table 6.13. A row of zeros appears in the s^5 row. Thus, the closed-loop transfer function denominator must have an even polynomial as a factor. Return to the s^6 row and form the even polynomial:

$$P(s) = s^6 + 8s^4 + 32s^2 + 64 \tag{6.18}$$

TABLE 6.13   Routh table for Example 6.8

s^8		1		10		48		128	128
s^7	~~3~~	1	~~24~~	8	~~96~~	32	~~192~~	64	
s^6	~~2~~	1	~~16~~	8	~~64~~	32	~~128~~	64	
s^5	~~0~~ ~~6~~	3	~~0~~ ~~32~~	16	~~0~~ ~~64~~	32	~~0~~ ~~0~~	0	
s^4	$\dfrac{8}{3}$	1	$\dfrac{64}{3}$	8	~~64~~	24			
s^3	~~8~~ 1		~~40~~ -5						
s^2	~~3~~	1	~~24~~	8					
s^1		3							
s^0		8							

Differentiate this polynomial with respect to s to form the coefficients that will replace the row of zeros:

$$\frac{dP(s)}{ds} = 6s^5 + 32s^3 + 64s + 0 \tag{6.19}$$

Replace the row of zeros at the s^5 row by the coefficients of Eq. (6.19) and multiply through by 1/2 for convenience. Then complete the table.

We note that there are two sign changes from the even polynomial at the s^6 row down to the end of the table. Hence, the even polynomial has two right–half-

TABLE 6.14   Summary of pole locations for Example 6.8

	Polynomial		
Location	Even (sixth-order)	Other (second-order)	Total (eighth-order)
Right half-plane	2	0	2
Left half-plane	2	2	4
$j\omega$	2	0	2

plane poles. Because of the symmetry about the origin, the even polynomial must have an equal number of left–half-plane poles. Therefore, the even polynomial has two left–half-plane poles. Since the even polynomial is of sixth order, the two remaining poles must be on the $j\omega$-axis.

There are no sign changes from the beginning of the table down to the even polynomial at the s^6 row. Therefore, the rest of the polynomial has no right–half-plane poles. The results are summarized in Table 6.14. The system has two poles in the right half-plane, four poles in the left half-plane, and two poles on the $j\omega$-axis, which are of unit multiplicity. The closed-loop system is unstable because of the right–half-plane poles.

The Routh-Hurwitz criterion gives vivid proof that changes in the gain of a feedback control system result in differences in transient response because of changes in closed-loop pole locations. The next example demonstrates this concept. We will see that for control systems, such as those shown in Figure 6.9, gain variations can move poles from stable regions of the s-plane onto the $j\omega$-axis and then into the right half-plane.
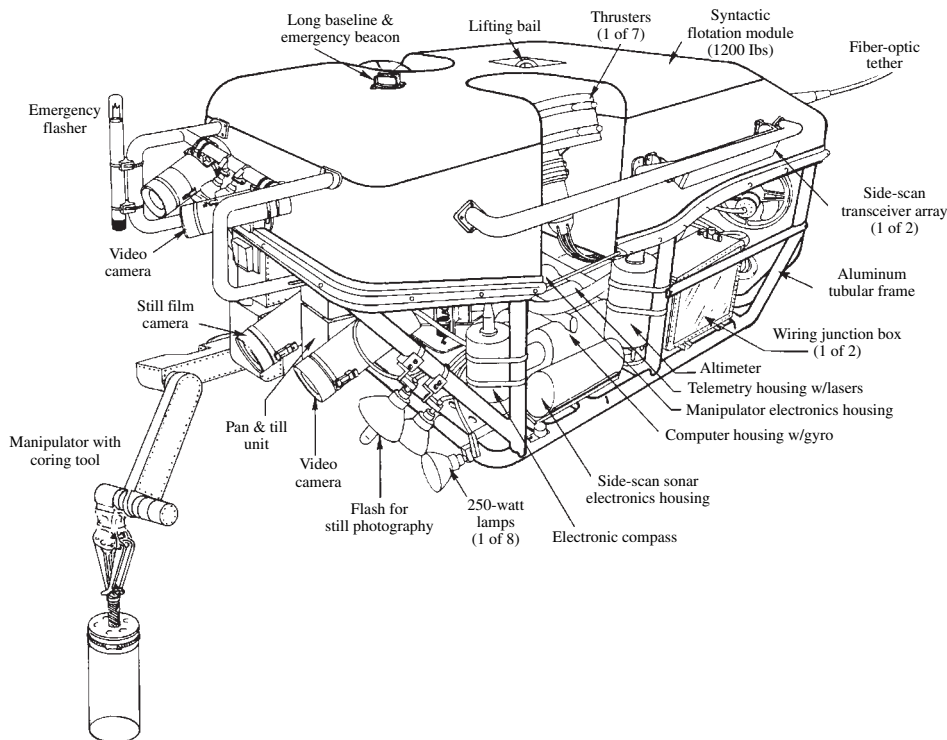
FIGURE 6.9   *Jason* is an underwater, remote-controlled vehicle that has been used to explore the wreckage of the *Lusitania*. The manipulator and cameras comprise some of the vehicle's control systems

Example 6.9

Stability Design via Routh-Hurwitz

PROBLEM: Find the range of gain, K, for the system of Figure 6.10 that will cause the system to be stable, unstable, and marginally stable. Assume $K > 0$.
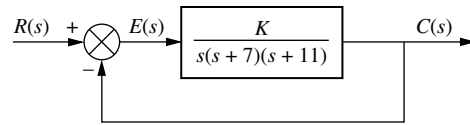
FIGURE 6.10 Feedback control system for Example 6.9

SOLUTION: First find the closed-loop transfer function as

$$T(s) = \frac{K}{s^3 + 18s^2 + 77s + K} \tag{6.20}$$

Next form the Routh table shown as Table 6.15.

TABLE 6.15 Routh table for Example 6.9

s^3	1	77
s^2	18	K
s^1	$\dfrac{1386 - K}{18}$	
s^0	K	

Since K is assumed positive, we see that all elements in the first column are always positive except the s^1 row. This entry can be positive, zero, or negative, depending upon the value of K. If $K < 1386$, all terms in the first column will be positive, and since there are no sign changes, the system will have three poles in the left half-plane and be *stable*.

If $K > 1386$, the s^1 term in the first column is negative. There are two sign changes, indicating that the system has two right–half-plane poles and one left–half-plane pole, which makes the system *unstable*.

If $K = 1386$, we have an entire row of zeros, which could signify $j\omega$ poles. Returning to the s^2 row and replacing K with 1386, we form the even polynomial

$$P(s) = 18s^2 + 1386 \tag{6.21}$$

Differentiating with respect to s, we have

$$\frac{dP(s)}{ds} = 36s + 0 \tag{6.22}$$

Replacing the row of zeros with the coefficients of Eq. (6.22), we obtain the Routh-Hurwitz table shown as Table 6.16 for the case of $K = 1386$.

TABLE 6.16 Routh table for Example 6.9 with $K = 1386$

s^3	1	77
s^2	18	1386
s^1	$\cancel{0}$ 36	
s^0	1386	

Since there are no sign changes from the even polynomial (s^2 row) down to the bottom of the table, the even polynomial has its two roots on the $j\omega$-axis of unit multiplicity. Since there are no sign changes above the even polynomial, the remaining root is in the left half-plane. Therefore the system is *marginally stable*.

```
Students who are using MATLAB should now run ch6p2 in Appendix B.
You will learn how to set up a loop to search for the range of gain to
yield stability. This exercise uses MATLAB to do Example 6.9.
```

MATLAB

ML

```
Students who are performing the MATLAB exercises and want to
explore the added capability of MATLAB's Symbolic Math Toolbox
should now run ch6sp2 in Appendix F at www.wiley.com/college/
nise. You will learn how to use the Symbolic Math Toolbox to
calculate the values of cells in a Routh table even if the table
contains symbolic objects, such as a variable gain, K. You will
see that the Symbolic Math Toolbox and MATLAB yield an alterna-
tive way to solve Example 6.9.
```

Symbolic Math

SM

The Routh-Hurwitz criterion is often used in limited applications to factor polynomials containing even factors. Let us look at an example.

Example 6.10

Factoring via Routh-Hurwitz

PROBLEM: Factor the polynomial

$$s^4 + 3s^3 + 30s^2 + 30s + 200 \tag{6.23}$$

SOLUTION: Form the Routh table of Table 6.17. We find that the s^1 row is a row of zeros. Now form the even polynomial at the s^2 row:

$$P(s) = s^2 + 10 \tag{6.24}$$

TABLE 6.17   Routh table for Example 6.10

s^4		1	30	200
s^3	~~3~~ 1		~~30~~ 10	
s^2	~~20~~ 1		~~200~~ 10	
s^1	~~0~~ 2		~~0~~ 0	
s^0		10		

This polynomial is differentiated with respect to s in order to complete the Routh table. However, since this polynomial is a factor of the original polynomial in Eq. (6.23), dividing Eq. (6.23) by (6.24) yields $(s^2 + 3s + 20)$ as the other factor. Hence,

$$s^4 + 3s^3 + 30s^2 + 30s + 200 = (s^2 + 10)(s^2 + 3s + 20)$$
$$= (s + j3.1623)(s - j3.1623) \tag{6.25}$$
$$\times (s + 1.5 + j4.213)(s + 1.5 - j4.213)$$

Skill-Assessment Exercise 6.3

PROBLEM: For a unity feedback system with the forward transfer function

$$G(s) = \frac{K(s+20)}{s(s+2)(s+3)}$$

find the range of K to make the system stable.

ANSWER: $0 < K < 2$

The complete solution is at www.wiley.com/college/nise.

6.5   Stability in State Space

State Space

SS

Up to this point we have examined stability from the s-plane viewpoint. Now we look at stability from the perspective of state space. In Section 4.10, we mentioned that the values of the system's poles are equal to the eigenvalues of the system matrix, **A**. We stated that the eigenvalues of the matrix **A** were solutions of the equation det $(s\mathbf{I} - \mathbf{A}) = 0$, which also yielded the poles of the transfer function. Eigenvalues appeared again in Section 5.8, where they were formally defined and used to diagonalize a matrix. Let us now formally show that the eigenvalues and the system poles have the same values.

Reviewing Section 5.8, the eigenvalues of a matrix, **A**, are values of λ that permit a nontrivial solution (other than **0**) for **x** in the equation

$$\mathbf{A}\mathbf{x} = \lambda\mathbf{x} \tag{6.26}$$

In order to solve for the values of λ that do indeed permit a solution for **x**, we rearrange Eq. (6.26) as follows:

$$\lambda\mathbf{x} - \mathbf{A}\mathbf{x} = \mathbf{0} \tag{6.27}$$

or

$$(\lambda\mathbf{I} - \mathbf{A})\mathbf{x} = \mathbf{0} \tag{6.28}$$

Solving for **x** yields

$$\mathbf{x} = (\lambda\mathbf{I} - \mathbf{A})^{-1}\mathbf{0} \tag{6.29}$$

or

$$\mathbf{x} = \frac{\text{adj}(\lambda\mathbf{I} - \mathbf{A})}{\det(\lambda\mathbf{I} - \mathbf{A})}\mathbf{0} \tag{6.30}$$

We see that all solutions will be the null vector except for the occurrence of zero in the denominator. Since this is the only condition where elements of **x** will be $0/0$, or indeterminate, it is the only case where a nonzero solution is possible.

The values of λ are calculated by forcing the denominator to zero:

$$\det(\lambda\mathbf{I} - \mathbf{A}) = 0 \tag{6.31}$$

This equation determines the values of λ for which a nonzero solution for **x** in Eq. (6.26) exists. In Section 5.8, we defined **x** as *eigenvectors* and the values of λ as the *eigenvalues* of the matrix **A**.

Let us now relate the eigenvalues of the system matrix, **A**, to the system's poles. In Chapter 3 we derived the equation of the system transfer function, Eq. (3.73), from the state equations. The system transfer function has $\det(s\mathbf{I} - \mathbf{A})$ in the denominator because of the presence of $(s\mathbf{I} - \mathbf{A})^{-1}$. Thus,

$$\det(s\mathbf{I} - \mathbf{A}) = 0 \tag{6.32}$$

is the characteristic equation for the system from which the system poles can be found.

Since Eqs. (6.31) and (6.32) are identical apart from a change in variable name, we conclude that the eigenvalues of the matrix **A** are identical to the system's poles before cancellation of common poles and zeroes in the transfer function. Thus, we can determine the stability of a system represented in state space by finding the eigenvalues of the system matrix, **A**, and determining their locations on the *s*-plane.

Example 6.11

Stability in State Space

PROBLEM: Given the system

$$\dot{\mathbf{x}} = \begin{bmatrix} 0 & 3 & 1 \\ 2 & 8 & 1 \\ -10 & -5 & -2 \end{bmatrix} \mathbf{x} + \begin{bmatrix} 10 \\ 0 \\ 0 \end{bmatrix} u \tag{6.33a}$$

$$y = \begin{bmatrix} 1 & 0 & 0 \end{bmatrix} \mathbf{x} \tag{6.33b}$$

find out how many poles are in the left half-plane, in the right half-plane, and on the $j\omega$-axis.

SOLUTION: First form $(s\mathbf{I} - \mathbf{A})$:

$$(s\mathbf{I} - \mathbf{A}) = \begin{bmatrix} s & 0 & 0 \\ 0 & s & 0 \\ 0 & 0 & s \end{bmatrix} - \begin{bmatrix} 0 & 3 & 1 \\ 2 & 8 & 1 \\ -10 & -5 & -2 \end{bmatrix} = \begin{bmatrix} s & -3 & -1 \\ -2 & s-8 & -1 \\ 10 & 5 & s+2 \end{bmatrix} \tag{6.34}$$

Now find the $\det(s\mathbf{I} - \mathbf{A})$:

$$\det(s\mathbf{I} - \mathbf{A}) = s^3 - 6s^2 - 7s - 52 \tag{6.35}$$

Using this polynomial, form the Routh table of Table 6.18.

TABLE 6.18   Routh table for Example 6.11

s^3	1	-7
s^2	$\cancel{6}\ -3$	$\cancel{52}\ -26$
s^1	$\cancel{\dfrac{47}{3}}\ -1$	$\cancel{0}\quad 0$
s^0	-26	

Since there is one sign change in the first column, the system has one right–half-plane pole and two left–half-plane poles. It is therefore unstable. Yet, you may question the possibility that if a nonminimum-phase zero cancels the unstable pole, the system will be stable. However, in practice, the nonminimum-phase zero or unstable pole will shift due to a slight change in the system's parameters. This change will cause the system to become unstable.

Students who are using MATLAB should now run ch6p3 in Appendix B. You will learn how to determine the stability of a system represented in state space by finding the eigenvalues of the system matrix. This exercise uses MATLAB to do Example 6.11.

Skill-Assessment Exercise 6.4

WileyPLUS

WPCS

Control Solutions

TryIt 6.3

Use the following MATLAB statements to find the eigenvalues of the system described in Skill-Assessment Exercise 6.4.

```
A=[2  1  1
   1  7  1
  −3  4  −5];
Eig=eig(A)
```

PROBLEM: For the following system represented in state space, find out how many poles are in the left half-plane, in the right half-plane, and on the $j\omega$-axis.

$$\dot{\mathbf{x}} = \begin{bmatrix} 2 & 1 & 1 \\ 1 & 7 & 1 \\ -3 & 4 & -5 \end{bmatrix} \mathbf{x} + \begin{bmatrix} 0 \\ 0 \\ 1 \end{bmatrix} r$$

$$\mathbf{y} = \begin{bmatrix} 0 & 1 & 0 \end{bmatrix} \mathbf{x}$$

ANSWER: Two rhp and one lhp.

The complete solution is at www.wiley.com/college/nise.

In this section, we have evaluated the stability of feedback control systems from the state-space perspective. Since the closed-loop poles and the eigenvalues of a system are the same, the stability requirement of a system represented in state space dictates that the eigenvalues cannot be in the right half of the *s*-plane or be multiple on the $j\omega$-axis.

We can obtain the eigenvalues from the state equations without first converting to a transfer function to find the poles: The equation $\det(s\mathbf{I} - \mathbf{A}) = 0$ yields the eigenvalues directly. If $\det(s\mathbf{I} - \mathbf{A})$, a polynomial in *s*, cannot be factored easily, we can apply the Routh-Hurwitz criterion to it to evaluate how many eigenvalues are in each region of the *s*-plane.

We now summarize this chapter, first with case studies and then with a written summary. Our case studies include the antenna azimuth position control system and the UFSS. Stability is as important to these systems as it is to the system shown in Figure 6.11.

Case Studies

Antenna Control: Stability Design via Gain

Design
D

This chapter has covered the elements of stability. We saw that stable systems have their closed-loop poles in the left half of the *s*-plane. As the loop gain is changed, the locations of the poles are also changed, creating the possibility that the poles can move into the right half of the *s*-plane, which yields instability. Proper gain settings are essential for the stability of closed-loop systems. The following case study demonstrates the proper setting of the loop gain to ensure stability.

PROBLEM: You are given the antenna azimuth position control system shown on the front endpapers, Configuration 1. Find the range of preamplifier gain required to keep the closed-loop system stable.

SOLUTION: The closed-loop transfer function was derived in the case studies in Chapter 5 as

$$T(s) = \frac{6.63K}{s^3 + 101.71s^2 + 171s + 6.63K} \tag{6.36}$$

Using the denominator, create the Routh table shown as Table 6.19. The third row of the table shows that a row of zeros occurs if $K = 2623$. This value of K makes the system marginally stable. Therefore, there will be no sign changes in the first column if $0 < K < 2623$. We conclude that, for stability, $0 < K < 2623$.

TABLE 6.19   Routh table for antenna control case study

s^3	1	171
s^2	101.71	$6.63K$
s^1	$17392.41{-}6.63K$	0
s^0	$6.63K$	

CHALLENGE: We now give you a problem to test your knowledge of this chapter's objectives. Refer to the antenna azimuth position control system shown on the front endpapers, Configuration 2. Find the range of preamplifier gain required to keep the closed-loop system stable.

UFSS Vehicle: Stability Design via Gain

For this case study, we return to the UFSS vehicle and study the stability of the pitch control system, which is used to control depth. Specifically, we find the range of pitch gain that keeps the pitch control loop stable.

PROBLEM: The pitch control loop for the UFSS vehicle (*Johnson*, *1980*) is shown on the back endpapers. Let $K_2 = 1$ and find the range of K_1 that ensures that the closed-loop pitch control system is stable.

SOLUTION: The first step is to reduce the pitch control system to a single, closed-loop transfer function. The equivalent forward transfer function, $G_e(s)$, is

$$G_e(s) = \frac{0.25K_1(s + 0.435)}{s^4 + 3.456s^3 + 3.457s^2 + 0.719s + 0.0416} \tag{6.37}$$

With unity feedback the closed-loop transfer function, $T(s)$, is

$$T(s) = \frac{0.25K_1(s + 0.435)}{s^4 + 3.456s^3 + 3.457s^2 + (0.719 + 0.25K_1)s + (0.0416 + 0.109K_1)} \tag{6.38}$$

The denominator of Eq. (6.38) is now used to form the Routh table shown as Table 6.20.

TABLE 6.20   Routh table for UFSS case study

s^4	1	3.457	$0.0416 + 0.109K_1$
s^3	3.456	$0.719 + 0.25K_1$	
s^2	$11.228 - 0.25K_1$	$0.144 + 0.377K_1$	
s^1	$\dfrac{-0.0625K_1^2 + 1.324K_1 + 7.575}{11.228 - 0.25K_1}$		
s^0	$0.144 + 0.377K_1$		

Note: Some rows have been multiplied by a positive constant for convenience.

Looking at the first column, the s^4 and s^3 rows are positive. Thus, all elements of the first column must be positive for stability. For the first column of the s^2 row to be positive, $-\infty < K_1 < 44.91$. For the first column of the s^1 row to be positive, the numerator must be positive, since the denominator is positive from the previous step. The solution to the quadratic term in the numerator yields roots of $K_1 = -4.685$ and 25.87. Thus, for a positive numerator, $-4.685 < K_1 < 25.87$. Finally, for the first column of the s^0 row to be positive, $-0.382 < K_1 < \infty$. Using all three conditions, stability will be ensured if $-0.382 < K_1 < 25.87$.

CHALLENGE: You are now given a problem to test your knowledge of this chapter's objectives. For the UFSS vehicle (*Johnson*, *1980*) heading control system shown on the back endpapers and introduced in the UFSS case study challenge in Chapter 5, do the following:

a. Find the range of heading gain that ensures the vehicle's stability. Let $K_2 = 1$

b. `Repeat Part a using MATLAB.`

In our case studies, we calculated the ranges of gain to ensure stability. The student should be aware that although these ranges yield stability, setting gain within these limits may not yield the desired transient response or steady-state error characteristics. In Chapters 9 and 11, we will explore design techniques, other than simple gain adjustment, that yield more flexibility in obtaining desired characteristics.

❨ Summary ❩

In this chapter, we explored the concepts of system stability from both the classical and the state-space viewpoints. We found that for linear systems, *stability* is based on a natural response that decays to zero as time approaches infinity. On the other hand, if the natural response increases without bound, the forced response is overpowered by the natural response, and we lose control. This condition is known as *instability*. A third possibility exists: The natural response may neither decay nor grow without bound but oscillate. In this case, the system is said to be *marginally stable*.

We also used an alternative definition of stability when the natural response is not explicitly available. This definition is based on the total response and says that a system is stable if every bounded input yields a bounded output (BIBO) and unstable if any bounded input yields an unbounded output.

Mathematically, stability for linear, time-invariant systems can be determined from the location of the closed-loop poles:

- If the poles are only in the left half-plane, the system is stable.
- If any poles are in the right half-plane, the system is unstable.
- If the poles are on the $j\omega$-axis and in the left half-plane, the system is marginally stable as long as the poles on the $j\omega$-axis are of unit multiplicity; it is unstable if there are any multiple $j\omega$ poles.

Unfortunately, although the open-loop poles may be known, we found that in higher-order systems it is difficult to find the closed-loop poles without a computer program.

The *Routh-Hurwitz criterion* lets us find how many poles are in each of the sections of the *s*-plane without giving us the coordinates of the poles. Just knowing that there are poles in the right half-plane is enough to determine that a system is unstable. Under certain limited conditions, when an even polynomial is present, the Routh table can be used to factor the system's characteristic equation.

Obtaining stability from the state-space representation of a system is based on the same concept—the location of the roots of the characteristic equation. These roots are equivalent to the eigenvalues of the system matrix and can be found by solving $\det(s\mathbf{I} - \mathbf{A}) = 0$. Again, the Routh-Hurwitz criterion can be applied to this polynomial. The point is that the state-space representation of a system need not be converted to a transfer function in order to investigate stability. In the next chapter, we will look at steady-state errors, the last of three important control system requirements we emphasize.

❨ Review Questions ❩

1. What part of the output response is responsible for determining the stability of a linear system?
2. What happens to the response named in Question 1 that creates instability?

3. What would happen to a physical system that becomes unstable?

4. Why are marginally stable systems considered unstable under the BIBO definition of stability?

5. Where do system poles have to be to ensure that a system is not unstable?

6. What does the Routh-Hurwitz criterion tell us?

7. Under what conditions would the Routh-Hurwitz criterion easily tell us the actual location of the system's closed-loop poles?

8. What causes a zero to show up only in the first column of the Routh table?

9. What causes an entire row of zeros to show up in the Routh table?

10. Why do we sometimes multiply a row of a Routh table by a positive constant?

11. Why do we not multiply a row of a Routh table by a negative constant?

12. If a Routh table has two sign changes above the even polynomial and five sign changes below the even polynomial, how many right–half-plane poles does the system have?

13. Does the presence of an entire row of zeros always mean that the system has $j\omega$ poles?

14. If a seventh-order system has a row of zeros at the s^3 row and two sign changes below the s^4 row, how many $j\omega$ poles does the system have?

State Space

SS

State Space

SS

15. Is it true that the eigenvalues of the system matrix are the same as the closed-loop poles?

16. How do we find the eigenvalues?

Problems

1. Tell how many roots of the following polynomial are in the right half-plane, in the left half-plane, and on the $j\omega$-axis: [Section: 6.2]

$$P(s) = s^5 + 3s^4 + 5s^3 + 4s^2 + s + 3$$

2. Tell how many roots of the following polynomial are in the right half-plane, in the left half-plane, and on the $j\omega$-axis: [Section: 6.3]

$$P(s) = s^5 + 6s^3 + 5s^2 + 8s + 20$$

3. Using the Routh table, tell how many poles of the following function are in the right half-plane, in the left half-plane, and on the $j\omega$-axis: [Section: 6.3]

WileyPLUS

WPCS

Control Solutions

$$T(s) = \frac{s + 8}{s^5 - s^4 + 4s^3 - 4s^2 + 3s - 2}$$

4. The closed-loop transfer function of a system is [Section: 6.3]

$$T(s) = \frac{s^3 + 2s^2 + 7s + 21}{s^5 - 2s^4 + 3s^3 - 6s^2 + 2s - 4}$$

Determine how many closed-loop poles lie in the right half-plane, in the left half-plane, and on the $j\omega$-axis.

5. How many poles are in the right half-plane, in the left half-plane, and on the $j\omega$-axis for the open-loop system of Figure P6.1? [Section: 6.3]

$R(s)$ → $\dfrac{s^2 + 4s - 3}{s^4 + 4s^3 + 8s^2 + 20s + 15}$ → $C(s)$

FIGURE P6.1

6. How many poles are in the right half-plane, the left half-plane, and on the $j\omega$-axis for the open-loop system of Figure P6.2? [Section: 6.3]
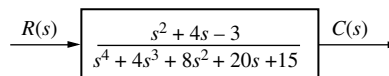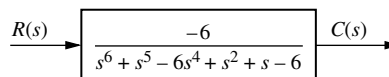
$R(s)$ → $\dfrac{-6}{s^6 + s^5 - 6s^4 + s^2 + s - 6}$ → $C(s)$

FIGURE P6.2

7. Use MATLAB to find the pole locations for the system of Problem 6.

MATLAB

ML

8. Use MATLAB and the Symbolic Math Toolbox to generate a Routh table to solve Problem 3.

9. Determine whether the unity feedback system of Figure P6.3 is stable if [Section: 6.2]
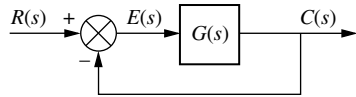
$$G(s) = \frac{240}{(s+1)(s+2)(s+3)(s+4)}$$

FIGURE P6.3

10. Use MATLAB to find the pole locations for the system of Problem 9.

11. Consider the unity feedback system of Figure P6.3 with

$$G(s) = \frac{1}{4s^2(s^2+1)}$$

Using the Routh-Hurwitz criterion, find the region of the s-plane where the poles of the closed-loop system are located. [Section: 6.3]

12. In the system of Figure P6.3, let

$$G(s) = \frac{K(s+2)}{s(s-1)(s+3)}$$

Find the range of K for closed-loop stability. [Section: 6.4]

13. Given the unity feedback system of Figure P6.3 with [Section: 6.3]

$$G(s) = \frac{84}{s(s^7 + 5s^6 + 12s^5 + 25s^4 + 45s^3 + 50s^2 + 82s + 60)}$$

tell how many poles of the closed-loop transfer function lie in the right half-plane, in the left half-plane, and on the $j\omega$-axis. [Section: 6.3]

14. Using the Routh-Hurwitz criterion and the unity feedback system of Figure P6.3 with

$$G(s) = \frac{1}{2s^4 + 5s^3 + s^2 + 2s}$$

tell whether or not the closed-loop system is stable. [Section: 6.2]

15. Given the unity feedback system of Figure P6.3 with

$$G(s) = \frac{8}{s(s^6 - 2s^5 - s^4 + 2s^3 + 4s^2 - 8s - 4)}$$

tell how many closed-loop poles are located in the right half-plane, in the left half-plane, and on the $j\omega$-axis. [Section: 6.3]

16. Repeat Problem 15 using MATLAB.

17. Consider the following Routh table. Notice that the s^5 row was originally all zeros. Tell how many roots of the original polynomial were in the right half-plane, in the left half-plane, and on the $j\omega$-axis. [Section: 6.3]

s^7	1	2	−1	−2
s^6	1	2	−1	−2
s^5	3	4	−1	0
s^4	1	−1	−3	0
s^3	7	8	0	0
s^2	−15	−21	0	0
s^1	−9	0	0	0
s^0	−21	0	0	0

18. For the system of Figure P6.4, tell how many closed-loop poles are located in the right half-plane, in the left half-plane, and on the $j\omega$-axis. Notice that there is positive feedback. [Section: 6.3]
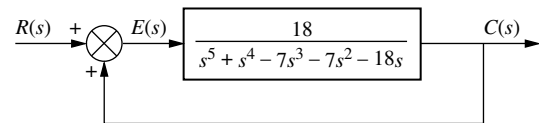
FIGURE P6.4

19. Using the Routh-Hurwitz criterion, tell how many closed-loop poles of the system shown in Figure P6.5 lie in the left half-plane, in the right half-plane, and on the $j\omega$-axis. [Section: 6.3]
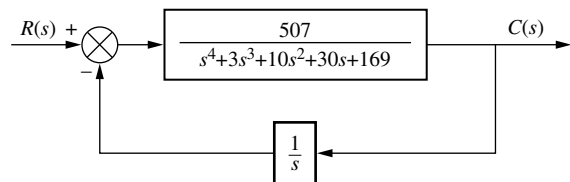

FIGURE P6.5

20. Determine if the unity feedback system of Figure P6.3 with

$$G(s) = \frac{K(s^2 + 1)}{(s+1)(s+2)}$$

can be unstable. [Section: 6.4]

21. For the unity feedback system of Figure P6.3 with

$$G(s) = \frac{K(s+6)}{s(s+1)(s+4)}$$

determine the range of K to ensure stability. [Section: 6.4]

22. In the system of Figure P6.3, let

$$G(s) = \frac{K(s-a)}{s(s-b)}$$

Find the range of K for closed-loop stability when: [Section: 6.4]

a. $a < 0, \quad b < 0$

b. $a < 0, \quad b > 0$

c. $a > 0, \quad b < 0$

d. $a > 0, \quad b > 0$

23. For the unity feedback system of Figure P6.3 with

WileyPLUS
WPCS
Control Solutions

$$G(s) = \frac{K(s+3)(s+5)}{(s-2)(s-4)}$$

determine the range of K for stability. [Section: 6.4]

24. Repeat Problem 23 using MATLAB.

MATLAB
ML

25. Use MATLAB and the Symbolic Math Toolbox to generate a Routh table in terms of K to solve Problem 23.

Symbolic Math
SM

26. Find the range of K for stability for the unity feedback system of Figure P6.3 with [Section: 6.4]

$$G(s) = \frac{K(s+4)(s-4)}{(s^2+3)}$$

27. For the unity feedback system of Figure P6.3 with

$$G(s) = \frac{K(s+1)}{s^4(s+2)}$$

find the range of K for stability. [Section: 6.4]

28. Find the range of gain, K, to ensure stability in the unity feedback system of Figure P6.3 with [Section: 6.4]

$$G(s) = \frac{K(s-2)(s+4)(s+5)}{(s^2+12)}$$

29. Find the range of gain, K, to ensure stability in the unity feedback system of Figure P6.3 with [Section: 6.4]

$$G(s) = \frac{K(s+2)}{(s^2+1)(s+4)(s-1)}$$

30. Using the Routh-Hurwitz criterion, find the value of K that will yield oscillations for the unity feedback system of Figure P6.3 with [Section: 6.4]

$$G(s) = \frac{K}{(s+77)(s+27)(s+38)}$$

31. Use the Routh-Hurwitz criterion to find the range of K for which the system of Figure P6.6 is stable. [Section: 6.4]
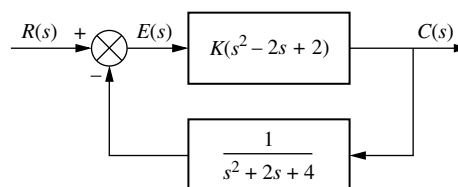
FIGURE P6.6

32. Repeat Problem 31 for the system of Figure P6.7. [Section: 6.4]

WileyPLUS
WPCS
Control Solutions

FIGURE P6.7

33. Given the unity feedback system of Figure P6.3 with

$$G(s) = \frac{K(s+4)}{s(s+1.2)(s+2)}$$

find the following: [Section: 6.4]

a. The range of K that keeps the system stable

b. The value of K that makes the system oscillate

c. The frequency of oscillation when K is set to the value that makes the system oscillate

34. Repeat Problem 33 for [Section: 6.4]

$$G(s) = \frac{K(s-1)(s-2)}{(s+2)(s^2+2s+2)}$$

35. For the system shown in Figure P6.8, find the value of gain, K, that will make the system oscillate. Also, find the frequency of oscillation. [Section: 6.4]
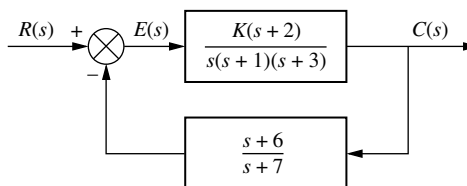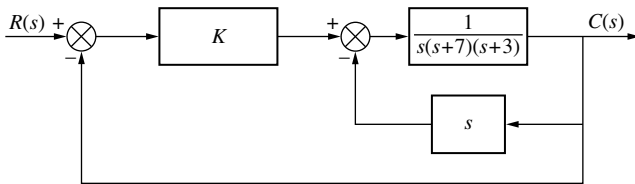

FIGURE P6.8

36. Given the unity feedback system of Figure P6.3 with [Section: 6.4]

WileyPLUS
WPCS
Control Solutions

$$G(s) = \frac{Ks(s+2)}{(s^2-4s+8)(s+3)}$$

a. Find the range of K for stability.

b. Find the frequency of oscillation when the system is marginally stable.

37. Repeat Problem 36 using MATLAB.

MATLAB
ML

38. For the unity feedback system of Figure P6.3 with

$$G(s) = \frac{K(s+2)}{(s^2+1)(s+4)(s-1)}$$

find the range of K for which there will be only two closed-loop, right–half-plane poles. [Section: 6.4]

39. For the unity feedback system of Figure P6.3 with [Section: 6.4]

$$G(s) = \frac{K}{(s+1)^3(s+4)}$$

a. Find the range of K for stability.

b. Find the frequency of oscillation when the system is marginally stable.

40. Given the unity feedback system of Figure P6.3 with [Section: 6.4]

$$G(s) = \frac{K}{(s+49)(s^2+4s+5)}$$

a. Find the range of K for stability.

b. Find the frequency of oscillation when the system is marginally stable.

41. Using the Routh-Hurwitz criterion and the unity feedback system of Figure P6.3 with [Section: 6.4]

$$G(s) = \frac{K}{s(s+1)(s+2)(s+5)}$$

a. Find the range of K for stability.

b. Find the value of K for marginal stability.

c. Find the actual location of the closed-loop poles when the system is marginally stable.

42. Find the range of K to keep the system shown in Figure P6.9 stable. [Section: 6.4]

FIGURE P6.9

43. Find the value of K in the system of Figure P6.10 that will place the closed-loop poles as shown. [Section: 6.4]

WileyPLUS
WPCS
Control Solutions

FIGURE P6.10 Closed-loop system with pole plot

44. The closed-loop transfer function of a system is

$$T(s) = \frac{s^2 + K_1 s + K_2}{s^4 + K_1 s^3 + K_2 s^2 + 5s + 1}$$

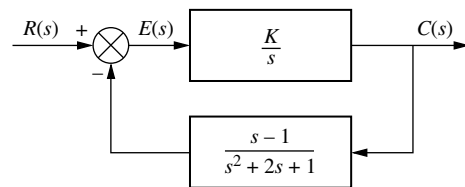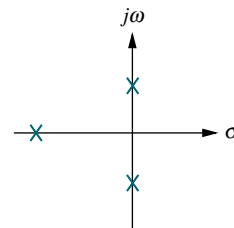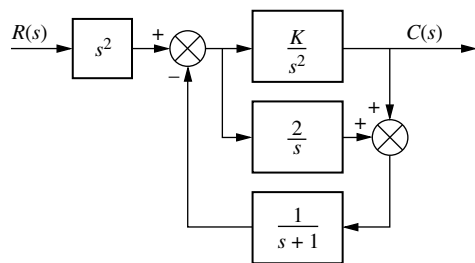Determine the range of K_1 in order for the system to be stable. What is the relationship between K_1 and K_2 for stability? [Section: 6.4]

45. For the transfer function below, find the constraints on K_1 and K_2 such that the function will have only two $j\omega$ poles. [Section: 6.4]

$$T(s) = \frac{K_1 s + K_2}{s^4 + K_1 s^3 + s^2 + K_2 s + 1}$$

46. The transfer function relating the output engine fan speed (rpm) to the input main burner fuel flow rate (lb/h) in a short takeoff and landing (STOL) fighter aircraft, ignoring the coupling between engine fan speed and the pitch control command, is (*Schierman*, *1992*) [Section: 6.4]

$$G(s) = \frac{1.3s^7 + 90.5s^6 + 1970s^5 + 15,000s^4 + 3120s^3 - 41,300s^2 - 5000s - 1840}{s^8 + 103s^7 + 1180s^6 + 4040s^5 + 2150s^4 - 8960s^3 - 10,600s^2 - 1550s - 415}$$

a. Find how many poles are in the right half-plane, in the left half-plane, and on the $j\omega$-axis.

b. Is this open-loop system stable?

47. An interval polynomial is of the form

$$P(s) = a_0 + a_1 s + a_2 s^2 + a_3 s^3 + a_4 s^4 + a_5 s^5 + \cdots$$

with its coefficients belonging to intervals $x_i \leq a_i \leq y_i$, where x_i, y_i are prescribed constants. Kharitonov's theorem says that an interval polynomial has all its roots in the left half-plane if each one of the following four polynomials has its roots in the left half-plane (*Minichelli*, *1989*):

$$K_1(s) = x_0 + x_1 s + y_2 s^2 + y_3 s^3 + x_4 s^4 + x_5 s^5 + y_6 s^6 + \cdots$$
$$K_2(s) = x_0 + y_1 s + y_2 s^2 + x_3 s^3 + x_4 s^4 + y_5 s^5 + y_6 s^6 + \cdots$$
$$K_3(s) = y_0 + x_1 s + x_2 s^2 + y_3 s^3 + y_4 s^4 + x_5 s^5 + x_6 s^6 + \cdots$$
$$K_4(s) = y_0 + y_1 s + x_2 s^2 + x_3 s^3 + y_4 s^4 + y_5 s^5 + x_6 s^6 + \cdots$$

Use Kharitonov's theorem and the Routh-Hurwitz criterion to find if the following polynomial has any zeros in the right–half-plane.

$$P(s) = a_0 + a_1 s + a_2 s^2 + a_3 s^3$$
$$2 \leq a_0 \leq 4; \quad 1 \leq a_1 \leq 2; \quad 4 \leq a_2 \leq 6; \quad a_3 = 1$$

48. A linearized model of a torque-controlled crane hoisting a load with a fixed rope length is

$$P(s) = \frac{X_T(s)}{F_T(s)} = \frac{1}{m_T} \frac{s^2 + \omega_0^2}{s^2(s^2 + a\omega_0^2)}$$

where $\omega_0 = \sqrt{\frac{g}{L}}$, $L =$ the rope length, $m_T =$ the mass of the car, $a =$ the combined rope and car mass, $f_T =$ the force input applied to the car, and $x_T =$ the resulting rope displacement (*Marttinen*, *1990*). If the system is controlled in a feedback configuration by placing it in a loop as shown in Figure P6.11, with $K > 0$, where will the closed-loop poles be located?
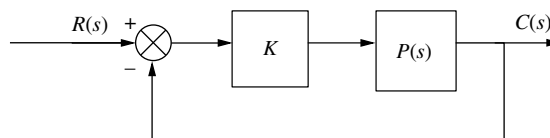
FIGURE P6.11

49. The read/write head assembly arm of a computer hard disk drive (HDD) can be modeled as a rigid rotating body with inertia I_b. Its dynamics can be described with the transfer function

$$P(s) = \frac{X(s)}{F(s)} = \frac{1}{I_b s^2}$$

where $X(s)$ is the displacement of the read/write head and $F(s)$ is the applied force (*Yan*, *2003*). Show that if the HDD is controlled in the configuration shown in Figure P6.11, the arm will oscillate and cannot be positioned with any precision over a HDD track. Find the oscillation frequency.

50. A system is represented in state space as   State Space
                                                      SS

$$\dot{\mathbf{x}} = \begin{bmatrix} 0 & 1 & 3 \\ 2 & 2 & -4 \\ 1 & -4 & 3 \end{bmatrix} \mathbf{x} + \begin{bmatrix} 0 \\ 1 \\ 0 \end{bmatrix} u$$
$$y = \begin{bmatrix} 1 & 1 & 0 \end{bmatrix} \mathbf{x}$$

Determine how many eigenvalues are in the right half-plane, in the left half-plane, and on the $j\omega$-axis. [Section: 6.5]

51. Use MATLAB to find the eigenvalues of the following system:

$$\dot{\mathbf{x}} = \begin{bmatrix} 0 & 1 & 0 \\ 0 & 1 & -4 \\ -1 & 1 & 8 \end{bmatrix} \mathbf{x} + \begin{bmatrix} 0 \\ 0 \\ 0 \end{bmatrix} u$$

$$y = \begin{bmatrix} 0 & 0 & 1 \end{bmatrix} \mathbf{x}$$

52. The following system in state space represents the forward path of a unity feedback system. Use the Routh-Hurwitz criterion to determine if the closed-loop system is stable. [Section: 6.5]

$$\dot{\mathbf{x}} = \begin{bmatrix} 0 & 1 & 0 \\ 0 & 1 & 3 \\ -3 & -4 & -5 \end{bmatrix} \mathbf{x} + \begin{bmatrix} 0 \\ 0 \\ 1 \end{bmatrix} u$$

$$y = \begin{bmatrix} 0 & 1 & 1 \end{bmatrix} \mathbf{x}$$

53. Repeat Problem 52 using MATLAB.

54. A Butterworth polynomial is of the form

$$B_n(s) = 1 + (-1)^n \left(\frac{s}{\omega_c} \right)^{2n}, \ n > 0.$$

Use the Routh-Hurwitz criteria to find the zeros of a Butterworth polynomial for:

a. $n = 1$;

b. $n = 2$

DESIGN PROBLEMS

55. A model for an airplane's pitch loop is shown in Figure P6.12. Find the range

of gain, K, that will keep the system stable. Can the system ever be unstable for positive values of K?

56. A common application of control systems is in regulating the temperature of a chemical process (Figure P6.13). The flow of a chemical reactant to a process is controlled by an actuator and valve. The reactant causes the temperature in the vat to change. This temperature is sensed and compared to a desired set-point temperature in a closed loop, where the flow of reactant is adjusted to yield the desired temperature. In Chapter 9, we will learn how a PID controller is used to improve the performance of such process control systems. Figure P6.13 shows the control system prior to the addition of the PID controller. The PID controller is replaced by the shaded box with a gain of unity. For this system, prior to the design of the PID controller, find the range of amplifier gain, K, to keep the system stable.

FIGURE P6.13 Block diagram of a chemical process control system

57. A robot arm called ISAC (Intelligent Soft Arm Control) can be used as part of a system to feed people with disabilities (see Figure P6.14(*a*)). The control system guides the spoon to the food and then to a position near the person's mouth. The arm uses a special pneumatically controlled actuator called a rubbertuator. Rubbertuators consist of rubber tubes covered with fiber cord. The actuator contracts in length when pneumatic pressure is increased and expands in length when pressure is decreased. This expansion and contraction in length can drive a pulley or other device. A video camera provides the sight for the robot and the tracking loop (*Kara*, *1992*). Assume the simplified block diagram shown in Figure P6.14(*b*) for regulating the spoon at a distance from the mouth. Find the range of K for stability. (Use of a program with symbolic capability is recommended.)

FIGURE P6.12 Aircraft pitch loop model
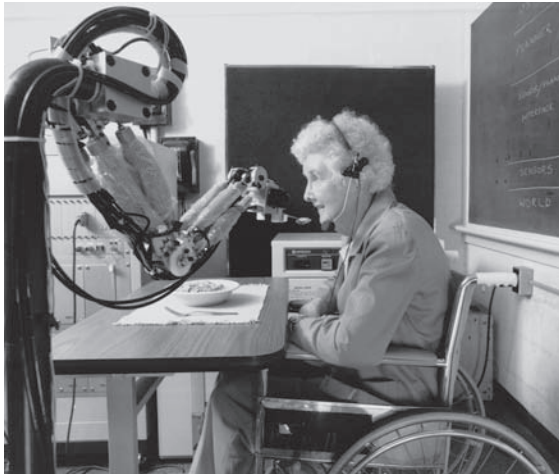
(*a*)
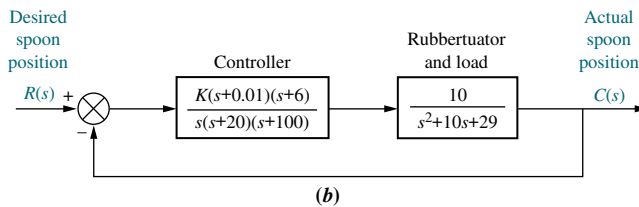
(*b*)

FIGURE P6.14   a. ISAC used for feeding (Courtesy of Kazuhiko Kawamura, Vanderbilt University.) **b.** simplified block diagram

58. Often an aircraft is required to tow another vehicle, such as a practice target or glider. To stabilize the towed vehicle and prevent it from rolling, pitching, and yawing, an autopilot is built into the towed vehicle. Assume the block diagram shown in Figure P6.15 represents the autopilot roll control system (*Cochran*, *1992*). Find the range of *K* to keep the roll angle stable.

WileyPLUS

WPCS

Control Solutions
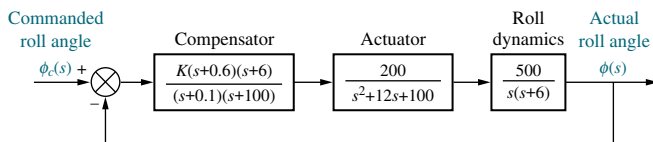
FIGURE P6.15   Towed vehicle roll control

59. Cutting forces should be kept constant during machining operations to prevent changes in spindle speeds or work position. Such changes would deteriorate the accuracy of the work's dimensions. A control system is proposed to control the cutting force. The plant is difficult to model, since the
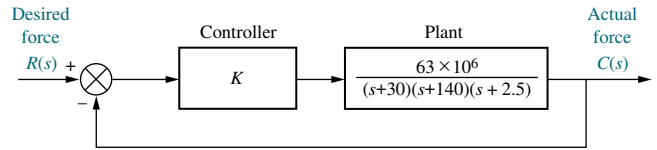
FIGURE P6.16   Cutting force control system (Reprinted with permission of ASME.)

factors that affect cutting force are time varying and not easily predicted. However, assuming the simplified force control model shown in Figure P6.16, use the Routh-Hurwitz criterion to find the range of *K* to keep the system stable (*Rober*, *1997*).

60. Transportation systems that use magnetic levitation can reach very high speeds, since contact friction at the rails is eliminated (see Figure P6.17(*a*)). Electromagnets can produce the force to elevate the vehicle. Figure P6.17(*b*) is a simulation model of a control system that can be used to regulate the magnetic gap. In the figure, $Z_{vin}(s)$ represents a voltage proportional to the desired amount of levitation, or gap. $Z_{vout}(s)$ represents a voltage proportional to the actual amount of levitation. The plant models the dynamic response of the vehicle to

(*a*)
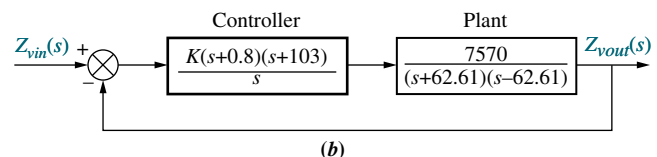
(*b*)

FIGURE P6.17   a. A magnetic levitation transportation system (© Japan Air Lines/Photo Researchers); **b.** simplified block diagram (© 1998 IEEE)

signals from the controller (*Bittar*, *1998*). Use the Routh-Hurwitz criterion to find the range of gain, K, to keep the closed loop system stable.

61. A transfer function from indoor radiator power, $\dot{Q}(s)$, to room temperature, $T(s)$, in an $11\,\mathrm{m}^2$ room is

$$P(s) = \frac{T(s)}{\dot{Q}(s)} = \frac{1 \times 10^{-6}s^2 + 1.314 \times 10^{-9}s + 2.66 \times 10^{-13}}{s^3 + 0.00163s^2 + 5.272 \times 10^{-7}s + 3.538 \times 10^{-11}}$$

where $\dot{Q}$ is in watts and T is in °C. (*Thomas*, *2005*). The room's temperature will be controlled by embedding it in a closed loop, such as that of Figure P6.11. Find the range of K for closed-loop stability.

62. During vertical spindle surface grinding, adjustments are made on a multi-axis computer numerical control (CNC) machine by measuring the applied force with a dynamometer and applying appropriate corrections. This feedback force control results in higher homogeneity and better tolerances in the resulting finished product. In a specific experiment with an extremely high feed rate, the transfer function from the desired depth of cut (DOC) to applied force was

$$\frac{F(s)}{DOC(s)} = \frac{K_C}{1 + \dfrac{K_C}{ms^2 + bs + k} - \dfrac{K_C}{K_f}\dfrac{1}{Ts + 1}}$$

where $k = 2.1 \times 10^4\,\mathrm{N/m}$, $b = 0.78\,\mathrm{Ns/m}$, $m = 1.2 \times 10^{-4}\,\mathrm{Kg}$, $K_C = 1.5 \times 10^4\,\mathrm{N/mm}$ and $T = 0.004$ s. K_f is a parameter that is varied to adjust the system. Find the range of K_f under which the system is stable (*Hekman*, *1999*).

63. Figure P6.18 depicts the schematic diagram of a phase shift oscillator.
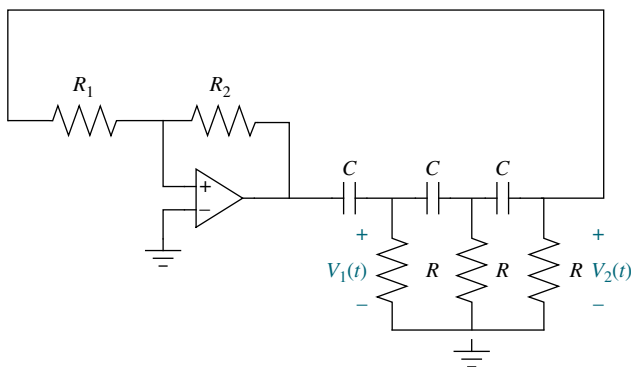
FIGURE P6.18 Phase shift oscillator

The circuit will oscillate if it is designed to have poles on the $j\omega$-axis.

a. Show that the transfer function for the passive network in the circuit is given by

$$\frac{V_2(s)}{V_1(s)} = \frac{-1}{\left(1 + \dfrac{1}{sRC}\right)\left(2 + \dfrac{1}{sRC}\right)^2 - 3 - \dfrac{2}{sRC}}$$

b. Show that the oscillator's characteristic equation is given by

$$1 - K\frac{1}{\left(1 + \dfrac{1}{sRC}\right)\left(2 + \dfrac{1}{sRC}\right)^2 - 3 - \dfrac{2}{sRC}} = 0,$$

where $K = \dfrac{R_2}{R_1}$

c. Use the Routh-Hurwitz criterion to obtain the oscillation condition and the oscillation frequency.

64. In order to obtain a low-cost lithium-ion battery charger, the feedback loop of Figure P6.3 is used, where $G(s) = G_c(s)P(s)$. The following transfer functions have been derived for $G(s)$ (*Tsang*, *2009*):

$$P(s) = \frac{R_1 R_2 C_1 C_2 s^2 + (R_1 C_1 + R_2 C_1 + R_2 C_2)s + 1}{C_1(1 + R_2 C_2)s}$$

$$G_c(s) = K_p + \frac{K_I}{s}$$

If $R_1 = 0.15\,\Omega; R_2 = 0.44\,\Omega; C_1 = 7200\,\mathrm{F}$; and $C_2 = 170\,\mathrm{F}$ use the Routh-Hurwitz criteria to find the range of positive K_P and K_I for which the system is closed-loop stable.

65. Figure P6.19 is a simplified and linearized block diagram of a cascade control system, which is used to control water level in a steam generator of a nuclear power plant (*Wang*, *2009,*).

In this system, the level controller, $G_{LC}(s)$, is the *master* controller and the feed-water flow controller, $G_{FC}(s)$ is the *slave* controller. Using mass balance equations, the water level would ordinarily be regarded as a simple integration process of water flow. In a steam generator, however, steam flow rate and the cooling effect of feed-water change the dynamics of that process. Taking the latter into account and ignoring the much-less pronounced impact of changes in steam flow rate, a first-order lag plus time delay is introduced into the transfer
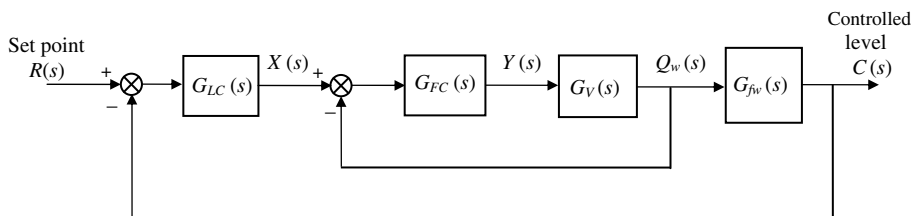
function, $G_{fw}(s)$, relating the controlled level, $C(s)$, to feed-water flow rate, $Q_w(s)$ as follows:

$$G_{fw}(s) = \frac{C(s)}{Q_w(s)} = \frac{K_1 e^{-\tau_1 S}}{s(T_1 s + 1)} = \frac{2e^{-2S}}{s(25s + 1)}$$

$$\approx \frac{2}{s(25s + 1)(2s^2 + 2s + 1)}$$

where $K_1 = 2$ is the process gain, $\tau_1 = 2$ is the pure time delay, and $T_1 = 25$ is the steam generator's time constant. (The expression $e^{-\tau_1 s}$ represents a time delay. This function can be represented by what is known as a *Pade approximation*. This approximation can take on many increasingly complicated forms, depending upon the degree of accuracy required. Here we use the Pade approximation, $e^{-x} \approx \dfrac{1}{1 + x + \dfrac{x^2}{2!}}$, and specific numerical values for the considered steam generator.)

The dynamic characteristics of the control valve are approximated by the transfer function: $G_v(s) = \dfrac{Q_w(s)}{Y(s)} = \dfrac{K_v}{T_v s + 1} = \dfrac{1}{3s + 1}$, where K_v is the valve gain and T_v is its time constant.

Given that: $G_{FC}(s) = K_{P_{FC}} + K_{D_{FC}} s = 0.5 + 2s$ and $G_{LC}(s) = K_{P_{LC}} + K_{D_{LC}} s = 0.5 + Ks$, use the Routh-Hurwitz criterion to find the range of the level controller's derivative gain, $K_{D_{LC}} = K > 0$, that will keep the system stable.

66. Look-ahead information can be used to automatically steer a bicycle in a closed-loop configuration. A line is drawn in the middle of the lane to be followed, and an arbitrary point is chosen in the vehicle's longitudinal axis. A look-ahead offset is calculated by measuring the distance between the look-ahead point and the reference line and is used by the system to correct the vehicle's trajectory. A linearized model of a particular bicycle traveling on a straight-line path at a fixed longitudinal speed is

$$\begin{bmatrix} \dot{V} \\ \dot{r} \\ \dot{\psi} \\ \dot{Y}_g \end{bmatrix} = \begin{bmatrix} -11.7 & 6.8 & 61.6K & 7.7K \\ -3.5 & -24 & -66.9K & 8.4K \\ 0 & 1 & 0 & 0 \\ 1 & 0 & -10 & 0 \end{bmatrix} \begin{bmatrix} V \\ r \\ \psi \\ Y_g \end{bmatrix}$$

In this model, $V =$ bicycle's lateral velocity, $r =$ bicycle's yaw velocity, $\psi =$ bicycle's yaw acceleration, and $Y_g =$ bicycle's center of gravity coordinate on the y-axis. K is a controller parameter to be chosen by the designer (*Özgüner, 1995*). Use the Routh-Hurwitz criterion to find the range of K for which the system is closed-loop stable.

PROGRESSIVE ANALYSIS AND DESIGN PROBLEMS

67. **High-speed rail pantograph.** Problem 21 in Chapter 1 discusses active control of a pantograph mechanism for high-speed rail systems. In Problem 79(*a*), Chapter 5, you found the block diagram for the active pantograph control system. Using your solution for Problem 79(*a*) in Chapter 5 and the Routh-Hurwitz criterion, find the range of controller gain, K, that will keep the system stable (*O'Connor, 1997*).

68. **Control of HIV/AIDS.** The HIV infection linearized model developed in Problem 82, Chapter 4, can be shown to have the transfer function

$$P(s) = \frac{Y(s)}{U_1(s)} = \frac{-520s - 10.3844}{s^3 + 2.6817s^2 + 0.11s + 0.0126}$$
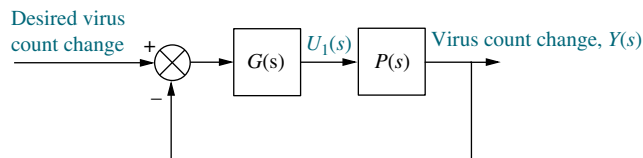
FIGURE P6.20

It is desired to develop a policy for drug delivery to maintain the virus count at prescribed levels. For the purpose of obtaining an appropriate $u_1(t)$, feedback will be used as shown in Figure P6.20 (*Craig, 2004*).
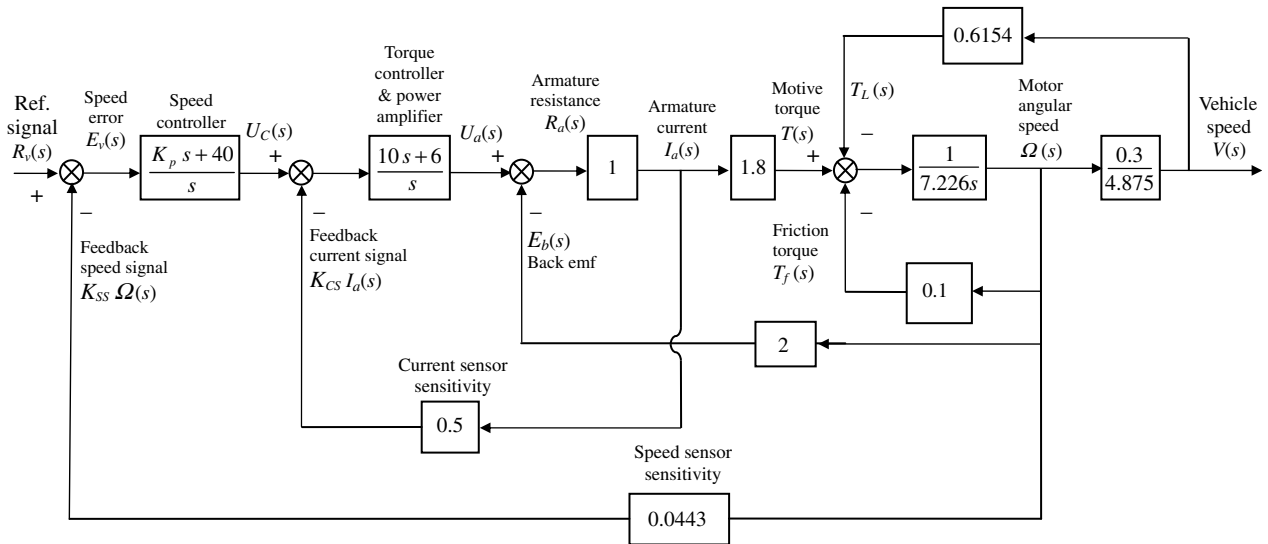
FIGURE P6.21

As a first approach, consider $G(s) = K$, a constant to be selected. Use the Routh-Hurwitz criteria to find the range of K for which the system is closed-loop stable.

69. **Hybrid vehicle.** Figure P6.21 shows the HEV system presented in Chapter 5, where parameter values have been substituted. It is assumed here that the speed controller has a proportional gain, K_p, to be adjusted. Use the Routh-Hurwitz stability method to find the range of positive K_p for which the system is closed-loop stable (*Graebe, 1995*).

Cyber Exploration Laboratory

Experiment 6.1

Objectives To verify the effect of pole location upon stability. To verify the effect upon stability of loop gain in a negative feedback system.

Minimum Required Software Packages MATLAB, Simulink, and the Control System Toolbox

Prelab

1. Find the equivalent transfer function of the negative feedback system of Figure P6.22 if

FIGURE P6.22

$$G(s) = \frac{K}{s(s+2)^2} \text{ and } H(s) = 1$$

2. For the system of Prelab 1, find two values of gain that will yield closed-loop, overdamped, second-order poles. Repeat for underdamped poles.

3. For the system of Prelab 1, find the value of gain, K, that will make the system critically damped.
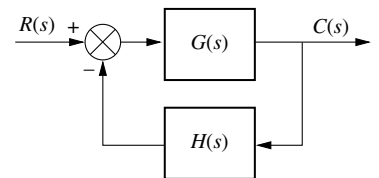
4. For the system of Prelab 1, find the value of gain, K, that will make the system marginally stable. Also, find the frequency of oscillation at that value of K that makes the system marginally stable.

5. For each of Prelab 2 through 4, plot on one graph the pole locations for each case and write the corresponding value of gain, K, at each pole.

Lab

1. Using Simulink, set up the negative feedback system of Prelab 1. Plot the step response of the system at each value of gain calculated to yield overdamped, underdamped, critically damped, and marginally stable responses.

2. Plot the step responses for two values of gain, K, above that calculated to yield marginal stability.

3. At the output of the negative feedback system, cascade the transfer function

$$G_1(s) = \frac{1}{s^2 + 4}$$

Set the gain, K, at a value below that calculated for marginal stability and plot the step response. Repeat for K calculated to yield marginal stability.

Postlab

1. From your plots, discuss the conditions that lead to unstable responses.

2. Discuss the effect of gain upon the nature of the step response of a closed-loop system.

Experiment 6.2

Objective   To use the LabVIEW Control Design and Simulation Module for stability analysis.

Minimum Required Software Package   LabVIEW with the Control Design and Simulation Module

Prelab   Select six transfer functions of various orders and use Routh-Hurwitz to determine their stability.

Lab   Create a LabVIEW VI that receives the order and the coefficients of the characteristic equation and outputs the location of the poles and information regarding stability.

Postlab   Verify the stability of the systems from your Prelab.

◖ Bibliography ◗

Ballard, R. D. The Riddle of the *Lusitania*. *National Geographic*, April 1994, National Geographic Society, Washington, D.C., 1994, pp. 68–85.

Bittar, A., and Sales, R. M. H_2 and H_2 Control for MagLev Vehicles. *IEEE Control Systems*, vol. 18, no. 4, August 1998, pp. 18–25.

Cochran, J. E., Innocenti, M., No, T. S., and Thukral, A. Dynamics and Control of Maneuverable Towed Flight Vehicles. *Journal of Guidance, Control, and Dynamics*, vol. 15, no. 5, September–October 1992, pp. 1245–1252.

Craig, I. K., Xia, X., and Venter, J. W. Introducing HIV/AIDS Education into the Electrical Engineering Curriculum at the University of Pretoria, *IEEE Transactions on Education*, vol. 47, no. 1, February 2004, pp. 65–73.

D'Azzo, J., and Houpis, C. H. *Linear Control System Analysis and Design*, 3d ed. McGraw-Hill, New York, 1988.

Dorf, R. C. *Modern Control Systems*, 5th ed. Addison-Wesley, Reading, MA, 1989.

Graebe, S. F., Goodwin, G. C., and Elsley, G. Control Design and Implementation in Continuous Steel Casting. *IEEE Control Systems, August 1995*, pp. 64–71.

Hekman, K. A., and Liang, S. Y. Compliance Feedback Control for Part Parallelism in Grinding. *International Journal of Manufacturing Technology*, vol. 15, 1999, pp. 64–69.

Hostetter, G. H., Savant, C. J., Jr., and Stefani, R. T. *Design of Feedback Control Systems*, 2d ed. Saunders College Publishing, New York, 1989.

Johnson, H., et al. *Unmanned Free-Swimming Submersible (UFSS) System Description*. NRL Memorandum Report 4393. Naval Research Laboratory, Washington, D.C., 1980.

Kara, A., Kawamura, K., Bagchi, S., and El-Gamal, M. Reflex Control of a Robotic Aid System to Assist the Physically Disabled. *IEEE Control Systems*, June 1992, pp. 71–77.

Martinnen, A., Virkkunen, J., and Salminen, R. T. Control Study with Pilot Crane. *IEEE Transactions on Education*, vol. 33, no. 3, August 1990, pp. 298–305.

Minnichelli, R. J., Anagnost, J. J., and Desoer, C. A. An Elementary Proof of Kharitonov's Stability Theorem with Extensions. *IEEE Transactions on Automatic Control*, vol. 34, 1989, pp. 995–998.

O'Connor, D. N., Eppinger, S. D., Seering, W. P., and Wormly, D. N. Active Control of a High-Speed Pantograph. *Journal of Dynamic Systems, Measurements, and Control*, vol. 119, March 1997, pp. 1–4.

Özgüner, Ű., Űnyelioĝlu, K. A., and Haptipoĝlu, C. An Analytical Study of Vehicle Steering Control. Proceedings of the 4th IEEE Conference Control Applications, 1995, pp. 125–130.

Phillips, C. L., and Harbor, R. D. *Feedback Control Systems*, 2d ed. Prentice Hall, Upper Saddle River, NJ, 1991.

Preitl, Z., Bauer, P., and J. Bokor, J. A Simple Control Solution for Traction Motor Used in Hybrid Vehicles. *4th International Symposium on Applied Computational Intelligence and Informatics*. IEEE. 2007.

Rober, S. J., Shin, Y. C., and Nwokah, O. D. I. A Digital Robust Controller for Cutting Force Control in the End Milling Process. *Journal of Dynamic Systems, Measurement, and Control*, vol. 119, June 1997, pp. 146–152.

Routh, E. J. *Dynamics of a System of Rigid Bodies*, 6th ed. Macmillan, London, 1905.

Schierman, J. D., and Schmidt, D. K. Analysis of Airframe and Engine Control Interactions and Integrated Flight/Propulsion Control. *Journal of Guidance, Control, and Dynamics*, vol. 15, no. 6, November–December 1992, pp. 1388–1396.

Thomas, B., Soleimani-Mosheni, M., and Fahlén, P., Feed-Forward in Temperature Control of Buildings. *Energy and Buildings*, vol. 37, 2005, pp. 755–761.

Timothy, L. K., and Bona, B. E. *State Space Analysis: An Introduction*. McGraw-Hill, New York, 1968.

Tsang, K. M., Chan, W. L. A Simple and Low-cost Charger for Lithium-Ion Batteries. *Journal of Power Sources*, vol. 191, 2009, pp. 633–635.

Wang, X.-K., Yang, X.-H., Liu, G., and Qian, H. Adaptive Neuro-Fuzzy Inference System PID controller for steam generator water level of nuclear power plant, Procedings of the Eighth International Conference on Machine Learning and Cybernetics, 2009, pp. 567–572.

Yan, T., and Lin, R. Experimental Modeling and Compensation of Pivot Nonlinearly in Hard Disk Drives. *IEEE Transactions on Magnetics*, vol. 39, 2003, pp. 1064–1069.
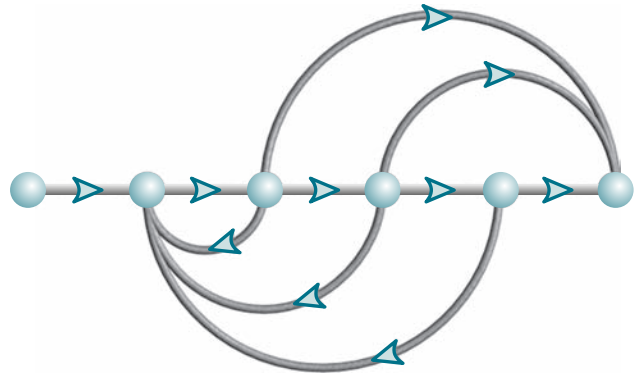
Steady-State Errors

7

Chapter Learning Outcomes

After completing this chapter the student will be able to:

- Find the steady-state error for a unity feedback system (Sections 7.1–7.2)
- Specify a system's steady-state error performance (Section 7.3)
- Design the gain of a closed-loop system to meet a steady-state error specification (Section 7.4)
- Find the steady-state error for disturbance inputs (Section 7.5)
- Find the steady-state error for nonunity feedback systems (Section 7.6)
- Find the steady-state error sensitivity to parameter changes (Section 7.7)
- Find the steady-state error for systems represented in state space (Section 7.8)

Case Study Learning Outcomes

You will be able to demonstrate your knowledge of the chapter objectives with case studies as follows:

- Given the antenna azimuth position control system shown on the front endpapers, you will be able to find the preamplifier gain to meet steady-state error performance specifications.
- Given a video laser disc recorder, you will be able to find the gain required to permit the system to record on a warped disc.

7.1   Introduction
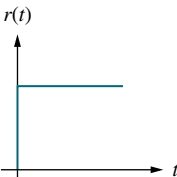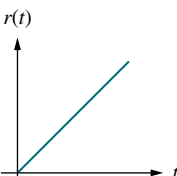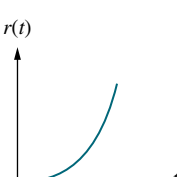
In Chapter 1, we saw that control systems analysis and design focus on three specifications: (1) transient response, (2) stability, and (3) steady-state errors, taking into account the robustness of the design along with economic and social considerations. Elements of transient analysis were derived in Chapter 4 for first- and second-order systems. These concepts are revisited in Chapter 8, where they are extended to higher-order systems. Stability was covered in Chapter 6, where we saw that forced responses were overpowered by natural responses that increase without bound if the system is unstable. Now we are ready to examine steady-state errors. We define the errors and derive methods of controlling them. As we progress, we find that control system design entails trade-offs between desired transient response, steady-state error, and the requirement that the system be stable.

Definition and Test Inputs

Steady-state error is the difference between the input and the output for a prescribed test input as $t \rightarrow \infty$. Test inputs used for steady-state error analysis and design are summarized in Table 7.1.

In order to explain how these test signals are used, let us assume a position control system, where the output position follows the input commanded position. Step inputs represent constant position and thus are useful in determining the ability of the control system to position itself with respect to a stationary target, such as a satellite in geostationary orbit (see Figure 7.1). An antenna position control is an example of a system that can be tested for accuracy using step inputs.

TABLE 7.1   Test waveforms for evaluating steady-state errors of position control systems

Waveform	Name	Physical interpretation	Time function	Laplace transform
	Step	Constant position	1	$\dfrac{1}{s}$
	Ramp	Constant velocity	t	$\dfrac{1}{s^2}$
	Parabola	Constant acceleration	$\dfrac{1}{2}t^2$	$\dfrac{1}{s^3}$
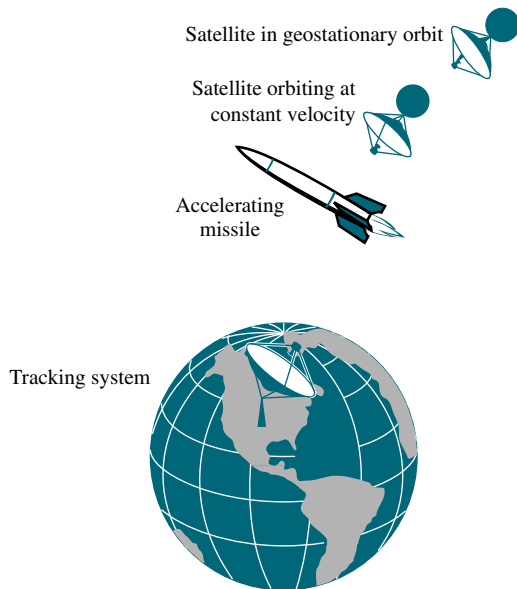
FIGURE 7.1 Test inputs for steady-state error analysis and design vary with target type

Ramp inputs represent constant-velocity inputs to a position control system by their linearly increasing amplitude. These waveforms can be used to test a system's ability to follow a linearly increasing input or, equivalently, to track a constant-velocity target. For example, a position control system that tracks a satellite that moves across the sky at a constant angular velocity, as shown in Figure 7.1, would be tested with a ramp input to evaluate the steady-state error between the satellite's angular position and that of the control system.

Finally, parabolas, whose second derivatives are constant, represent constant-acceleration inputs to position control systems and can be used to represent accelerating targets, such as the missile in Figure 7.1, to determine the steady-state error performance.

Application to Stable Systems

Since we are concerned with the difference between the input and the output of a feedback control system after the steady state has been reached, our discussion is limited to stable systems, where the natural response approaches zero as $t \to \infty$. Unstable systems represent loss of control in the steady state and are not acceptable for use at all. The expressions we derive to calculate the steady-state error can be applied erroneously to an unstable system. Thus, the engineer must check the system for stability while performing steady-state error analysis and design. However, in order to focus on the topic, we assume that all the systems in examples and problems in this chapter are stable. For practice, you may want to test some of the systems for stability.

Evaluating Steady-State Errors

Let us examine the concept of steady-state errors. In Figure 7.2(*a*) a step input and two possible outputs are shown. Output 1 has zero steady-state error, and output 2 has a finite steady-state error, $e_2(\infty)$. A similar example is shown in Figure 7.2(*b*), where a ramp input is compared with output 1, which has zero steady-state error, and output 2, which has a finite steady-state error, $e_2(\infty)$, as measured vertically between the input and output 2 after the transients have died down. For the ramp input
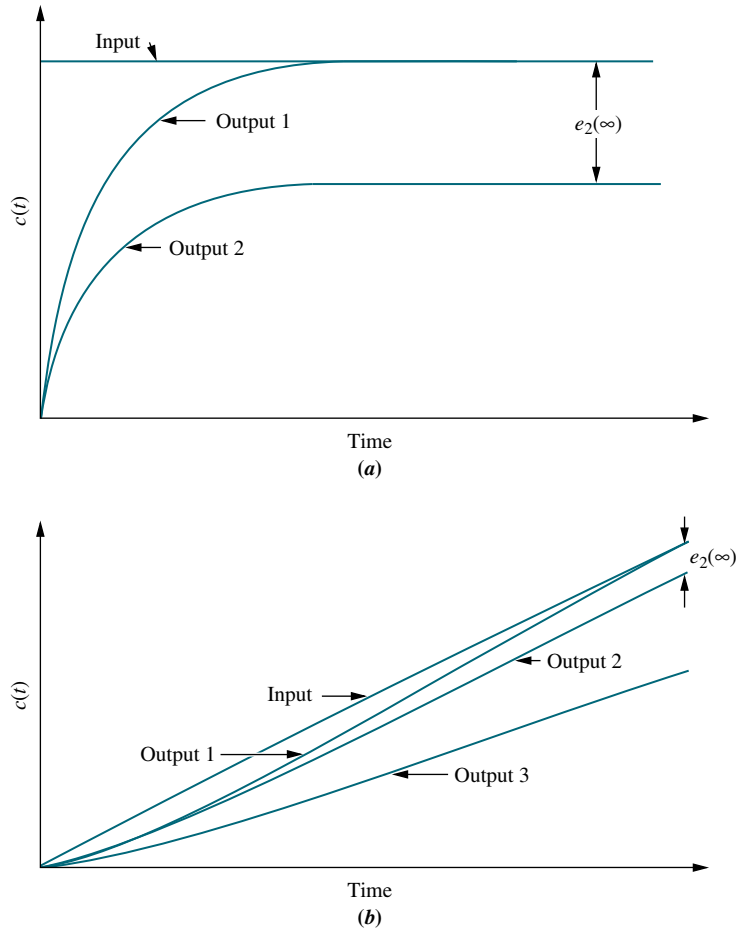
FIGURE 7.2   Steady-state error:
a. step input; **b.** ramp input

another possibility exists. If the output's slope is different from that of the input, then output 3, shown in Figure 7.2(*b*), results. Here the steady-state error is infinite as measured vertically between the input and output 3 after the transients have died down, and *t* approaches infinity.

Let us now look at the error from the perspective of the most general block diagram. Since the error is the difference between the input and the output of a system, we assume a closed-loop transfer function, $T(s)$, and form the error, $E(s)$, by taking the difference between the input and the output, as shown in Figure 7.3(*a*). Here we are interested in the steady-state, or final, value of $e(t)$. For unity feedback systems, $E(s)$ appears as shown in Figure 7.3(*b*). In this chapter, we study and derive expressions for the steady-state error for unity feedback systems first and then expand to nonunity feedback systems. Before we begin our study of steady-state errors for unity feedback systems, let us look at the sources of the errors with which we deal.

FIGURE 7.3   Closed-loop control system error: **a.** general representation; **b.** representation for unity feedback systems
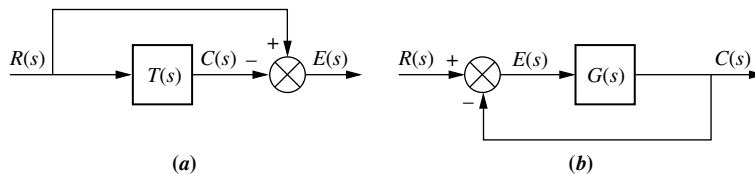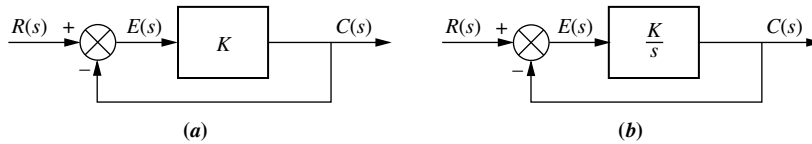
FIGURE 7.4   System with **a.** finite steady-state error for a step input; **b.** zero steady-state error for step input

Sources of Steady-State Error

Many steady-state errors in control systems arise from nonlinear sources, such as backlash in gears or a motor that will not move unless the input voltage exceeds a threshold. Nonlinear behavior as a source of steady-state errors, although a viable topic for study is beyond the scope of a text on linear control systems. The steady-state errors we study here are errors that arise from the configuration of the system itself and the type of applied input.

For example, look at the system of Figure 7.4(a), where $R(s)$ is the input, $C(s)$ is the output, and $E(s) = R(s) - C(s)$ is the error. Consider a step input. In the steady state, if $c(t)$ equals $r(t)$, $e(t)$ will be zero. But with a pure gain, K, the error, $e(t)$, cannot be zero if $c(t)$ is to be finite and nonzero. Thus, by virtue of the configuration of the system (a pure gain of K in the forward path), an error must exist. If we call $c_{\text{steady-state}}$ the steady-state value of the output and $e_{\text{steady-state}}$ the steady-state value of the error, then $c_{\text{steady-state}} = K e_{\text{steady-state}}$, or

$$e_{\text{steady-state}} = \frac{1}{K} c_{\text{steady-state}} \tag{7.1}$$

Thus, the larger the value of K, the smaller the value of $e_{\text{steady-state}}$ would have to be to yield a similar value of $c_{\text{steady-state}}$. The conclusion we can draw is that with a pure gain in the forward path, there will always be a steady-state error for a step input. This error diminishes as the value of K increases.

If the forward-path gain is replaced by an integrator, as shown in Figure 7.4(b), there will be zero error in the steady state for a step input. The reasoning is as follows: As $c(t)$ increases, $e(t)$ will decrease, since $e(t) = r(t) - c(t)$. This decrease will continue until there is zero error, but there will still be a value for $c(t)$ since an integrator can have a constant output without any input. For example, a motor can be represented simply as an integrator. A voltage applied to the motor will cause rotation. When the applied voltage is removed, the motor will stop and remain at its present output position. Since it does not return to its initial position, we have an angular displacement output without an input to the motor. Therefore, a system similar to Figure 7.4(b), which uses a motor in the forward path, can have zero steady-state error for a step input.

We have examined two cases qualitatively to show how a system can be expected to exhibit various steady-state error characteristics, depending upon the system configuration. We now formalize the concepts and derive the relationships between the steady-state errors and the system configuration generating these errors.

7.2   Steady-State Error for Unity Feedback Systems

Steady-state error can be calculated from a system's closed-loop transfer function, $T(s)$, or the open-loop transfer function, $G(s)$, for unity feedback systems. We begin by deriving the system's steady-state error in terms of the closed-loop transfer

function, $T(s)$, in order to introduce the subject and the definitions. Next we obtain insight into the factors affecting steady-state error by using the open-loop transfer function, $G(s)$, in unity feedback systems for our calculations. Later in the chapter we generalize this discussion to nonunity feedback systems.

Steady-State Error in Terms of *T(s)*

Consider Figure 7.3(*a*). To find $E(s)$, the error between the input, $R(s)$, and the output, $C(s)$, we write

$$E(s) = R(s) - C(s) \tag{7.2}$$

But

$$C(s) = R(s)T(s) \tag{7.3}$$

Substituting Eq. (7.3) into Eq. (7.2), simplifying, and solving for $E(s)$ yields

$$E(s) = R(s)[1 - T(s)] \tag{7.4}$$

Although Eq. (7.4) allows us to solve for $e(t)$ at any time, t, we are interested in the final value of the error, $e(\infty)$. Applying the final value theorem,[1] which allows us to use the final value of $e(t)$ without taking the inverse Laplace transform of $E(s)$, and then letting t approach infinity, we obtain

$$e(\infty) = \lim_{t \to \infty} e(t) = \lim_{s \to 0} sE(s) \tag{7.5}^{[2]}$$

Substituting Eq. (7.4) into Eq. (7.5) yields

$$e(\infty) = \lim_{s \to \infty} sR(s)[1 - T(s)] \tag{7.6}$$

Let us look at an example.

---

[1] The final value theorem is derived from the Laplace transform of the derivative. Thus,

$$\mathscr{L}[\dot{f}(t)] = \int_{0-}^{\infty} \dot{f}(t)e^{st}dt = sF(s) - f(0-)$$

As $\quad s \to 0$,

$$\int_{0-}^{\infty} \dot{f}(t)dt = f(\infty) - f(0-) = \lim_{s \to 0} sF(s) - f(0-)$$

or

$$f(\infty) = \lim_{s \to 0} sF(s)$$

For finite steady-state errors, the final value theorem is valid only if $F(s)$ has poles only in the left half-plane and, at most, one pole at the origin. However, correct results that yield steady-state errors that are infinite can be obtained if $F(s)$ has more than one pole at the origin (see *D'Azzo and Houpis*, *1988*). If $F(s)$ has poles in the right half-plane or poles on the imaginary axis other than at the origin, the final value theorem is invalid.

[2] Valid only if (1) $E(s)$ has poles only in the left half-plane and at the origin, and (2) the closed-loop transfer function, $T(s)$, is stable. Notice that by using Eq. (7.5), numerical results can be obtained for unstable systems. These results, however, are meaningless.

Example 7.1

Steady-State Error in Terms of *T(s)*

PROBLEM: Find the steady-state error for the system of Figure 7.3(*a*) if $T(s) = 5/(s^2 + 7s + 10)$ and the input is a unit step.

SOLUTION: From the problem statement, $R(s) = 1/s$ and $T(s) = 5/(s^2 + 7s + 10)$. Substituting into Eq. (7.4) yields

$$E(s) = \frac{s^2 + 7s + 5}{s(s^2 + 7s + 10)} \tag{7.7}$$

Since $T(s)$ is stable and, subsequently, $E(s)$ does not have right–half-plane poles or $j\omega$ poles other than at the origin, we can apply the final value theorem. Substituting Eq. (7.7) into Eq. (7.5) gives $e(\infty) = 1/2$.

Steady-State Error in Terms of *G(s)*

Many times we have the system configured as a unity feedback system with a forward transfer function, $G(s)$. Although we can find the closed-loop transfer function, $T(s)$, and then proceed as in the previous subsection, we find more insight for analysis and design by expressing the steady-state error in terms of $G(s)$ rather than $T(s)$.

Consider the feedback control system shown in Figure 7.3(*b*). Since the feedback, $H(s)$, equals 1, the system has unity feedback. The implication is that $E(s)$ is actually the error between the input, $R(s)$, and the output, $C(s)$. Thus, if we solve for $E(s)$, we will have an expression for the error. We will then apply the final value theorem, Item 11 in Table 2.2, to evaluate the steady-state error.

Writing $E(s)$ from Figure 7.3(*b*), we obtain

$$E(s) = R(s) - C(s) \tag{7.8}$$

But

$$C(s) = E(s)G(s) \tag{7.9}$$

Finally, substituting Eq. (7.9) into Eq. (7.8) and solving for $E(s)$ yields

$$E(s) = \frac{R(s)}{1 + G(s)} \tag{7.10}$$

We now apply the final value theorem, Eq. (7.5). At this point in a numerical calculation, we must check to see whether the closed-loop system is stable, using, for example, the Routh-Hurwitz criterion. For now, though, assume that the closed-loop system is stable and substitute Eq. (7.10) into Eq. (7.5), obtaining

$$e(\infty) = \lim_{s \to 0} \frac{sR(s)}{1 + G(s)} \tag{7.11}$$

Equation (7.11) allows us to calculate the steady-state error, $e(\infty)$, given the input, $R(s)$, and the system, $G(s)$. We now substitute several inputs for $R(s)$ and then

draw conclusions about the relationships that exist between the open-loop system, $G(s)$, and the nature of the steady-state error, $e(\infty)$.

The three test signals we use to establish specifications for a control system's steady-state error characteristics are shown in Table 7.1. Let us take each input and evaluate its effect on the steady-state error by using Eq. (7.11).

Step Input. Using Eq. (7.11) with $R(s) = 1/s$, we find

$$e(\infty) = e_{step}(\infty) = \lim_{s \to 0} \frac{s(1/s)}{1 + G(s)} = \frac{1}{1 + \lim_{s \to 0} G(s)} \qquad (7.12)$$

The term

$$\lim_{s \to 0} G(s)$$

is the dc gain of the forward transfer function, since s, the frequency variable, is approaching zero. In order to have zero steady-state error,

$$\lim_{s \to 0} G(s) = \infty \qquad (7.13)$$

Hence, to satisfy Eq. (7.13), $G(s)$ must take on the following form:

$$G(s) \equiv \frac{(s + z_1)(s + z_2) \cdots}{s^n(s + p_1)(s + p_2) \cdots} \qquad (7.14)$$

and for the limit to be infinite, the denominator must be equal to zero as s goes to zero. Thus, $n \geq 1$; that is, at least one pole must be at the origin. Since division by s in the frequency domain is integration in the time domain (see Table 2.2, Item 10), we are also saying that at least one pure integration must be present in the forward path. The steady-state response for this case of zero steady-state error is similar to that shown in Figure 7.2(a), output 1.

If there are no integrations, then $n = 0$. Using Eq. (7.14), we have

$$\lim_{s \to 0} G(s) = \frac{z_1 z_2 \cdots}{p_1 p_2 \cdots} \qquad (7.15)$$

which is finite and yields a finite error from Eq. (7.12). Figure 7.2(a), output 2, is an example of this case of finite steady-state error.

In summary, for a step input to a unity feedback system, the steady-state error will be zero if there is at least one pure integration in the forward path. If there are no integrations, then there will be a nonzero finite error. This result is comparable to our qualitative discussion in Section 7.1, where we found that a pure gain yields a constant steady-state error for a step input, but an integrator yields zero error for the same type of input. We now repeat the development for a ramp input.

Ramp Input. Using Eq. (7.11) with, $R(s) = 1/s^2$, we obtain

$$e(\infty) = e_{ramp}(\infty) = \lim_{s \to 0} \frac{s(1/s^2)}{1 + G(s)} = \lim_{s \to 0} \frac{1}{s + sG(s)} = \frac{1}{\lim_{s \to 0} sG(s)} \qquad (7.16)$$

To have zero steady-state error for a ramp input, we must have

$$\lim_{s \to 0} sG(s) = \infty \tag{7.17}$$

To satisfy Eq. (7.17), $G(s)$ must take the same form as Eq. (7.14), except that $n \geq 2$. In other words, there must be at least two integrations in the forward path. An example of zero steady-state error for a ramp input is shown in Figure 7.2(b), output 1.

If only one integration exists in the forward path, then, assuming Eq. (7.14),

$$\lim_{s \to 0} sG(s) = \frac{z_1 z_2 \cdots}{p_1 p_2 \cdots} \tag{7.18}$$

which is finite rather than infinite. Using Eq. (7.16), we find that this configuration leads to a constant error, as shown in Figure 7.2(b), output 2.

If there are no integrations in the forward path, then

$$\lim_{s \to 0} sG(s) = 0 \tag{7.19}$$

and the steady-state error would be infinite and lead to diverging ramps, as shown in Figure 7.2(b), output 3. Finally, we repeat the development for a parabolic input.

Parabolic Input. Using Eq. (7.11) with $R(s) = 1/s^3$, we obtain

$$e(\infty) = e_{\text{parabola}}(\infty) = \lim_{s \to 0} \frac{s(1/s^3)}{1 + G(s)} = \lim_{s \to 0} \frac{1}{s^2 + s^2 G(s)} = \frac{1}{\lim_{s \to 0} s^2 G(s)} \tag{7.20}$$

In order to have zero steady-state error for a parabolic input, we must have

$$\lim_{s \to 0} s^2 G(s) = \infty \tag{7.21}$$

To satisfy Eq. (7.21), $G(s)$ must take on the same form as Eq. (7.14), except that $n \geq 3$. In other words, there must be at least three integrations in the forward path.

If there are only two integrations in the forward path, then

$$\lim_{s \to 0} s^2 G(s) = \frac{z_1 z_2 \cdots}{p_1 p_2 \cdots} \tag{7.22}$$

is finite rather than infinite. Using Eq. (7.20), we find that this configuration leads to a constant error.

If there is only one or less integration in the forward path, then

$$\lim_{s \to 0} s^2 G(s) = 0 \tag{7.23}$$

and the steady-state error is infinite. Two examples demonstrate these concepts.

Example 7.2

Steady-State Errors for Systems with No Integrations

PROBLEM: Find the steady-state errors for inputs of $5u(t)$, $5tu(t)$, and $5t^2 u(t)$ to the system shown in Figure 7.5. The function $u(t)$ is the unit step.

$R(s)$ + → $E(s)$ → $\dfrac{120(s+2)}{(s+3)(s+4)}$ → $C(s)$

FIGURE 7.5   Feedback control system for Example 7.2

SOLUTION: First we verify that the closed-loop system is indeed stable. For this example we leave out the details. Next, for the input $5u(t)$, whose Laplace transform is $5/s$, the steady-state error will be five times as large as that given by Eq. (7.12), or

$$e(\infty) = e_{\text{step}}(\infty) = \frac{5}{1 + \lim_{s \to 0} G(s)} = \frac{5}{1 + 20} = \frac{5}{21} \qquad (7.24)$$

which implies a response similar to output 2 of Figure 7.2(a).

For the input $5tu(t)$, whose Laplace transform is $5/s^2$, the steady-state error will be five times as large as that given by Eq. (7.16), or

$$e(\infty) = e_{\text{ramp}}(\infty) = \frac{5}{\lim_{s \to 0} sG(s)} = \frac{5}{0} = \infty \qquad (7.25)$$

which implies a response similar to output 3 of Figure 7.2(b).

For the input $5t^2u(t)$, whose Laplace transform is $10/s^3$, the steady-state error will be 10 times as large as that given by Eq. (7.20), or

$$e(\infty) = e_{\text{parabola}}(\infty) = \frac{10}{\lim_{s \to 0} s^2 G(s)} = \frac{10}{0} = \infty \qquad (7.26)$$

Example 7.3

Steady-State Errors for Systems with One Integration

$R(s)$ + → $E(s)$ → $\dfrac{100(s+2)(s+6)}{s(s+3)(s+4)}$ → $C(s)$
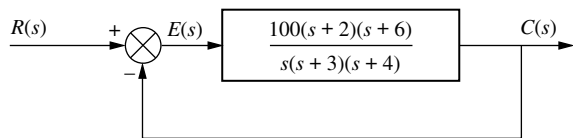
FIGURE 7.6   Feedback control system for Example 7.3

PROBLEM: Find the steady-state errors for inputs of $5u(t)$, $5tu(t)$, and $5t^2u(t)$ to the system shown in Figure 7.6. The function $u(t)$ is the unit step.
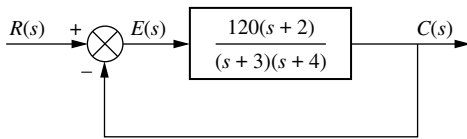
SOLUTION: First verify that the closed-loop system is indeed stable. For this example we leave out the details. Next note that since there is an integration in the forward path, the steady-state errors for some of the input waveforms will be less than those found in Example 7.2. For the input $5u(t)$, whose Laplace transform is $5/s$, the steady-state error will be five times as large as that given by Eq. (7.12), or

$$e(\infty) = e_{\text{step}}(\infty) = \frac{5}{1 + \lim_{s \to 0} G(s)} = \frac{5}{\infty} = 0 \qquad (7.27)$$

which implies a response similar to output 1 of Figure 7.2(a). Notice that the integration in the forward path yields zero error for a step input, rather than the finite error found in Example 7.2.

For the input $5tu(t)$, whose Laplace transform is $5/s^2$, the steady-state error will be five times as large as that given by Eq. (7.16), or

$$e(\infty) = e_{\text{ramp}}(\infty) = \frac{5}{\lim_{s \to 0} sG(s)} = \frac{5}{100} = \frac{1}{20} \qquad (7.28)$$

which implies a response similar to output 2 of Figure 7.2(*b*). Notice that the integration in the forward path yields a finite error for a ramp input, rather than the infinite error found in Example 7.2.

For the input, $5t^2u(t)$, whose Laplace transform is $10/s^3$, the steady-state error will be 10 times as large as that given by Eq. (7.20), or

$$e(\infty) = e_{\text{parabola}}(\infty) = \frac{10}{\lim_{s \to 0} s^2 G(s)} = \frac{10}{0} = \infty \tag{7.29}$$

Notice that the integration in the forward path does not yield any improvement in steady-state error over that found in Example 7.2 for a parabolic input.

Skill-Assessment Exercise 7.1

PROBLEM: A unity feedback system has the following forward transfer function:

$$G(s) = \frac{10(s+20)(s+30)}{s(s+25)(s+35)}$$

a. Find the steady-state error for the following inputs: $15u(t)$, $15tu(t)$, and $15t^2u(t)$.

b. Repeat for

$$G(s) = \frac{10(s+20)(s+30)}{s^2(s+25)(s+35)(s+50)}$$

ANSWERS:

a. The closed-loop system is stable. For $15u(t)$, $e_{\text{step}}(\infty) = 0$; for $15tu(t)$, $e_{\text{ramp}}(\infty) = 2.1875$; for $15(t^2)u(t)$, $e_{\text{parabola}}(\infty) = \infty$.

b. The closed-loop system is unstable. Calculations cannot be made.

The complete solution is at www.wiley.com/college/nise.

7.3   Static Error Constants and System Type

We continue our focus on unity negative feedback systems and define parameters that we can use as steady-state error performance specifications, just as we defined damping ratio, natural frequency, settling time, percent overshoot, and so on as performance specifications for the transient response. These steady-state error performance specifications are called *static error constants*. Let us see how they are defined, how to calculate them, and, in the next section, how to use them for design.

Static Error Constants

In the previous section we derived the following relationships for steady-state error. For a step input, $u(t)$,

$$e(\infty) = e_{\text{step}}(\infty) = \frac{1}{1 + \lim_{s \to 0} G(s)} \qquad (7.30)$$

For a ramp input, $tu(t)$,

$$e(\infty) = e_{\text{ramp}}(\infty) = \frac{1}{\lim_{s \to 0} sG(s)} \qquad (7.31)$$

For a parabolic input, $\frac{1}{2}t^2u(t)$.

$$e(\infty) = e_{\text{parabola}}(\infty) = \frac{1}{\lim_{s \to 0} s^2G(s)} \qquad (7.32)$$

The three terms in the denominator that are taken to the limit determine the steady-state error. We call these limits *static error constants*. Individually, their names are
position constant, K_p, where

$$K_p = \lim_{s \to 0} G(s) \qquad (7.33)$$

velocity constant, K_v, where

$$K_v = \lim_{s \to 0} sG(s) \qquad (7.34)$$

acceleration constant, K_a, where

$$K_a = \lim_{s \to 0} s^2G(s) \qquad (7.35)$$

As we have seen, these quantities, depending upon the form of $G(s)$, can assume values of zero, finite constant, or infinity. Since the static error constant appears in the denominator of the steady-state error. Eqs. (7.30) through (7.32), the value of the steady-state error decreases as the static error constant increases.

In Section 7.2, we evaluated the steady-state error by using the final value theorem. An alternate method makes use of the static error constants. A few examples follow.

Example 7.4

Steady-State Error via Static Error Constants

PROBLEM: For each system of Figure 7.7, evaluate the static error constants and find the expected error for the standard step, ramp, and parabolic inputs.

$$\frac{500(s+2)(s+5)}{(s+8)(s+10)(s+12)}$$

(a)

$$\frac{500(s+2)(s+5)(s+6)}{s(s+8)(s+10)(s+12)}$$

(b)

$$\frac{500(s+2)(s+4)(s+5)(s+6)(s+7)}{s^2(s+8)(s+10)(s+12)}$$

(c)
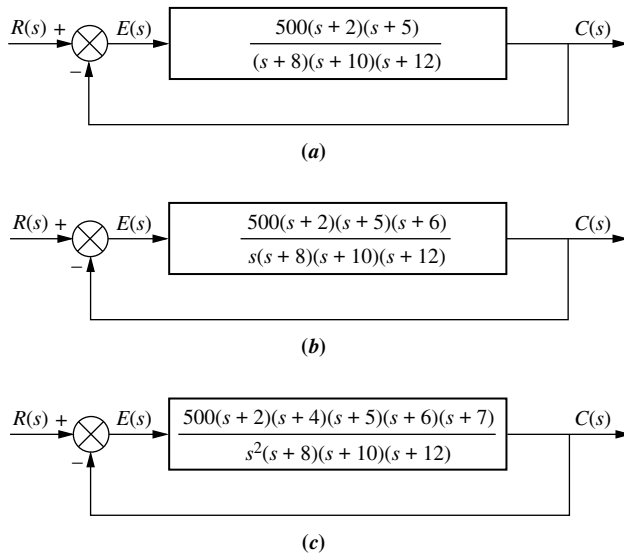
FIGURE 7.7 Feedback control systems for Example 7.4

SOLUTION: First verify that all closed-loop systems shown are indeed stable. For this example we leave out the details. Next, for Figure 7.7(a),

$$K_p = \lim_{s \to 0} G(s) = \frac{500 \times 2 \times 5}{8 \times 10 \times 12} = 5.208 \tag{7.36}$$

$$K_v = \lim_{s \to 0} sG(s) = 0 \tag{7.37}$$

$$K_a = \lim_{s \to 0} s^2 G(s) = 0 \tag{7.38}$$

Thus, for a step input,

$$e(\infty) = \frac{1}{1 + K_p} = 0.161 \tag{7.39}$$

For a ramp input,

$$e(\infty) = \frac{1}{K_v} = \infty \tag{7.40}$$

For a parabolic input,

$$e(\infty) = \frac{1}{K_a} = \infty \tag{7.41}$$

Now, for Figure 7.7(b),

$$K_p = \lim_{s \to 0} G(s) = \infty \tag{7.42}$$

$$K_v = \lim_{s \to 0} sG(s) = \frac{500 \times 2 \times 5 \times 6}{8 \times 10 \times 12} = 31.25 \tag{7.43}$$

and

$$K_a = \lim_{s \to 0} s^2 G(s) = 0 \tag{7.44}$$

Thus, for a step input,

$$e(\infty) = \frac{1}{1 + K_p} = 0 \tag{7.45}$$

For a ramp input,

$$e(\infty) = \frac{1}{K_v} = \frac{1}{31.25} = 0.032 \tag{7.46}$$

For a parabolic input,

$$e(\infty) = \frac{1}{K_a} = \infty \tag{7.47}$$

Finally, for Figure 7.7(c),

$$K_p = \lim_{s \to 0} G(s) = \infty \tag{7.48}$$

$$K_v = \lim_{s \to 0} s G(s) = \infty \tag{7.49}$$

and

$$K_a = \lim_{s \to 0} s^2 G(s) = \frac{500 \times 2 \times 4 \times 5 \times 6 \times 7}{8 \times 10 \times 12} = 875 \tag{7.50}$$

Thus, for a step input,

$$e(\infty) = \frac{1}{1 + K_p} = 0 \tag{7.51}$$

For a ramp input,

$$e(\infty) = \frac{1}{K_v} = 0 \tag{7.52}$$

For a parabolic input,

$$e(\infty) = \frac{1}{K_a} = \frac{1}{875} = 1.14 \times 10^{-3} \tag{7.53}$$

MATLAB
ML

Students who are using MATLAB should now run ch7p1 in Appendix B. You will learn how to test the system for stability, evaluate static error constants, and calculate steady-state error using MATLAB. This exercise applies MATLAB to solve Example 7.4 with System (b).

System Type

Let us continue to focus on a unity negative feedback system. The values of the static error constants, again, depend upon the form of $G(s)$, especially the number of pure integrations in the forward path. Since steady-state errors are dependent upon the

number of integrations in the forward path, we give a name to this system attribute. Given the system in Figure 7.8, we define *system type* to be the value of n in the denominator or, equivalently, the number of pure integrations in the forward path. Therefore, a system with $n = 0$ is a Type 0 system. If $n = 1$ or $n = 2$, the corresponding system is a Type 1 or Type 2 system, respectively.

FIGURE 7.8   Feedback control system for defining system type

Table 7.2 ties together the concepts of steady-state error, static error constants, and system type. The table shows the static error constants and the steady-state errors as functions of input waveform and system type.
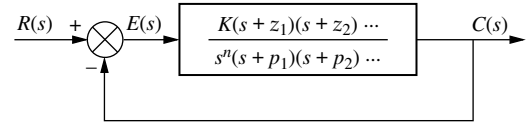
TABLE 7.2   Relationships between input, system type, static error constants, and steady-state errors

Input	Steady-state error formula	Type 0		Type 1		Type 2	
		Static error constant	Error	Static error constant	Error	Static error constant	Error
Step, $u(t)$	$\dfrac{1}{1 + K_p}$	$K_p = $ Constant	$\dfrac{1}{1 + K_p}$	$K_p = \infty$	0	$K_p = \infty$	0
Ramp, $tu(t)$	$\dfrac{1}{K_v}$	$K_v = 0$	∞	$K_v = $ Constant	$\dfrac{1}{K_v}$	$K_v = \infty$	0
Parabola, $\dfrac{1}{2}t^2 u(t)$	$\dfrac{1}{K_a}$	$K_a = 0$	∞	$K_a = 0$	∞	$K_a = $ Constant	$\dfrac{1}{K_a}$

Skill-Assessment Exercise 7.2

PROBLEM: A unity feedback system has the following forward transfer function:

$$G(s) = \frac{1000(s + 8)}{(s + 7)(s + 9)}$$

a. Evaluate system type, K_p, K_v, and K_a.

b. Use your answers to **a.** to find the steady-state errors for the standard step, ramp, and parabolic inputs.

ANSWERS:

a. The closed-loop system is stable. System type = Type 0. $K_p = 127$, $K_v = 0$, and $K_a = 0$.

b. $e_{step}(\infty) = 7.8 \times 10^{-3}$, $e_{ramp}(\infty) = \infty$, and $e_{parabola}(\infty) = \infty$

The complete solution is at www.wiley.com/college/nise.

TryIt 7.1

Use MATLAB, the Control System Toolbox, and the following statements to find K_p, $e_{step}(\infty)$, and the closed-loop poles to check for stability for the system of Skill-Assessment Exercise 7.2.

```
numg=1000*[1 8];
deng=poly([-7 -9]);
G=tf(numg,deng);
Kp=dcgain(G)
estep=1/(1+Kp)
T=feedback(G,1);
poles=pole(T)
```

In this section, we defined steady-state errors, static error constants, and system type. Now the specifications for a control system's steady-state errors will be formulated, followed by some examples.

7.4   Steady-State Error Specifications

Static error constants can be used to specify the steady-state error characteristics of control systems, such as that shown in Figure 7.9. Just as damping ratio, ζ, settling time, T_s, peak time, T_p, and percent overshoot, $\%OS$, are used as specifications for a

FIGURE 7.9   A robot used in the manufacturing of semiconductor random-access memories (RAMs) similar to those in personal computers. Steady-state error is an important design consideration for assembly-line robots.

control system's transient response, so the position constant, K_p, velocity constant, K_v, and acceleration constant, K_a, can be used as specifications for a control system's steady-state errors. We will soon see that a wealth of information is contained within the specification of a static error constant.

For example, if a control system has the specification $K_v = 1000$, we can draw several conclusions:

1. The system is stable.
2. The system is of Type 1, since only Type 1 systems have K_v's that are finite constants. Recall that $K_v = 0$ for Type 0 systems, whereas $K_v = \infty$ for Type 2 systems.
3. A ramp input is the test signal. Since K_v is specified as a finite constant, and the steady-state error for a ramp input is inversely proportional to K_v, we know the test input is a ramp.
4. The steady-state error between the input ramp and the output ramp is $1/K_v$ per unit of input slope.

Let us look at two examples that demonstrate analysis and design using static error constants.

Example 7.5

Interpreting the Steady-State Error Specification

PROBLEM: What information is contained in the specification $K_p = 1000$?

SOLUTION: The system is stable. The system is Type 0, since only a Type 0 system has a finite K_p. Type 1 and Type 2 systems have $K_p = \infty$. The input test signal is a step, since K_p is specified. Finally, the error per unit step is

$$e(\infty) = \frac{1}{1 + K_p} = \frac{1}{1 + 1000} = \frac{1}{1001} \tag{7.54}$$

<div style="border:1px solid #000;padding:10px;">

Example 7.6

Gain Design to Meet a Steady-State Error Specification

PROBLEM: Given the control system in Figure 7.10, find the value of K so that there is 10% error in the steady state.

FIGURE 7.10   Feedback control system for Example 7.6

SOLUTION: Since the system is Type 1, the error stated in the problem must apply to a ramp input; only a ramp yields a finite error in a Type 1 system. Thus,

$$e(\infty) = \frac{1}{K_v} = 0.1 \qquad (7.55)$$

Therefore,

$$K_v = 10 = \lim_{s \to 0} sG(s) = \frac{K \times 5}{6 \times 7 \times 8} \qquad (7.56)$$

which yields

$$K = 672 \qquad (7.57)$$

Applying the Routh-Hurwitz criterion, we see that the system is stable at this gain.

Although this gain meets the criteria for steady-state error and stability, it may not yield a desirable transient response. In Chapter 9 we will design feedback control systems to meet all three specifications.

```
Students who are using MATLAB should now run ch7 p2 in Appendix B.
You will learn how to find the gain to meet a steady-state error
specification using MATLAB. This exercise solves Example 7.6
using MATLAB.
```

MATLAB
ML

</div>

<div style="border:1px solid #000;padding:10px;">

Skill-Assessment Exercise 7.3

PROBLEM: A unity feedback system has the following forward transfer function:

$$G(s) = \frac{K(s + 12)}{(s + 14)(s + 18)}$$

Find the value of K to yield a 10% error in the steady state.

ANSWER: $K = 189$

The complete solution is at www.wiley.com/college/nise.

WileyPLUS
WPCS
Control Solutions

TryIt 7.2

Use MATLAB, the Control System Toolbox, and the following statements to solve Skill-Assessment Exercise 7.3 and check the resulting system for stability.

```
numg=[l 12];
deng=poly([-14 -18]);
G=tf(numg,deng);
Kpdk=dcgain(G);
estep=0.1;
K=(l/estep-1)/Kpdk
T=feedback(G,1);
poles=pole(T)
```

</div>

This example and exercise complete our discussion of unity feedback systems. In the remaining sections, we will deal with the steady-state errors for disturbances and the steady-state errors for feedback control systems in which the feedback is not unity.

◖ 7.5   Steady-State Error for Disturbances

Feedback control systems are used to compensate for disturbances or unwanted inputs that enter a system. The advantage of using feedback is that regardless of these disturbances, the system can be designed to follow the input with small or zero error, as we now demonstrate. Figure 7.11 shows a feedback control system with a disturbance, $D(s)$, injected between the controller and the plant. We now re-derive the expression for steady-state error with the disturbance included.
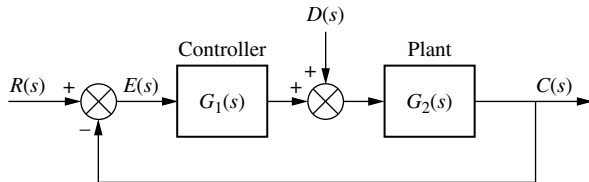
The transform of the output is given by

$$C(s) = E(s)G_1(s)G_2(s) + D(s)G_2(s) \qquad (7.58)$$

But

$$C(s) = R(s) - E(s) \qquad (7.59)$$

Substituting Eq. (7.59) into Eq. (7.58) and solving for $E(s)$, we obtain

$$E(s) = \frac{1}{1 + G_1(s)G_2(s)} R(s) - \frac{G_2(s)}{1 + G_1(s)G_2(s)} D(s) \qquad (7.60)$$

where we can think of $1/[1 + G_1(s)G_2(s)]$ as a transfer function relating $E(s)$ to $R(s)$ and $-G_2(s)/[1 + G_1(s)G_2(s)]$ as a transfer function relating $E(s)$ to $D(s)$.

To find the steady-state value of the error, we apply the final value theorem[3] to Eq. (7.60) and obtain

$$\boxed{\begin{aligned} e(\infty) = \lim_{s \to 0} sE(s) &= \lim_{s \to 0} \frac{s}{1 + G_1(s)G_2(s)} R(s) - \lim_{s \to 0} \frac{sG_2(s)}{1 + G_1(s)G_2(s)} D(s) \\ &= e_R(\infty) + e_D(\infty) \end{aligned}} \qquad (7.61)$$

where

$$\boxed{e_R(\infty) = \lim_{s \to 0} \frac{s}{1 + G_1(s)G_2(s)} R(s)}$$

and

$$\boxed{e_D(\infty) = -\lim_{s \to 0} \frac{sG_2(s)}{1 + G_1(s)G_2(s)} D(s)}$$

The first term, $e_R(\infty)$, is the steady-state error due to $R(s)$, which we have already obtained. The second term, $e_D(\infty)$, is the steady-state error due to the disturbance. Let us explore the conditions on $e_D(\infty)$ that must exist to reduce the error due to the disturbance.

At this point, we must make some assumptions about $D(s)$, the controller, and the plant. First we assume a step disturbance, $D(s) = 1/s$. Substituting this value into

FIGURE 7.11   Feedback control system showing disturbance

---
[3] Remember that the final value theorem can be applied only if the system is stable, with the roots of $[1 + G_1(s)G_2(s)]$ in the left–half–plane.

the second term of Eq. (7.61), $e_D(\infty)$, the steady-state error component due to a step disturbance is found to be

$$e_D(\infty) = -\frac{1}{\displaystyle\lim_{s\to 0}\frac{1}{G_2(s)} + \lim_{s\to 0} G_1(s)} \tag{7.62}$$

This equation shows that the steady-state error produced by a step disturbance can be reduced by increasing the dc gain of $G_1(s)$ or decreasing the dc gain of $G_2(s)$.

This concept is shown in Figure 7.12, where the system of Figure 7.11 has been rearranged so that the disturbance, $D(s)$, is depicted as the input and the error, $E(s)$, as the output, with $R(s)$ set equal to zero. If we want to minimize the steady-state value of $E(s)$, shown as the output in Figure 7.12, we must either increase the dc gain of $G_1(s)$ so that a lower value of $E(s)$ will be fed back to match the steady-state value of $D(s)$, or decrease the dc value of $G_2(s)$, which then yields a smaller value of $e(\infty)$ as predicted by the feedback formula.

Let us look at an example and calculate the numerical value of the steady-state error that results from a disturbance.
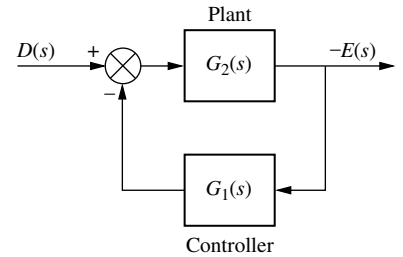
FIGURE 7.12   Figure 7.11 system rearranged to show disturbance as input and error as output, with $R(s) = 0$

Example 7.7

Steady-State Error Due to Step Disturbance

PROBLEM: Find the steady-state error component due to a step disturbance for the system of Figure 7.13.
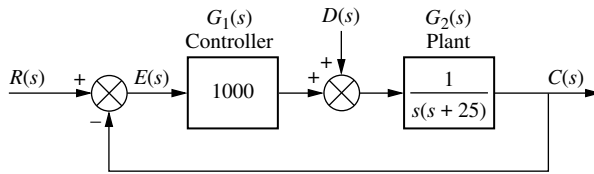
FIGURE 7.13   Feedback control system for Example 7.7

SOLUTION: The system is stable. Using Figure 7.12 and Eq. (7.62), we find

$$e_D(\infty) = -\frac{1}{\displaystyle\lim_{s\to 0}\frac{1}{G_2(s)} + \lim_{s\to 0} G_1(s)} = -\frac{1}{0 + 1000} = -\frac{1}{1000} \tag{7.63}$$

The result shows that the steady-state error produced by the step disturbance is inversely proportional to the dc gain of $G_1(s)$. The dc gain of $G_2(s)$ is infinite in this example.

**Virtual Experiment 7.1
Steady-State Error**

Put theory into practice finding the steady-state error of the Quanser Rotary Servo when subject to an input or a disturbance by simulating it in LabVIEW. This analysis becomes important when developing controllers for bottle labelling machines or robot joint control.
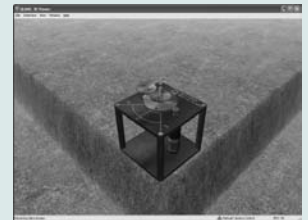
Virtual experiments are found on WileyPLUS.

Skill-Assessment Exercise 7.4

PROBLEM: Evaluate the steady-state error component due to a step disturbance for the system of Figure 7.14.
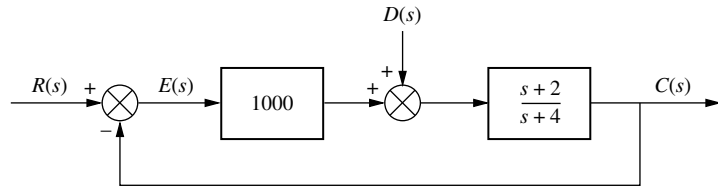
FIGURE 7.14   System for Skill-Assessment Exercise 7.4

ANSWER: $e_D(\infty) = -9.98 \times 10^{-4}$

The complete solution is at www.wiley.com/college/nise.

7.6   Steady-State Error for Nonunity Feedback Systems

Control systems often do not have unity feedback because of the compensation used to improve performance or because of the physical model for the system. The feedback path can be a pure gain other than unity or have some dynamic representation.

A general feedback system, showing the input transducer, $G_1(s)$, controller and plant, $G_2(s)$, and feedback, $H_1(s)$, is shown in Figure 7.15(a). Pushing the input transducer

(a)

(b)   (c)
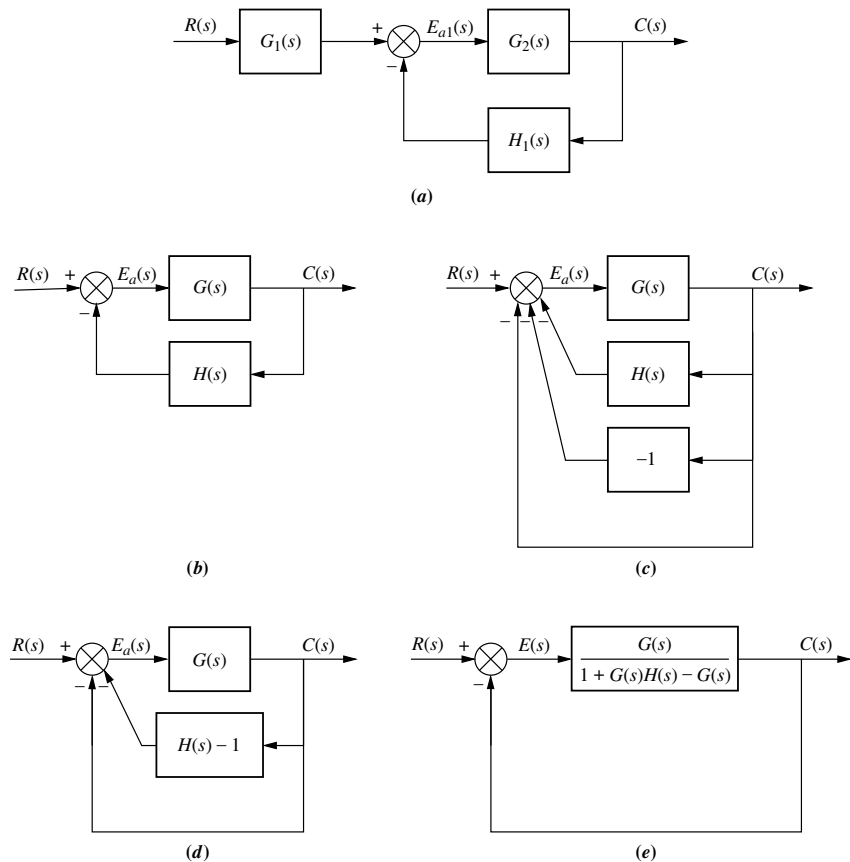
FIGURE 7.15   Forming an equivalent unity feedback system from a general nonunity feedback system

(d)   (e)

to the right past the summing junction yields the general nonunity feedback system shown in Figure 7.15(*b*), where $G(s) = G_1(s)G_2(s)$ and $H(s) = H_1(s)/G_1(s)$. Notice that unlike a unity feedback system, where $H(s) = 1$, the error is not the difference between the input and the output. For this case we call the signal at the output of the summing junction the *actuating signal,* $E_a(s)$. If $r(t)$ and $c(t)$ have the same units, we can find the steady-state error, $e(\infty) = r(\infty) - c(\infty)$. The first step is to show explicitly $E(s) = R(s) - C(s)$ on the block diagram.

Take the nonunity feedback control system shown in Figure 7.15(*b*) and form a unity feedback system by adding and subtracting unity feedback paths, as shown in Figure 7.15(*c*). This step requires that input and output units be the same. Next combine $H(s)$ with the negative unity feedback, as shown in Figure 7.15(*d*). Finally, combine the feedback system consisting of $G(s)$ and $[H(s) - 1]$, leaving an equivalent forward path and a unity feedback, as shown in Figure 7.15(*e*). Notice that the final figure shows $E(s) = R(s) - C(s)$ explicitly.

The following example summarizes the concepts of steady-state error, system type, and static error constants for nonunity feedback systems.

Example 7.8

Steady-State Error for Nonunity Feedback Systems

PROBLEM: For the system shown in Figure 7.16, find the system type, the appropriate error constant associated with the system type, and the steady-state error for a unit step input. Assume input and output units are the same.

SOLUTION: After determining that the system is indeed stable, one may impulsively declare the system to be Type 1. This may not be the case, since there is a nonunity feedback element, and the plant's actuating signal is not the difference between the input and the output.

FIGURE 7.16   Nonunity feedback control system for Example 7.8

The first step in solving the problem is to convert the system of Figure 7.16 into an equivalent unity feedback system. Using the equivalent forward transfer function of Figure 7.15(*e*) along with

$$G(s) = \frac{100}{s(s + 10)} \tag{7.64}$$

and

$$H(s) = \frac{1}{(s + 5)} \tag{7.65}$$

we find

$$G_e(s) = \frac{G(s)}{1 + G(s)H(s) - G(s)} = \frac{100(s + 5)}{s^3 + 15s^2 - 50s - 400} \tag{7.66}$$

Thus, the system is Type 0, since there are no pure integrations in Eq. (7.66). The appropriate static error constant is then K_p, whose value is

$$K_p = \lim_{s \to 0} G_e(s) = \frac{100 \times 5}{-400} = -\frac{5}{4} \tag{7.67}$$

TryIt 7.3
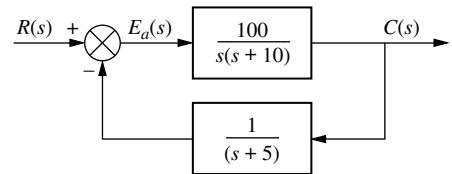
Use MATLAB, the Control System Toolbox, and the following statements to find $G_e(s)$ in Example 7.8.

```
G=zpk([ ],[0 -10],100);
H=zpk([ ],-5,1);
Ge=feedback...
  (G,(H-1));
'Ge(s)'
Ge=tf(Ge)
T=feedback(Ge,1);
'Poles of T(s)'
pole(T)
```

The steady-state error, $e(\infty)$, is

$$e(\infty) = \frac{1}{1 + K_p} = \frac{1}{1 - (5/4)} = -4 \qquad (7.68)$$

The negative value for steady-state error implies that the output step is larger than the input step.
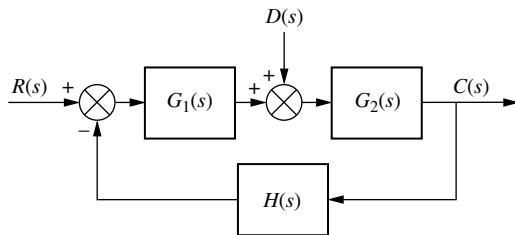

FIGURE 7.17 Nonunity feedback control system with disturbance

To continue our discussion of steady-state error for systems with nonunity feedback, let us look at the general system of Figure 7.17, which has both a disturbance and nonunity feedback. We will derive a general equation for the steady-state error and then determine the parameters of the system in order to drive the error to zero for step inputs and step disturbances.[4]

The steady-state error for this system, $e(\infty) = r(\infty) - c(\infty)$, is

$$e(\infty) = \lim_{s \to 0} sE(s) = \lim_{s \to 0} s \left\{ \left[1 - \frac{G_1(s)G_2(s)}{1 + G_1(s)G_2(s)H(s)} \right] R(s) \right.$$
$$\left. - \left[\frac{G_2(s)}{1 + G_1(s)G_2(s)H(s)} D(s) \right] \right\} \qquad (7.69)$$

Now limiting the discussion to step inputs and step disturbances, where $R(s) = D(s) = 1/s$, Eq. (7.69) becomes

$$e(\infty) = \lim_{s \to 0} sE(s) = \left\{ \left[1 - \frac{\lim_{s \to 0}[G_1(s)G_2(s)]}{\lim_{s \to 0}[1 + G_1(s)G_2(s)H(s)]} \right] \right.$$
$$\left. - \left[\frac{\lim_{s \to 0} G_2(s)}{\lim_{s \to 0}[1 + G_1(s)G_2(s)H(s)]} \right] \right\} \qquad (7.70)$$

For zero error,

$$\frac{\lim_{s \to 0}[G_1(s)G_2(s)]}{\lim_{s \to 0}[1 + G_1(s)G_2(s)H(s)]} = 1 \quad \text{and} \quad \frac{\lim_{s \to 0} G_2(s)}{\lim_{s \to 0}[1 + G_1(s)G_2(s)H(s)]} = 0 \qquad (7.71)$$

The two equations in Eq. (7.71) can always be satisfied if (1) the system is stable, (2) $G_1(s)$ is a Type 1 system, (3) $G_2(s)$ is a Type 0 system, and (4) $H(s)$ is a Type 0 system with a dc gain of unity.

To conclude this section, we discuss finding the steady-state value of the actuating signal, $E_{a1}(s)$, in Figure 7.15(a). For this task there is no restriction that the input and output units be the same, since we are finding the steady-state difference between signals at the summing junction, which do have the same units.[5] The steady-state

---

[4] Details of the derivation are included as a problem at the end of this chapter.

[5] For clarity, steady-state error is the steady-state difference between the input and the output. Steady-state actuating signal is the steady-state difference at the output of the summing junction. In questions asking for steady-state error in problems, examples, and skill-assessment exercises, it will be assumed that input and output units are the same.

actuating signal for Figure 7.15(a) is

$$e_{a1}(\infty) = \lim_{s \to 0} \frac{sR(s)G_1(s)}{1 + G_2(s)H_1(s)} \tag{7.72}$$

The derivation is left to the student in the problem set at the end of this chapter.

Example 7.9

Steady-State Actuating Signal for Nonunity Feedback Systems

PROBLEM: Find the steady-state actuating signal for the system of Figure 7.16 for a unit step input. Repeat for a unit ramp input.

SOLUTION: Use Eq. (7.72) with $R(s) = 1/s$, a unit step input, $G_1(s) = 1$, $G_2(s) = 100/[s(s+10)]$, and $H_1(s) = 1/(s+5)$. Also, realize that $e_{a1}(\infty) = e_a(\infty)$, since $G_1(s) = 1$. Thus,

$$e_a(\infty) = \lim_{s \to 0} \frac{s\left(\dfrac{1}{s}\right)}{1 + \left(\dfrac{100}{s(s+10)}\right)\left(\dfrac{1}{(s+5)}\right)} = 0 \tag{7.73}$$

Now use Eq. (7.72) with $R(s) = 1/s^2$, a unit ramp input, and obtain

$$e_a(\infty) = \lim_{s \to 0} \frac{s\left(\dfrac{1}{s^2}\right)}{1 + \left(\dfrac{100}{s(s+10)}\right)\left(\dfrac{1}{(s+5)}\right)} = \frac{1}{2} \tag{7.74}$$

Skill-Assessment Exercise 7.5

PROBLEM:

a. Find the steady-state error, $e(\infty) = r(\infty) - c(\infty)$, for a unit step input given the nonunity feedback system of Figure 7.18. Repeat for a unit ramp input. Assume input and output units are the same.

b. Find the steady-state actuating signal, $e_a(\infty)$, for a unit step input given the nonunity feedback system of Figure 7.18. Repeat for a unit ramp input.

FIGURE 7.18   Nonunity feedback system for Skill-Assessment Exercise 7.5

ANSWERS:

a. $e_{\text{step}}(\infty) = 3.846 \times 10^{-2}; e_{\text{ramp}}(\infty) = \infty$

b. For a unit step input, $e_a(\infty) = 3.846 \times 10^{-2}$; for a unit ramp input, $e_a(\infty) = \infty$

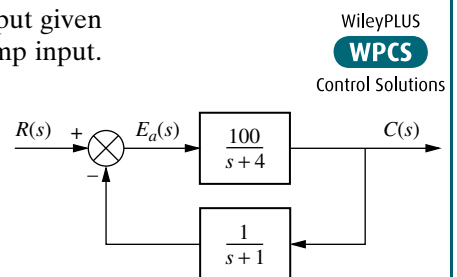The complete solution is at www.wiley.com/college/nise.

In this section, we have applied steady-state error analysis to nonunity feedback systems. When nonunity feedback is present, the plant's actuating signal is not

the actual error or difference between the input and the output. With nonunity feedback we may choose to (1) find the steady-state error for systems where the input and output units are the same or (2) find the steady-state actuating signal.

We also derived a general expression for the steady-state error of a nonunity feedback system with a disturbance. We used this equation to determine the attributes of the subsystems so that there was zero error for step inputs and step disturbances.

Before concluding this chapter, we will discuss a topic that is not only significant for steady-state errors but generally useful throughout the control systems design process.

7.7   Sensitivity

During the design process, the engineer may want to consider the extent to which changes in system parameters affect the behavior of a system. Ideally, parameter changes due to heat or other causes should not appreciably affect a system's perform-ance. The degree to which changes in system parameters affect system transfer functions, and hence performance, is called *sensitivity*. A system with zero sensitivity (that is, changes in the system parameters have no effect on the transfer function) is ideal. The greater the sensitivity, the less desirable the effect of a parameter change.

For example, assume the function $F = K/(K + a)$. If $K = 10$ and $a = 100$, then $F = 0.091$. If parameter a triples to 300, then $F = 0.032$. We see that a fractional change in parameter a of $(300 - 100)/100 = 2$ (a 200% change), yields a change in the function F of $(0.032 - 0.091)/0.091 = -0.65$ (-65% change). Thus, the function F has reduced sensitivity to changes in parameter a. As we proceed, we will see that another advantage of feedback is that in general it affords reduced sensitivity to parameter changes.

Based upon the previous discussion, let us formalize a definition of sensitivity: *Sensitivity* is the ratio of the fractional change in the function to the fractional change in the parameter as the fractional change of the parameter approaches zero. That is,

$$S_{F:P} = \lim_{\Delta P \to 0} \frac{\text{Fractional change in the function, } F}{\text{Fractional change in the parameter, } P}$$
$$= \lim_{\Delta P \to 0} \frac{\Delta F/F}{\Delta P/P}$$
$$= \lim_{\Delta P \to 0} \frac{P\Delta F}{F\Delta P}$$

which reduces to

$$S_{F:P} = \frac{P}{F}\frac{\delta F}{\delta P} \qquad (7.75)$$

Let us now apply the definition, first to a closed-loop transfer function and then to the steady-state error.

Example 7.10

Sensitivity of a Closed-Loop Transfer Function
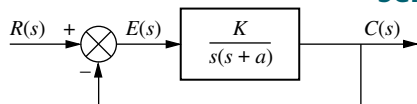

FIGURE 7.19   Feedback control system for Examples 7.10 and 7.11

PROBLEM: Given the system of Figure 7.19, calculate the sensitivity of the closed-loop transfer function to changes in the parameter a. How would you reduce the sensitivity?

SOLUTION: The closed-loop transfer function is

$$T(s) = \frac{K}{s^2 + as + K} \tag{7.76}$$

Using Eq. (7.75), the sensitivity is given by

$$S_{T:a} = \frac{a}{T}\,\frac{\delta T}{\delta a} = \frac{a}{\left(\dfrac{K}{s^2 + as + K}\right)}\left(\frac{-Ks}{(s^2 + as + K)^2}\right) = \frac{-as}{s^2 + as + K} \tag{7.77}$$

which is, in part, a function of the value of *s*. For any value of *s*, however, an increase in *K* reduces the sensitivity of the closed-loop transfer function to changes in the parameter *a*.

Example 7.11

Sensitivity of Steady-State Error with Ramp Input

PROBLEM: For the system of Figure 7.19, find the sensitivity of the steady-state error to changes in parameter *K* and parameter *a* with ramp inputs.

SOLUTION: The steady-state error for the system is

$$e(\infty) = \frac{1}{K_v} = \frac{a}{K} \tag{7.78}$$

The sensitivity of $e(\infty)$ to changes in parameter *a* is

$$S_{e:a} = \frac{a}{e}\,\frac{\delta e}{\delta a} = \frac{a}{a/K}\left[\frac{1}{K}\right] = 1 \tag{7.79}$$

The sensitivity of $e(\infty)$ to changes in parameter *K* is

$$S_{e:K} = \frac{K}{e}\,\frac{\delta e}{\delta K} = \frac{K}{a/K}\left[\frac{-a}{K^2}\right] = -1 \tag{7.80}$$

Thus, changes in either parameter *a* or parameter *K* are directly reflected in $e(\infty)$, and there is no reduction or increase in sensitivity. The negative sign in Eq. (7.80) indicates a decrease in $e(\infty)$ for an increase in *K*. Both of these results could have been obtained directly from Eq. (7.78) since $e(\infty)$ is directly proportional to parameter *a* and inversely proportional to parameter *K*.

Example 7.12

Sensitivity of Steady-State Error with Step Input

PROBLEM: Find the sensitivity of the steady-state error to changes in parameter *K* and parameter *a* for the system shown in Figure 7.20 with a step input.
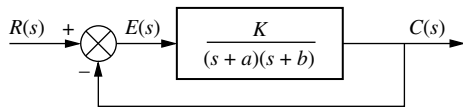
FIGURE 7.20 Feedback control system for Example 7.12

TryIt 7.4

Use MATLAB, the Symbolic Math Toolbox, and the following statements to find $S_{e:a}$ in Example 7.12.

```
syms K a b s
G=K/((s+a)*(s+b));
Kp=subs(G,s,o);
e=1/(1+Kp);
Sea=(a/e)*diff(e,a);
Sea=simple(Sea);
'Sea'
pretty(Sea)
```

SOLUTION: The steady-state error for this Type 0 system is

$$e(\infty) = \frac{1}{1 + K_p} = \frac{1}{1 + \dfrac{K}{ab}} = \frac{ab}{ab + K} \tag{7.81}$$

The sensitivity of $e(\infty)$ to changes in parameter a is

$$S_{e:a} = \frac{a}{e} \frac{\delta e}{\delta a} = \frac{a}{\left(\dfrac{ab}{ab + K}\right)} \frac{(ab + K)b - ab^2}{(ab + K)^2} = \frac{K}{ab + K} \tag{7.82}$$

The sensitivity of $e(\infty)$ to changes in parameter K is

$$S_{e:K} = \frac{K}{e} \frac{\delta e}{\delta K} = \frac{K}{\left(\dfrac{ab}{ab + K}\right)} \frac{-ab}{(ab + K)^2} = \frac{-K}{ab + K} \tag{7.83}$$

Equations (7.82) and (7.83) show that the sensitivity to changes in parameter K and parameter a is less than unity for positive a and b. Thus, feedback in this case yields reduced sensitivity to variations in both parameters.

Skill-Assessment Exercise 7.6
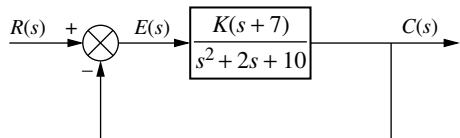
FIGURE 7.21 System for Skill-Assessment Exercise 7.6

PROBLEM: Find the sensitivity of the steady-state error to changes in K for the system of Figure 7.21.

ANSWER: $S_{e:k} = \dfrac{-7K}{10 + 7K}$

The complete solution is at www.wiley.com/college/nise.

In this section, we defined sensitivity and showed that in some cases feedback reduces the sensitivity of a system's steady-state error to changes in system parameters. The concept of sensitivity can be applied to other measures of control system performance, as well; it is not limited to the sensitivity of the steady-state error performance.

7.8 Steady-State Error for Systems in State Space

Up to this point, we have evaluated the steady-state error for systems modeled as transfer functions. In this section, we will discuss how to evaluate the steady-state error for systems represented in state space. Two methods for calculating the steady-state error will be covered: (1) analysis via final value theorem and (2) analysis via input substitution. We will consider these methods individually.

Analysis via Final Value Theorem
A single-input, single-output system represented in state space can be analyzed for steady-state error using the final value theorem and the closed-loop transfer

function, Eq. (3.73), derived in terms of the state-space representation. Consider the closed-loop system represented in state space:

$$\dot{\mathbf{x}} = \mathbf{A}\mathbf{x} + \mathbf{B}r \tag{7.84a}$$

$$y = \mathbf{C}\mathbf{x} \tag{7.84b}$$

The Laplace transform of the error is

$$E(s) = R(s) - Y(s) \tag{7.85}$$

But

$$Y(s) = R(s)T(s) \tag{7.86}$$

where $T(s)$ is the closed-loop transfer function. Substituting Eq. (7.86) into (7.85), we obtain

$$E(s) = R(s)[1 - T(s)] \tag{7.87}$$

Using Eq. (3.73) for $T(s)$, we find

$$E(s) = R(s)[1 - \mathbf{C}(s\mathbf{I} - \mathbf{A})^{-1}\mathbf{B}] \tag{7.88}$$

Applying the final value theorem, we have

$$\boxed{\lim_{s \to 0} sE(s) = \lim_{s \to 0} sR(s)[1 - \mathbf{C}(s\mathbf{I} - \mathbf{A})^{-1}\mathbf{B}]} \tag{7.89}$$

Let us apply the result to an example.

Example 7.13

Steady-State Error Using the Final Value Theorem

PROBLEM: Evaluate the steady-state error for the system described by Eqs. (7.90) for unit step and unit ramp inputs. Use the final value theorem.

$$\mathbf{A} = \begin{bmatrix} -5 & 1 & 0 \\ 0 & -2 & 1 \\ 20 & -10 & 1 \end{bmatrix}; \quad \mathbf{B} = \begin{bmatrix} 0 \\ 0 \\ 1 \end{bmatrix}; \quad \mathbf{C} = \begin{bmatrix} -1 & 1 & 0 \end{bmatrix} \tag{7.90}$$

SOLUTION: Substituting Eqs. (7.90) into (7.89), we obtain

$$
\begin{aligned}
e(\infty) &= \lim_{s \to 0} sR(s)\left(1 - \frac{s+4}{s^3 + 6s^2 + 13s + 20}\right) \\
&= \lim_{s \to 0} sR(s)\left(\frac{s^3 + 6s^2 + 12s + 16}{s^3 + 6s^2 + 13s + 20}\right)
\end{aligned} \tag{7.91}
$$

For a unit step, $R(s) = 1/s$, and $e(\infty) = 4/5$. For a unit ramp, $R(s) = 1/s^2$, and $e(\infty) = \infty$. Notice that the system behaves like a Type 0 system.

TryIt 7.5

Use MATLAB, the Symbolic Math Toolbox, and the following statements to find the steady-state error for a step input to the system of Example 7.13.

```
syms s
A=[-5 1 0
    0 -2 1
   20 -10 1];
B=[0;0;1];
C=[-1 1 0];
I=[1 0 0
   0 1 0
   0 0 1];
E=(1/s)*[1-C* ...
 [(s*I-A)^-1]*B];
%New command:
%subs(X,old,new):
%Replace old in ...
%X(old) with new.
error=subs(s*E,s,0)
```

Analysis via Input Substitution

Another method for steady-state analysis avoids taking the inverse of $(s\mathbf{I} - \mathbf{A})$ and can be expanded to multiple-input, multiple-output systems; it substitutes the input along with an assumed solution into the state equations (*Hostetter*, *1989*). We will derive the results for unit step and unit ramp inputs.

Step Inputs. Given the state Eqs. (7.84), if the input is a unit step where $r = 1$, a steady-state solution, $\mathbf{x}_{ss}$, for $\mathbf{x}$, is

$$\mathbf{x}_{ss} = \begin{bmatrix} V_1 \\ V_2 \\ \vdots \\ V_n \end{bmatrix} = \mathbf{V} \tag{7.92}$$

where V_i is constant. Also,

$$\dot{\mathbf{x}}_{ss} = \mathbf{0} \tag{7.93}$$

Substituting $r = 1$, a unit step, along with Eqs. (7.92) and (7.93), into Eqs. (7.84) yields

$$\mathbf{0} = \mathbf{A}\mathbf{V} + \mathbf{B} \tag{7.94a}$$

$$y_{ss} = \mathbf{C}\mathbf{V} \tag{7.94b}$$

where y_{ss} is the steady-state output. Solving for $\mathbf{V}$ yields

$$\mathbf{V} = -\mathbf{A}^{-1}\mathbf{B} \tag{7.95}$$

But the steady-state error is the difference between the steady-state input and the steady-state output. The final result for the steady-state error for a unit step input into a system represented in state space is

$$\boxed{e(\infty) = 1 - y_{ss} = 1 - \mathbf{C}\mathbf{V} = 1 + \mathbf{C}\mathbf{A}^{-1}\mathbf{B}} \tag{7.96}$$

Ramp Inputs. For unit ramp inputs, $r = t$, a steady-state solution for $\mathbf{x}$ is

$$\mathbf{x}_{ss} = \begin{bmatrix} V_1 t + W_1 \\ V_2 t + W_2 \\ \vdots \\ V_n t + W_n \end{bmatrix} = \mathbf{V}t + \mathbf{W} \tag{7.97}$$

where V_i and W_i are constants. Hence,

$$\dot{\mathbf{x}}_{ss} = \begin{bmatrix} V_1 \\ V_2 \\ \vdots \\ V_n \end{bmatrix} = \mathbf{V} \tag{7.98}$$

Substituting $r = t$ along with Eqs. (7.97) and (7.98) into Eqs. (7.84) yields

$$\mathbf{V} = \mathbf{A}(\mathbf{V}t + \mathbf{W}) + \mathbf{B}t \tag{7.99a}$$

$$y_{ss} = \mathbf{C}(\mathbf{V}t + \mathbf{W}) \tag{7.99b}$$

In order to balance Eq. (7.99a), we equate the matrix coefficients of t, $\mathbf{AV} = -\mathbf{B}$, or

$$\mathbf{V} = -\mathbf{A}^{-1}\mathbf{B} \tag{7.100}$$

Equating constant terms in Eq. (7.99a), we have $\mathbf{AW} = \mathbf{V}$, or

$$\mathbf{W} = \mathbf{A}^{-1}\mathbf{V} \tag{7.101}$$

Substituting Eqs. (7.100) and (7.101) into (7.99b) yields

$$y_{ss} = \mathbf{C}[-\mathbf{A}^{-1}\mathbf{B}t + \mathbf{A}^{-1}(-\mathbf{A}^{-1}\mathbf{B})] = -\mathbf{C}[\mathbf{A}^{-1}\mathbf{B}t + (\mathbf{A}^{-1})^2\mathbf{B}] \tag{7.102}$$

The steady-state error is therefore

$$e(\infty) = \lim_{t\to\infty}(t - y_{ss}) = \lim_{t\to\infty}[(1 + \mathbf{C}\mathbf{A}^{-1}\mathbf{B})t + \mathbf{C}(\mathbf{A}^{-1})^2\mathbf{B}] \tag{7.103}$$

Notice that in order to use this method, $\mathbf{A}^{-1}$ must exist. That is, $\det\mathbf{A} \neq 0$.

We now demonstrate the use of Eqs. (7.96) and (7.103) to find the steady-state error for step and ramp inputs.

Example 7.14

Steady-State Error Using Input Substitution

PROBLEM: Evaluate the steady-state error for the system described by the three equations in Eq. (7.90) for unit step and unit ramp inputs. Use input substitution.

SOLUTION: For a unit step input, the steady-state error given by Eq. (7.96) is

$$e(\infty) = 1 + \mathbf{C}\mathbf{A}^{-1}\mathbf{B} = 1 - 0.2 = 0.8 \tag{7.104}$$

where $\mathbf{C}$, $\mathbf{A}$, and $\mathbf{B}$ are as follows:

$$\mathbf{A} = \begin{bmatrix} -5 & 1 & 0 \\ 0 & -2 & 1 \\ 20 & -10 & 1 \end{bmatrix}; \quad \mathbf{B} = \begin{bmatrix} 0 \\ 0 \\ 1 \end{bmatrix}; \quad \mathbf{C} = \begin{bmatrix} -1 & 1 & 0 \end{bmatrix} \tag{7.105}$$

For a ramp input, using Eq. (7.103), we have

$$e(\infty) = [\lim_{t\to\infty}[(1 + \mathbf{C}\mathbf{A}^{-1}\mathbf{B})]t + \mathbf{C}(\mathbf{A}^{-1})^2\mathbf{B}] = \lim_{t\to\infty}(0.8t + 0.08) = \infty \tag{7.106}$$

Skill-Assessment Exercise 7.7

PROBLEM: Find the steady-state error for a step input given the system repre-
sented in state space below. Calculate the steady-state error using both the final
value theorem and input substitution methods.

$$\mathbf{A} = \begin{bmatrix} 0 & 1 \\ -3 & -6 \end{bmatrix}; \quad \mathbf{B} = \begin{bmatrix} 0 \\ 1 \end{bmatrix}; \quad \mathbf{C} = \begin{bmatrix} 1 & 1 \end{bmatrix}$$

ANSWER:

$$e_{\text{step}}(\infty) = \frac{2}{3}$$

The complete solution is at www.wiley.com/college/nise.

In this chapter, we covered the evaluation of steady-state error for systems
represented by transfer functions as well as systems represented in state space. For
systems represented in state space, two methods were presented: (1) final value
theorem and (2) input substitution.

Case Studies

Antenna Control: Steady-State Error Design via Gain

This chapter showed how to find steady-state errors for step, ramp, and parabolic
inputs to a closed-loop feedback control system. We also learned how to evaluate
the gain to meet a steady-state error requirement. This ongoing case study uses our
antenna azimuth position control system to summarize the concepts.

PROBLEM: For the antenna azimuth position control system shown on the front
endpapers, Configuration 1,

a. Find the steady-state error in terms of gain, *K*, for step, ramp, and parabolic
inputs.

b. Find the value of gain, *K*, to yield a 10% error in the steady state.

SOLUTION:

a. The simplified block diagram for the system is shown on the front endpapers.
The steady-state error is given by

$$e(\infty) = \lim_{s \to 0} sE(s) = \lim_{s \to 0} \frac{sR(s)}{1 + G(s)} \tag{7.107}$$

From the block diagram, after pushing the potentiometer to the right past the
summing junction, the equivalent forward transfer function is

$$G(s) = \frac{6.63K}{s(s + 1.71)(s + 100)} \tag{7.108}$$

To find the steady-state error for a step input, use $R(s) = 1/s$ along with Eq. (7.108), and substitute these in Eq. (7.107). The result is $e(\infty) = 0$.

To find the steady-state error for a ramp input, use $R(s) - 1/s^2$ along with Eq. (7.108), and substitute these in Eq. (7.107). The result is $e(\infty) = 25.79/K$.

To find the steady-state error for a parabolic input, use $R(s) = 1/s^3$ along with Eq. (7.108), and substitute these in Eq. (7.107). The result is $e(\infty) = \infty$.

b. Since the system is Type 1, a 10% error in the steady-state must refer to a ramp input. This is the only input that yields a finite, nonzero error. Hence, for a unit ramp input,

$$e(\infty) = 0.1 = \frac{1}{K_v} = \frac{(1.71)(100)}{6.63K} = \frac{25.79}{K} \tag{7.109}$$

from which $K = 257.9$. You should verify that the value of K is within the range of gains that ensures system stability. In the antenna control case study in the last chapter, the range of gain for stability was found to be $0 < K < 2623.29$. Hence, the system is stable for a gain of 257.9.

CHALLENGE: You are now given a problem to test your knowledge of this chapter's objectives: Referring to the antenna azimuth position control system shown on the front endpapers, Configuration 2, do the following:

a. Find the steady-state errors in terms of gain, K, for step, ramp, and parabolic inputs.

b. Find the value of gain, K, to yield a 20% error in the steady state.

Video Laser Disc Recorder: Steady-State Error Design via Gain

Design
D

As a second case study, let us look at a video laser disc focusing system for recording.

PROBLEM: In order to record on a video laser disc, a 0.5μm laser spot must be focused on the recording medium to burn pits that represent the program material. The small laser spot requires that the focusing lens be positioned to an accuracy of $\pm0.1\mu$m. A model of the feedback control system for the focusing lens is shown in Figure 7.22.

The detector detects the distance between the focusing lens and the video disc by measuring the degree of focus as shown in Figure 7.23(a). Laser light reflected from the disc, D, is split by beam splitters B_1 and B_2 and focused behind aperture A. The remainder is reflected by the mirror and focuses in front of aperture A. The amount of light of each beam that passes through the aperture depends on how far the beam's focal point is from the aperture. Each side of the split photodiode, P, measures the intensity of each beam. Thus, as the disc's distance from the recording
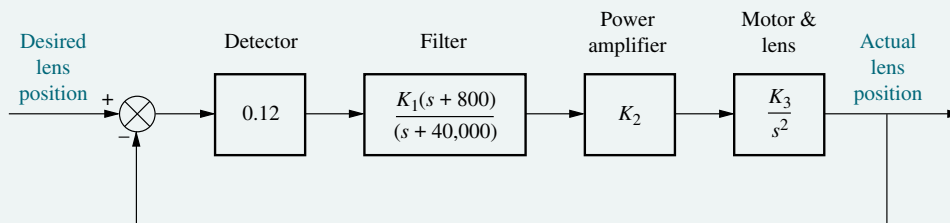

FIGURE 7.22 Video laser disc recording: control system for focusing write beam

Mirror

A, pinhole
aperture

P, split
photodiode

B_2, 50-50
beam splitter

Q–X/Y plate

L_1, condensing
lens

B_1, polarizing
beam splitter

L_2, recording
objective lens

D-Disc

(a)

Differential
voltage

0.6

Distance from
nominal focus
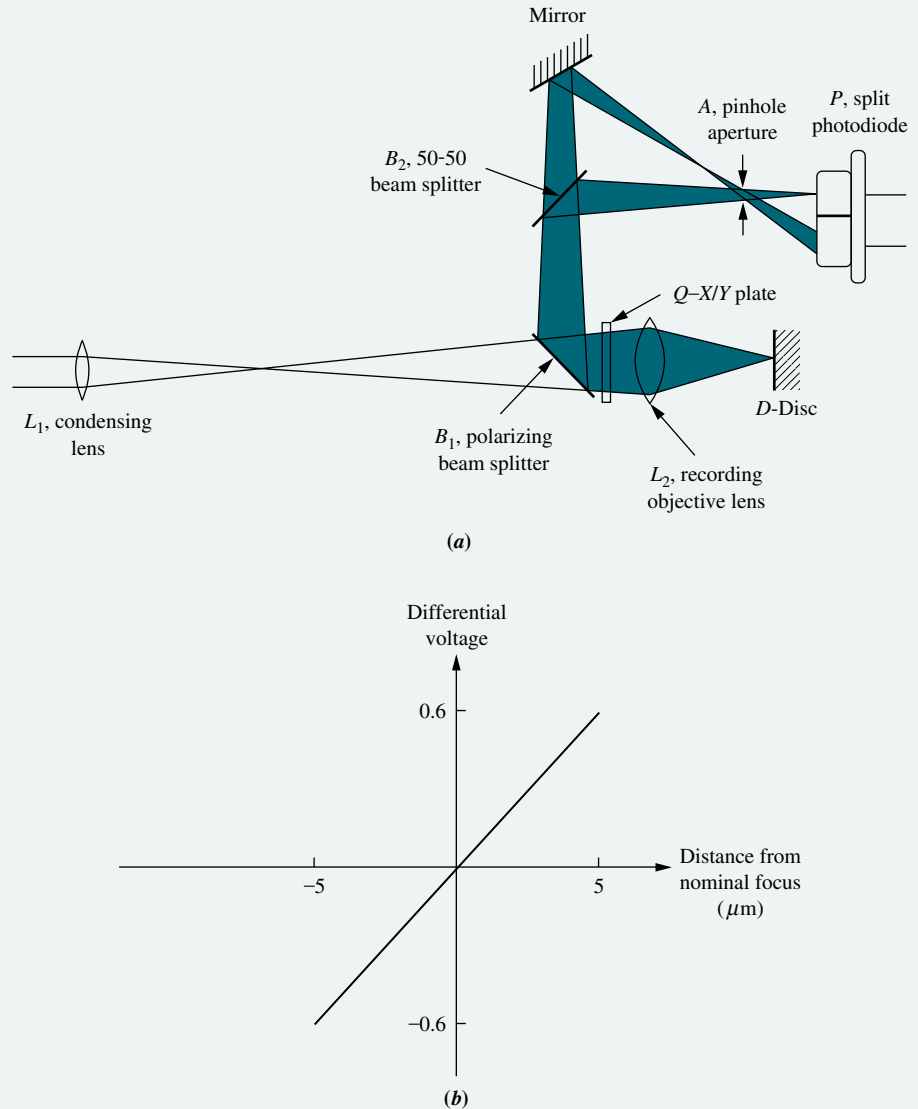(μm)

−5

5

−0.6

(b)

FIGURE 7.23   Video disc laser recording: **a.** focus detector optics; **b.** linearized transfer function for focus detector

objective lens changes, so does the focal point of each beam. As a result, the relative voltage detected by each part of the split photodiode changes. When the beam is out of focus, one side of the photodiode outputs a larger voltage. When the beam is in focus, the voltage outputs from both sides of the photodiode are equal.

A simplified model for the detector is a straight line relating the differential voltage output from the two elements to the distance of the laser disc from nominal focus. A linearized plot of the detector input-output relationship is shown in Figure 7.23(b) (*Isailović, 1985*). Assume that a warp on the disc yields a worst-case disturbance in the focus of $10\tau^2\mu$m. Find the value of $K_1K_2K_3$ in order to meet the focusing accuracy required by the system.

SOLUTION: Since the system is Type 2, it can respond to parabolic inputs with finite error. We can assume that the disturbance has the same effect as an input of $10t^2\mu$m. The Laplace transform of $10t^2$ is $20/s^3$, or 20 units greater than the unit acceleration used to derive the general equation of the error for a parabolic input. Thus, $e(\infty) = 20/K_a$. But $K_a = \lim\limits_{s\to 0} s^2 G(s)$.

From Figure 7.22, $K_a = 0.0024 K_1 K_2 K_3$. Also, from the problem statement, the error must be no greater than 0.1μm. Hence, $e(\infty) = 8333.33/K_1 K_2 K_3 = 0.1$. Thus, $K_1 K_2 K_3 \geq 83333.3$, and the system is stable.

CHALLENGE: You are now given a problem to test your knowledge of this chapter's objectives: Given the video laser disc recording system whose block diagram is shown in Figure 7.24, do the following:

a. If the focusing lens needs to be positioned to an accuracy of $\pm 0.005\mu$m, find the value of $K_1 K_2 K_3$ if the warp on the disc yields a worst-case disturbance in the focus of $15t^2\mu$m.

b. Use the Routh-Hurwitz criterion to show that the system is stable when the conditions of **a.** are met.

c. Use MATLAB to show that the system is stable when the conditions of **a.** are met.
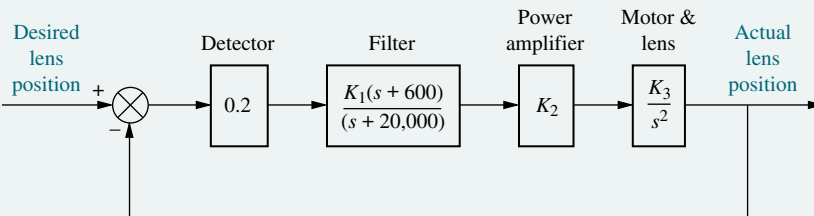
MATLAB
ML

FIGURE 7.24   Video laser disc recording focusing system

Summary

This chapter covered the analysis and design of feedback control systems for steady-state errors. The steady-state errors studied resulted strictly from the system configuration. On the basis of a system configuration and a group of selected test signals, namely steps, ramps, and parabolas, we can analyze or design for the system's steady-state error performance. The greater the number of pure integrations a system has in the forward path, the higher the degree of accuracy, assuming the system is stable.

The steady-state errors depend upon the type of test input. Applying the final value theorem to stable systems, the steady-state error for unit step inputs is

$$e(\infty) = \frac{1}{1 + \lim\limits_{s\to 0} G(s)} \qquad (7.110)$$

The steady-state error for ramp inputs of unit velocity is

$$e(\infty) = \frac{1}{\lim\limits_{s\to 0} sG(s)} \qquad (7.111)$$

and for parabolic inputs of unit acceleration, it is

$$e(\infty) = \frac{1}{\lim\limits_{s \to 0} s^2 G(s)} \tag{7.112}$$

The terms taken to the limit in Eqs. (7.110) through (7.112) are called *static error constants*. Beginning with Eq. (7.110), the terms in the denominator taken to the limit are called the *position constant, velocity constant*, and *acceleration constant*, respectively. The static error constants are the steady-state error specifications for control systems. By specifying a static error constant, one is stating the number of pure integrations in the forward path, the test signal used, and the expected steady-state error.

Another definition covered in this chapter was that of *system type*. The system type is the number of pure integrations in the forward path, assuming a unity feedback system. Increasing the system type decreases the steady-state error as long as the system remains stable.

Since the steady-state error is, for the most part, inversely proportional to the static error constant, the larger the static error constant, the smaller the steady-state error. Increasing system gain increases the static error constant. Thus, in general, increasing system gain decreases the steady-state error as long as the system remains stable.

Nonunity feedback systems were handled by deriving an equivalent unity feedback system whose steady-state error characteristics followed all previous development. The method was restricted to systems where input and output units are the same.

We also saw how feedback decreases a system's steady-state error caused by disturbances. With feedback, the effect of a disturbance can be reduced by system gain adjustments.

Finally, for systems represented in state space, we calculated the steady-state error using the final value theorem and input substitution methods.

In the next chapter, we will examine the root locus, a powerful tool for the analysis and design of control systems.

◀ Review Questions ▶

1. Name two sources of steady-state errors.
2. A position control, tracking with a constant difference in velocity, would yield how much position error in the steady state?
3. Name the test inputs used to evaluate steady-state error.
4. How many integrations in the forward path are required in order for there to be zero steady-state error for each of the test inputs listed in Question 3?
5. Increasing system gain has what effect upon the steady-state error?
6. For a step input, the steady-state error is approximately the reciprocal of the static error constant if what condition holds true?
7. What is the exact relationship between the static error constants and the steady-state errors for ramp and parabolic inputs?
8. What information is contained in the specification $K_p = 10,000$?
9. Define *system type*.

10. The forward transfer function of a control system has three poles at $-1, -2,$ and -3. What is the system type?

11. What effect does feedback have upon disturbances?

12. For a step input disturbance at the input to the plant, describe the effect of controller and plant gain upon minimizing the effect of the disturbance.

13. Is the forward-path actuating signal the system error if the system has nonunity feedback?

14. How are nonunity feedback systems analyzed and designed for steady-state errors?

15. Define, in words, *sensitivity* and describe the goal of feedback-control-system engineering as it applies to sensitivity.

16. Name two methods for calculating the steady-state error for systems represented in state space.

Problems

1. For the unity feedback system shown in Figure P7.1, where

WileyPLUS

WPCS

Control Solutions

$$G(s) = \frac{450(s+8)(s+12)(s+15)}{s(s+38)(s^2+2s+28)}$$

find the steady-state errors for the following test inputs: $25u(t)$, $37tu(t)$, $47t^2u(t)$. [Section: 7.2]
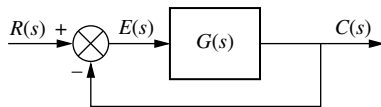

FIGURE P7.1

2. Figure P7.2 shows the ramp input $r(t)$ and the output $c(t)$ of a system. Assuming the output's steady state can be approximated by a ramp, find [Section: 7.1]

   a. the steady-state error;

   b. the steady-state error if the input becomes $r(t) = tu(t)$.
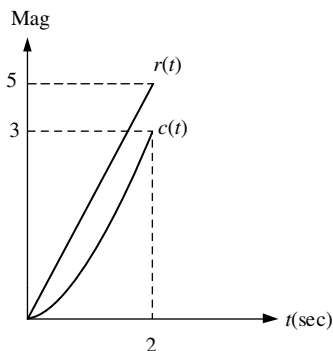
FIGURE P7.2

3. For the unity feedback system shown in Figure P7.1, where

$$G(s) = \frac{60(s+3)(s+4)(s+8)}{s^2(s+6)(s+17)}$$

find the steady-state error if the input is $80t^2u(t)$. [Section: 7.2]

4. For the system shown in Figure P7.3, what steady-state error can be expected for the following test inputs: $15u(t)$, $15tu(t)$, $15t^2u(t)$. [Section: 7.2]

FIGURE P7.3

5. For the unity feedback system shown in Figure P7.1, where

$$G(s) = \frac{500}{(s+24)(s^2+8s+14)}$$

find the steady-state error for inputs of $30u(t)$, $70tu(t)$, and $81t^2u(t)$. [Section: 7.3]

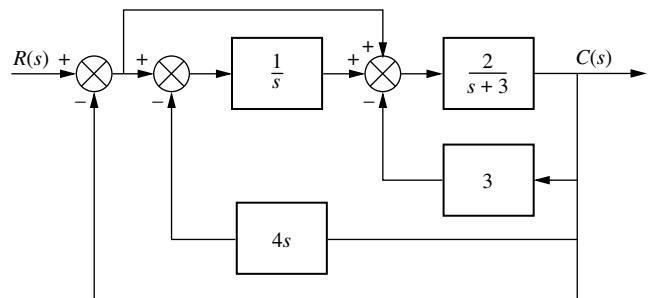6. An input of $25t^3u(t)$ is applied to the input of a Type 3 unity feedback system, as shown in Figure P7.1,

where

$$G(s) = \frac{210(s+4)(s+6)(s+11)(s+13)}{s^3(s+7)(s+14)(s+19)}$$

Find the steady-state error in position. [Section: 7.3]

7. The steady-state error in velocity of a system is defined to be

WileyPLUS

WPCS

Control Solutions

$$\left(\frac{dr}{dt} - \frac{dc}{dt}\right)\bigg|_{t\to\infty}$$

where r is the system input, and c is the system output. Find the steady-state error in velocity for an input of $t^3u(t)$ to a unity feedback system with a forward transfer function of [Section: 7.2]

$$G(s) = \frac{100(s+1)(s+2)}{s^2(s+3)(s+10)}$$

8. What is the steady-state error for a step input of 15 units applied to the unity feedback system of Figure P7.1, where [Section: 7.3]

$$G(s) = \frac{1020(s+13)(s+26)(s+33)}{(s+65)(s+75)(s+91)}$$

9. A system has $K_p = 4$. What steady-state error can be expected for inputs of $70u(t)$ and $70tu(t)$? [Section 7.3]

10. For the unity feedback system shown in Figure P7.1, where [Section: 7.3]

$$G(s) = \frac{5000}{s(s+75)}$$

a. What is the expected percent overshoot for a unit step input?

b. What is the settling time for a unit step input?

c. What is the steady-state error for an input of $5u(t)$?

d. What is the steady-state error for an input of $5tu(t)$?

e. What is the steady-state error for an input of $5t^2u(t)$?

11. Given the unity feedback system shown in Figure P7.1, where

$$G(s) = \frac{100500(s+5)(s+14)(s+23)}{s(s+27)(s+\alpha)(s+33)}$$

find the value of α to yield a $K_v = 25000$. [Section: 7.4]

12. For the unity feedback system of Figure P7.1, where

WileyPLUS

WPCS

Control Solutions

$$G(s) = \frac{K(s+2)(s+4)(s+6)}{s^2(s+5)(s+7)}$$

find the value of K to yield a static error constant of 10,000. [Section: 7.4]

13. For the system shown in Figure P7.4, [Section: 7.3]

a. Find K_p, K_v, and K_a.

b. Find the steady-state error for an input of $50u(t)$, $50tu(t)$, and $50t^2u(t)$.

c. State the system type.
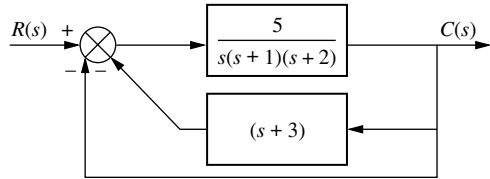
FIGURE P7.4

14. A Type 3 unity feedback system has $r(t) = 10t^3$ applied to its input. Find the steady-state position error for this input if the forward transfer function is [Section: 7.3]

$$G(s) = \frac{1030(s^2 + 8s + 23)(s^2 + 21s + 18)}{s^3(s+6)(s+13)}$$

15. Find the system type for the system of Figure P7.5. [Section: 7.3]

FIGURE P7.5

16. What are the restrictions on the feedforward transfer function $G_2(s)$ in the system of Figure P7.6 to obtain zero steady-state error for step inputs if: [Section: 7.3]

a. $G_1(s)$ is a Type 0 transfer function;

b. $G_1(s)$ is a Type 1 transfer function;

c. $G_1(s)$ is a Type 2 transfer function?

FIGURE P7.6

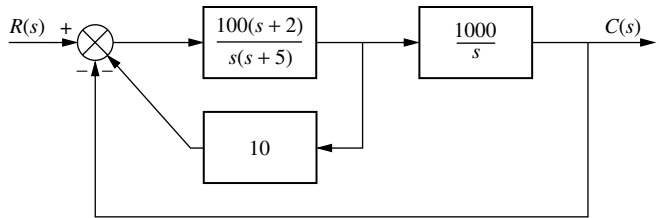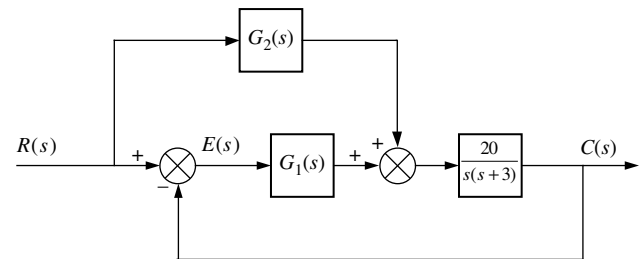**17.** The steady-state error is defined to be the difference in position between input and output as time approaches infinity. Let us define a steady-state velocity error, which is the difference in velocity between input and output. Derive an expression for the error in velocity, $\dot{e}(\infty) = \dot{r}(\infty) - \dot{c}(\infty)$, and complete Table P7.1 for the error in velocity. [Sections: 7.2, 7.3]

TABLE P7.1

		Type		
		0	1	2
Input	Step			
	Ramp			
	Parabola			

18. For the system shown in Figure P7.7, [Section: 7.4]

  a. What value of K will yield a steady-state error in position of 0.01 for an input of $(1/10)t$?

  b. What is the K_v for the value of K found in Part **a**?

  c. What is the minimum possible steady-state position error for the input given in Part **a**?

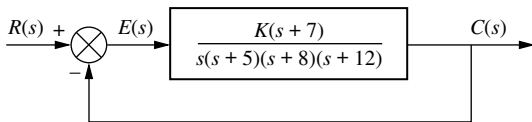$R(s) + \quad E(s) \quad \dfrac{K(s+7)}{s(s+5)(s+8)(s+12)} \quad C(s)$

FIGURE P7.7

19. Given the unity feedback system of Figure P7.1, where

$$G(s) = \frac{K(s+a)}{s(s+2)(s+13)}$$

find the value of Ka so that a ramp input of slope 40 will yield an error of 0.006 in the steady state when compared to the output. [Section: 7.4]

20. Given the system of Figure P7.8, design the value of K so that for an input of $100tu(t)$, there will be a 0.01 error in the steady state. [Section: 7.4]
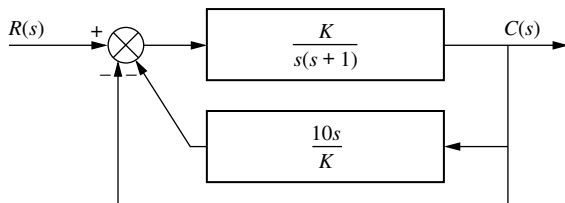

$R(s) + \quad \dfrac{K}{s(s+1)} \quad C(s)$

$\dfrac{10s}{K}$

FIGURE P7.8

21. Find the value of K for the unity feedback system shown in Figure P7.1, where

$$G(s) = \frac{K(s+3)}{s^2(s+7)}$$

if the input is $10t^2u(t)$, and the desired steady-state error is 0.061 for this input. [Section: 7.4]

22. The unity feedback system of Figure P7.1, where

$$G(s) = \frac{K(s^2 + 3s + 30)}{s^n(s+5)}$$

is to have $1/6000$ error between an input of $10tu(t)$ and the output in the steady state. [Section: 7.4]

  a. Find K and n to meet the specification.

  b. What are K_p, K_v, and K_a?

23. For the unity feedback system of Figure P7.1, where [Section: 7.3]

$$G(s) = \frac{K(s^2 + 6s + 6)}{(s+5)^2(s+3)}$$

  a. Find the system type.

  b. What error can be expected for an input of $12u(t)$?

  c. What error can be expected for an input of $12tu(t)$?

24. For the unity feedback system of Figure P7.1, where

$$G(s) = \frac{K(s+13)(s+19)}{s(s+6)(s+9)(s+22)}$$

find the value of K to yield a steady-state error of 0.4 for a ramp input of $27tu(t)$. [Section: 7.4]

25. Given the unity feedback system of Figure P7.1, where

$$G(s) = \frac{K(s+6)}{(s+2)(s^2 + 10s + 29)}$$

find the value of K to yield a steady-state error of 8%. [Section: 7.4]

26. For the unity feedback system of Figure P7.1, where

$$G(s) = \frac{K}{s(s+4)(s+8)(s+10)}$$

find the minimum possible steady-state position error if a unit ramp is applied. What places the constraint upon the error?

27. The unity feedback system of Figure P7.1, where

$$G(s) = \frac{K(s + \alpha)}{(s + \beta)^2}$$

is to be designed to meet the following specifications: steady-state error for a unit step input = 0.1; damping ratio = 0.5; natural frequency = $\sqrt{10}$. Find K, α, and β. [Section: 7.4]

28. A second-order, unity feedback system is to follow a ramp input with the following specifications: the steady-state output position shall differ from the input position by 0.01 of the input velocity; the natural frequency of the closed-loop system shall be 10 rad/s. Find the following:

  a. The system type

  b. The exact expression for the forward-path transfer function

  c. The closed-loop system's damping ratio

29. The unity feedback system of Figure P7.1, where

$$G(s) = \frac{K(s + \alpha)}{s(s + \beta)}$$

is to be designed to meet the following requirements: The steady-state position error for a unit ramp input equals 1/10; the closed-loop poles will be located at $-1 \pm j1$. Find K, α, and β in order to meet the specifications. [Section: 7.4]

30. Given the unity feedback control system of Figure P7.1, where

$$G(s) = \frac{K}{s^n(s + a)}$$

find the values of n, K, and a in order to meet specifications of 12% overshoot and $K_v = 110$. [Section: 7.4]

31. Given the unity feedback control system of Figure P7.1, where

$$G(s) = \frac{K}{s(s + a)}$$

find the following: [Section: 7.4]

  a. K and a to yield $K_v = 1000$ and a 20% overshoot

  b. K and a to yield a 1% error in the steady state and a 10% overshoot

32. Given the system in Figure P7.9, find the following: [Section: 7.3]

  a. The closed-loop transfer function

  b. The system type

  c. The steady-state error for an input of $5u(t)$

  d. The steady-state error for an input of $5tu(t)$

  e. Discuss the validity of your answers to Parts **c** and **d**.
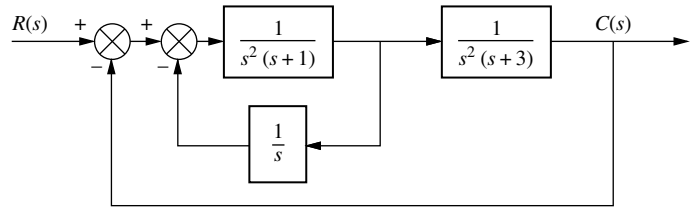
FIGURE P7.9

33. Repeat Problem 32 for the system shown in Figure P7.10. [Section: 7.3]
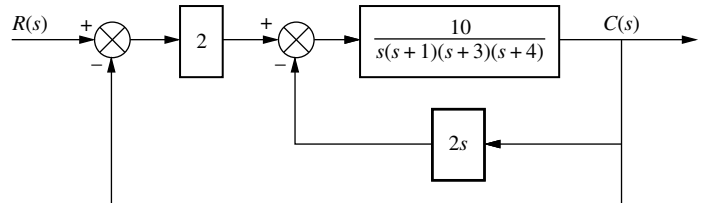
FIGURE P7.10

34. For the system shown in Figure P7.11, use MATLAB to find the following: [Section: 7.3]

  a. The system type

  b. K_p, K_v, and K_a

  c. The steady-state error for inputs of $100u(t)$, $100tu(t)$, and $100t^2u(t)$
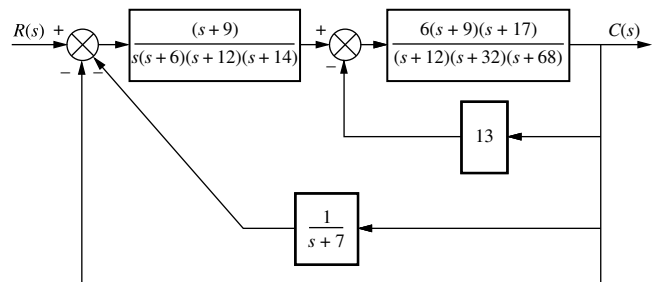
FIGURE P7.11

35. The system of Figure P7.12 is to have the following specifications: $K_v = 10$; $\zeta = 0.5$. Find the values of K_1 and K_f required for the specifications of the system to be met. [Section: 7.4]
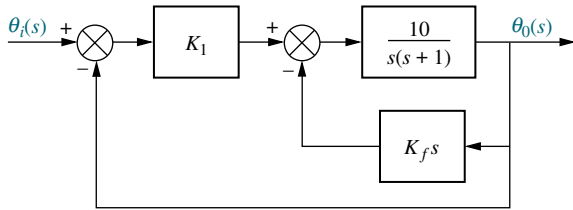
FIGURE P7.12

36. The transfer function from elevator deflection to altitude change in a Tower Trainer 60 Unmanned Aerial Vehicle is

$$P(s) = \frac{h(s)}{\delta(s)_e}$$

$$= \frac{-34.16s^3 - 144.4s^2 + 7047s + 557.2}{s^5 + 13.18s^4 + 95.93s^3 + 14.61s^2 + 31.94s}$$

An autopilot is built around the aircraft as shown in Figure P7.13, with $F(s) = H(s) = 1$ and

$$G(s) = \frac{0.00842(s + 7.895)(s^2 + 0.108s + 0.3393)}{(s + 0.07895)(s^2 + 4s + 8)}$$

(*Barkana*, *2005*). The steady-state error for a ramp input in this system is $e_{ss} = 25$. Find the slope of the ramp input.
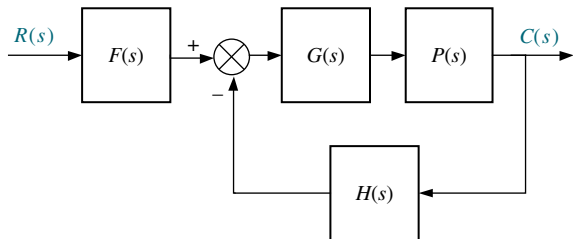
FIGURE P7.13

37. A block diagram representing the Ktesibios' water clock discussed in Section 1.2 is shown in Chapter 5, Problem 58, Figure P5.38(*b*) (*Lepschy*, *1992*).
  a. Find the system's type.
  b. For $h_r(t) = u(t)$, find the steady-state value of $e(t) = h_r(t) - h_f(t)$.

38. Find the total steady-state error due to a unit step input and a unit step disturbance in the system of Figure P7.14. [Section: 7.5]
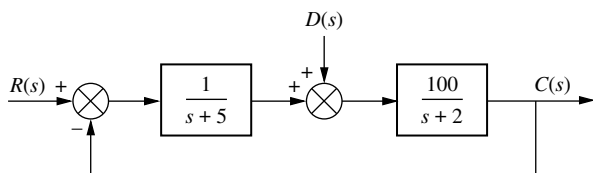
FIGURE P7.14

39. Design the values of K_1 and K_2 in the system of Figure P7.15 to meet the following specifications: Steady-state error component due to a unit step disturbance is -0.000012; steady-state error component due to a unit ramp input is 0.003. [Section: 7.5]
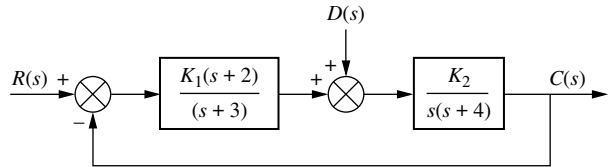
FIGURE P7.15

40. In Figure P7.16, let $G(s) = 5$ and $P(s) = \dfrac{7}{s + 2}$.
  a. Calculate the steady-state error due to a command input $R(s) = \dfrac{3}{s}$ with $D(s) = 0$.
  b. Verify the result of Part **a** using Simulink. Simulink **SL**
  c. Calculate the steady-state error due to a disturbance input $D(s) = -\dfrac{1}{s}$ with $R(s) = 0$.
  d. Verify the result of Part **c** using Simulink. Simulink **SL**
  e. Calculate the total steady-state error due to a command input $R(s) = \dfrac{3}{s}$ and a disturbance $D(s) = -\dfrac{1}{s}$ applied simultaneously.
  f. Verify the result of Part **e** using Simulink. Simulink **SL**
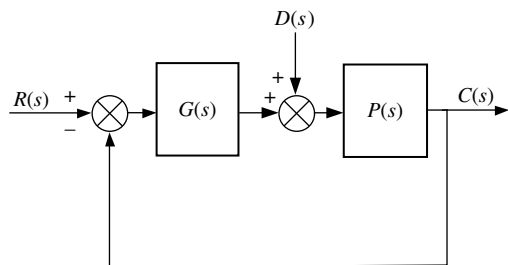
FIGURE P7.16

**41.** Derive Eq. (7.72) in the text, the final value of the actuating signal for nonunity feedback systems. [Section: 7.6]

42. For each of the systems shown in Figure P7.17, find the following: [Section: 7.6]
  a. The system type
  b. The appropriate static error constant
  c. The input waveform to yield a constant error

d. The steady-state error for a unit input of the waveform found in Part **c**

e. The steady-state value of the actuating signal
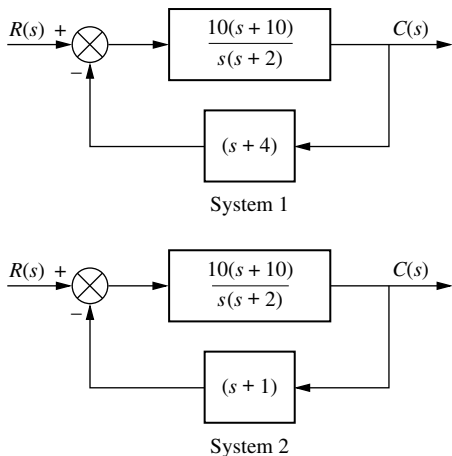
System 1

System 2

FIGURE P7.17 Closed-loop systems with nonunity feedback

43. For each of the systems shown in Figure P7.18, find the appropriate static error constant as well as the steady-state error, $r(\infty) - c(\infty)$, for unit step, ramp, and parabolic inputs. [Section: 7.6]
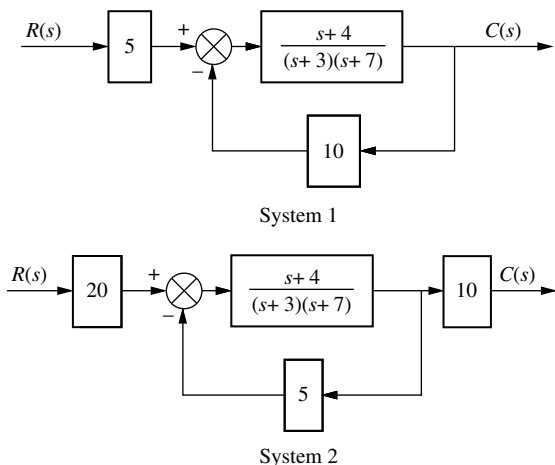
System 1

System 2

FIGURE P7.18

44. Given the system shown in Figure P7.19, find the following: [Section: 7.6]

WileyPLUS

WPCS

Control Solutions

a. The system type

b. The value of K to yield 0.1% error in the steady state
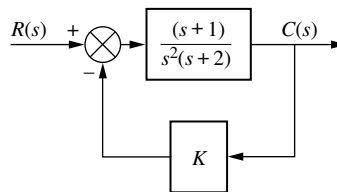
FIGURE P7.19

45. For the system shown in Figure P7.20, [Section: 7.6]

a. What is the system type?

b. What is the appropriate static error constant?

c. What is the value of the appropriate static error constant?

d. What is the steady-state error for a unit step input?
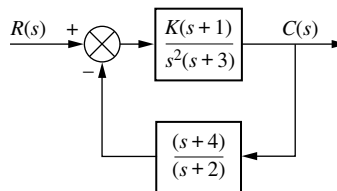
FIGURE P7.20

46. For the system shown in Figure P7.21, use MATLAB to find the following for $K = 10$, and $K = 10^6$: [Section: 7.6]

MATLAB

ML

a. The system type

b. K_p, K_v, and K_a

c. The steady-state error for inputs of $30u(t)$, $30tu(t)$, and $30t^2u(t)$
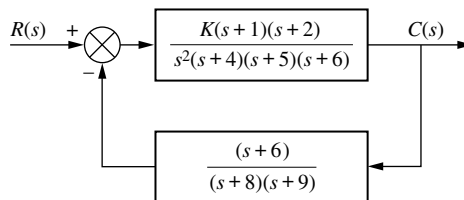
FIGURE P7.21

47. A dynamic voltage restorer (DVR) is a device that is connected in series to a power supply. It continuously monitors the voltage delivered to the load, and compensates voltage sags by applying the necessary extra voltage to maintain the load voltage constant.

In the model shown in Figure P7.22, u_r represents the desired reference voltage, u_o is the output

voltage, and Z_L is the load impedance. All other parameters are internal to the DVR (*Lam*, *2004*).

a. Assuming $Z_L = \dfrac{1}{sC_L}$, and $\beta \neq 1$, find the system's type.

b. Find the steady-state error to a unit step input as a function of β.
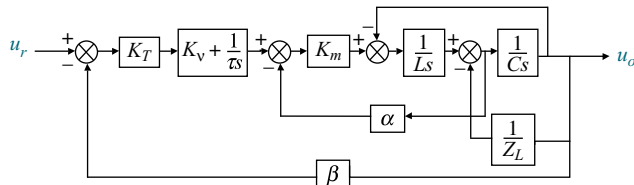
FIGURE P7.22 DVR Model

48. Derive Eq. (7.69) in the text. [Section: 7.6]

49. Given the system shown in Figure P7.23, do the following: [Section: 7.6]

a. Derive the expression for the error, $E(s) = R(s) - C(s)$, in terms of $R(s)$ and $D(s)$.

b. Derive the steady-state error, $e(\infty)$, if $R(s)$ and $D(s)$ are unit step functions.

c. Determine the attributes of $G_1(s)$, $G_2(s)$, and $H(s)$ necessary for the steady-state error to become zero.
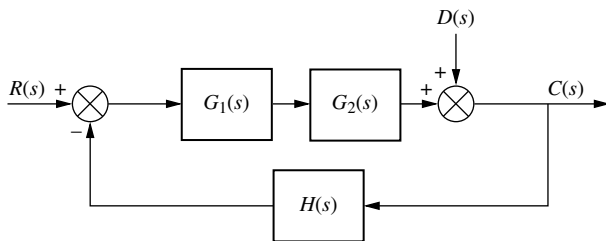
FIGURE P7.23 System with input and disturbance

50. Given the system shown in Figure P7.24, find the sensitivity of the steady-state error to parameter a. Assume a step input. Plot the sensitivity as a function of parameter a. [Section: 7.7]
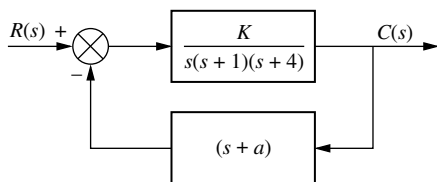
FIGURE P7.24

51. a. Show that the sensitivity to plant changes in the system of Figure P7.13 is

$$S_{T:P} = \frac{P}{T}\frac{\delta T}{\delta P} = \frac{1}{1 + L(s)}$$

where $L(s) = G(s)P(s)H(s)$ and

$$T(s) = \frac{C(s)}{R(s)} = \frac{F(s)L(s)}{1 + R(s)}.$$

b. Show that $S_{T:P}(s) + \dfrac{T(s)}{F(s)} = 1$ for all values of s.

**52.** In Figure P7.13, $P(s) = \dfrac{2}{s}$,

$$T(s) = \frac{C(s)}{R(s)} = \frac{14K}{(s + 1)(s + 2)(s^2 + 5s + 14)},$$

and

$$S_{T:P} = \frac{P}{T}\frac{\delta T}{\delta P} = \frac{s^2 + 5s}{s^2 + 5s + 14}.$$

a. Find $F(s)$ and $G(s)$.

b. Find the value of K that will result in zero steady-state error for a unit step input.

53. For the system shown in Figure P7.25, find the sensitivity of the steady-state error for changes in K_1 and in K_2, when $K_1 = 100$ and $K_2 = 0.1$. Assume step inputs for both the input and the disturbance. [Section: 7.7]
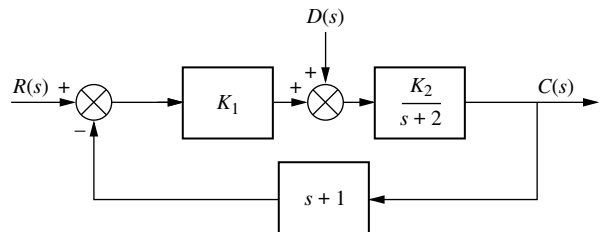
FIGURE P7.25 System with input and disturbance

54. Given the block diagram of the active suspension system shown in Figure P5.43 (*Lin*, *1997*):

a. Find the transfer function from a road disturbance r to the error signal e.

b. Use the transfer function in Part **a** to find the steady-state value of e for a unit step road disturbance.

c. Use the transfer function in Part **a** to find the steady-state value of e for a unit ramp road disturbance.

d. From your results in Parts **b** and **c**, what is the system's type for e?

55. For each of the following closed-loop systems, find the steady-state error for unit step and unit ramp

inputs. Use both the final value theorem and input substitution methods. [Section: 7.8]

a. $\dot{\mathbf{x}} = \begin{bmatrix} -5 & -4 & -2 \\ -3 & -10 & 0 \\ -1 & 1 & -5 \end{bmatrix}\mathbf{x} + \begin{bmatrix} 1 \\ 1 \\ 0 \end{bmatrix} r; \; y = \begin{bmatrix} -1 & 2 & 1 \end{bmatrix}\mathbf{x}$

b. $\dot{\mathbf{x}} = \begin{bmatrix} 0 & 1 & 0 \\ -5 & -9 & 7 \\ -1 & 0 & 0 \end{bmatrix}\mathbf{x} + \begin{bmatrix} 0 \\ 0 \\ 1 \end{bmatrix} r; \; y = \begin{bmatrix} 1 & 0 & 0 \end{bmatrix}\mathbf{x}$

c. $\dot{\mathbf{x}} = \begin{bmatrix} -9 & -5 & -1 \\ 1 & 0 & -2 \\ -3 & -2 & -5 \end{bmatrix}\mathbf{x} + \begin{bmatrix} 2 \\ 3 \\ 5 \end{bmatrix} r; \; y = \begin{bmatrix} 1 & -2 & 4 \end{bmatrix}\mathbf{x}$

56. An automobile guidance system yields an actual output distance, $X(s)$, for a desired input distance, $X_e(s)$, as shown in Figure P7.26(a). Any difference, $X_e(s)$, between the commanded distance and the actual distance is converted into a velocity command, $V_c(s)$, by the controller and applied to the vehicle accelerator. The vehicle responds to the velocity command with a velocity, $V(s)$, and a displacement, $X(s)$, is realized. The velocity control, $G_2(s)$, is itself a closed-loop system, as shown in Figure P7.26(b). Here the difference, $V_e(s)$, between the commanded velocity, $V_c(s)$, and the actual vehicle velocity, $V(s)$, drives a motor that displaces the automobile's accelerator by $Y_c(s)$ (*Stefani*, *1978*). Find the steady-state error for the velocity control loop if the motor and amplifier transfer function $G_3(s) = K/[s(s+1)]$. Assume $G_4(s)$ to be a first-order system, where a maximum possible 1-foot displacement of the accelerator linkage yields a steady-state velocity of 100 miles/hour, with the automobile reaching 60 miles/hour in 10 seconds.

(a)

(b)
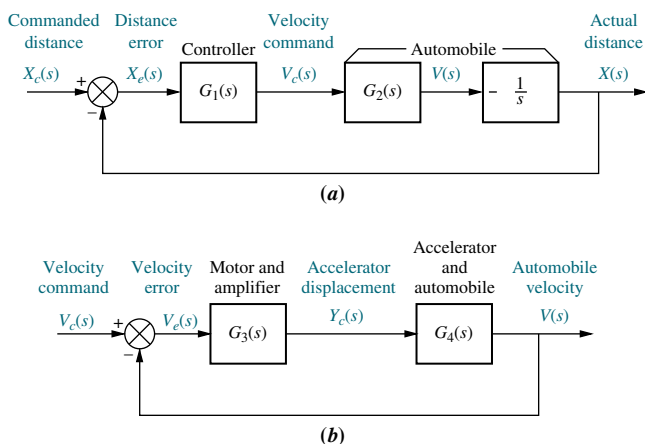
FIGURE P7.26   Automobile guidance system: **a.** displacement control system; **b.** velocity control loop

57. A simplified block diagram of a meter used to measure oxygen concentration is shown in Figure P7.27. The meter uses the paramagnetic properties of a stream of
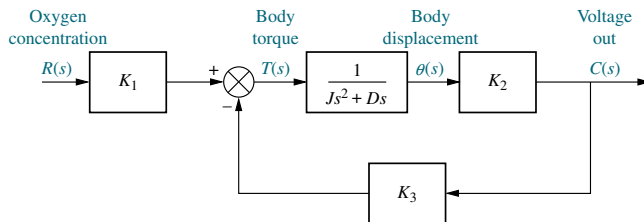
FIGURE P7.27   Block diagram of a paramagnetic oxygen analyzer

oxygen. A small body is placed in a stream of oxygen whose concentration is $R(s)$, and it is subjected to a magnetic field. The torque on the body, $K_1R(s)$, due to the magnetic field is a function of the concentration of the oxygen. The displacement of the body, $\theta(s)$, is detected, and a voltage, $C(s)$, is developed proportional to the displacement. This voltage is used to develop an electrostatic field that places a torque, $K_3C(s)$, on the body opposite to that developed by the magnetic field. When the body comes to rest, the output voltage represents the strength of the magnetic torque, which in turn is related to the concentration of the oxygen (*Chesmond*, *1982*). Find the steady-state error between the output voltage, representing oxygen concentration, and the input oxygen concentration. How would you reduce the error to zero?

58. A space station, shown in Figure P7.28(a), will keep its solar arrays facing the Sun. If we assume that the simplified block diagram of Figure P7.28(b) represents the solar tracking control system that will be used to rotate the array via rotary joints called *solar alpha rotary joints* (Figure P7.28(c)). Find (*Kumar*, *1992*)

a. The steady-state error for step commands

b. The steady-state error for ramp commands

c. The steady-state error for parabolic commands

d. The range of K_c/J to make the system stable

(a)
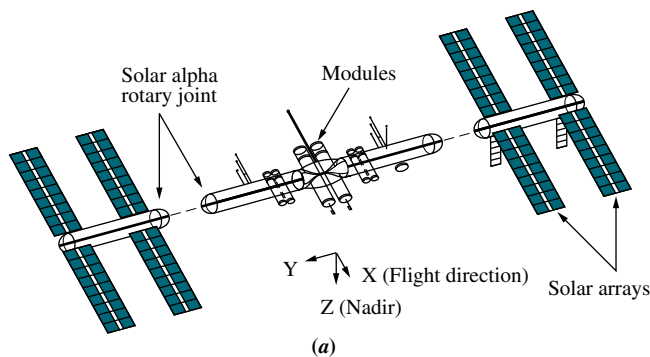
FIGURE P7.28   A space station: **a.** configuration (© 1992 AIAA); (*figure continues*)

(b)

(c)

FIGURE P7.28 *(Continued)* **b.** simplified block diagram; **c.** alpha joint drive train and control system (© 1992 AIAA)

59. A simplified model of the steering of a four-wheel drive vehicle is shown in Figure P7.29.

In this block diagram, the output r is the vehicle's yaw rate, while δ_f and δ_r are the steering angles of the front and rear tires respectively. In this model,

$$r^*(s) = \frac{\frac{s}{300} + 0.8}{\frac{s}{10} + 1}, \quad G_f(s) = \frac{h_1 s + h_2}{s^2 + a_1 s + a_2},$$

$$G_r(s) = \frac{h_3 s + b_1}{s^2 + a_1 s + a_2}$$

and $K(s)$ is a controller to be designed. (*Yin, 2007*).

FIGURE P7.29 Steering model for a four-wheel drive vehicle (© 2007 IEEE)

a. Assuming a step input for δ_f, find the minimum system type of the controller $K(s)$ necessary so that in steady-state the error as defined by the signal e in Figure P7.29 is zero if at all possible.

b. Assuming a step input for δ_f, find the system type of the controller $K(s)$ necessary so that in steady state the error as defined by $\delta_f(\infty) - r(\infty)$ is zero if at all possible.

DESIGN PROBLEMS

60. The following specification applies to a position control: $K_v = 10$. On hand is an amplifier with a variable gain, K_2, with which to drive a motor. Two one-turn pots to convert shaft position into voltage are also available, where $\pm 3\pi$ volts are placed across the pots. A motor is available whose transfer function is

$$\frac{\theta_m(s)}{E_a(s)} = \frac{K}{s(s + \alpha)}$$

where $\theta_m(s)$ is the motor armature position and $E_a(s)$ is the armature voltage. The components are interconnected as shown in Figure P7.30.
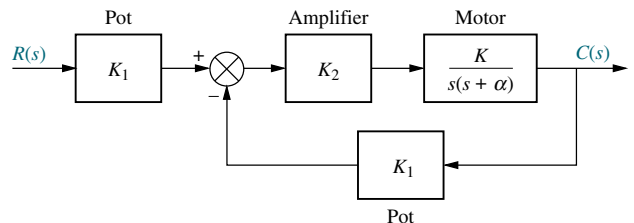
FIGURE P7.30 Position control system

The transfer function of the motor is found experimentally as follows. The motor and load are driven separately by applying a large, short square wave (a unit impulse) to the armature. An oscillograph of the response shows that the motor reached 63% of its final output value 0.5 second after application of the impulse. Furthermore, with 10 volts dc applied to the armature, the constant output speed was 100 rad/s. Draw the completed block diagram of the system, specifying the transfer function of each component of the block diagram.

61. A boat is circling a ship that is using a tracking radar. The speed of the boat is 20 knots, and it is circling

the ship at a distance of 1 nautical mile, as shown in Figure P7.31(a). A simplified model of the tracking system is shown in Figure P7.31(b). Find the value of K so that the boat is kept in the center of the radar beam with no more than 0.1 degree error.

(a)

(b)
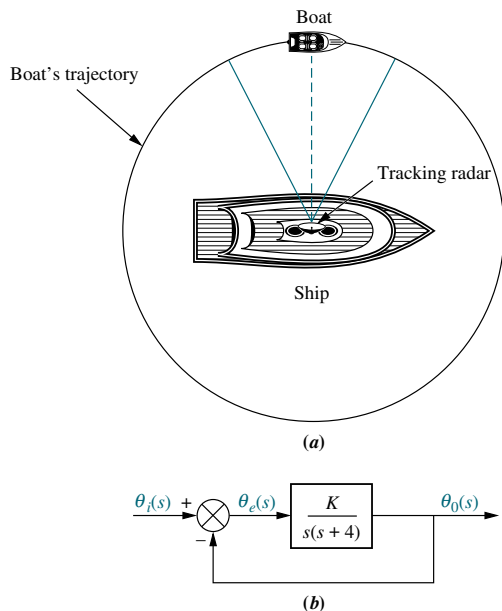
FIGURE P7.31   Boat tracked by ship's radar: **a.** physical arrangement; **b.** block diagram of tracking system

62. Figure P7.32 shows a simplified block diagram of a pilot in a loop to control the roll attitude of an Army UH-60A Black Hawk twin-engine helicopter with a single main rotor (*Hess*, *1993*).

   a. Find the system type.

   b. The pilot's response determines K_1. Find the value of K_1 if an appropriate static error constant value of 700 is required.

   c. Would a pilot whose K_1 is the value found in Part **b** be hired to fly the helicopter?

Note: In the block diagram $G_D(s)$ is a delay of about 0.154 second and can be represented by a Pade approximation of $G_D(s) = -(s - 13)/(s + 13)$.

63. Motion control, which includes position or force control, is used in robotics and machining. Force control requires the designer to consider two phases: contact and non-contact motions. Figure P7.33(a) is a diagram of a mechanical system for force control under contact motion. A force command, $F_{cmd}(s)$, is the input to the system, while the output, $F(s)$, is the controlled contact force.

   In the figure a motor is used as the force actuator. The force output from the actuator is applied to the

WileyPLUS

WPCS

Control Solutions

(a)

(b)
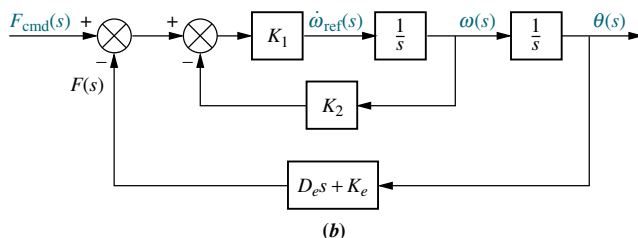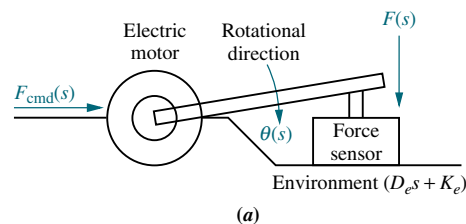
FIGURE P7.33   **a.** Force control mechanical loop under contact motion (© 1996 IEEE); **b.** block diagram (© 1996 IEEE)

FIGURE P7.32   Simplified block diagram of a pilot in a loop (© 1992 AIAA)

object through a force sensor. A block diagram representation of the system is shown in Figure P7.33(*b*). K_2 is velocity feedback used to improve the transient response. The loop is actually implemented by an electrical loop (not shown) that controls the armature current of the motor to yield the desired torque at the output. Recall that $T_m = K_t i_a$ (*Ohnishi*, *1996*). Find an expression for the range of K_2 to keep the steady-state force error below 10% for ramp inputs of commanded force.

64. Problem 50 in Chapter 4 describes an open-loop swivel controller and plant for an industrial robot. The transfer function for the controller and plant is

$$G_e(s) = \frac{\omega_o(s)}{V_i(s)} = \frac{K}{(s + 10)(s^2 + 4s + 10)}$$

where $\omega_o(s)$ is the Laplace transform of the robot's angular swivel velocity and $V_i(s)$ is the input voltage to the controller. Assume $G_e(s)$ is the forward transfer function of a velocity control loop with an input transducer and sensor, each represented by a constant gain of 3 (*Schneider*, *1992*).

   a. Find the value of gain, K, to minimize the steady-state error between the input commanded angular swivel velocity and the output actual angular swivel velocity.

   b. What is the steady-state error for the value of K found in Part **a**?

   c. For what kind of input does the design in Part **a** apply?

65. Packet information flow in a router working under TCP/IP can be modeled using the linearized transfer function

$$P(s) = \frac{Q(s)}{f(s)} = \frac{\dfrac{C^2}{2N} e^{-sR}}{\left(s + \dfrac{2N}{R^2 C}\right)\left(s + \dfrac{1}{R}\right)}$$

where

$C =$ link capacity (packets/second).

$N =$ load factor (number of TCP sessions)

$Q =$ expected queue length

$R =$ round trip time (second)

$p =$ probability of a packet drop

The objective of an active queue management (AQM) algorithm is to automatically choose a packet-drop probability, p, so that the queue length is maintained at a desired level. This system can be represented by the block diagram of Figure P7.13 with the plant model in the $P(s)$ block, the AQM algorithm in the $G(s)$ block, and $F(s) = H(s) = 1$.

Several AQM algorithms are available, but one that has received special attention in the literature is the random early detection (RED) algorithm. This algorithm can be approximated with $G(s) = \dfrac{LK}{s + K}$, where L and K are constants (*Hollot*, *2001*). Find the value of L required to obtain a 10% steady-state error for a unit step input when $C = 3750$ packets/s, $N = 50$ TCP sessions, $R = 0.1$ s, and $K = 0.005$.

66. In Figure P7.16, the plant, $P(s) = \dfrac{48,500}{s^2 + 2.89s}$, represents the dynamics of a robotic manipulator joint. The system's output, $C(s)$, is the joint's angular position (*Low*, *2005*). The system is controlled in a closed-loop configuration as shown with $G(s) = K_P + \dfrac{K_I}{s}$, a proportional-plus-integral (PI) controller to be discussed in Chapter 9. $R(s)$ is the joint's desired angular position. $D(s)$ is an external disturbance, possibly caused by improper dynamics modeling, Coulomb friction, or other external forces acting on the joint.

   a. Find the system's type.

   b. Show that for a step disturbance input, $e_{ss} = 0$ when $K_I \neq 0$.

   c. Find the value of K_I that will result in $e_{ss} = 5\%$ for a parabolic input.

   d. Using the value of K_I found in Part **c**, find the range of K_P for closed-loop stability.

PROGRESSIVE ANALYSIS AND DESIGN PROBLEMS

67. **High-speed rail pantograph.** Problem 21 in Chapter 1 discusses the active control of a pantograph mechanism for high-speed rail systems. In Problem 79(*a*), Chapter 5, you found the block diagram for the active pantograph control system. Use your solution for Problem 79(*a*) in Chapter 5 to perform steady-state error analysis and design as follows (*O'Connor*, *1997*):

   a. Find the system type.

   b. Find the value of controller gain, K, that minimizes the steady-state force error.

   c. What is the minimum steady-state force error?

68. **Control of HIV/AIDS.** Consider the HIV infection model of Problem 68 in Chapter 6 and its block diagram in Figure P6.20 (*Craig*, *2004*).

   a. Find the system's type if $G(s)$ is a constant.

   b. It was shown in Problem 68, Chapter 6, that when $G(s) = K$ the system will be stable when $K < 2.04 \times 10^{-4}$. What value of K will result in a unit step input steady-state error of 10%?

c. It is suggested that to reduce the steady-state error the system's type should be augmented by making $G(s) = \dfrac{K}{s}$. Is this a wise choice? What is the resulting stability range for K?

69. Hybrid vehicle. Figure P7.34 shows the block diagram of the speed control of an HEV taken from Figure P5.54, and rearranged as a unity feedback system (*Preitl, 2007*). Here the system output is, $C(s) = K_{SS} V(s)$, the output voltage of the speed sensor/transducer.
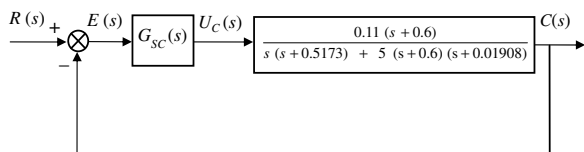
FIGURE P7.34

a. Assume the speed controller is given as $G_{SC}(s) = K_{P_{SC}}$. Find the gain, $K_{P_{SC}}$, that yields a steady-state error, $e_{step}(\infty) = 1\%$.

b. Now assume that in order to reduce the steady-state error for step inputs, integration is added to the controller yielding $G_{SC}(s) = K_{P_{SC}} + (K_{I_{SC}}/s) = 100 + (K_{I_{SC}}/s))$. Find the value of the integral gain, $K_{I_{SC}}$, that results in a steady-state error, $e_{ramp}(\infty) = 2.5\%$.

c. In Parts **a** and **b**, the HEV was assumed to be driven on level ground. Consider the case when, after reaching a steady-state speed with a controller given by $G_{SC}(s) = 100 + \dfrac{40}{s}$, the car starts climbing up a hill with a gradient angle, $\alpha = 5°$. For small angles $\sin\alpha = \alpha$ (in radians) and, hence, when reflected to the motor shaft the climbing torque is:

$$T_{st} = \frac{F_{st} r}{i_{tot}} = \frac{mgr}{i_{tot}}\sin\alpha = \frac{mgr\alpha}{i_{tot}} = \frac{1590 \times 9.8 \times 0.3 \times 5}{4.875 \times 57.3} = 83.7\,\text{Nm}.$$

The block diagram in Figure P7.35 represents the control system of the HEV rearranged for Part **c**.

$G_1(s)$ = Transfer function representation of torque & speed controllers
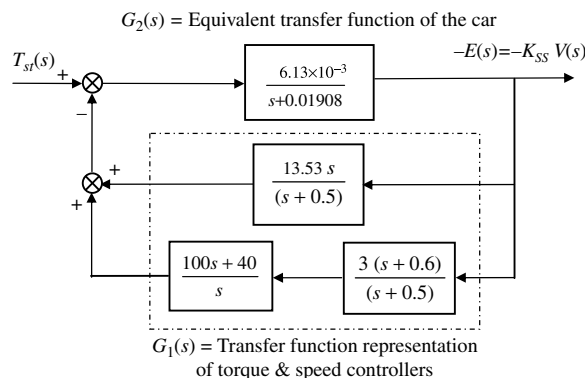
FIGURE P7.35

In this diagram, the input is $T_{st}(t) = 83.7\,u(t)$, corresponding to $\alpha = 5°$, and the output is the negative error, $-e(t) = -c(t) = -K_{SS}\,v(t)$, proportional to the change in car speed, $v(t)$. Find the steady-state error $e(\infty)$ due to a step change in the disturbance; e.g., the climbing torque, $T_{st}(t) = 83.7\,u(t)$.

Cyber Exploration Laboratory

Experiment 7.1

Objective To verify the effect of input waveform, loop gain, and system type upon steady-state errors.

Minimum Required Software Packages MATLAB, Simulink, and the Control System Toolbox

Prelab
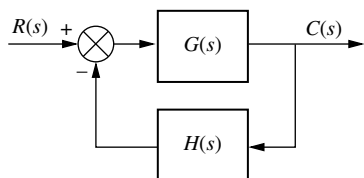
FIGURE P7.36

1. What system types will yield zero steady-state error for step inputs?

2. What system types will yield zero steady-state error for ramp inputs?

3. What system types will yield infinite steady-state error for ramp inputs?

4. What system types will yield zero steady-state error for parabolic inputs?

5. What system types will yield infinite steady-state error for parabolic inputs?

6. For the negative feedback system of Figure P7.36, where $G(s) = \dfrac{K(s + 6)}{(s + 4)(s + 7)(s + 9)(s + 12)}$ and $H(s) = 1$, calculate the steady-state error in terms of K for the following inputs: $5u(t)$, $5tu(t)$, and $5t^2 u(t)$.

7. Repeat Prelab 6 for $G(s) = \dfrac{K(s+6)(s+8)}{s(s+4)(s+7)(s+9)(s+12)}$ and $H(s) = 1$.

8. Repeat Prelab 6 for $G(s) = \dfrac{K(s+1)(s+6)(s+8)}{s^2(s+4)(s+7)(s+9)(s+12)}$ and $H(s) = 1$.

Lab

1. Using Simulink, set up the negative feedback system of Prelab 6. Plot on one graph the error signal of the system for an input of $5u(t)$ and $K = 50$, 500, 1000, and 5000. Repeat for inputs of $5tu(t)$ and $5t^2u(t)$.

2. Using Simulink, set up the negative feedback system of Prelab 7. Plot on one graph the error signal of the system for an input of $5u(t)$ and $K = 50$, 500, 1000, and 5000. Repeat for inputs of $5tu(t)$ and $5t^2u(t)$.

3. Using Simulink, set up the negative feedback system of Prelab 8. Plot on one graph the error signal of the system for an input of $5u(t)$ and $K = 200$, 400, 800, and 1000. Repeat for inputs of $5tu(t)$ and $5t^2u(t)$.

Postlab

1. Use your plots from Lab 1 and compare the expected steady-state errors to those calculated in the Prelab. Explain the reasons for any discrepancies.

2. Use your plots from Lab 2 and compare the expected steady-state errors to those calculated in the Prelab. Explain the reasons for any discrepancies.

3. Use your plots from Lab 3 and compare the expected steady-state errors to those calculated in the Prelab. Explain the reasons for any discrepancies.

Experiment 7.2

Objective To use the LabVIEW Control Design and Simulation Module for analysis of steady-state performance for step and ramp inputs.

Minimum Required Software Package Lab VIEW with the Control Design and Simulation Module

Prelab You are given the model of a single joint of a robotic manipulator shown in Figure P7.37 (*Spong, 2005*), where B is the coefficient of viscous friction, $\theta_d(s)$ is the desired angle, $\theta(s)$ is the output angle, and $D(s)$ is the disturbance. We want to track the joint angle using a PD controller, which we will study in Chapter 9.
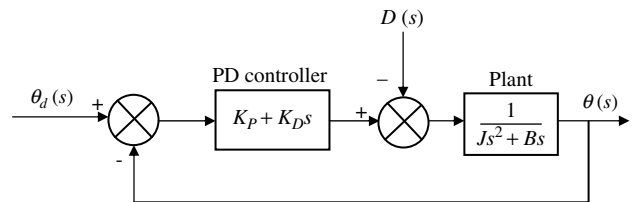
FIGURE P7.37

Assume $J = B = 1$. Find the step and ramp responses of this system for the following combinations of PD gains (K_P, K_D): (16, 7), (64, 15), and (144, 23).

Lab

1. Create a LabVIEW VI to simulate the response of this system to a step and a ramp inputs, under no-disturbance conditions. Use the functions available in the **Control Design and Simulation/Control Design** palette.

2. Create a LabVIEW VI using the functions available in the **Control Design and Simulation/Simulation** palette, to track an input set-point of 10 under a disturbance of $D = 40$.

Postlab Compare your results with those of the Prelab. What conclusions can you draw from the various responses of this system to different inputs and different PD parameters? What is the system type? Does the steady-state behavior corroborate the theory you learned regarding system type and the steady-state error for various inputs? Explain your answer.

Bibliography

Barkana, I. Classical and Simple Adaptive Control of Nonminimum Phase Autopilot Design. *Journal of Guidance, Control, and Dynamics*, vol. 28, 2005, pp. 631–638.

Chesmond, C. J., *Control System Technology*. E. Arnold, London, 1982.

Craig, I. K., Xia, X., and Venter, J. W., Introducing HIV/AIDS Education into the Electrical Engineering Curriculum at the University of Pretoria. *IEEE Transactions on Education*, vol. 47, no. 1, February 2004, pp. 65–73.

D'Azzo, J. J., and Houpis, C. H., *Feedback Control System Analysis and Design Conventional and Modern*, 3d ed. McGraw-Hill, New York, 1988.

Hess, R. A., Malsbury, T., and Atencio, A., Jr. Flight Simulator Fidelity Assessment in a Rotorcraft Lateral Translation Maneuver. *Journal of Guidance, Control, and Dynamics*, vol. 16, no. 1, January–February 1993, pp. 79–85.

Hollot, C. V., Misra, V., Towsley, D., and Gong, W., A Control Theoretic Analysis of RED. *Proceedings of IEEE INFOCOM*, 2001, pp. 1510–1519.

Hostetter, G. H., Savant, C. J., Jr., and Stefani, R. T. *Design of Feedback Control Systems*, 2d ed. Saunders College Publishing, New York, 1989.

Isailović, J. *Videodisc and Optical Memory Systems*. Prentice Hall, Upper Saddle River, NJ, 1985.

Kumar, R. R., Cooper, P. A., and Lim, T. W. Sensitivity of Space Station Alpha Joint Robust Controller to Structural Modal Parameter Variations. *Journal of Guidance, Control, and Dynamics*, vol. 15, no. 6, November–December 1992, pp. 1427–1433.

Lam, C. S., Wong, M. C., and Han, Y. D. Stability Study on Dynamic Voltage Restorer (DVR). *Power Electronics Systems and Applications, 2004; Proceedings First International Conference on Power Electronics*, 2004, pp. 66–71.

Lepschy, A. M., Mian, G. A., and Viaro, U. Feedback Control in Ancient Water and Mechanical Clocks. *IEEE Transactions on Education*, vol. 35, 1992, pp. 3–10.

Lin, J.-S., and Kanellakopoulos, I. Nonlinear Design of Active Suspensions. *IEEE Control Systems*, vol. 17, issue 3, June 1997, pp. 45–59.

Low, K. H., Wang, H., Liew, K. M., and Cai, Y. Modeling and Motion Control of Robotic Hand for Telemanipulation Application. *International Journal of Software Engineering and Knowledge Engineering*, vol. 15, 2005, pp. 147–152.

O'Connor, D. N., Eppinger, S. D., Seering, W. P., and Wormly, D. N. Active Control of a High-Speed Pantograph. *Journal of Dynamic Systems, Measurements, and Control*, vol. 119, March 1997, pp. 1–4.

Ohnishi, K., Shibata, M., and Murakami, T. Motion Control for Advanced Mechatronics. *IEEE/ASME Transactions on Mechatronics*, vol. 1, no. 1, March 1996, pp. 56–67.

Preitl, Z., Bauer, P., and Bokor, J. A Simple Control Solution for Traction Motor Used in Hybrid Vehicles. *Fourth International Symposium on Applied Computational Intelligence and Informatics*. IEEE, 2007.

Schneider, R. T. Pneumatic Robots Continue to Improve. *Hydraulics & Pneumatics*, October 1992, pp. 38–39.

Spong, M., Hutchinson, S., and Vidyasagar, M. *Robot Modeling and Control*. John Wiley & Sons. Hoboken, NJ, 2006.

Stefani, R. T. Design and Simulation of an Automobile Guidance and Control System. *Transactions, Computers in Education Division of ASEE*, January 1978, pp. 1–9.

Yin, G., Chen, N., and Li, P. Improving Handling Stability Performance of Four-Wheel Steering Vehicle via μ-Synthesis Robust Control. *Ieee Transactions on Vehicular Technology*, vol. 56, no. 5, 2007, pp. 2432–2439.

Root Locus Techniques

<div style="text-align:right">

8

</div>

(Chapter Learning Outcomes)

After completing this chapter the student will be able to:

- Define a root locus (Sections 8.1–8.2)
- State the properties of a root locus (Section 8.3)
- Sketch a root locus (Section 8.4)
- Find the coordinates of points on the root locus and their associated gains (Sections 8.5–8.6)
- Use the root locus to design a parameter value to meet a transient response specification for systems of order 2 and higher (Sections 8.7–8.8)
- Sketch the root locus for positive-feedback systems (Section 8.9)
- Find the root sensitivity for points along the root locus (Section 8.10)

(Case Study Learning Outcomes)

You will be able to demonstrate your knowledge of the chapter objectives with case studies as follows:

- Given the antenna azimuth position control system shown on the front endpapers, you will be able to find the preamplifier gain to meet a transient response specification.
- Given the pitch or heading control system for the Unmanned Free-Swimming Submersible vehicle shown on the back endpapers, you will be able to plot the root locus and design the gain to meet a transient response specification. You will then be able to evaluate other performance characteristics.

8.1 Introduction

Root locus, a graphical presentation of the closed-loop poles as a system parameter is varied, is a powerful method of analysis and design for stability and transient response (*Evans*, *1948*; *1950*). Feedback control systems are difficult to comprehend from a qualitative point of view, and hence they rely heavily upon mathematics. The root locus covered in this chapter is a graphical technique that gives us the qualitative description of a control system's performance that we are looking for and also serves as a powerful quantitative tool that yields more information than the methods already discussed.

Up to this point, gains and other system parameters were designed to yield a desired transient response for only first- and second-order systems. Even though the root locus can be used to solve the same kind of problem, its real power lies in its ability to provide solutions for systems of order higher than 2. For example, under the right conditions, a fourth-order system's parameters can be designed to yield a given percent overshoot and settling time using the concepts learned in Chapter 4.

The root locus can be used to describe qualitatively the performance of a system as various parameters are changed. For example, the effect of varying gain upon percent overshoot, settling time, and peak time can be vividly displayed. The qualitative description can then be verified with quantitative analysis.

Besides transient response, the root locus also gives a graphical representation of a system's stability. We can clearly see ranges of stability, ranges of instability, and the conditions that cause a system to break into oscillation.

Before presenting root locus, let us review two concepts that we need for the ensuing discussion: (1) the control system problem and (2) complex numbers and their representation as vectors.

The Control System Problem

We have previously encountered the control system problem in Chapter 6: Whereas the poles of the open-loop transfer function are easily found (typically, they are known by inspection and do not change with changes in system gain), the poles of the closed-loop transfer function are more difficult to find (typically, they cannot be found without factoring the closed-loop system's characteristic polynomial, the denominator of the closed-loop transfer function), and further, the closed-loop poles change with changes in system gain.

A typical closed-loop feedback control system is shown in Figure 8.1(*a*). The open-loop transfer function was defined in Chapter 5 as $KG(s)H(s)$. Ordinarily, we
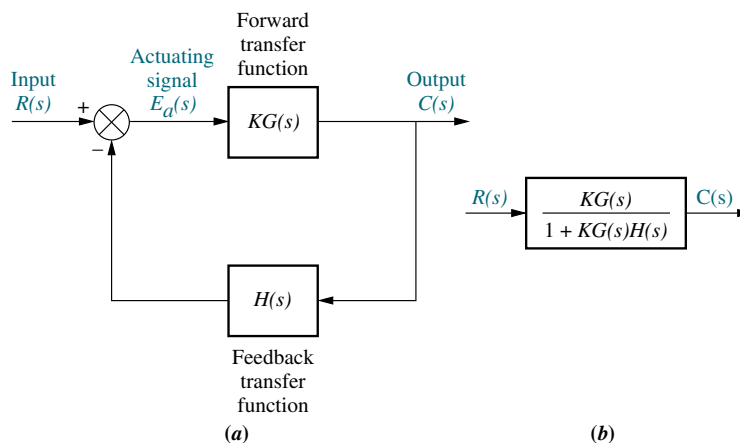

FIGURE 8.1   **a.** Closed-loop system; **b.** equivalent transfer function

can determine the poles of $KG(s)H(s)$, since these poles arise from simple cascaded first- or second-order subsystems. Further, variations in K do not affect the location of any pole of this function. On the other hand, we cannot determine the poles of $T(s) = KG(s)/[1 + KG(s)H(s)]$ unless we factor the denominator. Also, the poles of $T(s)$ change with K.

Let us demonstrate. Letting

$$G(s) = \frac{N_G(s)}{D_G(s)} \qquad (8.1)$$

and

$$H(s) = \frac{N_H(s)}{D_H(s)} \qquad (8.2)$$

then

$$T(s) = \frac{KN_G(s)D_H(s)}{D_G(s)D_H(s) + KN_G(s)N_H(s)} \qquad (8.3)$$

where N and D are factored polynomials and signify numerator and denominator terms, respectively. We observe the following: Typically, we know the factors of the numerators and denominators of $G(s)$ and $H(s)$. Also, the zeros of $T(s)$ consist of the zeros of $G(s)$ and the poles of $H(s)$. The poles of $T(s)$ are not immediately known and in fact can change with K. For example, if $G(s) = (s + 1)/[s(s + 2)]$ and $H(s) = (s + 3)/(s + 4)$, the poles of $KG(s)H(s)$ are $0, -2$, and -4. The zeros of $KG(s)H(s)$ are -1 and -3. Now, $T(s) = K(s + 1)(s + 4)/[s^3 + (6 + K)s^2 + (8 + 4K)s + 3K]$. Thus, the zeros of $T(s)$ consist of the zeros of $G(s)$ and the poles of $H(s)$. The poles of $T(s)$ are not immediately known without factoring the denominator, and they are a function of K. Since the system's transient response and stability are dependent upon the poles of $T(s)$, we have no knowledge of the system's performance unless we factor the denominator for specific values of K. The root locus will be used to give us a vivid picture of the poles of $T(s)$ as K varies.

Vector Representation of Complex Numbers

Any *complex number*, $\sigma + j\omega$, described in Cartesian coordinates can be graphically represented by a vector, as shown in Figure 8.2(a). The complex number also can be described in polar form with magnitude M and angle θ, as $M\angle\theta$. If the complex number is substituted into a complex function, $F(s)$, another complex number will result. For example, if $F(s) = (s + a)$, then substituting the complex number $s = \sigma + j\omega$ yields $F(s) = (\sigma + a) + j\omega$, another complex number. This number is shown in Figure 8.2(b). Notice that $F(s)$ has a zero at $-a$. If we translate the vector a units to the left, as in Figure 8.2(c), we have an alternate representation of the complex number that originates at the zero of $F(s)$ and terminates on the point $s = \sigma + j\omega$.

We conclude that $(s + a)$ *is a complex number and can be represented by a vector drawn from the zero of the function to the point s*. For example, $(s + 7)|_{s \rightarrow 5+j2}$ is a complex number drawn from the zero of the function, -7, to the point s, which is $5 + j2$, as shown in Figure 8.2(d).
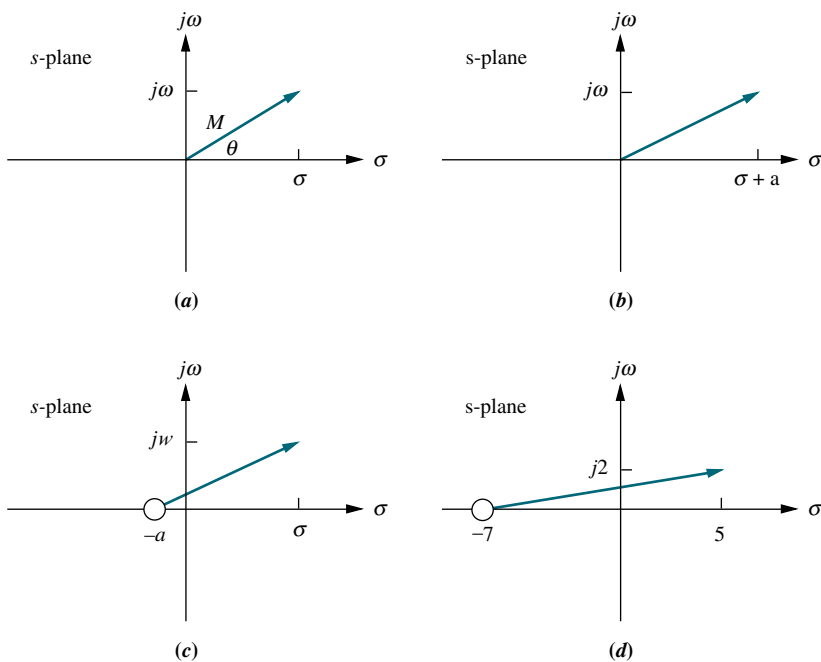
FIGURE 8.2 Vector representation of complex numbers: **a.** $s = \sigma + j\omega$; **b.** $(s + a)$; **c.** alternate representation of $(s + a)$; **d.** $(s + 7)|_{s \to 5 + j2}$

Now let us apply the concepts to a complicated function. Assume a function

$$F(s) = \frac{\prod\limits_{i=1}^{m}(s + z_i)}{\prod\limits_{j=1}^{n}(s + p_j)} = \frac{\prod \text{numerator's complex factors}}{\prod \text{denominator's complex factors}} \tag{8.4}$$

where the symbol $\prod$ means "product," $m =$ number of zeros, and $n =$ number of poles. Each factor in the numerator and each factor in the denominator is a complex number that can be represented as a vector. The function defines the complex arithmetic to be performed in order to evaluate $F(s)$ at any point, s. Since each complex factor can be thought of as a vector, the magnitude, M, of $F(s)$ at any point, s, is

$$M = \frac{\prod \text{zero lengths}}{\prod \text{pole lengths}} = \frac{\prod\limits_{i=1}^{m}|(s + z_i)|}{\prod\limits_{j=1}^{n}|(s + p_j)|} \tag{8.5}$$

where a zero length, $|(s + z_i)|$, is the magnitude of the vector drawn from the zero of $F(s)$ at $-z_i$ to the point s, and a pole length, $|(s + p_j)|$, is the magnitude of the vector drawn from the pole of $F(s)$ at $-p_j$ to the point s. The angle, θ, of $F(s)$ at any point, s, is

$$\theta = \sum \text{zero angles} - \sum \text{pole angles}$$
$$= \sum_{i=1}^{m} \angle(s + z_i) - \sum_{j=1}^{n} \angle(s + p_j) \tag{8.6}$$

where a zero angle is the angle, measured from the positive extension of the real axis, of a vector drawn from the zero of $F(s)$ at $-z_i$ to the point s, and a pole angle is the

angle, measured from the positive extension of the real axis, of the vector drawn from the pole of $F(s)$ at $-p_j$ to the point s.

As a demonstration of the above concept, consider the following example.

Example 8.1

Evaluation of a Complex Function via Vectors

PROBLEM: Given

$$F(s) = \frac{(s+1)}{s(s+2)} \qquad (8.7)$$

find $F(s)$ at the point $s = -3 + j4$.

SOLUTION: The problem is graphically depicted in Figure 8.3, where each vector, $(s+\alpha)$, of the function is shown terminating on the selected point $s = -3 + j4$. The vector originating at the zero at -1 is

$$\sqrt{20}\angle116.6° \qquad (8.8)$$

The vector originating at the pole at the origin is

$$5\angle126.9° \qquad (8.9)$$

The vector originating at the pole at -2 is

$$\sqrt{17}\angle104.0° \qquad (8.10)$$

Substituting Eqs. (8.8) through (8.10) into Eqs. (8.5) and (8.6) yields

$$M\angle\theta = \frac{\sqrt{20}}{5\sqrt{17}}\angle116.6° - 126.9° - 104.0° = 0.217\angle-114.3° \qquad (8.11)$$

as the result for evaluating $F(s)$ at the point $-3 + j4$.
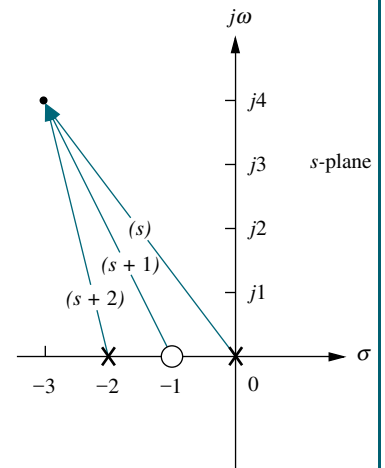
FIGURE 8.3   Vector representation of Eq. (8.7)

Skill-Assessment Exercise 8.1

PROBLEM: Given

$$F(s) = \frac{(s+2)(s+4)}{s(s+3)(s+6)}$$

find $F(s)$ at the point $s = -7 + j9$ the following ways:

   a. Directly substituting the point into $F(s)$

   b. Calculating the result using vectors

ANSWER:

$$-0.0339 - j0.0899 = 0.096\angle-110.7°$$

The complete solution is at www.wiley.com/college/nise.

TryIt 8.1

Use the following MATLAB statements to solve the problem given in Skill-Assessment Exercise 8.1.

```
s=-7+9j;
G=(s+2)*(s+4)/...
 (s*(s+3)*(s+6));
Theta=(180/pi)*...
 angle(G)
M=abs(G)
```

We are now ready to begin our discussion of the root locus.

8.2 Defining the Root Locus

A security camera system similar to that shown in Figure 8.4(*a*) can automatically follow a subject. The tracking system monitors pixel changes and positions the camera to center the changes.

The root locus technique can be used to analyze and design the effect of loop gain upon the system's transient response and stability. Assume the block diagram representation of a tracking system as shown in Figure 8.4(*b*), where the closed-loop poles of the system change location as the gain, K, is varied. Table 8.1, which was formed by applying the quadratic formula to the denominator of the transfer function in Figure 8.4(*c*), shows the variation of pole location for different values of gain, K. The data of Table 8.1 is graphically displayed in Figure 8.5(*a*), which shows each pole and its gain.

As the gain, K, increases in Table 8.1 and Figure 8.5(*a*), the closed-loop pole, which is at -10 for $K = 0$, moves toward the right, and the closed-loop pole, which is at 0 for $K = 0$, moves toward the left. They meet at -5, break away from the real axis, and move into the complex plane. One closed-loop pole moves upward while the other moves downward. We cannot tell which pole moves up or which moves down. In Figure 8.5(*b*), the individual closed-loop pole locations are removed and their paths are represented with solid lines. It is this *representation of the paths of the*
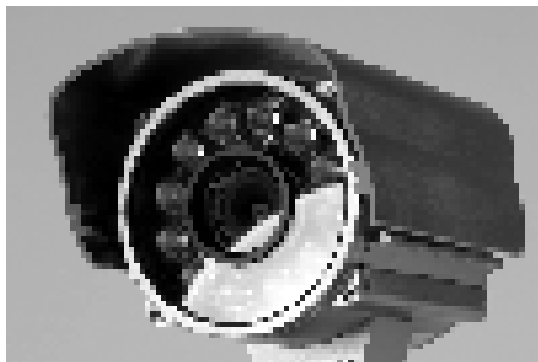
(*a*)
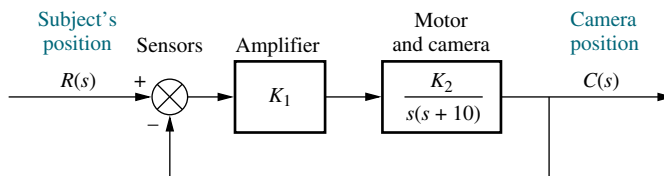
(*b*)
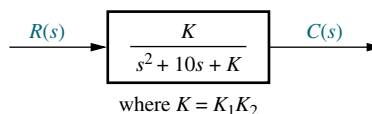
(*c*)

FIGURE 8.4 **a.** Security cameras with auto tracking can be used to follow moving objects automatically; **b.** block diagram; **c.** closed-loop transfer function

TABLE 8.1 Pole location as function of gain for the system of Figure 8.4

K	Pole 1	Pole 2
0	−10	0
5	−9.47	−0.53
10	−8.87	−1.13
15	−8.16	−1.84
20	−7.24	−2.76
25	−5	−5
30	−5 + j2.24	−5 − j2.24
35	−5 + j3.16	−5 − j3.16
40	−5 + j3.87	−5 − j3.87
45	−5 + j4.47	−5 − j4.47
50	−5 + j5	−5 − j5
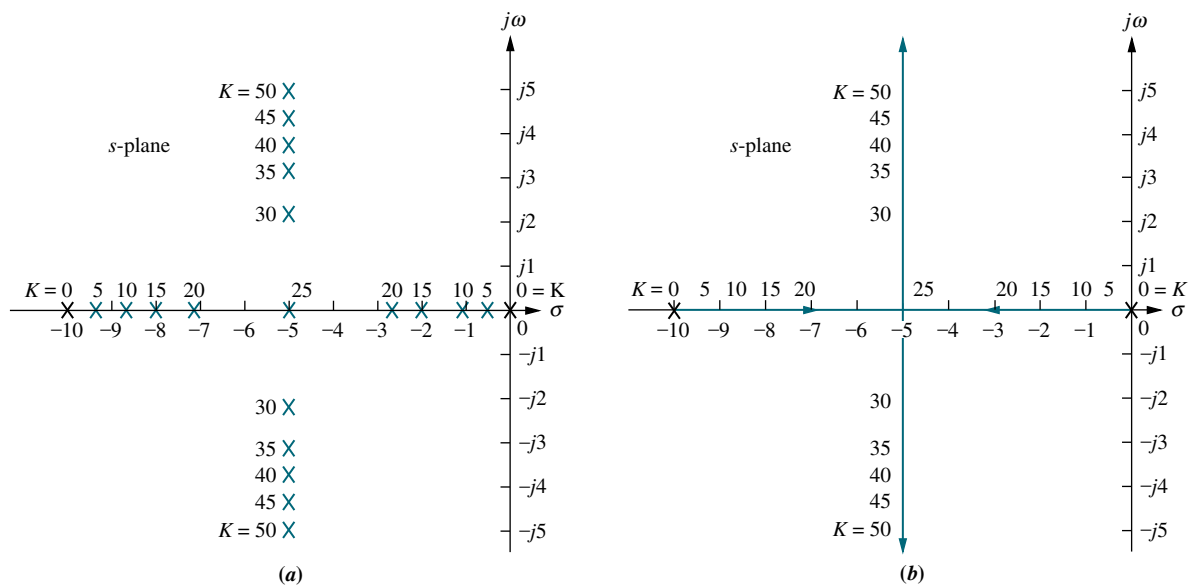
FIGURE 8.5 **a.** Pole plot from Table 8.1; **b.** root locus

closed-loop poles as the gain is varied that we call a *root locus*. For most of our work, the discussion will be limited to positive gain, or $K \geq 0$.

The root locus shows the changes in the transient response as the gain, K, varies. First of all, the poles are real for gains less than 25. Thus, the system is overdamped. At a gain of 25, the poles are real and multiple and hence critically damped. For gains above 25, the system is underdamped. Even though these preceding conclusions were available through the analytical techniques covered in Chapter 4, the following conclusions are graphically demonstrated by the root locus.

Directing our attention to the underdamped portion of the root locus, we see that regardless of the value of gain, the real parts of the complex poles are always the same.

Since the settling time is inversely proportional to the real part of the complex poles for this second-order system, the conclusion is that regardless of the value of gain, the settling time for the system remains the same under all conditions of underdamped responses.

Also, as we increase the gain, the damping ratio diminishes, and the percent overshoot increases. The damped frequency of oscillation, which is equal to the imaginary part of the pole, also increases with an increase in gain, resulting in a reduction of the peak time. Finally, since the root locus never crosses over into the right half-plane, the system is always stable, regardless of the value of gain, and can never break into a sinusoidal oscillation.

These conclusions for such a simple system may appear to be trivial. What we are about to see is that the analysis is applicable to systems of order higher than 2. For these systems, it is difficult to tie transient response characteristics to the pole location. The root locus will allow us to make that association and will become an important technique in the analysis and design of higher-order systems.

8.3   Properties of the Root Locus

In Section 8.2, we arrived at the root locus by factoring the second-order polynomial in the denominator of the transfer function. Consider what would happen if that polynomial were of fifth or tenth order. Without a computer, factoring the polynomial would be quite a problem for numerous values of gain.

We are about to examine the properties of the root locus. From these properties we will be able to make a rapid *sketch* of the root locus for higher-order systems without having to factor the denominator of the closed-loop transfer function.

The properties of the root locus can be derived from the general control system of Figure 8.1(a). The closed-loop transfer function for the system is

$$T(s) = \frac{KG(s)}{1 + KG(s)H(s)} \tag{8.12}$$

From Eq. (8.12), a pole, s, exists when the characteristic polynomial in the denominator becomes zero, or

$$KG(s)H(s) = -1 = 1\angle(2k+1)180° \quad k = 0, \pm1, \pm2, \pm3, \ldots \tag{8.13}$$

where -1 is represented in polar form as $1\angle(2k+1)180°$. Alternately, a value of s is a closed-loop pole if

$$|KG(s)H(s)| = 1 \tag{8.14}$$

and

$$\angle KG(s)H(s) = (2k+1)180° \tag{8.15}$$

Equation (8.13) implies that if a value of s is substituted into the function $KG(s)H(s)$, a complex number results. If the angle of the complex number is an odd multiple of $180°$, that value of s is a system pole for some particular value of K. What

value of K? Since the angle criterion of Eq. (8.15) is satisfied, all that remains is to satisfy the magnitude criterion, Eq. (8.14). Thus,

$$K = \frac{1}{|G(s)||H(s)|} \tag{8.16}$$

We have just found that a pole of the closed-loop system causes the angle of $KG(s)H(s)$, or simply $G(s)H(s)$ since K is a scalar, to be an odd multiple of $180°$. Furthermore, the magnitude of $KG(s)H(s)$ must be unity, implying that the value of K is the reciprocal of the magnitude of $G(s)H(s)$ when the pole value is substituted for s.

Let us demonstrate this relationship for the second-order system of Figure 8.4. The fact that closed-loop poles exist at -9.47 and -0.53 when the gain is 5 has already been established in Table 8.1. For this system,

$$KG(s)H(s) = \frac{K}{s(s+10)} \tag{8.17}$$

Substituting the pole at -9.47 for s and 5 for K yields $KG(s)H(s) = -1$. The student can repeat the exercise for other points in Table 8.1 and show that each case yields $KG(s)H(s) = -1$.

It is helpful to visualize graphically the meaning of Eq. (8.15). Let us apply the complex number concepts reviewed in Section 8.1 to the root locus of the system shown in Figure 8.6. For this system the open-loop transfer function is

$$KG(s)H(s) = \frac{K(s+3)(s+4)}{(s+1)(s+2)} \tag{8.18}$$

The closed-loop transfer function, $T(s)$, is

$$T(s) = \frac{K(s+3)(s+4)}{(1+K)s^2 + (3+7K)s + (2+12K)} \tag{8.19}$$

If point s is a closed-loop system pole for some value of gain, K, then s must satisfy Eqs. (8.14) and (8.15).
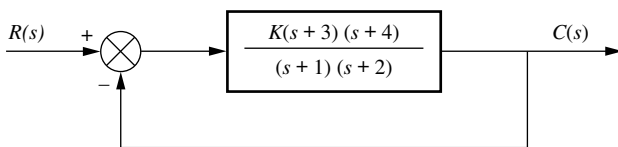
(a)
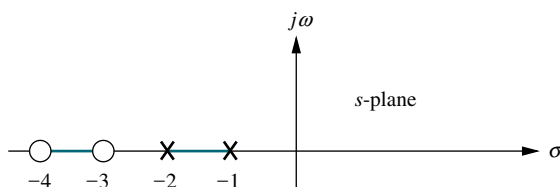
(b)

FIGURE 8.6   a. Example system; **b.** pole-zero plot of $G(s)$
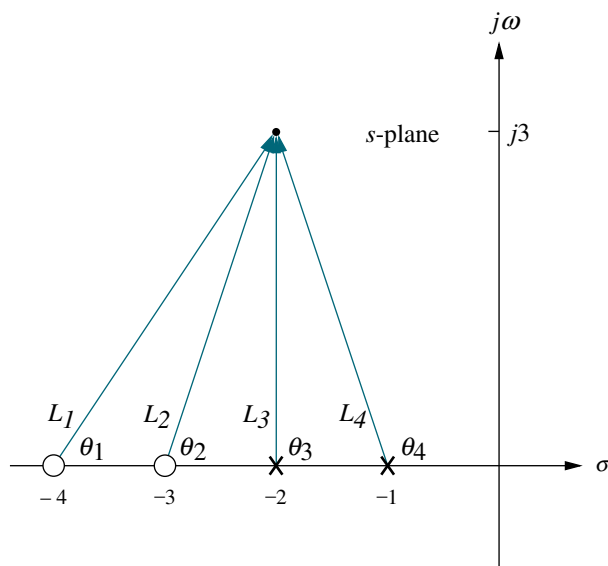
FIGURE 8.7   Vector representation of $G(s)$ from Figure 8.6(a) at $-2 + j3$

Consider the point $-2 + j3$. If this point is a closed-loop pole for some value of gain, then the angles of the zeros minus the angles of the poles must equal an odd multiple of $180°$. From Figure 8.7,

$$\theta_1 + \theta_2 - \theta_3 - \theta_4 = 56.31° + 71.57° - 90° - 108.43° = -70.55° \qquad (8.20)$$

Therefore, $-2 + j3$ is not a point on the root locus, or alternatively, $-2 + j3$ is not a closed-loop pole for any gain.

If these calculations are repeated for the point $-2 + j(\sqrt{2}/2)$, the angles do add up to $180°$. That is, $-2 + j(\sqrt{2}/2)$ is a point on the root locus for some value of gain. We now proceed to evaluate that value of gain.

From Eqs. (8.5) and (8.16),

$$K = \frac{1}{|G(s)H(s)|} = \frac{1}{M} = \frac{\prod \text{pole lengths}}{\prod \text{zero lengths}} \qquad (8.21)$$

Looking at Figure 8.7 with the point $-2 + j3$ replaced by $-2 + j(\sqrt{2}/2)$, the gain, K, is calculated as

$$K = \frac{L_3 L_4}{L_1 L_2} = \frac{\dfrac{\sqrt{2}}{2}(1.22)}{(2.12)(1.22)} = 0.33 \qquad (8.22)$$

Thus, the point $-2 + j(\sqrt{2}/2)$ is a point on the root locus for a gain of 0.33.

We summarize what we have found as follows: Given the poles and zeros of the open-loop transfer function, $KG(s)H(s)$, a point in the s-plane is on the root locus for a particular value of gain, K, if the angles of the zeros minus the angles of the poles, all drawn to the selected point on the s-plane, add up to $(2k + 1)180°$. Furthermore, gain K at that point for which the angles add up to $(2k + 1)180°$ is found by dividing the product of the pole lengths by the product of the zero lengths.

Skill-Assessment Exercise 8.2

PROBLEM: Given a unity feedback system that has the forward transfer function

$$G(s) = \frac{K(s+2)}{(s^2 + 4s + 13)}$$

do the following:

a. Calculate the angle of $G(s)$ at the point $(-3 + j0)$ by finding the algebraic sum of angles of the vectors drawn from the zeros and poles of $G(s)$ to the given point.

b. Determine if the point specified in **a** is on the root locus.

c. If the point specified in **a** is on the root locus, find the gain, K, using the lengths of the vectors.

ANSWERS:

a. Sum of angles $= 180°$

b. Point is on the root locus

c. $K = 10$

The complete solution is at www.wiley.com/college/nise.

TryIt 8.2

Use MATLAB and the following statements to solve Skill-Assessment Exercise 8.2.

```
s=-3+0j;
G=(s+2)/(s^2+4*s+13);
Theta=(180/pi)*...
 angle(G)
M=abs(G);
K=1/M
```

8.4   Sketching the Root Locus

It appears from our previous discussion that the root locus can be obtained by sweeping through every point in the *s*-plane to locate those points for which the angles, as previously described, add up to an odd multiple of $180°$. Although this task is tedious without the aid of a computer, the concept can be used to develop rules that can be used to *sketch* the root locus without the effort required to *plot* the locus. Once a sketch is obtained, it is possible to accurately plot just those points that are of interest to us for a particular problem.

The following five rules allow us to sketch the root locus using minimal calculations. The rules yield a sketch that gives intuitive insight into the behavior of a control system. In the next section, we refine the sketch by finding actual points or angles on the root locus. These refinements, however, require some calculations or the use of computer programs, such as MATLAB.

1. **Number of branches.** Each closed-loop pole moves as the gain is varied. If we define a *branch* as the path that one pole traverses, then there will be one branch for each closed-loop pole. Our first rule, then, defines the number of branches of the root locus:

   The number of branches of the root locus equals the number of closed-loop poles.

   As an example, look at Figure 8.5(*b*), where the two branches are shown. One originates at the origin, the other at -10.

2. **Symmetry.** If complex closed-loop poles do not exist in conjugate pairs, the resulting polynomial, formed by multiplying the factors containing the closed-loop poles,

would have complex coefficients. Physically realizable systems cannot have complex coefficients in their transfer functions. Thus, we conclude:

The root locus is symmetrical about the real axis.

An example of symmetry about the real axis is shown in Figure 8.5(*b*).

3. **Real-axis segments.** Let us make use of the angle property, Eq. (8.15), of the points on the root locus to determine where the real-axis segments of the root locus exist. Figure 8.8 shows the poles and zeros of a general open-loop system. If an attempt is made to calculate the angular contribution of the poles and zeros at each point, P_1, P_2, P_3, and P_4, along the real axis, we observe the following: (1) At each point the angular contribution of a pair of open-loop complex poles or zeros is zero, and (2) the contribution of the open-loop poles and open-loop zeros to the left of the respective point is zero. The conclusion is that the only contribution to the angle at any of the points comes from the open-loop, real-axis poles and zeros that exist to the right of the respective point. If we calculate the angle at each point using only the open-loop, real-axis poles and zeros to the right of each point, we note the following: (1) The angles on the real axis alternate between $0°$ and $180°$, and (2) the angle is $180°$ for regions of the real axis that exist to the left of an odd number of poles and/or zeros. The following rule summarizes the findings:

FIGURE 8.8 Poles and zeros of a general open-loop system with test points, P_i, on the real axis

On the real axis, for K > 0 the root locus exists to the left of an odd number of real-axis, finite open-loop poles and/or finite open-loop zeros.

Examine Figure 8.6(*b*). According to the rule just developed, the real-axis segments of the root locus are between -1 and -2 and between -3 and -4 as shown in Figure 8.9.

4. **Starting and ending points.** Where does the root locus begin (zero gain) and end (infinite gain)? The answer to this question will enable us to expand the sketch of the root locus beyond the real-axis segments. Consider the closed-loop transfer function, $T(s)$, described by Eq. (8.3). $T(s)$ can now be evaluated for both large and small gains, K. As K approaches zero (small gain),

$$T(s) \approx \frac{K N_G(s) D_H(s)}{D_G(s) D_H(s) + \epsilon} \tag{8.23}$$

From Eq. (8.23) we see that the closed-loop system poles at small gains approach the combined poles of $G(s)$ and $H(s)$. We conclude that the root locus begins at the poles of $G(s)H(s)$, the open-loop transfer function.
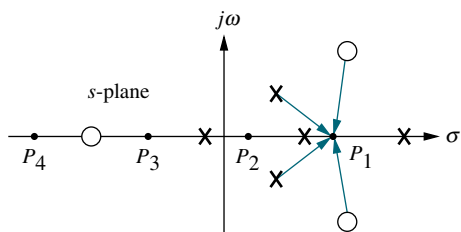

FIGURE 8.9 Real-axis segments of the root locus for the system of Figure 8.6

At high gains, where K is approaching infinity,

$$T(s) \approx \frac{KN_G(s)D_H(s)}{\epsilon + KN_G(s)N_H(s)} \tag{8.24}$$

From Eq. (8.24) we see that the closed-loop system poles at large gains approach the combined zeros of $G(s)$ and $H(s)$. Now we conclude that the root locus ends at the zeros of $G(s)H(s)$, the open-loop transfer function.

Summarizing what we have found:

The root locus begins at the finite and infinite poles of $G(s)H(s)$ and ends at the finite and infinite zeros of $G(s)H(s)$.

Remember that these poles and zeros are the open-loop poles and zeros.

In order to demonstrate this rule, look at the system in Figure 8.6(*a*), whose real-axis segments have been sketched in Figure 8.9. Using the rule just derived, we find that the root locus begins at the poles at -1 and -2 and ends at the zeros at -3 and -4 (see Figure 8.10). Thus, the poles start out at -1 and -2 and move through the real-axis space between the two poles. They meet somewhere between the two poles and break out into the complex plane, moving as complex conjugates. The poles return to the real axis somewhere between the zeros at -3 and -4, where their path is completed as they move away from each other, and end up, respectively, at the two zeros of the open-loop system at -3 and -4.

5. **Behavior at infinity.** Consider applying Rule 4 to the following open-loop transfer function:

$$KG(s)H(s) = \frac{K}{s(s+1)(s+2)} \tag{8.25}$$

There are three finite poles, at $s = 0, -1,$ and -2, and no finite zeros.

A function can also have *infinite* poles and zeros. If the function approaches infinity as s approaches infinity, then the function has a pole at infinity. If the function approaches zero as s approaches infinity, then the function has a zero at infinity. For example, the function $G(s) = s$ has a pole at infinity, since $G(s)$ approaches infinity as s approaches infinity. On the other hand, $G(s) = 1/s$ has a zero at infinity, since $G(s)$ approaches zero as s approaches infinity.

Every function of s has an equal number of poles and zeros if we include the infinite poles and zeros as well as the finite poles and zeros. In this example,
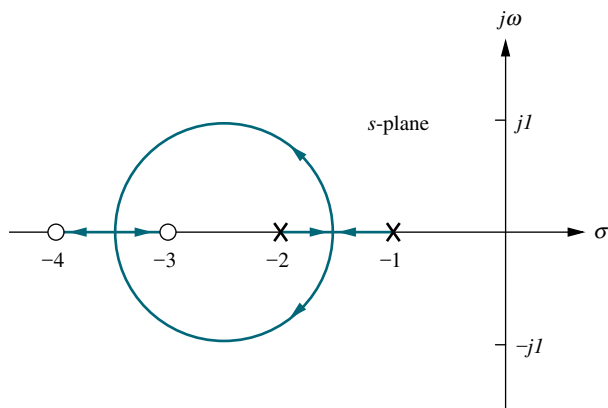
FIGURE 8.10   Complete root locus for the system of Figure 8.6

Eq. (8.25) contains three finite poles and three infinite zeros. To illustrate, let *s* approach infinity. The open-loop transfer function becomes

$$KG(s)H(s) \approx \frac{K}{s^3} = \frac{K}{s \cdot s \cdot s} \tag{8.26}$$

Each *s* in the denominator causes the open-loop function, $KG(s)H(s)$, to become zero as that *s* approaches infinity. Hence, Eq. (8.26) has three zeros at infinity.

   Thus, for Eq. (8.25), the root locus begins at the finite poles of $KG(s)H(s)$ and ends at the infinite zeros. The question remains: Where are the infinite zeros? We must know where these zeros are in order to show the locus moving from the three finite poles to the three infinite zeros. Rule 5 helps us locate these zeros at infinity. Rule 5 also helps us locate poles at infinity for functions containing more finite zeros than finite poles.[1]

   We now state Rule 5, which will tell us what the root locus looks like as it approaches the zeros at infinity or as it moves from the poles at infinity. The derivation can be found in Appendix M.1 at www.wiley.com/college/nise.

The root locus approaches straight lines as asymptotes as the locus approaches infinity. Further, the equation of the asymptotes is given by the real-axis intercept, σ_a and angle, θ_a as follows:

$$\sigma_a = \frac{\sum \text{finite poles} - \sum \text{finite zeros}}{\#\text{finite poles} - \#\text{finite zeros}} \tag{8.27}$$

$$\theta_a = \frac{(2k+1)\pi}{\#\text{finite poles} - \#\text{finite zeros}} \tag{8.28}$$

where $k = 0, \pm1, \pm2, \pm3$ and the angle is given in radians with respect to the positive extension of the real axis.

Notice that the running index, *k*, in Eq. (8.28) yields a multiplicity of lines that account for the many branches of a root locus that approach infinity. Let us demonstrate the concepts with an example.

Example 8.2

Sketching a Root Locus with Asymptotes

PROBLEM: Sketch the root locus for the system shown in Figure 8.11.
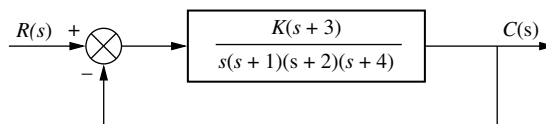
FIGURE 8.11   System for Example 8.2.

---

[1] Physical systems, however, have more finite poles than finite zeros, since the implied differentiation yields infinite output for discontinuous input functions, such as step inputs.

SOLUTION: Let us begin by calculating the asymptotes. Using Eq. (8.27), the real-axis intercept is evaluated as

$$\sigma_a = \frac{(-1 - 2 - 4) - (-3)}{4 - 1} = -\frac{4}{3} \tag{8.29}$$

The angles of the lines that intersect at $-4/3$, given by Eq. (8.28), are

$$\theta_a = \frac{(2k + 1)\pi}{\#\text{finite poles} - \#\text{finite zeros}} \tag{8.30a}$$

$$= \pi/3 \qquad \text{for } k = 0 \tag{8.30b}$$

$$= \pi \qquad \text{for } k = 1 \tag{8.30c}$$

$$= 5\pi/3 \qquad \text{for } k = 2 \tag{8.30d}$$

If the value for k continued to increase, the angles would begin to repeat. The number of lines obtained equals the difference between the number of finite poles and the number of finite zeros.

Rule 4 states that the locus begins at the open-loop poles and ends at the open-loop zeros. For the example there are more open-loop poles than open-loop zeros. Thus, there must be zeros at infinity. The asymptotes tell us how we get to these zeros at infinity.

Figure 8.12 shows the complete root locus as well as the asymptotes that were just calculated. Notice that we have made use of all the rules learned so far. The real-axis segments lie to the left of an odd number of poles and/or zeros. The locus starts at the open-loop poles and ends at the open-loop zeros. For the example there is only one open-loop finite zero and three infinite zeros. Rule 5, then, tells us that the three zeros at infinity are at the ends of the asymptotes.
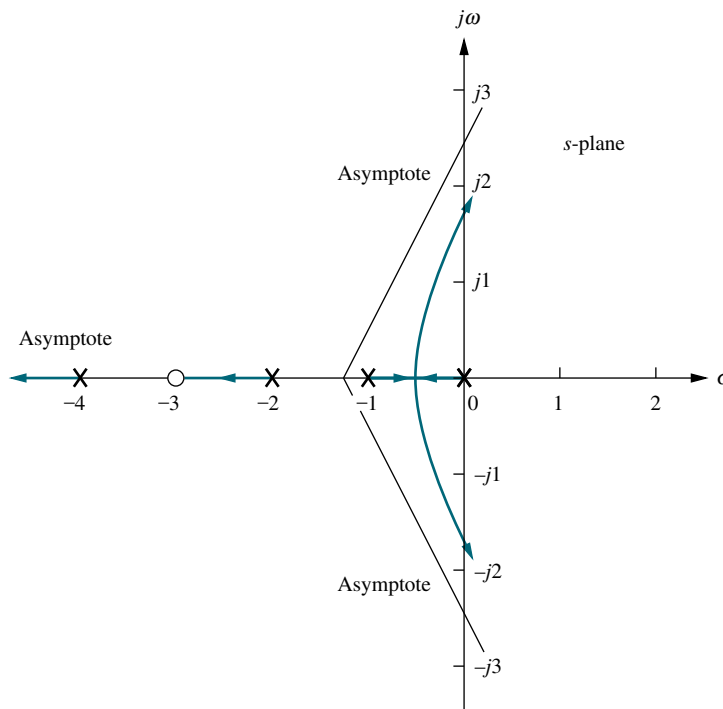
FIGURE 8.12 Root locus and asymptotes for the system of Figure 8.11

Skill-Assessment Exercise 8.3

PROBLEM: Sketch the root locus and its asymptotes for a unity feedback system that has the forward transfer function

$$G(s) = \frac{K}{(s+2)(s+4)(s+6)}$$

ANSWER: The complete solution is at www.wiley.com/college/nise.

8.5   Refining the Sketch

The rules covered in the previous section permit us to sketch a root locus rapidly. If we want more detail, we must be able to accurately find important points on the root locus along with their associated gain. Points on the real axis where the root locus enters or leaves the complex plane—real-axis breakaway and break-in points—and the $j\omega$-axis crossings are candidates. We can also derive a better picture of the root locus by finding the angles of departure and arrival from complex poles and zeros, respectively.

In this section, we discuss the calculations required to obtain specific points on the root locus. Some of these calculations can be made using the basic root locus relationship that the sum of the zero angles minus the sum of the pole angles equals an odd multiple of $180°$, and the gain at a point on the root locus is found as the ratio of (1) the product of pole lengths drawn to that point to (2) the product of zero lengths drawn to that point. We have yet to address how to implement this task. In the past, an inexpensive tool called a Spirule™ added the angles together rapidly and then quickly multiplied and divided the lengths to obtain the gain. Today we can rely on hand-held or programmable calculators as well as personal computers.

Students pursuing MATLAB will learn how to apply it to the root locus at the end of Section 8.6. Other alternatives are discussed in Appendix H.2 at www.wiley.com/college/nise. The discussion can be adapted to programmable hand-held calculators. All readers are encouraged to select a computational aid at this point. Root locus calculations can be labor intensive if hand calculations are used.

We now discuss how to refine our root locus sketch by calculating real-axis breakaway and break-in points, $j\omega$-axis crossings, angles of departure from complex poles, and angles of arrival to complex zeros. We conclude by showing how to find accurately any point on the root locus and calculate the gain.

Real-Axis Breakaway and Break-In Points

Numerous root loci appear to break away from the real axis as the system poles move from the real axis to the complex plane. At other times the loci appear to return to the real axis as a pair of complex poles becomes real. We illustrate this in Figure 8.13. This locus is sketched using the first four rules: (1) number of branches, (2) symmetry, (3) real-axis segments, and (4) starting and ending points. The figure shows a root locus leaving the real axis between -1 and -2 and returning to the real axis between $+3$ and $+5$. The point where the locus leaves the real axis, $-\sigma_1$, is called the *breakaway point*, and the point where the locus returns to the real axis, σ_2, is called the *break-in point*.
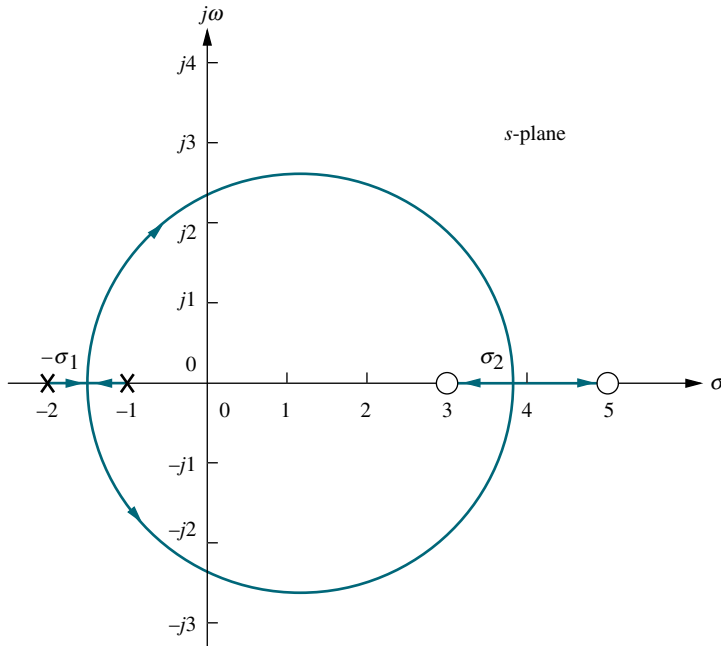
FIGURE 8.13   Root locus example showing real-axis breakaway ($-\sigma_1$) and break-in points (σ_2)

At the breakaway or break-in point, the branches of the root locus form an angle of $180°/n$ with the real axis, where n is the number of closed-loop poles arriving at or departing from the single breakaway or break-in point on the real axis (*Kuo, 1991*). Thus, for the two poles shown in Figure 8.13, the branches at the breakaway point form $90°$ angles with the real axis.

We now show how to find the breakaway and break-in points. As the two closed-loop poles, which are at -1 and -2 when $K = 0$, move toward each other, the gain increases from a value of zero. We conclude that the gain must be maximum along the real axis at the point where the breakaway occurs, somewhere between -1 and -2. Naturally, the gain increases above this value as the poles move into the complex plane. We conclude that the breakaway point occurs at a point of maximum gain on the real axis between the open-loop poles.

Now let us turn our attention to the break-in point somewhere between $+3$ and $+5$ on the real axis. When the closed-loop complex pair returns to the real axis, the gain will continue to increase to infinity as the closed-loop poles move toward the open-loop zeros. It must be true, then, that the gain at the break-in point is the minimum gain found along the real axis between the two zeros.

The sketch in Figure 8.14 shows the variation of real-axis gain. The breakaway point is found at the maximum gain between -1 and -2, and the break-in point is found at the minimum gain between $+3$ and $+5$.

There are three methods for finding the points at which the root locus breaks away from and breaks into the real axis. The first method is to maximize and minimize the gain, K, using differential calculus. For all points on the root locus, Eq. (8.13) yields

$$K = -\frac{1}{G(s)H(s)} \tag{8.31}$$
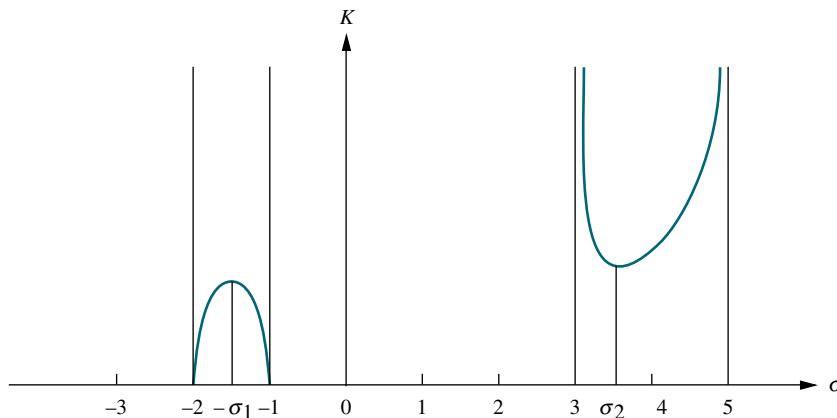
FIGURE 8.14 Variation of gain along the real axis for the root locus of Figure 8.13

For points along the real-axis segment of the root locus where breakaway and break-in points could exist, $s = \sigma$. Hence, along the real axis Eq. (8.31) becomes

$$K = -\frac{1}{G(\sigma)H(\sigma)} \tag{8.32}$$

This equation then represents a curve of K versus σ similar to that shown in Figure 8.14. Hence, if we differentiate Eq. (8.32) with respect to σ and set the derivative equal to zero, we can find the points of maximum and minimum gain and hence the breakaway and break-in points. Let us demonstrate.

Example 8.3

Breakaway and Break-in Points via Differentiation

PROBLEM: Find the breakaway and break-in points for the root locus of Figure 8.13, using differential calculus.

SOLUTION: Using the open-loop poles and zeros, we represent the open-loop system whose root locus is shown in Figure 8.13 as follows:

$$KG(s)H(s) = \frac{K(s-3)(s-5)}{(s+1)(s+2)} = \frac{K(s^2 - 8s + 15)}{(s^2 + 3s + 2)} \tag{8.33}$$

But for all points along the root locus, $KG(s)H(s) = -1$, and along the real axis, $s = \sigma$. Hence,

$$\frac{K(\sigma^2 - 8\sigma + 15)}{(\sigma^2 + 3\sigma + 2)} = -1 \tag{8.34}$$

Solving for K, we find

$$K = \frac{-(\sigma^2 + 3\sigma + 2)}{(\sigma^2 - 8\sigma + 15)} \tag{8.35}$$

Differentiating K with respect to σ and setting the derivative equal to zero yields

$$\frac{dK}{d\sigma} = \frac{(11\sigma^2 - 26\sigma - 61)}{(\sigma^2 - 8\sigma + 15)^2} = 0 \tag{8.36}$$

Solving for σ, we find $\sigma = -1.45$ and 3.82, which are the breakaway and break-in points.

The second method is a variation on the differential calculus method. Called the *transition method*, it eliminates the step of differentiation (*Franklin, 1991*). This method, derived in Appendix M.2 at www.wiley.com/college/nise, is now stated:

Breakaway and break-in points satisfy the relationship

$$\sum_{1}^{m} \frac{1}{\sigma + z_i} = \sum_{1}^{n} \frac{1}{\sigma + p_i} \qquad (8.37)$$

where z_i and p_i are the negative of the zero and pole values, respectively, of $G(s)H(s)$.

Solving Eq. (8.37) for σ, the real-axis values that minimize or maximize K, yields the breakaway and break-in points without differentiating. Let us look at an example.

Example 8.4

Breakaway and Break-in Points Without Differentiation

PROBLEM: Repeat Example 8.3 without differentiating.

SOLUTION: Using Eq. (8.37),

$$\frac{1}{\sigma - 3} + \frac{1}{\sigma - 5} = \frac{1}{\sigma + 1} + \frac{1}{\sigma + 2} \qquad (8.38)$$

Simplifying,

$$11\sigma^2 - 26\sigma - 61 = 0 \qquad (8.39)$$

Hence, $\sigma = -1.45$ and 3.82, which agrees with Example 8.3.

For the third method, the root locus program discussed in Appendix H.2 at www.wiley.com/college/nise can be used to find the breakaway and break-in points. Simply use the program to search for the point of maximum gain between -1 and -2 and to search for the point of minimum gain between $+3$ and $+5$. Table 8.2 shows the results of the search. The locus leaves the axis at -1.45, the point of maximum gain between -1 and -2, and reenters the real axis at $+3.8$, the point of minimum gain between $+3$ and $+5$. These results are the same as those obtained using the first two methods. MATLAB also has the capability of finding breakaway and break-in points.

The $j\omega$-Axis Crossings

We now further refine the root locus by finding the imaginary-axis crossings. The importance of the $j\omega$-axis crossings should be readily apparent. Looking at Figure 8.12, we see that the system's poles are in the left half-plane up to a particular value of gain. Above this value of gain, two of the closed-loop system's poles move into the right half-plane, signifying that the system is unstable. The $j\omega$-axis crossing is a point on the root locus that separates the stable operation of the system from the unstable operation. The value of ω at the axis crossing yields the frequency of oscillation, while the gain at the $j\omega$-axis crossing yields, for this example, the maximum positive gain for system stability. We should note here that other examples

TABLE 8.2   Data for breakaway and break-in points for the root locus of Figure 8.13

Real-axis value	Gain		Comment
−1.41	0.008557		
−1.42	0.008585		
−1.43	0.008605		
−1.44	0.008617		
−1.45	0.008623	←	Max. gain: breakaway
−1.46	0.008622		
3.3	44.686		
3.4	37.125		
3.5	33.000		
3.6	30.667		
3.7	29.440		
3.8	29.000	←	Min. gain: break-in
3.9	29.202		

illustrate instability at small values of gain and stability at large values of gain. These systems have a root locus starting in the right–half-plane (unstable at small values of gain) and ending in the left–half-plane (stable for high values of gain).

To find the $j\omega$-axis crossing, we can use the Routh-Hurwitz criterion, covered in Chapter 6, as follows: Forcing a row of zeros in the Routh table will yield the gain; going back one row to the even polynomial equation and solving for the roots yields the frequency at the imaginary-axis crossing.

Example 8.5

Frequency and Gain at Imaginary-Axis Crossing

PROBLEM: For the system of Figure 8.11, find the frequency and gain, K, for which the root locus crosses the imaginary axis. For what range of K is the system stable?

SOLUTION: The closed-loop transfer function for the system of Figure 8.11 is

$$T(s) = \frac{K(s+3)}{s^4 + 7s^3 + 14s^2 + (8+K)s + 3K} \tag{8.40}$$

Using the denominator and simplifying some of the entries by multiplying any row by a constant, we obtain the Routh array shown in Table 8.3.

A complete row of zeros yields the possibility for imaginary axis roots. For positive values of gain, those for which the root locus is plotted, only the s^1 row can yield a row of zeros. Thus,

$$-K^2 - 65K + 720 = 0 \tag{8.41}$$

From this equation K is evaluated as

$$K = 9.65 \tag{8.42}$$

TABLE 8.3   Routh table for Eq. (8.40)

s^4	1	14	$3K$
s^3	7	$8 + K$	
s^2	$90 - K$	$21K$	
s^1	$\dfrac{-K^2 - 65K + 720}{90 - K}$		
s^0	$21K$		

Forming the even polynomial by using the s^2 row with $K = 9.65$, we obtain

$$(90 - K)s^2 + 21K = 80.35s^2 + 202.7 = 0 \qquad (8.43)$$

and s is found to be equal to $\pm j1.59$. Thus the root locus crosses the $j\omega$-axis at $\pm j1.59$ at a gain of 9.65. We conclude that the system is stable for $0 \leq K < 9.65$.

Another method for finding the $j\omega$-axis crossing (or any point on the root locus, for that matter) uses the fact that at the $j\omega$-axis crossing, the sum of angles from the finite open-loop poles and zeros must add to $(2k + 1)180°$. Thus, we can search $j\omega$-axis until we find the point that meets this angle condition. A computer program, such as the root locus program discussed in Appendix H.2 at www.wiley.com/college/nise or MATLAB, can be used for this purpose. Subsequent examples in this chapter use this method to determine the $j\omega$-axis crossing.

Angles of Departure and Arrival

In this subsection, we further refine our sketch of the root locus by finding angles of departure and arrival from complex poles and zeros. Consider Figure 8.15, which shows the open-loop poles and zeros, some of which are complex. The root locus starts at the open-loop poles and ends at the open-loop zeros. In order to sketch the root locus more accurately, we want to calculate the root locus departure angle from the complex poles and the arrival angle to the complex zeros.

If we assume a point on the root locus ϵ close to a complex pole, the sum of angles drawn from all finite poles and zeros to this point is an odd multiple of 180°. Except for the pole that is ϵ close to the point, we assume all angles drawn from all other poles and zeros are drawn directly to the pole that is near the point. Thus, the only unknown angle in the sum is the angle drawn from the pole that is ϵ close. We can solve for this unknown angle, which is also the angle of departure from this complex pole. Hence, from Figure 8.15(a),

$$-\theta_1 + \theta_2 + \theta_3 - \theta_4 - \theta_5 + \theta_6 = (2k + 1)180° \qquad (8.44a)$$

or

$$\theta_1 = \theta_2 + \theta_3 - \theta_4 - \theta_5 + \theta_6 - (2k + 1)180° \qquad (8.44b)$$

If we assume a point on the root locus ϵ close to a complex zero, the sum of angles drawn from all finite poles and zeros to this point is an odd multiple of 180°. Except for the zero that is ϵ close to the point, we can assume all angles drawn from all other poles and zeros are drawn directly to the zero that is near the point. Thus,
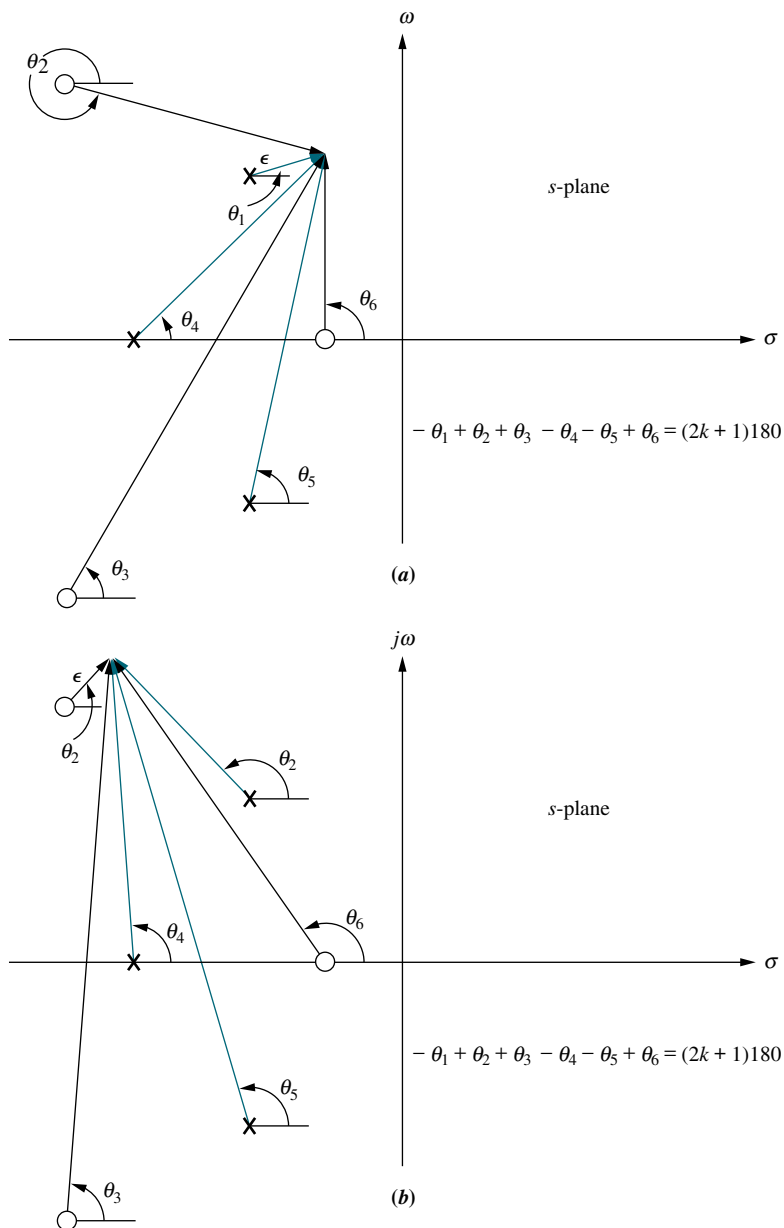
FIGURE 8.15   Open-loop poles and zeros and calculation of **a.** angle of departure; **b.** angle of arrival

the only unknown angle in the sum is the angle drawn from the zero that is ϵ close. We can solve for this unknown angle, which is also the angle of arrival to this complex zero. Hence, from Figure 8.15(*b*),

$$-\theta_1 + \theta_2 + \theta_3 - \theta_4 - \theta_5 + \theta_6 = (2k+1)180° \qquad (8.45a)$$

or

$$\theta_2 = \theta_1 - \theta_3 + \theta_4 + \theta_5 - \theta_6 + (2k+1)180° \qquad (8.45b)$$

Let us look at an example.

Example 8.6

Angle of Departure from a Complex Pole

PROBLEM: Given the unity feedback system of Figure 8.16, find the angle of departure from the complex poles and sketch the root locus.
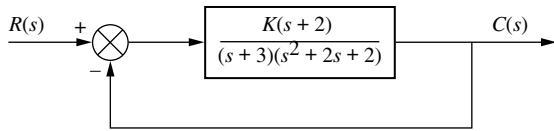
FIGURE 8.16   Unity feedback system with complex poles

SOLUTION: Using the poles and zeros of $G(s) = (s + 2)/[(s + 3)(s^2 + 2s + 2)]$ as plotted in Figure 8.17, we calculate the sum of angles drawn to a point ϵ close to the complex pole, $-1 + j1$, in the second quadrant. Thus,

$$-\theta_1 - \theta_2 + \theta_3 - \theta_4 = -\theta_1 - 90° + \tan^{-1}\left(\frac{1}{1}\right) - \tan^{-1}\left(\frac{1}{2}\right) = 180° \qquad (8.46)$$

from which $\theta = -251.6° = 108.4°$. A sketch of the root locus is shown in Figure 8.17. Notice how the departure angle from the complex poles helps us to refine the shape.
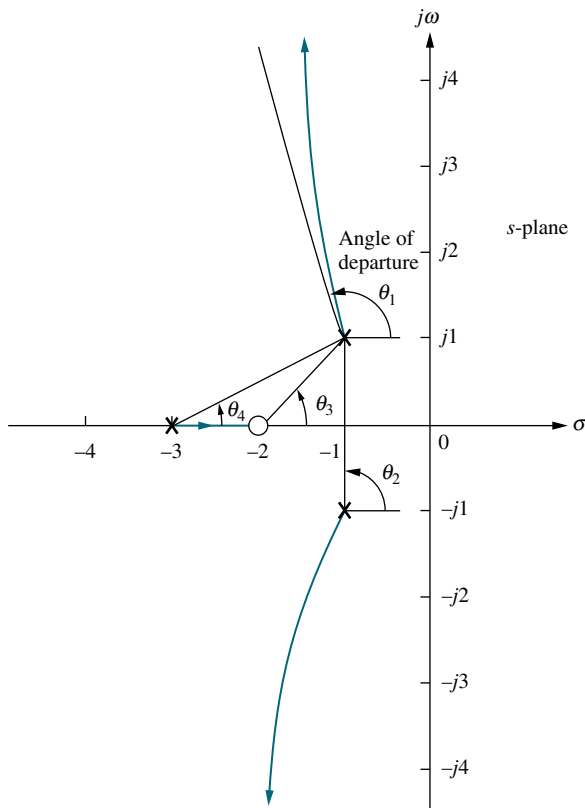
FIGURE 8.17   Root locus for system of Figure 8.16 showing angle of departure

Plotting and Calibrating the Root Locus

Once we sketch the root locus using the rules from Section 8.4, we may want to accurately locate points on the root locus as well as find their associated gain. For example, we might want to know the exact coordinates of the root locus as it crosses the radial line representing 20% overshoot. Further, we also may want the value of gain at that point.

Consider the root locus shown in Figure 8.12. Let us assume we want to find the exact point at which the locus crosses the 0.45 damping ratio line and the gain at that point. Figure 8.18 shows the system's open-loop poles and zeros along with the $\zeta = 0.45$ line. If a few test points along the $\zeta = 0.45$ line are selected, we can evaluate their angular sum and locate that point where the angles add up to an odd multiple of $180°$. It is at this point that the root locus exists. Equation (8.20) can then be used to evaluate the gain, K, at that point.

Selecting the point at radius 2 ($r = 2$) on the $\zeta = 0.45$ line, we add the angles of the zeros and subtract the angles of the poles, obtaining

$$\theta_2 - \theta_1 - \theta_3 - \theta_4 - \theta_5 = -251.5° \tag{8.47}$$

Since the sum is not equal to an odd multiple of $180°$, the point at radius $= 2$ is not on the root locus. Proceeding similarly for the points at radius $= 1.5$, 1, 0.747, and 0.5, we obtain the table shown in Figure 8.18. This table lists the points, giving their radius, r, and the sum of angles indicated by the symbol $\angle$. From the table we see that the point at radius 0.747 is on the root locus, since the angles add up to $-180°$. Using Eq. (8.21), the gain, K, at this point is

$$K = \frac{|A||C||D||E|}{|B|} = 1.71 \tag{8.48}$$

In summary, *we search a given line for the point yielding a summation of angles (zero angles–pole angles) equal to an odd multiple* of $180°$. We conclude that the point is on the root locus. The gain at that point is then found by *multiplying the pole lengths drawn to that point and dividing by the product of the zero lengths drawn to that point*. A computer program, such as that discussed in Appendix H.2 at www.wiley.com/college/nise or MATLAB, can be used.
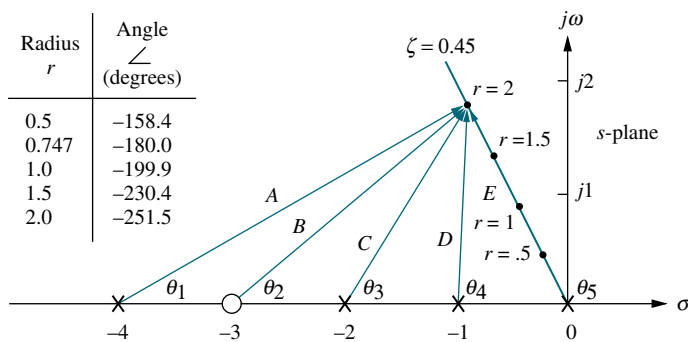

FIGURE 8.18   Finding and calibrating exact points on the root locus of Figure 8.12

Skill-Assessment Exercise 8.4

PROBLEM: Given a unity feedback system that has the forward transfer function

$$G(s) = \frac{K(s+2)}{(s^2 - 4s + 13)}$$

do the following:

   a. Sketch the root locus.
   b. Find the imaginary-axis crossing.
   c. Find the gain, K, at the $j\omega$-axis crossing.
   d. Find the break-in point.
   e. Find the angle of departure from the complex poles.

ANSWERS:

   a. See solution at www.wiley.com/college/nise.
   b. $s = \pm j\sqrt{21}$
   c. $K = 4$
   d. Break-in point $= -7$
   e. Angle of departure $= -233.1°$

The complete solution is at www.wiley.com/college/nise.

8.6   An Example

We now review the rules for sketching and finding points on the root locus, as well as present an example. The root locus is the path of the closed-loop poles of a system as a parameter of the system is varied. Each point on the root locus satisfies the angle condition, $\angle G(s)H(s) = (2k + 1)180°$. Using this relationship, rules for sketching and finding points on the root locus were developed and are now summarized:

Basic Rules for Sketching the Root Locus

Number of branches   The number of branches of the root locus equals the number of closed-loop poles.

Symmetry   The root locus is symmetrical about the real axis.

Real-axis segments   On the real axis, for $K > 0$ the root locus exists to the left of an odd number of real-axis, finite open-loop poles and/or finite open-loop zeros.

Starting and ending points   The root locus begins at the finite and infinite poles of $G(s)H(s)$ and ends at the finite and infinite zeros of $G(s)H(s)$.

Behavior at infinity   The root locus approaches straight lines as asymptotes as the locus approaches infinity. Further, the equations of the asymptotes are given by

the real-axis intercept and angle in radians as follows:

$$\sigma_a = \frac{\sum \text{finite poles} - \sum \text{finite zeros}}{\#\text{finite poles} - \#\text{finite zeros}} \tag{8.49}$$

$$\theta_a = \frac{(2k+1)\pi}{\#\text{finite poles} - \#\text{finite zeros}} \tag{8.50}$$

where $k = 0, \pm 1, \ \pm 2, \ \pm 3, \ldots$.

Additional Rules for Refining the Sketch

Real-axis breakaway and break-in points The root locus breaks away from the real axis at a point where the gain is maximum and breaks into the real axis at a point where the gain is minimum.

Calculation of $j\omega$-axis crossings The root locus crosses the $j\omega$-axis at the point where $\angle G(s)H(s) = (2k+1)180°$. Routh-Hurwitz or a search of the $j\omega$-axis for $(2k+1)180°$ can be used to find the $j\omega$-axis crossing.

Angles of departure and arrival The root locus departs from complex, open-loop poles and arrives at complex, open-loop zeros at angles that can be calculated as follows. Assume a point ϵ close to the complex pole or zero. Add all angles drawn from all open-loop poles and zeros to this point. The sum equals $(2k+1)180°$. The only unknown angle is that drawn from the ϵ close pole or zero, since the vectors drawn from all other poles and zeros can be considered drawn to the complex pole or zero that is ϵ close to the point. Solving for the unknown angle yields the angle of departure or arrival.

Plotting and calibrating the root locus All points on the root locus satisfy the relationship $\angle G(s)H(s) = (2k+1)180°$. The gain, K, at any point on the root locus is given by

$$K = \frac{1}{|G(s)H(s)|} = \frac{1}{M} - \frac{\prod \text{finite pole lengths}}{\prod \text{finite zero lengths}} \tag{8.51}$$

Let us now look at a summary example.

Example 8.7

Sketching a Root Locus and Finding Critical Points

PROBLEM: Sketch the root locus for the system shown in Figure 8.19(*a*) and find the following:

    a. The exact point and gain where the locus crosses the 0.45 damping ratio line

    b. The exact point and gain where the locus crosses the $j\omega$-axis

    c. The breakaway point on the real axis

    d. The range of K within which the system is stable

$$\frac{K(s^2 - 4s + 20)}{(s + 2)(s + 4)}$$

(*a*)

(*b*)
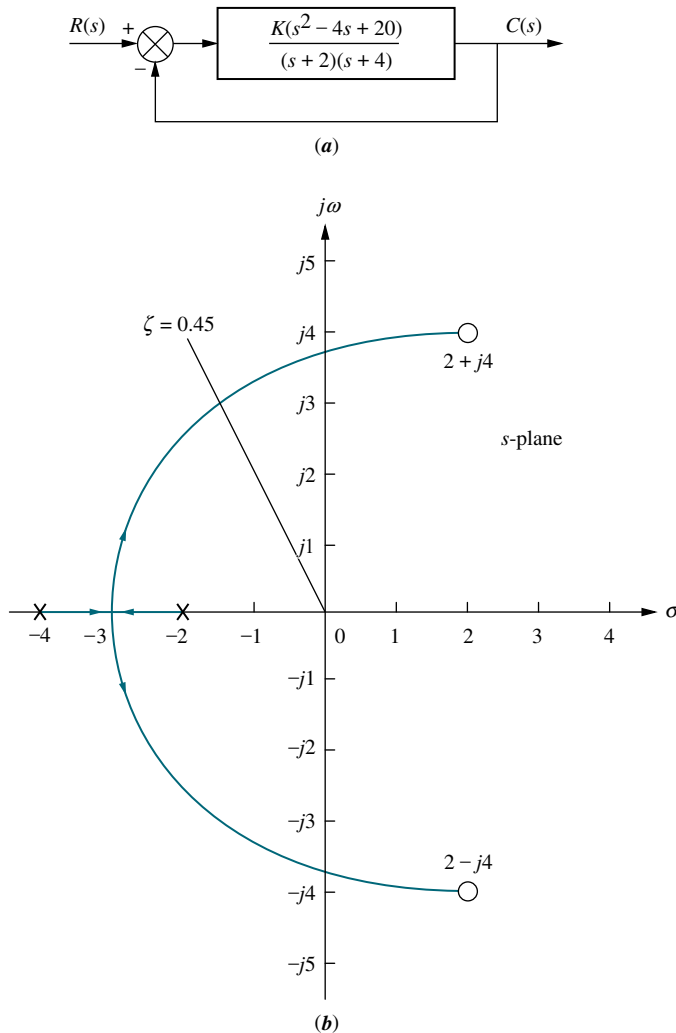
FIGURE 8.19   **a.** System for Example 8.7; **b.** root locus sketch.

SOLUTION: The problem solution is shown, in part, in Figure 8.19(*b*). First sketch the root locus. Using Rule 3, the real-axis segment is found to be between -2 and -4. Rule 4 tells us that the root locus starts at the open-loop poles and ends at the open-loop zeros. These two rules alone give us the general shape of the root locus.

a. To find the exact point where the locus crosses the $\zeta = 0.45$ line, we can use the root locus program discussed in Appendix H.2 at www.wiley.com/college/nise to search along the line

$$\theta = 180° - \cos^{-1} 0.45 = 116.7° \qquad (8.52)$$

for the point where the angles add up to an odd multiple of 180°. Searching in polar coordinates, we find that the root locus crosses the $\zeta = 0.45$ line at $3.4 \angle 116.7°$ with a gain, K, of 0.417.

b. To find the exact point where the locus crosses the $j\omega$-axis, use the root locus program to search along the line

$$\theta = 90° \qquad (8.53)$$

for the point where the angles add up to an odd multiple of 180°. Searching in polar coordinates, we find that the root locus crosses the $j\omega$-axis at $\pm j3.9$ with a gain of $K = 1.5$.

c. To find the breakaway point, use the root locus program to search the real axis between -2 and -4 for the point that yields maximum gain. Naturally, all points will have the sum of their angles equal to an odd multiple of 180°. A maximum gain of 0.0248 is found at the point -2.88. Therefore, the breakaway point is between the open-loop poles on the real axis at -2.88.

d. From the answer to **b**, the system is stable for K between 0 and 1.5.

Students who are using MATLAB should now run ch8p1 in Appendix B. You will learn how to use MATLAB to plot and title a root locus, overlay constant ζ and ω_n curves, zoom into and zoom out from a root locus, and interact with the root locus to find critical points as well as gains at those points. This exercise solves Example 8.7 using MATLAB.

Skill-Assessment Exercise 8.5

PROBLEM: Given a unity feedback system that has the forward transfer function

$$G(s) = \frac{K(s-2)(s-4)}{(s^2 + 6s + 25)}$$

TryIt 8.3

Use MATLAB, the Control System Toolbox, and the following statements to plot the root locus for Skill-Assessment Exercise 8.5. Solve the remaining parts of the problem by clicking on the appropriate points on the plotted root locus.

```
numg=poly([2 4]);
deng=[1 6 25];
G=tf(numg,deng)
rlocus(G)
z=0.5
sgrid(z,0)
```

do the following:

a. Sketch the root locus.

b. Find the imaginary-axis crossing.

c. Find the gain, K, at the $j\omega$-axis crossing.

d. Find the break-in point.

e. Find the point where the locus crosses the 0.5 damping ratio line.

f. Find the gain at the point where the locus crosses the 0.5 damping ratio line.

g. Find the range of gain, K, for which the system is stable.

ANSWERS:

a. See solution at www.wiley.com/college/nise.

b. $s = \pm j4.06$

c. $K = 1$

d. Break-in point $= +2.89$

e. $s = -2.42 + j4.18$

f. $K = 0.108$

g. $K < 1$

The complete solution is at www.wiley.com/college/nise.

8.7 Transient Response Design via Gain Adjustment

Now that we know how to sketch a root locus, we show how to use it for the design of transient response. In the last section we found that the root locus crossed the 0.45 damping ratio line with a gain of 0.417. Does this mean that the system will respond with 20.5% overshoot, the equivalent to a damping ratio of 0.45? It must be emphasized that the formulas describing percent overshoot, settling time, and peak time were derived only for a system with two closed-loop complex poles and no closed-loop zeros. The effect of additional poles and zeros and the conditions for justifying an approximation of a two-pole system were discussed in Sections 4.7 and 4.8 and apply here to closed-loop systems and their root loci. The conditions justifying a second-order approximation are restated here:

1. Higher-order poles are much farther into the left half of the *s*-plane than the dominant second-order pair of poles. The response that results from a higher-order pole does not appreciably change the transient response expected from the dominant second-order poles.

2. Closed-loop zeros near the closed-loop second-order pole pair are nearly canceled by the close proximity of higher-order closed-loop poles.

3. Closed-loop zeros not canceled by the close proximity of higher-order closed-loop poles are far removed from the closed-loop second-order pole pair.

The first condition as it applies to the root locus is shown graphically in Figure 8.20(*a*) and (*b*). Figure 8.20(*b*) would yield a much better second-order approximation than Figure 8.20(*a*), since closed-loop pole p_3 is farther from the dominant, closed-loop second-order pair, p_1 and p_2.

The second condition is shown graphically in Figure 8.20(*c*) and (*d*). Figure 8.20(*d*) would yield a much better second-order approximation than Figure 8.20(*c*), since closed-loop pole p_3 is closer to canceling the closed-loop zero.
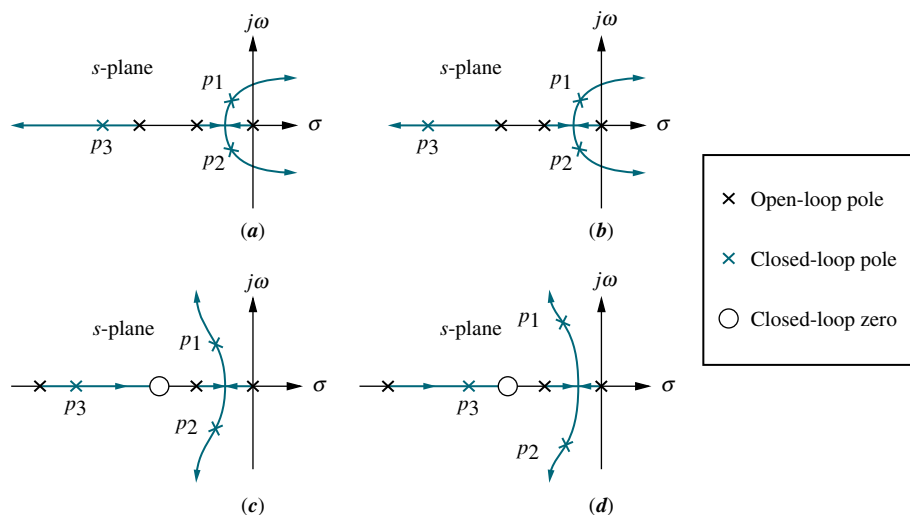

FIGURE 8.20 Making second-order approximations

Summarizing the design procedure for higher-order systems, we arrive at the following:

1. Sketch the root locus for the given system.

2. Assume the system is a second-order system without any zeros and then find the gain to meet the transient response specification.

3. Justify your second-order assumption by finding the location of all higher-order poles and evaluating the fact that they are much farther from the $j\omega$-axis than the dominant second-order pair. As a rule of thumb, this textbook assumes a factor of five times farther. Also, verify that closed-loop zeros are approximately canceled by higher-order poles. If closed-loop zeros are not canceled by higher-order closed-loop poles, be sure that the zero is far removed from the dominant second-order pole pair to yield approximately the same response obtained without the finite zero.

4. If the assumptions cannot be justified, your solution will have to be simulated in order to be sure it meets the transient response specification. It is a good idea to simulate all solutions, anyway.

We now look at a design example to show how to make a second-order approximation and then verify whether or not the approximation is valid.

Example 8.8

Third-Order System Gain Design

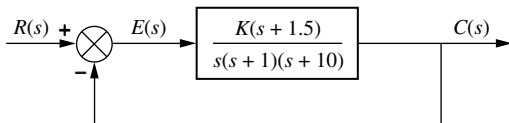**FIGURE 8.21**   System for Example 8.8

PROBLEM: Consider the system shown in Figure 8.21. Design the value of gain, K, to yield 1.52% overshoot. Also estimate the settling time, peak time, and steady-state error.

SOLUTION: The root locus is shown in Figure 8.22. Notice that this is a third-order system with one zero. Breakaway points on the real
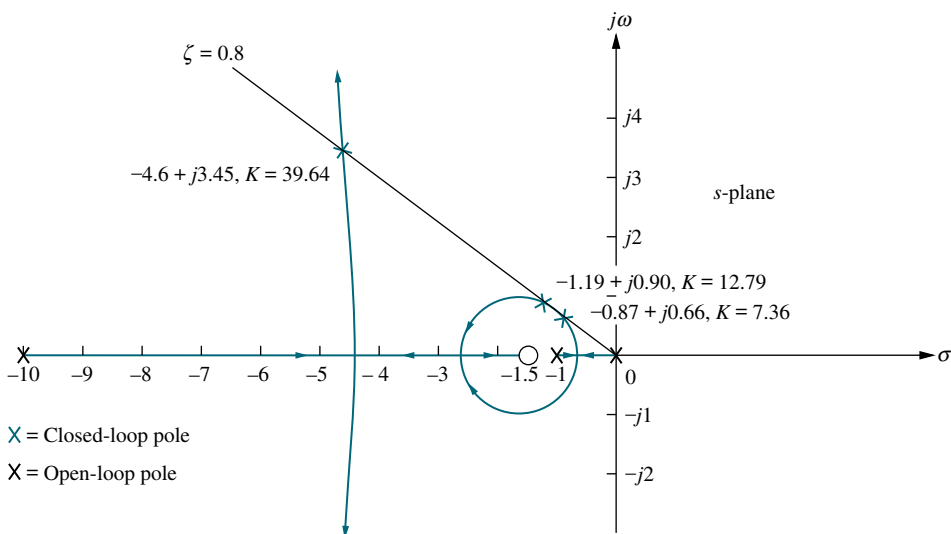

FIGURE 8.22   Root locus for Example 8.8

axis can occur between 0 and −1 and between −1.5 and −10, where the gain reaches a peak. Using the root locus program and searching in these regions for the peaks in gain, breakaway points are found at −0.62 with a gain of 2.511 and at −4.4 with a gain of 28.89. A break-in point on the real axis can occur between −1.5 and −10, where the gain reaches a local minimum. Using the root locus program and searching in these regions for the local minimum gain, a break-in point is found at −2.8 with a gain of 27.91.

Next assume that the system can be approximated by a second-order, underdamped system without any zeros. A 1.52% overshoot corresponds to a damping ratio of 0.8. Sketch this damping ratio line on the root locus, as shown in Figure 8.22.

Use the root locus program to search along the 0.8 damping ratio line for the point where the angles from the open-loop poles and zeros add up to an odd multiple of 180°. This is the point where the root locus crosses the 0.8 damping ratio or 1.52 percent overshoot line. Three points satisfy this criterion: $-0.87 \pm j0.66$, $-1.19 \pm j0.90$, and $-4.6 \pm j3.45$ with respective gains of 7.36, 12.79, and 39.64. For each point the settling time and peak time are evaluated using

$$T_s = \frac{4}{\zeta\omega_n} \tag{8.54}$$

where $\zeta\omega_n$ is the real part of the closed-loop pole, and also using

$$T_p = \frac{\pi}{\omega_n\sqrt{1-\zeta^2}} \tag{8.55}$$

where $\omega_n\sqrt{1-\zeta^2}$ is the imaginary part of the closed-loop pole.

To test our assumption of a second-order system, we must calculate the location of the third pole. Using the root locus program, search along the negative extension of the real axis between the zero at −1.5 and the pole at −10 for points that match the value of gain found at the second-order dominant poles. For each of the three crossings of the 0.8 damping ratio line, the third closed-loop pole is at −9.25, −8.6, and −1.8, respectively. The results are summarized in Table 8.4.

Finally, let us examine the steady-state error produced in each case. Note that we have little control over the steady-state error at this point. When the gain is set to meet the transient response, we have also designed the steady-state error. For the example, the steady-state error specification is given by K_v and is calculated as

$$K_v = \lim_{s \to 0} sG(s) = \frac{K(1.5)}{(1)(10)} \tag{8.56}$$

The results for each case are shown in Table 8.4.

How valid are the second-order assumptions? From Table 8.4, Cases 1 and 2 yield third closed-loop poles that are relatively far from the closed-loop zero. For these two cases there is no pole-zero cancellation, and a second-order system

TABLE 8.4 Characteristics of the system of Example 8.8

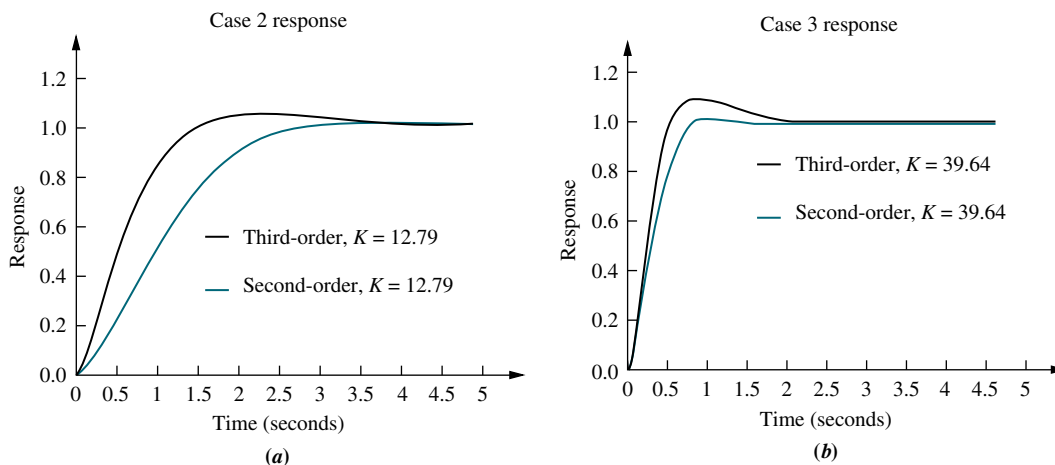| Case	Closed-loop poles	Closed-loop zero	Gain	Third closed-loop pole	Settling time	Peak time	K_v
1	$-0.87 \pm j0.66$	$-1.5 + j0$	7.36	-9.25	4.60	4.76	1.1
2	$-1.19 \pm j0.90$	$-1.5 + j0$	12.79	-8.61	3.36	3.49	1.9
3	$-4.60 \pm j3.45$	$-1.5 + j0$	39.64	-1.80	0.87	0.91	5.9

FIGURE 8.23   Second- and third-order responses for Example 8.8: **a.** Case 2; **b.** Case 3

approximation is not valid. In Case 3, the third closed-loop pole and the closed-loop zero are relatively close to each other, and a second-order system approximation can be considered valid. In order to show this, let us make a partial-fraction expansion of the closed-loop step response of Case 3 and see that the amplitude of the exponential decay is much less than the amplitude of the underdamped sinusoid. The closed-loop step response, $C_3(s)$, formed from the closed-loop poles and zeros of Case 3 is

$$
\begin{aligned}
C_3(s) &= \frac{39.64(s+1.5)}{s(s+1.8)(s+4.6+j3.45)(s+4.6-j3.45)} \\[2mm]
&= \frac{39.64(s+1.5)}{s(s+1.8)(s^2+9.2s+33.06)} \\[2mm]
&= \frac{1}{s} + \frac{0.3}{s(s+18)} - \frac{1.3(s+4.6)+1.6(3.45)}{(s+4.6)^2+3.45^2}
\end{aligned}
\tag{8.57}
$$

Thus, the amplitude of the exponential decay from the third pole is 0.3, and the amplitude of the underdamped response from the dominant poles is $\sqrt{1.3^2+1.6^2}=2.06$. Hence, the dominant pole response is 6.9 times as large as the nondominant exponential response, and we assume that a second-order approximation is valid.

Using a simulation program, we obtain Figure 8.23, which shows comparisons of step responses for the problem we have just solved. Cases 2 and 3 are plotted for both the third-order response and a second-order response, assuming just the dominant pair of poles calculated in the design problem. Again, the second-order approximation was justified for Case 3, where there is a small difference in percent overshoot. The second-order approximation is not valid for Case 2. Other than the excess overshoot, Case 3 responses are similar.

MATLAB
ML

Students who are using MATLAB should now run ch8p2 in Appendix B. You will learn how to use MATLAB to enter a value of percent overshoot from the keyboard. MATLAB will then draw the root locus and overlay the percent overshoot line requested. You will then interact with MATLAB and select the point of intersection of the

root locus with the requested percent overshoot line. MATLAB
will respond with the value of gain, all closed-loop poles at that
gain, and a closed-loop step response plot corresponding to the
selected point. This exercise solves Example 8.8 using MATLAB.

Students who are using MATLAB may want to explore the SISO Design
Tool described in Appendix E at www.wiley.com/college/nise. The
SISO Design Tool is a convenient and intuitive way to obtain, view,
and interact with a system's root locus. Section D.7 describes the
advantages of using the tool, while Section D.8 describes how to
use it. For practice, you may want to apply the SISO Design Tool to
some of the problems at the end of this chapter.

Gui Tool

GUIT

Skill-Assessment Exercise 8.6

PROBLEM: Given a unity feedback system that has the forward-path transfer
function

$$G(s) = \frac{K}{(s+2)(s+4)(s+6)}$$

do the following:

   a. Sketch the root locus.

   b. Using a second-order approximation, design the value of K to yield 10%
overshoot for a unit-step input.

   c. Estimate the settling time, peak time, rise time, and steady-state error for the
value of K designed in (b).

   d. Determine the validity of your second-order approximation.

ANSWERS:

   a. See solution located at www.wiley.com/college/nise.

   b. $K = 45.55$

   c. $T_s = 1.97\,\text{s}$, $T_p = 1.13\,s$, $T_r = 0.53\text{s}$, and $e_{\text{step}}(\infty) = 0.51$

   d. Second-order approximation is not valid.

The complete solution is located at www.wiley.com/college/nise.

8.8   Generalized Root Locus

Up to this point we have always drawn the root locus as a function of the forward-
path gain, K. The control system designer must often know how the closed-loop
poles change as a function of another parameter. For example, in Figure 8.24, the
parameter of interest is the open-loop pole at $-p_1$. How can we obtain a root locus
for variations of the value of p_1?

If the function $KG(s)H(s)$ is formed as

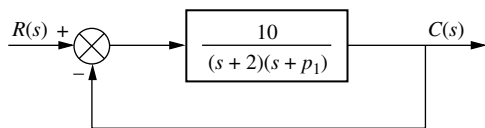$$KG(s)H(s) = \frac{10}{(s+2)(s+p_1)} \tag{8.58}$$

FIGURE 8.24 System requiring a root locus calibrated with p_1 as a parameter

the problem is that p_1 is not a multiplying factor of the function, as the gain, K, was in all of the previous problems. The solution to this dilemma is to create an equivalent system where p_1 appears as the forward-path gain. Since the closed-loop transfer function's denominator is $1 + KG(s)H(s)$, we effectively want to create an equivalent system whose denominator is $1 + p_1 G(s)H(s)$.

For the system of Figure 8.24, the closed-loop transfer function is

$$T(s) = \frac{KG(s)}{1 + KG(s)H(s)} = \frac{10}{s^2 + (p_1 + 2)s + 2p_1 + 10} \tag{8.59}$$

Isolating p_1, we have

$$T(s) = \frac{10}{s^2 + 2s + 10 + p_1(s+2)} \tag{8.60}$$

Converting the denominator to the form $[1 + p_1 G(s)H(s)]$ by dividing numerator and denominator by the term not included with p_1, $s^2 + 2s + 10$, we obtain

$$T(s) = \frac{\dfrac{10}{s^2 + 2s + 10}}{1 + \dfrac{p_1(s+2)}{s^2 + 2s + 10}} \tag{8.61}$$

Conceptually, Eq. (8.61) implies that we have a system for which

$$KG(s)H(s) = \frac{p_1(s+2)}{s^2 + 2s + 10} \tag{8.62}$$

The root locus can now be sketched as a function of p_1, assuming the open-loop system of Eq. (8.62). The final result is shown in Figure 8.25.
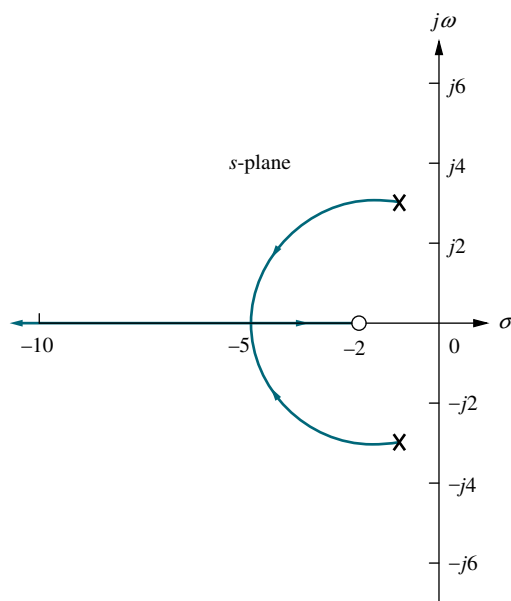

FIGURE 8.25 Root locus for the system of Figure 8.24, with p_1 as a parameter

In this section, we learned to plot the root locus as a function of any system parameter. In the next section we will learn how to plot root loci for positive-feedback systems.

8.9   Root Locus for Positive-Feedback Systems

The properties of the root locus were derived from the system of Figure 8.1. This is a negative-feedback system because of the negative summing of the feedback signal to the input signal. The properties of the root locus change dramatically if the feedback signal is added to the input rather than subtracted. A positive-feedback system can be thought of as a negative-feedback system with a negative value of $H(s)$. Using this concept, we find that the transfer function for the positive-feedback system shown in Figure 8.26 is
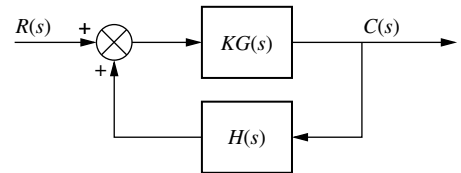
FIGURE 8.26   Positive-feedback system

$$T(s) = \frac{KG(s)}{1 - KG(s)H(s)} \tag{8.63}$$

We now retrace the development of the root locus for the denominator of Eq. (8.63). Obviously, a pole, s, exists when

$$KG(s)H(s) = 1 = 1\angle k360° \quad k = 0, \pm1, \pm2, \pm3, \ldots \tag{8.64}$$

Therefore, the root locus for positive-feedback systems consists of all points on the s-plane where the angle of $KG(s)H(s) = k360°$. How does this relationship change the rules for sketching the root locus presented in Section 8.4?

1. **Number of branches.** The same arguments as for negative feedback apply to this rule. There is no change.
2. **Symmetry.** The same arguments as for negative feedback apply to this rule. There is no change.
3. **Real-axis segments.** The development in Section 8.4 for the real-axis segments led to the fact that the angles of $G(s)H(s)$ along the real axis added up to either an odd multiple of $180°$ or a multiple of $360°$. Thus, for positive-feedback systems the

root locus exists on the real axis along sections where the locus for negative-feedback systems does not exist. The rule follows:

Real-axis segments: On the real axis, the root locus for positive-feedback systems exists to the left of an even number of real-axis, finite open-loop poles and/or finite open-loop zeros.

The change in the rule is the word *even;* for negative-feedback systems the locus existed to the left of an *odd* number of real-axis, finite open-loop poles and/or zeros.

4. **Starting and ending points.** You will find no change in the development in Section 8.4 if Eq. (8.63) is used instead of Eq. (8.12). Therefore, we have the following rule.

Starting and ending points: The root locus for positive-feedback systems begins at the finite and infinite poles of G(s)H(s) and ends at the finite and infinite zeros of G(s)H(s).

5. **Behavior at infinity.** The changes in the development of the asymptotes begin at Eq. (M.4) in Appendix M at www.wiley.com/college/nise since positive-feedback systems follow the relationship in Eq. (8.64). That change yields a different slope for the asymptotes. The value of the real-axis intercept for the asymptotes remains unchanged. The student is encouraged to go through the development in detail and show that the behavior at infinity for positive-feedback systems is given by the following rule:

The root locus approaches straight lines as asymptotes as the locus approaches infinity. Further, the equations of the asymptotes for positive-feedback systems are given by the real-axis intercept, σ_a, and angle, θ_a, as follows:

$$\sigma_a = \frac{\sum \text{finite poles} - \sum \text{finite zeros}}{\# \text{ finite poles} - \# \text{ finite zeros}} \qquad (8.65)$$

$$\theta_a = \frac{k2\pi}{\# \text{ finite poles} - \# \text{ finite zeros}} \qquad (8.66)$$

where $k = 0, \ \pm 1, \ \pm 2, \ \pm 3, \ldots$, and the angle is given in radians with respect to the positive extension of the real axis.

The change we see is that the numerator of Eq. (8.66) is $k2\pi$ instead of $(2k + 1)\pi$.

What about other calculations? The imaginary-axis crossing can be found using the root locus program. In a search of the $j\omega$-axis, you are looking for the point where the angles add up to a multiple of $360°$ instead of an odd multiple of $180°$. The breakaway points are found by looking for the maximum value of K. The break-in points are found by looking for the minimum value of K.

When we were discussing *negative*-feedback systems, we always made the root locus plot for positive values of gain. Since *positive*-feedback systems can also be thought of as *negative*-feedback systems with negative gain, the rules developed in this section apply equally to *negative*-feedback systems with negative gain. Let us look at an example.

Example 8.9

Root Locus for a Positive-Feedback System

PROBLEM: Sketch the root locus as a function of negative gain, K, for the system shown in Figure 8.11.

SOLUTION: The equivalent positive-feedback system found by pushing -1, associated with K, to the right past the pickoff point is shown in Figure 8.27(a).
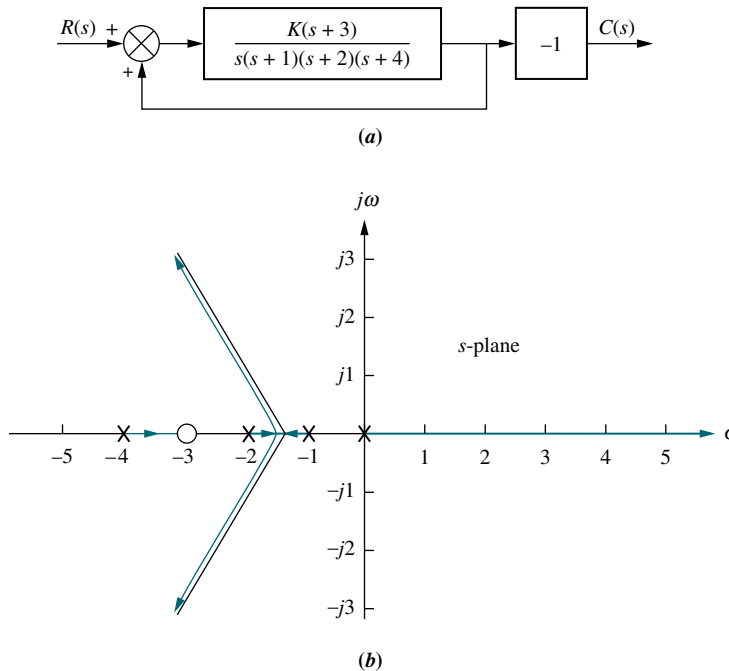

(a)

(b)

FIGURE 8.27 **a.** Equivalent positive-feedback system for Example 8.9; **b.** root locus

Therefore, as the gain of the equivalent system goes through positive values of K, the root locus will be equivalent to that generated by the gain, K, of the original system in Figure 8.11 as it goes through negative values.

The root locus exists on the real axis to the left of an even number of real, finite open-loop poles and/or zeros. Therefore, the locus exists on the entire positive extension of the real axis, between -1 and -2 and between -3 and -4. Using Eq. (8.27), the σ_a intercept is found to be

$$\sigma_a = \frac{(-1-2-4)-(-3)}{4-1} = -\frac{4}{3} \tag{8.67}$$

The angles of the lines that intersect at $-4/3$ are given by

$$\theta_a = \frac{k2\pi}{\#\text{ finite poles} - \#\text{ finite zeros}} \tag{8.68a}$$

$$= 0 \qquad \text{for } k = 0 \tag{8.68b}$$

$$= 2\pi/3 \qquad \text{for } k = 1 \tag{8.68c}$$

$$= 4\pi/3 \qquad \text{for } k = 2 \tag{8.68d}$$

The final root locus sketch is shown in Figure 8.27(b)

Skill-Assessment Exercise 8.8

PROBLEM: Sketch the root locus for the positive-feedback system whose forward transfer function is

$$G(s) = \frac{K(s+4)}{(s+1)(s+2)(s+3)}$$

The system has unity feedback.

ANSWER: The complete solution is at www.wiley.com/college/nise.

8.10 Pole Sensitivity

The root locus is a plot of the closed-loop poles as a system parameter is varied. Typically, that system parameter is gain. Any change in the parameter changes the closed-loop poles and, subsequently, the performance of the system. Many times the parameter changes against our wishes, due to heat or other environmental conditions. We would like to find out the extent to which changes in parameter values affect the performance of our system.

The root locus exhibits a nonlinear relationship between gain and pole location. Along some sections of the root locus, (1) very small changes in gain yield very large changes in pole location and hence performance; along other sections of the root locus, (2) very large changes in gain yield very small changes in pole location. In the first case we say that the system has a high sensitivity to changes in gain. In the second case, the system has a low sensitivity to changes in gain. We prefer systems with low sensitivity to changes in gain.

In Section 7.7, we defined sensitivity as the ratio of the fractional change in a function to the fractional change in a parameter as the change in the parameter approaches zero. Applying the same definition to the closed-loop poles of a system that vary with a parameter, we define *root sensitivity* as the ratio of the fractional change in a closed-loop pole to the fractional change in a system parameter, such as gain. Using Eq. (7.75), we calculate the sensitivity of a closed-loop pole, *s*, to gain, *K:*

$$S_{s:K} = \frac{K}{s}\frac{\delta s}{\delta K} \qquad (8.69)$$

where *s* is the current pole location, and *K* is the current gain. Using Eq. (8.69) and converting the partials to finite increments, the actual change in the closed-loop poles can be approximated as

$$\Delta s = s(S_{s:K})\frac{\Delta K}{K} \qquad (8.70)$$

where Δ*s* is the change in pole location, and Δ*K*/*K* is the fractional change in the gain, *K*. Let us demonstrate with an example. We begin with the characteristic equation from which δ*s*/δ*K* can be found. Then, using Eq. (8.69) with the current closed-loop pole, *s*, and its associated gain, *K*, we can find the sensitivity.

Example 8.10

Root Sensitivity of a Closed-Loop System to Gain Variations

PROBLEM: Find the root sensitivity of the system in Figure 8.4 at $s = -9.47$ and $-5 + j5$. Also calculate the change in the pole location for a 10% change in K.

SOLUTION: The system's characteristic equation, found from the closed-loop transfer function denominator, is $s^2 + 10s + K = 0$. Differentiating with respect to K, we have

$$2s\frac{\delta s}{\delta K} + 10\frac{\delta s}{\delta K} + 1 = 0 \tag{8.71}$$

from which

$$\frac{\delta s}{\delta K} = \frac{-1}{2s + 10} \tag{8.72}$$

Substituting Eq. (8.72) into Eq. (8.69), the sensitivity is found to be

$$S_{s:K} = \frac{K}{s}\frac{-1}{2s + 10} \tag{8.73}$$

For $s = -9.47$, Table 8.1 shows $K = 5$. Substituting these values into Eq. (8.73) yields $S_{s:K} = -0.059$. The change in the pole location for a 10% change in K can be found using Eq. (8.70), with $s = -9.47$, $\Delta K/K = 0.1$, and $S_{s:K} = -0.059$. Hence, $\Delta s = 0.056$, or the pole will move to the right by 0.056 units for a 10% change in K.

For $s = -5 + j5$, Table 8.1 shows $K = 50$. Substituting these values into Eq. (8.73) yields $S_{s:K} = 1/(1 + j1) = (1/\sqrt{2})\angle - 45°$. The change in the pole location for a 10% change in K can be found using Eq. (8.70), with $s = -5 + j5$, $\Delta K/K = 0.1$, and $S_{s:K} = (1/\sqrt{2})\angle - 45°$. Hence, $\Delta s = -j5$, or the pole will move vertically by 0.5 unit for a 10% change in K.

In summary, then, at $K = 5$, $S_{s:K} = -0.059$. At $K = 50$, $S_{s:K} = (1/\sqrt{2})\angle - 45°$. Comparing magnitudes, we conclude that the root locus is less sensitive to changes in gain at the lower value of K. Notice that root sensitivity is a complex quantity possessing both the magnitude and direction information from which the change in poles can be calculated.

Skill-Assessment Exercise 8.9

PROBLEM: A negative unity feedback system has the forward transfer function

$$G(s) = \frac{K(s + 1)}{s(s + 2)}$$

If K is set to 20, find the changes in closed-loop pole location for a 5% change in K.

ANSWER: For the closed-loop pole at -21.05, $\Delta s = -0.9975$; for the closed-loop pole at -0.95, $\Delta s = -0.0025$.

The complete solution is at www.wiley.com/college/nise.

Case Studies

Antenna Control: Transient Design via Gain

Design
D

The main thrust of this chapter is to demonstrate design of higher-order systems (higher than two) through gain adjustment. Specifically, we are interested in determining the value of gain required to meet transient response requirements, such as percent overshoot, settling time, and peak time. The following case study emphasizes this design procedure, using the root locus.

PROBLEM: Given the antenna azimuth position control system shown on the front endpapers, Configuration 1, find the preamplifier gain required for 25% overshoot.

SOLUTION: The block diagram for the system was derived in the Case Studies section in Chapter 5 and is shown in Figure 5.34(c), where $G(s) = 6.63K/[s(s + 1.71)(s + 100)]$.

First a sketch of the root locus is made to orient the designer. The real-axis segments are between the origin and -1.71 and from -100 to infinity. The locus begins at the open-loop poles, which are all on the real axis at the origin, -1.71, and -100. The locus then moves toward the zeros at infinity by following asymptotes that, from Eqs. (8.27) and (8.28), intersect the real axis at -33.9 at angles of $60°$, $180°$, and $-60°$. A portion of the root locus is shown in Figure 8.28.
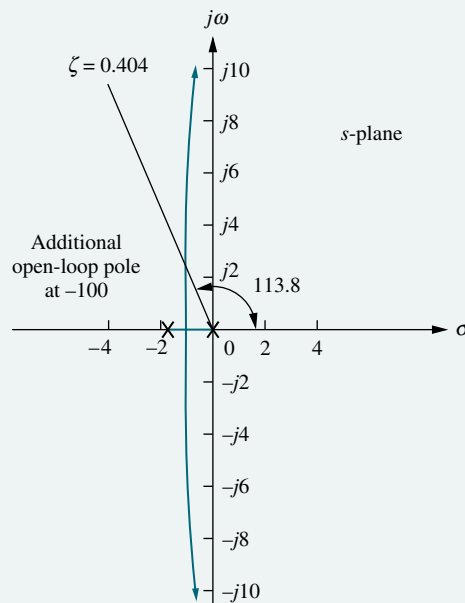

FIGURE 8.28   Portion of the root locus for the antenna control system

From Eq. (4.39), 25% overshoot corresponds to a damping ratio of 0.404. Now draw a radial line from the origin at an angle of $\cos^{-1} \zeta = 113.8$. The intersection of this line with the root locus locates the system's dominant, second-order closed-loop poles. Using the root locus program discussed in Appendix H.2 at www.wiley.com/college/nise to search the radial line for $180°$ yields the closed-loop dominant poles as $2.063 \angle 113.8° = -0.833 \pm j1.888$. The gain value yields $6.63K = 425.7$, from which $K = 64.21$.

Checking our second-order assumption, the third pole must be to the left of the open-loop pole at -100 and is thus greater than five times the real part of the dominant pole pair, which is -0.833. The second-order approximation is thus valid.

The computer simulation of the closed-loop system's step response in Figure 8.29 shows that the design requirement of 25% overshoot is met.
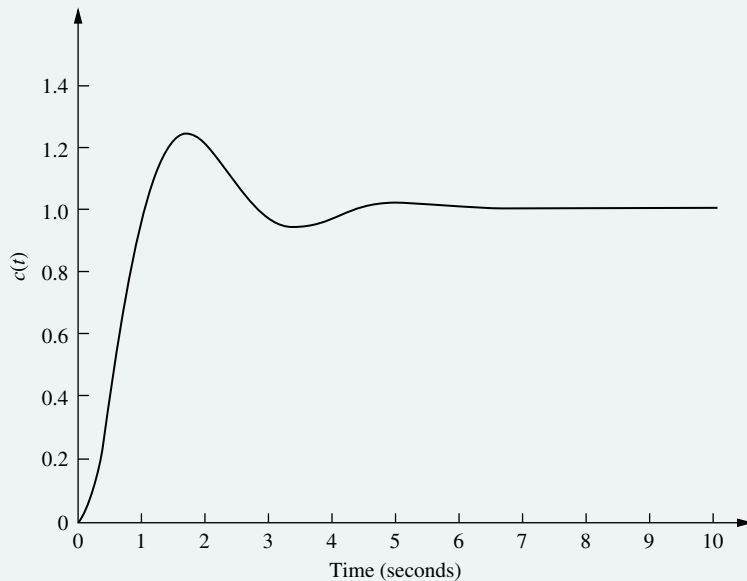

FIGURE 8.29 Step response of the gain-adjusted antenna control system

CHALLENGE: You are now given a problem to test your knowledge of this chapter's objectives. Referring to the antenna azimuth position control system shown on the front endpapers, Configuration 2, do the following:

a. Find the preamplifier gain, K, required for an 8-second settling time.

b. Repeat, using MATLAB.

MATLAB
ML

UFSS Vehicle: Transient Design via Gain

Design
D

In this case study, we apply the root locus to the UFSS vehicle pitch control loop. The pitch control loop is shown with both rate and position feedback on the back endpapers. In the example that follows, we plot the root locus without the rate feedback and then with the rate feedback. We will see the stabilizing effect that rate feedback has upon the system.

PROBLEM: Consider the block diagram of the pitch control loop for the UFSS vehicle shown on the back endpapers (*Johnson*, *1980*).

a. If $K_2 = 0$ (no rate feedback), plot the root locus for the system as a function of pitch gain, K_1, and estimate the settling time and peak time of the closed-loop response with 20% overshoot.

b. Let $K_2 = K_1$ (add rate feedback) and repeat **a**.

SOLUTION:

a. Letting $K_2 = 0$, the open-loop transfer function is

$$G(s)H(s) = \frac{0.25K_1(s + 0.435)}{(s + 1.23)(s + 2)(s^2 + 0.226s + 0.0169)} \tag{8.74}$$

from which the root locus is plotted in Figure 8.30. Searching along the 20% overshoot line evaluated from Eq. (4.39), we find the dominant second-order poles to be $-0.202 \pm j0.394$ with a gain of $K = 0.25K_1 = 0.706$, or $K_1 = 2.824$.
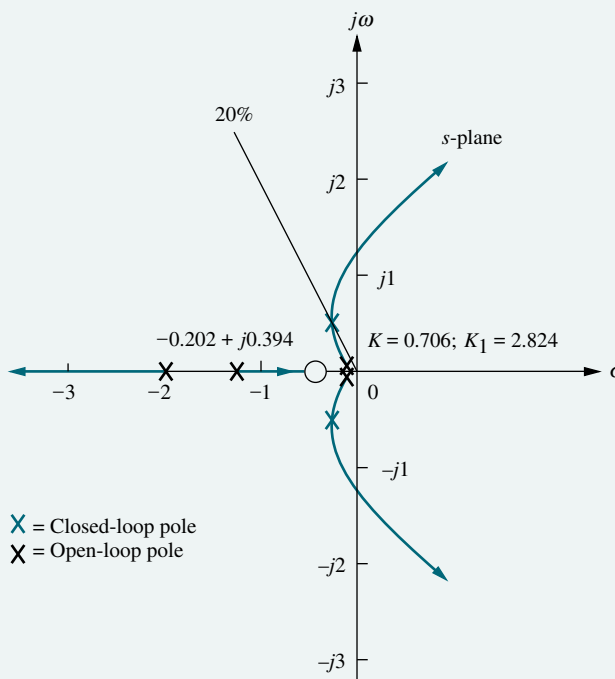

FIGURE 8.30   Root locus of pitch control loop without rate feedback, UFSS vehicle

From the real part of the dominant pole, the settling time is estimated to be $T_s = 4/0.202 = 19.8$ seconds. From the imaginary part of the dominant pole, the peak time is estimated to be $T_p = \pi/0.394 = 7.97$ seconds. Since our estimates are based upon a second-order assumption, we now test our assumption by finding the third closed-loop pole location between -0.435 and -1.23 and the fourth closed-loop pole location between -2 and infinity. Searching each of these regions for a gain of $K = 0.706$, we find the third and fourth poles at -0.784 and -2.27, respectively. The third pole, at -0.784, may not be close enough to the zero at -0.435, and thus the system should be simulated. The fourth pole, at -2.27, is 11 times as far from the imaginary axis as the dominant poles and thus meets the requirement of at least five times the real part of the dominant poles.

A computer simulation of the step response for the system, which is shown in Figure 8.31, shows a 29% overshoot above a final value of 0.88, approximately 20-second settling time, and a peak time of approximately 7.5 seconds.
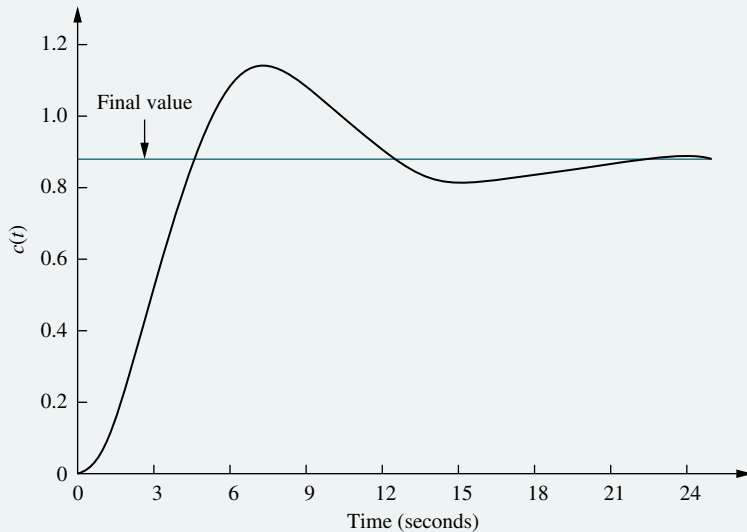
FIGURE 8.31 Computer simulation of step response of pitch control loop without rate feedback, UFSS vehicle

b. Adding rate feedback by letting $K_2 = K_1$ in the pitch control system shown on the back endpapers, we proceed to find the new open-loop transfer function. Pushing $-K_1$ to the right past the summing junction, dividing the pitch rate sensor by $-K_1$, and combining the two resulting feedback paths obtaining $(s + 1)$ give us the following open-loop transfer function:

$$G(s)H(s) = \frac{0.25K_1(s + 0.435)(s + 1)}{(s + 1.23)(s + 2)(s^2 + 0.226s + 0.0169)} \tag{8.75}$$

Notice that the addition of rate feedback adds a zero to the open-loop transfer function. The resulting root locus is shown in Figure 8.32. Notice that this root locus, unlike the root locus in **a**, is stable for all values of gain, since the locus does not enter the right half of the s-plane for any value of positive gain,
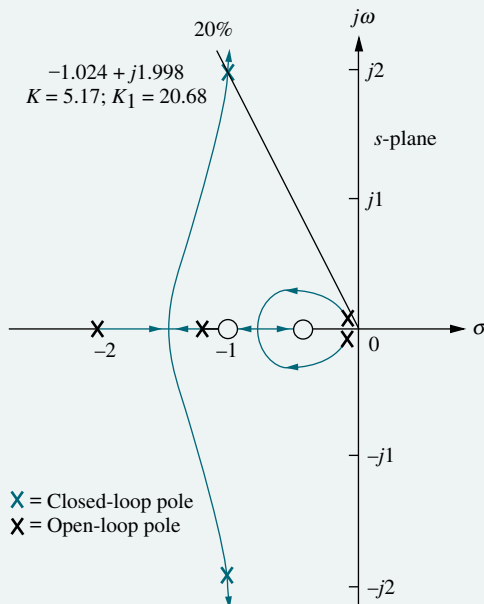

FIGURE 8.32 Root locus of pitch control loop with rate feedback, UFSS vehicle
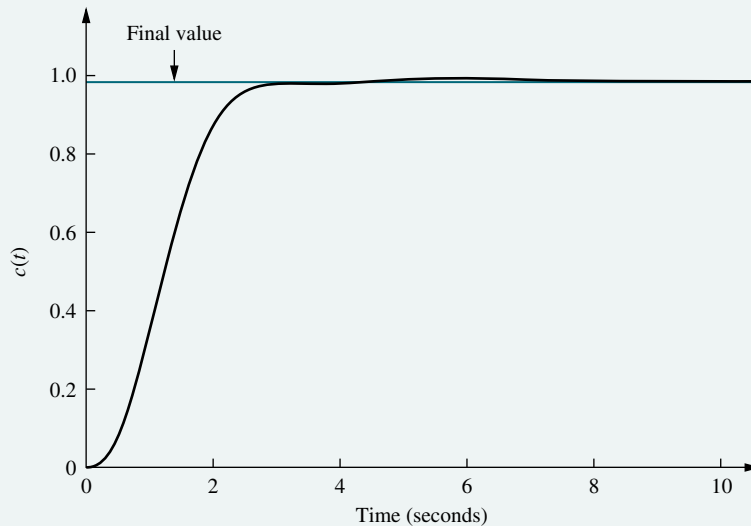
FIGURE 8.33 Computer simulation of step response of pitch control loop with rate feedback, UFSS vehicle

$K = 0.25K_1$. Also notice that the intersection with the 20% overshoot line is much farther from the imaginary axis than is the case without rate feedback, resulting in a faster response time for the system.

The root locus intersects the 20% overshoot line at $-1.024 \pm j1.998$ with a gain of $K = 0.25K_1 = 5.17$, or $K_1 = 20.68$. Using the real and imaginary parts of the dominant pole location, the settling time is predicted to be $T_s = 4/1.024 = 3.9$ seconds, and the peak time is estimated to be $T_p = \pi/1.998 = 1.57$ seconds. The new estimates show considerable improvement in the transient response as compared to the system without the rate feedback.

Now we test our second-order approximation by finding the location of the third and fourth poles between -0.435 and -1. Searching this region for a gain of $K = 5.17$, we locate the third and fourth poles at approximately -0.5 and -0.91. Since the zero at -1 is a zero of $H(s)$, the student can verify that this zero is not a zero of the closed-loop transfer function. Thus, although there may be pole-zero cancellation between the closed-loop pole at -0.5 and the closed-loop zero at -0.435, there is no *closed-loop* zero to cancel the closed-loop pole at -0.91.[2] Our second-order approximation is not valid.

A computer simulation of the system with rate feedback is shown in Figure 8.33. Although the response shows that our second-order approximation is invalid, it still represents a considerable improvement in performance over the system without rate feedback; the percent overshoot is small, and the settling time is about 6 seconds instead of about 20 seconds.

CHALLENGE: You are now given a problem to test your knowledge of this chapter's objectives. For the UFSS vehicle (*Johnson*, *1980*) heading control system shown on the back endpapers, and introduced in the case study challenge in Chapter 5, do the following:

a. Let $K_2 = K_1$ and find the value of K_1 that yields 10% overshoot.

MATLAB
ML

b. Repeat, using MATLAB.

---

[2] The zero at -1 shown on the root locus plot of Figure 8.32 is an open-loop zero since it comes from the numerator of $H(s)$.

We have concluded the chapter with two case studies showing the use and application of the root locus. We have seen how to plot a root locus and estimate the transient response by making a second-order approximation. We saw that the second-order approximation held when rate feedback was not used for the UFSS. When rate feedback was used, an open-loop zero from $H(s)$ was introduced. Since it was not a closed-loop zero, there was no pole-zero cancellation, and a second-order approximation could not be justified. In this case, however, the transient response with rate feedback did represent an improvement in transient response over the system without rate feedback. In subsequent chapters we will see why rate feedback yields an improvement. We will also see other methods of improving the transient response.

Summary

In this chapter, we examined the *root locus*, a powerful tool for the analysis and design of control systems. The root locus empowers us with qualitative and quantitative information about the stability and transient response of feedback control systems. The root locus allows us to find the poles of the closed-loop system by starting from the open-loop system's poles and zeros. It is basically a graphical root-solving technique.

We looked at ways to sketch the root locus rapidly, even for higher-order systems. The sketch gave us qualitative information about changes in the transient response as parameters were varied. From the locus we were able to determine whether a system was unstable for any range of gain.

Next we developed the criterion for determining whether a point in the *s*-plane was on the root locus: The angles from the open-loop zeros, minus the angles from the open-loop poles drawn to the point in the *s*-plane, add up to an odd multiple of $180°$.

The computer program discussed in Appendix G.2 at www.wiley.com/college/nise helps us to search rapidly for points on the root locus. This program allows us to find points and gains to meet certain transient response specifications as long as we are able to justify a second-order assumption for higher-order systems. Other computer programs, such as MATLAB, plot the root locus and allow the user to interact with the display to determine transient response specifications and system parameters.

Our method of design in this chapter is gain adjustment. We are limited to transient responses governed by the poles on the root locus. Transient responses represented by pole locations outside of the root locus cannot be obtained by a simple gain adjustment. Further, once the transient response has been established, the gain is set, and so is the steady-state error performance. In other words, by a simple gain adjustment, we have to trade off between a specified transient response and a specified steady-state error. Transient response and steady-state error cannot be designed independently with a simple gain adjustment.

We also learned how to plot the root locus against system parameters other than gain. In order to make this root locus plot, we must first convert the closed-loop transfer function into an equivalent transfer function that has the desired system parameter in the same position as the gain. The chapter discussion concluded with positive-feedback systems and how to plot the root loci for these systems.

The next chapter extends the concept of the root locus to the design of compensation networks. These networks have as an advantage the separate design of transient performance and steady-state error performance.

(Review Questions)

1. What is a root locus?
2. Describe two ways of obtaining the root locus.
3. If $KG(s)H(s) = 5\angle 180°$, for what value of gain is s a point on the root locus?
4. Do the zeros of a system change with a change in gain?
5. Where are the zeros of the closed-loop transfer function?
6. What are two ways to find where the root locus crosses the imaginary axis?
7. How can you tell from the root locus if a system is unstable?
8. How can you tell from the root locus if the settling time does not change over a region of gain?
9. How can you tell from the root locus that the natural frequency does not change over a region of gain?
10. How would you determine whether or not a root locus plot crossed the real axis?
11. Describe the conditions that must exist for all closed-loop poles and zeros in order to make a second-order approximation.
12. What rules for plotting the root locus are the same whether the system is a positive- or a negative-feedback system?
13. Briefly describe how the zeros of the open-loop system affect the root locus and the transient response.

(Problems)

1. For each of the root loci shown in Figure P8.1, tell whether or not the sketch can be a root locus. If the sketch cannot be a root locus, explain why. Give *all* reasons. [Section: 8.4]
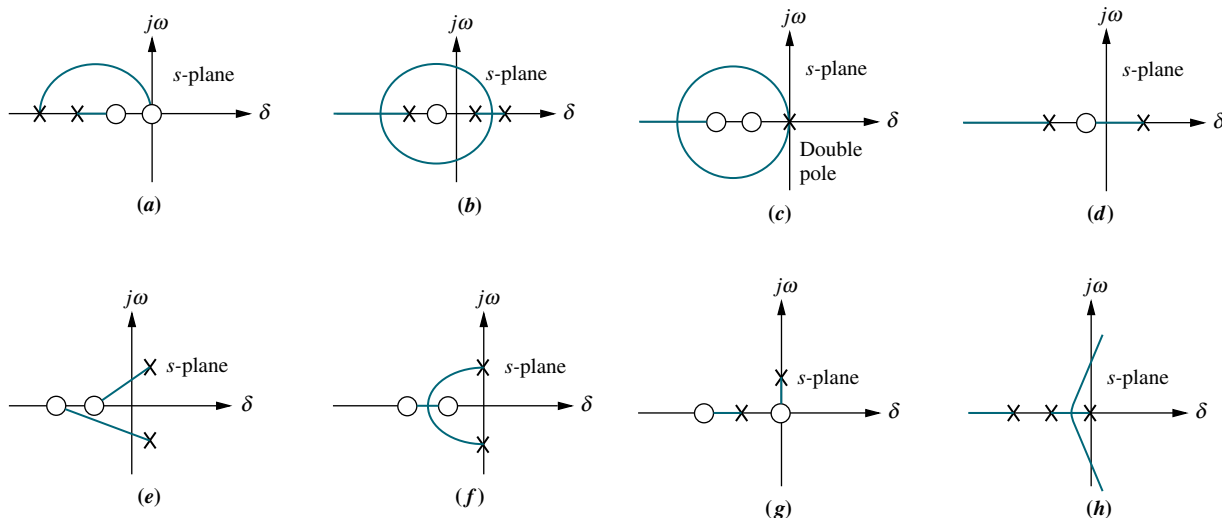

FIGURE P8.1

2. Sketch the general shape of the root locus for each of the open-loop pole-zero plots shown in Figure P8.2. [Section: 8.4]
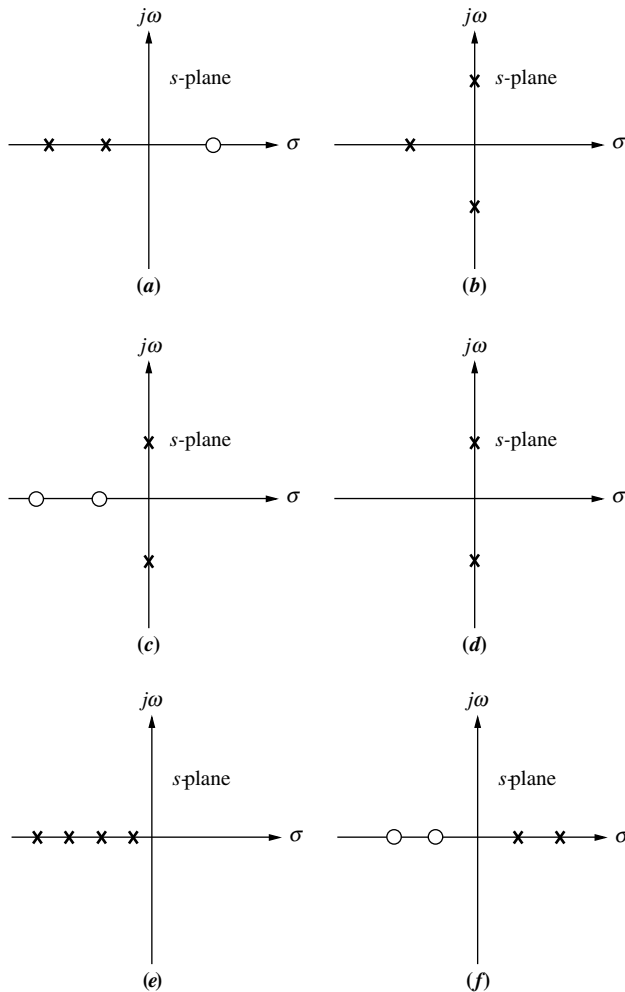
WileyPLUS

WPCS

Control Solutions

(a)

(b)

(c)

(d)

(e)

(f)

FIGURE P8.2

3. Sketch the root locus for the unity feedback system shown in Figure P8.3 for the following transfer functions: [Section: 8.4]

a. $G(s) = \dfrac{K(s+2)(s+6)}{s^2 + 8s + 25}$

b. $G(s) = \dfrac{K(s^2 + 4)}{(s^2 + 1)}$

c. $G(s) = \dfrac{K(s^2 + 1)}{s^2}$

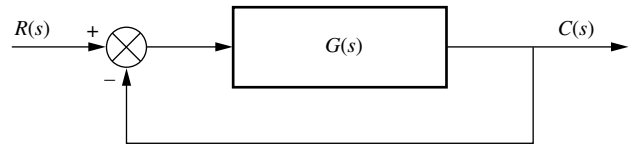**d.** $G(s) = \dfrac{K}{(s+1)^3(s+4)}$

FIGURE P8.3

4. Let

$$G(s) = \frac{K\left(s + \dfrac{2}{3}\right)}{s^2(s+6)}$$

in Figure P8.3. [Section: 8.5]

a. Plot the root locus.

b. Write an expression for the closed-loop transfer function at the point where the three closed-loop poles meet.

5. Let

$$G(s) = \frac{-K(s+1)^2}{s^2 + 2s + 2}$$

with $K > 0$ in Figure P8.3. [Sections: 8.5, 8.9]

a. Find the range of K for closed-loop stability.

b. Sketch the system's root locus.

c. Find the position of the closed-loop poles when $K = 1$ and $K = 2$.

6. For the open-loop pole-zero plot shown in Figure P8.4, sketch the root locus and find the break-in point. [Section: 8.5]
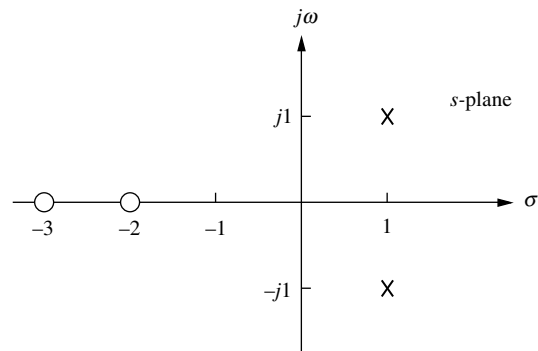
FIGURE P8.4

7. Sketch the root locus of the unity feedback system shown in Figure P8.3, where

$$G(s) = \frac{K(s+3)(s+5)}{(s+1)(s-7)}$$

and find the break-in and breakaway points. [Section: 8.5]

8. The characteristic polynomial of a feedback control system, which is the denominator of the closed-loop transfer function, is given by $s^3 + 2s^2 + (20K + 7)s + 100K$. Sketch the root locus for this system. [Section: 8.8]

9. Figure P8.5 shows open-loop poles and zeros. There are two possibilities for the sketch of the root locus. Sketch each of the two possibilities. Be aware that only one can be the *real* locus for specific open-loop pole and zero values. [Section: 8.4]
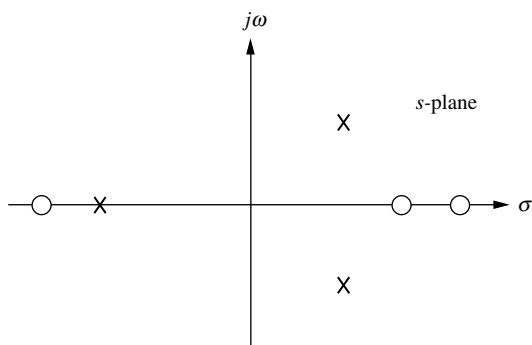

FIGURE P8.5

10. Plot the root locus for the unity feedback system shown in Figure P8.3, where

$$G(s) = \frac{K(s+2)(s^2+4)}{(s+5)(s-3)}$$

For what range of K will the poles be in the right half-plane? [Section: 8.5]

11. For the unity feedback system shown in Figure P8.3, where

$$G(s) = \frac{K(s^2-9)}{(s^2+4)}$$

sketch the root locus and tell for what values of K the system is stable and unstable. [Section: 8.5]

12. Sketch the root locus for the unity feedback system shown in Figure P8.3, where

$$G(s) = \frac{K(s^2+2)}{(s+3)(s+4)}$$

Give the values for all critical points of interest. Is the system ever unstable? If so, for what range of K? [Section: 8.5]

13. For each system shown in Figure P8.6, make an accurate plot of the root locus and find the following: [Section: 8.5]

a. The breakaway and break-in points

b. The range of K to keep the system stable

c. The value of K that yields a stable system with critically damped second-order poles

d. The value of K that yields a stable system with a pair of second-order poles that have a damping ratio of 0.707
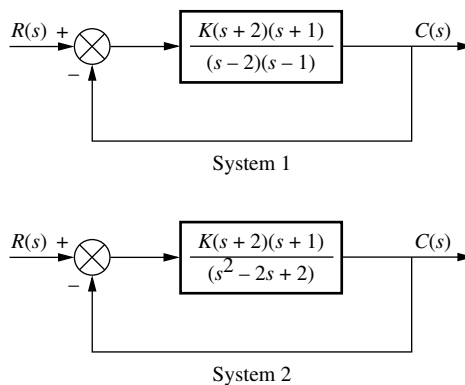
FIGURE P8.6

14. Sketch the root locus and find the range of K for stability for the unity feedback system shown in Figure P8.3 for the following conditions: [Section: 8.5]

a. $G(s) = \dfrac{K(s^2+1)}{(s-1)(s+2)(s+3)}$

b. $G(s) = \dfrac{K(s^2-2s+2)}{s(s+1)(s+2)}$

15. For the unity feedback system of Figure P8.3, where

$$G(s) = \frac{K(s+3)}{(s^2+2)(s-2)(s+5)}$$

sketch the root locus and find the range of K such that there will be only two right–half-plane poles for the closed-loop system. [Section: 8.5]

16. For the unity feedback system of Figure P8.3, where

$$G(s) = \frac{K}{s(s+6)(s+9)}$$

plot the root locus and calibrate your plot for gain. Find all the critical points, such as breakaways, asymptotes, $j\omega$-axis crossing, and so forth. [Section: 8.5]

17. Given the unity feedback system of Figure P8.3, make an accurate plot of the root locus for the following:

a. $G(s) = \dfrac{K(s^2 - 2s + 2)}{(s+1)(s+2)}$

b. $G(s) = \dfrac{K(s-1)(s-2)}{(s+1)(s+2)}$

Calibrate the gain for at least four points for each case. Also find the breakaway points, the $j\omega$-axis crossing, and the range of gain for stability for each case. Find the angles of arrival for Part **a**. [Section: 8.5]

18. Given the root locus shown in Figure P8.7, [Section: 8.5]

a. Find the value of gain that will make the system marginally stable.

b. Find the value of gain for which the closed-loop transfer function will have a pole on the real axis at -5.
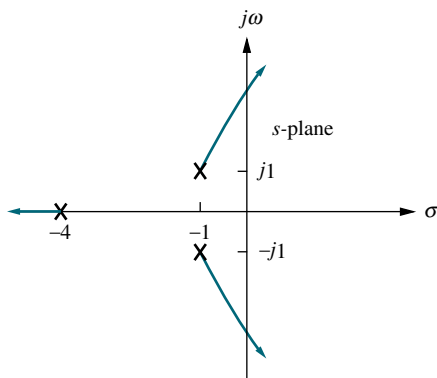
FIGURE P8.7

19. Given the unity feedback system of Figure P8.3, where

$$G(s) = \frac{K(s+1)}{s(s+2)(s+3)(s+4)}$$

do the following: [Section: 8.5]

a. Sketch the root locus.

b. Find the asymptotes.

c. Find the value of gain that will make the system marginally stable.

d. Find the value of gain for which the closed-loop transfer function will have a pole on the real axis at -0.5.

20. For the unity feedback system of Figure P8.3, where

$$G(s) = \frac{K(s+\alpha)}{s(s+3)(s+6)}$$

find the values of α and K that will yield a second-order closed-loop pair of poles at $-1 \pm j100$. [Section: 8.5]

21. For the unity feedback system of Figure P8.3, where

$$G(s) = \frac{K(s-1)(s-2)}{s(s+1)}$$

sketch the root locus and find the following: [Section: 8.5]

a. The breakaway and break-in points

b. The $j\omega$-axis crossing

c. The range of gain to keep the system stable

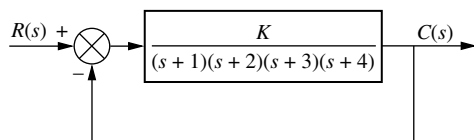**d.** The value of K to yield a stable system with second-order complex poles, with a damping ratio of 0.5

22. For the unity feedback system shown in Figure P8.3, where

$$G(s) = \frac{K(s+10)(s+20)}{(s+30)(s^2 - 20s + 200)}$$

do the following: [Section: 8.7]

a. Sketch the root locus.

b. Find the range of gain, K, that makes the system stable.

c. Find the value of K that yields a damping ratio of 0.707 for the system's closed-loop dominant poles.

d. Find the value of K that yields closed-loop critically damped dominant poles.

23. For the system of Figure P8.8(a), sketch the root locus and find the following: [Section: 8.7]

a. Asymptotes

b. Breakaway points

c. The range of K for stability

d. The value of K to yield a 0.7 damping ratio for the dominant second-order pair

To improve stability, we desire the root locus to cross the $j\omega$-axis at $j5.5$. To accomplish this, the open-loop function is cascaded with a zero, as shown in Figure P8.8(b).
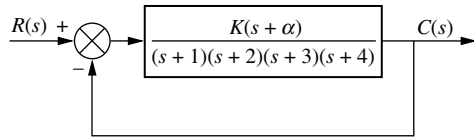
FIGURE P8.8

e. Find the value of α and sketch the new root locus.

f. Repeat Part **c** for the new locus.

g. Compare the results of Part **c** and Part **f**. What improvement in transient response do you notice?

24. Sketch the root locus for the positive-feedback system shown in Figure P8.9. [Section: 8.9]
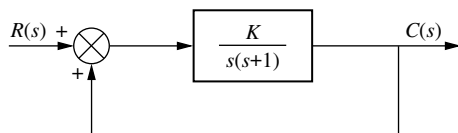
FIGURE P8.9

25. Root loci are usually plotted for variations in the gain. Sometimes we are interested in the variation of the closed-loop poles as other parameters are changed. For the system shown in Figure P8.10, sketch the root locus as α is varied. [Section: 8.8]
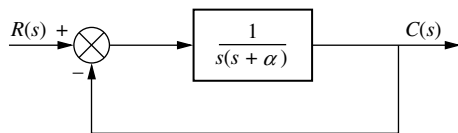
FIGURE P8.10

26. Given the unity feedback system shown in Figure P8.3, where

$$G(s) = \frac{K}{(s+1)(s+2)(s+3)}$$

do the following problem parts by first making a second-order approximation. After you are finished with all of the parts, justify your second-order approximation. [Section: 8.7]

a. Sketch the root locus.

b. Find K for 20% overshoot.

c. For K found in Part **b**, what is the settling time, and what is the peak time?

d. Find the locations of higher-order poles for K found in Part **b**.

e. Find the range of K for stability.

27. For the unity feedback system shown in Figure P8.3, where

$$G(s) = \frac{K(s^2 - 2s + 2)}{(s+2)(s+4)(s+5)(s+6)}$$

do the following: [Section: 8.7]

a. Sketch the root locus.

b. Find the asymptotes.

c. Find the range of gain, K, that makes the system stable.

d. Find the breakaway points.

e. Find the value of K that yields a closed-loop step response with 25% overshoot.

f. Find the location of higher-order closed-loop poles when the system is operating with 25% overshoot.

g. Discuss the validity of your second-order approximation.

h. Use MATLAB to obtain the closed-loop step re- sponse to validate or refute your second-order approximation.

MATLAB

ML

28. The unity feedback system shown in Figure P8.3, where

$$G(s) = \frac{K(s+2)(s+3)}{s(s+1)}$$

is to be designed for minimum damping ratio. Find the following: [Section: 8.7]

a. The value of K that will yield minimum damping ratio

b. The estimated percent overshoot for that case

c. The estimated settling time and peak time for that case

d. The justification of a second-order approxima- tion (discuss)

e. The expected steady-state error for a unit ramp input for the case of minimum damping ratio

29. For the unity feedback system shown in Figure P8.3, where

$$G(s) = \frac{K(s+2)}{s(s+6)(s+10)}$$

find K to yield closed-loop complex poles with a damping ratio of 0.55. Does your solution require a justification of a second-order approximation? Explain. [Section: 8.7]

30. For the unity feedback system shown in Figure P8.3, where

WileyPLUS
WPCS
Control Solutions

$$G(s) = \frac{K(s+\alpha)}{s(s+1)(s+10)}$$

find the value of α so that the system will have a settling time of 4 seconds for large values of K. Sketch the resulting root locus. [Section: 8.8]

31. For the unity feedback system shown in Figure 8.3, where

$$G(s) = \frac{K(s+6)}{(s^2+10s+26)(s+1)^2(s+\alpha)}$$

design K and α so that the dominant complex poles of the closed-loop function have a damping ratio of 0.45 and a natural frequency of 9/8 rad/s.

32. For the unity feedback system shown in Figure 8.3, where

$$G(s) = \frac{K}{s(s+3)(s+4)(s+8)}$$

do the following: [Section: 8.7]

a. Sketch the root locus.

b. Find the value of K that will yield a 10% overshoot.

c. Locate all nondominant poles. What can you say about the second-order approximation that led to your answer in Part **b**?

d. Find the range of K that yields a stable system.

33. Repeat Problem 32 using MATLAB. Use one program to do the following:

MATLAB
ML

a. Display a root locus and pause.

b. Draw a close-up of the root locus where the axes go from −2 to 0 on the real axis and −2 to 2 on the imaginary axis.

c. Overlay the 10% overshoot line on the close-up root locus.

d. Select interactively the point where the root locus crosses the 10% over-shoot line, and respond with the gain at that point as well as all of the closed-loop poles at that gain.

e. Generate the step response at the gain for 10% overshoot.

34. For the unity feedback system shown in Figure 8.3, where

WileyPLUS
WPCS
Control Solutions

$$G(s) = \frac{K(s^2+4s+5)}{(s^2+2s+5)(s+3)(s+4)}$$

do the following: [Section: 8.7]

a. Find the gain, K, to yield a 1-second peak time if one assumes a second-order approximation.

b. Check the accuracy of the second-order approximation using MATLAB to simulate the system.

MATLAB
ML

35. For the unity feedback system shown in Figure P8.3, where

$$G(s) = \frac{K(s+2)(s+3)}{(s^2+2s+2)(s+4)(s+5)(s+6)}$$

do the following: [Section: 8.7]

a. Sketch the root locus.

b. Find the $j\omega$-axis crossing and the gain, K, at the crossing.

c. Find all breakaway and break-in points.

d. Find angles of departure from the complex poles.

e. Find the gain, K, to yield a damping ratio of 0.3 for the closed-loop dominant poles.

36. Repeat Parts **a** through **c** and **e** of Problem 35 for [Section: 8.7]

$$G(s) = \frac{K(s+8)}{s(s+2)(s+4)(s+6)}$$

37. For the unity feedback system shown in Figure P8.3, where

$$G(s) = \frac{K}{(s+3)(s^2+4s+5)}$$

do the following: [Section: 8.7]

a. Find the location of the closed-loop dominant poles if the system is operating with 15% overshoot.

b. Find the gain for Part **a.**

c. Find all other closed-loop poles.

d. Evaluate the accuracy of your second-order approximation.

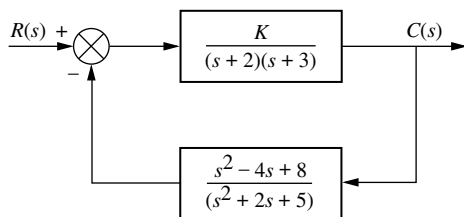**38.** For the system shown in Figure P8.11, do the following: [Section: 8.7]

$$\frac{K}{(s+2)(s+3)}$$

$$\frac{s^2 - 4s + 8}{(s^2 + 2s + 5)}$$

FIGURE P8.11

a. Sketch the root locus.

b. Find the $j\omega$-axis crossing and the gain, K, at the crossing.

c. Find the real-axis breakaway to two-decimal-place accuracy.

d. Find angles of arrival to the complex zeros.

e. Find the closed-loop zeros.

f. Find the gain, K, for a closed-loop step response with 30% overshoot.

g. Discuss the validity of your second-order approximation.

39. Sketch the root locus for the system of Figure P8.12 and find the following: [Section: 8.7]
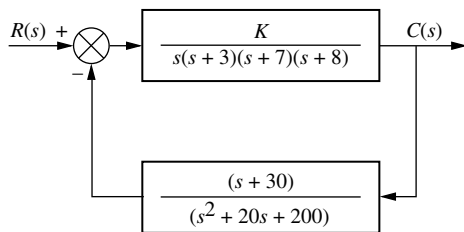

$$\frac{K}{s(s+3)(s+7)(s+8)}$$

$$\frac{(s+30)}{(s^2 + 20s + 200)}$$

FIGURE P8.12

a. The range of gain to yield stability

b. The value of gain that will yield a damping ratio of 0.707 for the system's dominant poles

c. The value of gain that will yield closed-loop poles that are critically damped

40. Repeat Problem 39 using MATLAB. The program will do the following in one program:

a. Display a root locus and pause.

b. Display a close-up of the root locus where the axes go from −2 to 2 on the real axis and −2 to 2 on the imaginary axis.

c. Overlay the 0.707 damping ratio line on the close-up root locus.

d. Allow you to select interactively the point where the root locus crosses the 0.707 damping ratio line, and respond by displaying the gain at that point as well as all of the closed-loop poles at that gain. The program will then allow you to select interactively the imaginary-axis crossing and respond with a display of the gain at that point as well as all of the closed-loop poles at that gain. Finally, the program will repeat the evaluation for critically damped dominant closed-loop poles.

e. Generate the step response at the gain for 0.707 damping ratio.

41. Given the unity feedback system shown in Figure P8.3, where

$$G(s) = \frac{K(s+z)}{s^2(s+20)}$$

do the following: [Section: 8.7]

a. If $z = 6$, find K so that the damped frequency of oscillation of the transient response is 10 rad/s.

b. For the system of Part **a**, what static error constant (finite) can be specified? What is its value?

c. The system is to be redesigned by changing the values of z and K. If the new specifications are $\%OS = 4.32\%$ and $T_s = 0.4$ s, find the new values of z and K.

42. Given the unity feedback system shown in Figure P8.3, where

$$G(s) = \frac{K}{(s+1)(s+3)(s+6)^2}$$

find the following: [Section: 8.7]

a. The value of gain, K, that will yield a settling time of 4 seconds

b. The value of gain, K, that will yield a critically damped system

43. Let

$$G(s) = \frac{K(s-1)}{(s+2)(s+3)}$$

in Figure P8.3. [Section: 8.7].

a. Find the range of K for closed-loop stability.

b. Plot the root locus for $K > 0$.

c. Plot the root locus for $K < 0$.

d. Assuming a step input, what value of K will result in the smallest attainable settling time?

e. Calculate the system's e_{ss} for a unit step input assuming the value of K obtained in Part **d**.

f. Make an approximate hand sketch of the unit step response of the system if K has the value obtained in Part **d**.

44. Given the unity feedback system shown in Figure P8.3, where

$$G(s) = \frac{K}{s(s+1)(s+5)}$$

evaluate the pole sensitivity of the closed-loop system if the second-order, underdamped closed-loop poles are set for [Section: 8.10]

a. $\zeta = 0.591$

b. $\zeta = 0.456$

c. Which of the two previous cases has more desirable sensitivity?

45. Figure P8.13(*a*) shows a robot equipped to perform arc welding. A similar device can be configured as a six-degrees-of-freedom industrial robot that can transfer objects according to a desired program. Assume the block diagram of the swing motion system shown in Figure P8.13(*b*). If $K = 64,510$, make a second-order approximation and estimate the following (*Hardy, 1967*):
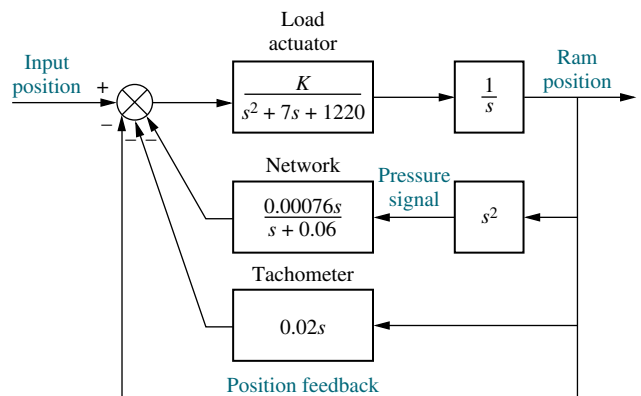
a. Damping ratio

b. Percent overshoot

c. Natural frequency

d. Settling time

e. Peak time

What can you say about your original second-order approximation?

46. During ascent, the automatic steering program aboard the space shuttle provides the interface

(*a*)

(*b*)

FIGURE P8.13   a. Robot equipped to perform arc welding; **b.** block diagram for swing motion system

between the low-rate processing of guidance (commands) and the high-rate processing of flight control (steering in response to the commands). The function performed is basically that of smoothing. A simplified representation of a maneuver smoother linearized for coplanar maneuvers is shown in Figure P8.14. Here $\theta_{CB}(s)$ is the commanded body angle as calculated by guidance, and $\theta_{CB}(s)$ is the desired body angle sent to flight control after smoothing.[3] Using the methods of Section 8.8, do the following:
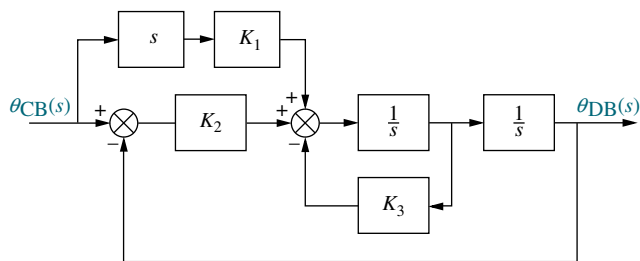
---

[3] Source: Rockwell International.

FIGURE P8.14   Block diagram of smoother

a. Sketch a root locus where the roots vary as a function of K_3.

b. Locate the closed-loop zeros.

c. Repeat Parts **a** and **b** for a root locus sketched as a function of K_2.

47. Repeat Problem 3 but sketch your root loci for negative values of K. [Section: 8.9]

48. Large structures in space, such as the space station, have to be stabilized against unwanted vibration. One method is to use an active vibration absorber to control the structure, as shown in Figure P8.15(a) (*Bruner*, *1992*). Assuming that all values except the mass of the active vibration absorber are known and are equal to unity, do the following:
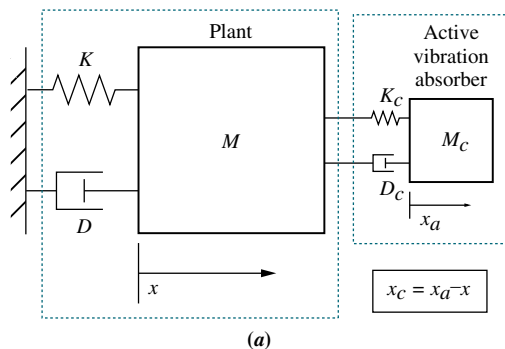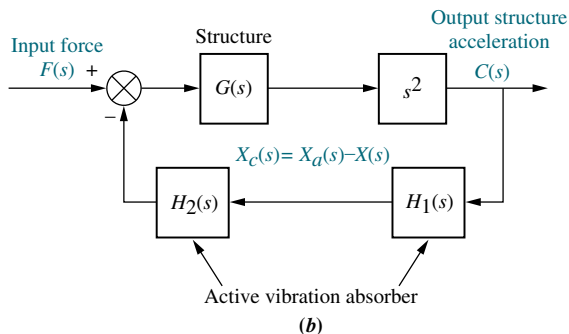
FIGURE P8.15   a. Active vibration absorber (© 1992 AIAA); **b.** control system block diagram

a. Obtain $G(s)$ and $H(s) = H_1(s)H_2(s)$ in the block diagram representation of the system of Figure 8.15(*b*), which shows that the active vibration absorber acts as a feedback element to control the structure. (Hint: Think of K_c and D_c as producing inputs to the structure.)

b. Find the steady-state position of the structure for a force disturbance input.

c. Sketch the root locus for the system as a function of active vibration absorber mass, M_c.

49. Figure P8.16 shows the block diagram of the closed-loop control of the linearized magnetic levitation system described in Chapter 2, Problem 58. (*Galvão*, *2003*).
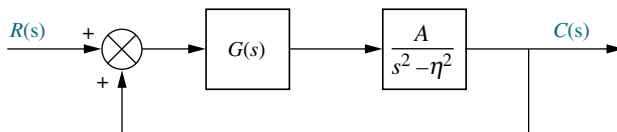

FIGURE P8.16   Linearized magnetic levitation system block diagram

Assuming $A = 1300$ and $\eta = 860$, draw the root locus and find the range of K for closed-loop stability when:

a. $G(s) = K$;

b. $G(s) = \dfrac{K(s + 200)}{s + 1000}$

50. The simplified transfer function model from steering angle $\delta(s)$ to tilt angle $\varphi(s)$ in a bicycle is given by

$$G(s) = \frac{\varphi(s)}{\delta(s)} = \frac{aV}{bh}\frac{s + \dfrac{V}{a}}{s^2 - \dfrac{g}{h}}$$

In this model, h represents the vertical distance from the center of mass to the floor, so it can be readily verified that the model is open-loop unstable. (*Åström*, *2005*). Assume that for a specific bicycle, $a = 0.6$ m, $b = 1.5$ m, $h = 0.8$ m, and $g = 9.8$ m/sec. In order to stabilize the bicycle, it is assumed that the bicycle is placed in the closed-loop configuration shown in Figure P8.3 and that the only available control variable is V, the rear wheel velocity.

a. Find the range of V for closed-loop stability.

b. Explain why the methods presented in this chapter cannot be used to obtain the root locus.

c. Use MATLAB to obtain the system's root locus.

MATLAB
ML

51. A technique to control the steering of a vehicle that follows a line located in the middle of a lane is to define a look-ahead point and measure vehicle deviations with respect to the point. A linearized model for such a vehicle is

$$
\begin{bmatrix} \dot{V} \\ \dot{r} \\ \dot{\psi} \\ \dot{Y_g} \end{bmatrix} = \begin{bmatrix} a_{11} & a_{12} & -b_1 K & \dfrac{b_1 K}{d} \\ a_{21} & a_{22} & -b_2 K & \dfrac{b_2 K}{d} \\ 0 & 1 & 0 & 0 \\ 1 & 0 & U & 0 \end{bmatrix} \begin{bmatrix} V \\ r \\ \psi \\ Y_g \end{bmatrix}
$$

where V = vehicle's lateral velocity, r = vehicle's yaw velocity, ψ = vehicle's yaw position, and Y_g = the y-axis coordinate of the vehicle's center of gravity. K is a parameter to be varied depending upon trajectory changes. In a specific vehicle traveling at a speed of $U = -10$ m/sec, the parameters are $a_{11} = -11.6842$, $a_{12} = 6.7632$, $b_1 = -61.5789$, $a_{21} = -3.5143$, $a_{22} = 24.0257$, and $b_2 = 66.8571$. $d = 5$ m is the look-ahead distance (*Ünyelioğlu, 1997*). Assuming the vehicle will be controlled in closed loop:

a. Find the system's characteristic equation as a function of K.

b. Find the system's root locus as K is varied.

c. Using the root locus found in Part **b**, show that the system will be unstable for all values K.

52. It is known that mammals have hormonal regulation mechanisms that help maintain almost constant calcium plasma levels (0.08–0.1 g/L in dairy cows). This control is necessary to maintain healthy functions, as calcium is responsible for diverse physiological functions, such as bone formation, intracellular communications, and blood clotting. It has been postulated that the mechanism of calcium control resembles that of a PI (proportional-plus-integral) controller. PI controllers (discussed in detail in Chapter 9) are placed in cascade with the plant and used to improve steady-state error. Assume that the PI controller has the form $G_c(s) = \left[K_P + \dfrac{K_I}{S} \right]$ where K_P and K_I are constants. Also assume that the mammal's system accumulates calcium in an integrator-like fashion, namely $P(s) = \dfrac{1}{V_s}$, where V is the plasma volume. The closed-loop model is similar to that of Figure P8.3, where $G(s) = G_c(s)P(s)$ (*Khammash, 2004*).

a. Sketch the system's root locus as a function of K_P, assuming $K_I > 0$ is constant.

b. Sketch the system's root locus as a function of K_I, assuming $K_P > 0$ is constant.

53. Problem 65 in Chapter 7 introduced the model of a TCP/IP router whose packet-drop probability is controlled by using a random early detection (RED) algorithm (*Hollot, 2001*). Using Figure P8.3 as a model, a specific router queue's open-loop transfer function is

$$
G(s) = \frac{7031250 L e^{-0.2s}}{(s + 0.667)(s + 5)(s + 50)}
$$

The function $e^{-0.2s}$ represents delay. To apply the root locus method, the delay function must be replaced with a rational function approximation. A first-order Padé approximation can be used for this purpose. Let $e^{-sD} \approx 1 - Ds$. Using this approximation, plot the root locus of the system as a function of L.

54. For the dynamic voltage restorer (DVR) discussed in Problem 47, Chapter 7, do the following:

a. When $Z_L = \dfrac{1}{sC_L}$, a pure capacitance, the system is more inclined toward instability. Find the system's characteristic equation for this case.

b. Using the characteristic equation found in Part **a**, sketch the root locus of the system as a function of C_L. Let $L = 7.6$ mH, $C = 11$ μF, $\alpha = 26.4$, $\beta = 1$, $K_m = 25$, $K_v = 15$, $K_T = 0.09565$, and $\tau = 2$ ms (*Lam, 2004*).

55. The closed-loop vehicle response in stopping a train depends on the train's dynamics and the driver, who is an integral part of the feedback loop. In Figure P8.3, let the input be $R(s) = v_r$ the reference velocity, and the output $C(s) = v$, the actual vehicle velocity. (*Yamazaki, 2008*) shows that such dynamics can be modeled by $G(s) = G_d(s)G_t(s)$ where

$$
G_d(s) = h\left(1 + \frac{K}{s}\right) \frac{s - \dfrac{L}{2}}{s + \dfrac{L}{2}}
$$

represents the driver dynamics with h, K, and L parameters particular to each individual driver. We assume here that $h = 0.003$ and $L = 1$. The train dynamics are given by

$$
G_t(s) = \frac{k_b f K_p}{M(1 + k_e)s(\tau s + 1)}
$$

where $M = 8000$ kg, the vehicle mass; $k_e = 0.1$ the inertial coefficient; $k_b = 142.5$, the brake gain; $K_p = 47.5$, the pressure gain; $\tau = 1.2$ sec, a time constant; and $f = 0.24$, the normal friction coefficient.

a. Make a root locus plot of the system as a function of the driver parameter K.

b. Discuss why this model may not be an accurate description of a real driver-train situation.

56. Voltage droop control is a technique in which loads are driven at lower voltages than those provided by the source. In general, the voltage is decreased as current demand increases in the load. The advantage of voltage droop is that it results in lower sensitivity to load current variations.

Voltage droop can be applied to the power distribution of several generators and loads linked through a dc bus. In (*Karlsson, 2003*) generators and loads are driven by 3-phase ac power, so they are interfaced to the bus through ac/dc converters. Since each one of the loads works independently, a feedback system shown in Figure P8.17 is used in each to respond equally to bus voltage variations. Given that $C_s = C_r = 8,000\,\mu\text{F}$, $L_{cable} = 50\,\mu\text{H}$, $R_{cable} = 0.06\,\Omega$, $Z_r = R_r = 5\,\Omega$, $\omega_{lp} = 200$ rad/s, $G_{conv}(s) = 1$, $V_{dc-ref} = 750$ V, and $P_{ref-ext} = 0$, do the following:

a. If $Z_{r_{eq}}$ is the parallel combination of R_r and C_r, and $G_{conv}(s) = 1$, find

$$G(s) = \frac{V_s(s)}{I_s(s)} = \frac{V_s(s)}{I_{s-ref}(s)}.$$

b. Write a MATLAB M-file to plot and copy the full root locus for that system, then zoom-in the locus by setting the x-axis (real-axis) limits to -150 to 0 and the y-axis (imaginary-axis) limits to -150 to 150. Copy that plot, too, and find and record the following:

MATLAB
ML

(1) The gain, K, at which the system would have complex-conjugate

closed-loop dominant poles with a damping ratio $\zeta = 0.707$

(2) The coordinates of the corresponding point selected on the root-locus

(3) The values of all closed-loop poles at that gain

(4) The output voltage $v_s(t)$ for a step input voltage $v_{dc-ref}(t) = 750\,u(t)$ volts

c. Plot that step response and use MATLAB **Characteristics** tool (in the graph window) to note on the curve the following parameters:

(1) The actual percent overshoot and the corresponding peak time, T_p

(2) The rise time, T_r, and the settling time, T_s

(3) The final steady-state value in volts

DESIGN PROBLEMS

57. A disk drive is a position control system in which a read/write head is positioned over a magnetic disk. The system responds to a command from a computer to position itself at a particular track on the disk. A physical representation of the system and a block diagram are shown in Figure P8.18.

a. Find K to yield a settling time of 0.1 second.

b. What is the resulting percent overshoot?

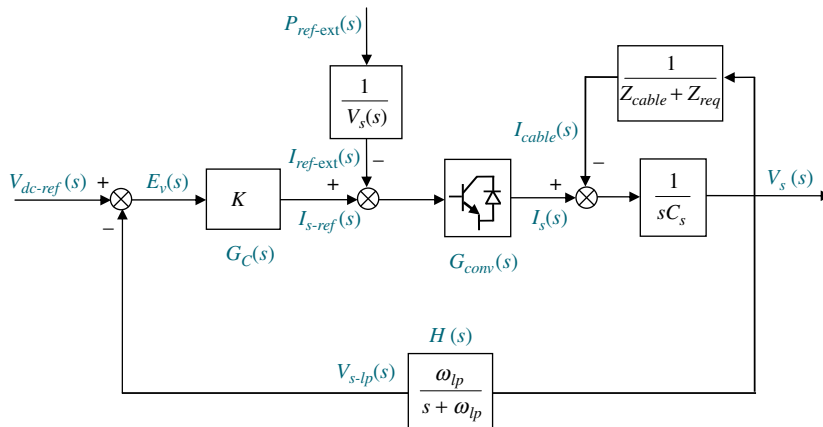**c.** What is the range of K that keeps the system stable?
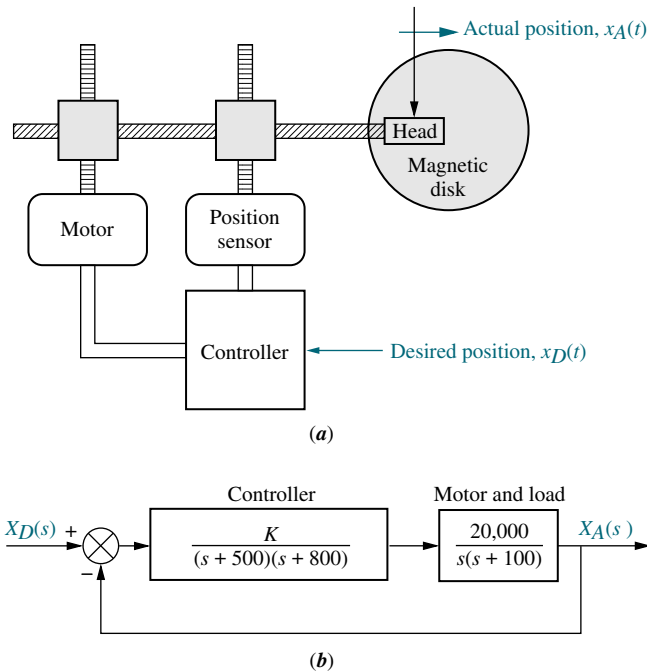

FIGURE P8.17   (© 2003 IEEE)

FIGURE P8.18   Disk drive: **a.** physical representation;
b. block diagram

58. A simplified block diagram of a human
pupil servomechanism is shown in Figure
P8.19. The term $e^{-0.18s}$ represents a time
delay. This function can be approximated by what is
known as a Padé approximation. This approximation
can take on many increasingly complicated forms,
depending upon the degree of accuracy required. If
we use the Padé approximation

WileyPLUS
WPCS
Control Solutions

$$e^{-x} = \cfrac{1}{1 + x + \cfrac{x^2}{2!}}$$

then

$$e^{-0.18s} = \frac{61.73}{s^2 + 11.11s + 61.73}$$

Since the retinal light flux is a function of the
opening of the iris, oscillations in the amount of
retinal light flux imply oscillations of the iris (*Guy*,
1976). Find the following:

a. The value of K that will yield oscillations

b. The frequency of these oscillations

c. The settling time for the iris if K is such that the
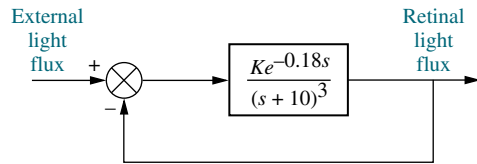eye is operating with 20% overshoot

FIGURE P8.19   Simplified block diagram of pupil
servomechanism

59. An active suspension system for AMTRAK trains
has been proposed. The system uses a pneumatic
actuator in parallel with the passive suspension sys-
tem, as shown in Figure P8.20. The force of the
actuator subtracts from the force applied by the
ground, as represented by displacement, $y_g(t)$. Ac-
celeration is sensed by an accelerometer, and signals
proportional to acceleration and velocity are fed
back to the force actuator. The transfer function
relating acceleration to ground displacement is

$$\frac{\ddot{Y}_m(s)}{Y_g(s)} = \frac{s^2(D_s + K)}{(C_a + M)s^2 + (C_v + D)s + K}$$

Assuming that $M = 1$ and $D = K = C_v = 2$, do the
following (*Cho*, *1985*):

a. Sketch a root locus for this system as C_a varies
from zero to infinity.

b. Find the value of C_a that would yield a damping
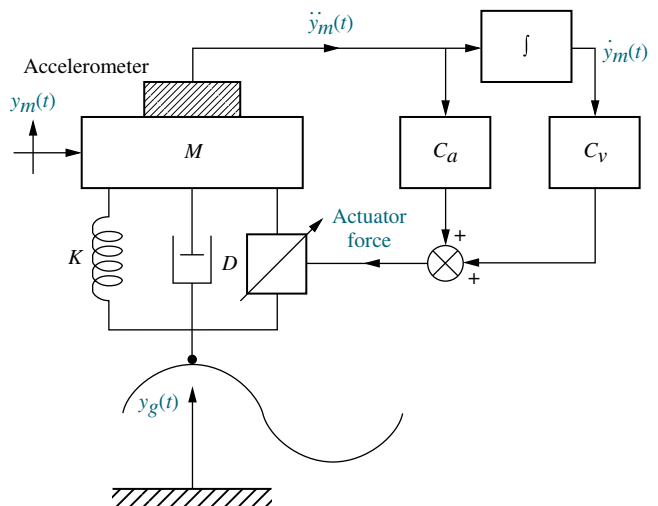ratio of 0.69 for the closed-loop poles.

FIGURE P8.20   Active suspension system (Reprinted with
permission of ASME)

60. The pitch stabilization loop for an F4-E military
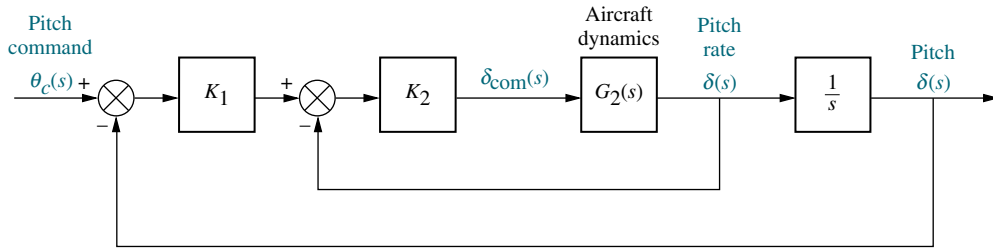aircraft is shown in Figure P8.21. δ_{com} is the elevator

FIGURE P8.21 F4-E pitch stabilization loop

and canard input deflection command to create a pitch rate (see Problem 22, Chapter 3). If

$$G_2(s) = \frac{-508(s+1.6)}{(s+14)(s-1.8)(s+4.9)}$$

do the following (*Cavallo, 1992*):

a. Sketch the root locus of the inner loop.

b. Find the range of K_2 to keep the inner loop stable with just pitch-rate feedback.

c. Find the value of K_2 that places the inner-loop poles to yield a damping ratio of 0.5.

d. For your answer to Part **c**, find the range of K_1 that keeps the system stable.

e. Find the value of K_1 that yields closed-loop poles with a damping ratio of 0.45.

61. Accurate pointing of spacecraft is required for communication and mapping. Attitude control can be implemented by exchanging angular momentum between the body of the spacecraft and an onboard momentum wheel. The block diagram for the pitch axis attitude control is shown in Figure P8.22, where $\theta_c(s)$ is a commanded pitch angle and $\theta(s)$ is the actual pitch angle of the spacecraft. The compensator, which improves pointing accuracy, provides a commanded momentum, $H_c(s)$, to the momentum wheel assembly. The spacecraft momentum, $H_{sys}(s)$, is an additional input to the momentum wheel. This

WileyPLUS

WPCS

Control Solutions

body momentum is given by

$$h_{sys}(t) = I_2\dot{\theta}(t) + h_w(t)$$

where I_2 is the spacecraft moment of inertia about the pitch axis and $h_w(t)$ is the momentum of the wheel. The total torque output from the momentum wheel, T_w, as shown in Figure P8.22, is

$$T_w(t) = \frac{h_{sys}(t) - h_w(t) + h_c(t)}{\tau}$$

If $\tau = 23$ seconds and $I_2 = 9631$ in-lb-s^2, do the following (*Piper, 1992*):

a. Sketch the root locus for the pitch axis control system.

b. Find the value of K to yield a closed-loop step response with 25% overshoot.

c. Evaluate the accuracy of any second-order approximations that were made.

62. During combustion in such devices as gas turbines and jet engines, acoustic waves are generated. These pressure waves can lead to excessive noise as well as mechanical failure. Active control is proposed to reduce this thermoacoustic effect. Specifically, a microphone is used as a sensor to read the sound waves, while a loudspeaker is used as an actuator to set up opposing pressure waves to reduce the effect. A proposed diagram showing the microphone and loudspeaker positioned in the combustion chamber is
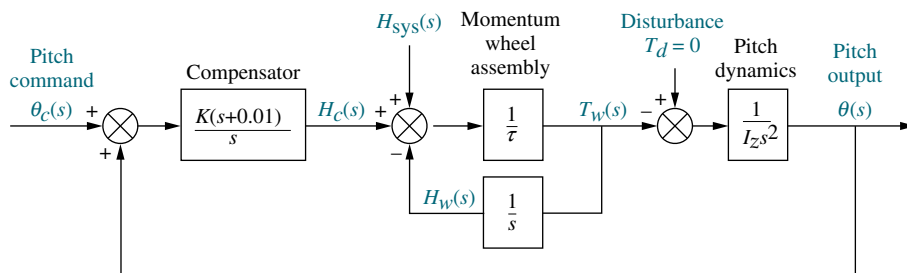

FIGURE P8.22 Pitch axis attitude control system utilizing momentum wheel
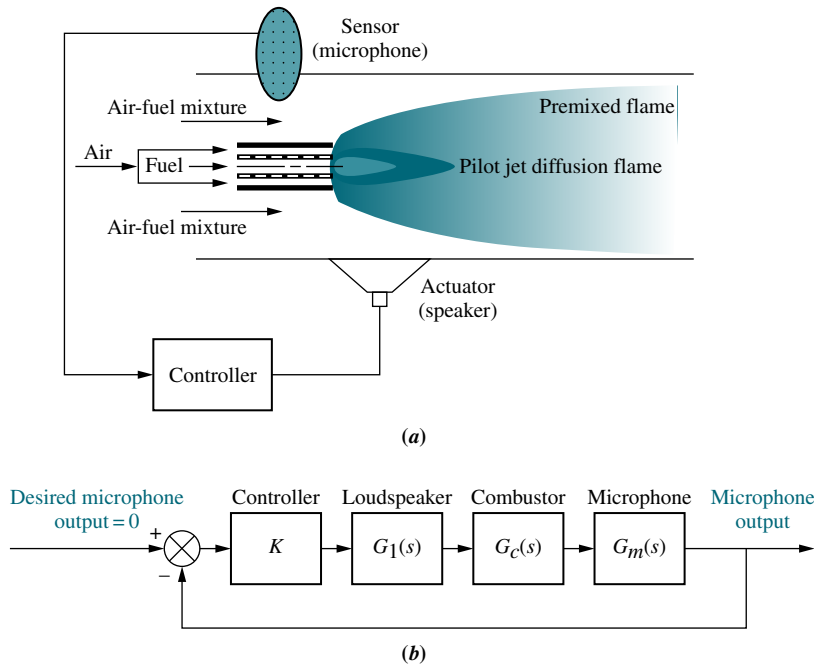
FIGURE P8.23 **a.** Combustor with microphone and loudspeaker (© 1995 IEEE); **b.** block diagram (© 1995 IEEE)

shown in Figure P8.23(*a*). A simplified block diagram of the active control system is shown in Figure P8.23(*b*). The transfer functions are dependent upon microphone and loudspeaker placement and parameters as well as flame placement and parameters. The forward-path transfer function is of the form

$$G(s) = KG_1(s)G_c(s)G_m(s)$$

$$= \frac{K(s + z_f)(s^2 + 2\zeta_2\omega_2 s + \omega_2^2)}{(s + p_f)(s^2 - 2\zeta_1\omega_1 s + \omega_1^2)(s^2 + 2\zeta_2\omega_2 s + \omega_2^2)}$$

where the values for three configurations (A, B, and C) are given in the following table for Part **b** (*Annaswamy, 1995*).

|	**A**	**B**	**C**
z_f	1500	1500	1500
p_f	1000	1000	1000
ζ_z	0.45	0.45	−0.45
ω_z	4500	4500	4500
ζ_1	0.5	−0.5	−0.5
ω_1	995	995	995
ζ_2	0.3	0.3	0.3
ω_2	3500	3500	3500

a. Draw the root locus for each configuration.

b. For those configurations where stable regions of operation are possible, evaluate the range of gain, *K*, for stability.

63. Wind turbines, such as the one shown in Figure P8.24(*a*), are becoming popular as a way of generating electricity. Feedback control loops are designed to control the output power of the turbine, given an input power demand. Blade-pitch control may be used as part of the control loop for a constant-speed, pitch-controlled wind turbine, as shown in Figure P8.24(*b*). The drivetrain, consisting of the windmill rotor, gearbox, and electric generator (see Figure P8.24(*c*)), is part of the control loop. The torque created by the wind drives the rotor. The windmill rotor is connected to the generator through a gearbox.

The transfer function of the drivetrain is

$$\frac{P_o(s)}{T_R(s)} = G_{dt}(s)$$

$$= \frac{3.92 K_{LSS} K_{HSS} K_G N^2 s}{\{N^2 K_{HSS}(J_R s^2 + K_{LSS})(J_G s^2[\tau_{el}s + 1] + K_G) + J_R s^2 K_{LSS}[(J_G s^2 + K_{HSS}) (\tau_{el}s + 1) + K_G s]\}}$$
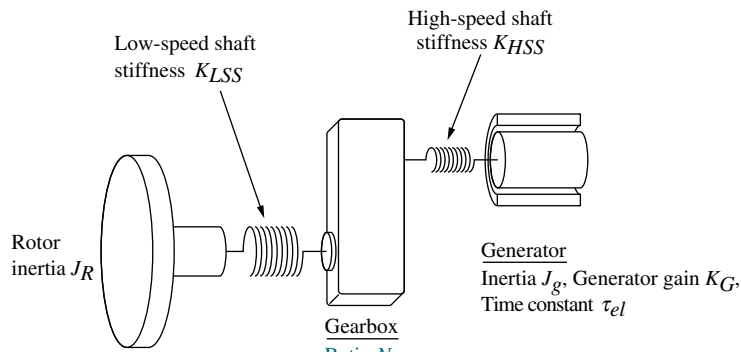
where $P_o(s)$ is the Laplace transform of the output power from the generator and $T_R(s)$ is the Laplace

(*a*)
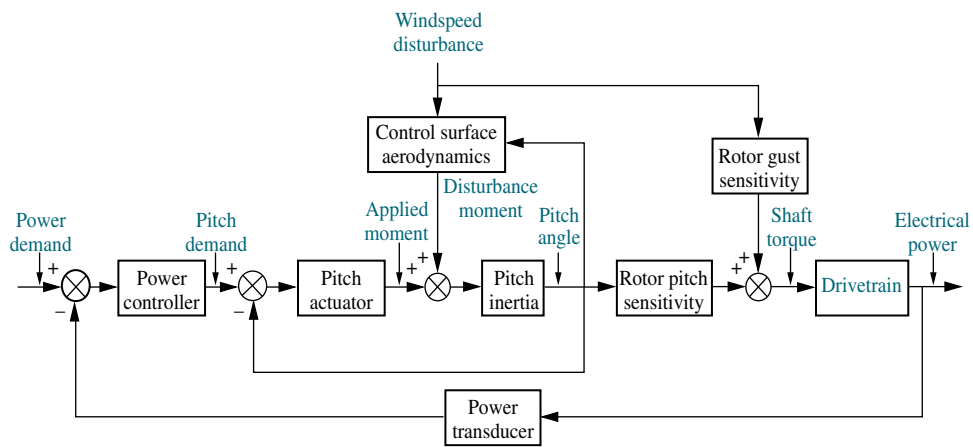
(*b*)

(*c*)

FIGURE P8.24 **a.** Wind turbines generating electricity near Palm Springs, California **b.** control loop for a constant-speed pitch-controlled wind turbine (© 1998 IEEE); **c.** drivetrain (© 1998 IEEE)

transform of the input torque on the rotor. Substituting typical numerical values into the transfer function yields

$$\frac{P_o(s)}{T_R(s)} = G_{dt}(s)$$

$$= \frac{(3.92)(12.6 \times 10^6)(301 \times 10^3)(688)N^2 s}{\{N^2(301 \times 10^3)(190,120s^2 + 12.6 \times 10^6)}$$
$$\times (3.8s^2[20 \times 10^{-3}s + 1] + 668s)$$
$$+ 190,120s^2(12.6 \times 10^6)$$
$$\times [(3.8s^2 + 301 \times 10^3)$$
$$\times (20 \times 10^{-3}s + 1) + 668s]\}$$

(*Anderson*, *1998*). Do the following for the drive-train dynamics, making use of any computational aids at your disposal:

a. Sketch a root locus that shows the pole locations of $G_{dt}(s)$ for different values of gear ratio, N.

b. Find the value of N that yields a pair of complex poles of $G_{dt}(s)$ with a damping ratio of 0.5.

64. A hard disk drive (HDD) arm has an open-loop unstable transfer function,

$$P(s) = \frac{X(s)}{F(s)} = \frac{1}{I_b s^2}$$

where $X(s)$ is arm displacement and $F(s)$ is the applied force (*Yan*, *2003*). Assume the arm has an inertia of $I_b = 3 \times 10^{-5}$ kg-m^2 and that a lead controller, $G_c(s)$ (used to improve transient response and discussed in Chapter 9), is placed in cascade to yield

$$P(s)G_c(s) = G(s) = \frac{K}{I_b}\frac{(s+1)}{s^2(s+10)}$$

as in Figure P8.3.

a. Plot the root locus of the system as a function of K.

b. Find the value of K that will result in dominant complex conjugate poles with a $\zeta = 0.7$ damping factor.

65. A robotic manipulator together with a cascade PI controller (used to improve steady-state response and discussed in Chapter 9) has a transfer function (*Low*, *2005*)

$$G(s) = \left(K_p + \frac{K_1}{s}\right)\frac{48,500}{s^2 + 2.89s}$$

Assume the robot's joint will be controlled in the configuration shown in Figure P8.3.

a. Find the value of K_I that will result in $e_{ss} = 2\%$ for a parabolic input.

b. Using the value of K_I found in Part **a**, plot the root locus of the system as a function of K_P.

c. Find the value of K_P that will result in a real pole at -1. Find the location of the other two poles.

66. An active system for the elimina- Gui Tool tion of floor vibrations due to **GUIT** human presence is presented in (*Nyawako, 2009*). The system consists of a sensor that measures the floor's vertical acceleration and an actuator that changes the floor characteristics. The open-loop transmission of the particular setup used can be described by $G(s) = KG_a(s)F(s)G_m(s)$, where the actuator's transfer function is

$$G_a(s) = \frac{10.26}{s^2 + 11.31s + 127.9}$$

The floor's dynamic charactristics can be modeled by

$$F(s) = \frac{6.667 \times 10^{-5}s^2}{s^2 + 0.2287s + 817.3}$$

The sensor's transfer function is

$$G_m(s) = \frac{s}{s^2 + 5.181s + 22.18}$$

and K is the gain of the controller. The system operations can be described by the unity-gain feedback loop of Figure P8.3.

a. Use MATLAB's SISO Design Tool to obtain the root locus of the system in terms of K.

b. Find the range of K for closed-loop stability.

c. Find, if possible, a value of K that will yield a closed-loop overdamped response.

67. Many implantable medical devices such as pacemakers, retinal implants, deep brain stimulators, and spinal cord stimulators are powered by an in-body battery that can be charged through a transcutaneous inductive device. Optimal battery charge can be obtained when the out-of-body charging circuit is in resonance with the implanted charging circuit (*Baker, 2007*). Under certain conditions, the coupling of both resonant circuits can be modeled by the feedback system in Figure P8.3 where

$$G(s) = \frac{Ks^4}{\left(s^2 + 2\zeta\omega_n s + \omega_n^2\right)^2}$$

The gain K is related to the magnetic coupling between the external and in-body circuits. K may vary due to positioning, skin conditions, and other variations. For this problem let $\zeta = 0.5$ and $\omega_n = 1$.

a. Find the range of K for closed-loop stability.

b. Draw the corresponding root locus.

68. It is important to precisely control the amount of organic fertilizer applied to a specific crop area in order to provide specific nutrient quantities and to avoid unnecessary environmental pollution. A precise delivery liquid manure machine has been developed for this purpose (*Saeys, 2008*). The system consists of a pressurized tank, a valve, and a rheological flow sensor. After simplification, the system can be modeled as a closed-loop negative-feedback system with a forward-path transfer function

MATLAB
ML

Gui Tool
GUIT

$$G(s) = \frac{2057.38K(s^2 - 120s + 4800)}{s(s + 13.17)(s^2 + 120s + 4800)}$$

consisting of an electrohydraulic system in cascade with the gain of the manure flow valve and a variable gain, K. The feedback path is comprised of

$$H(s) = \frac{10(s^2 - 4s + 5.333)}{(s + 10)(s^2 + 4s + 5.333)}$$

a. Use the SISO Design Tool in MATLAB to obtain the root locus of the system.

b. Use the SISO Design Tool to find the range of K for closed-loop stability.

c. Find the value of K that will result in the smallest settling time for this system.

d. Calculate the expected settling time for a step input with the value of K obtained in Part **c**.

e. Check your result through a step-response simulation.

69. Harmonic drives are very popular for use in robotic manipulators due to their low backlash, high torque transmission, and compact size (*Spong, 2006*). The problem of joint flexibility is sometimes a limiting factor in achieving good performance. Consider

MATLAB
ML

that the idealized model representing joint flexibility is shown in Figure P8.25. The input to the drive is from an actuator and is applied at θ_m. The output is connected to a load at θ_l. The spring represents the joint flexibility and B_m and B_l represent the viscous damping of the actuator and load, respectively. Now we insert the device into the feedback loop shown in Figure P8.26. The first block in the forward path is a PD controller, which we will study in the next chapter. The PD controller is used to improve transient response performance.
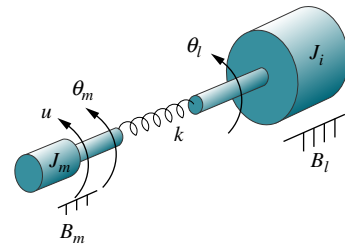

FIGURE P8.25 Idealized model representing joint flexibility (Reprinted with permission of John Wiley & Sons, Inc.)
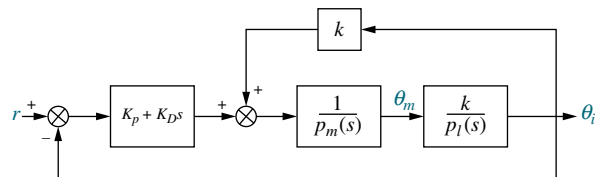

FIGURE P8.26 Joint flexibility model inserted in feedback loop. (Reprinted with permission of John Wiley & Sons, Inc.)

Use MATLAB to find the gain K_D to yield an approximate 5% overshoot in the step response given the following parameters: J_l=10; B_l=1; k=100; J_m=2; B_m=0.5; $\dfrac{K_P}{K_D} = 0.25$; $p_l(s) = J_l s^2 + B_l s + k$; and $p_m(s) = J_m s^2 + B_m s + k$

70. Using LabVIEW, the Control Design and Simulation Module, and the MathScript RT Module, open and customize the Interactive Root Locus VI from the Examples to implement the system of Problem 69. Select the parameter K_D to meet the requirement of Problem 69 by varying the location of the closed-loop poles on the root locus. Be sure

LabVIEW
LV

your front panel shows the following: (1) open-loop transfer function, (2) closed-loop transfer function, (3) root locus, (4) list of closed-loop poles, and (5) step response.

71. An automatic regulator is used to control the field current of a three-phase synchronous machine with identical symmetrical armature windings (*Stapleton, 1964*). The purpose of the regulator is to maintain the system voltage constant within certain limits. The transfer function of the synchronous machine is

`MATLAB`
`ML`

$$G_{sm}(s) = \frac{\Delta\delta(s)}{\Delta P_m(s)} = \frac{M(s - z_1)(s - z_2)}{(s - p_1)(s - p_2)(s - p_3)}$$

which relates the variation of rotor angle, $\Delta\delta(s)$, to the change in the synchronous machine's shaft power, $\Delta P_m(s)$. The closed-loop system is shown in Figure P8.3, where $G(s) = KG_C(s)G_{sm}(s)$ and K is a gain to be adjusted. The regulator's transfer function, $G_c(s)$, is given by:

$$G_c(s) = \frac{\mu/T_e}{s + \frac{1}{T_e}}$$

Assume the following parameter values:

$\mu = 4, M = 0.117, T_e = 0.5, z_{1,2} = -0.071 \pm j6.25,$
$p_1 = -0.047,$ and $p_{2,3} = -0.262 \pm j5.1,$

and do the following:

Write a MATLAB M-file to plot the root locus for the system and to find the following:

a. The gain K at which the system becomes marginally stable

b. The closed-loop poles, p, and transfer function, $T(s)$, corresponding to a 16% overshoot

c. The coordinates of the point selected on the root-locus corresponding to 16% overshoot

d. A simulation of the unit-step response of the closed-loop system corresponding to your 16% overshoot design. Note in your simulation the following values: (1) actual percent overshoot, (2)

corresponding peak time, T_p, (2) rise time, T_r, (3) settling time, T_s, and (4) final steady-state value.

PROGRESSIVE ANALYSIS AND DESIGN PROBLEMS

72. **High-speed rail pantograph.** Problem 21 in Chapter 1 discusses the active control of a pantograph mechanism for high-speed rail systems. In Problem 79, Chapter 5, you found the block diagram for the active pantograph control system. Use your block diagram to do the following (*O'Connor, 1997*):

a. Sketch the root locus.

b. Assume a second-order approximation and find the gain, K, to yield a closed-loop step response that has 38% overshoot.

c. Estimate settling time and peak time for the response designed in Part **b.**

d. Discuss the validity of your second-order approximation.

e. Use MATLAB to plot the closed-loop step response for the value of K found in Part **b.** Compare the plot to predicted values found in Parts **b** and **c.**

`MATLAB`
`ML`

73. **Control of HIV/AIDS.** In the linearized model of Chapter 6, Problem 68, where virus levels are controlled by means of RTIs, the open-loop plant transfer function was shown to be

$$P(s) = \frac{Y(s)}{U_1(s)} = \frac{-520s - 10.3844}{s^3 + 2.6817s^2 + 0.11s + 0.0126}$$

The amount of RTIs delivered to the patient will automatically be calculated by embedding the patient in the control loop as $G(s)$ shown in Figure P6.20 (*Craig, 2004*).

a. In the simplest case, $G(s) = K$, with $K > 0$. Note that this effectively creates a positive-feedback loop because the negative sign in the numerator of $P(s)$ cancels out with the negative-feedback sign in the summing junction. Use positive-feedback rules to plot the root locus of the system.

b. Now assume $G(s) = -K$ with $K > 0$. The system is now a negative-feedback system. Use negative-feed-back rules to draw the root locus. Show that in this case the system will be closed-loop stable for all $K > 0$.

74. **Hybrid vehicle.** In chapter 7, Figure P7.34 shows the block diagram of the speed control of

`MATLAB`
`ML`

an HEV rearranged as a unity feedback system (*Preitl, 2007*).

Let the transfer function of the speed controller be

$$G_{SC}(s) = K_{P_{sc}} + \frac{K_{I_{sc}}}{s} = \frac{K_{P_{sc}}\left(s + \frac{K_{I_{sc}}}{K_{P_{sc}}}\right)}{s}$$

a. Assume first that the speed controller is configured as a proportional controller ($K_{I_{sc}} = 0$ and $G_{SC}(s) = K_{P_{sc}}$). Calculate the forward-path open-loop poles. Now use MATLAB to plot the system's root locus and find the gain, $K_{P_{sc}}$ that yields a critically damped closed-loop response. Finally, plot the time-domain response, $c(t)$, for a unit-step input using MATLAB. Note on the curve the rise time, T_r, and settling time, T_s.

b. Now add an integral gain, $K_{I_{sc}}$, to the controller, such that $K_{I_{sc}}/K_{P_{sc}} = 0.4$. Use MATLAB to plot the root locus and find the proportional gain, $K_{P_{sc}}$, that could lead to a closed-loop unit-step response with 10% overshoot. Plot $c(t)$ using MATLAB and note on the curve the peak time, T_p, and settling time, T_s. Does the response obtained resemble a second-order underdamped response?

Cyber Exploration Laboratory

Experiment 8.1

Objective To verify the effect of open-loop poles and zeros upon the shape of the root locus. To verify the root locus as a tool for estimating the effect of open-loop gain upon the transient response of closed-loop systems.

Minimum Required Software Packages MATLAB and the Control System Toolbox

Prelab

1. Sketch two possibilities for the root locus of a unity negative-feedback system with the open-loop pole-zero configuration shown in Figure P8.27.
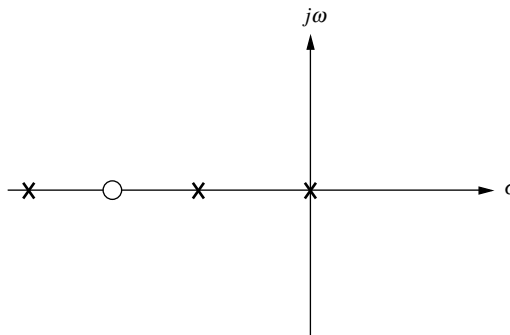

FIGURE P8.27

2. If the open-loop system of Prelab 1 is $G(s) = \dfrac{K(s + 1.5)}{s(s + 0.5)(s + 10)}$, estimate the percent overshoot at the following values of gain, *K*: 20, 50, 85, 200, and 700.

Lab

1. Using Matlab's SISO Design Tool, set up a negative unity feedback system with $G(s) = \dfrac{K(s + 6)}{s(s + 0.5)(s + 10)}$ to produce a root locus. For convenience, set up the zero

at -6 using SISO Design Tool's compensator function by simply dragging a zero to -6 on the resulting root locus. Print the root locus for the zero at -6. Move the zero to the following locations and print out a root locus at each location: -2, -1.5, -1.37, and -1.2.

2. Using Matlab's SISO Design Tool, set up a negative unity feedback system with $G(s) = \dfrac{K(s+1.5)}{s(s+0.5)(s+10)}$ to produce a root locus. Open the LTI Viewer for SISO Design Tool to show step responses. Using the values of K specified in Prelab 2, record the percent overshoot and settling time and print the root loci and step response for each value of K.

Postlab

1. Discuss your findings from Prelab 1 and Lab 1. What conclusions can you draw?

2. Make a table comparing percent overshoot and settling time from your calculations in Prelab 2 and your experimental values found in Lab 2. Discuss the reasons for any discrepancies. What conclusions can you draw?

Experiment 8.2

Objective   To use MATLAB to design the gain of a controller via root locus.

Minimum Required Software Package   MATLAB with the Control Systems Toolbox.

Prelab   The open-loop system dynamics model for the NASA eight-axis Advanced Research Manipulator II (ARM II) electromechanical shoulder joint/link, actuated by an armature-controlled dc servomotor is shown in Figure P8.28.

The ARM II shoulder joint constant parameters are $K_a = 12$, $L = 0.006$ H, $R = 1.4\,\Omega$, $K_b = 0.00867$, $n = 200$, $K_m = 4.375$, $J = J_m + J_L/n^2$, $D = D_m + D_L/n^2$, $J_L = 1$, $D_L = 0.5$, $J_m = 0.00844$, and $D_m = 0.00013$ (*Craig, 2005*), (*Nyzen, 1999*), (*Williams, 1994*).

a. Obtain the equivalent open-loop transfer function, $G(s) = \dfrac{\theta_L(s)}{V_{ref}(s)}$.

b. The loop is to be closed by cascading a controller, $G_c(s) = K_D s + K_P$, with $G(s)$ in the forward path forming an equivalent forward-transfer function, $G_e(s) = G_c(s)G(s)$. Parameters of $G_c(s)$ will be used to design a desired transient performance. The input to the closed-loop system is a voltage, $V_I(s)$, representing the desired angular displacement of the robotic joint with a ratio of 1 volt equals 1 radian. The output of the closed-loop system is the actual angular displacement of the joint, $\theta_L(s)$. An encoder in the feedback path, K_e, converts the actual joint displacement to a voltage with a ratio of 1 radian equals 1 volt. Draw the closed-loop system showing all transfer functions.
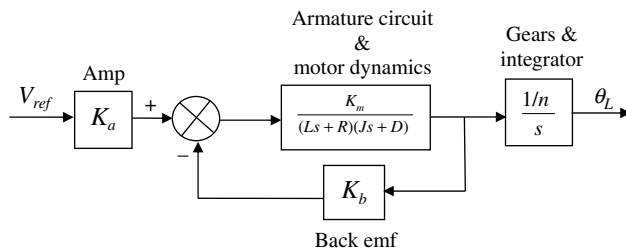
c. Find the closed-loop transfer function.

FIGURE P8.28   Open-loop model for ARM ll

Lab Let $\dfrac{K_P}{K_D} = 4$ and use MATLAB to design the value of K_D to yield a step response with a maximum percent overshoot of 0.2%.

Postlab

1. Discuss the success of your design.

2. Is the steady-state error what you would expect? Give reasons for your answer.

Experiment 8.3

Objective   To use LabVIEW to design the gain of a controller via root locus.

Minimum Required Software Package   LabVIEW with the Control Design and Simulation Module, and the MathScript RT Module.

Prelab   Complete the Prelab to Experiment 8.2 if you have not already done so.

Lab   Let $\dfrac{K_P}{K_D} = 4$. Use LabVIEW to open and customize the Interactive Root Locus VI from the Examples in order to implement a design of K_D to yield a step response with a maximum percent overshoot of 0.2%. Use a hybrid graphical/ MathScript approach.

Postlab

1. Discuss the success of your design.

2. Is the steady-state error what you would expect? Give reasons for your answer.

Bibliography

Anderson, C. G., Richon, J.-B., and Campbell, T. J. An Aerodynamic Moment-Controlled Surface for Gust Load Alleviation on Wind Turbine Rotors. *IEEE Transactions on Control System Technology*, vol. 6, no. 5, September 1998, pp. 577–595.

Annaswamy, A. M., and Ghonien, A. F. Active Control in Combustion Systems. *IEEE Control Systems*, December 1995, pp. 49–63.

Åström, K., Klein, R. E., and Lennartsson, A. Bicycle Dynamics and Control. *IEEE Control Systems*, August 2005, pp. 26–47.

Baker, M. W., and Sarpeshkar, R. Feedback Analysis and Design of RF Power Links for Low-Power Bionic Systems. *IEEE Transactions on Biomedical, Circuits and Systems*. vol. 1, 2007, pp. 28–38.

Bruner, A. M., Belvin, W. K., Horta, L. G., and Juang, J. Active Vibration Absorber for the CSI Evolutionary Model: Design and Experimental Results. *Journal of Guidance, Control, and Dynamics*, vol. 15, no. 5, September–October 1992, pp. 1253–1257.

Cavallo, A., De Maria, G., and Verde, L. Robust Flight Control Systems: A Parameter Space Design. *Journal of Guidance, Control, and Dynamics*, vol. 15, no. 5, September–October 1992, pp. 1207–1215.

Cho, D., and Hedrick, J. K. Pneumatic Actuators for Vehicle Active Suspension Applications. *Journal of Dynamic Systems, Measurement, and Control*, March 1985, pp. 67–72.

Craig, I. K., Xia, X., and Venter, J. W., Introducing HIV/AIDS Education into the Electrical Engineering Curriculum at the University of Pretoria. *IEEE Transactions on Education*, vol. 47, no. 1, February 2004, pp. 65–73.

Craig, J. J, *Introduction to Robotics. Mechanics and Control*, 3d ed. Prentice Hall, Upper Saddle River, NJ, 2005.

Dorf, R. C. *Modern Control Systems*, 5th ed. Addison-Wesley, Reading, MA., 1989.

Evans, W. R. Control System Synthesis by Root Locus Method. *AIEE Transactions*, vol. 69, 1950, pp. 66–69.

Evans, W. R. Graphical Analysis of Control Systems. *AIEE Transactions*, vol. 67, 1948, pp. 547–551.

Franklin, G. F., Powell, J. D., and Emami-Naeini, A. *Feedback Control of Dynamic Systems*, 2d ed. Addison-Wesley, Reading, MA., 1991.

Galvão, K. H. R., Yoneyama, T., and de Araújo, F. M. U. A Simple Technique for Identifying a Linearized Model for a Didactic Magnetic Levitation System. *IEEE Transactions on Education*, vol. 46, no. 1, February 2003, pp. 22–25.

Guy, W., *The Human Pupil Servomechanism*. Computers in Education Division of ASEE, Application Note No. 45, 1976.

Hardy, H. L. Multi-Loop Servo Controls Programmed Robot. *Instruments and Control Systems*, June 1967, pp. 105–111.

Hollot, C. V., Misra, V., Towsley, D., and Gong, W. A Control Theoretic Analysis of RED. *Proceedings of IEEE INFOCOM*, 2001, pp. 1510–1519.

Johnson, H., et al. *Unmanned Free-Swimming Submersible(UFSS) System Description*. NRL Memorandum Report 4393. Naval Research Laboratory, Washington, D.C., 1980.

Karlsson, P., and Svesson, J. DC Bus Voltage Control for a Distributed Power System, *IEEE Trans. on Power Electronics*, vol. 18, no. 6, 2003, pp. 1405–1412.

Khammash, M., and El-Samad, H. Systems Biology: From Physiology to Gene Regulation. *IEEE Control Systems*, August 2004, pp. 62–76.

Kuo, B. C. *Automatic Control Systems*, 6th ed. Prentice Hall, Upper Saddle River, NJ, 1991.

Lam, C. S., Wong, M. C., and Han, Y. D. Stability Study on Dynamic Voltage Restorer (DVR). Power Electronics Systems and Applications 2004; Proceedings of the First International Conference on Power Electronics, 2004, pp. 66–71.

Low, K. H., Wang, H., Liew, K. M., and Cai, Y. Modeling and Motion Control of Robotic Hand for Telemanipulation Application. *International Journal of Software Engineering and Knowledge Engineering*, vol. 15, 2005, pp. 147–152.

Nyawako, D., and Reynolds, P. Response-Dependent Velocity Feedback Control for Mitigation of Human-Induced Floor Vibrations, *Smart Materials and Structures*, vol. 18, IOP Publishing Ltd., UK, 2009, pp. 1–13.

Nyzen, R. J. *Analysis and Control of an Eight-Degree-of-Freedom Manipulator*, Ohio University Masters Thesis, Mechanical Engineering, Dr. Robert L. Williams II, advisor, August 1999.

O'Connor, D. N., Eppinger, S. D., Seering, W. P., and Wormly, D. N. Active Control of a High-Speed Pantograph. *Journal of Dynamic Systems, Measurements, and Control*, vol. 119, March 1997, pp. 1–4.

Piper, G. E., and Kwatny, H. G. Complicated Dynamics in Spacecraft Attitude Control Systems. *Journal of Guidance, Control, and Dynamics*, vol. 15, no. 4, July–August 1992, pp. 825–831.

Preitl, Z., Bauer, P., and Bokor, J. A Simple Control Solution for Traction Motor Used in Hybrid Vehicles. *Fourth International Symposium on Applied Computational Intelligence and Informatics*. IEEE, 2007.

Saeys, W., Deblander, J., Ramon, H., and Anthonis, J. High-Performance Flow Control for Site-Specific Application of Liquid Manure, *Biosystems Engineering*, vol. 99, 2008, pp. 22–34.

Spong, M., Hutchinson, S., and Vidyasagar, M. *Robot Modeling and Control*. John Wiley & Sons, Hoboken, NJ, 2006.

Stapleton, C.A. Root-Locus Study of Synchronous-Machine Regulation. *IEE Proceedings*, vol. 111, issue 4, 1964, pp. 761–768.

Ünyelioğlu, K. A., Hatopoğlu, C., and Özgüner, Ü. Design and Stability Analysis of a Lane Following Controller. *IEEE Transactions on Control Systems Technology*, vol. 5, 1997, pp. 127–134.

Williams, R. L. II. Local Performance Optimization for a Class of Redundant Eight-Degree-of-Freedom Manipulators. *NASA Technical Paper 3417*, NASA Langley Research Center, Hampton VA, March 1994.

Yamazaki, H., Marumo, Y., Iizuka, Y., and Tsunashima, H. Driver Model Simulation for Railway Brake Systems, *Fourth IET Int. Conf. on Railway Condition Monitoring*, 2008.

Yan, T., and Lin, R. Experimental Modeling and Compensation of Pivot Nonlinearity in Hard Disk Drives. *IEEE Transactions on Magnetics*, vol. 39, 2003, pp. 1064–1069.

Design via Root Locus
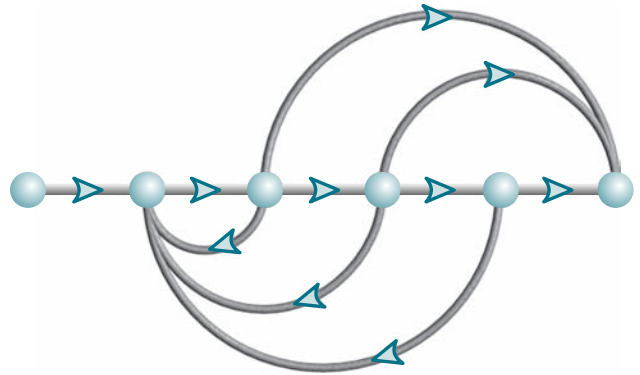
Chapter Learning Outcomes

After completing this chapter the student will be able to:

- Use the root locus to design cascade compensators to improve the steady-state error (Sections 9.1–9.2)
- Use the root locus to design cascade compensators to improve the transient response (Section 9.3)
- Use the root locus to design cascade compensators to improve both the steady-state error and the transient response (Section 9.4)
- Use the root locus to design feedback compensators to improve the transient response (Section 9.5)
- Realize the designed compensators physically (Section 9.6)

Case Study Learning Outcomes

You will be able to demonstrate your knowledge of the chapter objectives with case studies as follows:

- Given the antenna azimuth position control system shown on the front endpapers, you will be able to design a cascade compensator to meet transient response and steady-state error specifications.
- Given the pitch or heading control system for the UFSS vehicle shown on the back endpapers, you will be able to design a cascade or feedback compensator to meet transient response specifications.

9.1 Introduction

In Chapter 8, we saw that the root locus graphically displayed both transient response and stability information. The locus can be sketched quickly to get a general idea of the changes in transient response generated by changes in gain. Specific points on the locus also can be found accurately to give quantitative design information.

   The root locus typically allows us to choose the proper loop gain to meet a transient response specification. As the gain is varied, we move through different regions of response. Setting the gain at a particular value yields the transient response dictated by the poles at that point on the root locus. Thus, *we are limited to those responses that exist along the root locus.*

Improving Transient Response

Flexibility in the design of a desired transient response can be increased if we can design for transient responses that are not on the root locus. Figure 9.1(*a*) illustrates the concept. Assume that the desired transient response, defined by percent overshoot and settling time, is represented by point *B*. Unfortunately, on the current root locus at the specified percent overshoot, we only can obtain the settling time represented by point *A* after a simple gain adjustment. Thus, our goal is to speed up the response at *A* to that of *B*, without affecting the percent overshoot. This increase in speed cannot be accomplished by a simple gain adjustment, since point *B* does not lie on the root locus. Figure 9.1(*b*) illustrates the improvement in the transient response we seek: The faster response has the same percent overshoot as the slower response.
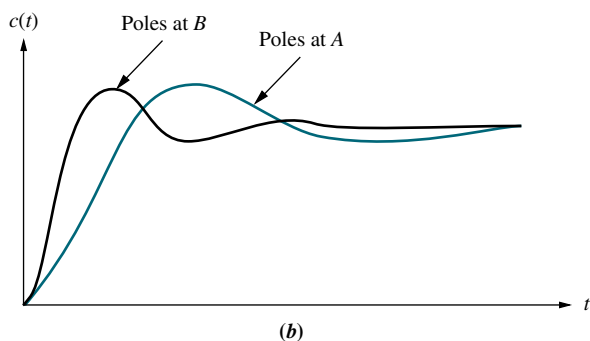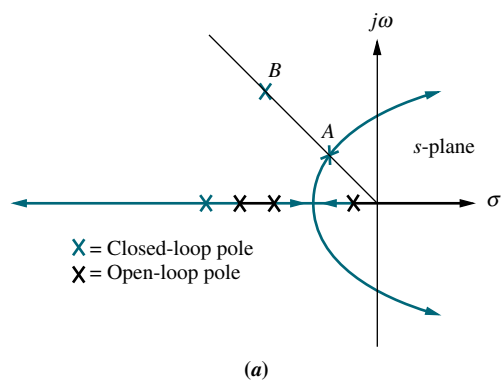

(*a*)

FIGURE 9.1   a. Sample root locus, showing possible design point via gain adjustment (*A*) and desired design point that cannot be met via simple gain adjustment (*B*); **b.** responses from poles at *A* and *B*

(*b*)

One way to solve our problem is to replace the existing system with a system whose root locus intersects the desired design point, *B*. Unfortunately, this replacement is expensive and counterproductive. Most systems are chosen for characteristics other than transient response. For example, an elevator cage and motor are chosen for speed and power. Components chosen for their transient response may not necessarily meet, for example, power requirements.

Rather than change the existing system, we augment, or *compensate*, the system with *additional* poles and zeros, so that the compensated system has a root locus that goes through the desired pole location for some value of gain. One of the advantages of compensating a system in this way is that additional poles and zeros can be added at the low-power end of the system before the plant. Addition of compensating poles and zeros need not interfere with the power output requirements of the system or present additional load or design problems. The compensating poles and zeros can be generated with a passive or an active network.

A possible disadvantage of compensating a system with additional open-loop poles and zeros is that the system order can increase, with a subsequent effect on the desired response. In Chapters 4 and 8, we discussed the effect of additional closed-loop poles and zeros on the transient response. At the beginning of the design process discussed in this chapter, we determine the proper location of additional *open-loop* poles and zeros to yield the desired second-order *closed-loop* poles. However, we do not know the location of the higher-order *closed-loop* poles until the end of the design. Thus, we should evaluate the transient response through simulation after the design is complete to be sure the requirements have been met.

In Chapter 12, when we discuss state-space design, the disadvantage of finding the location of higher-order closed-loop poles after the design will be eliminated by techniques that allow the designer to specify and design the location of all the closed-loop poles at the beginning of the design process.

One method of compensating for transient response that will be discussed later is to insert a differentiator in the forward path in parallel with the gain. We can visualize the operation of the differentiator with the following example. Assuming a position control with a step input, we note that the error undergoes an initial large change. Differentiating this rapid change yields a large signal that drives the plant. The output from the differentiator is much larger than the output from the pure gain. This large, initial input to the plant produces a faster response. As the error approaches its final value, its derivative approaches zero, and the output from the differentiator becomes negligible compared to the output from the gain.

Improving Steady-State Error

Compensators are not only used to improve the transient response of a system; they are also used *independently* to improve the steady-state error characteristics. Previously, when the system gain was adjusted to meet the transient response specification, steady-state error performance deteriorated, since both the transient response and the static error constant were related to the gain. The higher the gain, the smaller the steady-state error, but the larger the percent overshoot. On the other hand, reducing gain to reduce overshoot increased the steady-state error. If we use dynamic compensators, compensating networks can be designed that will allow us to meet transient and steady-state error specifications *simultaneously*.[1] We no longer

---

[1] The word *dynamic* describes compensators with noninstantaneous transient response. The transfer functions of such compensators are functions of the Laplace variable, *s*, rather than pure gain.
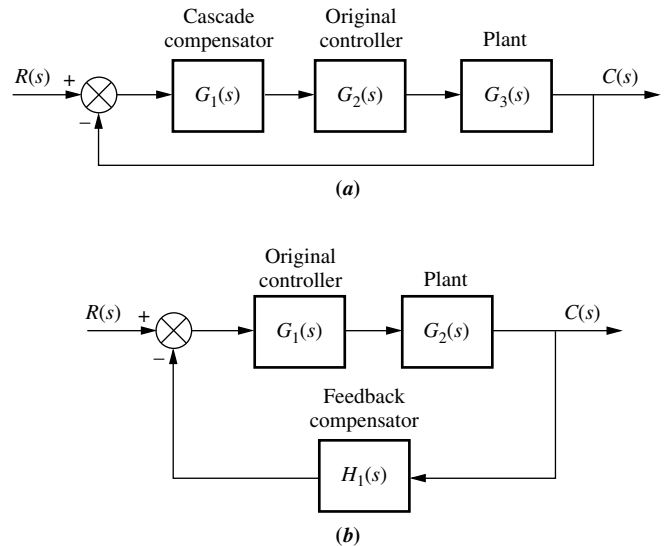
FIGURE 9.2 Compensation techniques: **a.** cascade; **b.** feedback

need to compromise between transient response and steady-state error, as long as the system operates in its linear range.

In Chapter 7, we learned that steady-state error can be improved by adding an open-loop pole at the origin in the forward path, thus increasing the system type and driving the associated steady-state error to zero. This additional pole at the origin requires an integrator for its realization.

In summary, then, transient response is improved with the addition of differentiation, and steady-state error is improved with the addition of integration in the forward path.

Configurations

Two configurations of compensation are covered in this chapter: cascade compensation and feedback compensation. These methods are modeled in Figure 9.2. With cascade compensation, the compensating network, $G_1(s)$, is placed at the low-power end of the forward path in cascade with the plant. If feedback compensation is used, the compensator, $H_1(s)$, is placed in the feedback path. Both methods change the open-loop poles and zeros, thereby creating a new root locus that goes through the desired closed-loop pole location.

Compensators

Compensators that use pure integration for improving steady-state error or pure differentiation for improving transient response are defined as *ideal compensators*. Ideal compensators must be implemented with active networks, which, in the case of electric networks, require the use of active amplifiers and possible additional power sources. An advantage of ideal integral compensators is that steady-state error is reduced to zero. Electromechanical ideal compensators, such as tachometers, are often used to improve transient response, since they can be conveniently interfaced with the plant.

Other design techniques that preclude the use of active devices for compensation can be adopted. These compensators, which can be implemented with passive elements such as resistors and capacitors, do not use pure integration and differentiation and are not ideal compensators. Advantages of passive networks are that they

are less expensive and do not require additional power sources for their operation. Their disadvantage is that the steady-state error is not driven to zero in cases where ideal compensators yield zero error.

Thus, the choice between an active or a passive compensator revolves around cost, weight, desired performance, transfer function, and the interface between the compensator and other hardware. In Sections 9.2, 9.3, and 9.4, we first discuss cascade compensator design using ideal compensation and follow with cascade compensation using compensators that are not implemented with pure integration and differentiation.

9.2   Improving Steady-State Error via Cascade Compensation

In this section, we discuss two ways to improve the steady-state error of a feedback control system using cascade compensation. One objective of this design is to improve the steady-state error without appreciably affecting the transient response.

The first technique is *ideal integral compensation*, which uses a pure integrator to place an open-loop, forward-path pole at the origin, thus increasing the system type and reducing the error to zero. The second technique does not use pure integration. This compensation technique places the pole near the origin, and although it does not drive the steady-state error to zero, it does yield a measurable reduction in steady-state error.

While the first technique reduces the steady-state error to zero, the compensator must be implemented with active networks, such as amplifiers. The second technique, although it does not reduce the error to zero, does have the advantage that it can be implemented with a less expensive passive network that does not require additional power sources.

The names associated with the compensators come either from the method of implementing the compensator or from the compensator's characteristics. Systems that feed the error forward to the plant are called *proportional control systems*. Systems that feed the integral of the error to the plant are called *integral control systems*. Finally, systems that feed the derivative of the error to the plant are called *derivative control systems*. Thus, in this section we call the ideal integral compensator a *proportional-plus-integral (PI) controller*, since the implementation, as we will see, consists of feeding the error (proportional) plus the integral of the error forward to the plant. The second technique uses what we call a *lag compensator*. The name of this compensator comes from its frequency response characteristics, which will be discussed in Chapter 11. Thus, we use the name *PI controller* interchangeably with *ideal integral compensator*, and we use the name *lag compensator* when the cascade compensator does not employ pure integration.

Ideal Integral Compensation (PI)

Steady-state error can be improved by placing an open-loop pole at the origin, because this increases the system type by one. For example, a Type 0 system responding to a step input with a finite error responds with zero error if the system type is increased by one. Active circuits can be used to place poles at the origin. Later in this chapter, we show how to build an integrator with active electronic circuits.

To see how to improve the steady-state error without affecting the transient response, look at Figure 9.3(*a*). Here we have a system operating with a desirable
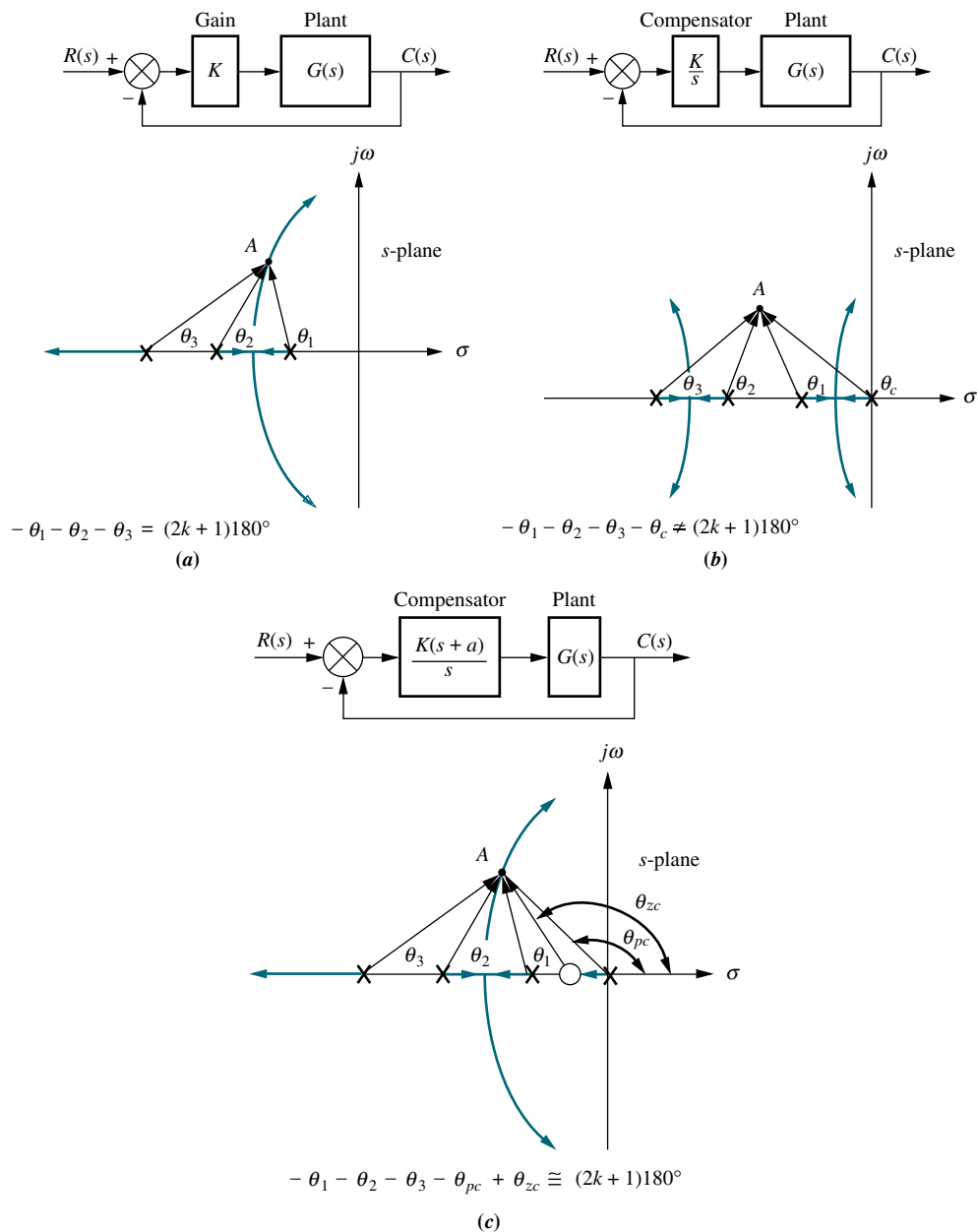
$$-\theta_1 - \theta_2 - \theta_3 = (2k+1)180°$$
(a)

$$-\theta_1 - \theta_2 - \theta_3 - \theta_c \neq (2k+1)180°$$
(b)

$$-\theta_1 - \theta_2 - \theta_3 - \theta_{pc} + \theta_{zc} \cong (2k+1)180°$$
(c)

FIGURE 9.3 Pole at A is **a.** on the root locus without compensator; **b.** not on the root locus with compensator pole added; **c.** approximately on the root locus with compensator pole and zero added

transient response generated by the closed-loop poles at A. If we add a pole at the origin to increase the system type, the angular contribution of the open-loop poles at point A is no longer $180°$, and the root locus no longer goes through point A, as shown in Figure 9.3(b).

To solve the problem, we also add a zero close to the pole at the origin, as shown in Figure 9.3(c). Now the angular contribution of the compensator zero and compensator pole cancel out, point A is still on the root locus, and the system type has been increased. Furthermore, the required gain at the dominant pole is about the same as

before compensation, since the ratio of lengths from the compensator pole and the compensator zero is approximately unity. Thus, we have improved the steady-state error without appreciably affecting the transient response. A compensator with a pole at the origin and a zero close to the pole is called an *ideal integral compensator*.

In the example that follows, we demonstrate the effect of ideal integral compensation. An open-loop pole will be placed at the origin to increase the system type and drive the steady-state error to zero. An open-loop zero will be placed very close to the open-loop pole at the origin so that the original closed-loop poles on the original root locus still remain at approximately the same points on the compensated root locus.

Example 9.1

Effect of an Ideal Integral Compensator

PROBLEM: Given the system of Figure 9.4(*a*), operating with a damping ratio of 0.174, show that the addition of the ideal integral compensator shown in Figure 9.4(*b*) reduces the steady-state error to zero for a step input without appreciably affecting transient response. The compensating network is chosen with a pole at the origin to increase the system type and a zero at -0.1, close to the compensator pole, so that the angular contribution of the compensator evaluated at the original, dominant, second-order poles is approximately zero. Thus, the original, dominant, second-order closed-loop poles are still approximately on the new root locus.

SOLUTION: We first analyze the uncompensated system and determine the location of the dominant, second-order poles. Next we evaluate the uncompensated steady-state error for a unit step input. The root locus for the uncompensated system is shown in Figure 9.5.

A damping ratio of 0.174 is represented by a radial line drawn on the *s*-plane at $100.02°$. Searching along this line with the root locus program discussed in Appendix H at www.wiley.com/college/nise, we find that the dominant poles are $0.694 \pm j3.926$ for a gain, K, of 164.6. Now look for the third pole on the root locus beyond -10 on the real axis. Using the root locus program and searching for the same gain as that of the dominant pair, $K = 164.6$, we find that the third pole is approximately at -11.61. This gain yields $K_p = 8.23$. Hence, the steady-state error is

$$e(\infty) = \frac{1}{1 + K_p} = \frac{1}{1 + 8.23} = 0.108 \tag{9.1}$$
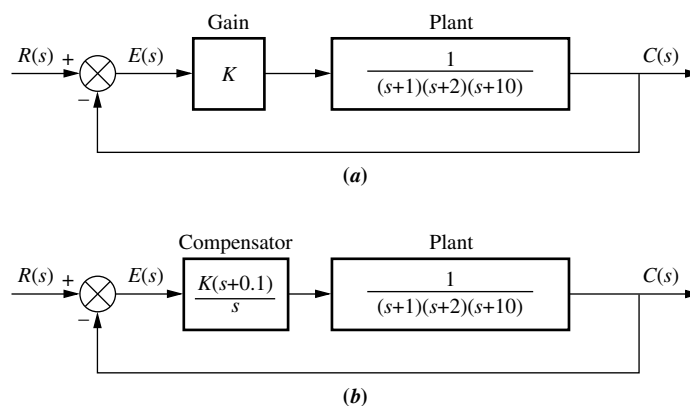

FIGURE 9.4   Closed-loop system for Example 9.1: **a.** before compensation; **b.** after ideal integral compensation
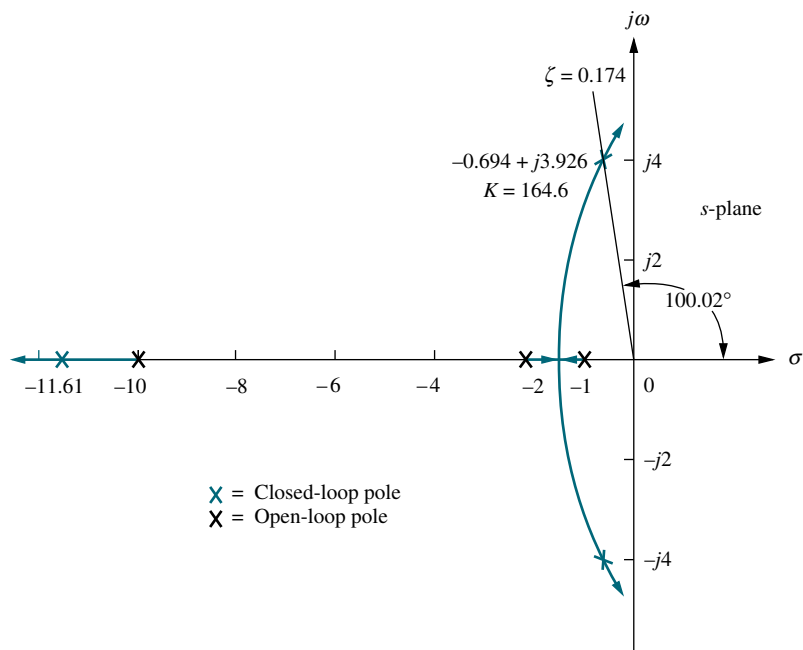
FIGURE 9.5   Root locus for uncompensated system of Figure 9.4(*a*)

Adding an ideal integral compensator with a zero at −0.1, as shown in Figure 9.4(*b*), we obtain the root locus shown in Figure 9.6. The dominant second-order poles, the third pole beyond −10, and the gain are approximately the same as for the uncompensated system. Another section of the compensated root locus is between the origin and −0.1. Searching this region for the same gain at the dominant pair, $K = 158.2$, the fourth closed-loop pole is found at −0.0902, close
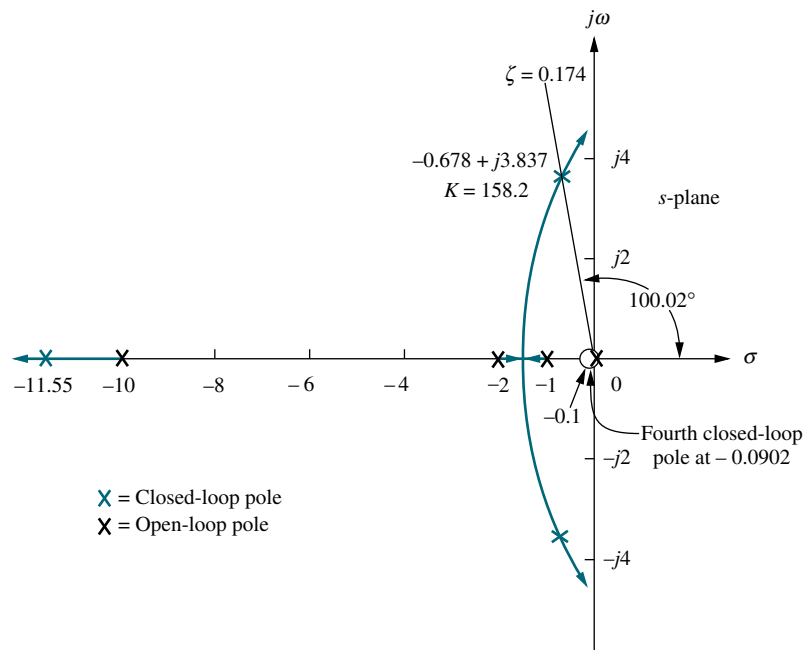
FIGURE 9.6   Root locus for compensated system of Figure 9.4(*b*)
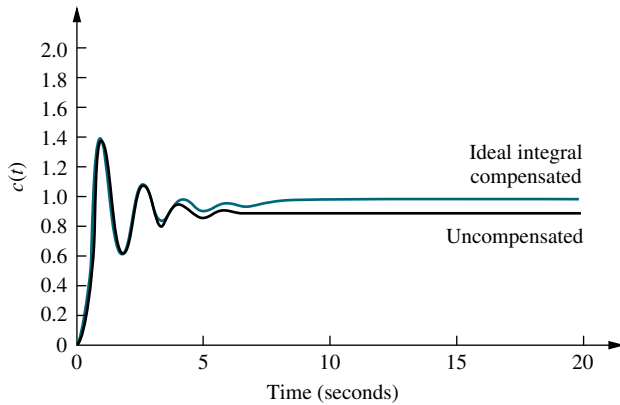
FIGURE 9.7   Ideal integral compensated system response and the uncompensated system response of Example 9.1

enough to the zero to cause pole-zero cancellation. Thus, the compensated system's closed-loop poles and gain are approximately the same as the un-compensated system's closed-loop poles and gain, which indicates that the transient response of the compensated system is about the same as the un-compensated system. However, the compensated system, with its pole at the origin, is a Type 1 system; unlike the uncompensated system, it will respond to a step input with zero error.

Figure 9.7 compares the uncompensated response with the ideal integral compensated response. The step response of the ideal integral compensated system approaches unity in the steady state, while the uncompensated system approaches 0.892. Thus, the ideal integral compensated system responds with zero steady-state error. The transient response of both the uncompensated and the ideal integral compensated systems is the same up to approximately 3 seconds. After that time the integrator in the compensator, shown in Figure 9.4(b), slowly compensates for the error until zero error is finally reached. The simulation shows that it takes 18 seconds for the compensated system to reach to within $\pm2\%$ of the final value of unity, while the uncompensated system takes about 6 seconds to settle to within $\pm2\%$ of its final value of 0.892. The compensation at first may appear to yield deterioration in the settling time. However, notice that the compensated system reaches the un-compensated system's final value in about the same time. The remaining time is used to improve the steady-state error over that of the uncompensated system.

A method of implementing an ideal integral compensator is shown in Figure 9.8. The compensating network precedes $G(s)$ and is an ideal integral compensator since

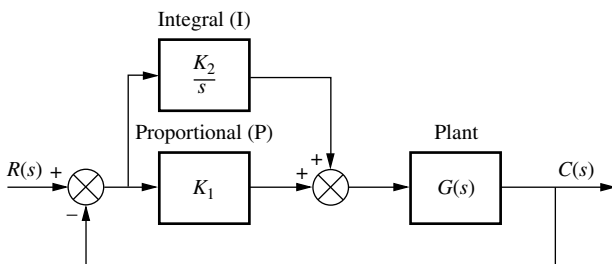$$G_c(s) = K_1 + \frac{K_2}{s} = \frac{K_1\left(s + \frac{K_2}{K_1}\right)}{s} \tag{9.2}$$

FIGURE 9.8   PI controller

The value of the zero can be adjusted by varying K_2/K_1. In this implementation, the error and the integral of the error are fed forward to the plant, $G(s)$. Since Figure 9.8 has both proportional and integral control, the ideal integral controller, or compensator, is given the alternate name *PI controller*. Later in the chapter we will see how to implement each block, K_1 and K_2/s.

Lag Compensation

Ideal integral compensation, with its pole on the origin, requires an active integrator. If we use passive networks, the pole and zero are moved to the left, close to the origin, as shown in Figure 9.9(c). One may guess that this placement of the pole, although it does not increase the system type, does yield an improvement in the static error constant over an uncompensated system. Without loss of generality, we demonstrate that this improvement is indeed realized for a Type 1 system.

Assume the uncompensated system shown in Figure 9.9(a). The static error constant, K_{v_O}, for the system is

$$K_{v_O} = \frac{K z_1 z_2 \cdots}{p_1 p_2 \cdots} \tag{9.3}$$

Assuming the lag compensator shown in Figure 9.9(b) and (c), the new static error constant is

$$K_{v_N} = \frac{(K z_1 z_2 \cdots)(z_c)}{(p_1 p_2 \cdots)(p_c)} \tag{9.4}$$

What is the effect on the transient response? Figure 9.10 shows the effect on the root locus of adding the lag compensator. The uncompensated system's root locus is shown in Figure 9.10(a), where point P is assumed to be the dominant pole. If the lag compensator pole and zero are close together, the angular contribution of the
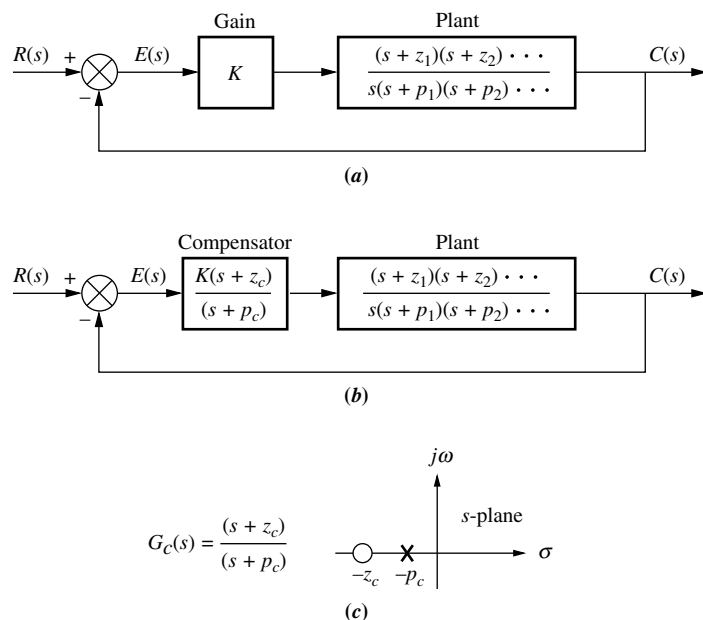

FIGURE 9.9 **a.** Type 1 uncompensated system; **b.** Type 1 compensated system; **c.** compensator pole-zero plot
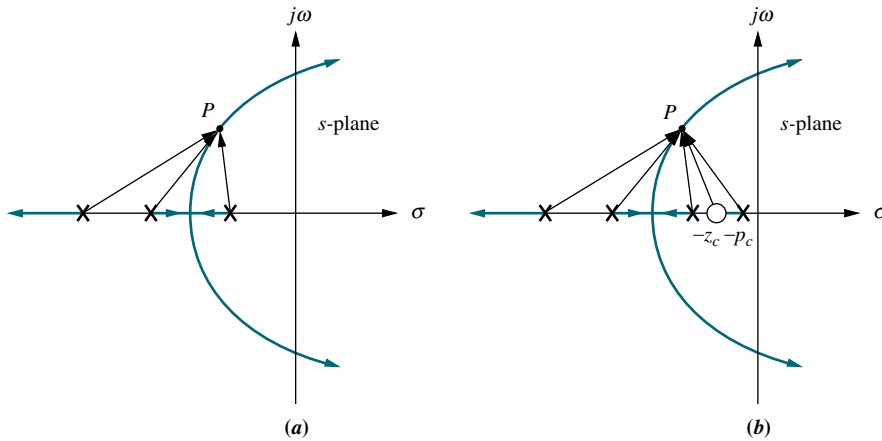
FIGURE 9.10   Root locus: **a.** before lag compensation; **b.** after lag compensation

compensator to point *P* is approximately zero degrees. Thus, in Figure 9.10(*b*), where the compensator has been added, point *P* is still at approximately the same location on the compensated root locus.

What is the effect on the required gain, *K*? After inserting the compensator, we find that *K* is virtually the same for the uncompensated and compensated systems, since the lengths of the vectors drawn from the lag compensator are approximately equal and all other vectors have not changed appreciably.

Now, what improvement can we expect in the steady-state error? Since we established that the gain, *K*, is about the same for the uncompensated and compensated systems, we can substitute Eq. (9.3) into (9.4) and obtain

$$K_{v_N} = K_{v_O} \frac{z_c}{p_c} > K_{v_O} \qquad (9.5)$$

Equation (9.5) shows that the improvement in the compensated system's K_v over the uncompensated system's K_v is equal to the ratio of the magnitude of the compensator zero to the compensator pole. In order to keep the transient response unchanged, we know the compensator pole and zero must be close to each other. The only way the ratio of z_c to p_c can be large in order to yield an appreciable improvement in steady-state error and simultaneously have the compensator's pole and zero close to each other to minimize the angular contribution is to place the compensator's pole-zero pair close to the origin. For example, the ratio of z_c to p_c can be equal to 10 if the pole is at −0.001 and the zero is at −0.01. Thus, the ratio is 10, yet the pole and zero are very close, and the angular contribution of the compensator is small.

In conclusion, although the ideal compensator drives the steady-state error to zero, a lag compensator with a pole that is not at the origin will improve the static error constant by a factor equal to z_c/p_c. There also will be a minimal effect upon the transient response if the pole-zero pair of the compensator is placed close to the origin. Later in the chapter we show circuit configurations for the lag compensator. These circuit configurations can be obtained with passive networks and thus do not require the active amplifiers and possible additional power supplies that are required by the ideal integral (PI) compensator. In the following example we design a lag compensator to yield a specified improvement in steady-state error.

Example 9.2

Lag Compensator Design

PROBLEM: Compensate the system of Figure 9.4(a), whose root locus is shown in Figure 9.5, to improve the steady-state error by a factor of 10 if the system is operating with a damping ratio of 0.174.

SOLUTION: The uncompensated system error from Example 9.1 was 0.108 with $K_p = 8.23$. A tenfold improvement means a steady-state error of

$$e(\infty) = \frac{0.108}{10} = 0.0108 \tag{9.6}$$

Since

$$e(\infty) = \frac{1}{1 + K_p} = 0.0108 \tag{9.7}$$

rearranging and solving for the required K_p yields

$$K_p = \frac{1 - e(\infty)}{e(\infty)} = \frac{1 - 0.0108}{0.0108} = 91.59 \tag{9.8}$$

The improvement in K_p from the uncompensated system to the compensated system is the required ratio of the compensator zero to the compensator pole, or

$$\frac{z_c}{p_c} = \frac{K_{p_N}}{K_{p_O}} = \frac{91.59}{8.23} = 11.13 \tag{9.9}$$

Arbitrarily selecting

$$p_c = 0.01 \tag{9.10}$$

we use Eq. (9.9) and find

$$z_c = 11.13 p_c \approx 0.111 \tag{9.11}$$

Let us now compare the compensated system, shown in Figure 9.11, with the uncompensated system. First sketch the root locus of the compensated system, as shown in Figure 9.12. Next search along the $\zeta = 0.174$ line for a multiple of $180°$ and find that the second-order dominant poles are at $-0.678 \pm j3.836$ with a gain, K, of 158.1. The third and fourth closed-loop poles are at -11.55 and -0.101, respectively, and are found by searching the real axis for a gain equal to that of the dominant poles. All transient and steady-state results for both the uncompensated and the compensated systems are shown in Table 9.1.

The fourth pole of the compensated system cancels its zero. This leaves the remaining three closed-loop poles of the compensated system very close in value to the three closed-loop poles of the uncompensated system. Hence, the transient
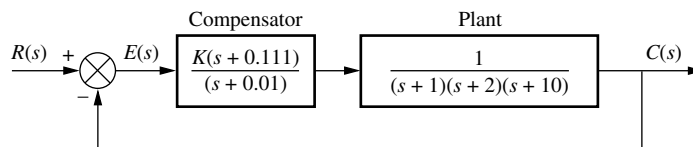

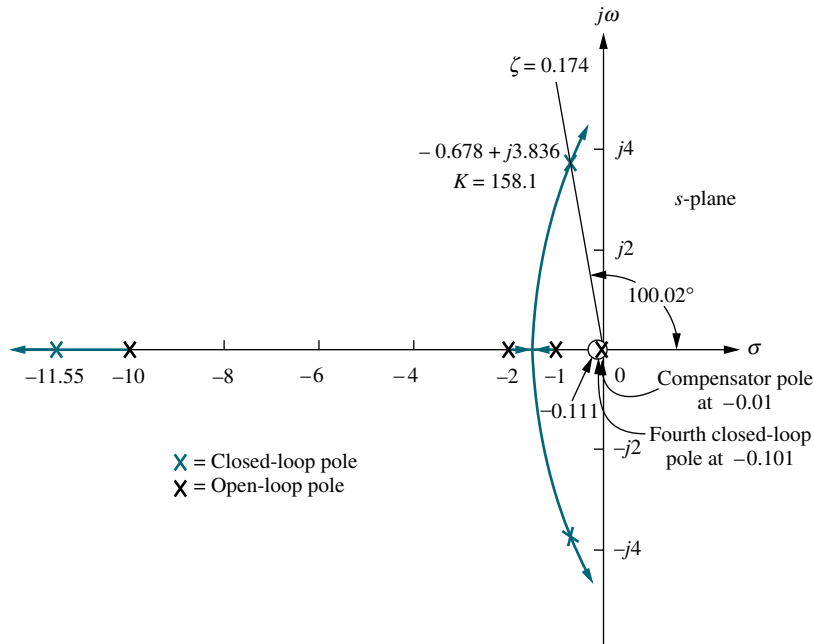**FIGURE 9.11** Compensated system for Example 9.2

FIGURE 9.12   Root locus for compensated system of Figure 9.11

response of both systems is approximately the same, as is the system gain, but notice that the steady-state error of the compensated system is 1/9.818 that of the uncompensated system and is close to the design specification of a tenfold improvement.

Figure 9.13 shows the effect of the lag compensator in the time domain. Even though the transient responses of the uncompensated and lag-compensated systems are the same, the lag-compensated system exhibits less steady-state error by approaching unity more closely than the uncompensated system.

We now examine another design possibility for the lag compensator and compare the response to Figure 9.13. Let us assume a lag compensator whose pole and zero are 10 times as close to the origin as in the previous design. The results are compared in Figure 9.14. Even though both responses will eventually reach approximately the same steady-state value, the lag compensator previously designed, $G_c(s) = (s + 0.111)/(s + 0.01)$, approaches the final value faster than the proposed lag compensator, $G_c(s) = (s + 0.0111)/(s + 0.001)$. We can explain this phenomenon as follows. From Table 9.1, the previously designed lag compensator

TryIt 9.1

Use the following MATLAB and Control System Toolbox statements to reproduce Figure 9.13.

```
Gu=zpk([],...
 [-1 -2 -10],164.6);
Gc=zpk([-0.111],...
 [-0.01],1);
Gce=Gu*Gc;
Tu=feedback(Gu,1);
Tc=feedback(Gce,1);
step(Tu)
hold
step(Tc)
```

TABLE 9.1   Predicted characteristics of uncompensated and lag-compensated systems for Example 9.2

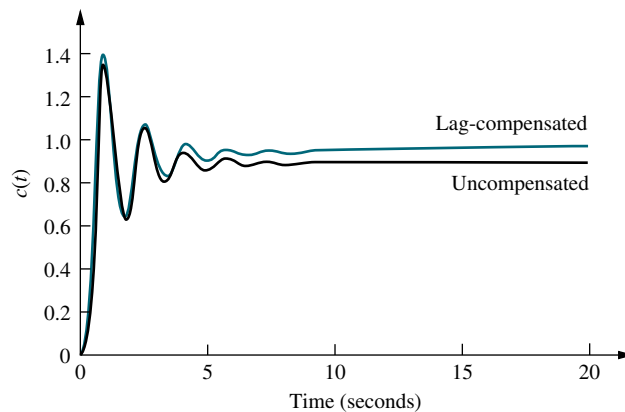| Parameter	Uncompensated	Lag-compensated
Plant and compensator	$\dfrac{K}{(s+1)(s+2)(s+10)}$	$\dfrac{K(s+0.111)}{(s+1)(s+2)(s+10)(s+0.01)}$
K	164.6	158.1
K_p	8.23	87.75
$e(\infty)$	0.108	0.011
Dominant second-order poles	$-0.694 \pm j3.926$	$-0.678 \pm j3.836$
Third pole	-11.61	-11.55
Fourth pole	None	-0.101
Zero	None	-0.111

FIGURE 9.13   Step responses of uncompensated and lag-compensated systems for Example 9.2
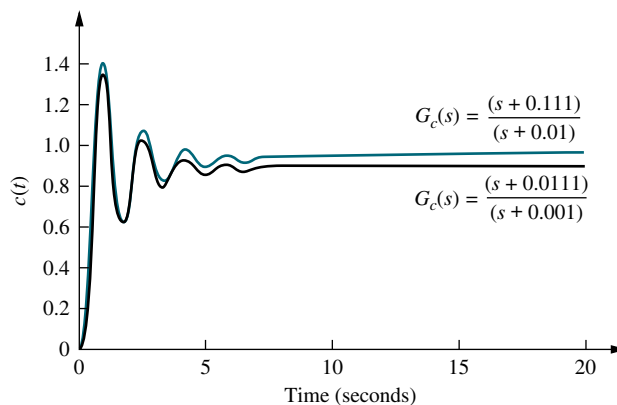

FIGURE 9.14   Step responses of the system for Example 9.2 using different lag compensators

has a fourth closed-loop pole at -0.101. Using the same analysis for the new lag compensator with its open-loop pole 10 times as close to the imaginary axis, we find its fourth closed-loop pole at -0.01. Thus, the new lag compensator has a closed-loop pole closer to the imaginary axis than the original lag compensator. This pole at -0.01 will produce a longer transient response than the original pole at -0.101, and the steady-state value will not be reached as quickly.

Skill-Assessment Exercise 9.1

PROBLEM: A unity feedback system with the forward transfer function

$$G(s) = \frac{K}{s(s+7)}$$

is operating with a closed-loop step response that has 15% overshoot. Do the following:

   a. Evaluate the steady-state error for a unit ramp input.

   b. Design a lag compensator to improve the steady-state error by a factor of 20.

c. Evaluate the steady-state error for a unit ramp input to your compensated system.

d. Evaluate how much improvement in steady-state error was realized.

ANSWERS:

a. $e_{\text{ramp}}(\infty) = 0.1527$

b. $G_{\text{lag}}(s) = \dfrac{s + 0.2}{s + 0.01}$

c. $e_{\text{ramp}}(\infty) = 0.0078$

d. 19.58 times improvement

The complete solution is at www.wiley.com/college/nise.

9.3 Improving Transient Response via Cascade Compensation

Since we have solved the problem of improving the steady-state error without affecting the transient response, let us now improve the transient response itself. In this section, we discuss two ways to improve the transient response of a feedback control system by using cascade compensation. Typically, the objective is to design a response that has a desirable percent overshoot and a shorter settling time than the uncompensated system.

The first technique we will discuss is *ideal derivative compensation*. With ideal derivative compensation, a pure differentiator is added to the forward path of the feedback control system. We will see that the result of adding differentiation is the addition of a zero to the forward-path transfer function. This type of compensation requires an active network for its realization. Further, differentiation is a noisy process; although the level of the noise is low, the frequency of the noise is high compared to the signal. Thus, differentiating high-frequency noise yields a large, unwanted signal.

The second technique does not use pure differentiation. Instead, it approximates differentiation with a passive network by adding a zero and a more distant pole to the forward-path transfer function. The zero approximates pure differentiation as described previously.

As with compensation to improve steady-state error, we introduce names associated with the implementation of the compensators. We call an ideal derivative compensator a *proportional-plus-derivative* (*PD*) *controller*, since the implementation, as we will see, consists of feeding the error (proportional) plus the derivative of the error forward to the plant. The second technique uses a passive network called a *lead compensator*. As with the lag compensator, the name comes from its frequency response, which is discussed in Chapter 11. Thus, we use the name *PD controller* interchangeably with *ideal derivative compensator*, and we use the name *lead compensator* when the cascade compensator does not employ pure differentiation.

Ideal Derivative Compensation (PD)

The transient response of a system can be selected by choosing an appropriate closed-loop pole location on the *s*-plane. If this point is on the root locus, then a simple gain adjustment is all that is required in order to meet the transient response specification. If the closed-loop pole location is not on the root locus, then the root locus must be reshaped so that the compensated (new) root locus goes through the selected closed-loop pole location. In order to accomplish the latter task, poles and zeros can be added in the forward path to produce a new open-loop function whose root locus goes through the design point on the *s*-plane. One way to speed up the original system that generally works is to add a single zero to the forward path.

This zero can be represented by a compensator whose transfer function is

$$G_c(s) = s + z_c \tag{9.12}$$

This function, the sum of a differentiator and a pure gain, is called an *ideal derivative*, or *PD controller*. Judicious choice of the position of the compensator zero can quicken the response over the uncompensated system. In summary, transient responses unattainable by a simple gain adjustment can be obtained by augmenting the system's poles and zeros with an ideal derivative compensator.

We now show that ideal derivative compensation speeds up the response of a system. Several simple examples are shown in Figure 9.15, where the uncompensated system of Figure 9.15(*a*), operating with a damping ratio of 0.4, becomes a compensated system by the addition of a compensating zero at $-2, -3$, and -4 in Figures 9.15(*b*), (*c*), and (*d*), respectively. In each design, the zero is moved to a different position, and the root locus is shown. For each compensated case, the dominant, second-order poles are farther out along the 0.4 damping ratio line than the uncompensated system.

Each of the compensated cases has dominant poles with the same damping ratio as the uncompensated case. Thus, we predict that the percent overshoot will be the same for each case.

Also, the compensated, dominant, closed-loop poles have more negative real parts than the uncompensated, dominant, closed-loop poles. Hence, we predict that the settling times for the compensated cases will be shorter than for the
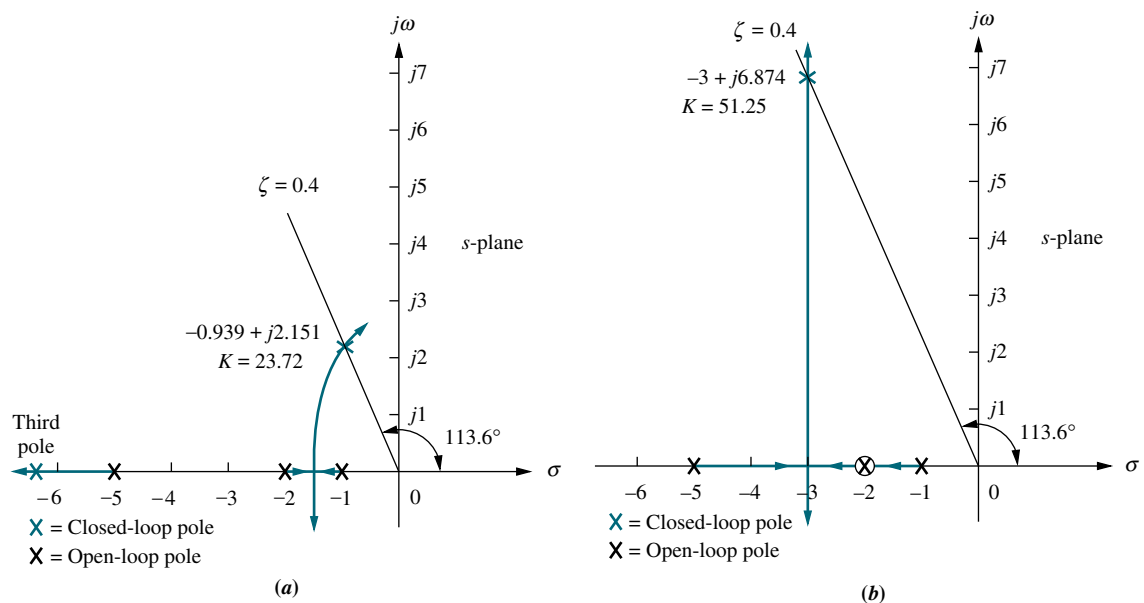

FIGURE 9.15   Using ideal derivative compensation: **a.** uncompensated; **b.** compensator zero at -2; (figure continues)
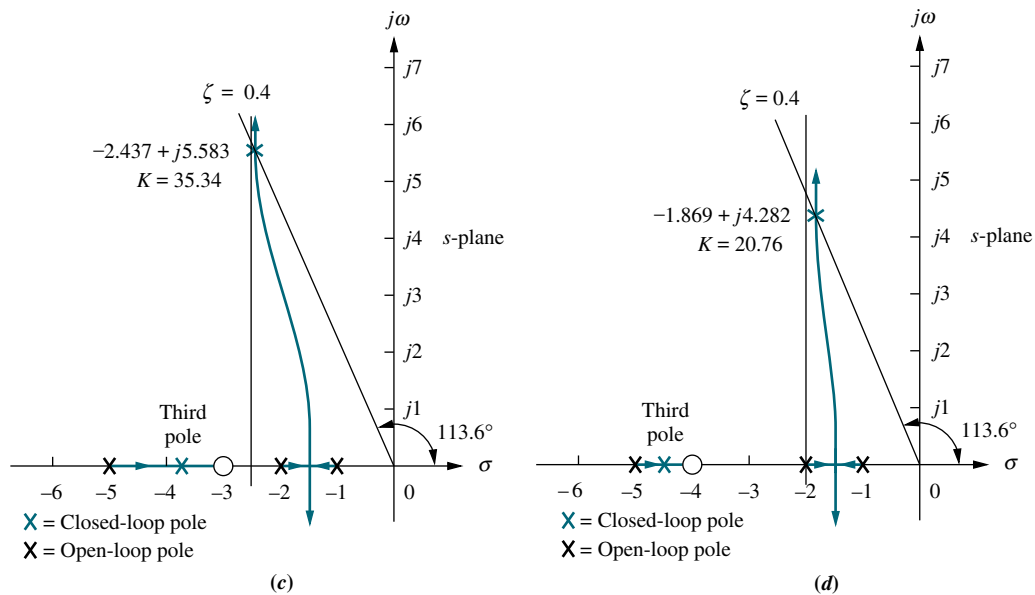
FIGURE 9.15   (*Continued*) **c.** compensator zero at −3; **d.** compensator zero at −4.

uncompensated case. The compensated, dominant, closed-loop poles with the more negative real parts will have the shorter settling times. The system in Figure 9.15(*b*) will have the shortest settling time.

All of the compensated systems will have smaller peak times than the uncompensated system, since the imaginary parts of the compensated systems are larger. The system of Figure 9.15(*b*) will have the smallest peak time.

Also notice that as the zero is placed farther from the dominant poles, the closed-loop, compensated dominant poles move closer to the origin and to the uncompensated, dominant closed-loop poles. Table 9.2 summarizes the

TABLE 9.2   Predicted characteristics for the systems of Figure 9.15

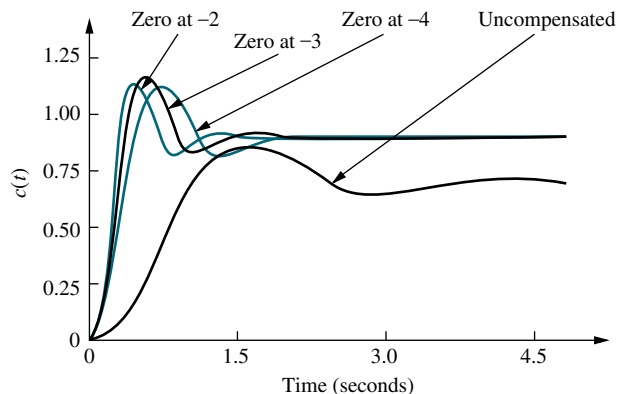|	**Uncompensated**	**Compensation b**	**Compensation c**	**Compensation d**
Plant and compensator	$\dfrac{K}{(s+1)(s+2)(s+5)}$	$\dfrac{K(s+2)}{(s+1)(s+2)(s+5)}$	$\dfrac{K(s+3)}{(s+1)(s+2)(s+5)}$	$\dfrac{K(s+4)}{(s+1)(s+2)(s+5)}$
Dom, poles	$-0.939 \pm j2.151$	$-3 \pm j6.874$	$-2.437 \pm j5.583$	$-1.869 \pm j4.282$
K	23.72	51.25	35.34	20.76
ζ	0.4	0.4	0.4	0.4
ω_n	2.347	7.5	6.091	4.673
%OS	25.38	25.38	25.38	25.38
T_s	4.26	1.33	1.64	2.14
T_p	1.46	0.46	0.56	0.733
K_p	2.372	10.25	10.6	8.304
$e(\infty)$	0.297	0.089	0.086	0.107
Third pole	−6.123	None	−3.127	−4.262
Zero	None	None	−3	−4
Comments	Second-order approx. OK	Pure second-order	Second-order approx. OK	Second-order approx. OK

FIGURE 9.16 Uncompensated system and ideal derivative compensation solutions from Table 9.2

results obtained from the root locus of each of the design cases shown in Figure 9.15.

In summary, although compensation methods *c* and *d* yield slower responses than method *b*, the addition of ideal derivative compensation shortened the response time in each case while keeping the percent overshoot the same. This change can best be seen in the settling time and peak time, where there is at least a doubling of speed across all of the cases of compensation. An added benefit is the improvement in the steady-state error, even though lag compensation was not used. Here the steady-state error of the compensated system is at least one-third that of the uncompensated system, as seen by $e(\infty)$ and K_p. All systems in Table 9.2 are Type 0, and some steady-state error is expected. The reader must not assume that, in general, improvement in transient response always yields an improvement in steady-state error.

The time response of each case in Table 9.2 is shown in Figure 9.16. We see that the compensated responses are faster and exhibit less error than the uncompensated response.

Now that we have seen what ideal derivative compensation can do, we are ready to design our own ideal derivative compensator to meet a transient response specification. Basically, we will evaluate the sum of angles from the open-loop poles and zeros to a design point that is the closed-loop pole that yields the desired transient response. The difference between 180° and the calculated angle must be the angular contribution of the compensator zero. Trigonometry is then used to locate the position of the zero to yield the required difference in angle.

Example 9.3

Ideal Derivative Compensator Design

PROBLEM: Given the system of Figure 9.17, design an ideal derivative compensator to yield a 16% overshoot, with a threefold reduction in settling time.
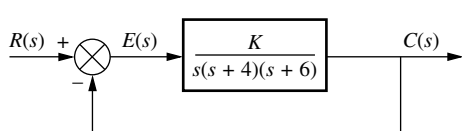

FIGURE 9.17 Feedback control system for Example 9.3

SOLUTION: Let us first evaluate the performance of the uncompensated system operating with 16% overshoot. The root locus for the uncompensated system is shown in Figure 9.18. Since 16% overshoot is equivalent to $\zeta = 0.504$, we search along that damping ratio line for an odd multiple of 180° and find that the dominant, second-order pair of poles is at $-1.205 \pm j2.064$. Thus, the settling
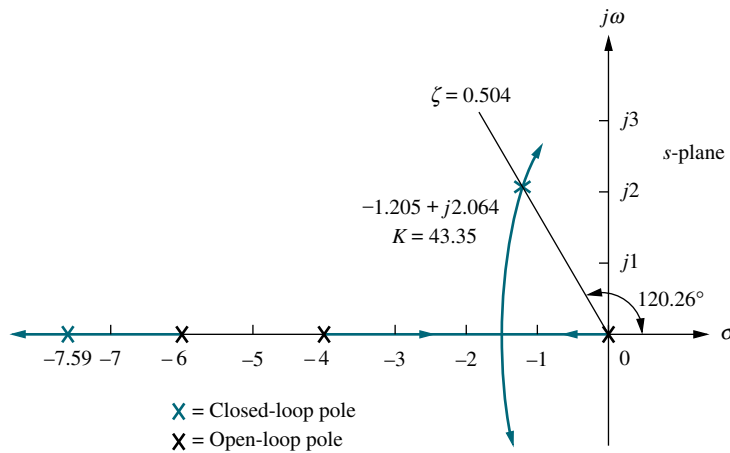
FIGURE 9.18   Root locus for uncompensated system shown in Figure 9.17

time of the uncompensated system is

$$T_s = \frac{4}{\zeta \omega_n} = \frac{4}{1.205} = 3.320 \tag{9.13}$$

Since our evaluation of percent overshoot and settling time is based upon a second-order approximation, we must check the assumption by finding the third pole and justifying the second-order approximation. Searching beyond −6 on the real axis for a gain equal to the gain of the dominant, second-order pair, 43.35, we find a third pole at −7.59, which is over six times as far from the $j\omega$-axis as the dominant, second-order pair. We conclude that our approximation is valid. The transient and steady-state error characteristics of the uncompensated system are summarized in Table 9.3.

TABLE 9.3   Uncompensated and compensated system characteristic of Example 9.3

	Uncompensated	Simulation	Compensated	Simulation
Plant and compensator	$\dfrac{K}{s(s+4)(s+6)}$		$\dfrac{K(s+3.006)}{s(s+4)(s+6)}$	
Dominant poles	$-1.205 \pm j2.064$		$-3.613 \pm j6.193$	
K	43.35		47.45	
ζ	0.504		0.504	
ω_n	2.39		7.17	
$\%OS$	16	14.8	16	11.8
T_s	3.320	3.6	1.107	1.2
T_p	1.522	1.7	0.507	0.5
K_v	1.806		5.94	
$e(\infty)$	0.554		0.168	
Third pole	−7.591		−2.775	
Zero	None		−3.006	
Comments	Second-order approx. OK		Pole-zero not canceling	
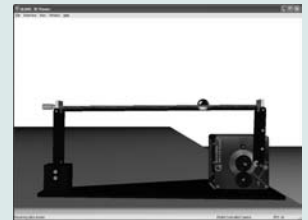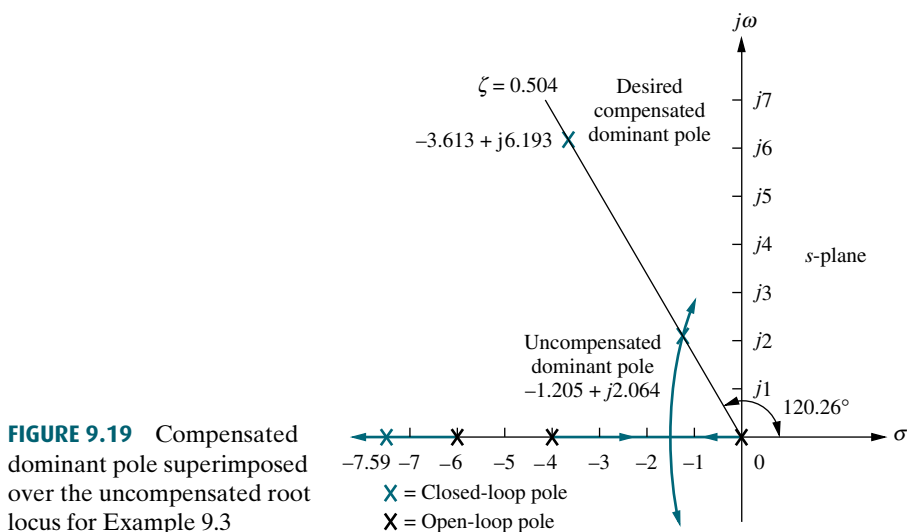
Now we proceed to compensate the system. First we find the location of the compensated system's dominant poles. In order to have a threefold reduction in the settling time, the compensated system's settling time will be one-third of Eq. (9.13). The new settling time will be 1.107. Therefore, the real part of the compensated system's dominant, second-order pole is

$$\sigma = \frac{4}{T_s} = \frac{4}{1.107} = 3.613 \tag{9.14}$$

Figure 9.19 shows the designed dominant, second-order pole, with a real part equal to -3.613 and an imaginary part of

$$\omega_d = 3.613 \tan(180° - 120.26°) = 6.193 \tag{9.15}$$

Next we design the location of the compensator zero. Input the uncompensated system's poles and zeros in the root locus program as well as the design point $-3.613 \pm j6.193$ as a test point. The result is the sum of the angles to the design point of all the poles and zeros of the compensated system except for those of the compensator zero itself. The difference between the result obtained and $180°$ is the angular contribution required of the compensator zero. Using the open-loop poles shown in Figure 9.19 and the test point, $-3.613 + j6.193$, which is the desired dominant second-order pole, we obtain the sum of the angles as $-275.6°$. Hence, the angular contribution required from the compensator zero for the test point to be on the root locus is $+275.6° - 180° = 95.6°$. The geometry is shown in Figure 9.20, where we now must solve for $-\sigma$, the location of the compensator zero.

From the figure,

$$\frac{6.193}{3.613 - \sigma} = \tan(180° - 95.6°) \tag{9.16}$$

Thus, $\sigma = 3.006$. The complete root locus for the compensated system is shown in Figure 9.21.

Table 9.3 summarizes the results for both the uncompensated system and the compensated system. For the uncompensated system, the estimate of the transient
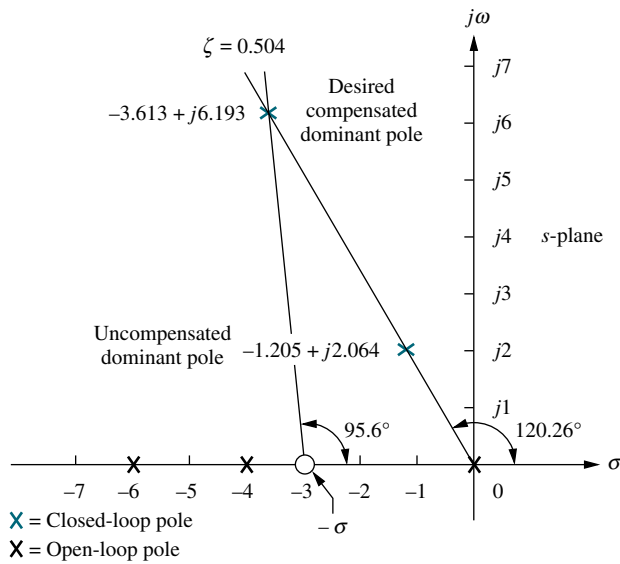
FIGURE 9.20   Evaluating the location of the compensating zero for Example 9.3

response is accurate since the third pole is at least five times the real part of the dominant, second-order pair. The second-order approximation for the compensated system, however, may be invalid because there is no approximate closed-loop third-pole and zero cancellation between the closed-loop pole at -2.775 and the closed-loop zero at -3.006. A simulation or a partial-fraction expansion of the closed-loop response to compare the residue of the pole at -2.775 to the residues of the dominant poles at $-3.613 \pm j6.193$ is required. The results of a simulation are shown in the table's second column for the uncompensated system and the fourth column for the compensated system. The simulation results can be obtained using MATLAB (discussed at the end of this example) or a program
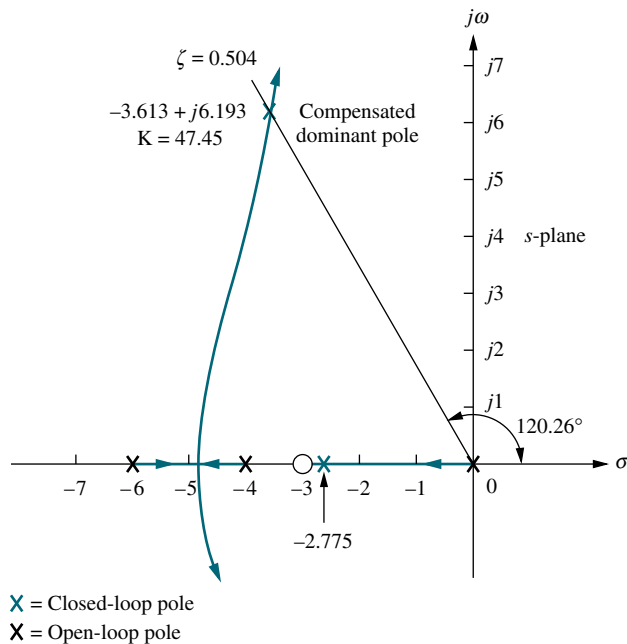

FIGURE 9.21   Root locus for the compensated system of Example 9.3
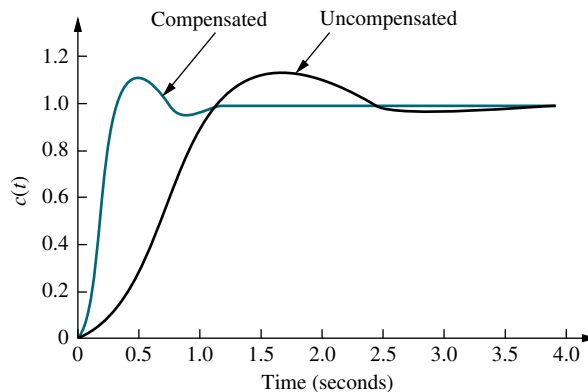
FIGURE 9.22 Uncompensated and compensated system step responses of Example 9.3

like the state-space step-response program described in Appendix H.1 at www. wiley.com/college/nise. The percent overshoot differs by 3% between the uncompensated and compensated systems, while there is approximately a threefold improvement in speed as evaluated from the settling time.

The final results are displayed in Figure 9.22, which compares the uncompensated system and the faster compensated system.

MATLAB
ML

Students who are using MATLAB should now run ch9p1 in Appendix B. MATLAB will be used to design a PD controller. You will input the desired percent overshoot from the keyboard. MATLAB will plot the root locus of the uncompensated system and the percent overshoot line. You will interactively select the gain, after which MATLAB will display the performance characteristics of the uncompensated system and plot its step response. Using these characteristics, you will input the desired settling time. MATLAB will design the PD controller, enumerate its performance characteristics, and plot a step response. This exercise solves Example 9.3 using MATLAB.
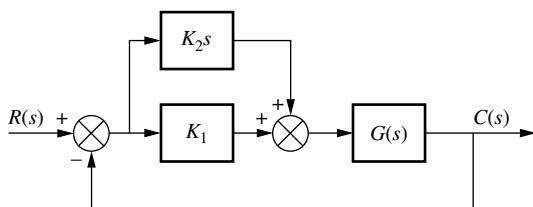

FIGURE 9.23 PD controller

Once we decide on the location of the compensating zero, how do we implement the ideal derivative, or PD controller? The ideal integral compensator that improved steady-state error was implemented with a proportional-plus-integral (PI) controller. The ideal derivative compensator used to improve the transient response is implemented with a proportional-plus-derivative (PD) controller. For example, in Figure 9.23 the transfer function of the controller is

$$G_c(s) = K_2 s + K_1 = K_2 \left(s + \frac{K_1}{K_2} \right) \tag{9.17}$$

Hence, K_1/K_2 is chosen to equal the negative of the compensator zero, and K_2 is chosen to contribute to the required loop-gain value. Later in the chapter, we will study circuits that can be used to approximate differentiation and produce gain.

While the ideal derivative compensator can improve the transient response of the system, it has two drawbacks. First, it requires an active circuit to perform the

differentiation. Second, as previously mentioned, differentiation is a noisy process: The level of the noise is low, but the frequency of the noise is high compared to the signal. Differentiation of high frequencies can lead to large unwanted signals or saturation of amplifiers and other components. The lead compensator is a passive network used to overcome the disadvantages of ideal differentiation and still retain the ability to improve the transient response.

Lead Compensation

Just as the active ideal integral compensator can be approximated with a passive lag network, an active ideal derivative compensator can be approximated with a passive lead compensator. When passive networks are used, a single zero cannot be produced; rather, a compensator zero and a pole result. However, if the pole is farther from the imaginary axis than the zero, the angular contribution of the compensator is still positive and thus approximates an equivalent single zero. In other words, the angular contribution of the compensator pole subtracts from the angular contribution of the zero but does not preclude the use of the compensator to improve transient response, since the net angular contribution is positive, just as for a single PD controller zero.

The advantages of a passive lead network over an active PD controller are that (1) no additional power supplies are required and (2) noise due to differentiation is reduced. The disadvantage is that the additional pole does not reduce the number of branches of the root locus that cross the imaginary axis into the right–half-plane, while the addition of the single zero of the PD controller tends to reduce the number of branches of the root locus that cross into the right half-plane.

Let us first look at the concept behind lead compensation. If we select a desired dominant, second-order pole on the *s*-plane, the sum of the angles from the uncompensated system's poles and zeros to the design point can be found. The difference between $180°$ and the sum of the angles must be the angular contribution required of the compensator.

For example, looking at Figure 9.24, we see that

$$\theta_2 - \theta_1 - \theta_3 - \theta_4 + \theta_5 = (2k + 1)180° \qquad (9.18)$$

where $(\theta_2 - \theta_1) = \theta_c$ is the angular contribution of the lead compensator. From Figure 9.24 we see that θ_c is the angle of a ray extending from the design point and intersecting the real axis at the pole value and zero value of the compensator. Now visualize this ray rotating about the desired closed-loop pole location and
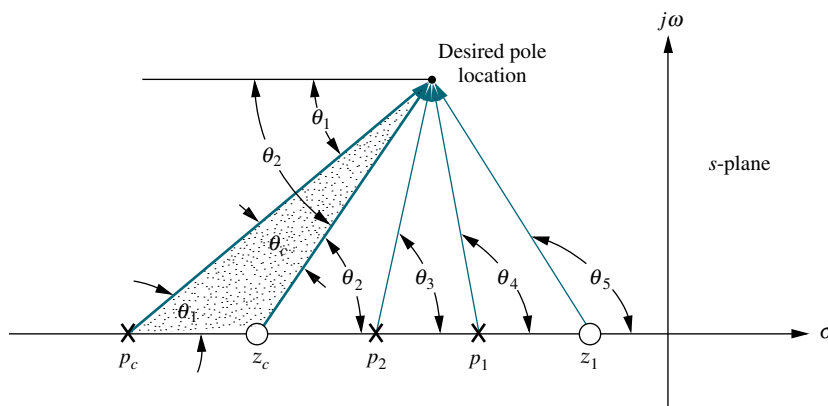

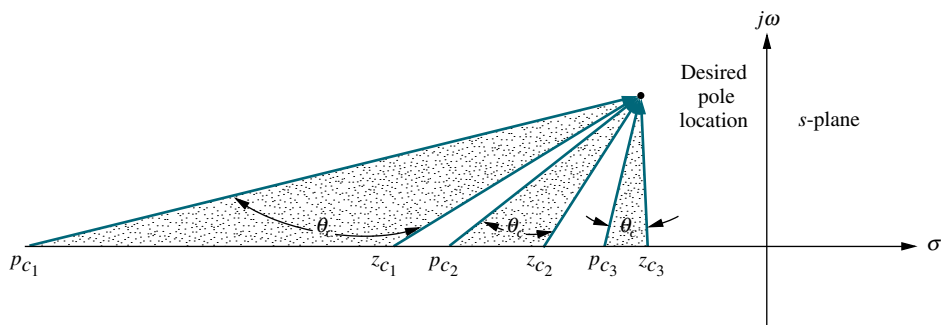**FIGURE 9.24** Geometry of lead compensation

FIGURE 9.25 Three of the infinite possible lead compensator solutions

intersecting the real axis at the compensator pole and zero, as illustrated in Figure 9.25. We realize that an infinite number of lead compensators could be used to meet the transient response requirement.

How do the possible lead compensators differ? The differences are in the values of static error constants, the gain required to reach the design point on the compensated root locus, the difficulty in justifying a second-order approximation when the design is complete, and the ensuing transient response.

For design, we arbitrarily select either a lead compensator pole or zero and find the angular contribution at the design point of this pole or zero along with the system's open-loop poles and zeros. The difference between this angle and $180°$ is the required contribution of the remaining compensator pole or zero. Let us look at an example.

Example 9.4

Lead Compensator Design

PROBLEM: Design three lead compensators for the system of Figure 9.17 that will reduce the settling time by a factor of 2 while maintaining 30% overshoot. Compare the system characteristics between the three designs.
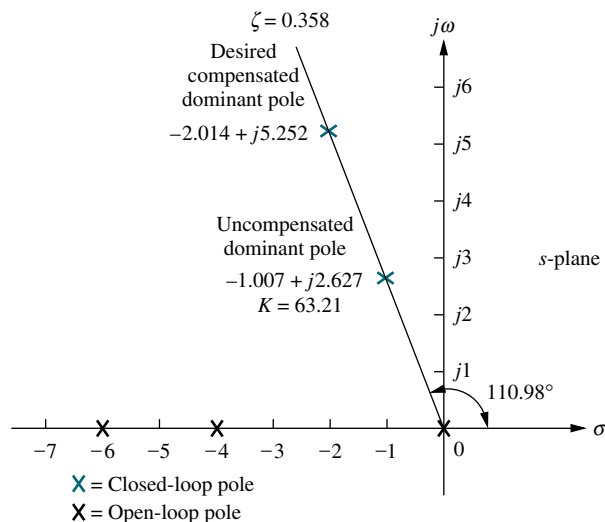
FIGURE 9.26 Lead compensator design, showing evaluation of uncompensated and compensated dominant poles for Example 9.4

SOLUTION: First determine the characteristics of the uncompensated system operating at 30% overshoot to see what the uncompensated settling time is. Since 30% overshoot is equivalent to a damping ratio of 0.358, we search along the $\zeta = 0.358$ line for the uncompensated dominant poles on the root locus, as shown in Figure 9.26. From the pole's real part, we calculate the uncompensated settling time as $T_s = 4/1.007 = 3.972$ seconds. The remaining characteristics of the uncompensated system are summarized in Table 9.4.

Next we find the design point. A twofold reduction in settling time yields $T_s = 3.972/2 = 1.986$ seconds, from which the real part of the desired pole location is $-\zeta\omega_n = -4/T_s = -2.014$. The imaginary part is $\omega_d = -2.014 \tan(110.98°) = 5.252$.

We continue by designing the lead compensator. Arbitrarily assume a compensator zero at -5 on the real axis as a possible solution. Using the root locus program, sum the angles from both this zero and the

TABLE 9.4   Comparison of lead compensation designs for Example 9.4

	Uncompensated	**Compensation a**	**Compensation b**	**Compensation c**
Plant and compensator	$\dfrac{K}{s(s+4)(s+6)}$	$\dfrac{K(s+5)}{s(s+4)(s+6)(s+42.96)}$	$\dfrac{K(s+4)}{s(s+4)(s+6)(s+20.09)}$	$\dfrac{K(s+2)}{s(s+4)(s+6)(s+8.971)}$
Dominant poles	$-1.007 \pm j2.627$	$-2.014 \pm j5.252$	$-2.014 \pm j5.252$	$-2.014 \pm j5.252$
K	63.21	1423	698.1	345.6
ζ	0.358	0.358	0.358	0.358
ω_n	2.813	5.625	5.625	5.625
$\%OS^*$	30 (28)	30 (30.7)	30 (28.2)	30 (14.5)
T_s^*	3.972 (4)	1.986 (2)	1.986 (2)	1.986 (1.7)
T_p^*	1.196 (1.3)	0.598 (0.6)	0.598 (0.6)	0.598 (0.7)
K_v	2.634	6.9	5.791	3.21
$e(\infty)$	0.380	0.145	0.173	0.312
Other poles	-7.986	$-43.8, -5.134$	-22.06	$-13.3, -1.642$
Zero	None	-5	None	-2
Comments	Second-order approx. OK	Second-order approx. OK	Second-order approx. OK	No pole-zero cancellation

*Simulation results are shown in parentheses.

uncompensated system's poles and zeros, using the design point as a test point. The resulting angle is $-172.69°$. The difference between this angle and $180°$ is the angular contribution required from the compensator pole in order to place the design point on the root locus. Hence, an angular contribution of $-7.31°$ is required from the compensator pole.

The geometry shown in Figure 9.27 is used to calculate the location of the compensator pole. From the figure,

$$\frac{5.252}{p_c - 2.014} = \tan 7.31° \qquad (9.19)$$

from which the compensator pole is found to be

$$p_c = 42.96 \qquad (9.20)$$

The compensated system root locus is sketched in Figure 9.28.

X = Closed-loop pole
X = Open-loop pole
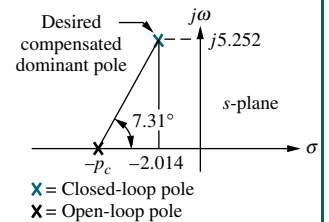
Note: This figure is not drawn to scale.

FIGURE 9.27   *s*-plane picture used to calculate the location of the compensator pole for Example 9.4
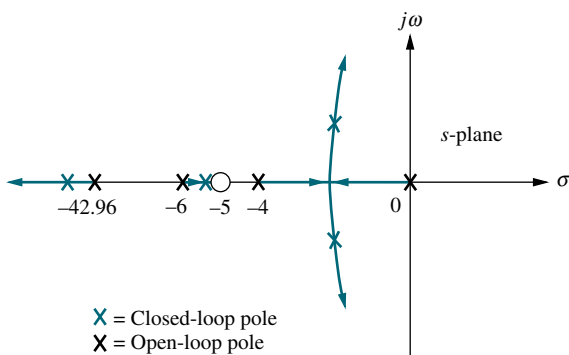
X = Closed-loop pole
X = Open-loop pole

Note: This figure is not drawn to scale.

FIGURE 9.28   Compensated system root locus

In order to justify our estimates of percent overshoot and settling time, we must show that the second-order approximation is valid. To perform this validity check, we search for the third and fourth closed-loop poles found beyond -42.96 and between -5 and -6 in Figure 9.28. Searching these regions for the gain equal to that of the compensated dominant pole, 1423, we find that the third and fourth poles are at -43.8 and -5.134, respectively. Since -43.8 is more than 20 times the real part of the dominant pole, the effect of the third closed-loop pole is negligible. Since the closed-loop pole at -5.134 is close to the zero at -5, we have pole-zero cancellation, and the second-order approximation is valid.

All results for this design and two other designs, which place the compensator zero arbitrarily at -2 and -4 and follow similar design techniques, are summarized in Table 9.4. Each design should be verified by a simulation, which could consist of using MATLAB (discussed at the end of this example) or the state-space model and the step-response program discussed in Appendix H.1 at www.wiley.com/college/nise. We have performed a simulation for this design problem, and the results are shown by parenthetical entries next to the estimated values in the table. The only design that disagrees with the simulation is the case where the compensator zero is at -2. For this case the closed-loop pole and zero do not cancel.

A sketch of the root locus, which you should generate, shows why the effect of the zero is pronounced, causing the response to be different from that predicted. Placing the zero to the right of the pole at -4 creates a portion of the root locus that is between the origin and the zero. In other words, there is a closed-loop pole closer to the origin than the dominant poles, with little chance of pole-zero cancellation except at high gain. Thus, a quick sketch of the root locus gives us information from which we can make better design decisions. For this example, we want to place the zero on, or to the left of, the pole at -4, which gives a better chance for pole-zero cancellation and for a higher-order pole that is to the left of the dominant poles and subsequently faster. This is verified by the fact that our results show good second-order approximations for the cases where the zero was placed at -4 and -5. Again, decisions about where to place the zero are based on simple rules of thumb and must be verified by simulations at the end of the design.

Let us now summarize the results shown in Table 9.4. First we notice differences in the following:

1. The position of the arbitrarily selected zero
2. The amount of improvement in the steady-state error
3. The amount of required gain, K
4. The position of the third and fourth poles and their relative effect upon the second-order approximation. This effect is measured by their distance from the dominant poles or the degree of cancellation with the closed-loop zero.

Once a simulation verifies desired performance, the choice of compensation can be based upon the amount of gain required or the improvement in steady-state error that can be obtained without a lag compensator.

The results of Table 9.4 are supported by simulations of the step response, shown in Figure 9.29 for the uncompensated system and the three lead compensation solutions.

MATLAB
ML

Students who are using MATLAB should now run ch9p2 in Appendix B. MATLAB will be used to design a lead compensator. You will input the desired percent overshoot from the keyboard. MATLAB
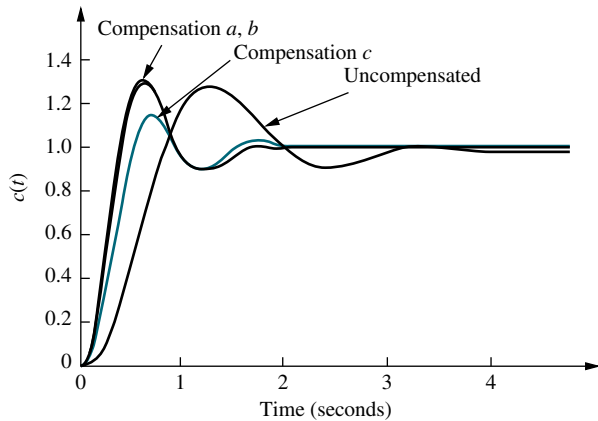
FIGURE 9.29   Uncompensated system and lead compensation responses for Example 9.4

will plot the root locus of the uncompensated system and the
percent overshoot line. You will interactively select the gain,
after which MATLAB will display the performance characteris-
tics of the uncompensated system and plot its step response.
Using these characteristics,you will input the desired set-
tling time and a zero value for the lead compensator.You will
then interactively select a value for the compensator pole.
MATLAB will respond with a root locus.You can then continue
selecting pole values until the root locus goes through the
desired point.MATLAB will display the lead compensator,enu-
merate its performance characteristics,and plot a step re-
sponse.This exercise solves Example 9.4 using MATLAB.

Skill-Assessment Exercise 9.2

PROBLEM: A unity feedback system with the forward transfer function

$$G(s) = \frac{K}{s(s+7)}$$

is operating with a closed-loop step response that has 15% overshoot. Do the
following:

- **a.** Evaluate the settling time.
- **b.** Design a lead compensator to decrease the settling time by three times.
   Choose the compensator's zero to be at -10.

ANSWERS:

- **a.** $T_s = 1.143$ s
- **b.** $G_{\text{lead}}(s) = \dfrac{s+10}{s+25.52}$, $K = 476.3$

The complete solution is at www.wiley.com/college/nise.

◖ 9.4 Improving Steady-State Error and Transient Response

We now combine the design techniques covered in Sections 9.2 and 9.3 to obtain improvement in steady-state error and transient response *independently*. Basically, we first improve the transient response by using the methods of Section 9.3. Then we improve the steady-state error of this compensated system by applying the methods of Section 9.2. A disadvantage of this approach is the slight decrease in the speed of the response when the steady-state error is improved.

As an alternative, we can improve the steady-state error first and then follow with the design to improve the transient response. A disadvantage of this approach is that the improvement in transient response in some cases yields deterioration in the improvement of the steady-state error, which was designed first. In other cases, the improvement in transient response yields further improvement in steady-state errors. Thus, a system can be overdesigned with respect to steady-state errors. Overdesign is usually not a problem unless it affects cost or produces other design problems. In this textbook, we first design for transient response and then design for steady-state error.

The design can use either active or passive compensators, as previously described. If we design an active PD controller followed by an active PI controller, the resulting compensator is called a *proportional-plus-integral-plus-derivative* (*PID*) *controller*. If we first design a passive lead compensator and then design a passive lag compensator, the resulting compensator is called a *lag-lead compensator*.

PID Controller Design

A PID controller is shown in Figure 9.30. Its transfer function is

$$G_c(s) = K_1 + \frac{K_2}{s} + K_3 s = \frac{K_1 s + K_2 + K_3 s^2}{s} = \frac{K_3 \left(s^2 + \frac{K_1}{K_3} s + \frac{K_2}{K_3} \right)}{s} \qquad (9.21)$$

which has two zeros plus a pole at the origin. One zero and the pole at the origin can be designed as the ideal integral compensator; the other zero can be designed as the ideal derivative compensator.

The design technique, which is demonstrated in Example 9.5, consists of the following steps:

1. Evaluate the performance of the uncompensated system to determine how much improvement in transient response is required.

2. Design the PD controller to meet the transient response specifications. The design includes the zero location and the loop gain.
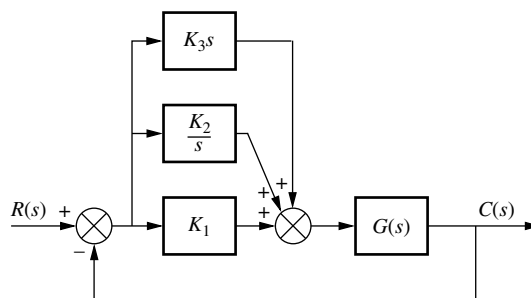

FIGURE 9.30   PID controller

3. Simulate the system to be sure all requirements have been met.
4. Redesign if the simulation shows that requirements have not been met.
5. Design the PI controller to yield the required steady-state error.
6. Determine the gains, K_1, K_2, and K_3, in Figure 9.30.
7. Simulate the system to be sure all requirements have been met.
8. Redesign if simulation shows that requirements have not been met.

Example 9.5

PID Controller Design

PROBLEM: Given the system of Figure 9.31, design a PID controller so that the system can operate with a peak time that is two-thirds that of the uncompensated system at 20% overshoot and with zero steady-state error for a step input.
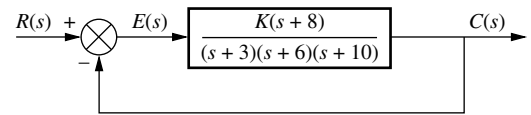
FIGURE 9.31   Uncompensated feedback control system for Example 9.5

SOLUTION: Note that our solution follows the eight-step procedure described earlier.

Step 1   Let us first evaluate the uncompensated system operating at 20% overshoot. Searching along the 20% overshoot line ($\zeta = 0.456$) in Figure 9.32, we find the dominant poles to be $-5.415 \pm j10.57$ with a gain of 121.5. A third pole, which exists at -8.169, is found by searching the region

FIGURE 9.32   Root locus for the uncompensated system of Example 9.5

TABLE 9.5 Predicted characteristics of uncompensated, PD-, and PID-compensated systems of Example 9.5

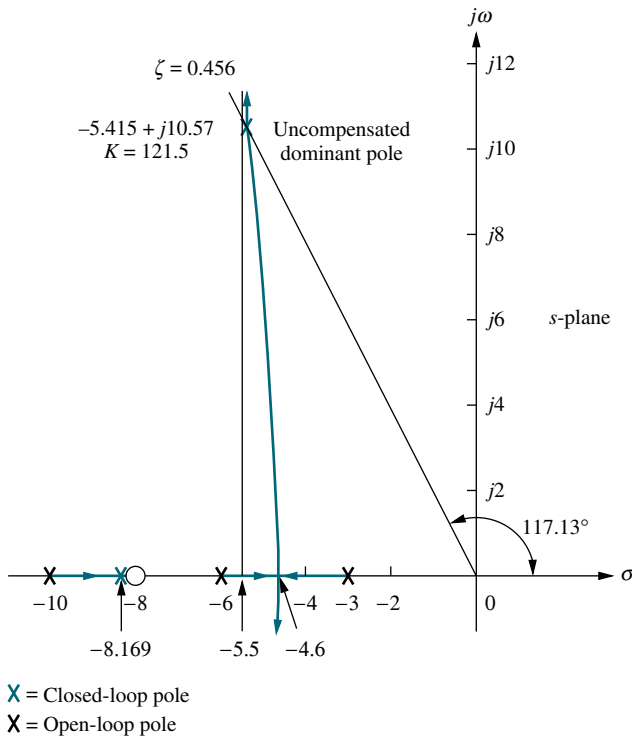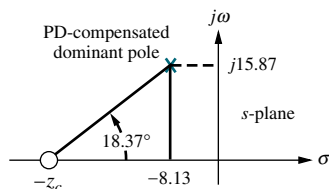|	**Uncompensated**	**PD-compensated**	**PID-compensated**
Plant and compensator	$\dfrac{K(s+8)}{(s+3)(s+6)(s+10)}$	$\dfrac{K(s+8)(s+55.92)}{(s+3)(s+6)(s+10)}$	$\dfrac{K(s+8)(s+55.92)(s+0.5)}{(s+3)(s+6)(s+10)s}$
Dominant poles	$-5.415 \pm j10.57$	$-8.13 \pm j15.87$	$-7.516 \pm j14.67$
K	121.5	5.34	4.6
ζ	0.456	0.456	0.456
ω_n	11.88	17.83	16.49
$\%OS$	20	20	20
T_s	0.739	0.492	0.532
T_p	0.297	0.198	0.214
K_p	5.4	13.27	∞
$e(\infty)$	0.156	0.070	0
Other poles	-8.169	-8.079	$-8.099, -0.468$
Zeros	-8	$-8, -55.92$	$-8, -55.92, -0.5$
Comments	Second-order approx. OK	Second-order approx. OK	Zeros at -55.92 and -0.5 not canceled

between -8 and -10 for a gain equivalent to that at the dominant poles. The complete performance of the uncompensated system is shown in the first column of Table 9.5, where we compare the calculated values to those obtained through simulation (Figure 9.35). We estimate that the uncompensated system has a peak time of 0.297 second at 20% overshoot.

Step 2 To compensate the system to reduce the peak time to two-thirds of that of the uncompensated system, we must first find the compensated system's dominant pole location. The imaginary part of the compensated dominant pole is

$$\omega_d = \frac{\pi}{T_p} = \frac{\pi}{(2/3)(0.297)} = 15.87 \qquad (9.22)$$

Thus, the real part of the compensated dominant pole is

$$\sigma = \frac{\omega_d}{\tan 117.13°} = -8.13 \qquad (9.23)$$

Next we design the compensator. Using the geometry shown in Figure 9.33, we calculate the compensating zero's location. Using the root locus program, we find the sum of angles from the uncompensated system's poles and zeros to the desired compensated dominant pole to be $-198.37°$. Thus, the contribution required from the compensator zero is $198.37° - 180° = 18.37°$. Assume that the compensator zero is located at $-z_c$, as shown in Figure 9.33. Since

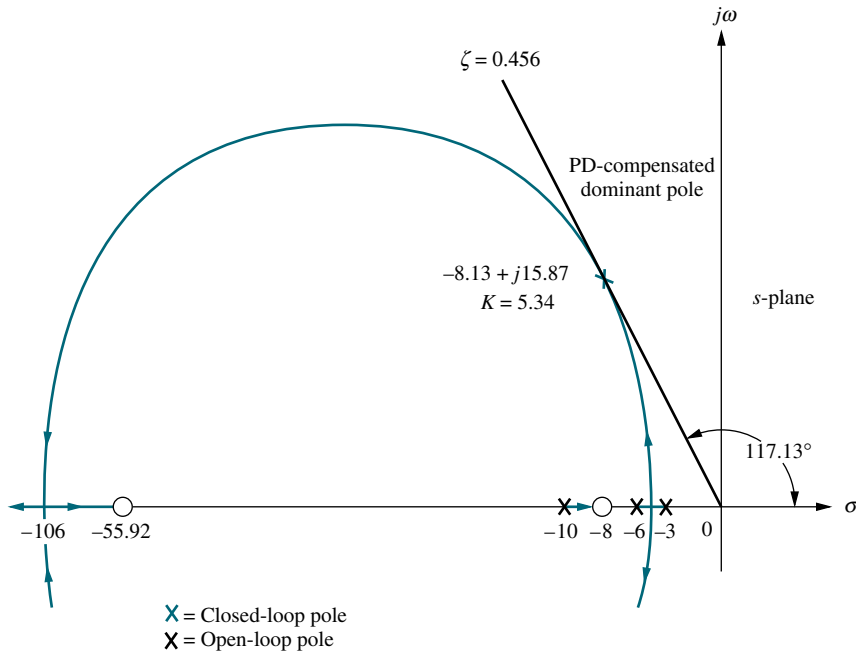$$\frac{15.87}{z_c - 8.13} = \tan 18.37° \qquad (9.24)$$

then

$$z_c = 55.92 \qquad (9.25)$$

Thus, the PD controller is

$$G_{\text{PD}}(s) = (s + 55.92) \qquad (9.26)$$

FIGURE 9.33 Calculating the PD compensator zero for Example 9.5

PD-compensated dominant pole

$j\omega$

$j15.87$

s-plane

$18.37°$

$-z_c$ -8.13 σ

X = Closed-loop pole

Note: This figure is not drawn to scale.

FIGURE 9.34   Root locus for PD-compensated system of Example 9.5

The complete root locus for the PD-compensated system is sketched in Figure 9.34. Using a root locus program, the gain at the design point is 5.34. Complete specifications for ideal derivative compensation are shown in the third column of Table 9.5.

Steps 3 and 4   We simulate the PD-compensated system, as shown in Figure 9.35. We see the reduction in peak time and the improvement in steady-state error over the uncompensated system.

Step 5   After we design the PD controller, we design the ideal integral compensator to reduce the steady-state error to zero for a step input. Any ideal integral compensator zero will work, as long as the zero is placed close to the origin. Choosing the ideal integral compensator to be
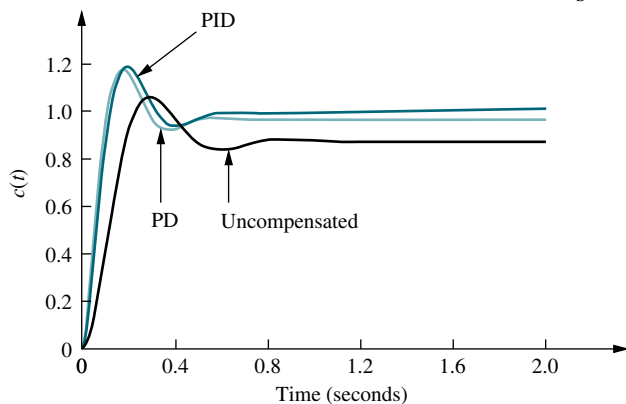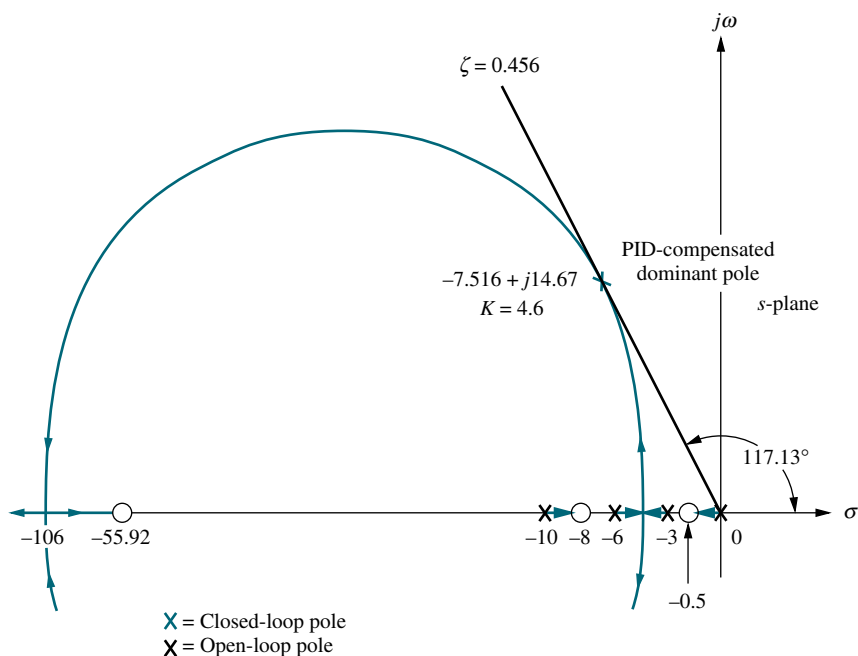
$$G_{PI}(s) = \frac{s + 0.5}{s} \qquad (9.27)$$

FIGURE 9.35   Step responses for uncompensated, PD-compensated, and PID-compensated systems of Example 9.5

FIGURE 9.36 Root locus for PID-compensated system of Example 9.5

we sketch the root locus for the PID-compensated system, as shown in Figure 9.36. Searching the 0.456 damping ratio line, we find the dominant, second-order poles to be $-7.516 \pm j14.67$, with an associated gain of 4.6. The remaining characteristics for the PID-compensated system are summarized in the fourth column of Table 9.5.

Step 6 Now we determine the gains, K_1, K_2, and K_3, in Figure 9.30. From Eqs. (9.26) and (9.27), the product of the gain and the PID controller is

$$
\begin{aligned}
G_{\text{PID}}(s) &= \frac{K(s + 55.92)(s + 0.5)}{s} = \frac{4.6(s + 55.92)(s + 0.5)}{s} \\
&= \frac{4.6(s^2 + 56.42s + 27.96)}{s}
\end{aligned}
\tag{9.28}
$$

Matching Eqs. (9.21) and (9.28), $K_1 = 259.5$, $K_2 = 128.6$, and $K_3 = 4.6$

Steps 7 and 8 Returning to Figure 9.35, we summarize the results of our design. PD compensation improved the transient response by decreasing the time required to reach the first peak as well as yielding some improvement in the steady-state error. The complete PID controller further improved the steady-state error without appreciably changing the transient response designed with the PD controller. As we have mentioned before, the PID controller exhibits a slower response, reaching the final value of unity at approximately 3 seconds. If this is undesirable, the speed of the system must be increased by redesigning the ideal derivative compensator or moving the PI controller zero farther from the origin. Simulation plays an important role in this type of design since our derived equation for settling time is not applicable for this part of the response, where there is a slow correction of the steady-state error.

Lag-Lead Compensator Design

In the previous example, we serially combined the concepts of ideal derivative and ideal integral compensation to arrive at the design of a PID controller that improved both the transient response and the steady-state error performance. In the next example, we improve both transient response and the steady-state error by using a lead compensator and a lag compensator rather than the ideal PID. Our compensator is called a *lag-lead compensator*.

We first design the lead compensator to improve the transient response. Next we evaluate the improvement in steady-state error still required. Finally, we design the lag compensator to meet the steady-state error requirement. Later in the chapter we show circuit designs for the passive network. The following steps summarize the design procedure:

1. Evaluate the performance of the uncompensated system to determine how much improvement in transient response is required.
2. Design the lead compensator to meet the transient response specifications. The design includes the zero location, pole location, and the loop gain.
3. Simulate the system to be sure all requirements have been met.
4. Redesign if the simulation shows that requirements have not been met.
5. Evaluate the steady-state error performance for the lead-compensated system to determine how much more improvement in steady-state error is required.
6. Design the lag compensator to yield the required steady-state error.
7. Simulate the system to be sure all requirements have been met.
8. Redesign if the simulation shows that requirements have not been met.

Example 9.6

Lag-Lead Compensator Design

PROBLEM: Design a lag-lead compensator for the system of Figure 9.37 so that the system will operate with 20% overshoot and a twofold reduction in settling time. Further, the compensated system will exhibit a tenfold improvement in steady-state error for a ramp input.

FIGURE 9.37   Uncompensated system for Example 9.6

SOLUTION: Again, our solution follows the steps just described.

Step 1   First we evaluate the performance of the uncompensated system. Searching along the 20% overshoot line ($\zeta = 0.456$) in Figure 9.38, we find the dominant poles at $-1.794 \pm j3.501$, with a gain of 192.1. The performance of the uncompensated system is summarized in Table 9.6.

Step 2   Next we begin the lead compensator design by selecting the location of the compensated system's dominant poles. In order to realize a twofold reduction in settling time, the real part of the dominant pole must be increased by a factor of 2, since the settling time is inversely proportional to the real part. Thus,

$$-\zeta\omega_n = -2(1.794) = -3.588 \tag{9.29}$$

The imaginary part of the design point is

$$\omega_d = \zeta\omega_n \tan 117.13° = 3.588 \tan 117.13° = 7.003 \tag{9.30}$$

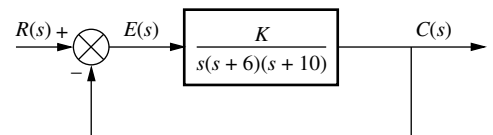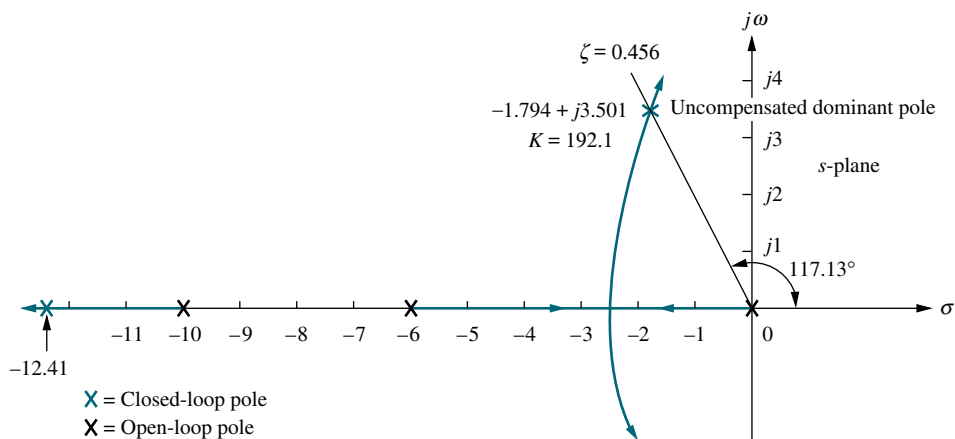**FIGURE 9.38** Root locus for uncompensated system of Example 9.6

Now we design the lead compensator. Arbitrarily select a location for the lead compensator zero. For this example, we select the location of the compensator zero coincident with the open-loop pole at −6. This choice will eliminate a zero and leave the lead-compensated system with three poles, the same number that the uncompensated system has.

We complete the design by finding the location of the compensator pole. Using the root locus program, sum the angles to the design point from the uncompensated system's poles and zeros and the compensator zero and get −164.65°. The difference between 180° and this quantity is the angular contribution required from the compensator pole, or −15.35°. Using the geometry shown in Figure 9.39,

$$\frac{7.003}{p_c - 3.588} = \tan 15.35° \tag{9.31}$$

from which the location of the compensator pole, p_c, is found to be −29.1.

TABLE 9.6 Predicted characteristics of uncompensated, lead-compensated, and lag-lead-compensated systems of Example 9.6

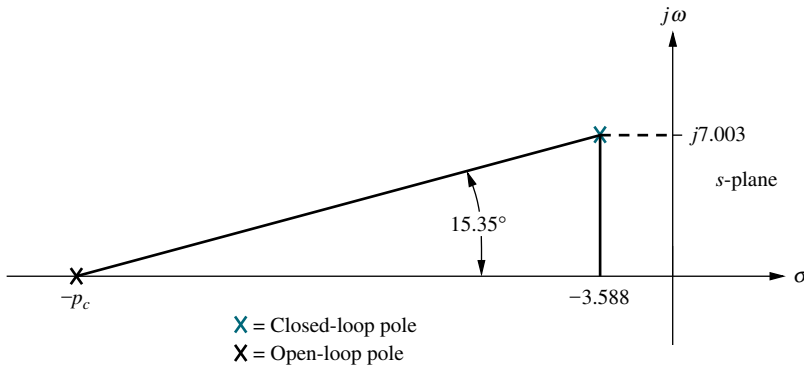|	**Uncompensated**	**Lead-compensated**	**Lag-lead-compensated**
Plant and compensator	$\dfrac{K}{s(s+6)(s+10)}$	$\dfrac{K}{s(s+10)(s+29.1)}$	$\dfrac{K(s+0.04713)}{s(s+10)(s+29.1)(s+0.01)}$
Dominant poles	$-1.794 \pm j3.501$	$-3.588 \pm j7.003$	$-3.574 \pm j6.976$
K	192.1	1977	1971
ζ	0.456	0.456	0.456
ω_n	3.934	7.869	7.838
$\%OS$	20	20	20
T_s	2.230	1.115	1.119
T_p	0.897	0.449	0.450
K_v	3.202	6.794	31.92
$e(\infty)$	0.312	0.147	0.0313
Third pole	-12.41	-31.92	$-31.91, -0.0474$
Zero	None	None	-0.04713
Comments	Second-order approx. OK	Second-order approx. OK	Second-order approx. OK

FIGURE 9.39   Evaluating the compensator pole for Example 9.6

The complete root locus for the lead-compensated system is sketched in Figure 9.40. The gain setting at the design point is found to be 1977.

Steps 3 and 4   Check the design with a simulation. (The result for the lead-compensated system is shown in Figure 9.42 and is satisfactory.)

Step 5   Continue by designing the lag compensator to improve the steady-state error. Since the uncompensated system's open-loop transfer function is

$$G(s) = \frac{192.1}{s(s+6)(s+10)} \tag{9.32}$$

the static error constant, K_v, which is inversely proportional to the steady-state error, is 3.201. Since the open-loop transfer function of the lead-compensated system is

$$G_{LC}(s) = \frac{1977}{s(s+10)(s+29.1)} \tag{9.33}$$

the static error constant, K_v, which is inversely proportional to the steady-state error, is 6.794. Thus, the addition of lead compensation has improved the steady-state error by a factor of 2.122. Since the requirements of the problem specified a tenfold improvement, the lag compensator must be designed to improve the steady-state error by a factor of 4.713 ($10/2.122 = 4.713$) over the lead-compensated system.
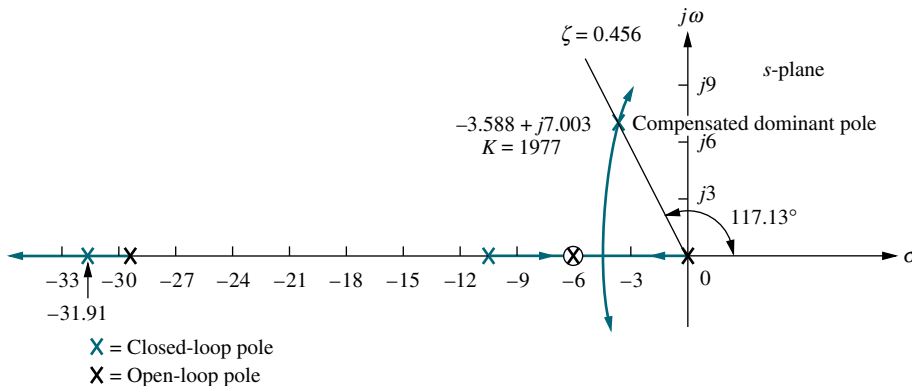

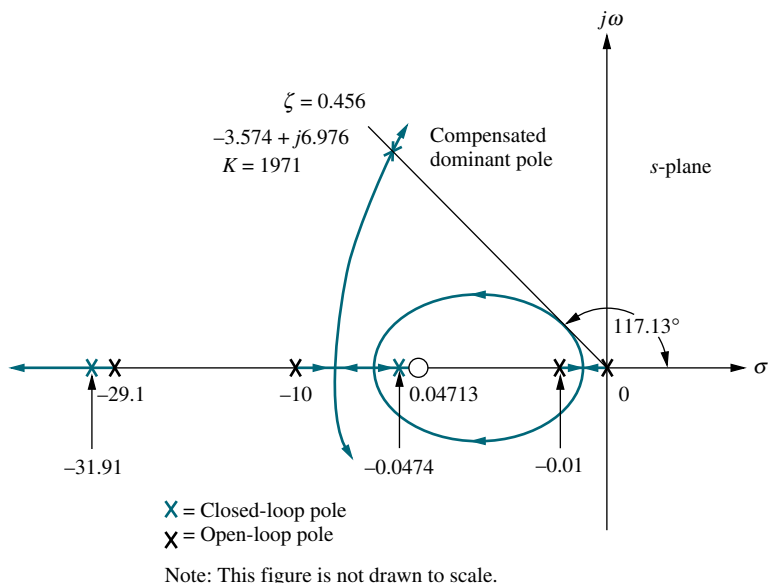**FIGURE 9.40**   Root locus for lead-compensated system of Example 9.6

FIGURE 9.41   Root locus for lag-lead-compensated system of Example 9.6

Step 6   We arbitrarily choose the lag compensator pole at 0.01, which then places the lag compensator zero at 0.04713, yielding

$$G_{\text{lag}}(s) = \frac{(s + 0.04713)}{(s + 0.01)} \tag{9.34}$$

as the lag compensator. The lag-lead-compensated system's open-loop transfer function is

$$G_{\text{LLC}}(s) = \frac{K(s + 0.04713)}{s(s + 10)(s + 29.1)(s + 0.01)} \tag{9.35}$$

where the uncompensated system pole at -6 canceled the lead compensator zero at -6. By drawing the complete root locus for the lag-lead-compensated system and by searching along the 0.456 damping ratio line, we find the dominant, closed-loop poles to be at $-3.574 \pm j6.976$, with a gain of 1971. The lag-lead-compensated root locus is shown in Figure 9.41.

A summary of our design is shown in Table 9.6. Notice that the lag-lead compensation has indeed increased the speed of the system, as witnessed by the settling time or the peak time. The steady-state error for a ramp input has also decreased by about 10 times, as seen from $e(\infty)$.

Step 7   The final proof of our designs is shown by the simulations of Figures 9.42 and 9.43. The improvement in the transient response is shown in Figure 9.42, where we see the peak time occurring sooner in the lag-lead-compensated system. Improvement in the steady-state error for a ramp input is seen in Figure 9.43, where each step of our design yields more improvement. The improvement for the lead-compensated system is shown in Figure 9.43(a), and the final improvement due to the addition of the lag is shown in Figure 9.43(b).
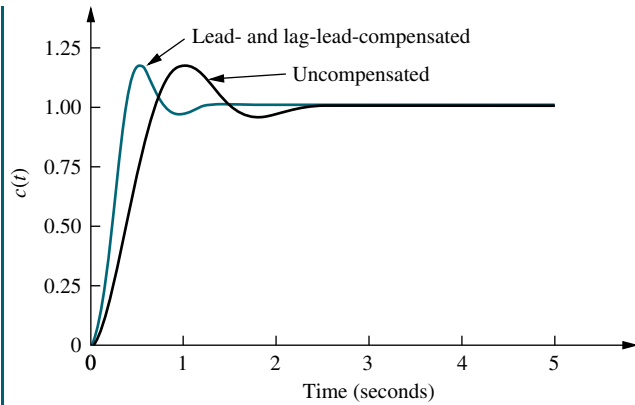
FIGURE 9.42   Improvement in step response for lag-lead-compensated system of Example 9.6
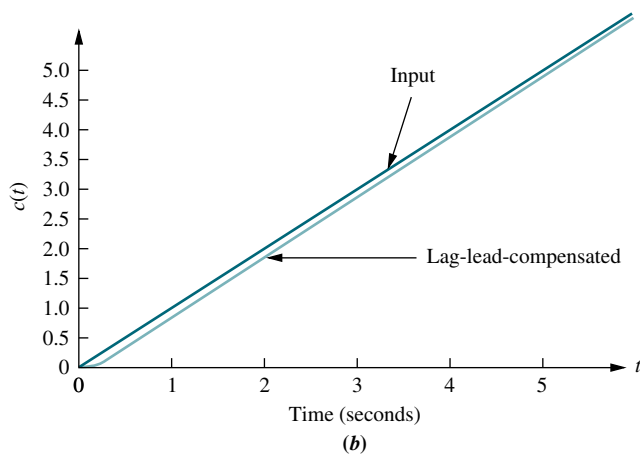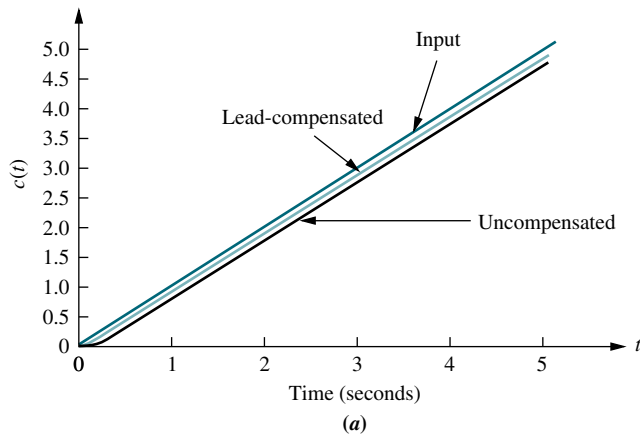
FIGURE 9.43   Improvement in ramp response error for the system of Example 9.6:
a. lead-compensated;
b. lag-lead-compensated

In the previous example, we canceled the system pole at −6 with the lead compensator zero. The design technique is the same if you place the lead compensator zero at a different location. Placing a zero at a different location and not canceling the open-loop pole yields a system with one more pole than the example. This increased complexity could make it more difficult to justify a second-order approximation. In any case, simulations should be used at each step to verify performance.

Notch Filter

If a plant, such as a mechanical system, has high-frequency vibration modes, then a desired closed-loop response may be difficult to obtain. These high-frequency vibration modes can be modeled as part of the plant's transfer function by pairs of complex poles near the imaginary axis. In a closed-loop configuration, these poles can move closer to the imaginary axis or even cross into the right half-plane, as shown in Figure 9.44(*a*). Instability or high-frequency oscillations superimposed over the desired response can result (see Figure 9.44(*b*)).

One way of eliminating the high-frequency oscillations is to cascade a *notch filter*[2] with the plant (*Kuo, 1995*), as shown in Figure 9.44(*c*). The notch filter has
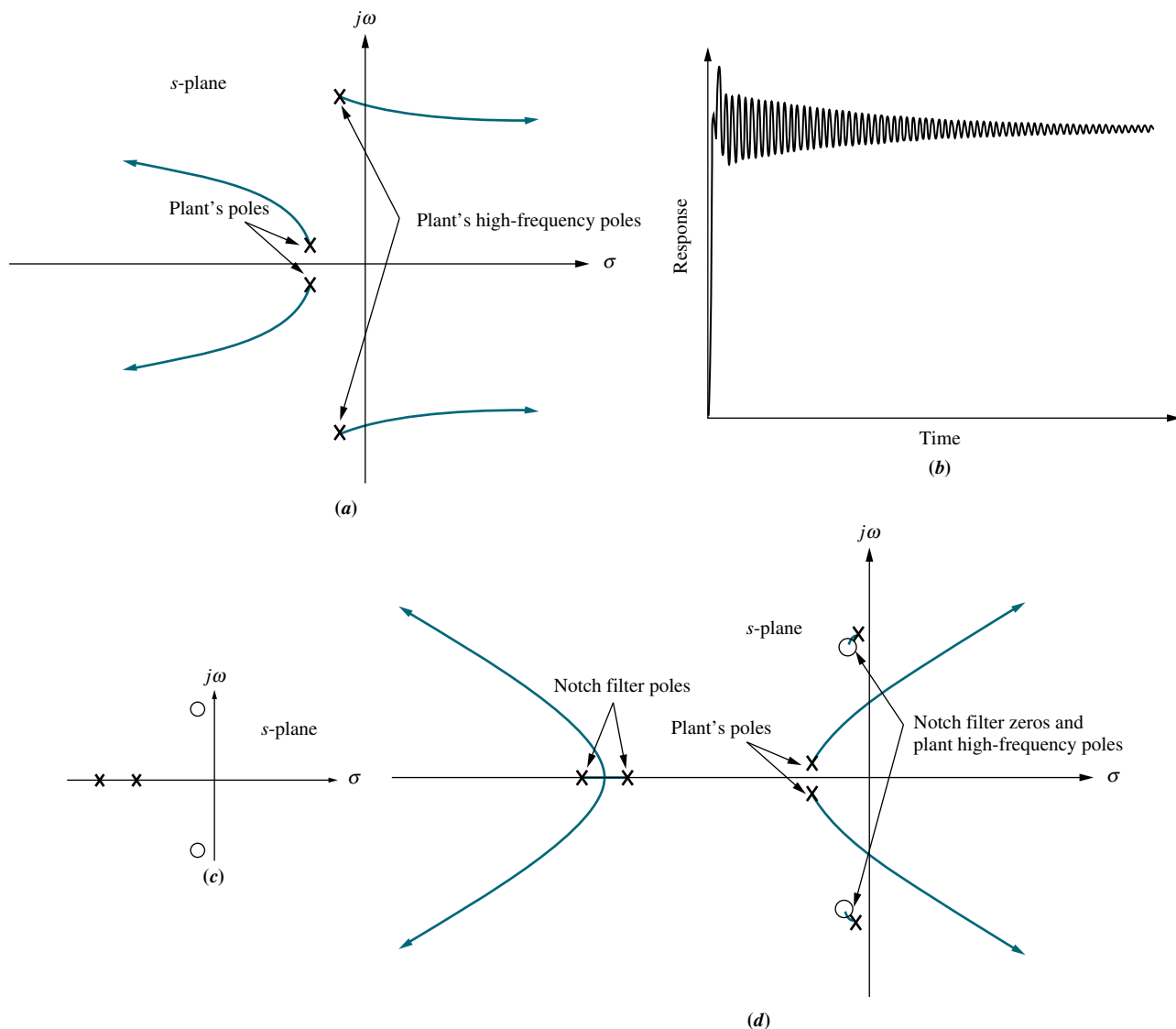
FIGURE 9.44 **a.** Root locus before cascading notch filter; **b.** typical closed-loop step response before cascading notch filter; **c.** pole-zero plot of a notch filter; **d.** root locus after cascading notch filter; (*figure continues*)

[2] The name of this filter comes from the shape of its magnitude frequency response characteristics, which shows a dip near the damped frequency of the high-frequency poles. Magnitude frequency response is discussed in Chapter 10.
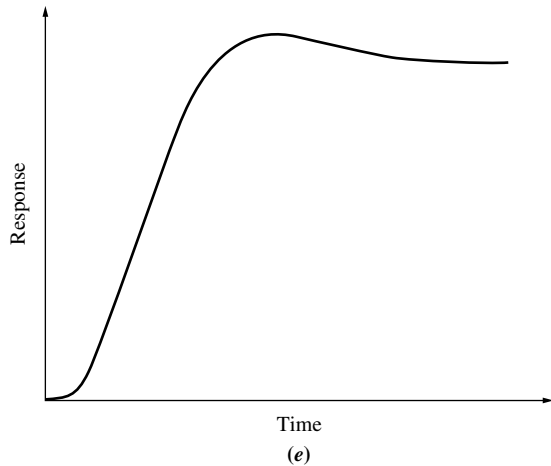
FIGURE 9.44   (*Continued*)
e. closed-loop step response
after cascading notch filter

zeros close to the low-damping-ratio poles of the plant as well as two real poles.
Figure 9.44(*d*) shows that the root locus branch from the high-frequency poles now
goes a short distance from the high-frequency pole to the notch filter's zero. The
high-frequency response will now be negligible because of the pole-zero cancellation
(see Figure 9.44(*e*)). Other cascade compensators can now be designed to yield a
desired response. The notch filter will be applied to Progressive Analysis and Design
Problem 55 near the end of this chapter.

Skill-Assessment Exercise 9.3

WileyPLUS

WPCS

Control Solutions

PROBLEM: A unity feedback system with forward transfer function

$$G(s) = \frac{K}{s(s+7)}$$

is operating with a closed-loop step response that has 20% overshoot. Do the
following:

a. Evaluate the settling time.
b. Evaluate the steady-state error for a unit ramp input.
c. Design a lag-lead compensator to decrease the settling time by 2 times and
   decrease the steady-state error for a unit ramp input by 10 times. Place the
   lead zero at -3.

ANSWERS:

a. $T_s = 1.143$ s
b. $e_{\text{ramp}}(\infty) = 0.1189$
c. $G_c(s) = \dfrac{(s+3)(s+0.092)}{(s+9.61)(s+0.01)}, \quad K = 205.4$

The complete solution is at www.wiley.com/college/nise.

Before concluding this section, let us briefly summarize our discussion of
cascade compensation. In Sections 9.2, 9.3, and 9.4, we used cascade compensators to
improve transient response and steady-state error. Table 9.7 itemizes the types,
functions, and characteristics of these compensators.

TABLE 9.7   Types of cascade compensators

Function	Compensator	Transfer function	Characteristics
Improve steady-state error	PI	$K\dfrac{s + z_c}{s}$	1. Increases system type. 2. Error becomes zero. 3. Zero at $-z_c$ is small and negative. 4. Active circuits are required to implement.
Improve steady-state error	Lag	$K\dfrac{s + z_c}{s + p_c}$	1. Error is improved but not driven to zero. 2. Pole at $-p_c$ is small and negative. 3. Zero at $-z_c$ is close to, and to the left of, the pole at $-p_c$. 4. Active circuits are not required to implement.
Improve transient response	PD	$K(s + z_c)$	1. Zero at $-z_c$ is selected to put design point on root locus. 2. Active circuits are required to implement. 3. Can cause noise and saturation; implement with rate feedback or with a pole (lead).
Improve transient response	Lead	$K\dfrac{s + z_c}{s + p_c}$	1. Zero at $-z_c$ and pole at $-p_c$ are selected to put design point on root locus. 2. Pole at $-p_c$ is more negative than zero at $-z_c$. 3. Active circuits are not required to implement.
Improve steady-state error and transient response	PID	$K\dfrac{(s + z_{\text{lag}})(s + z_{\text{lead}})}{s}$	1. Lag zero at $-z_{\text{lag}}$ and pole at origin improve steady-state error. 2. Lead zero at $-z_{\text{lead}}$ improves transient response. 3. Lag zero at $-z_{\text{lag}}$ is close to, and to the left of, the origin. 4. Lead zero at $-z_{\text{lead}}$ is selected to put design point on root locus. 5. Active circuits required to implement. 6. Can cause noise and saturation; implement with rate feedback or with an additional pole.
Improve steady-state error and transient response	Lag-lead	$K\dfrac{(s + z_{\text{lag}})(s + z_{\text{lead}})}{(s + p_{\text{lag}})(s + p_{\text{lead}})}$	1. Lag pole at $-p_{\text{lag}}$ and lag zero at $-z_{\text{lag}}$ are used to improve steady-state error. 2. Lead pole at $-p_{\text{lead}}$ and lead zero at $-z_{\text{lead}}$ are used to improve transient response. 3. Lag pole at $-p_{\text{lag}}$ is small and negative. 4. Lag zero at $-z_{\text{lag}}$ is close to, and to the left of, lag pole at $-p_{\text{lag}}$. 5. Lead zero at $-z_{\text{lead}}$ and lead pole at $-p_{\text{lead}}$ are selected to put design point on root locus. 6. Lead pole at $-p_{\text{lead}}$ is more negative than lead zero at $-z_{\text{lead}}$. 7. Active circuits are not required to implement.

9.5   Feedback Compensation

In Section 9.4, we used cascade compensation as a way to improve transient response and steady-state response independently. Cascading a compensator with the plant is not the only way to reshape the root locus to intersect the closed-loop *s*-plane poles that yield a desired transient response. Transfer functions designed to be placed in a feedback path can also reshape the root locus. Figure 9.45 is a generic configuration showing a compensator, $H_c(s)$, placed in the *minor loop* of a feedback control system. Other configurations arise if we consider K unity, $G_2(s)$ unity, or both unity.

The design procedures for feedback compensation can be more complicated than for cascade compensation. On the other hand, feedback compensation can yield faster responses. Thus, the engineer has the luxury of designing faster responses into portions of a control loop in order to provide isolation. For example, the transient response of the ailerons and rudder control systems of an aircraft can be designed separately to be fast in order to reduce the effect of their dynamic response on the steering control loop. Feedback compensation can be used in cases where noise problems preclude the use of cascade compensation. Also, feedback compensation may not require additional amplification, since the signal passing through the compensator originates at the high-level output of the forward path and is delivered to a low-level input in the forward path. For example, let K and $G_2(s)$ in Figure 9.45 be unity. The input to the feedback compensator, $K_f H_c(s)$, is from the high-level output of $G_1(s)$, while the output of $K_f H_c(s)$ is one of the low-level inputs into K_1. Thus, there is a reduction in level through $K_f H_c(s)$, and amplification is usually not required.

A popular feedback compensator is a rate sensor that acts as a differentiator. In aircraft and ship applications, the rate sensor can be a rate gyro that responds with an output voltage proportional to the input angular velocity. In many other systems this rate sensor is implemented with a tachometer. A tachometer is a voltage generator that yields a voltage output proportional to input rotational speed. This compensator can easily be geared to the position output of a system. Figure 9.46 is a position
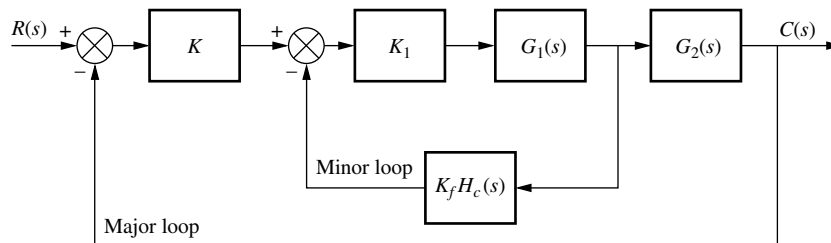

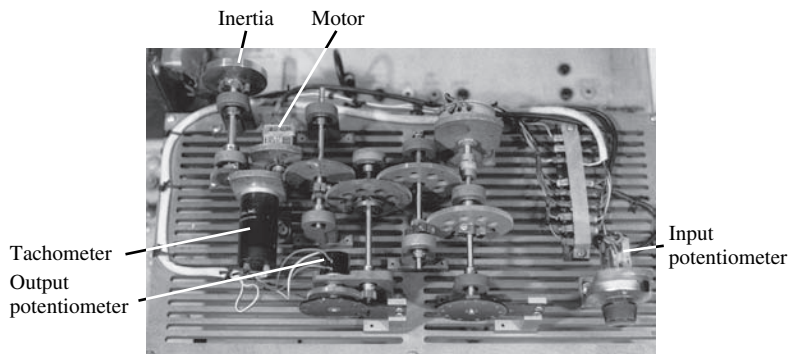**FIGURE 9.45**   Generic control system with feedback compensation.

FIGURE 9.46   A position control system that uses a tachometer as a differentiator in the feedback path. Can you see the similarity between this system and the schematic on the front endpapers?
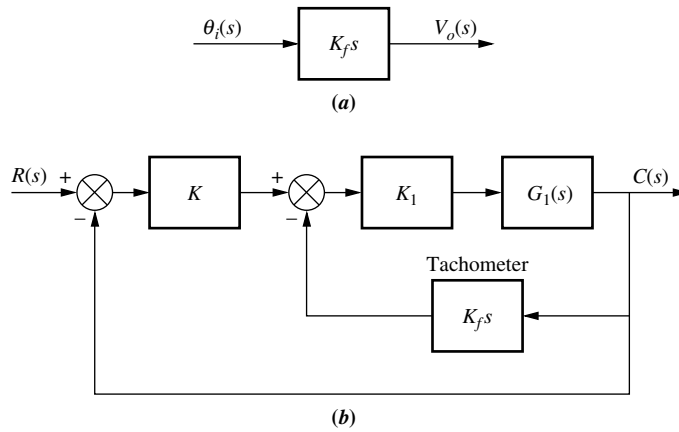
FIGURE 9.47   **a.** Transfer function of a tachometer; **b.** tachometer feed-back compensation

control system showing the gearing of the tachometer to the motor. You can see the input and output potentiometers as well as the motor and inertial load. The block diagram representation of a tachometer is shown in Figure 9.47(a), and its typical position within a control loop is shown in Figure 9.47(b).

While this section shows methods for designing systems using rate feedback, it also sets the stage for compensation techniques in Chapter 12, where not only rate but all states including position will be fed back for proper control system performance.

We now discuss design procedures. Typically, the design of feedback compensation consists of finding the gains, such as K, K_1, and K_f in Figure 9.45, after establishing a dynamic form for $H_c(s)$. There are two approaches. The first is similar to cascade compensation. Assume a typical feedback system, where $G(s)$ is the forward path and $H(s)$ is the feedback. Now consider that a root locus is plotted from $G(s)H(s)$. With cascade compensation we added poles and zeros to $G(s)$. With feedback compensation, poles and zeros are added via H(s).

With the second approach, we design a specified performance for the minor loop, shown in Figure 9.45, followed by a design of the major loop. Thus, the minor loop, such as ailerons on an aircraft, can be designed with its own performance specifications and operate within the major loop.
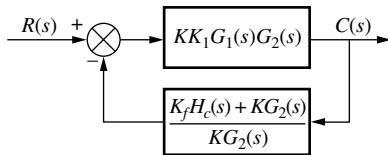
FIGURE 9.48 Equivalent block diagram of Figure 9.45

Approach 1

The first approach consists of reducing Figure 9.45 to Figure 9.48 by pushing K to the right past the summing junction, pushing $G_2(s)$ to the left past the pickoff point, and then adding the two feedback paths. Figure 9.48 shows that the loop gain, $G(s)H(s)$, is

$$G(s)H(s) = K_1G_1(s)[K_fH_c(s) + KG_2(s)] \tag{9.36}$$

Without feedback, $K_fH_c(s)$, the loop gain is

$$G(s)H(s) = KK_1G_1(s)G_2(s) \tag{9.37}$$

Thus, the effect of adding feedback is to replace the poles and zeros of $G_2(s)$ with the poles and zeros of $[K_fH_c(s) + KG_2(s)]$. Hence, this method is similar to cascade compensation in that we add new poles and zeros via $H(s)$ to reshape the root locus to go through the design point. However, one must remember that zeros of the equivalent feedback shown in Figure 9.48, $H(s) = [K_fH_c(s) + KG_2(s)]/KG_2(s)$, are not closed-loop zeros.

For example, if $G_2(s) = 1$ and the minor-loop feedback, $K_f H_c(s)$, is a rate sensor, $K_f H_c(s) = K_f s$, then from Eq. (9.36) the loop gain is

$$G(s)H(s) = K_f K_1 G_1(s)\left(s + \frac{K}{K_f}\right) \tag{9.38}$$

Thus, a zero at $-K/K_f$ is added to the existing open-loop poles and zeros. This zero reshapes the root locus to go through the desired design point. A final adjustment of the gain, K_1, yields the desired response. Again, you should verify that this zero is not a closed-loop zero. Let us look at a numerical example.

Example 9.7

Compensating Zero via Rate Feedback

PROBLEM: Given the system of Figure 9.49(a), design rate feedback compensation, as shown in Figure 9.49(b), to reduce the settling time by a factor of 4 while continuing to operate the system with 20% overshoot.

SOLUTION: First design a PD compensator. For the uncompensated system, search along the 20% overshoot line ($\zeta = 0.456$) and find that the dominant poles are at $-1.809 \pm j3.531$, as shown in Figure 9.50. The estimated specifications for the
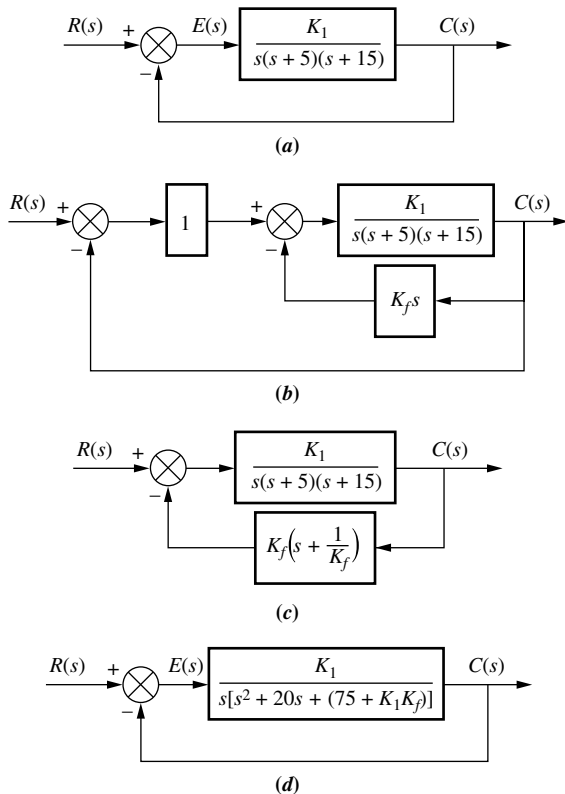
FIGURE 9.49 **a.** System for Example 9.7; **b.** system with rate feedback compensation; **c.** equivalent compensated system; **d.** equivalent compensated system showing unity feedback

FIGURE 9.50 Root locus for uncompensated system of Example 9.7
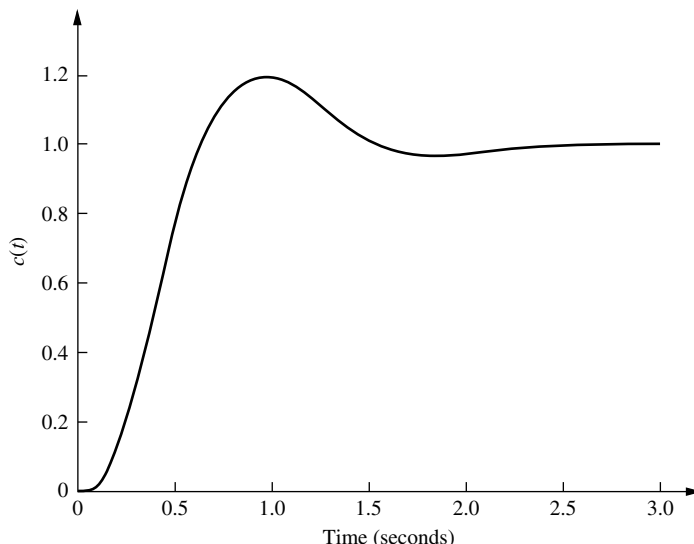
FIGURE 9.51 Step response for uncompensated system of Example 9.7

uncompensated system are shown in Table 9.8, and the step response is shown in Figure 9.51. The settling time is 2.21 seconds and must be reduced by a factor of 4 to 0.55 second.

Next determine the location of the dominant poles for the compensated system. To achieve a fourfold decrease in the settling time, the real part of the pole must be increased by a factor of 4. Thus, the compensated pole has a real part of $4(-1.809) = -7.236$. The imaginary part is then

$$\omega_d = -7.236 \tan 117.13° = 14.12 \tag{9.39}$$

where $117.13°$ is the angle of the 20% overshoot line.

TABLE 9.8 Predicted characteristics of uncompensated and compensated systems of Example 9.7

	Uncompensated	**Compensated**
Plant and compensator	$\dfrac{K_1}{s(s+5)(s+15)}$	$\dfrac{K_1}{s(s+5)(s+15)}$
Feedback	1	$0.185(s+5.42)$
Dominant poles	$-1.809 \pm j3.531$	$-7.236 \pm j14.12$
K_1	257.8	1388
ζ	0.456	0.456
ω_n	3.97	15.87
%OS	20	20
T_s	2.21	0.55
T_p	0.89	0.22
K_v	3.44	4.18
$e(\infty)$ (ramp)	0.29	0.24
Other poles	-16.4	-5.53
Zero	None	None
Comments	Second-order approx. OK	Simulate

Using the compensated dominant pole position of $-7.236 \pm j14.12$, we sum the angles from the uncompensated system's poles and obtain $-277.33°$. This angle requires a compensator zero contribution of $+97.33°$ to yield $180°$ at the design point. The geometry shown in Figure 9.52 leads to the calculation of the compensator's zero location. Hence,

$$\frac{14.12}{7.236 - z_c} = \tan(180° - 97.33°) \tag{9.40}$$

from which $z_c = 5.42$.

The root locus for the equivalent compensated system of Figure 9.49(c) is shown in Figure 9.53. The gain at the design point, which is $K_1 K_f$ from Figure 9.49(c), is found to be 256.7. Since K_f is the reciprocal of the compensator zero, $K_f = 0.185$. Thus, $K_1 = 1388$.

In order to evaluate the steady-state error characteristic, K_v is found from Figure 9.49(d) to be

$$K_v = \frac{K_1}{75 + K_1 K_f} = 4.18 \tag{9.41}$$

Predicted performance for the compensated system is shown in Table 9.8. Notice that the higher-order pole is not far enough away from the dominant poles and thus cannot be neglected. Further, from Figure 9.49(d), we see that the closed-loop transfer function is

$$T(s) = \frac{G(s)}{1 + G(s)H(s)} = \frac{K_1}{s^3 + 20s^2 + (75 + K_1 K_f)s + K_1} \tag{9.42}$$

Thus, as predicted, the open-loop zero is not a closed-loop zero, and there is no pole-zero cancellation. Hence, the design must be checked by simulation.

The results of the simulation are shown in Figure 9.54 and show an over-damped response with a settling time of 0.75 second, compared to the uncompensated system's settling time of approximately

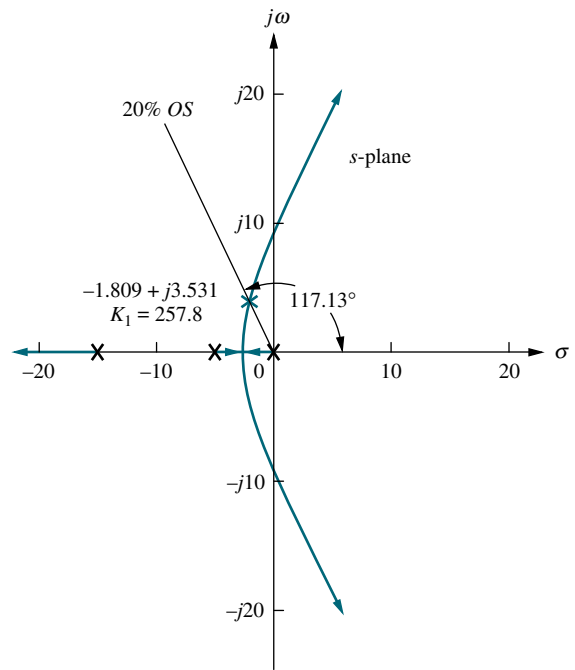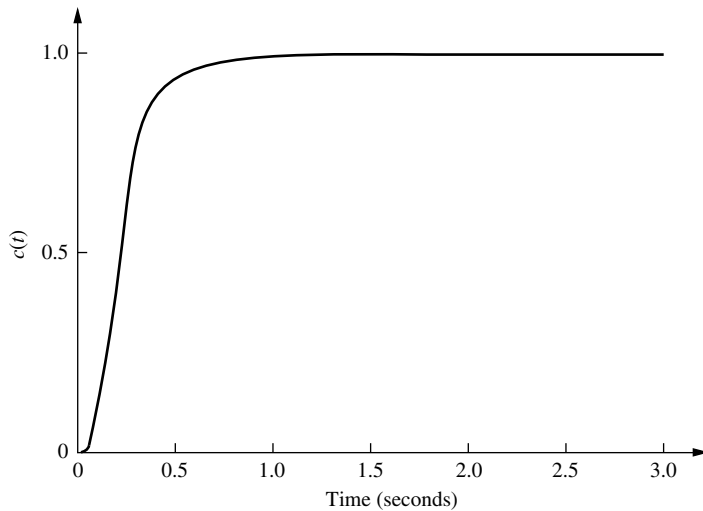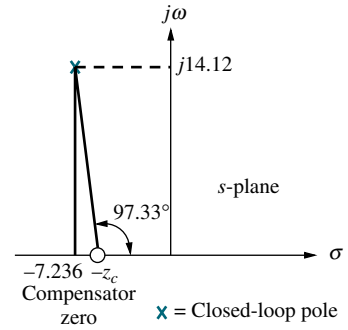**FIGURE 9.52**   Finding the compensator zero in Example 9.7
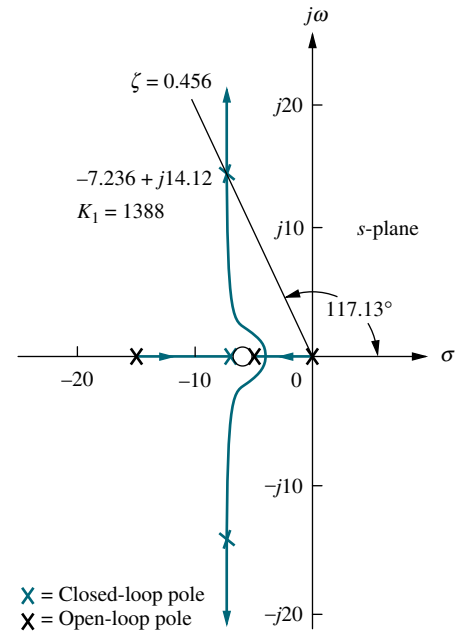
FIGURE 9.53   Root locus for the compensated system of Example 9.7

FIGURE 9.54   Step response for the compensated system of Example 9.7

2.2 seconds. Although not meeting the design requirements, the response still represents an improvement over the uncompensated system of Figure 9.51. Typically, less overshoot is acceptable. The system should be redesigned for further reduction in settling time.

You may want to do Problem 8 at the end of this chapter, where you can repeat this example using PD cascade compensation. You will see that the compensator zero for cascade compensation is a closed-loop zero, yielding the possibility of pole-zero cancellation. However, PD compensation is usually noisy and not always practical.

Approach 2

The second approach allows us to use feedback compensation to design a minor loop's transient response separately from the closed-loop system response. In the case of an aircraft, the minor loop may control the position of the aerosurfaces, while the entire closed-loop system may control the entire aircraft's pitch angle.

We will see that the minor loop of Figure 9.45 basically represents a forward-path transfer function whose poles can be adjusted with the minor-loop gain. These poles then become the open-loop poles for the entire control system. In other words, rather than reshaping the root locus with additional poles and zeros, as in cascade compensation, we can actually change the plant's poles through a gain adjustment. Finally, the closed-loop poles are set by the loop gain, as in cascade compensation.

Example 9.8

Minor-Loop Feedback Compensation

PROBLEM: For the system of Figure 9.55(*a*), design minor-loop feedback compensation, as shown in Figure 9.55(*b*), to yield a damping ratio of 0.8 for the minor loop and a damping ratio of 0.6 for the closed-loop system.

(*a*)

(*b*)

FIGURE 9.55   **a.** Uncompensated system and **b.** feedback-compensated system for Example 9.8

SOLUTION: The minor loop is defined as the loop containing the plant, $1/[s(s+5)(s+15)]$, and the feedback compensator, $K_f s$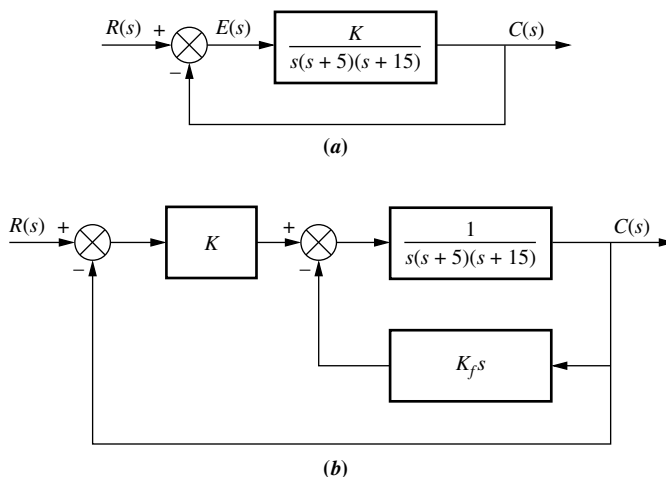. The value of K_f will be adjusted to set the location of the minor-loop poles, and then K will be adjusted to yield the desired closed-loop response.

The transfer function of the minor loop, $G_{\mathrm{ML}}(S)$, is

$$G_{\mathrm{ML}}(s) = \frac{1}{s[s^2 + 20s + (75 + K_f)]} \qquad (9.43)$$

The poles of $G_{\mathrm{ML}}(s)$ can be found analytically or via the root locus. The root locus for the minor loop, where $K_f s/[s(s+5)(s+15)]$ is the open-loop transfer function, is shown in Figure 9.56. Since the zero at the origin comes from the feedback transfer function of the minor loop, this zero is not a zero of the closed-loop transfer function of the minor loop. Hence, the pole at the origin appears to remain stationary, and there is no pole-zero cancellation at the origin. Eq. (9.43) also shows this phenomenon. We see a stationary pole at the origin and two complex poles that change with gain. Notice that the compensator gain, K_f, varies the natural frequency, ω_n, of the minor-loop poles as seen from Eq. (9.43). Since the real parts of the complex poles are constant at $\zeta\omega_n = -10$, the damping ratio must also be varying to keep $2\zeta\omega_n = 20$, a constant. Drawing the $\zeta = 0.8$ line in Figure 9.56 yields the complex poles at $-10 \pm j7.5$. The gain, K_f, which equals 81.25, places the minor-loop poles in a position to meet the specifications. The poles just found, $-10 \pm j7.5$, as well as the pole at the origin (Eq. (9.43)), act as open-loop poles that generate a root locus for variations of the gain, K.

The final root locus for the system is shown in Figure 9.57. The $\zeta = 0.6$ damping ratio line is drawn and searched. The closed-loop complex poles are found to be $-4.535 \pm j6.046$, with a required gain of 624.3. A third pole is at -10.93.

FIGURE 9.56   Root locus for minor loop of Example 9.8
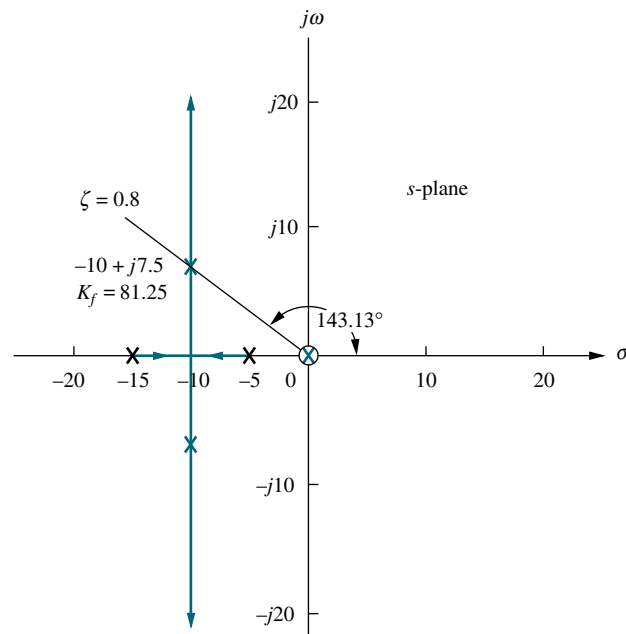
X = Closed-loop pole (minor loop)
X = Open-loop pole

Virtual Experiment 9.2 Improving Transient Response and Steady-State Error Using Rate Feedback and PD Control

Put theory into practice and design a compensator in LabVIEW that controls the ball position in the Quanser Magnetic Levitation system. Magnetic Levitation technology is used for modern transportation systems that suspend, such as the high speed Magnetic Levitation train.

Virtual experiments are found on WileyPLUS.
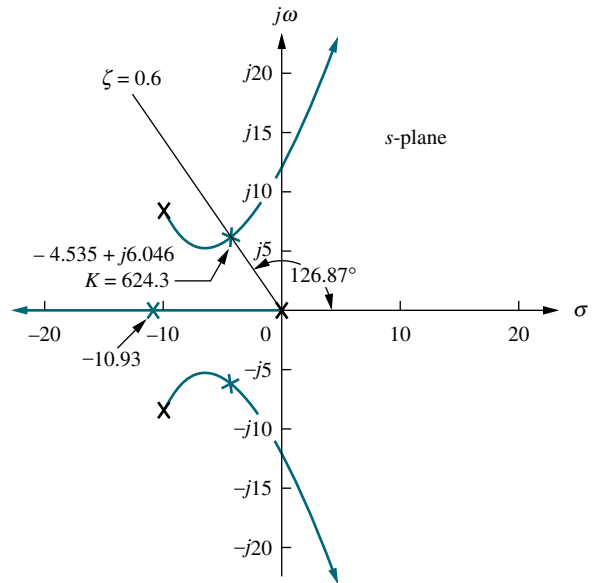
FIGURE 9.57 Root locus for closed-loop system of Example 9.8

X = Closed-loop pole
X = Open-loop pole

The results are summarized in Table 9.9. We see that the compensated system, although having the same damping ratio as the uncompensated system, is much faster and also has a smaller steady-state error. The results, however, are predicted results and must be simulated to verify percent overshoot, settling time, and peak time, since the third pole is not far enough from the dominant poles. The step response is shown in Figure 9.58 and closely matches the predicted performance.

TABLE 9.9 Predicted characteristics of the uncompensated and compensated systems of Example 9.8

	Uncompensated	**Compensated**
Plant and compensator	$\dfrac{K_1}{s(s+5)(s+15)}$	$\dfrac{K}{s(s^2+20s+156.25)}$
Feedback	1	1
Dominant poles	$-1.997 \pm j2.662$	$-4.535 \pm j6.046$
K	177.3	624.3
ζ	0.6	0.6
ω_n	3.328	7.558
%OS	9.48	9.48
T_s	2	0.882
T_p	1.18	0.52
K_v	2.364	3.996
$e(\infty)$(ramp)	0.423	0.25
Other poles	-16	-10.93
Zero	None	None
Comments	Second-order approx. OK	Simulate
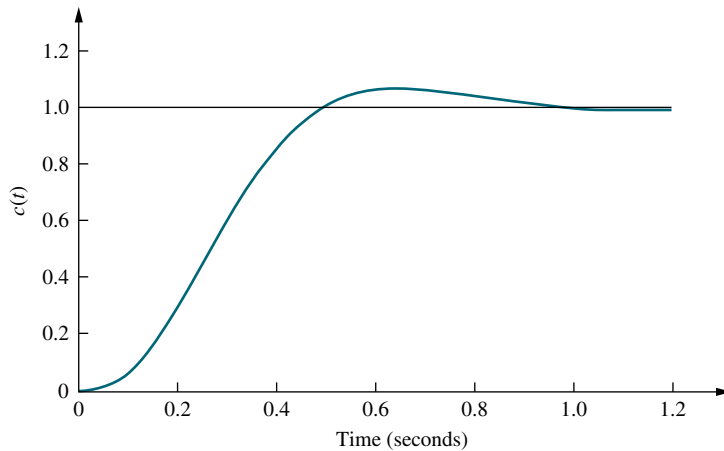
FIGURE 9.58   Step response simulation for Example 9.8

Skill-Assessment Exercise 9.4

PROBLEM: For the system of Figure 9.59, design minor-loop rate feedback compensation to yield a damping ratio of 0.7 for the minor loop's dominant poles and a damping ratio of 0.5 for the closed-loop system's dominant poles.
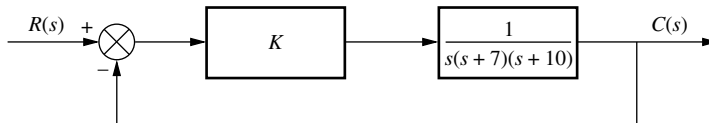
FIGURE 9.59   System for Skill-Assessment Exercise 9.4

ANSWER: The system is configured similar to Figure 9.55(b) with $K_f = 77.42$ and $K = 626.3$.

The complete solution is at www.wiley.com/college/nise.

Our discussion of compensation methods is now complete. We studied both cascade and feedback compensation and compared and contrasted them. We are now ready to show how to physically realize the controllers and compensators we designed.

9.6   Physical Realization of Compensation

In this chapter, we derived compensation to improve transient response and steady-state error in feedback control systems. Transfer functions of compensators used in cascade with the plant or in the feedback path were derived. These compensators were defined by their pole-zero configurations. They were either active PI, PD, or PID controllers or passive lag, lead, or lag-lead compensators. In this section, we show how to implement the active controllers and the passive compensators.

Active-Circuit Realization

In Chapter 2, we derived
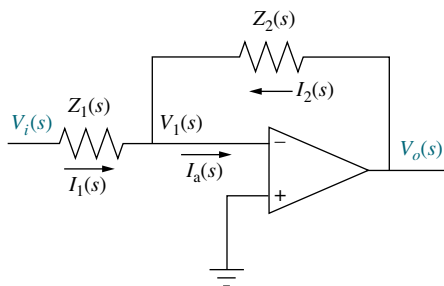
FIGURE 9.60 Operational amplifier configured for transfer function realization

$$\frac{V_o(s)}{V_i(s)} = -\frac{Z_2(s)}{Z_1(s)} \tag{9.44}$$

as the transfer function of an inverting operational amplifier whose configuration is repeated here in Figure 9.60. By judicious choice of $Z_1(s)$ and $Z_2(s)$, this circuit can be used as a building block to implement the compensators and controllers, such as PID controllers, discussed in this chapter. Table 9.10 summarizes the realization of PI, PD, and PID controllers as well as lag, lead, and lag-lead compensators using operational amplifiers. You can verify the table by using the methods of Chapter 2 to find the impedances.

TABLE 9.10   Active realization of controllers and compensators, using an operational amplifier

Function	$Z_1(s)$	$Z_2(s)$	$G_c(s) = -\frac{Z_2(s)}{Z_1(s)}$
Gain	R_1	R_2	$-\dfrac{R_2}{R_1}$
Integration	R	C	$-\dfrac{\frac{1}{RC}}{s}$
Differentiation	C	R	$-RCs$
PI controller	R_1	R_2 C	$-\dfrac{R_2}{R_1}\dfrac{\left(s+\frac{1}{R_2C}\right)}{s}$
PD controller	C / R_1	R_2	$-R_2C\left(s+\dfrac{1}{R_1C}\right)$
PID controller	C_1 / R_1	R_2 C_2	$-\left[\left(\dfrac{R_2}{R_1}+\dfrac{C_1}{C_2}\right)+R_2C_1s+\dfrac{\frac{1}{R_1C_2}}{s}\right]$
Lag compensation	C_1 / R_1	C_2 / R_2	$-\dfrac{C_1}{C_2}\dfrac{\left(s+\frac{1}{R_1C_1}\right)}{\left(s+\frac{1}{R_2C_2}\right)}$ where $R_2C_2 > R_1C_1$
Lead compensation	C_1 / R_1	C_2 / R_2	$-\dfrac{C_1}{C_2}\dfrac{\left(s+\frac{1}{R_1C_1}\right)}{\left(s+\frac{1}{R_2C_2}\right)}$ where $R_1C_1 > R_2C_2$
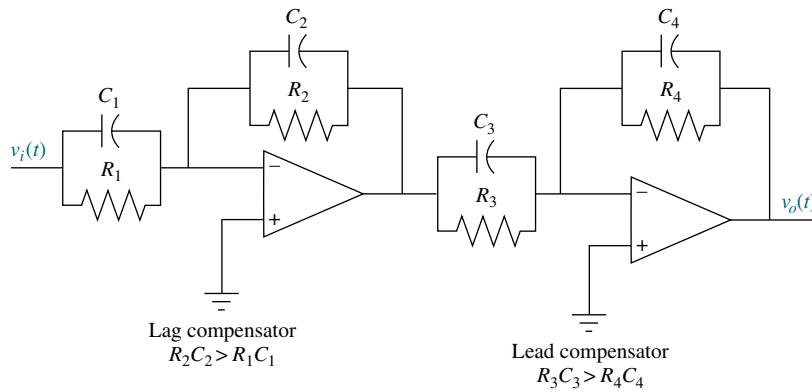
FIGURE 9.61   Lag-lead compensator implemented with operational amplifiers

Other compensators can be realized by cascading compensators shown in the table. For example, a lag-lead compensator can be formed by cascading the lag compensator with the lead compensator, as shown in Figure 9.61. As an example, let us implement one of the controllers we designed earlier in the chapter.

Example 9.9

Implementing a PID Controller

PROBLEM: Implement the PID controller of Example 9.5.

SOLUTION: The transfer function of the PID controller is

$$G_c(s) = \frac{(s + 55.92)(s + 0.5)}{s} \tag{9.45}$$

which can be put in the form

$$G_c(s) = s + 56.42 + \frac{27.96}{s} \tag{9.46}$$

Comparing the PID controller in Table 9.10 with Eq. (9.46), we obtain the following three relationships:

$$\frac{R_2}{R_1} + \frac{C_1}{C_2} = 56.42 \tag{9.47}$$

$$R_2 C_1 = 1 \tag{9.48}$$

and

$$\frac{1}{R_1 C_2} = 27.96 \tag{9.49}$$

Since there are four unknowns and three equations, we arbitrarily select a practical value for one of the elements. Selecting $C_2 = 0.1\ \mu F$, the remaining values are found to be $R_1 = 357.65\ k\Omega$, $R_2 = 178{,}891\ k\Omega$, and $C_1 = 5.59\ \mu F$.

The complete circuit is shown in Figure 9.62, where the circuit element values have been rounded off.
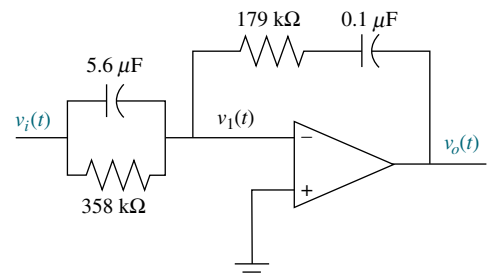
FIGURE 9.62   PID controller

Passive-Circuit Realization

Lag, lead, and lag-lead compensators can also be implemented with passive networks. Table 9.11 summarizes the networks and their transfer functions. The transfer functions can be derived with the methods of Chapter 2.
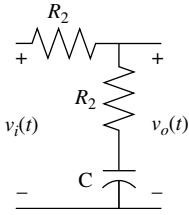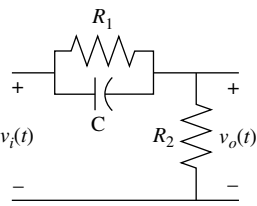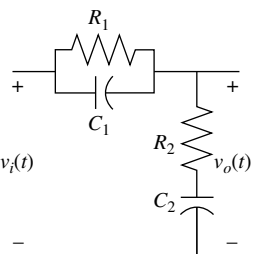
The lag-lead transfer function can be put in the following form:

$$G_c(s) = \frac{\left(s + \dfrac{1}{T_1}\right)\left(s + \dfrac{1}{T_2}\right)}{\left(s + \dfrac{1}{\alpha T_1}\right)\left(s + \dfrac{\alpha}{T_2}\right)} \tag{9.50}$$

where $\alpha < 1$. Thus, the terms with T_1 form the lead compensator, and the terms with T_2 form the lag compensator. Equation (9.50) shows a restriction inherent in using this passive realization. We see that the ratio of the lead compensator zero to the lead compensator pole must be the same as the ratio of the lag compensator pole to the lag compensator zero. In Chapter 11 we design a lag-lead compensator with this restriction.

A lag-lead compensator without this restriction can be realized with an active network as previously shown or with passive networks by cascading the lead and lag networks shown in Table 9.11. Remember, though, that the two networks must be isolated to ensure that one network does not load the other. If the networks load each other, the transfer function will not be the product of the individual transfer functions. A possible realization using the passive networks uses an operational amplifier to provide isolation. The circuit is shown in Figure 9.63. Example 9.10 demonstrates the design of a passive compensator.

TABLE 9.11   Passive realization of compensators

Function	Network	Transfer function, $\dfrac{V_o(s)}{V_i(s)}$
Lag compensation		$\dfrac{R_2}{R_1 + R_2} \dfrac{s + \dfrac{1}{R_2 C}}{s + \dfrac{1}{(R_1 + R_2)C}}$
Lead compensation		$\dfrac{s + \dfrac{1}{R_1 C}}{s + \dfrac{1}{R_1 C} + \dfrac{1}{R_2 C}}$
Lag-lead compensation		$\dfrac{\left(s + \dfrac{1}{R_1 C_1}\right)\left(s + \dfrac{1}{R_2 C_2}\right)}{s^2 + \left(\dfrac{1}{R_1 C_1} + \dfrac{1}{R_2 C_2} + \dfrac{1}{R_2 C_1}\right)s + \dfrac{1}{R_1 R_2 C_1 C_2}}$
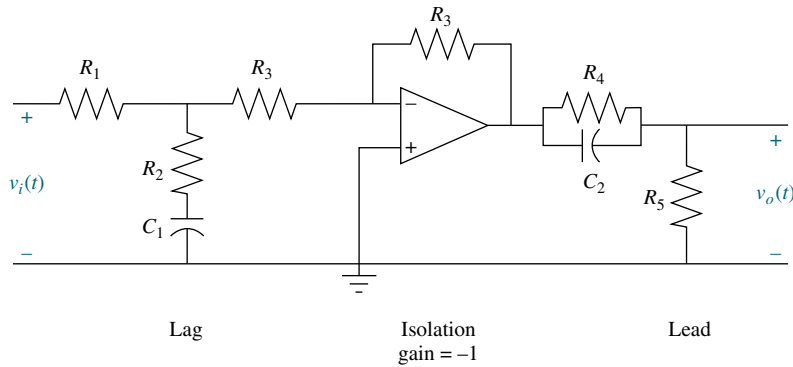
FIGURE 9.63   Lag-lead compensator implemented with cascaded lag and lead networks with isolation

Example 9.10

Realizing a Lead Compensator

PROBLEM: Realize the lead compensator designed in Example 9.4 (Compensator *b*).

SOLUTION: The transfer function of the lead compensator is

$$G_c(s) = \frac{s+4}{s+20.09} \tag{9.51}$$

Comparing the transfer function of a lead network shown in Table 9.11 with Eq. (9.51), we obtain the following two relationships:

$$\frac{1}{R_1 C} = 4 \tag{9.52}$$

and

$$\frac{1}{R_1 C} + \frac{1}{R_2 C} = 20.09 \tag{9.53}$$

Hence, $R_1 C = 0.25$, and $R_2 C = 0.0622$. Since there are three network elements and two equations, we may select one of the element values arbitrarily. Letting $C = 1\,\mu\text{F}$, then $R_1 = 250\,\text{k}\Omega$ and $R_2 = 62.2\,\text{k}\Omega$.

Skill-Assessment Exercise 9.5

PROBLEM: Implement the compensators shown in **a**. and **b**. below. Choose a passive realization if possible.

a. $G_c(s) = \dfrac{(s+0.1)(s+5)}{s}$

b. $G_c(s) = \dfrac{(s+0.1)(s+2)}{(s+0.01)(s+20)}$

ANSWERS:

a. $G_c(s)$ is a PID controller and thus requires active realization. Use Figure 9.60 with the PID controller circuits shown in Table 9.10. One possible set of approximate component values is

$$C_1 = 10\,\mu\text{F}, \quad C_2 = 100\,\mu\text{F}, \quad R_1 = 20\,\text{k}\Omega, \quad R_2 = 100\,\text{k}\Omega$$

b. $G_c(s)$ is a lag-lead compensator that can be implemented with a passive network because the ratio of the lead pole to zero is the inverse of the ratio of the lag pole to zero. Use the lag-lead compensator circuit shown in Table 9.11. One possible set of approximate component values is

$$C_1 = 100\,\mu\mathrm{F}, \quad C_2 = 900\,\mu\mathrm{F}, \quad R_1 = 100\,\mathrm{k\Omega}, \quad R_2 = 560\,\Omega$$

The complete solution is at www.wiley.com.college/nise.

Case Studies

Antenna Control: Lag-Lead Compensation

Design

D

For the antenna azimuth position control system case study in Chapter 8, we obtained a 25% overshoot using a simple gain adjustment. Once this percent overshoot was obtained, the settling time was determined. If we try to improve the settling time by increasing the gain, the percent overshoot also increases. In this section, we continue with the antenna azimuth position control by designing a cascade compensator that yields 25% overshoot at a reduced settling time. Further, we effect an improvement in the steady-state error performance of the system.

PROBLEM: Given the antenna azimuth position control system shown on the front endpapers, Configuration 1, design cascade compensation to meet the following requirements: (1) 25% overshoot, (2) 2-second settling time, and (3) $K_v = 20$.

SOLUTION: For the case study in Chapter 8, a preamplifier gain of 64.21 yielded 25% overshoot, with the dominant, second-order poles at $-0.833 \pm j1.888$. The settling time is thus $4/\zeta\omega_n = 4/.833 = 4.8$ seconds. The open-loop function for the system as derived in the case study in Chapter 5 is $G(s) = 6.63K/[s(s + 1.71)(s + 100)]$. Hence $K_v = 6.63K/(1.71 \times 100) = 2.49$. Comparing these values to this example's problem statement, we want to improve the settling time by a factor of 2.4, and we want approximately an eightfold improvement in K_v.

Lead compensator design to improve transient response: First locate the dominant second-order pole. To obtain a settling time, T_s, of 2 seconds and a percent overshoot of 25%, the real part of the dominant second-order pole should be at $-4/T_s = -2$. Locating the pole on the 113.83° line ($\zeta = 0.404$, corresponding to 25% overshoot) yields an imaginary part of 4.529 (see Figure 9.64).

Second, assume a lead compensator zero and find the compensator pole. Assuming a compensator zero at -2, along with the uncompensated system's open-loop poles and zeros, use the root locus program in Appendix H.2 at www.wiley.com/college/nise to find that there is an angular contribution of $-120.14°$ at the design point of $-2 \pm j4.529$. Therefore, the compensator's pole must contribute $120.14° - 180° = -59.86°$ for the design point to be on the compensated system's root locus. The geometry is shown in Figure 9.64. To calculate the compensator pole, we use $4.529/(p_c - 2) = \tan 59.86°$ or $p_c = 4.63$.
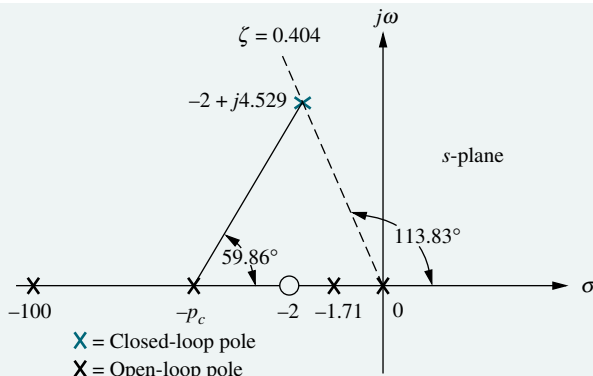
FIGURE 9.64 Locating compensator pole

X = Closed-loop pole
X = Open-loop pole

Note: This figure is not drawn to scale.

Now determine the gain. Using the lead-compensated system's open-loop function,

$$G(s) = \frac{6.63K(s+2)}{s(s+1.71)(s+100)(s+4.63)} \qquad (9.54)$$

and the design point $-2 + j4.529$ as the test point in the root locus program, the gain, $6.63K$, is found to be 2549.

Lag compensator design to improve the steady-state error: K_v for the lead-compensated system is found using Eq. (9.54). Hence,

$$K_v = \frac{2549(2)}{(1.71)(100)(4.63)} = 6.44 \qquad (9.55)$$

Since we want $K_v = 20$, the amount of improvement required over the lead-compensated system is $20/6.44 = 3.1$. Choose $p_c = -0.01$ and calculate $z_c = 0.031$, which is 3.1 times larger.

Determine gain: The complete lag-lead-compensated open-loop function, $G_{LLC}(s)$, is

$$G_{LLC}(s) = \frac{6.63K(s+2)(s+0.031)}{s(s+.01)(s+1.71)(s+4.63)(s+100)} \qquad (9.56)$$

Using the root locus program in Appendix H.2 at www.wiley.com/college/nise and the poles and zeros of Eq. (9.56), search along the 25% overshoot line ($113.83°$) for the design point. This point has moved slightly with the addition of the lag compensator to $-1.99 \pm j4.51$. The gain at this point equals 2533, which is $6.63K$. Solving for K yields $K = 382.1$.

Realization of the compensator: A realization of the lag-lead compensator is shown in Figure 9.63. From Table 9.11 the lag portion has the following transfer function:

$$G_{lag}(s) = \frac{R_2}{R_1 + R_2} \frac{s + \dfrac{1}{R_2 C}}{s + \dfrac{1}{(R_1 + R_2)C}} = \frac{R_2}{R_1 + R_2} \frac{(s+0.031)}{(s+0.01)} \qquad (9.57)$$
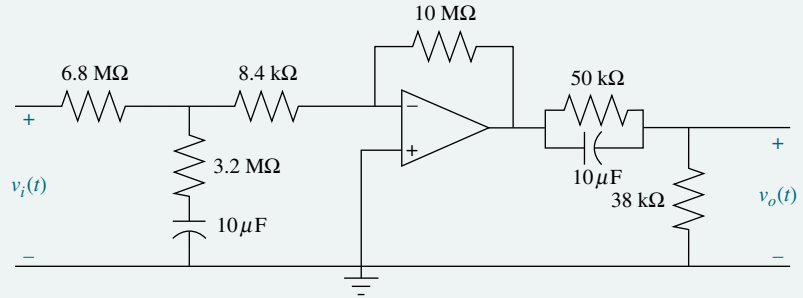
FIGURE 9.65   Realization of lag-lead compensator

Selecting $C = 10\,\mu\text{F}$, we find $R_2 = 3.2\,\text{M}\Omega$ and $R_1 = 6.8\,\text{M}\Omega$.

From Table 9.11 the lead compensator portion has the following transfer function:

$$G_{\text{lead}}(s) = \frac{s + \dfrac{1}{R_1 C}}{s + \dfrac{1}{R_1 C} + \dfrac{1}{R_2 C}} = \frac{(s + 2)}{(s + 4.63)} \tag{9.58}$$

Selecting $C = 10\,\mu\text{F}$, we find $R_1 = 50\,\text{k}\Omega$ and $R_2 = 38\,\text{k}\Omega$.

The total loop gain required by the system is 2533. Hence,

$$6.63K \frac{R_2}{R_1 + R_2} = 2533 \tag{9.59}$$

where K is the gain of the preamplifier, and $R_2/(R_1 + R_2)$ is the gain of the lag portion. Using the values of R_1 and R_2 found during the realization of the lag portion, we find $K = 1194$.

The final circuit is shown in Figure 9.65, where the preamplifier is implemented with an operational amplifier whose feedback and input resistor ratio approximately equals 1194, the required preamplifier gain. The preamplifier isolates the lag and lead portions of the compensator.

Summary of the design results: Using Eq. (9.56) along with $K = 382.1$ yields the compensated value of K_v. Thus,

$$K_v = \lim_{s \to 0} sG_{\text{LLC}}(s) = \frac{2533(2)(0.031)}{(0.01)(1.71)(4.63)(100)} = 19.84 \tag{9.60}$$

which is an improvement over the gain-compensated system in the case study of Chapter 8, where $K_v = 2.49$. This value is calculated from the uncompensated $G(s)$ by letting $K = 64.21$, as found in the Case Study of Chapter 8.

Finally, checking the second-order approximation via simulation, we see in Figure 9.66 the actual transient response. Compare this to the gain-compensated system response of Figure 8.29 to see the improvement effected by cascade compensation over simple gain adjustment. The gain-compensated system yielded 25%, with a settling time of about 4 seconds. The lag-lead-compensated system yields 28% overshoot, with a settling time of about 2 seconds. If the results are not adequate for the application, the system should be redesigned to reduce the percent overshoot.
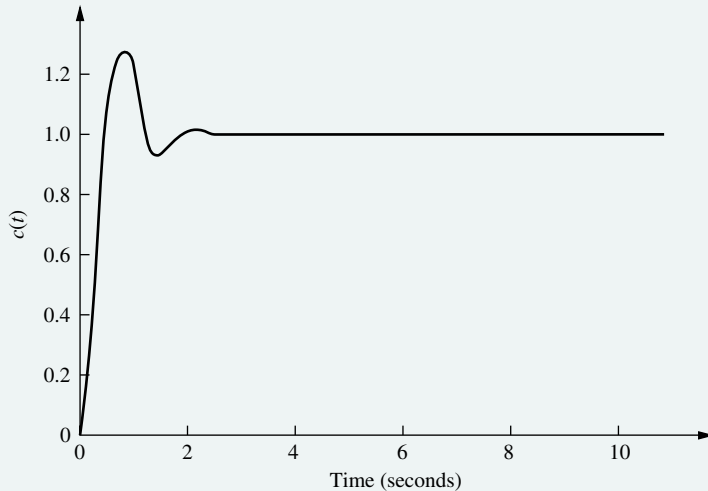
FIGURE 9.66   Step response of lag-lead-compensated antenna control

CHALLENGE: You are now given a problem to test your knowledge of this chapter's objectives. You are given the antenna azimuth position control system shown on the front endpapers, Configuration 2. In the challenge in Chapter 8, you were asked to design, via gain adjustment, an 8-second settling time.

a. For your solution to the challenge in Chapter 8, evaluate the percent overshoot and the value of the appropriate static error constant.

b. Design a cascade compensator to reduce the percent overshoot by a factor of 4 and the settling time by a factor of 2. Also, improve the appropriate static error constant by a factor of 2.

c. Repeat Part **b** using MATLAB.

MATLAB
ML

UFSS Vehicle: Lead and Feedback Compensation

As a final look at this case study, we redesign the pitch control loop for the UFSS vehicle. For the case study in Chapter 8, we saw that rate feedback improved the transient response. In this chapter's case study, we replace the rate feedback with a cascade compensator.

PROBLEM: Given the pitch control loop without rate feedback ($K_2 = 0$) for the UFSS vehicle shown on the back endpapers, design a compensator to yield 20% overshoot and a settling time of 4 seconds (*Johnson*, *1980*).

SOLUTION: First determine the location of the dominant closed-loop poles. Using the required 20% overshoot and a 4-second settling time, a second-order approximation shows the dominant closed-loop poles are located at $-1 \pm j1.951$. From the uncompensated system analyzed in the Chapter 8 case study, the estimated settling time was 19.8 seconds for dominant closed-loop poles of $-0.202 \pm j0.394$. Hence, a lead compensator is required to speed up the system.

Arbitrarily assume a lead compensator zero at -1. Using the root locus program in Appendix H.2 at www.wiley.com/college/nise, we find that this compensator zero, along with the open-loop poles and zeros of the system, yields an angular contribution at the design point, $-1 + j1.951$, of $-178.92°$. The difference between this angle and $180°$, or $-1.08°$, is the angular contribution required from the compensator pole.

$\zeta = 0.456$

$j\omega$

$-1 + j1.951$

s-plane

$117.13°$

$1.08°$

$-p_c$

0

σ
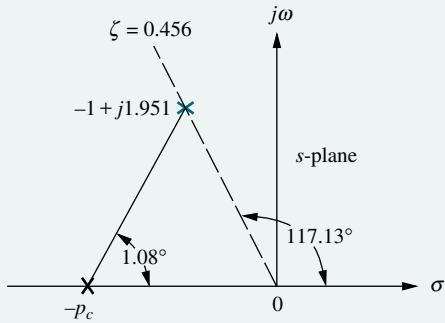
X = Closed-loop pole
X = Open-loop pole
Note: This figure is not drawn to scale.

FIGURE 9.67 Locating compensator pole

Using the geometry shown in Figure 9.67, where $-p_c$ is the compensator pole location, we find that

$$\frac{1.951}{p_c - 1} = \tan 1.08° \tag{9.61}$$

from which $p_c = 104.5$. The compensated open-loop transfer function is thus

$$G(s) = \frac{0.25K_1(s + 0.435)(s + 1)}{(s + 1.23)(s + 2)(s^2 + 0.226s + 0.0169)(s + 104.5)} \tag{9.62}$$

where the compensator is

$$G_c(s) = \frac{(s + 1)}{(s + 104.5)} \tag{9.63}$$

Using all poles and zeros shown in Eq. (9.62), the root locus program shows that a gain of 516.5 is required at the design point, $-1 \pm j1.951$. The root locus of the compensated system is shown in Figure 9.68.

A test of the second-order approximation shows three more closed-loop poles at -0.5, -0.9, and -104.5. Since the open-loop zeros are at -0.435 and -1, simulation is required to see if there is effectively closed-loop pole-zero cancellation with the closed-loop poles at -0.5 and -0.9, respectively. Further, the closed-loop pole at -104.5 is more than five times the real part of the dominant closed-loop pole, $-1 \pm j1.951$, and its effect on the transient response is therefore negligible.

The step response of the closed-loop system is shown in Figure 9.69, where we see a 26% overshoot and a settling time of about 4.5 seconds. Comparing this

FIGURE 9.68 Root locus for lead-compensated system

FIGURE 9.69 Step response of lead-compensated UFSS vehicle

response with Figure 8.31, the response of the uncompensated system, we see considerable improvement in the settling time and steady-state error. However, the transient response performance does not meet the design r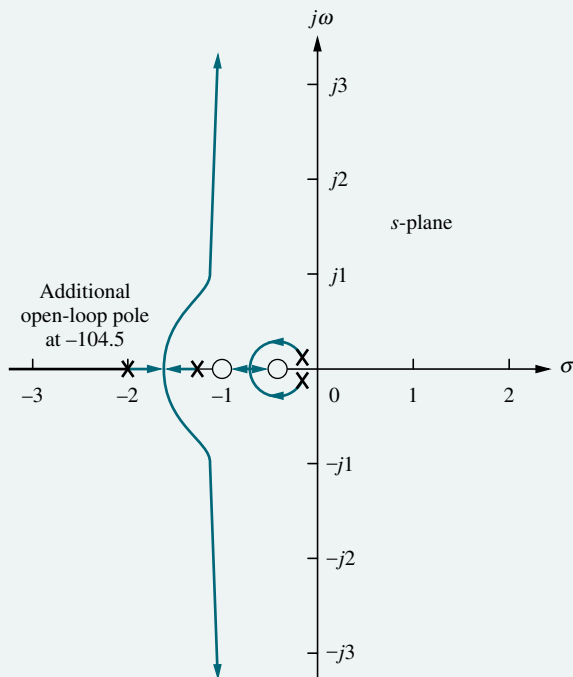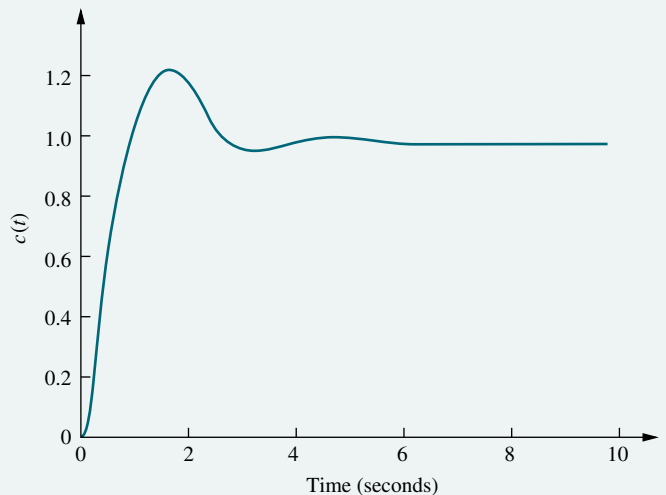equirements. Thus, a redesign of the system to reduce the percent overshoot is suggested if required by the application.

CHALLENGE: You are now given a problem to test your knowledge of this chapter's objectives. The heading control system for the UFSS vehicle is shown on the back endpapers. The minor loop contains the rudder and vehicle dynamics, and the major loop relates output and input heading (*Johnson*, *1980*).

a. Find the values of K_1 and K_2 so that the minor-loop dominant poles have a damping ratio of 0.6 and the major-loop dominant poles have a damping ratio of 0.5.

b. Repeat, using MATLAB.

MATLAB

ML

Summary

In this chapter, we learned how to design a system to meet transient and steady-state specifications. These design techniques overcame limitations in the design methodology covered in Chapter 8, whereby a transient response could be created only if the poles generating that response were on the root locus. Subsequent gain adjustment yielded the desired response. Since this value of gain dictated the amount of steady-state error in the response, a trade-off was required between the desired transient response and the desired steady-state error.

    Cascade or *feedback compensation* is used to overcome the disadvantages of gain adjustment as a compensating technique. In this chapter, we saw that the transient response and the steady-state error can be designed separately from each other. No longer was a trade-off between these two specifications required. Further, we were able to design for a transient response that was not represented on the original root locus.

    The transient response design technique covered in this chapter is based upon reshaping the root locus to go through a desired transient response point, followed by a gain adjustment. Typically, the resulting gain is much higher than the original if the compensated system response is faster than the uncompensated response.

    The root locus is reshaped by adding additional poles and zeros via a cascade or feedback compensator. The additional poles and zeros must be checked to see that any second-order approximations used in the design are valid. All poles besides the dominant second-order pair must yield a response that is much faster than the designed response. Thus, nondominant poles must be at least five times as far from the imaginary axis as the dominant pair. Further, any zeros of the system must be close to a nondominant pole for pole-zero cancellation, or far from the dominant pole pair. The resulting system can then be approximated by two dominant poles.

    The steady-state response design technique is based upon placing a pole on or near the origin in order to increase or nearly increase the system type, and then placing a zero near this pole so that the effect upon the transient response is negligible. However, final reduction of steady-state error occurs with a long-time

constant. The same arguments about other poles yielding fast responses and about zeros being cancelled in order to validate a second-order approximation also hold true for this technique. If the second-order approximations cannot be justified, then a simulation is required to make sure the design is within tolerance.

Steady-state design compensators are implemented via *PI controllers* or *lag compensators*. PI controllers add a pole at the origin, thereby increasing the system type. Lag compensators, usually implemented with passive networks, place the pole off the origin but near it. Both methods add a zero very close to the pole in order not to affect the transient response.

The transient response design compensators are implemented through *PD controllers* or *lead compensators*. PD controllers add a zero to compensate the transient response; they are considered *ideal*. Lead compensators, on the other hand, are not ideal since they add a pole along with the zero. Lead compensators are usually passive networks.

We can correct both transient response and steady-state error with a *PID* or *lag-lead compensator*. Both of these are simply combinations of the previously described compensators. Table 9.7 summarized the types of cascade compensators.

Feedback compensation can also be used to improve the transient response. Here the compensator is placed in the feedback path. The feedback gain is used to change the compensator zero or the system's open-loop poles, giving the designer a wide choice of various root loci. The system gain is then varied to move along the selected root locus to the design point. An advantage of feedback compensation is the ability to design a fast response into a subsystem independently of the system's total response.

In the next chapter, we look at another method of design, frequency response, which is an alternate method to the root locus.

❰ Review Questions ❱

1. Briefly distinguish between the design techniques in Chapter 8 and Chapter 9.
2. Name two major advantages of the design techniques of Chapter 9 over the design techniques of Chapter 8.
3. What kind of compensation improves the steady-state error?
4. What kind of compensation improves transient response?
5. What kind of compensation improves both steady-state error and transient response?
6. Cascade compensation to improve the steady-state error is based upon what pole-zero placement of the compensator? Also, state the reasons for this placement.
7. Cascade compensation to improve the transient response is based upon what pole-zero placement of the compensator? Also, state the reasons for this placement.
8. What difference on the *s*-plane is noted between using a PD controller or using a lead network to improve the transient response?
9. In order to speed up a system without changing the percent overshoot, where must the compensated system's poles on the *s*-plane be located in comparison to the uncompensated system's poles?

10. Why is there more improvement in steady-state error if a PI controller is used instead of a lag network?

11. When compensating for steady-state error, what effect is sometimes noted in the transient response?

12. A lag compensator with the zero 25 times as far from the imaginary axis as the compensator pole will yield approximately how much improvement in steady-state error?

13. If the zero of a feedback compensator is at -3 and a closed-loop system pole is at -3.001, can you say there will be pole-zero cancellation? Why?

14. Name two advantages of feedback compensation.

Problems

1. Design a PI controller to drive the step response error to zero for the unity feedback system shown in Figure P9.1, where

   WileyPLUS
   WPCS
   Control Solutions

$$G(s) = \frac{K}{(s+1)(s+3)(s+10)}$$

   The system operates with a damping ratio of 0.5. Compare the specifications of the uncompensated and compensated systems. [Section: 9.2]
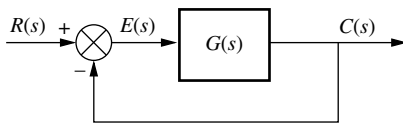
   FIGURE P9.1

2. Consider the unity feedback system shown in Figure P9.1, where

$$G(s) = \frac{K}{s(s+3)(s+6)}$$

   a. Design a PI controller to drive the ramp response error to zero for any K that yields stability. [Section: 9.2]

   b. Use MATLAB to simulate your design for $K = 1$. Show both the input ramp and the output response on the same plot.

   MATLAB
   ML

3. The unity feedback system shown in Figure P9.1 with

$$G(s) = \frac{K}{(s+2)(s+3)(s+7)}$$

   is operating with 10% overshoot. [Section: 9.2]

   a. What is the value of the appropriate static error constant?

   b. Find the transfer function of a lag network so that the appropriate static error constant equals 4 without appreciably changing the dominant poles of the uncompensated system.

   c. Use MATLAB or any other computer program to simulate the system to see the effect of your compensator.

   MATLAB
   ML

4. Repeat Problem 3 for $G(s) = \dfrac{K}{s(s+3)(s+7)}$. [Section: 9.2]

5. Consider the unity feedback system shown in Figure P9.1 with

$$G(s) = \frac{K}{(s+3)(s+5)(s+7)}$$

   a. Design a compensator that will yield $K_p = 20$ without appreciably changing the dominant pole location that yields a 10% overshoot for the uncompensated system. [Section: 9.2]

   b. Use MATLAB or any other computer program to simulate the un-compensated and compensated systems.

   MATLAB
   ML

   c. Use MATLAB or any other computer program to determine how much time it takes the slow response of the lag compensator to bring the output to within 2% of its final compensated value.

   MATLAB
   ML

6. The unity feedback system shown Figure P9.1 with

   WileyPLUS
   WPCS
   Control Solutions

$$G(s) = \frac{K(s+6)}{(s+2)(s+3)(s+5)}$$

is operating with a dominant-pole damping ratio of 0.707. Design a PD controller so that the settling time is reduced by a factor of 2. Compare the transient and steady-state performance of the uncompensated and compensated systems. Describe any problems with your design. [Section: 9.3]

7. Redo Problem 6 using MATLAB in the following way:

> **MATLAB**
> **ML**

  a. MATLAB will generate the root locus for the uncompensated system along with the 0.707 damping ratio line. You will interactively select the operating point. MATLAB will then inform you of the coordinates of the operating point, the gain at the operating point, as well as the estimated %OS, T_s, T_p, ζ, ω_n, and K_p represented by a second-order approximation at the operating point.

  b. MATLAB will display the step response of the uncompensated system.

  c. Without further input, MATLAB will calculate the compensated design point and will then ask you to input a value for the PD compensator zero from the keyboard. MATLAB will respond with a plot of the root locus showing the compensated design point. MATLAB will then allow you to keep changing the PD compensator value from the keyboard until a root locus is plotted that goes through the design point.

  d. For the compensated system, MATLAB will inform you of the coordinates of the operating point, the gain at the operating point, as well as the estimated %OS, T_s, T_p, ζ, ω_n, and K_p represented by a second-order approximation at the operating point.

  e. MATLAB will then display the step response of the compensated system.

8. Design a PD controller for the system shown in Figure P9.2 to reduce the settling time by a factor of 4 while continuing to operate the system with 20% overshoot. Compare your performance to that obtained in Example 9.7.

$$R(s) \xrightarrow{\;+\;} \bigotimes \xrightarrow{} \boxed{\dfrac{K}{s(s+10)(s+20)}} \xrightarrow{} C(s)$$
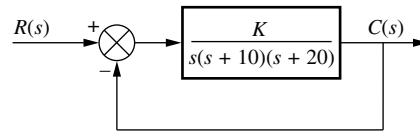
FIGURE P9.2

9. Consider the unity feedback system shown in Figure P9.1 with [Section: 9.3]

$$G(s) = \frac{K}{(s+4)^3}$$

  a. Find the location of the dominant poles to yield a 1.6 second settling time and an overshoot of 25%.

  b. If a compensator with a zero at -1 is used to achieve the conditions of Part **a**, what must the angular contribution of the compensator pole be?

  c. Find the location of the compensator pole.

  d. Find the gain required to meet the requirements stated in Part **a**.

  e. Find the location of other closed-loop poles for the compensated system.

  f. Discuss the validity of your second-order approximation.

  g. Use MATLAB or any other computer program to simulate the compensated system to check your design.

> **MATLAB**
> **ML**

10. The unity feedback system shown in Figure P9.1 with

> **WileyPLUS**
> **WPCS**
> Control Solutions

$$G(s) = \frac{K}{s^2}$$

is to be designed for a settling time of 1.667 seconds and a 16.3% overshoot. If the compensator zero is placed at -1, do the following: [Section: 9.3]

  a. Find the coordinates of the dominant poles.

  b. Find the compensator pole.

  c. Find the system gain.

  d. Find the location of all nondominant poles.

  e. Estimate the accuracy of your second-order approximation.

  f. Evaluate the steady-state error characteristics.

  g. Use MATLAB or any other computer program to simulate the system and evaluate the actual transient response characteristics for a step input.

> **MATLAB**
> **ML**

11. Given the unity feedback system of Figure P9.1, with

$$G(s) = \frac{K(s+6)}{(s+3)(s+4)(s+7)(s+9)}$$

do the following: [Section: 9.3]

a. Sketch the root locus.

b. Find the coordinates of the dominant poles for which $\zeta = 0.8$.

c. Find the gain for which $\zeta = 0.8$.

d. If the system is to be cascade-compensated so that $T_s = 1$ second and $\zeta = 0.8$, find the compensator pole if the compensator zero is at -4.5.

e. Discuss the validity of your second-order approximation.

f. Use MATLAB or any other computer program to simulate the compensated and uncompensated systems and compare the results to those expected. `MATLAB` `ML`

12. Redo Problem 11 using MATLAB in the following way: `MATLAB` `ML`

a. MATLAB will generate the root locus for the uncompensated system along with the 0.8 damping ratio line. You will interactively select the operating point. MATLAB will then inform you of the coordinates of the operating point, the gain at the operating point, as well as the estimated %OS, T_s, T_p, ζ, ω_n, and K_p represented by a second-order approximation at the operating point.

b. MATLAB will display the step response of the uncompensated system.

c. Without further input, MATLAB will calculate the compensated design point and will then ask you to input a value for the lead compensator pole from the keyboard. MATLAB will respond with a plot of the root locus showing the compensated design point. MATLAB will then allow you to keep changing the lead compensator pole value from the keyboard until a root locus is plotted that goes through the design point.

d. For the compensated system, MATLAB will inform you of the coordinates

of the operating point, the gain at the operating point, as well as the estimated %OS, T_s, T_p, ζ, ω_n, and K_p represented by a second-order approximation at the operating point.

e. MATLAB will then display the step response of the compensated system.

f. Change the compensator's zero location a few times and collect data on the compensated system to see if any other choices of compensator zero yield advantages over the original design.

13. Consider the unity feedback system of Figure P9.1 with

$$G(s) = \frac{K}{s(s+20)(s+40)}$$

The system is operating at 20% overshoot. Design a compensator to decrease the settling time by a factor of 2 without affecting the percent overshoot and do the following: [Section: 9.3]

a. Evaluate the uncompensated system's dominant poles, gain, and settling time.

b. Evaluate the compensated system's dominant poles and settling time.

c. Evaluate the compensator's pole and zero. Find the required gain.

d. Use MATLAB or any other computer program to simulate the compensated and uncompensated systems' step response. `MATLAB` `ML`

14. The unity feedback system shown in Figure P9.1 with

$$G(s) = \frac{K}{(s+15)(s^2+6s+13)}$$

is operating with 30% overshoot. [Section: 9.3]

a. Find the transfer function of a cascade compensator, the system gain, and the dominant pole location that will cut the settling time in half if the compensator zero is at -7.

b. Find other poles and zeros and discuss your second-order approximation.

c. Use MATLAB or any other computer program to simulate both the uncompensated and compensated systems to see the effect of your compensator. `MATLAB` `ML`

15. For the unity feedback system of Figure P9.1 with

$$G(s) = \frac{K}{s(s+1)(s^2+10s+26)}$$

do the following: [Section: 9.3]

a. Find the settling time for the system if it is operating with 15% overshoot.

b. Find the zero of a compensator and the gain, K, so that the settling time is 7 seconds. Assume that the pole of the compensator is located at -15.

c. Use MATLAB or any other computer program to simulate the system's step response to test the compensator.

MATLAB
ML

16. A unity feedback control system has the following forward transfer function: [Section: 9.3]

WileyPLUS
WPCS
Control Solutions

$$G(s) = \frac{K}{s^2(s+4)(s+12)}$$

a. Design a lead compensator to yield a closed-loop step response with 20.5% overshoot and a settling time of 3 seconds. Be sure to specify the value of K.

b. Is your second-order approximation valid?

c. Use MATLAB or any other computer program to simulate and compare the transient response of the compensated system to the predicted transient response.

MATLAB
ML

17. For the unity feedback system of Figure P9.1, with

$$G(s) = \frac{K}{(s^2+20s+101)(s+20)}$$

the damping ratio for the dominant poles is to be 0.4, and the settling time is to be 0.5 second. [Section: 9.3]

a. Find the coordinates of the dominant poles.

b. Find the location of the compensator zero if the compensator pole is at -15.

c. Find the required system gain.

d. Compare the performance of the uncompensated and compensated systems.

e. Use MATLAB or any other computer program to simulate the system to check your design. Redesign if necessary.

MATLAB
ML

18. Consider the unity feedback system of Figure P9.1, with

$$G(s) = \frac{K}{(s+3)(s+5)}$$

a. Show that the system cannot operate with a settling time of 2/3 second and a percent overshoot of 1.5 % with a simple gain adjustment.

b. Design a lead compensator so that the system meets the transient response characteristics of Part **a.** Specify the compensator's pole, zero, and the required gain.

19. Given the unity feedback system of Figure P9.1 with

$$G(s) = \frac{K}{(s+2)(s+4)(s+6)(s+8)}$$

Find the transfer function of a lag-lead compensator that will yield a settling time 0.5 second shorter than that of the uncompensated system, with a damping ratio of 0.5, and improve the steady-state error by a factor of 30. The compensator zero is at -5. Also, find the compensated system's gain. Justify any second-order approximations or verify the design through simulation. [Section: 9.4]

20. Redo Problem 19 using a lag-lead compensator and MATLAB in the following way:

MATLAB
ML

a. MATLAB will generate the root locus for the uncompensated system along with the 0.5 damping-ratio line. You will interactively select the operating point. MATLAB will then proceed to inform you of the coordinates of the operating point, the gain at the operating point, as well as the estimated %OS, T_s, T_p, ζ, ω_n, and K_p represented by a second-order approximation at the operating point.

b. MATLAB will display the step response of the uncompensated system.

c. Without further input, MATLAB will calculate the compensated design point and will then ask you to input a value for the lead compensator pole from the keyboard. MATLAB will respond with a plot of the root locus showing the compensated design point. MATLAB will then allow you to keep changing the lead compensator pole value from the keyboard

until a root locus is plotted that goes through the design point.

d. For the compensated system, MATLAB will inform you of the coordinates of the operating point, the gain at the operating point, as well as the estimated $\%OS, T_s, T_p, \zeta, \omega_n,$ and K_p represented by a second-order approximation at the operating point.

e. MATLAB will then display the step response of the compensated system.

f. Change the compensator's zero location a few times and collect data on the compensated system to see if any other choices of the compensator zero yield advantages over the original design.

g. Using the steady-state error of the uncompensated system, add a lag compensator to yield an improvement of 30 times over the uncompensated system's steady-state error, with minimal effect on the designed transient response. Have MATLAB plot the step response. Try several values for the lag compensator's pole and see the effect on the step response.

21. Given the uncompensated unity feedback system of Figure P9.1, with

$$G(s) = \frac{K}{s(s+1)(s+3)}$$

do the following: [Section: 9.4]

a. Design a compensator to yield the following specifications: settling time = 2.86 seconds; percent overshoot = 4.32%; the steady-state error is to be improved by a factor of 2 over the uncompensated system.

b. Compare the transient and steady-state error specifications of the uncompensated and compensated systems.

c. Compare the gains of the uncompensated and compensated systems.

d. Discuss the validity of your second-order approximation.

e. Use MATLAB or any other computer program to simulate the uncompensated and compensated systems and verify the specifications.   MATLAB **ML**

22. For the unity feedback system given in Figure P9.1 with   WileyPLUS **WPCS** Control Solutions

$$G(s) = \frac{K}{s(s+5)(s+11)}$$

do the following: [Section: 9.4]

a. Find the gain, K, for the uncompensated system to operate with 30% overshoot.

b. Find the peak time and K_v for the uncompensated system.

c. Design a lag-lead compensator to decrease the peak time by a factor of 2, decrease the percent overshoot by a factor of 2, and improve the steady-state error by a factor of 30. Specify all poles, zeros, and gains.

23. The unity feedback system shown in Figure P9.1 with

$$G(s) = \frac{K}{(s^2 + 4s + 8)(s + 10)}$$

is to be designed to meet the following specifications:

Overshoot: Less than 25%

Settling time: Less than 1 second

$K_p = 10$

Do the following: [Section: 9.4]

a. Evaluate the performance of the uncompensated system operating at 10% overshoot.

b. Design a passive compensator to meet the desired specifications.

c. Use MATLAB to simulate the compensated system. Compare the response with the desired specifications.   MATLAB **ML**

24. Consider the unity feedback system in Figure P9.1, with

$$G(s) = \frac{K}{(s+2)(s+4)}$$

The system is operated with 4.32% overshoot. In order to improve the steady-state error, K_p is to be increased by at least a factor of 5. A lag compensator of the form

$$G_c(s) = \frac{(s+0.5)}{(s+0.1)}$$

is to be used. [Section: 9.4]

a. Find the gain required for both the compensated and the uncompensated systems.

b. Find the value of K_p for both the compensated and the uncompensated systems.

c. Estimate the percent overshoot and settling time for both the compensated and the uncompensated systems.

d. Discuss the validity of the second-order approximation used for your results in Part **c**.

e. Use MATLAB or any other computer program to simulate the step response for the uncompensated and compensated systems. What do you notice about the compensated system's response?

MATLAB **ML**

f. Design a lead compensator that will correct the objection you notice in Part **e**.

25. For the unity feedback system in Figure P9.1, with

$$G(s) = \frac{K}{(s+1)(s+4)}$$

design a PID controller that will yield a peak time of 1.047 seconds and a damping ratio of 0.8, with zero error for a step input. [Section: 9.4]

26. For the unity feedback system in Figure P9.1, with

$$G(s) = \frac{K}{(s+4)(s+6)(s+10)}$$

WileyPLUS **WPCS** Control Solutions

do the following:

a. Design a controller that will yield no more than 25% overshoot and no more than a 2-second settling time for a step input and zero steady-state error for step and ramp inputs.

b. Use MATLAB and verify your design.

MATLAB **ML**

27. Redo Problem 26 using MATLAB in the following way:

MATLAB **ML**

a. MATLAB will ask for the desired percent over shoot, settling time, and PI compensator zero.

b. MATLAB will design the PD controller's zero.

c. MATLAB will display the root locus of the PID-compensated system with the desired percent overshoot line.

d. The user will interactively select the intersection of the root locus

and the desired percent over shoot line.

e. MATLAB will display the gain and transient response characteristics of the PID-compensated system.

f. MATLAB will display the step response of the PID-compensated system.

g. MATLAB will display the ramp response of the PID-compensated system.

28. If the system of Figure P9.3 operates with a damping ratio of 0.517 for the dominant second-order poles, find the location of all closed-loop poles and zeros.
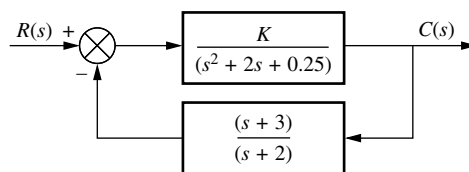

FIGURE P9.3

29. For the unity feedback system in Figure P9.1, with

$$G(s) = \frac{K}{s(s+2)(s+4)(s+6)}$$

do the following: [Section: 9.5]

a. Design rate feedback to yield a step response with no more than 15% overshoot and no more than 3 seconds settling time. Use Approach 1.

b. Use MATLAB and simulate your compensated system.

MATLAB **ML**

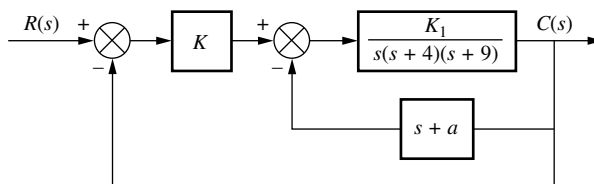**30.** Given the system of Figure P9.4: [Section: 9.5]

FIGURE P9.4

a. Design the value of K_1, as well as a in the feedback path of the minor loop, to yield a settling time of 1 second with 5% overshoot for the step response.

b. Design the value of K to yield a major-loop response with 10% overshoot for a step input.

c. Use MATLAB or any other computer program to simulate the step response to the entire closed-loop system. **MATLAB ML**

d. Add a PI compensator to reduce the major-loop steady-state error to zero and simulate the step response using MATLAB or any other computer program. **MATLAB ML**

31. Identify and realize the following controllers with operational amplifiers. [Section: 9.6]

a. $\dfrac{s + 0.01}{s}$

b. $s + 2$

32. Identify and realize the following compensators with passive networks. [Section: 9.6] **WileyPLUS WPCS** **Control Solutions**

a. $\dfrac{s + 0.1}{s + 0.01}$

b. $\dfrac{s + 2}{s + 5}$

c. $\left(\dfrac{s + 0.1}{s + 0.01}\right)\left(\dfrac{s + 1}{s + 10}\right)$

33. Repeat Problem 32 using operational amplifiers. [Section: 9.6]

DESIGN PROBLEMS

34. The room temperature of an 11 m^2 room is to be controlled by varying the power of an indoor radiator. For this specific room the open-loop transfer function from radiator power, $\dot{Q}(s)$, to temperature, $T(s)$, is (*Thomas, 2005*)

$$G(s) = \frac{T(s)}{\dot{Q}(s)} = \frac{(1 \times 10^{-6})s^2 + (1.314 \times 10^{-9})s + (2.66 \times 10^{-13})}{s^3 + 0.00163s^2 + (5.272 \times 10^{-7})s + (3.538 \times 10^{-11})}$$

The system is assumed to be in the closed-loop configuration shown in Figure P9.1.

a. For a unit step input, calculate the steady-state error of the system.

b. Try using the procedure of Section 9.2 to design a PI controller to obtain zero steady-state error for step inputs without appreciably changing the transient response. Then explain why it is not possible to do so.

c. Design a PI controller of the form $G_c(s) = \dfrac{K(s + z)}{s}$ that will reduce the step-response error to zero while not changing significantly the transient response. (Hint: Place the zero of the compensator in a position where the closed-loop poles of the uncompensated root locus will not be affected significantly.)

d. Use Simulink to simulate the systems of Parts **b** and **c** and to verify the correctness of your design in Part **c**. **Simulink SL**

35. Figure P9.5 shows a two-tank system. The liquid inflow to the upper tank can be controlled using a valve and is represented by F_0. The upper tank's outflow equals the lower tank's inflow and is represented by F_1. The outflow of the lower tank is F_2. The objective of the design is to control the liquid level, $y(t)$, in the lower tank. The open-loop transmission for this system is $\dfrac{Y(s)}{F_o(s)} = \dfrac{a_2 a_3}{s^2 + (a_1 + a_4)s + a_1 a_4}$ (*Romagnoli, 2006*). The system will be controlled in a loop analogous to that of Figure P9.1, where the lower liquid level will be measured and compared to a set point. The resulting error will be fed to a controller, which in turn will open or close the valve feeding the upper tank.

a. Assuming $a_1 = 0.04$, $a_2 = 0.0187$, $a_3 = 1$, and $a_4 = 0.227$, design a lag compensator to obtain a step-response steady-state error of 10% without affecting the system's transient response appreciably.

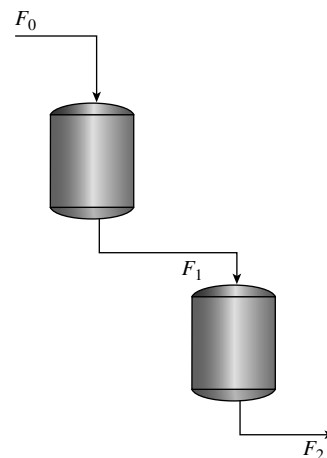**b.** Verify your design through MATLAB simulations. **MATLAB ML**

FIGURE P9.5

36. Figure P9.6(*a*) shows a heat-exchanger process whose purpose is to maintain the temperature of a liquid at a prescribed temperature.

The temperature is measured using a sensor and a transmitter, TT 22, that sends the measurement to a
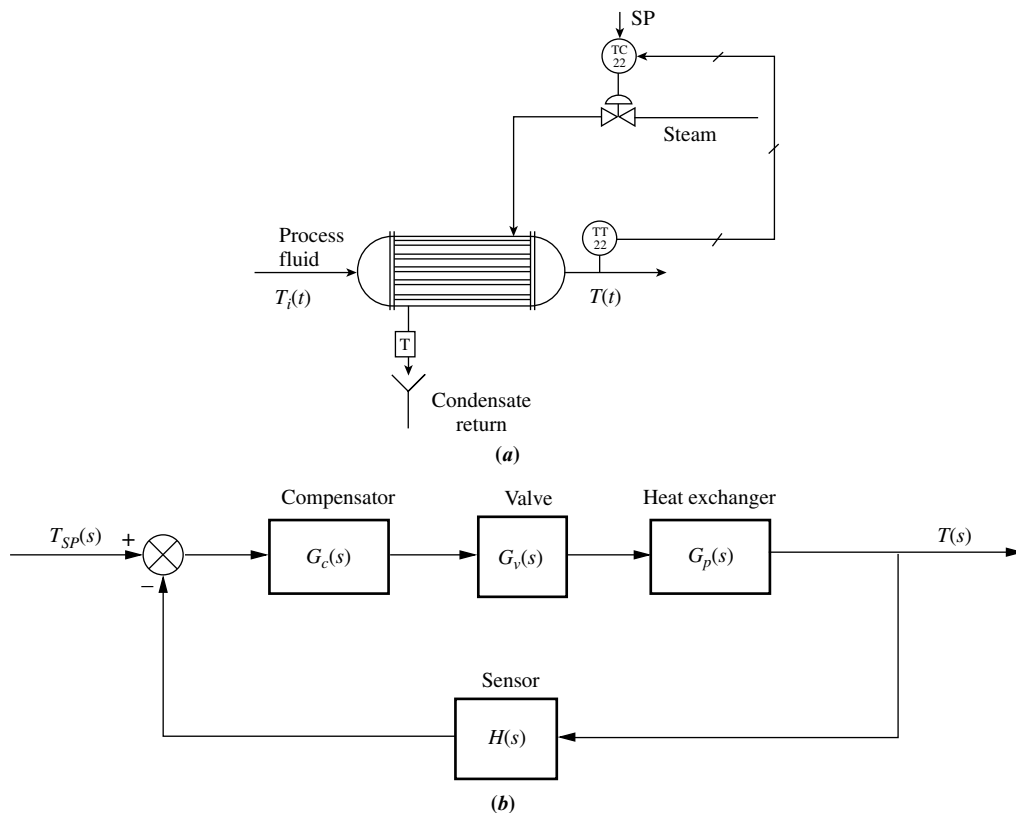
FIGURE P9.6   **a.** Heat-exchanger process (Reprinted with permission of John Wiley & Sons, Inc.); **b.** block diagram

corresponding controller, TC 22, that compares the actual temperature with a desired temperature set point, SP. The controller automatically opens or closes a valve to allow or prevent the flow of steam to change the temperature in the tank. The corresponding block diagram for this system is shown in Figure P9.6(*b*) (*Smith 2002*). Assume the following transfer functions:

$$G_v(s) = \frac{0.02}{4s + 1}; \quad G_1(s) = \frac{70}{50s + 1}; \quad H(s) = \frac{1}{12s + 1}.$$

a. Assuming $G_c(s) = K$, find the value of K that will result in a dominant pole with $\zeta = 0.7$. Obtain the corresponding T_s.

b. Design a PD controller to obtain the same damping factor as Part **a** but with a settling time 20% smaller.

c. Verify your results through MATLAB simulation. **MATLAB** **ML**

37. Repeat Problem 36, Parts **b** and **c**, using a lead compensator.

38. a. Find the transfer function of a motor whose torque-speed curve and load are given in Figure P9.7.
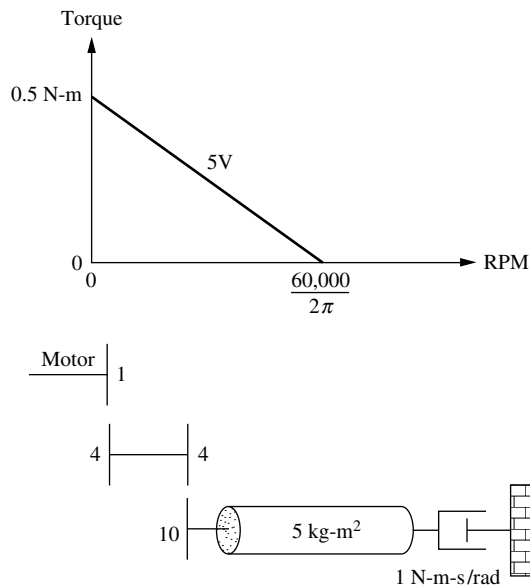

FIGURE P9.7

b. Design a tachometer compensator to yield a damping ratio of 0.5 for a position control

employing a power amplifier of gain 1 and a preamplifier of gain 5000.

c. Compare the transient and steady-state characteristics of the uncompensated system and the compensated system.

39. You are given the motor whose transfer function is shown in Figure P9.8(*a*).

$$E_a(s) \quad \boxed{\dfrac{25}{s(s+1)}} \quad \theta_o(s)$$
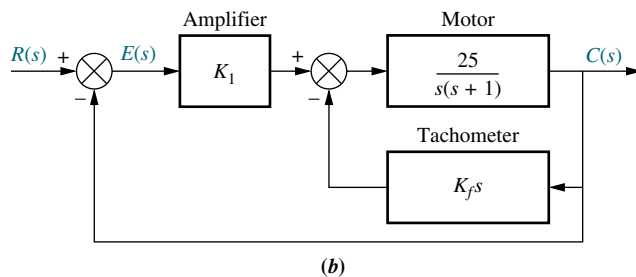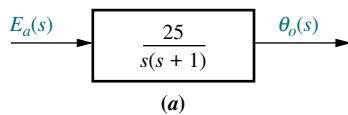
(*a*)

(*b*)

FIGURE P9.8

a. If this motor were the forward transfer function of a unity feedback system, calculate the percent overshoot and settling time that could be expected.

b. You want to improve the closed-loop response. Since the motor constants cannot be changed and you cannot use a different motor, an amplifier and tachometer are inserted into the loop as shown in Figure P9.8(*b*). Find the values of K_1 and K_f to yield a percent overshoot of 25% and a settling time of 0.2 second.

c. Evaluate the steady-state error specifications for both the uncompensated and the compensated systems.

40. A position control is to be designed with a 20% overshoot and a settling time of 2 seconds. You have on hand an amplifier and a power amplifier whose cascaded transfer function is $K_1/(s+20)$ with which to drive the motor. Two 10-turn pots are available to convert shaft position into voltage. A voltage of $\pm 5\pi$ volts is placed across the pots. A dc motor whose transfer function is of the form

$$\frac{\theta_o(s)}{E_a(s)} = \frac{K}{s(s+a)}$$

is also available. The transfer function of the motor is found experimentally as follows. The motor and geared load are driven open-loop by applying a large, short, rectangular pulse to the armature. An oscillo-gram of the response shows that the motor reached 63% of its final output value at 1/2 second after the application of the pulse. Further, with a constant 10 volts dc applied to the armature, the constant output speed was 100 rad/s.

a. Draw a complete block diagram of the system, specifying the transfer function of each component when the system is operating with 20% overshoot.

b. What will the steady-state error be for a unit ramp input?

c. Determine the transient response characteristics.

d. If tachometer feedback is used around the motor, as shown in Figure P9.9, find the tachometer and the amplifier gain to meet the original specifications. Summarize the transient and steady-state characteristics.
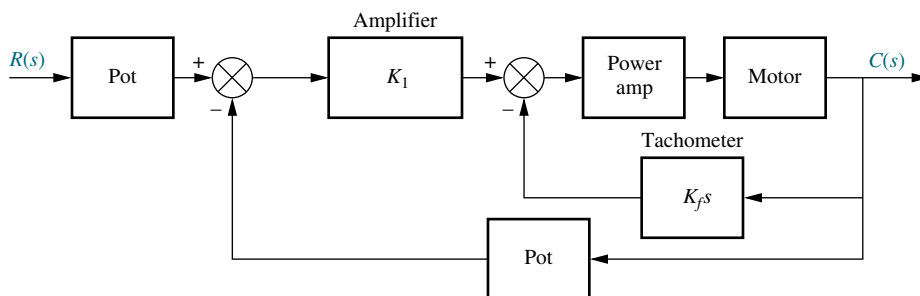

FIGURE P9.9

41. A position control is to be designed with a 10% overshoot, a settling time of 1 second, and $K_v = 1000$. You have on hand an amplifier and a power amplifier whose cascaded transfer function is $K_1/(s + 40)$ with which to drive the motor. Two 10-turn pots are available to convert shaft position into voltage. A voltage of $\pm 20\pi$ volts is placed across the pots. A dc motor whose transfer function is of the form

$$\frac{\theta_o(s)}{E_a(s)} = \frac{K}{s(s + a)}$$

is also available. The following data are observed from a dynamometer test at 50 V. At 25 N-m of torque, the motor turns at 1433 rpm. At 75 N-m of torque, the motor turns at 478 rpm. The speed measured at the load is 0.1 that of the motor. The equivalent inertia, including the load, at the motor armature is 100 kg-m², and the equivalent viscous damping, including the load, at the motor armature is 50 N-m-s/rad.

a. Draw a complete block diagram of the system, specifying the transfer function of each component.

b. Design a passive compensator to meet the requirements in the problem statement.

c. Draw the schematic of the compensator showing all component values. Use an operational amplifier for isolation where necessary.

d. Use MATLAB or any other computer program to simulate your system and show that all requirements have been met.

MATLAB
ML

42. Given the system shown in Figure P9.10, find the values of K and K_f so that the closed-loop dominant poles will have a damping ratio of 0.5 and the underdamped poles of the minor loop will have a damping ratio of 0.8.
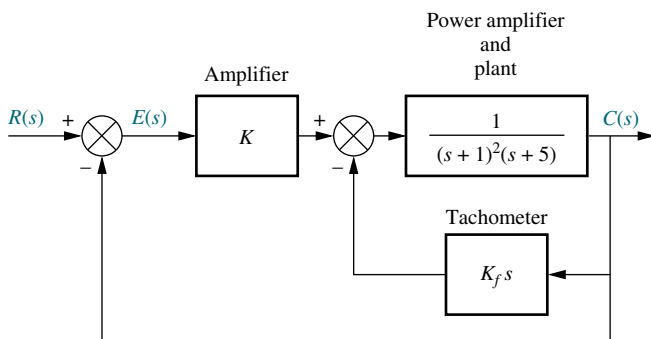

FIGURE P9.10

43. Given the system in Figure P9.11, find the values of K and K_f so that the closed-loop system will have a 4.32% overshoot and the minor loop will have a damping ratio of 0.8. Compare the expected performance of the system without tachometer compensation to the expected performance with tachometer compensation.
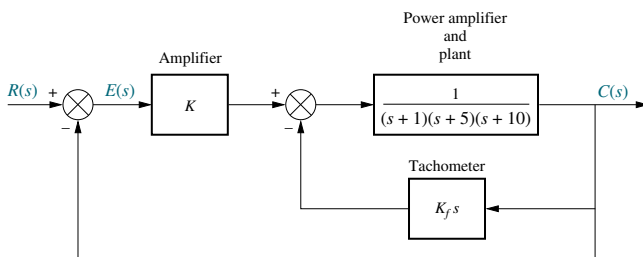

FIGURE P9.11

44. In Problem 57 of Chapter 8, a head-position control system for a floppy disk drive was designed to yield a settling time of 0.1 second through gain adjustment alone. Design a lead compensator to decrease the settling time to 0.05 second without changing the percent overshoot. Also, find the required loop gain.

45. Consider the temperature control system for a chemical process shown in Figure P9.12. The uncompensated system is operating with a rise time approximately the same as a second-order system with a peak time of 16 seconds and 5% overshoot. There is also considerable steady-state error. Design a PID controller so that the compensated system will have a rise time approximately equivalent to a second-order system with a peak time of 8 seconds and 5% overshoot, and zero steady-state error for a step input.

WileyPLUS
WPCS
Control Solutions

46. Steam-driven power generators rotate at a constant speed via a governor that maintains constant steam pressure in the turbine. In addition, automatic generation control (AGC) or load frequency control (LFC) is added to ensure reliability and consistency despite load variations or other disturbances that can affect the distribution line frequency output. A specific turbine-governor system can be described only using the block diagram of Figure P9.1 in which $G(s) = G_c(s)G_g(s)G_t(s)G_m(s)$, where (*Khoda-bakhshian, 2005*)
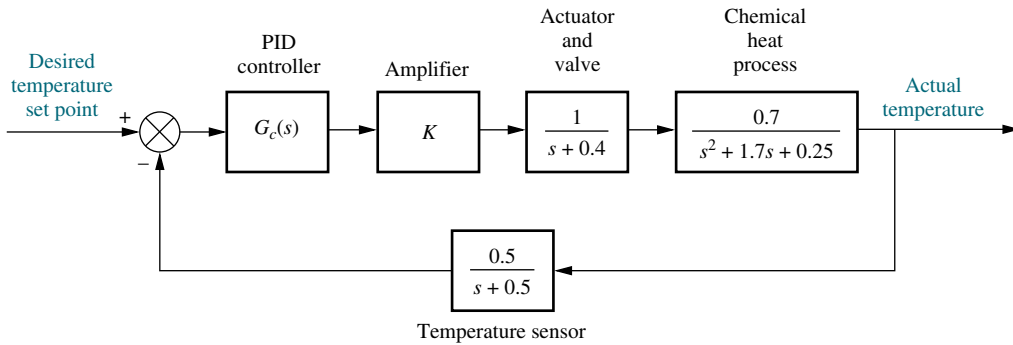
FIGURE P9.12 Chemical process temperature control system

$G_g(s) = \dfrac{1}{0.2s + 1}$ is the governor's transfer function

$G_t(s) = \dfrac{1}{0.5s + 1}$ is the turbine transfer function

$G_m(s) = \dfrac{1}{10s + 0.8}$ represents the machine and load transfer functions

$G_c(s)$ is the LFC compensation to be designed

   a. Assuming $G_c(s) = K$, find the value of K that will result in a dominant pole with $\zeta = 0.7$. Obtain the corresponding T_s.

   b. Design a PID controller to obtain the same damping factor as in Part **a**, but with a settling time of 2 seconds and zero steady-state error to step input commands.

   c. Verify your results using a MATLAB simuation.   MATLAB **ML**

47. Repeat Problem 46 using a lag-lead compensator instead of a PID controller. Design for a steady-state error of 1% for a step input command.

48. Digital versatile disc (DVD) players incorporate several control systems for their operations. The control tasks include (1) keeping the laser beam focused on the disc surface, (2) fast track selection, (3) disc rotation speed control, and (4) following a track accurately. In order to follow a track, the pickup-head radial position is controlled via a voltage that operates a voice coil embedded in a magnet configuration. For a specific DVD player, the transfer function is given by

$$P(s) = \frac{X(s)}{V(s)}$$

$$= \frac{0.63}{\left(1 + \dfrac{0.36}{305.4}s + \dfrac{s^2}{305.4^2}\right)\left(1 + \dfrac{0.04}{248.2}s + \dfrac{s^2}{248.2^2}\right)}$$

where $x(t)$ = radial pickup position and $v(t)$ = the coil input voltage (*Bittanti*, *2002*).

   a. Assume that the system will be controlled in a closed-loop configuration, such as the one shown in Figure P9.1. Assuming that the plant, $P(s)$, is cascaded with a proportional compensator, $G_c(s) = K$, plot the root locus of the system.

   b. Repeat Part **a** using MATLAB if your root locus plot was created by any other tool.   MATLAB **ML**

   c. Find the range of K for closed-loop stability, the resulting damping factor range, and the smallest settling time.

   d. Design a notch filter compensator so that the system's dominant poles have a damping factor of $\zeta = 0.7$ with a closed-loop settling time of 0.1 second.

   e. Simulate the system's step response for Part **c** using MATLAB.   MATLAB **ML**

   f. Add a PI compensator to the system to achieve zero steady-state error for a step input without appreciably affecting the transient response achieved in Part **b**.

   g. Simulate the system's step response for Part **e** using MATLAB.   MATLAB **ML**

49. A coordinate measuring machine (CMM) measures coordinates on three-dimensional objects. The accuracy of CMMs is affected by temperature changes as well as by mechanical resonances due to joint elasticity. These resonances are more pronounced when the machine has to go over abrupt changes of dimension, such as sharp corners at high speed. Each of the machine links can be controlled in a closed-loop configuration, such as the one shown in
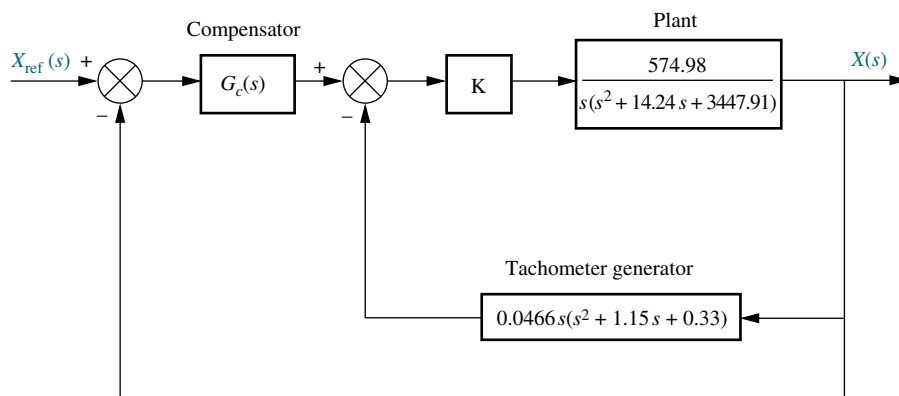
Figure P9.13 for a specific machine with prismatic (sliding) links. In the figure, $X_{ref}(s)$ is the commanded position and $X(s)$ is the actual position. The minor loop uses a tachometer generator to obtain the joint speed, while the main loop controls the joint's position (*Özel*, *2003*).

a. Find the value of K that will result in a minor loop with $\zeta = 0.5$.

b. Use a notch filter compensator, $G_c(s)$, for the external loop so that it results in a closed-loop damping factor of $\zeta = 0.7$ with $T_s \approx 4$ seconds.

c. Use MATLAB to simulate the compensated system's closed-loop step response.

MATLAB
ML

50. Magnetic levitation systems are now used to elevate and propel trains along tracks. A diagram of a demonstration magnetic levitation system is shown in Figure P9.14(*a*). Action between a permanent magnet attached to the Ping-Pong ball, the object to be levitated, and an electromagnet provides the lift. The amount of elevation can be controlled through V_a applied to the electromagnet as shown in Figure P9.14(*a*). The elevation is controlled by using a photo-detector pair to detect the elevation of the Ping-Pong ball. Assume that the elevation control system is represented by Figure P9.14(*b*) and do the following (*Cho*, *1993*):

a. Design a compensator, $G_c(s)$, to yield a settling time of 0.1 second or less if the step response is to have no more than 1% overshoot. Specify the compensator's poles, zeros, and gain.

b. Cascade another compensator to minimize the steady-state error and have the total settling time
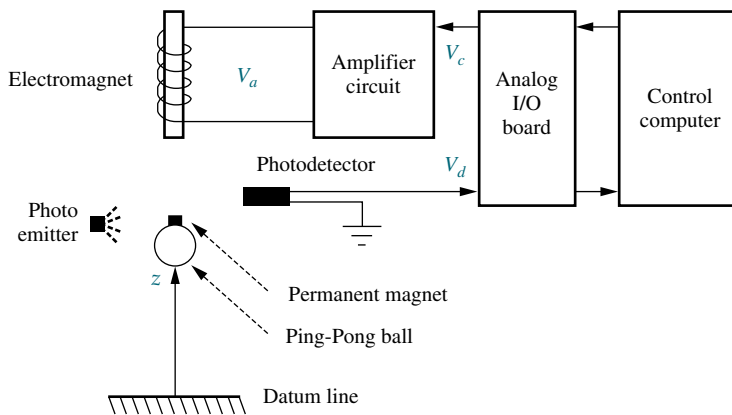
(*a*)

FIGURE P9.14   **a.** Magnetic levitation system (© 1993 IEEE); (*figure continues*)
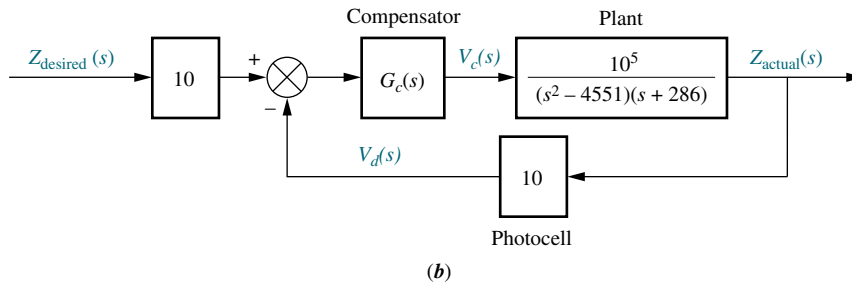
FIGURE P9.14 (*Continued*) **b.** block diagram

not exceed 0.5 second. This compensator should not appreciably affect the transient response designed in Part **a**. Specify the poles and zeros of this compensator.

c. Use MATLAB or any other computer program to simulate the system to check your design. **ML**

51. The transfer function for an AFTI/F-16 aircraft relating angle of attack, $\alpha(t)$, to elevator deflection, $\delta_e(t)$, is given by

$$G(s) = \frac{\alpha(s)}{\delta_e(s)}$$
$$= 0.072 \frac{(s+23)(s^2+0.05s+0.04)}{(s-0.7)(s+1.7)(s^2+0.08s+0.04)}$$

Assume the block diagram shown in Figure P9.15 for controlling the angle of attack, α, and do the following (*Monahemi*, 1992):

a. Find the range of K for stability.

b. Plot or sketch a root locus.

c. Design a cascade compensator to yield zero steady-state error, a settling time of about 0.05 second, and a percent overshoot not greater than 20%.

d. Use MATLAB or any other computer program to simulate the system to check your design. **ML**
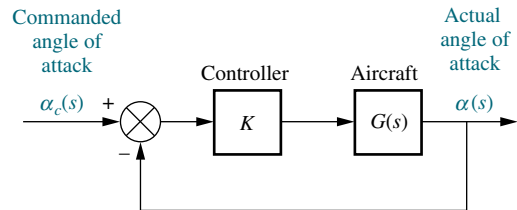

FIGURE P9.15 Simplified block diagram for angle of attack control

52. Figure P9.16 is a simplified block diagram of a self-guiding vehicle's bearing angle control. Design a lead compensator to yield a closed-loop step response with 10% overshoot and a settling time of 1.5 seconds.

53. An X-4 quadrotor flyer is designed as a small-sized unmanned autonomous vehicle (UAV) that flies mainly indoors and can help in search and recognizance missions. To minimize mechanical problems and for simplicity, this aircraft uses fixed pitch rotors with specially designed blades. Therefore, for thrust it is necessary to add a fifth propeller. A simplified design of the thrust control design can be modeled
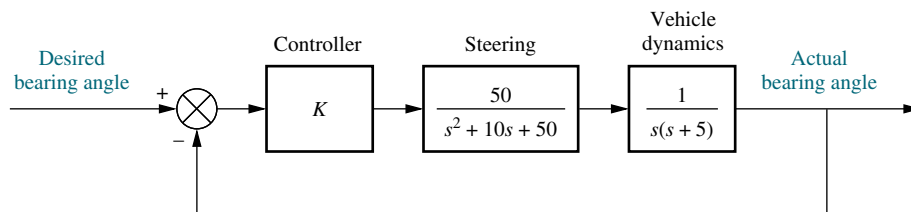

FIGURE P9.16 Simplified block diagram of a self-guiding vehicle's bearing angle control

as in Figure 9.1 with $G(s) = G_c(s)P(s)$ where

$$P(s) = \frac{1.90978\left(\dfrac{s}{0.43} + 1\right)}{\left(\dfrac{s}{9.6} + 1\right)\left(\dfrac{s}{0.54} + 1\right)}$$

represents the dynamics of the thruster rotor gain, the motor, and the battery dynamics. Initially, the system is designed using a proportional compensator given by $G_c(s) = 3$ (*Pounds, 2009*).

a. Calculate the resulting steady-state error for a unit step input.

b. Design a lag compensator to yield half the steady-state error of the proportional compensator, without appreciably affecting the system's transient response.

c. Use MATLAB to simulate the original design and the lag compensated design. Verify your results.

MATLAB
ML

54. Problem 8.56 described an ac/dc conversion and power distribution system for which droop control is implemented through the use of a proportional controller to stabilize the dc-bus voltage. For simplification, a system with only one source converter and one load converter was considered. The parameters and design considerations presented in that problem, along with some solution results, allow us to represent the block-diagram of that system as shown in the Figure P9.17.
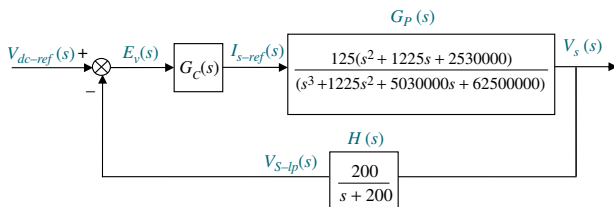

FIGURE P9.17

Here $G_c(s)$ is the transfer function of the controller, $G_p(s)$ represents the forward path of the controlled plant (a conversion and power distribution unit), and $H(s)$ is the transfer function of the feedback low-pass filter (*Karlsson, 2003*).

Prepare a table, such as Table 9.5, where the first column, headed *Uncompensated*, is filled in with your results from the proportional design of

Problem 8.56, assuming an input step, $v_{dc-ref}(t) = 750\, u(t)$.

Follow Steps 2–8 as described in Section 9.4 (Example 9.5), to design a proportional-plus-integral-plus-derivative (PID) controller so that the system can operate with a percent overshoot $\leq 4.4\%$, a peak time 20% smaller than that of the uncompensated system, and zero steady-state error, $e_{V\text{step}}(\infty) = 0$. Fill in the remaining two columns of your table, *PD-compensated* and *PID-compensated*.

PROGRESSIVE ANALYSIS AND DESIGN PROBLEMS

55. **High-speed rail pantograph.** Problem 21 in Chapter 1 discusses the active control of a pantograph mechanism for high-speed rail systems. In Problem 79(*b*), Chapter 5, you found the block diagram for the active pantograph control system. In Chapter 8, Problem 72, you designed the gain to yield a closed-loop step response with 38% overshoot. A plot of the step response should have shown a settling time greater than 0.5 second as well as a high-frequency oscillation superimposed over the step response (*O'Conner, 1997*). We want to reduce the settling time to about 0.3 second, reduce the step response steady-state error to zero, and eliminate the high-frequency oscillation. A way of eliminating the high-frequency oscillation is to cascade a notch filter with the plant. Using the notch filter,

$$G_n(s) = \frac{s^2 + 16s + 9200}{(s + 60)^2}$$

do the following:

a. Design a PD controller to yield a settling time of approximately 0.3 second with no more then 60% overshoot.

b. Add a PI controller to yield zero steady-state error for step inputs.

c. Use MATLAB to plot the PID/notch-compensated closed-loop step response.

MATLAB
ML

56. **Control of HIV/AIDS**. It was shown in Chapter 6, Problem 68, that when the virus levels in an HIV/AIDS patient are controlled using RTIs the linearized plant model is

$$P(s) = \frac{Y(s)}{U_1(s)} = \frac{-520s - 10.3844}{s^3 + 2.6817s^2 + 0.11s + 0.0126}$$

Assume that the system is embedded in a configuration, such as the one shown in Figure P9.1, where $G(s) = G_c(s) P(s)$. Here, $G_c(s)$ is a cascade compensator. For simplicity in this problem, choose the dc gain of $G_c(s)$ less than zero to obtain a negative-feedback system (the negative signs of $G_c(s)$ and $P(s)$ cancel out) (*Craig, I. K., 2004*).

a. Consider the uncompensated system with $G_c(s) = -K$. Find the value of K that will place all closed-loop poles on the real axis.

b. Use MATLAB to simulate the unit step response of the gain-compensated system. Note the %OS and the T_s from the simulation.

MATLAB

ML

c. Design a PI compensator so that the steady-state error for step inputs is zero. Choose a gain value to make all poles real.

d. Use MATLAB to simulate the design in Part c for a unit step input. Compare the simulation to Part b.

MATLAB

ML

57. Hybrid vehicle. In the previous chapter, we used the root locus to design a proportional controller for the speed control of an HEV. We rearranged the block diagram to be a unity feedback system, as shown in the block diagram of Figure P7.34 (*Preitl, 2007*). The plant and compensator resulted in

$$G(s) = \frac{K(s + 0.60)}{(s + 0.5858)(s + 0.0163)}$$

and we found that $K = 0.78$ resulted in a critically damped system.

a. Use this design to itemize the performance specifications by filling in a table, similar to Table 9.5, under the column *Uncompensated*. Take advantage of the results from Chapter 8 or use MATLAB to find the entries. Plot $c(t)$ for $r(t) = 4 \ u(t)$ volts.

b. Now assume that the system specifications require zero steady-state error for step inputs, a steady-state error for ramp inputs $\leq 2\%$, a %OS $\leq 4.32\%$, and a settling time ≤ 4 sec. It should be evident that this is not accomplished with a proportional controller. Thus, start by designing a PI controller to meet the

MATLAB

ML

requirements. If necessary add a PD mode to get a PID controller. Simulate your final design using MATLAB. Fill in the results of this design in the second column of your table with the heading *Compensated*.

c. Now note the following limitations of linear control system modeling:

(1) No limit is set on system variables. For example, vehicle acceleration as well as motor and power amplifier current, torque or power do not have upper limits.

(2) It is assumed that to improve the speed of response in Part **b**, we could place the PI controller's zero on top of the pole closest to the origin. Realistically, such pole-zero cancellation is not always possible to maintain.

If you do not expand your model beyond the described limitations if required for accuracy, unrealistic response characteristics, such as rise and settling times could result. Look at your design results including response curves. Are they realistic? If not, revise your Simulink model, which you developed for Problem 5.81, as follows:

Simulink

SL

i. Represent the motor armature as a first-order system with a unity steady-state gain and a time constant of 50 ms, which avoids the creation of internal algebraic closed-loops and should have negligible effect on system response;

ii. Add a saturation element at the output of the motor armature and set it to an upper limit of 250 A;

iii. Use the following PI settings. The PI settings of the speed controller are P = 61 and I = 0.795. The PI settings of the torque controller are P = 10 and I = 6;

iv. Run the modified model and comment on the graphs obtained for motor current, car acceleration, and speed.

Cyber Exploration Laboratory

Experiment 9.1

Objectives   To perform a trade-off study for lead compensation. To design a PI controller and see its effect upon steady-state error.

Minimum Required Software Packages   MATLAB, and the Control System Toolbox

Prelab

1. How many lead compensator designs will meet the transient response specifications of a system?
2. What differences do the lead compensators of Prelab 1 make?
3. Design a lead compensator for a unity negative feedback system with a forward transfer function of $G(s) = \dfrac{K}{s(s+3)(s+6)}$ to meet the following specifications: percent overshoot $= 20\%$; settling time $= 2$ seconds. Specify the required gain, K. Estimate the validity of the second-order approximation.
4. What is the total angular contribution of the lead compensator of Prelab 3?
5. Determine the pole and zero of two more lead compensators that will meet the requirements of Prelab 3.
6. What is the expected steady-state error for a step input for each of the lead-compensated systems?
7. What is the expected steady-state error for a ramp input for each of the lead-compensated systems?
8. Select one of the lead compensator designs and specify a PI controller that can be cascaded with the lead compensator that will produce a system with zero steady-state error for both step and ramp inputs.

Lab

1. Using the SISO Design Tool, create the design in Prelab 3 and plot the root locus, step response, and ramp response. Take data to determine the percent overshoot, settling time, and step and ramp steady-state errors. Record the gain, K.
2. Repeat Lab 1 for each of the designs in Prelab 5.
3. For the design selected in Prelab 8, use the SISO Design Tool and insert the PI controller. Plot the step response and measure the percent overshoot, settling time, and steady-state error. Also, plot the ramp response for the design and measure the steady-state error.
4. Plot the step and ramp responses for two more values of the PI controller zero.

Postlab

1. Make a table showing calculated and actual values for percent overshoot, settling time, gain, K, steady-state error for step inputs, and steady-state error for ramp inputs. Use the three systems without the PI controller and the single system with the PI controller from Lab 3.
2. Itemize the benefits of each system without the PI controller.
3. Choose a final design and discuss the reasons for your choice.